ISSN 1007-9327 (print)
ISSN 2219-2840 (online)

World Journal of *Gastroenterology*

World J Gastroenterol 2023 May 7; 29(17): 2515-2703

Published by Baishideng Publishing Group Inc

World Journal of Gastroenterology

Contents

Weekly Volume 29 Number 17 May 7, 2023

REVIEW

MINIREVIEWS

ORIGINAL ARTICLE

Basic Study

Retrospective Study

Randomized Controlled Trial

SYSTEMATIC REVIEWS

LETTER TO THE EDITOR

World Journal of Gastroenterology

Weekly Volume 29 Number 17 May 7, 2023

Contents

ABOUT COVER

Editorial Board Member of *World Journal of Gastroenterology*, Mohamad Amin Pourhoseingholi, PhD, Associate Professor, Gastroenterology and Liver Diseases Research Center, Research Institute for Gastroenterology and Liver Diseases, Shahid Beheshti University of Medical Sciences, Tehran 19835, Iran. aminphg@gmail.com

AIMS AND SCOPE

The primary aim of *World Journal of Gastroenterology* (*WJG*, *World J Gastroenterol*) is to provide scholars and readers from various fields of gastroenterology and hepatology with a platform to publish high-quality basic and clinical research articles and communicate their research findings online. *WJG* mainly publishes articles reporting research results and findings obtained in the field of gastroenterology and hepatology and covering a wide range of topics including gastroenterology, hepatology, gastrointestinal endoscopy, gastrointestinal surgery, gastrointestinal oncology, and pediatric gastroenterology.

INDEXING/ABSTRACTING

The *WJG* is now abstracted and indexed in Science Citation Index Expanded (SCIE, also known as SciSearch®), Current Contents/Clinical Medicine, Journal Citation Reports, Index Medicus, MEDLINE, PubMed, PubMed Central, Scopus, Reference Citation Analysis, China National Knowledge Infrastructure, China Science and Technology Journal Database, and Superstar Journals Database. The 2022 edition of Journal Citation Reports® cites the 2021 impact factor (IF) for *WJG* as 5.374; IF without journal self cites: 5.187; 5-year IF: 5.715; Journal Citation Indicator: 0.84; Ranking: 31 among 93 journals in gastroenterology and hepatology; and Quartile category: Q2. The *WJG*'s CiteScore for 2021 is 8.1 and Scopus CiteScore rank 2021: Gastroenterology is 18/149.

RESPONSIBLE EDITORS FOR THIS ISSUE

NAME OF JOURNAL
World Journal of Gastroenterology

ISSN
ISSN 1007-9327 (print) ISSN 2219-2840 (online)

LAUNCH DATE
October 1, 1995

FREQUENCY
Weekly

EDITORS-IN-CHIEF
Andrzej S Tarnawski

EDITORIAL BOARD MEMBERS
http://www.wjgnet.com/1007-9327/editorialboard.htm

PUBLICATION DATE
May 7, 2023

INSTRUCTIONS TO AUTHORS
https://www.wjgnet.com/bpg/gerinfo/204

GUIDELINES FOR ETHICS DOCUMENTS
https://www.wjgnet.com/bpg/GerInfo/287

GUIDELINES FOR NON-NATIVE SPEAKERS OF ENGLISH
https://www.wjgnet.com/bpg/gerinfo/240

PUBLICATION ETHICS
https://www.wjgnet.com/bpg/GerInfo/288

PUBLICATION MISCONDUCT
https://www.wjgnet.com/bpg/gerinfo/208

ARTICLE PROCESSING CHARGE
https://www.wjgnet.com/bpg/gerinfo/242

STEPS FOR SUBMITTING MANUSCRIPTS
https://www.wjgnet.com/bpg/GerInfo/239

ONLINE SUBMISSION
https://www.f6publishing.com

World Journal of Gastroenterology

Submit a Manuscript: https://www.f6publishing.com

World J Gastroenterol 2023 May 7; 29(17): 2515-2533

DOI: 10.3748/wjg.v29.i17.2515

ISSN 1007-9327 (print) ISSN 2219-2840 (online)

REVIEW

Novel biomarkers for early detection of gastric cancer

Tasuku Matsuoka, Masakazu Yashiro

Specialty type: Gastroenterology and hepatology

Provenance and peer review: Invited article; Externally peer reviewed.

Peer-review model: Single blind

Peer-review report's scientific quality classification

Grade A (Excellent): 0
Grade B (Very good): B, B
Grade C (Good): C, C
Grade D (Fair): 0
Grade E (Poor): 0

P-Reviewer: Chen X, China; Li DH, China; Zhang Y, China; Zhao Q, China

Received: November 19, 2022
Peer-review started: November 19, 2022
First decision: January 2, 2023
Revised: January 31, 2023
Accepted: April 13, 2023
Article in press: April 13, 2023
Published online: May 7, 2023

Tasuku Matsuoka, Masakazu Yashiro, Molecular Oncology and Therapeutics, Osaka Metropolitan University Graduate School of Medicine, Osaka 5458585, Japan

Corresponding author: Masakazu Yashiro, MD, PhD, Assistant Professor, Molecular Oncology and Therapeutics, Osaka Metropolitan University Graduate School of Medicine, 1-4-3 Asahi-machi, Abeno-ku, Osaka 5458585, Japan. i21496f@omu.ac.jp

Abstract

Gastric cancer (GC) remains a leading cause of cancer-related death worldwide. Less than half of GC cases are diagnosed at an advanced stage due to its lack of early symptoms. GC is a heterogeneous disease associated with a number of genetic and somatic mutations. Early detection and effective monitoring of tumor progression are essential for reducing GC disease burden and mortality. The current widespread use of semi-invasive endoscopic methods and radiologic approaches has increased the number of treatable cancers: However, these approaches are invasive, costly, and time-consuming. Thus, novel molecular noninvasive tests that detect GC alterations seem to be more sensitive and specific compared to the current methods. Recent technological advances have enabled the detection of blood-based biomarkers that could be used as diagnostic indicators and for monitoring postsurgical minimal residual disease. These biomarkers include circulating DNA, RNA, extracellular vesicles, and proteins, and their clinical applications are currently being investigated. The identification of ideal diagnostic markers for GC that have high sensitivity and specificity would improve survival rates and contribute to the advancement of precision medicine. This review provides an overview of current topics regarding the novel, recently developed diagnostic markers for GC.

Key Words: Gastric cancer; Diagnostic biomarkers; Early detection; Liquid biopsy

Core Tip: Gastric cancer (GC) is a major unsolved clinical problem. It is the fifth most diagnosed cancer in the world, and the fourth most frequent cause of cancer-related deaths worldwide. The outcome of advanced GC remains tremendously poor despite the use of surgery and adjuvant therapy. Therefore, the detection new biomarkers for early diagnosis will be potential therapeutic strategies for improving survival of GC patients. The aim of this review is to summarizes the current status and approaches for novel biomarkers, which could be useful for early diagnosis.

Citation: Matsuoka T, Yashiro M. Novel biomarkers for early detection of gastric cancer. *World J Gastroenterol* 2023; 29(17): 2515-2533
URL: https://www.wjgnet.com/1007-9327/full/v29/i17/2515.htm
DOI: https://dx.doi.org/10.3748/wjg.v29.i17.2515

INTRODUCTION

Gastric cancer (GC) is the fifth most common cancer and the fourth most common cause of cancer-related death worldwide[1]. The overall survival rate of individuals with GC remains poor, because it is often diagnosed at an advanced stage or even as metastasis. One strategy for lowering the burden of GC is early screening and diagnosis. Even though upper gastrointestinal endoscopy has been well established as the standard for GC screening, capturing a concealed tumor in the stomach requires higher sensitivity and specificity. Upper gastrointestinal endoscopies also involve high costs with regard to cost and human resources, requiring experienced endoscopists and patient understanding.

To achieve large-scale GC screening among healthy individuals in the future, a more general and cost-effective approach is needed. Cancer biomarkers (tumor markers) are molecules indicative of the presence and progression of cancer; as such, they play a crucial role in cancer diagnoses and treatment selection[2]. Their applications are rapidly expanding owning to advances in genetic analysis technology and molecular targeting. There are at present no biomarkers with sufficient sensitivity and specificity for the diagnosis of GC that could be applied in clinical settings. Biomarkers are needed for every stage of GC to improve its clinical course. The emergence of liquid biopsy technology, which enables the detection of specific molecular information of solid tumors from body fluids, has provided major changes in cancer diagnosis and treatment[3]. There are many studies on biomarkers for GC screening. However, many of these candidate biomarkers identified thus far are preferentially expressed at advanced stages, and thus unsuitable for early detection. Moreover, a comprehensive review focusing on early detection of GC is still lacking. Herein, we review novel candidates of biomarkers focusing on early detection of GC comprehensively, from the laboratory to the clinical prevalence and the future prospects. This information will contribute to further research on GC biomarkers and their clinical applications.

METHODS

A non-systematic review was performed based on an electronic search through the medical literature using PubMed and Google Scholar. The keywords "biomarker", "gastric cancer", "early detection", "diagnostics", "liquid biopsy" were used. Review articles and guidelines investigating the values of biomarker for early detection of GC from gastroenterology, oncology and genetics were included in this review. When more than one guideline concerning the same subject was available, the most up-to-date one was selected. Only full articles in the English language published in the last ten years were considered for further review. Great importance was also given to "Clinical study" and "Review" articles dealing with the topic. The exclusion criteria comprised duplicated articles, studies absent of diagnostic outcomes. Case reports, correspondences, letters, and non-human research were not included.

LIQUID BIOPSY

Various diverse molecules in blood (serum/plasma) have been said to be correlated with GC carcinogenesis. Among them, DNA, proteins, and noncoding RNA (ncRNA) molecules have been focused. These molecules allow the dependable finding of new noninvasive biomarkers for GC in plasma/serum. Liquid biopsy has shown good potential in detecting circulating tumor cells (CTCs) from any bodily fluid, including peripheral blood, urine and cerebrospinal fluid, ascites, pleural effusion, *etc*., and includes a genomic, proteomic and metabolite assessment. It is a quick, easy and inexpensive method

with minimal invasiveness, making it widely accepted by patients, without major side effects[4]. Liquid biopsy (using mainly peripheral blood) can be used as a screening method to detect early GC (EGC) and minimal residual disease (MRD) after surgery and can create an appropriate treatment plan in GC patients.

CTCs/circulating tumor DNA

CTCs defined as tumor cells that have been detached from the primary tumor or metastases and shed in patient's bloodstream, characterize an easily attainable sample of cancer specimens. As a liquid biopsy, emerging technologies for CTC isolation have enabled the research on the pathology of CTCs and have prompted the clinical uses of CTCs in the diagnosis of malignancies[5]. Although many researchers have come to the same conclusion that CTCs positivity was associated with prognosis, few researches were found for the early diagnosis, especially in the last several years.

Circulating cell-free DNA (cfDNA) consists of fragments of extracellular DNA that can be found in the blood[6]. cfDNA changes across different pathological states have been successfully exploited as noninvasive biomarkers for liquid biopsies. Particularly, the cfDNA that is identified from tumors and shows tumor-specific mutations is named circulating tumor DNA (ctDNA)[7]. The analysis of ctDNA has been predominantly of interest over a decade as its remarkable stability in body fluids. Besides, accumulating evidences showed that ctDNA is useful for early incidence during disease progress after surgical procedure. Further improvement of the ctDNA detection system is progressing. The cfDNA-based liquid biopsy for early diagnosis is mostly restrained by the low signals shed from early-stage cancer, which directly influence the sensitivity of sequencing analyses.

Recent paper has described that the circulating biomarkers, such as cfDNA was highly expressed in stage I GC patients compared with those in benign gastric disease patients and health controls, suggesting the potential for their use for the early detection of GC[8,9]. The human epidermal growth factor receptor 2 (HER2) gene copy number detected in ctDNA was higher in GC patients compared to healthy control. Elucidation of HER2 copy number variation could distinguish healthy individuals and patients with GCs with 58% sensitivity and 98% specificity [area under curve (AUC) = 0.707, 95% confidence interval (CI): 0.593-0.821][10]. ctDNA sequencing identifies fibroblast growth factor receptor 2 (FGFR2) amplification missed by tissue testing in patients with advanced GC, and these patients may respond to FGFR inhibition. ctDNA can detect plasma *FGFR2* alterations, occasionally at a higher frequency than tissue testing, identify patients and these patients may respond to FGFR inhibition[11].

Current cancer biomarkers can be categorized into two groups: (1) Biomarkers generally used for the detection of specific cancer types; and (2) Biomarkers to be aimed to decide personalized medicine, such as companion diagnostics. Even when surgical procedure is successfully carried out, detecting MRD after surgery is still challenging for doctors, and it is difficult to detect MRD in time using radiologic imaging or tissue biopsy. Recent studies presented that ctDNA-based testing were able to detect MRD several weeks earlier than imaging[12]. Another study monitoring ctDNA in postoperative blood has verified that, the median duration from positive ctDNA detection to relapse was 4.05 mo[13]. Moreover, the postoperative positive ctDNA was significantly correlated with tumor recurrence within 12 mo after surgery, suggesting that postoperative ctDNA monitoring possess clinical application value in the prediction of postoperative GC recurrence[13]. In a similar, ctDNA positivity preceded radiographic recurrence by a median of 6 mo, suggesting that, ctDNA is a sensitive and specific biomarker for finding patients at high risk for relapse after curative treatment[14]. ctDNA-positive patients were at higher risk of relapse and exhibited worse outcome compared to the ctDNA-negative group, implying that ctDNA monitoring in the post-treatment setting is predicted to offer knowledge about necessity for further therapy[15]. The clinical usefulness of ctDNA as biomarker for longitudinal disease monitoring and identification of MRD in GC was assessed by ultra-deep sequencing methods. The occurrence of relapse was 100% (7 of 7), 100% (5 of 5), and 94% (16 of 17), respectively in patients with measurable ctDNA at the post-operative, post-adjuvant chemotherapy, and consequent longitudinal time spots. To date, novel high throughput sequencing techniques such as next-generation sequencing (NGS) or whole exosome sequence can identify mutations in multiple genetic regions[16]. Recent study conducted surveillance for recurrent disease after curative surgical resection analyzed by whole genome sequence. For 1630 patients with GC and esophageal adenocarcinomas, detection of MRD after successful surgical procedure is intensely correlated with an enhanced risk of relapse by utilizing a Guardant 360, ctDNA-NGS assay[17]. These studies elucidate that risk stratification of patients for adjuvant chemotherapy escalation/de-escalation could be predicted by incorporation of ctDNA. ctDNA-guided treatment strategy in post-surgery surveillance for patients with GC is a novel emerging strategy that will likely replace the current treatment decision, as outlined in Figure 1.

NC RNA

Diverse ncRNAs, such as microRNA (miRNA), circular RNA (circRNA), and long ncRNA (lncRNA), are implicated in GC carcinogenesis[18]. MiRNAs are small ncRNA molecules of approximately 18-22 nucleotides that regulate cell differentiation, proliferation, apoptosis and gene regulation[19]. Currently, due to the stability and specificity of expression in circulation, accumulating evidences suggest that miRNAs can serve as novel biomarkers with a prospective clinical significance tool for patient with GC. MiRNAs are very stable in blood and can be identified by various assays such as reverse transcription

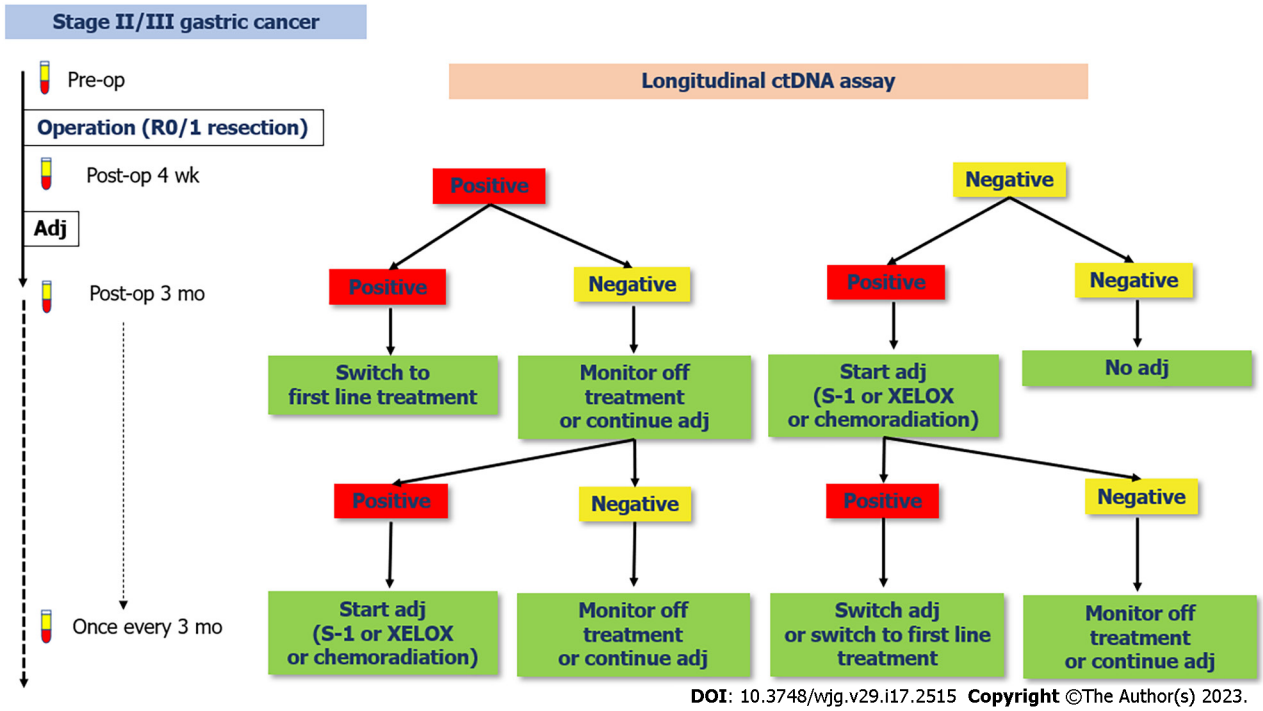

Figure 1 Proposed design of circulating tumor DNA-guided treatment strategy in gastric cancer. Schematic presentation of proposed circulating tumor DNA (ctDNA) guided treatment strategy in gastric cancer evaluating tailored treatment based on ctDNA detection. ctDNA positivity was determined by accessing the presence of plasma mutations, which indicates the existence of minimal residual disease. Adapted from Chakrabarti *et al*[100], and Kasi *et al*[101]. ctDNA: Circulating tumor DNA; Op: Operative; Adj: Ajuvant chemotherapy.

quantitative real-time polymerase chain reaction, and NGS. Recent studies challenged to verify the importance of various miRNAs in human plasma/serum as diagnostic markers for early-stage GC, including miR-17, miR-25, and miR-133b[20], miR-425-5p, miR-1180-3p, miR-122-5p, miR-24-3p, and miR-4632-5p[21]. A recent distinctive expression study of miRNA profiles utilizing two datasets from plasma samples identified hsa-miR-320a, hsa-miR-1260b, and hsa-miR-6515.5p as potential biomarkers for primary diagnosis of GC, with an AUC higher than 0.95 in all cases. Furthermore, hsa-miR-320a and hsa-miR-1260b was more stable in all the discovery and validation datasets[22]. Similarly, a recent study developed an EGC index to differentiate EGC from non-cancer controls based on the serum levels of four miRNAs (miR-4257, miR-6785-5p, miR-187-5p, and miR-5739). This index provided a sensitivity of 0.996 and a specificity of 0.953, with an AUC of 0.998 for the detection of EGC in a large sample size study (n = 1417)[23]. These results suggest that miRNAs could act as promising biomarkers for the early detection of GC. Nevertheless, further research is needed to optimize their detection methods and reproducibility of accrued results to meet the rigorous requirements for clinical setting.

LncRNAs are the transcripts of more than 200 nucleotides that have been found to participate widely in various pathological processes of organisms[24]. In colon cancer, LncRNA small nucleolar RNA host gene 11 has been presented as a promising biomarker for early detection of this malignancy[25]. Meanwhile, hepatocellular carcinoma upregulated lncRNA and ZNFX1 antisense RNA 1 have been shown to distinguish GC patients from healthy subjects and proposed as novel diagnostic biomarkers of GC[26]. LncRNAs promoter of CDKN1A antisense DNA damage activated RNA, FOXD2 adjacent opposite strand RNA 1, and SWI/SN F related, matrix associated, actin dependent regulator of chromatin subfamily c member 2 in plasma may serve as novel biomarkers for early detection of GC. The combined these three lncRNAs offer a high sufficient diagnostic sensitivity[27]. LncRNA B3GALT5 antisense RNA 1 was shown to be better than carcinoembryonic antigen (CEA) and carbohydrate antigen 19-9 (CA19-9) and may serve as a diagnostic biomarker of GC[28]. Distinct levels of serum C5orf66 antisense RNA 1 (C5orf66-AS1) were shown between patients with GC and gastritis. A risk of gastric dysplasia and GC negatively associated with serum expression of C5orf66-AS1, implying that C5orf66-AS1 a potential biomarker for predicting EGC[29]. Combined lncRNAs have been displayed to improve biomarker values for early detection of GC. LncRNA HLA Complex P5 (HCP5) is a kind of RNA gene without protein-coding. The AUC of serum lncRNA HCP5 was 0.818 (95%CI: 0.757-0.880, 80% sensitivity, and 70% specificity) in distinguishing between GC and healthy controls. Besides, the highest AUC of 0.870 (95%CI: 0.819-0.921) with 81% sensitivity and 79% specificity were revealed by the combination of three diagnoses, HCP5, CEA, and CA19-9[30]. Thus, the results above indicate that lncRNAs possess the diagnostic potential for early diagnosis of GC.

CircRNAs are also generally categorized as a ncRNA and physically vigorous nucleic acid molecules that construct closed loop RNA and require polyadenylated tails unlike messenger RNAs[31]. CircRNAs are more stable in tissues, have a superior life period and are more resistant to Ribonuclease R compared with linear RNAs[32]. In a recent, the rapid development of high-throughput sequencing has promoted the detection of circRNAs and their roles in physiological and pathological processes, including GC carcinogenesis, have been evaluated. A recent study found circRNA Has_circ_0000745 was downregulated in GC tissues and in plasma from patients with GC. Therefore, the use of these circRNAs has great potential as a new biomarker for diagnosis of GC[33]. The expression of hsa_circ_0001789 in 24 paired of cancerous and paracancerous plasma specimens were examined. A down-regulated expression of hsa_circ_0001789 was detected in GC plasma samples in comparison to the healthy controls, indicating that hsa_circ_0001789 has the potential to be a novel GC diagnostic biomarker[34]. CircPTPN22 is an outstanding diagnostic marker for GC. Utilizing receiver operator characteristic (ROC) analysis of circPTPN22 expression in GC patients, gastritis patients, and healthy controls, showed that its AUC was higher than that of traditional tumor markers CEA and CA19-9, and the AUC reached 0.892 after combined use[35]. 8-circRNA biomarker panel (hsa_circ_0001013, hsa_circ_0052001, hsa_circ_0034398, circ_0006089, hsa_circ_0002019, hsa_circ_0007380, hsa_circ_0008768, hsa_circ_0045602) discriminated patients with GC from normal control tissues, with an AUC value of 0.87 (95%CI: 0.82-0.93, sensitivity 78.3%, specificity 78.3%). Interestingly, 7 of 8 circRNA markers significantly lower expressed in serum specimens after surgery. Furthermore, 8-circRNA panel showed a greater specificity for the identification of patients with GC *vs* all other gastrointestinal cancers, such as colorectal cancer, pancreatic cancer, esophageal cancer, and hepatocellular carcinoma[36]. Studies using ncRNAs in screening/diagnostics of GC in the past 5 years are collected in Table 1.

Exosome

Exosomes are lipid bilayer-enclosed extracellular vehicles (EVs) approximately 30-150 nm in size, consist of a lipid bilayer interspersed with various membrane proteins, and which contain a variety of nucleic acids, proteins, and lipids[37]. Exosomes are secreted continuously by all cells and offer distinct prospects for clinically relevant diagnostic content, including DNA, RNA, and proteins[37]. Exosomes have been said to be associated with driving key features of cancer activity, including facilitation of tumor cell proliferation, suppression of the immune response, stimulation of tumor cell migration, initiation of angiogenesis, and formation of metastases[38]. Recently, growing evidences have established the latent diagnostic value of EVs or circulating exosomes for early diagnosis of GC. Due to the easiness to isolate exosomes compared with CTCs and cfDNA in malignant tumors, an growing number of studies will be highlighted on exosomes in the diagnosis of EGC in the next several decades. Exosomal lncUEGC1 exhibited an AUC of 0.8760 and 0.8406 in distinguishing EGC patients from normal subjects and those with atrophic gastritis, respectively, implying that exosomal lncUEGC1 had higher diagnostic reliability compared with CEA[39]. Circulating exosomal lncRNA proprotein convertase subtilisin/kexin type 2-2:1, G protein subunit alpha q-6:1 and GC-associated lncRNA1 (lncRNA-GC1) have been reported as better biomarkers for distinguishing GC patients from healthy people, compared with CEA, CA19-9, and CA72-4[40-42]. Similarly, serum four exosoms, miR-92b-3p, miR-146b-5p, miR-9-5p, and miR-let-7g-5p have been shown to be latent biomarkers for early detection of GC[43]. Likewise, the ROC showed that serum exosomal miR-590-5p showed a good classifier with an AUC of 0.810 (95%CI: 0.751-0.860) with a sensitivity of 63.7% and specificity of 86.0%, suggesting that serum exosomal miR-590-5p expression may be a noninvasive diagnostic biomarker of GC[44]. MiR-195-5p and miR-211-5p in GC patients' plasma exosomes have shown to be upregulated compared to healthy controls. The AUC values of plasma exosomal 2-miRNAs signature was 0.820, which was more meaningful to discriminate the GC patients from the healthy samples, compared to the AUC values obtained for combined CEA, CA19-9[45]. circ_0065149 levels in plasma exosomes from EGC patients were significantly lower than those from healthy individuals. Thus, circ_0065149 revealed distinguished diagnostic accuracy, with an AUC of 0.64, sensitivity of 48.7%, and specificity of 90.2%[46]. Piwi-interacting RNAs (piRNAs) are another class of small ncRNAs that are 26-31 nucleotides in length, and quite comparable in size to miRNAs. PiRNAs are distinctly different from miRNA counterparts because they lack the sequence conservation present in miRNAs. As a source for liquid biopsy, piRNAs have similar properties to miRNAs and stabile in the blood flow and resistant to ribonuclease mediated degradation. Therefore, piRNAs can be used as effective biomarkers for the early detection of GC. Serum exosomal piR-019308, piR-004918 and piR-018569 can be utilized for the diagnosis of GC with the AUC value of 0.820, 0.754 and 0.732, respectively. Diagnostic value of these piRNAs were much better than that of CEA, CA19-9 and alpha-fetoprotein[47]. Collectively, circulating exosome has clinical potentials in the early diagnosis of GC, which may lead to the identification of cancer subtypes. Exosome investigated as potential diagnostic GC markers are listed in Table 2.

Collectively, this section highlights the developments in the ncRNAs as a source for the development of non-invasive diagnostic biomarkers for GC patients. NcRNAs appear to have a crucial potential to be implemented into biomarker development for early detection of GC. On the other hand, a variety of circulating biomarkers have been reported in different research team. The clinical value of all these factors is not still defined. Some discrepancies among different studies can be caused by the hetero-

Table 1 Overview of non-coding RNAs for early detection of GC in the past 5 years

Circulating biomarkers	Alterations	Patients	Controls (normal)	Sample	Methods	Sensitivity (%)	Specificity (%)	AUC	Ref.
miRNA									
miR-25	Upregulated	65	65	Plasma	qRT-PCR	87.6	76.9	0.817	[102]
miR-214	Downregulated	168	74	Plasma	qRT-PCR	73.2	91.9	0.880	[103]
miR-376c	Upregulated	47	67	Plasma	qRT-PCR	71.0	78.0	0.77	[104]
miR-381	Downregulated	40	40	Serum	qRT-PCR	83.6	97.5	0.931	[105]
miR-200c	Upregulated	200	250	Tissue and blood	Micoarrayand qRT-PCR	74.0	66.0	0.75	[106]
miR-551b-5p	Downregulated	40	40	Serum	qRT-PCR	77.5	80.0	0.84	[107]
Combination of miR-21, miR-93, miR-106a, and miR-196b	Upregulated	11	17	Plasma	qRT-PCR	84.8	79.2	0.887	[108]
Combination of miR-16, miR-25, miR-92a, miR-451 and miR-486-5p	Upregulated	40	40	Plasma	qRT-PCR	72.9	89.2	0.812	[109]
Combination of miR-4257, miR-6785-5p, miR-187-5p and miR-5739	Upregulated	1417	1417	Serum	microarray analysis	0.996 (index)	0.953 (index)	0998	[23]
Combination of miR-18a, miR-181b, and miR-335	Upregulated	176	173	Serum	qRT-PCR	71.6	87.9	0.86	[95]
Combination of miR-425-5p, miR-1180-3p. miR-122-5p, miR-24-3p and miR-4632-5p	Downregulated	30	90	Plasma	qRT-PCR	NA	NA	0829	[21]
Combination of miRNA-3185, miRNA-6083, miRNA-6792-3p, and miRNA-659-3p	Upregulated	52	30	Plasma	qRT-PCR	NA	NA	0.825	[110]
Combination of miRNA-936, miRNA-1306-3p	Downregulated	52	30	Plasma	qRT-PCR	NA	NA	0.730	[110]
Long non-coding RNAs									
ZNFX1-AS1	Upregulated	50	50	Plasma	qRT-PCR	84	68	0.85	[26]
LINC00978	Upregulated	38	31	Serum	qRT-PCR	80	70	0.831	[111]
CTC-501O10.1	Upregulated	100	100	Plasma	qRT-PCR	90	51	0.74	[112]
AC100830.4	Upregulated	100	100	Plasma	qRT-PCR	84	58	0.73	[112]
RP11-210K20.5	Upregulated	100	100	Plasma	qRT-PCR	89	55	0.737	[112]
CTC-497E21.4	Upregulated	110	84	Serum	qRT-PCR	81.8	75.0	0.896	[113]
SNHG17	Upregulated	67	67	Plasma	qRT-PCR	NA	NA	0.748	[114]
ARHGAP27P1	Downregulated	53	53	Plasma	qRT-PCR	75,5	60.4	0.732	[115]
PANDAR	Upregulated	109	106	Plasma	qRT-PCR	NA	NA	0.767	[27]
FOXD2-AS1	Upregulated	109	106	Plasma	qRT-PCR	NA	NA	0.700	[27]
SMARCC2	Upregulated	109	106	Plasma	qRT-PCR	NA	NA	0.748	[27]
LINC00086	Downregulated	168	74	Plasma	qRT-PCR	72.6	83.8	0.86	[103]
B3GALT5-AS1	Upregulated	107	87	Serum	qRT-PCR	87.4	74.7	0.816	[28]
C5orF66-AS1	Downregulated	200	278	Serum	qRT-PCR	77.5	53.6	0.668	[29]

HCP5	Upregulated	98	82	Serum	qRT-PCR	80	70	0.818	[30]
Combined of lnc-MB21D1-3:5, lnc-PSCA-4:2 and lnc-ABCC5-2:1	Upregulated	52	30	Plasma	qRT-PCR	NA	NA	0904	[110]
circular RNAs									
has_circ_0000745	Downregulated	60	60	Plasma	qRT-PCR	85.5	45,0	0.683	[33]
circPTPN22	Upregulated	120	104	Plasma	qRT-PCR	78.0	84.0	0.857	[35]
hsa_circ_0001789	Downregulated	24	24	Plasma	qRT-PCR	84.0	50.0	0.82	[34]
8-circRNA biomarker panel	Upregulated	92	46	Serum	qRT-PCR	78.3	78.3	0.87	[36]

miRNA: Micro RNA; qRT-PCR: Quantitative reverse transcriptase polymerase chain reaction; AUC: Area under curve; HCP5: HLA Complex P5; lncRNA: Long non-coding RNA; circ RNA: Circular RNA; NA: Not applicable; ZNFX1-AS1: ZNFX1 antisense RNA 1; PANDAR: Promoter of CDKN1A antisense DNA damage activated RNA; FOXD2-AS1: FOXD2 adjacent opposite strand RNA 1; SMARCC2: SWI/SN F related, matrix associated, actin dependent regulator of chromatin subfamily c member 2; B3GALT5-AS1: B3GALT5 antisense RNA 1; C5orf66-AS1: C5orf66 antisense RNA 1.

Table 2 Overview of exosome associated with early detection of gastric cancer

Marker	Alterations	Patients	Controls (normal)	Sample	Methods	Sensitivity (%)	Specificity (%)	AUC	Ref.
miRNA									
miR-590-5p	Downregulated	168	50	Serum	qRT-PCR	63.7	86.0	0.810	[44]
miR-92a-3p	Downregulated	131	122	Serum	qRT-PCR	NA	NA	0.829	[116]
Combination of miR-92b-3p, let-7g-5p, miR-146b-5p, and miR-9-5p	Upregulated	36	12	Serum	qRT-PCR	60	84	0.773	[43]
LncRNA									
HOTTIP	Upregulated	126	120	Serum	qRT-PCR	69.8	85.0	0.827	[117]
UEGC1	Upregulated	51	60	Plasma	qRT-PCR	NA	NA	0.876	[39]
Pcsk2-2:1	Upregulated	63	29	Serum	qRT-PCR	84	86.5	0.896	[40]
GNAQ-6:1	Downregulated	43	27	Serum	qRT-PCR	83.7	55.6	0.736	[41]
RNA-GC1	Upregulated	522	219	Serum	qRT-PCR	88.2	82.3	0.90	[42]
piRNAs									
piR-019308	Upregulated	70	60	Serum	qRT-PCR	57.14	91.67	0.820	[47]
piR-004918	Upregulated	70	60	Serum	qRT-PCR	42.86	95.0	0.754	
piR-018569	Upregulated	70	60	Serum	qRT-PCR	44.29	96.67	0.732	

miRNA: MicroRNA; lncRNA: Long non-coding RNA; circRNA: Circular RNA; piRNA: Piwi-interacting RNAs; qRT-PCR: Quantitative reverse transcriptase polymerase chain reaction; NA: Not applicable; GNAQ-6:1: G protein subunit alpha q-6:1.

geneity of GC. Thus, a more precise patient inclusion criteria or enlarging of the cohort size could overcome the differences in ncRNAs expression caused by the intrinsic heterogeneity of the disease. More multicenter, greater, longer-term studies are warranted to apply liquid biopsies in clinical settings, in terms of early diagnosis of GC. We systematically summarized the ncRNAs as biomarker for early detection of GC in Figure 2.

DNA METHYLATION

DNA methylation is an epigenetic mechanism which lead to oncogenesis in GC through activation of oncogenes and silencing of tumor-suppressor genes[48]. In a recent, a variety of studies demonstrated that aberrant epigenetic regulations, such as DNA methylation, histone posttranslational modifications,

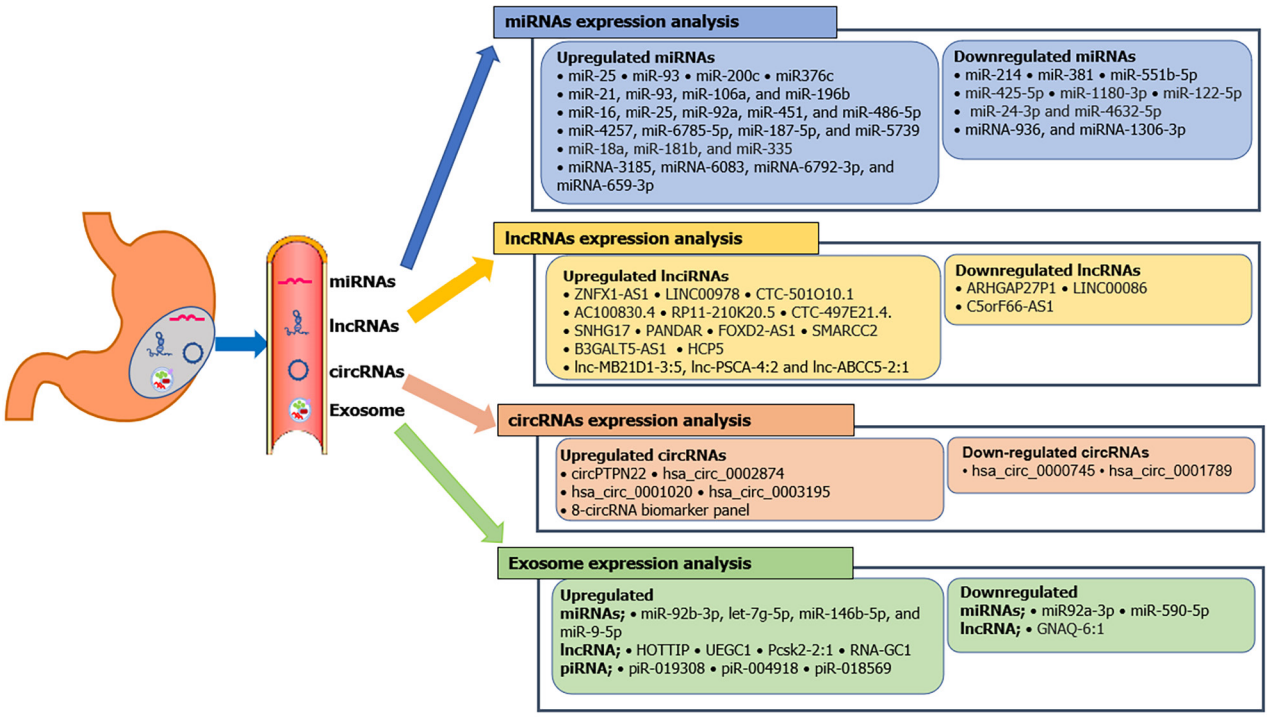

DOI: 10.3748/wjg.v29.i17.2515

Figure 2 The summary of non-coding RNAs as biomarker for early detection of gastric cancer. Schematic of the non-coding RNAs composition. Liquid biopsy obtained from peripheral blood is composed of different tumoral components such as micro-RNA, long non-coding RNAs, and circular RNAs. miRNA: MicroRNA; lncRNA: Long non-coding RNA; circRNA: Circular RNA; piRNA: Piwi-interacting RNAs.

ncRNAs and chromatin remodeling, have a pivotal influence on the pathogenesis of GC. DNA methylation is well-investigated epigenetic change among the epigenetic modifications[49]. Nowadays, the importance of aberrant DNA methylation is identified by liquid biopsy, including plasma/serum and gastric juice. Tumor suppressor genes methylation in peripheral blood has been examined most broadly. Aberrant gene methylation identified in body fluids could be a useful biomarker for the early detection of GC, likewise SEPT9 in CRC. Numerous methylated gene promoters detected in ctDNA have been proposed for GC detection as a latent diagnostic marker[50]. Among them, aberrant methylation of Reprimo, RUNX3, RASSF1A, SFRP2, PCDH10, H19, and MALAT1 show high sensitivity and specificity, suggesting that they have superiority in the early detection of GC[51-55]. A recent study elucidated the association of aberrant DNA methylation with the risk of GC. Hypermethylation of SOCS3 promoter in blood extensively facilitated GC risk[56]. Genome-wide hypomethylation commonly occurs in repeated components that are normally hypermethylated to keep genomic stability. Long interspersed nucleotide element 1, Alu repetitive elements and human endogenous retroviruses are the main components of scattered repeated sequences[57]. Although a number of studies examined the perspective of DNA methylation as a biomarker in GC, the methylation levels in those studies were mainly shown from the tissues. Thus, novel aberrantly methylated genes whose roles in GC should be investigated, especially those detected by non-invasive methods.

DNA methylation is major epigenetic changes when pathogens invade to gastric mucosa, which allows the infection to persist and promotes the development of GC[58]. *Helicobacter pylori* (*H. pylori*) is one of the most important pathogens for GC. Previous studies have demonstrated that Alu and Satα hypomethylation was significantly correlated with *H. pylori* infection in patients with GC[59]. Although numerous studies were examined to elucidate the mechanism of epigenetic changes induced by *H. pylori* infection, useful biomarker for early detection in GC is still not applied in clinical setting. Most recent report demonstrated that FGFR4 activation was interacted with signal transducer and activator of transcription 3 thorough steroid receptor coactivator in response to *H. pylori* infection, suggesting that FGFR4 could be a candidate of biomarker for early detection of GC[60].

NOVEL BIOMAKER IDENTIFIED FROM MULTI-OMICS DATA

Previous classifications of GC have quite restricted achievement in advocating the advancement of subtype-specific treatment applies due to the heterogeneity of GC and their incapacity to detect latent molecular targets. With NGS, omics technologies have offered beneficial tools to examine the molecular basis of GC. Multiple omics-based studies have been used to evaluate the biofluids of GC patients,

which resulted in numerous novel biomarkers due to rapid progress in machine learning approaches [61]. A number of mutations, gene alteration, protein abundance differences, epigenetic mutations, and metabolite concentrations which is linked to GC heterogeneity and staging, leading to improve our understanding of GC, have been successfully identified. NGS has high throughput and can screen unknown variants. A variety of methods are applying NGS to target panel, namely Tagged-Amplicon deep sequencing, Safe-Sequencing System, and Cancer Personalized Profiling by deep sequencing. The developments of NGS enable many applications in both DNA and RNA sequencing (RNA-seq), such as whole-genome, whole-exome, and targeted sequencing of DNA, and total RNA, mRNA, and small RNA [62].

Proteins contribute to determine the identity of a cell[63]. Cell function can be affected by aberrant protein expression, or altered post-translational arrangements. Proteomic signatures can afford complementary information for patient stratification to genetic signature. Besides, proteins can be a useful tool as a biomarker for malignances[63]. The development of proteomics technologies, such as mass-spectrometry (MS), has made it easier to identify protein biomarkers applied to tumor diagnosis. Liquid chromatography-MS (LC-MS) of digested proteins conducted with high-resolution instruments enable to quantitate thousands of proteins from complex biological specimens. Study using LC-MS/MS combined with TMT labeling, found that 11 proteins differentially expressed in plasma from EGC patients and healthy controls identified from the total of 2040 proteins. This model presented that the altered proteins found by plasma proteomics could provide a resource of potential biomarkers for diagnosis of EGC[64]. Isobaric tags for relative and absolute quantification (iTRAQ) are said to be the most widely used method for high-throughput protein quantification. The study using iTRAQ-labeled quantitative proteomics revealed that NAD(P)-dependent steroid dehydrogenase-like (NSDHL) and neutral cholesterol ester hydrolase 1 (NCEH1), key enzymes in cholesterol metabolism, were aberrantly expressed in patients with GC. Moreover, the combined analysis of NSDHL and NCEH1 showed high sensitivity compared with a single marker in detecting GC, indicating that NSDHL and NCEH1 may be adequate for novel biomarkers in the screening[65]. Identically, thioredoxin reductase 1 was aberrantly expressed in GC by using Itraq-labelling and/or LC-MS, supporting that these proteins are an important target for early determining and follow-up monitoring for GC[66]. Integration of phosphoproteome data with other types of omics data from young diffuse-type GC patients provided links of somatic mutations to phosphorylation changes in signaling pathways, association of mRNA-protein abundance correlations with survivals, and four subtypes of young diffuse-type GC patients characterized by genomic and proteomic signatures, which may contribute to have a deep insight into diffuse-type GCs[67]. More recent study using proteomics methods of serum based on high-resolution MS with ion mobility separation followed by multivariate statistics and network analysis presented that a 29-protein marker panel containing, integrin β6 and glutathione peroxidase, and ten serum markers specific for GC (ITIH1, FZD6, DPP10, SERPINA4, AKAP12, S100A9, POTEF, CACNB1, CRP KIAA1328), which were independent of *H. pylori* infection[68]. Multi-omic analysis characterizing the intricate relationships between the intragastric microbiome and gastric mucosal gene expression revealed higher abundances in several bacterial taxa (*Pasteurellaceae*, *Enterococcaceae*, *Helicobacteraceae*, *Gemellales* and *Neisseriaceae*) and genes (*SOCS3* and *ITM2A*) were shown in GC patients. In turn, *Lachnospiraceae* was closely associated with the expression of *Ubiquitin D*, which regulates mitosis and cell cycle time in GC [69]. Besides, lower abundances of B cell signatures in GC compared to gastritis may suggest a previously unidentified immune evasion process in gastric carcinogenesis. These results suggest that a combined analysis of microbiome and gene expression may help to devise a diagnostic kit that screens for high-risk patients of GC who require surveillance endoscopy.

STOMACH SPECIFIC BIOMARKER

The measurement of a biomarker in a gastric juice sample should be specific for early-stage GC than the same biomarker measured in plasma/serum because it is obtained directly from the area of the lesion, which would lead to avoid dilution of the biomarkers and their lack of specificity[70]. Because DNA is easily degraded due to gastric juice acidity, the main part of biomarkers identified in gastric juice are ncRNAs and some proteins. A significantly increased miR-135b-3p and miR-199a-3p, and a decreased miR-451a levels in gastric juice-derived EVs from GC patients was shown compared to non-cancer individuals[71]. LncRNAs in gastric juice and urine have also been reported as biomarkers of GC and urinary system cancer, respectively[72]. On the other hand, a recent study revealed that the levels of SNCG in gastric juice detected by enzyme-linked immunosorbent assay were significantly higher in the GC group compared with the control group[73]. Analysis using gastric juice-derived exosomal DNA samples presented that BARHL2 methylation had an area under the curve of 0.923 with 90% sensitivity and 100% specificity which suggested the feasibility of the application of BARHL2 methylation for screening for GC biomarker[74]. Although a number of studies elucidating the value of gastric juice as a biomarker for early detection of GC were carried out, the limitation is the tolerance of the patients as a usual examination due to the discomfort of gastroscopy.

Serological examinations, which are noninvasive and relatively convenient. can offer efficient indicators of gastrointestinal diseases. Markers of gastric function such as pepsinogen (PG)-I, PG-II, PG-I/PG-II ratio, gastrin 17, anti-*H. pylori* antibodies are used to cooperatively diagnose chronic atrophic gastritis (CAG)[75]. A recent meta-analysis has presented the use of serum pepsinogens revealed significant diagnostic accuracy for the early detection of gastric CAG or GC[76]. Among the various cut-off values investigation, PG rate ≤ 3 and PG-I ≤ 70 ng/mL have been proposed for CAG and GC prediction. Although there are numerous studies for evaluating PG as biomarker for early detection of GC, the potential use of pepsinogens in GC prevention is still not well-established.

DISCUSSION AND FUTURE PERSPECTIVE

Biomarkers are biological molecules implicated in the initiation and progression of cancer, and determination of their levels can clarify abnormal molecular changes in patients[77]. Morphological detection of diseased gastric epithelial cells using upper gastrointestinal endoscopy has always been the standard method for diagnosis of GC. However, the false-positive rates for endoscopic screening in the first round are said to be 14.9%. Notably, endoscopy is easily missed during screening, even when it is performed by qualified endoscopists. In this review, we describe the comprehensive and systematic search for and development of blood-based biomarkers for early detection of GC. Identification of highly sensitive biomarkers for GC screening might render upper gastrointestinal endoscopy unnecessary. Biomarker has assisted in the advancement of new DNA, RNA, and protein-based cancer biomarkers that can be detected from noninvasive, sensitive, specific, and cost-effective body fluids. These include the OncoBEAM™ RAS CRC liquid biopsy assay approved by the European Commission as an *in vitro* diagnostic tool for colorectal cancer therapy, and this has led to the early detection of emergent resistance to anti-epidermal growth factor receptor treatment and the assessment of genomic profile during treatment in clinical settings[78]. Such assays may also enable us to abandon approved but useless treatments for patients resistant to molecular targeted agents or immunosuppressants. For instance, with this technology the future patients with stage II or III GC with a low risk of postoperative recurrence may be simply monitored under active surveillance without adjuvant chemotherapy and possibly be started to treat from when MRD is detected (Figure 1). Although ctDNA for detection of MRD can be an emerging clinical biomarker for disease monitoring in GC, applications of ctDNA in clinical practice require more comprehensive examination in prospective trials.

However, several technical factors are hindering the use of liquid biopsy biomarkers in clinical use. A major challenge is the very low levels of peripheral DNA/RNA[79]. In 2022, ESMO published recommendations on the use of ctDNA in genomic testing and clinical practice. Based on its review of the different aspects of ctDNA, the ESMO Precision Medicine Working Group provides some outlook on the future of ctDNA examination. Considering deficient sensitivity in clinical practice for gene fusions and copy number variations and advancing tests to discriminate accurate results for more progressive genotyping are included in their recommendations[80]. To overcome these issues, several upgraded liquid biopsy approaches for cancer diagnosis are under development. It is likely that precancerous and cancerous lesions can be detected by combinations of biomarkers with superior sensitivity and specificity, fulfilling an unmet need in clinical practice. Combining biomarkers, such as ncRNAs, can enhance the sensitivity and specificity for detecting EGC. However, it would be difficult to identify the ideal combination of other biomarkers that can enhance the overall detection performance. Correlations between different types of biomarkers like the association pattern to guide the choice of panels can be effectively identified using biostatistical approaches. For example, a serum biomarker miRNA panel consisting of 12 miRNAs was developed for risk assessment in patients with GC. With the use of a multitarget miRNA assay in more than 5000 individuals in Singapore and Korea, this panel showed an AUC of 0.848 and 87% sensitivity and 68.4% specificity values to distinguish GC patients from healthy controls. Moreover, upgrading of the AUC to 0.884 and specificity to 69.4% for GC detection were achieved by the combination of this 12-miRNA panel with patient age, *H. pylori* serology, and the plasminogen I:II ratio[81]. Combinations of ctDNA mutations with other biomarkers, such as protein or methylation have been examined toward the goal of improving the overall sensitivity. It has been demonstrated that the combination of ctDNA and protein biomarkers can markedly increase the sensitivity[82]. Genome-wide methylation and protein marker profiles have been validated for a combination of *mSEPT9*, *mRNF180* and CA724 for the detection of GC, and the combination of all three markers detected 68.6% of GC cases[83].

Another important strategy for improving the sensitivity and specificity of GC detection is the use of innovative bioinformatic algorithms. Machine learning involves various computational techniques that are used to simplify large numbers of measurements into lower-dimensional outputs that are more explainable[84]. In the case of GC, a combination of artificial intelligence (AI)-based endoscopy and miR148a methylation has been evaluated for the diagnosis of gastric indefinite dysplasia[85]. Interestingly, a recent study using the microbial compositions of the Cancer Genome Atlas (TCGA) of 18116 human blood samples across 33 cancer types and stochastic gradient-boosting machine learning models effectively discriminated cancer-free individuals, patients with cancer, and patients with

multiple types of cancer[86]. A new concept of cfDNA is also expected to be applied to cancer diagnoses in the near future.

Unfortunately, there is a lack of standardized technique for isolation, amplification and detection in the use liquid biopsies for early diagnoses in clinical settings. One of the most meaningful accomplishments regarding biomarkers for early cancer detection is the emergence of high-throughput technological platforms such as NGS, which allows comprehensive quantification of whole genome or transcriptome. The cost of NGS has greatly declined over the past several decades, which has allowed the sequencing of a larger number of clinical biospecimens, as well as the ability to generate datasets with higher depth of coverage. The opportunity to generate higher resolution data for low expressing transcripts improves the ability to detect rare cancer-derived transcripts in circulation. A study aiming to found the latent miRNA for predicting GC by AI in the Gene Expression Omnibus (GEO) datasets, particularly with several states of the machine learning methods and the Boruta algorithm, demonstrated that the use of hsa-miR-1343-3p could predict GC with the AUC of 100% (sensitivity 100%, specificity 100%, ROC 100%)[87]. In a recent study using high-throughput RNA-seq, the expression profiles of circRNAs in serum EV between GC patients and healthy individuals were examined. The results demonstrated that the circRNA, Chr10q11, Chr1p11, and Chr7q11 were upregulated in GC; the AUC of the three combined circRNAs was 0.839 (95%CI: 0.772-0.893) with 73.2% sensitivity and 84.1% specificity. The construction of a circRNA-miRNA-mRNA network predicted that the three identified circRNAs interact with 13 miRNAs and 91 mRNAs. These findings suggest that panels of EV circRNAs may provide new insights into the early diagnosis of GC[88]. With the use of publicly available gene expression profiles from the TCGA and GEO datasets, a recent study explored the circRNA-miRNA-mRNA interaction axis by constructing a competing endogenous (ce)RNA network. On the basis of the hub RNAs included in ceRNA, the screening of the model for predicting the mRNA signature and miRNA signature by LASSO regression analysis found that both five mRNA-based signatures (CTF1, FKBP5, RNF128, GSTM2 and ADAMTS1) and five miRNA-based signatures (miR-145-5p, miR-615-3p, miR-6507-5p, miR-937-3p and miR-99a-3p) had superior capacity to predict the diagnosis of GC patients with the AUC of 0.9975[89]. Similarly, a study using regulatory networks for circRNA-miRNA-immune-related mRNA validated in the new GEO and TCGA datasets identified various ceRNA (circRNA-miRNA-immune-related mRNA) regulatory networks in GC constructed by hsa_circ_0050102–hsa-miR-4537-NRAS-Tgd cells, hsa_circ_0001013-hsa-miR-485-3p-MAP2K1-Tgd cells, hsa_circ_0003763-hsa-miR-145-5p-FGF10-StromaScore, hsa_circ_0001789-hsa-miR-1269b-MET-adipocytes, hsa_circ_0040573-hsa-miR-3686-RAC1-Tgd cells, and hsa_circ_0006089-hsa-miR-5584-3p-LYN-neurons, among which FGF10, MET, NRAS, RAC1, MAP2K1, and LYN showed promising diagnostic significance for GC patients[90]. In a study based solely on bioinformatics models constructed a circRNA-miRNA-mRNA network based on three circRNAs, 43 miRNAs, and 119 mRNAs, and upregulations of hsa_circ_0001013, hsa_circ_0007376, and hsa_circ_0043947 were observed, which may offer a new pathway for mechanical examinations and provide possible biomarkers for early detection of GC[91]. Likewise, in a bioinformatics circRNA-miRNA-gene interaction network analysis, two circRNAs (CircCEACAM5 and CircCOL1A1) cooperated with GC correlated miRNAs and their host genes were suggested as the pivotal diagnostic biomarker for GC[92]. The emergence of single-cell sequencing technologies has markedly improved the resolution of low-input sequencing. The recent introduction of single-cell DNA/RNA-seq provides an opportunity to detect cell types and cell status. For example, a single-cell expression atlas of gastric premalignant gastric lesions and EGC identified the expression signatures of multiple cell types across different lesions, as well as a panel of six high-confidence markers that could serve as specific biomarkers for early diagnosis of GC[93]. A weighted gene co-expression network analysis (WGCNA) aims to: (1) Identify co-expressed modules in multiple biological samples based on correlations between different gene expression profiles; and (2) Explore the relationship between gene networks and phenotypes of interest, as well as the hub genes in the network[94]. Performing a WGCNA can prevent the false-negative and false-positive results of previous biological methods. WGCNA data from the GEO database revealed hub genes involved in GC and identified four functional genes (*ITGAX*, *CCL14*, *ADHFE1*, and *HOXB13*) that were differentially expressed in tumor and normal gastric samples. Another study applying a WGCNA to screen potential biomarkers for EGC using RNA-seq and clinical data from the TCGA database identified five hub genes, *MS4A1*, *THBS2*, *VCAN*, *PDGFRB*, and *KCNA3*[94]. These technological developments will allow more researchers to conduct comprehensive assessment of molecular profiles in the human circulatory system.

Systematic studies applying the molecular profiling of ncRNAs for cancer biomarker have been developed. Several investigations have used tissue profiling data to identify ncRNA as a potential biomarker, leading to the evaluation of these cancer-associated ncRNA signatures in blood cohorts. Multiple tissue sequencing datasets were recently used to identify highly overexpressed miRNAs in GC tissues. Risk probabilities using quantitative reverse transcriptase polymerase chain reaction data for three miRNAs (miR-18a, miR-181b, and miR-335) were validated and showed much better diagnostic performance than the conventional tumor markers CEA and CA19-9 currently in use. Moreover, the three-miRNA signature discriminated between patients with stage I GC and cancer-free individuals. More importantly, using the miRNA signature was significantly more cost-effective relative to the current clinical practice of endoscopic screening, suggesting the robustness of a GC associated miRNA signature in multiple cohorts[95].

Table 3 Clinical trials of blood-based biofluid biomarkers for gastric cancer detection

Clinical trials	Type of trial	Phase	Results	Participants (estimated)	Assay	Comments
ctDNA						
NCT05027347	Cohort	NA	Recruiting	200	Ultradeep massive parallel sequencing assay	Development of a protocol for detection of ctDNA in plasma of patients with early stages of GC
NCT04511559	Cohort	NA	Not yet recruiting	540	ctDNA methylation sequencing	The correlation between the plasma ctDNA methylation status and the diagnosis of patients with early GC
NCT05208372	Case-control	NA	Recruiting	200	CTC and ctDNA test	Investigation of the value of CTCs and ctDNA in the diagnosis of metastasis of GC in peritoneal flushing fluid and blood
NCT04665687	Cohort	NA	Recruiting	1730	Illumina HiSeq2000/2500-based, MiSeq NGS targeted sequencing	Identification whether tumor's molecular profiling based on blood could be used for diagnosis of EGC and precancerous gastric adenoma
NCT05029869	Cohort	NA	Recruiting	100	NGS technologies	Study aims to evaluate the use of NGS to detect ctDNA in GC patients after gastrectomy
NCT05224596	Case-control	NA	Recruiting	498	Blood draw and blood-based biomarkers analyses	Multi-omics 498 study aimed at detecting GC by combined assays for serum protein markers, deep sequencing of cfDNA, ctDNA mutation and RNA
miRNAs						
NCT04329299	Cohort	NA	Completed	6862	Blood-based biomarkers analyses	Validation of the predictive value of various blood biomarkers, such as miRNA
lncRNAs						
NCT05397548	Cohort	NA	Recruiting	700	RT-PCR	Study to investigate the predictive value of circulating exosomal lncRNA-GC1 for early-detection and monitoring progression of GC
Methylation						
NCT04511559	Cohort	NA	Not yet recruiting	540	ctDNA methylation sequencing	Methylation analysis of ct DNA in early diagnosis in patients with GC
NCT03076567	Observational	NA	Completed	440	NA	Discovery and validation of plasma DNA methylation biomarker for detection of GC
NCT05336058	Cohort	NA	Recruiting	1240	Multi-target PCR	Exploration of the clinical performance of polygene methylation in the adjunctive diagnosis of GC
NCT04253106	Non-randomized	NA	Recruiting	10	NGS	Activating methylation profiles identified by liquid biopsies could identify CDH1 and CTNNA1 pathogenic variants carriers with DGC
Multi-omics						
NCT04947995	Case-control	NA	Recruiting	450	ctDNA multi-omics test	Exploration of a blood-based multi-omics assay and computational model for early detection of GC
NCT05347524	Observational	NA	Recruiting	384	Blood draw and blood-based biomarkers analyses	Detection of peritoneal metastasis of GC by combined assays for methylation of cfDNA and other blood-based biomarkers

GC: Gastric cancer; NGS: Next generation sequencing; PCR: Polymerase chain reaction; DGC: Diffuse gastric cancer; ctDNA: Circulating tumor DNA; cfDNA: Cell-free DNA; miRNA: MicroRNA; lncRNA: Long non-coding RNA; NA: Not applicable; lncRNA-GC1: Gastric cancer-associated lncRNA1.

More multicenter studies and prospective evaluations in large clinical trials are necessary for the integrations of such biomarkers into GC screening platforms supporting the daily clinical treatments of GC patients. Several clinical trials have explored the use of a liquid biopsy for early diagnosis of setting for patients with GC (Table 3). However, all of the trials were either observational, case-control, or cohort trials; no randomized control trial assessing liquid biopsy have been conducted to date. Hence, incorporating liquid biopsies into clinical practice for GC may be difficult.

Regarding the development of a circulating non-invasive biomarkers for early detection of GC, specificity for stomach would provide an additional confidence and suggested robustness of GC biomarkers. Biomarkers that are highly specific to GC will reduce the false positive rates, and thus are helpful in clinical practice. The detection of dysregulated genes that are highly expressed specifically in distinct organ could make it easier to find the locations of cancer. For example, KRAS mutations are rarely identified in healthy individuals, which makes these mutations highly cancer-specific. Nevertheless, detecting KRAS mutations in the circulation does not help identify the location of cancer as KRAS mutations can occur in multiple cancer types. Using candidates for GC specific driver genes, such as CDH1 and RhoA, may be possible to increase the specificity as diagnostic biomarkers of GC [96]. Growing evidences suggest that some EVs released from specific organs retain tissue-specific molecular features. It was recently reported that tumor cell-specific molecules, *i.e.*, circulating exosome-derived lncRNA-GC1 can be used as a biomarker to detect EGC and monitor disease progression[42]. Interestingly, a clinical study (ClinicalTrials.gov identifier NCT05397548) investigated whether circulating exosomal lncRNA-GC1 could support the early-detection and progression monitoring of GC. It is thus possible to measure ncRNA content of cancer-specific exosomes to further increase cancer specificity as biomarkers for GC diagnosis. The status of acquired DNA methylation can be tissue-specific and maintained during carcinogenesis, and examination of this status could allow the discovery of the tumor of origin[97], suggesting that biomarkers based on DNA methylation could have the additional potential to provide key information to guide follow-up clinical decision making. Multiple cancer types have been identified *via* high-depth, targeted bisulfite sequencing analysis of a large panel of methylation sites that have signals specific to certain organs; these panels include DEEPGEN™, CancerSEEK, PanSEER, cfMeDIP-se,q GRAIL, IvyGene®, and stMCEDs. Using these panels, excellent rates of detection in individuals with cancer were obtained[98]. However, the specificity of GC in individuals with early disease have been limited. A cost-effective experimental assay, called cell-free DNA Methylome Sequencing (cfMethyl-Seq) profiles the genome-wide methylation of cfDNA, offering > 12 × enrichment over whole-genome bisulfite sequencing in CpG islands[99]. By integrating four marker types, namely cancer-specific hypermethylation markers, tissue hypermethylation markers, cancer-specific hypomethylation markers types, and tissue hypomethylation markers, a cfMethyl-Seq model showed an AUR of 0.974 (95%CI: 0.926-0.998), yielding a sensitivity of 80.7% (95%CI: 68.6%-90.7%) at 97.9% specificity in multiple organs, including those with GC.

Collectively, the combination of multiple parameters and multiple analytes obtained by emerging machine learning methods will help address the challenges of EGC detection. Overcoming the limitation of cancer biomarker translation into clinical practice will require the development of high throughput, multiplexing techniques that can be easily incorporated into clinical settings as well as large-scale prospective research and interventional clinical trials with standardized specimen processing and data collection procedures.

CONCLUSION

Increased understanding of the molecular genetics and epigenetics of GC has led to the progress of molecular marker assays for GC screening. Liquid biopsy is emerging as a promising future screening technique for clinical testing owing to the use of a single sample and ease of specimen collection. The advancement of new technologies with improved sensitivity, such as methylation sequencing and multi-omics analysis, and rapid, global detection capacities that allowed the identification of novel potential biomarkers for early detection of GC.

FOOTNOTES

Author contributions: Matsuoka T and Yashiro M performed literature research; Matsuoka T wrote the manuscript and performed the revision and approval of the final version; Yashiro M designed research, coordinated and corrected the writing of the paper.

Supported by the National Cancer Center Research and Development Fund, No. 23-A-9.

Conflict-of-interest statement: All the authors report no relevant conflicts of interest for this article.

Country/Territory of origin: Japan

ORCID number: Tasuku Matsuoka 0000-0001-5019-8519; Masakazu Yashiro 0000-0001-5743-7228.

S-Editor: Wang JJ
L-Editor: A
P-Editor: Yu HG

REFERENCES

1 **Siegel RL**, Miller KD, Fuchs HE, Jemal A. Cancer statistics, 2022. *CA Cancer J Clin* 2022; **72**: 7-33 [PMID: 35020204 DOI: 10.3322/caac.21708]
2 **Matsuoka T**, Yashiro M. Biomarkers of gastric cancer: Current topics and future perspective. *World J Gastroenterol* 2018; **24**: 2818-2832 [PMID: 30018477 DOI: 10.3748/wjg.v24.i26.2818]
3 **Alix-Panabières C**, Pantel K. Liquid Biopsy: From Discovery to Clinical Application. *Cancer Discov* 2021; **11**: 858-873 [PMID: 33811121 DOI: 10.1158/2159-8290.CD-20-1311]
4 **Heitzer E**, Haque IS, Roberts CES, Speicher MR. Current and future perspectives of liquid biopsies in genomics-driven oncology. *Nat Rev Genet* 2019; **20**: 71-88 [PMID: 30410101 DOI: 10.1038/s41576-018-0071-5]
5 **Joosse SA**, Gorges TM, Pantel K. Biology, detection, and clinical implications of circulating tumor cells. *EMBO Mol Med* 2015; **7**: 1-11 [PMID: 25398926 DOI: 10.15252/emmm.201303698]
6 **Wan JCM**, Massie C, Garcia-Corbacho J, Mouliere F, Brenton JD, Caldas C, Pacey S, Baird R, Rosenfeld N. Liquid biopsies come of age: towards implementation of circulating tumour DNA. *Nat Rev Cancer* 2017; **17**: 223-238 [PMID: 28233803 DOI: 10.1038/nrc.2017.7]
7 **Pessoa LS**, Heringer M, Ferrer VP. ctDNA as a cancer biomarker: A broad overview. *Crit Rev Oncol Hematol* 2020; **155**: 103109 [PMID: 33049662 DOI: 10.1016/j.critrevonc.2020.103109]
8 **Qian C**, Ju S, Qi J, Zhao J, Shen X, Jing R, Yu J, Li L, Shi Y, Zhang L, Wang Z, Cong H. Alu-based cell-free DNA: a novel biomarker for screening of gastric cancer. *Oncotarget* 2017; **8**: 54037-54045 [PMID: 28903321 DOI: 10.18632/oncotarget.11079]
9 **Lan YT**, Chen MH, Fang WL, Hsieh CC, Lin CH, Jhang FY, Yang SH, Lin JK, Chen WS, Jiang JK, Lin PC, Chang SC. Clinical relevance of cell-free DNA in gastrointestinal tract malignancy. *Oncotarget* 2017; **8**: 3009-3017 [PMID: 27936467 DOI: 10.18632/oncotarget.13821]
10 **Grenda A**, Wojas-Krawczyk K, Skoczylas T, Krawczyk P, Sierocińska-Sawa J, Wallner G, Milanowski J. HER2 gene assessment in liquid biopsy of gastric and esophagogastric junction cancer patients qualified for surgery. *BMC Gastroenterol* 2020; **20**: 382 [PMID: 33198632 DOI: 10.1186/s12876-020-01531-5]
11 **Jogo T**, Nakamura Y, Shitara K, Bando H, Yasui H, Esaki T, Terazawa T, Satoh T, Shinozaki E, Nishina T, Sunakawa Y, Komatsu Y, Hara H, Oki E, Matsuhashi N, Ohta T, Kato T, Ohtsubo K, Kawakami T, Okano N, Yamamoto Y, Yamada T, Tsuji A, Odegaard JI, Taniguchi H, Doi T, Fujii S, Yoshino T. Circulating Tumor DNA Analysis Detects FGFR2 Amplification and Concurrent Genomic Alterations Associated with FGFR Inhibitor Efficacy in Advanced Gastric Cancer. *Clin Cancer Res* 2021; **27**: 5619-5627 [PMID: 34376535 DOI: 10.1158/1078-0432.CCR-21-1414]
12 **Reinert T**, Schøler LV, Thomsen R, Tobiasen H, Vang S, Nordentoft I, Lamy P, Kannerup AS, Mortensen FV, Stribolt K, Hamilton-Dutoit S, Nielsen HJ, Laurberg S, Pallisgaard N, Pedersen JS, Ørntoft TF, Andersen CL. Analysis of circulating tumour DNA to monitor disease burden following colorectal cancer surgery. *Gut* 2016; **65**: 625-634 [PMID: 25654990 DOI: 10.1136/gutjnl-2014-308859]
13 **Kim YW**, Kim YH, Song Y, Kim HS, Sim HW, Poojan S, Eom BW, Kook MC, Joo J, Hong KM. Monitoring circulating tumor DNA by analyzing personalized cancer-specific rearrangements to detect recurrence in gastric cancer. *Exp Mol Med* 2019; **51**: 1-10 [PMID: 31395853 DOI: 10.1038/s12276-019-0292-5]
14 **Yang J**, Gong Y, Lam VK, Shi Y, Guan Y, Zhang Y, Ji L, Chen Y, Zhao Y, Qian F, Chen J, Li P, Zhang F, Wang J, Zhang X, Yang L, Kopetz S, Futreal PA, Zhang J, Yi X, Xia X, Yu P. Deep sequencing of circulating tumor DNA detects molecular residual disease and predicts recurrence in gastric cancer. *Cell Death Dis* 2020; **11**: 346 [PMID: 32393783 DOI: 10.1038/s41419-020-2531-z]
15 **Chae YK**, Oh MS. Detection of Minimal Residual Disease Using ctDNA in Lung Cancer: Current Evidence and Future Directions. *J Thorac Oncol* 2019; **14**: 16-24 [PMID: 30296486 DOI: 10.1016/j.jtho.2018.09.022]
16 **Koldby KM**, Mortensen MB, Detlefsen S, Pfeiffer P, Thomassen M, Kruse TA. Tumor-specific genetic aberrations in cell-free DNA of gastroesophageal cancer patients. *J Gastroenterol* 2019; **54**: 108-121 [PMID: 30242476 DOI: 10.1007/s00535-018-1508-5]
17 **Maron SB**, Chase LM, Lomnicki S, Kochanny S, Moore KL, Joshi SS, Landron S, Johnson J, Kiedrowski LA, Nagy RJ, Lanman RB, Kim ST, Lee J, Catenacci DVT. Circulating Tumor DNA Sequencing Analysis of Gastroesophageal Adenocarcinoma. *Clin Cancer Res* 2019; **25**: 7098-7112 [PMID: 31427281 DOI: 10.1158/1078-0432.CCR-19-1704]
18 **Zhang M**, Du X. Noncoding RNAs in gastric cancer: Research progress and prospects. *World J Gastroenterol* 2016; **22**: 6610-6618 [PMID: 27547004 DOI: 10.3748/wjg.v22.i29.6610]
19 **Finnegan EF**, Pasquinelli AE. MicroRNA biogenesis: regulating the regulators. *Crit Rev Biochem Mol Biol* 2013; **48**: 51-68 [PMID: 23163351 DOI: 10.3109/10409238.2012.738643]
20 **ZiaSarabi P**, Sorayayi S, Hesari A, Ghasemi F. Circulating microRNA-133, microRNA-17 and microRNA-25 in serum and its potential diagnostic value in gastric cancer. *J Cell Biochem* 2019; **120**: 12376-12381 [PMID: 30861177 DOI: 10.1002/jcb.28503]
21 **Zhu XL**, Ren LF, Wang HP, Bai ZT, Zhang L, Meng WB, Zhu KX, Ding FH, Miao L, Yan J, Wang YP, Liu YQ, Zhou WC, Li X. Plasma microRNAs as potential new biomarkers for early detection of early gastric cancer. *World J Gastroenterol* 2019; **25**: 1580-1591 [PMID: 30983818 DOI: 10.3748/wjg.v25.i13.1580]

22 **Yao Y**, Ding Y, Bai Y, Zhou Q, Lee H, Li X, Teng L. Identification of Serum Circulating MicroRNAs as Novel Diagnostic Biomarkers of Gastric Cancer. *Front Genet* 2020; **11**: 591515 [PMID: 33597967 DOI: 10.3389/fgene.2020.591515]

23 **Abe S**, Matsuzaki J, Sudo K, Oda I, Katai H, Kato K, Takizawa S, Sakamoto H, Takeshita F, Niida S, Saito Y, Ochiya T. A novel combination of serum microRNAs for the detection of early gastric cancer. *Gastric Cancer* 2021; **24**: 835-843 [PMID: 33743111 DOI: 10.1007/s10120-021-01161-0]

24 **Fang XY**, Pan HF, Leng RX, Ye DQ. Long noncoding RNAs: novel insights into gastric cancer. *Cancer Lett* 2015; **356**: 357-366 [PMID: 25444905 DOI: 10.1016/j.canlet.2014.11.005]

25 **Xu W**, Zhou G, Wang H, Liu Y, Chen B, Chen W, Lin C, Wu S, Gong A, Xu M. Circulating lncRNA SNHG11 as a novel biomarker for early diagnosis and prognosis of colorectal cancer. *Int J Cancer* 2020; **146**: 2901-2912 [PMID: 31633800 DOI: 10.1002/ijc.32747]

26 **Xian HP**, Zhuo ZL, Sun YJ, Liang B, Zhao XT. Circulating long non-coding RNAs HULC and ZNFX1-AS1 are potential biomarkers in patients with gastric cancer. *Oncol Lett* 2018; **16**: 4689-4698 [PMID: 30197680 DOI: 10.3892/ol.2018.9199]

27 **Yang Z**, Sun Y, Liu R, Shi Y, Ding S. Plasma long noncoding RNAs PANDAR, FOXD2-AS1, and SMARCC2 as potential novel diagnostic biomarkers for gastric cancer. *Cancer Manag Res* 2019; **11**: 6175-6184 [PMID: 31308753 DOI: 10.2147/CMAR.S201935]

28 **Feng W**, Zong W, Li Y, Shen X, Cui X, Ju S. Abnormally expressed long noncoding RNA B3GALT5-AS1 may serve as a biomarker for the diagnostic and prognostic of gastric cancer. *J Cell Biochem* 2020; **121**: 557-565 [PMID: 31338903 DOI: 10.1002/jcb.29296]

29 **Zhou Q**, Li H, Jing J, Yuan Y, Sun L. Evaluation of C5orf66-AS1 as a Potential Biomarker for Predicting Early Gastric Cancer and Its Role in Gastric Carcinogenesis. *Onco Targets Ther* 2020; **13**: 2795-2805 [PMID: 32308414 DOI: 10.2147/OTT.S239965]

30 **Qin S**, Yang L, Kong S, Xu Y, Liang B, Ju S. LncRNA HCP5 : A Potential Biomarker for Diagnosing Gastric Cancer. *Front Oncol* 2021; **11**: 684531 [PMID: 34222007 DOI: 10.3389/fonc.2021.684531]

31 **Li X**, Yang L, Chen LL. The Biogenesis, Functions, and Challenges of Circular RNAs. *Mol Cell* 2018; **71**: 428-442 [PMID: 30057200 DOI: 10.1016/j.molcel.2018.06.034]

32 **Enuka Y**, Lauriola M, Feldman ME, Sas-Chen A, Ulitsky I, Yarden Y. Circular RNAs are long-lived and display only minimal early alterations in response to a growth factor. *Nucleic Acids Res* 2016; **44**: 1370-1383 [PMID: 26657629 DOI: 10.1093/nar/gkv1367]

33 **Huang M**, He YR, Liang LC, Huang Q, Zhu ZQ. Circular RNA hsa_circ_0000745 may serve as a diagnostic marker for gastric cancer. *World J Gastroenterol* 2017; **23**: 6330-6338 [PMID: 28974900 DOI: 10.3748/wjg.v23.i34.6330]

34 **Lu H**, Zhang Z, Yuan X, Song H, Li P. The role of circular RNA hsa_circ_0001789 as a diagnostic biomarker in gastric carcinoma. *Scand J Gastroenterol* 2023; **58**: 248-253 [PMID: 36111683 DOI: 10.1080/00365521.2022.2122865]

35 **Ma S**, Kong S, Gu X, Xu Y, Tao M, Shen L, Shen X, Ju S. As a biomarker for gastric cancer, circPTPN22 regulates the progression of gastric cancer through the EMT pathway. *Cancer Cell Int* 2021; **21**: 44 [PMID: 33430866 DOI: 10.1186/s12935-020-01701-1]

36 **Roy S**, Kanda M, Nomura S, Zhu Z, Toiyama Y, Taketomi A, Goldenring J, Baba H, Kodera Y, Goel A. Diagnostic efficacy of circular RNAs as noninvasive, liquid biopsy biomarkers for early detection of gastric cancer. *Mol Cancer* 2022; **21**: 42 [PMID: 35139874 DOI: 10.1186/s12943-022-01527-7]

37 **Yu W**, Hurley J, Roberts D, Chakrabortty SK, Enderle D, Noerholm M, Breakefield XO, Skog JK. Exosome-based liquid biopsies in cancer: opportunities and challenges. *Ann Oncol* 2021; **32**: 466-477 [PMID: 33548389 DOI: 10.1016/j.annonc.2021.01.074]

38 **Xu R**, Rai A, Chen M, Suwakulsiri W, Greening DW, Simpson RJ. Extracellular vesicles in cancer - implications for future improvements in cancer care. *Nat Rev Clin Oncol* 2018; **15**: 617-638 [PMID: 29795272 DOI: 10.1038/s41571-018-0036-9]

39 **Lin LY**, Yang L, Zeng Q, Wang L, Chen ML, Zhao ZH, Ye GD, Luo QC, Lv PY, Guo QW, Li BA, Cai JC, Cai WY. Tumor-originated exosomal lncUEGC1 as a circulating biomarker for early-stage gastric cancer. *Mol Cancer* 2018; **17**: 84 [PMID: 29690888 DOI: 10.1186/s12943-018-0834-9]

40 **Cai C**, Zhang H, Zhu Y, Zheng P, Xu Y, Sun J, Zhang M, Lan T, Gu B, Li S, Ma P. Serum Exosomal Long Noncoding RNA pcsk2-2:1 As A Potential Novel Diagnostic Biomarker For Gastric Cancer. *Onco Targets Ther* 2019; **12**: 10035-10041 [PMID: 31819499 DOI: 10.2147/OTT.S229033]

41 **Li S**, Zhang M, Zhang H, Hu K, Cai C, Wang J, Shi L, Ma P, Xu Y, Zheng P. Exosomal long noncoding RNA lnc-GNAQ-6:1 may serve as a diagnostic marker for gastric cancer. *Clin Chim Acta* 2020; **501**: 252-257 [PMID: 31730812 DOI: 10.1016/j.cca.2019.10.047]

42 **Guo X**, Lv X, Ru Y, Zhou F, Wang N, Xi H, Zhang K, Li J, Chang R, Xie T, Wang X, Li B, Chen Y, Yang Y, Chen L. Circulating Exosomal Gastric Cancer-Associated Long Noncoding RNA1 as a Biomarker for Early Detection and Monitoring Progression of Gastric Cancer: A Multiphase Study. *JAMA Surg* 2020; **155**: 572-579 [PMID: 32520332 DOI: 10.1001/jamasurg.2020.1133]

43 **Tang S**, Cheng J, Yao Y, Lou C, Wang L, Huang X, Zhang Y. Combination of Four Serum Exosomal MiRNAs as Novel Diagnostic Biomarkers for Early-Stage Gastric Cancer. *Front Genet* 2020; **11**: 237 [PMID: 32256526 DOI: 10.3389/fgene.2020.00237]

44 **Zheng GD**, Xu ZY, Hu C, Lv H, Xie HX, Huang T, Zhang YQ, Chen GP, Fu YF, Cheng XD. Exosomal miR-590-5p in Serum as a Biomarker for the Diagnosis and Prognosis of Gastric Cancer. *Front Mol Biosci* 2021; **8**: 636566 [PMID: 33681295 DOI: 10.3389/fmolb.2021.636566]

45 **Yang J**, Li X, Wei S, Peng L, Sang H, Jin D, Chen M, Dang Y, Zhang G. Evaluation of the Diagnostic Potential of a Plasma Exosomal miRNAs Panel for Gastric Cancer. *Front Oncol* 2021; **11**: 683465 [PMID: 34422636 DOI: 10.3389/fonc.2021.683465]

46 **Ni D**, Zhang Z, Liu X. Benthic ecological quality assessment of the Bohai Sea, China using marine biotic indices. *Mar*

Pollut Bull 2019; **142**: 457-464 [PMID: 31232324 DOI: 10.1016/j.marpolbul.2019.03.055]
47 **Ge L**, Zhang N, Li D, Wu Y, Wang H, Wang J. Circulating exosomal small RNAs are promising non-invasive diagnostic biomarkers for gastric cancer. *J Cell Mol Med* 2020; **24**: 14502-14513 [PMID: 33169519 DOI: 10.1111/jcmm.16077]
48 **Puneet**, Kazmi HR, Kumari S, Tiwari S, Khanna A, Narayan G. Epigenetic Mechanisms and Events in Gastric Cancer-Emerging Novel Biomarkers. *Pathol Oncol Res* 2018; **24**: 757-770 [PMID: 29552712 DOI: 10.1007/s12253-018-0410-z]
49 **Skvortsova K**, Stirzaker C, Taberlay P. The DNA methylation landscape in cancer. *Essays Biochem* 2019; **63**: 797-811 [PMID: 31845735 DOI: 10.1042/EBC20190037]
50 **Zeng Y**, Rong H, Xu J, Cao R, Li S, Gao Y, Cheng B, Zhou T. DNA Methylation: An Important Biomarker and Therapeutic Target for Gastric Cancer. *Front Genet* 2022; **13**: 823905 [PMID: 35309131 DOI: 10.3389/fgene.2022.823905]
51 **Alarcón MA**, Olivares W, Córdova-Delgado M, Muñoz-Medel M, de Mayo T, Carrasco-Aviño G, Wichmann I, Landeros N, Amigo J, Norero E, Villarroel-Espíndola F, Riquelme A, Garrido M, Owen GI, Corvalán AH. The Reprimo-Like Gene Is an Epigenetic-Mediated Tumor Suppressor and a Candidate Biomarker for the Non-Invasive Detection of Gastric Cancer. *Int J Mol Sci* 2020; **21** [PMID: 33322837 DOI: 10.3390/ijms21249472]
52 **Wen J**, Zheng T, Hu K, Zhu C, Guo L, Ye G. Promoter methylation of tumor-related genes as a potential biomarker using blood samples for gastric cancer detection. *Oncotarget* 2017; **8**: 77783-77793 [PMID: 29100425 DOI: 10.18632/oncotarget.20782]
53 **Wu S**, Zhang Y, Zhang L, Ma JL, Zhou T, Li ZX, Liu WD, Li WQ, You WC, Pan KF. Methylation and Expression of Nonclustered Protocadherins Encoding Genes and Risk of Precancerous Gastric Lesions in a High-Risk Population. *Cancer Prev Res (Phila)* 2018; **11**: 717-726 [PMID: 30213786 DOI: 10.1158/1940-6207.CAPR-18-0119]
54 **Miao J**, Liu Y, Zhao G, Liu X, Ma Y, Li H, Li S, Zhu Y, Xiong S, Zheng M, Fei S. Feasibility of Plasma-Methylated SFRP2 for Early Detection of Gastric Cancer. *Cancer Control* 2020; **27**: 1073274820922559 [PMID: 32379490 DOI: 10.1177/1073274820922559]
55 **Hu D**, Lou X, Meng N, Li Z, Teng Y, Zou Y, Wang F. Peripheral Blood-Based DNA Methylation of Long Non-Coding RNA H19 and Metastasis-Associated Lung Adenocarcinoma Transcript 1 Promoters are Potential Non-Invasive Biomarkers for Gastric Cancer Detection. *Cancer Control* 2021; **28**: 10732748211043667 [PMID: 34615385 DOI: 10.1177/10732748211043667]
56 **Han Q**, Zhou H, Xie W, Sun T, Wei R, Nie C, Hong J, Zhu L, Tian W. Association between the methylation of the STAT1 and SOCS3 in peripheral blood and gastric cancer. *J Gastroenterol Hepatol* 2020; **35**: 1347-1354 [PMID: 32108380 DOI: 10.1111/jgh.15021]
57 **Chansangpetch S**, Prombhul S, Tantisevi V, Sodsai P, Manassakorn A, Hirankarn N, Lin SC. DNA Methylation Status of the Interspersed Repetitive Sequences for LINE-1, Alu, HERV-E, and HERV-K in Trabeculectomy Specimens from Glaucoma Eyes. *J Ophthalmol* 2018; **2018**: 9171536 [PMID: 29651348 DOI: 10.1155/2018/9171536]
58 **Fattahi S**, Kosari-Monfared M, Ghadami E, Golpour M, Khodadadi P, Ghasemiyan M, Akhavan-Niaki H. Infection-associated epigenetic alterations in gastric cancer: New insight in cancer therapy. *J Cell Physiol* 2018; **233**: 9261-9270 [PMID: 30076708 DOI: 10.1002/jcp.27030]
59 **Yoshida T**, Yamashita S, Takamura-Enya T, Niwa T, Ando T, Enomoto S, Maekita T, Nakazawa K, Tatematsu M, Ichinose M, Ushijima T. Alu and Satα hypomethylation in Helicobacter pylori-infected gastric mucosae. *Int J Cancer* 2011; **128**: 33-39 [PMID: 20602342 DOI: 10.1002/ijc.25534]
60 **Zhang X**, Soutto M, Chen Z, Bhat N, Zhu S, Eissmann MF, Ernst M, Lu H, Peng D, Xu Z, El-Rifai W. Induction of Fibroblast Growth Factor Receptor 4 by Helicobacter pylori *via* Signal Transducer and Activator of Transcription 3 With a Feedforward Activation Loop Involving Steroid Receptor Coactivator Signaling in Gastric Cancer. *Gastroenterology* 2022; **163**: 620-636.e9 [PMID: 35588797 DOI: 10.1053/j.gastro.2022.05.016]
61 **Shi XJ**, Wei Y, Ji B. Systems Biology of Gastric Cancer: Perspectives on the Omics-Based Diagnosis and Treatment. *Front Mol Biosci* 2020; **7**: 203 [PMID: 33005629 DOI: 10.3389/fmolb.2020.00203]
62 **Morganti S**, Tarantino P, Ferraro E, D'Amico P, Viale G, Trapani D, Duso BA, Curigliano G. Complexity of genome sequencing and reporting: Next generation sequencing (NGS) technologies and implementation of precision medicine in real life. *Crit Rev Oncol Hematol* 2019; **133**: 171-182 [PMID: 30661654 DOI: 10.1016/j.critrevonc.2018.11.008]
63 **Ren AH**, Diamandis EP, Kulasingam V. Uncovering the Depths of the Human Proteome: Antibody-based Technologies for Ultrasensitive Multiplexed Protein Detection and Quantification. *Mol Cell Proteomics* 2021; **20**: 100155 [PMID: 34597790 DOI: 10.1016/j.mcpro.2021.100155]
64 **Zhou B**, Zhou Z, Chen Y, Deng H, Cai Y, Rao X, Yin Y, Rong L. Plasma proteomics-based identification of novel biomarkers in early gastric cancer. *Clin Biochem* 2020; **76**: 5-10 [PMID: 31765635 DOI: 10.1016/j.clinbiochem.2019.11.001]
65 **Xiao Y**, Xie J, Liu L, Huang W, Han Q, Qin J, Liu S, Jiang Z. NAD(P)-dependent steroid dehydrogenase-like protein and neutral cholesterol ester hydrolase 1 serve as novel markers for early detection of gastric cancer identified using quantitative proteomics. *J Clin Lab Anal* 2021; **35**: e23652 [PMID: 33219617 DOI: 10.1002/jcla.23652]
66 **Zhu Y**, Hu Y, Zhu X, Zhang J, Yuwen D, Wei X, Tang C, Zhang W. Plasma thioredoxin reductase: a potential diagnostic biomarker for gastric cancer. *Carcinogenesis* 2022; **43**: 736-745 [PMID: 35709525 DOI: 10.1093/carcin/bgac052]
67 **Mun DG**, Bhin J, Kim S, Kim H, Jung JH, Jung Y, Jang YE, Park JM, Lee H, Bae J, Back S, Kim SJ, Kim J, Park H, Li H, Hwang KB, Park YS, Yook JH, Kim BS, Kwon SY, Ryu SW, Park DY, Jeon TY, Kim DH, Lee JH, Han SU, Song KS, Park D, Park JW, Rodriguez H, Kim KP, Yang EG, Kim HK, Paek E, Lee S, Lee SW, Hwang D. Proteogenomic Characterization of Human Early-Onset Gastric Cancer. *Cancer Cell* 2019; **35**: 111-124.e10 [PMID: 30645970 DOI: 10.1016/j.ccell.2018.12.003]
68 **Aziz S**, Rasheed F, Zahra R, König S. Gastric Cancer Pre-Stage Detection and Early Diagnosis of Gastritis Using Serum Protein Signatures. *Molecules* 2022; **27** [PMID: 35566209 DOI: 10.3390/molecules27092857]
69 **Park CH**, Hong C, Lee AR, Sung J, Hwang TH. Multi-omics reveals microbiome, host gene expression, and immune landscape in gastric carcinogenesis. *iScience* 2022; **25**: 103956 [PMID: 35265820 DOI: 10.1016/j.isci.2022.103956]
70 **Kon OL**, Yip TT, Ho MF, Chan WH, Wong WK, Tan SY, Ng WH, Kam SY, Eng AKh, Ho P, Viner R, Ong HS,

Kumarasinghe MP. The distinctive gastric fluid proteome in gastric cancer reveals a multi-biomarker diagnostic profile. *BMC Med Genomics* 2008; **1**: 54 [PMID: 18950519 DOI: 10.1186/1755-8794-1-54]

71 **Skryabin GO**, Vinokurova SV, Galetsky SA, Elkin DS, Senkovenko AM, Denisova DA, Komelkov AV, Stilidi IS, Peregorodiev IN, Malikhova OA, Imaraliev OT, Enikeev AD, Tchevkina EM. Isolation and Characterization of Extracellular Vesicles from Gastric Juice. *Cancers (Basel)* 2022; **14** [PMID: 35884376 DOI: 10.3390/cancers14143314]

72 **Shao Y**, Ye M, Li Q, Sun W, Ye G, Zhang X, Yang Y, Xiao B, Guo J. LncRNA-RMRP promotes carcinogenesis by acting as a miR-206 sponge and is used as a novel biomarker for gastric cancer. *Oncotarget* 2016; **7**: 37812-37824 [PMID: 27192121 DOI: 10.18632/oncotarget.9336]

73 **Pan Y**, Zheng Y, Yang J, Wei Y, Wu H, Liu S, Yin A, Hu J, Zeng Y. A new biomarker for the early diagnosis of gastric cancer: gastric juice- and serum-derived SNCG. *Future Oncol* 2022; **18**: 3179-3190 [PMID: 35947016 DOI: 10.2217/fon-2022-0253]

74 **Yamamoto H**, Watanabe Y, Oikawa R, Morita R, Yoshida Y, Maehata T, Yasuda H, Itoh F. BARHL2 Methylation Using Gastric Wash DNA or Gastric Juice Exosomal DNA is a Useful Marker For Early Detection of Gastric Cancer in an H. pylori-Independent Manner. *Clin Transl Gastroenterol* 2016; **7**: e184 [PMID: 27441821 DOI: 10.1038/ctg.2016.40]

75 **Botezatu A**, Bodrug N. Chronic atrophic gastritis: an update on diagnosis. *Med Pharm Rep* 2021; **94**: 7-14 [PMID: 33629042 DOI: 10.15386/mpr-1887]

76 **Bang CS**, Lee JJ, Baik GH. Prediction of Chronic Atrophic Gastritis and Gastric Neoplasms by Serum Pepsinogen Assay: A Systematic Review and Meta-Analysis of Diagnostic Test Accuracy. *J Clin Med* 2019; **8** [PMID: 31083485 DOI: 10.3390/jcm8050657]

77 **Sarhadi VK**, Armengol G. Molecular Biomarkers in Cancer. *Biomolecules* 2022; **12** [PMID: 35892331 DOI: 10.3390/biom12081021]

78 **Nakajima H**, Kotani D, Bando H, Kato T, Oki E, Shinozaki E, Sunakawa Y, Yamazaki K, Yuki S, Nakamura Y, Yamanaka T, Yoshino T, Ohta T, Taniguchi H, Kagawa Y. REMARRY and PURSUIT trials: liquid biopsy-guided rechallenge with anti-epidermal growth factor receptor (EGFR) therapy with panitumumab plus irinotecan for patients with plasma RAS wild-type metastatic colorectal cancer. *BMC Cancer* 2021; **21**: 674 [PMID: 34098908 DOI: 10.1186/s12885-021-08395-2]

79 **Ignatiadis M**, Sledge GW, Jeffrey SS. Liquid biopsy enters the clinic - implementation issues and future challenges. *Nat Rev Clin Oncol* 2021; **18**: 297-312 [PMID: 33473219 DOI: 10.1038/s41571-020-00457-x]

80 **Pascual J**, Attard G, Bidard FC, Curigliano G, De Mattos-Arruda L, Diehn M, Italiano A, Lindberg J, Merker JD, Montagut C, Normanno N, Pantel K, Pentheroudakis G, Popat S, Reis-Filho JS, Tie J, Seoane J, Tarazona N, Yoshino T, Turner NC. ESMO recommendations on the use of circulating tumour DNA assays for patients with cancer: a report from the ESMO Precision Medicine Working Group. *Ann Oncol* 2022; **33**: 750-768 [PMID: 35809752 DOI: 10.1016/j.annonc.2022.05.520]

81 **So JBY**, Kapoor R, Zhu F, Koh C, Zhou L, Zou R, Tang YC, Goo PCK, Rha SY, Chung HC, Yoong J, Yap CT, Rao J, Chia CK, Tsao S, Shabbir A, Lee J, Lam KP, Hartman M, Yong WP, Too HP, Yeoh KG. Development and validation of a serum microRNA biomarker panel for detecting gastric cancer in a high-risk population. *Gut* 2021; **70**: 829-837 [PMID: 33028667 DOI: 10.1136/gutjnl-2020-322065]

82 **Cohen JD**, Li L, Wang Y, Thoburn C, Afsari B, Danilova L, Douville C, Javed AA, Wong F, Mattox A, Hruban RH, Wolfgang CL, Goggins MG, Dal Molin M, Wang TL, Roden R, Klein AP, Ptak J, Dobbyn L, Schaefer J, Silliman N, Popoli M, Vogelstein JT, Browne JD, Schoen RE, Brand RE, Tie J, Gibbs P, Wong HL, Mansfield AS, Jen J, Hanash SM, Falconi M, Allen PJ, Zhou S, Bettegowda C, Diaz LA Jr, Tomasetti C, Kinzler KW, Vogelstein B, Lennon AM, Papadopoulos N. Detection and localization of surgically resectable cancers with a multi-analyte blood test. *Science* 2018; **359**: 926-930 [PMID: 29348365 DOI: 10.1126/science.aar3247]

83 **Xu J**, Song J, Wang T, Zhu W, Zuo L, Wu J, Guo J, Yang X. A combination of methylation and protein markers is capable of detecting gastric cancer detection by combined markers. *Epigenomics* 2021; **13**: 1557-1570 [PMID: 34632818 DOI: 10.2217/epi-2021-0080]

84 **Ko J**, Baldassano SN, Loh PL, Kording K, Litt B, Issadore D. Machine learning to detect signatures of disease in liquid biopsies - a user's guide. *Lab Chip* 2018; **18**: 395-405 [PMID: 29192299 DOI: 10.1039/c7lc00955k]

85 **Watanabe Y**, Oikawa R, Agawa S, Matsuo Y, Oda I, Futagami S, Yamamoto H, Tada T, Itoh F. Combination of artificial intelligence-based endoscopy and miR148a methylation for gastric indefinite dysplasia diagnosis. *J Clin Lab Anal* 2022; **36**: e24122 [PMID: 34811809 DOI: 10.1002/jcla.24122]

86 **Poore GD**, Kopylova E, Zhu Q, Carpenter C, Fraraccio S, Wandro S, Kosciolek T, Janssen S, Metcalf J, Song SJ, Kanbar J, Miller-Montgomery S, Heaton R, Mckay R, Patel SP, Swafford AD, Knight R. Microbiome analyses of blood and tissues suggest cancer diagnostic approach. *Nature* 2020; **579**: 567-574 [PMID: 32214244 DOI: 10.1038/s41586-020-2095-1]

87 **Gilani N**, Arabi Belaghi R, Aftabi Y, Faramarzi E, Edgünlü T, Somi MH. Identifying Potential miRNA Biomarkers for Gastric Cancer Diagnosis Using Machine Learning Variable Selection Approach. *Front Genet* 2021; **12**: 779455 [PMID: 35082831 DOI: 10.3389/fgene.2021.779455]

88 **Xiao K**, Li S, Ding J, Wang Z, Wang D, Cao X, Zhang Y, Dong Z. Expression and clinical value of circRNAs in serum extracellular vesicles for gastric cancer. *Front Oncol* 2022; **12**: 962831 [PMID: 36059681 DOI: 10.3389/fonc.2022.962831]

89 **Ding W**, Wu L, Li X, Chang L, Liu G, Du H. Comprehensive analysis of competitive endogenous RNAs network: Identification and validation of prediction model composed of mRNA signature and miRNA signature in gastric cancer. *Oncol Lett* 2022; **23**: 150 [PMID: 35350591 DOI: 10.3892/ol.2022.13270]

90 **Wu Z**, Liu P, Zhang G. Identification of circRNA-miRNA-Immune-Related mRNA Regulatory Network in Gastric Cancer. *Front Oncol* 2022; **12**: 816884 [PMID: 35280778 DOI: 10.3389/fonc.2022.816884]

91 **Gong Y**, Jiao Y, Qi X, Fu J, Qian J, Zhu J, Yang H, Tang L. Construction of a circRNA-miRNA-mRNA network based on differentially co-expressed circular RNA in gastric cancer tissue and plasma by bioinformatics analysis. *World J Surg Oncol* 2022; **20**: 34 [PMID: 35164778 DOI: 10.1186/s12957-022-02503-7]

92 **Hossain MT**, Li S, Reza MS, Feng S, Zhang X, Jin Z, Wei Y, Peng Y. Identification of circRNA Biomarker for Gastric Cancer through Integrated Analysis. *Front Mol Biosci* 2022; **9**: 857320 [PMID: 35359600 DOI: 10.3389/fmolb.2022.857320]

93 **Zhang P**, Yang M, Zhang Y, Xiao S, Lai X, Tan A, Du S, Li S. Dissecting the Single-Cell Transcriptome Network Underlying Gastric Premalignant Lesions and Early Gastric Cancer. *Cell Rep* 2019; **27**: 1934-1947.e5 [PMID: 31067475 DOI: 10.1016/j.celrep.2019.04.052]

94 **Tan R**, Zhang G, Liu R, Hou J, Dong Z, Deng C, Wan S, Lai X, Cui H. Identification of Early Diagnostic and Prognostic Biomarkers *via* WGCNA in Stomach Adenocarcinoma. *Front Oncol* 2021; **11**: 636461 [PMID: 34221961 DOI: 10.3389/fonc.2021.636461]

95 **Izumi D**, Zhu Z, Chen Y, Toden S, Huo X, Kanda M, Ishimoto T, Gu D, Tan M, Kodera Y, Baba H, Li W, Chen J, Wang X, Goel A. Assessment of the Diagnostic Efficiency of a Liquid Biopsy Assay for Early Detection of Gastric Cancer. *JAMA Netw Open* 2021; **4**: e2121129 [PMID: 34427680 DOI: 10.1001/jamanetworkopen.2021.21129]

96 **Dong Y**, Song N, Wang J, Shi L, Zhang Z, Du J. Driver Gene Alterations in Malignant Progression of Gastric Cancer. *Front Oncol* 2022; **12**: 920207 [PMID: 35903675 DOI: 10.3389/fonc.2022.920207]

97 **Flavahan WA**, Gaskell E, Bernstein BE. Epigenetic plasticity and the hallmarks of cancer. *Science* 2017; **357** [PMID: 28729483 DOI: 10.1126/science.aal2380]

98 **Liu MC**, Oxnard GR, Klein EA, Swanton C, Seiden MV; CCGA Consortium. Sensitive and specific multi-cancer detection and localization using methylation signatures in cell-free DNA. *Ann Oncol* 2020; **31**: 745-759 [PMID: 33506766 DOI: 10.1016/j.annonc.2020.02.011]

99 **Stackpole ML**, Zeng W, Li S, Liu CC, Zhou Y, He S, Yeh A, Wang Z, Sun F, Li Q, Yuan Z, Yildirim A, Chen PJ, Winograd P, Tran B, Lee YT, Li PS, Noor Z, Yokomizo M, Ahuja P, Zhu Y, Tseng HR, Tomlinson JS, Garon E, French S, Magyar CE, Dry S, Lajonchere C, Geschwind D, Choi G, Saab S, Alber F, Wong WH, Dubinett SM, Aberle DR, Agopian V, Han SB, Ni X, Li W, Zhou XJ. Cost-effective methylome sequencing of cell-free DNA for accurately detecting and locating cancer. *Nat Commun* 2022; **13**: 5566 [PMID: 36175411 DOI: 10.1038/s41467-022-32995-6]

100 **Chakrabarti S**, Kasi AK, Parikh AR, Mahipal A. Finding Waldo: The Evolving Paradigm of Circulating Tumor DNA (ctDNA)-Guided Minimal Residual Disease (MRD) Assessment in Colorectal Cancer (CRC). *Cancers (Basel)* 2022; **14** [PMID: 35804850 DOI: 10.3390/cancers14133078]

101 **Kasi PM**, Fehringer G, Taniguchi H, Starling N, Nakamura Y, Kotani D, Powles T, Li BT, Pusztai L, Aushev VN, Kalashnikova E, Sharma S, Malhotra M, Demko ZP, Aleshin A, Rodriguez A, Billings PR, Grothey A, Taieb J, Cunningham D, Yoshino T, Kopetz S. Impact of Circulating Tumor DNA-Based Detection of Molecular Residual Disease on the Conduct and Design of Clinical Trials for Solid Tumors. *JCO Precis Oncol* 2022; **6**: e2100181 [PMID: 35263168 DOI: 10.1200/PO.21.00181]

102 **Kong Y**, Ning L, Qiu F, Yu Q, Cao B. Clinical significance of serum miR-25 as a diagnostic and prognostic biomarker in human gastric cancer. *Cancer Biomark* 2019; **24**: 477-483 [PMID: 30909187 DOI: 10.3233/CBM-182213]

103 **Ji B**, Huang Y, Gu T, Zhang L, Li G, Zhang C. Potential diagnostic and prognostic value of plasma long noncoding RNA LINC00086 and miR-214 expression in gastric cancer. *Cancer Biomark* 2019; **24**: 249-255 [PMID: 30689553 DOI: 10.3233/CBM-181486]

104 **Hung PS**, Chen CY, Chen WT, Kuo CY, Fang WL, Huang KH, Chiu PC, Lo SS. miR-376c promotes carcinogenesis and serves as a plasma marker for gastric carcinoma. *PLoS One* 2017; **12**: e0177346 [PMID: 28486502 DOI: 10.1371/journal.pone.0177346]

105 **Li Y**, Sun H, Guan J, Ji T, Wang X. Serum microRNA-381: A Potential Marker for Early Diagnosis of Gastric Cancer. *Yonsei Med J* 2019; **60**: 720-726 [PMID: 31347326 DOI: 10.3349/ymj.2019.60.8.720]

106 **Huang ZS**, Guo XW, Zhang G, Liang LX, Nong B. The Diagnostic and Prognostic Value of miR-200c in Gastric Cancer: A Meta-Analysis. *Dis Markers* 2019; **2019**: 8949618 [PMID: 31089400 DOI: 10.1155/2019/8949618]

107 **Jiang X**, Jiang M, Xu M, Xu J, Li Y. Identification of diagnostic utility and molecular mechanisms of circulating miR-551b-5p in gastric cancer. *Pathol Res Pract* 2019; **215**: 900-904 [PMID: 30732916 DOI: 10.1016/j.prp.2019.01.035]

108 **Zhao G**, Jiang T, Liu Y, Huai G, Lan C, Li G, Jia G, Wang K, Yang M. Droplet digital PCR-based circulating microRNA detection serve as a promising diagnostic method for gastric cancer. *BMC Cancer* 2018; **18**: 676 [PMID: 29929476 DOI: 10.1186/s12885-018-4601-5]

109 **Herrera-Pariente C**, Montori S, Llach J, Bofill A, Albeniz E, Moreira L. Biomarkers for Gastric Cancer Screening and Early Diagnosis. *Biomedicines* 2021; **9** [PMID: 34680565 DOI: 10.3390/biomedicines9101448]

110 **Yu Z**, Rong Z, Sheng J, Luo Z, Zhang J, Li T, Zhu Z, Fu Z, Qiu Z, Huang C. Aberrant Non-Coding RNA Expressed in Gastric Cancer and Its Diagnostic Value. *Front Oncol* 2021; **11**: 606764 [PMID: 34295803 DOI: 10.3389/fonc.2021.606764]

111 **Fu M**, Huang Z, Zang X, Pan L, Liang W, Chen J, Qian H, Xu W, Jiang P, Zhang X. Long noncoding RNA LINC00978 promotes cancer growth and acts as a diagnostic biomarker in gastric cancer. *Cell Prolif* 2018; **51** [PMID: 29271006 DOI: 10.1111/cpr.12425]

112 **Liu J**, Wang J, Song Y, Ma B, Luo J, Ni Z, Gao P, Sun J, Zhao J, Chen X, Wang Z. A panel consisting of three novel circulating lncRNAs, is it a predictive tool for gastric cancer? *J Cell Mol Med* 2018; **22**: 3605-3613 [PMID: 29700972 DOI: 10.1111/jcmm.13640]

113 **Zong W**, Feng W, Jiang Y, Ju S, Cui M, Jing R. Evaluating the diagnostic and prognostic value of serum long non-coding RNA CTC-497E21.4 in gastric cancer. *Clin Chem Lab Med* 2019; **57**: 1063-1072 [PMID: 30763257 DOI: 10.1515/cclm-2018-0929]

114 **Zhang G**, Xu Y, Wang S, Gong Z, Zou C, Zhang H, Ma G, Zhang W, Jiang P. LncRNA SNHG17 promotes gastric cancer progression by epigenetically silencing of p15 and p57. *J Cell Physiol* 2019; **234**: 5163-5174 [PMID: 30256413 DOI: 10.1002/jcp.27320]

115 **Zhang G**, Xu Y, Zou C, Tang Y, Lu J, Gong Z, Ma G, Zhang W, Jiang P. Long noncoding RNA ARHGAP27P1 inhibits gastric cancer cell proliferation and cell cycle progression through epigenetically regulating p15 and p16. *Aging (Albany NY)* 2019; **11**: 9090-9110 [PMID: 31665700 DOI: 10.18632/aging.102377]

116 **Lu X**, Lu J, Wang S, Zhang Y, Ding Y, Shen X, Jing R, Ju S, Chen H, Cong H. Circulating serum exosomal miR-92a-3p as a novel biomarker for early diagnosis of gastric cancer. *Future Oncol* 2021; **17**: 907-919 [PMID: 33533649 DOI: 10.2217/fon-2020-0792]

117 **Zhao R**, Zhang Y, Zhang X, Yang Y, Zheng X, Li X, Liu Y. Exosomal long noncoding RNA HOTTIP as potential novel diagnostic and prognostic biomarker test for gastric cancer. *Mol Cancer* 2018; **17**: 68 [PMID: 29486794 DOI: 10.1186/s12943-018-0817-x]

World Journal of Gastroenterology

Submit a Manuscript: https://www.f6publishing.com

World J Gastroenterol 2023 May 7; 29(17): 2534-2550

DOI: 10.3748/wjg.v29.i17.2534

ISSN 1007-9327 (print) ISSN 2219-2840 (online)

REVIEW

Non-invasive evaluation of liver steatosis with imaging modalities: New techniques and applications

Ke-Yu Zeng, Wu-Yong-Ga Bao, Yun-Han Wang, Min Liao, Jie Yang, Jia-Yan Huang, Qiang Lu

Specialty type: Gastroenterology and hepatology

Provenance and peer review: Invited article; Externally peer reviewed.

Peer-review model: Single blind

Peer-review report's scientific quality classification

Grade A (Excellent): A, A
Grade B (Very good): B, B
Grade C (Good): C
Grade D (Fair): 0
Grade E (Poor): 0

P-Reviewer: Losurdo G, Italy; Tai DI, Taiwan; Uhlmann D, Germany

Received: December 23, 2022
Peer-review started: December 23, 2022
First decision: February 16, 2023
Revised: February 26, 2023
Accepted: April 11, 2023
Article in press: April 11, 2023
Published online: May 7, 2023

Ke-Yu Zeng, Wu-Yong-Ga Bao, Yun-Han Wang, Min Liao, Jie Yang, Jia-Yan Huang, Qiang Lu, Department of Medical Ultrasound, West China Hospital of Sichuan University, Chengdu 610041, Sichuan Province, China

Corresponding author: Qiang Lu, MD, Professor, Department of Medical Ultrasound, West China Hospital of Sichuan University, No. 37 Guoxue Xiang, Chengdu 610041, Sichuan Province, China. luqiang@scu.edu.cn

Abstract

In the world, nonalcoholic fatty liver disease (NAFLD) accounts for majority of diffuse hepatic diseases. Notably, substantial liver fat accumulation can trigger and accelerate hepatic fibrosis, thus contributing to disease progression. Moreover, the presence of NAFLD not only puts adverse influences for liver but is also associated with an increased risk of type 2 diabetes and cardiovascular diseases. Therefore, early detection and quantified measurement of hepatic fat content are of great importance. Liver biopsy is currently the most accurate method for the evaluation of hepatic steatosis. However, liver biopsy has several limitations, namely, its invasiveness, sampling error, high cost and moderate intraobserver and interobserver reproducibility. Recently, various quantitative imaging techniques have been developed for the diagnosis and quantified measurement of hepatic fat content, including ultrasound- or magnetic resonance-based methods. These quantitative imaging techniques can provide objective continuous metrics associated with liver fat content and be recorded for comparison when patients receive check-ups to evaluate changes in liver fat content, which is useful for longitudinal follow-up. In this review, we introduce several imaging techniques and describe their diagnostic performance for the diagnosis and quantified measurement of hepatic fat content.

Key Words: Non-alcoholic fatty liver disease; Hepatic steatosis; Imaging techniques; Quantitative evaluation; Ultrasound; Quantitative ultrasound

Core Tip: Accurate evaluation of the hepatic steatosis is important. The conventional gray scale ultrasound has the limitation of low diagnostic accuracy for mild hepatic steatosis and inability to make quantification evaluations. Quantification imaging techniques including ultrasound-based techniques and magnetic resonance imaging-based techniques can provide objective continuous numbers associated with liver fat content and past records can be found when patients receiving check-ups to evaluate change of liver fat content, which is useful for the longitudinal follow-up to monitor the impact of clinical interventions.

Citation: Zeng KY, Bao WYG, Wang YH, Liao M, Yang J, Huang JY, Lu Q. Non-invasive evaluation of liver steatosis with imaging modalities: New techniques and applications. *World J Gastroenterol* 2023; 29(17): 2534-2550
URL: https://www.wjgnet.com/1007-9327/full/v29/i17/2534.htm
DOI: https://dx.doi.org/10.3748/wjg.v29.i17.2534

INTRODUCTION

There are several types of chronic liver diseases, but nonalcoholic fatty liver disease (NAFLD) is the broadest state[1,2]. NAFLD represents a wide range of liver abnormalities[3]. Over 25% of general population is influenced by NAFLD, while affected proportion of type 2 diabetes population is 55%-80% [1]. Simple fatty liver may progress to non-alcoholic steatohepatitis (NASH), which is a severe form of fatty liver characterized by inflammation of hepatocyte. This form may result in cirrhosis with portal hypertension or liver dysfunction or even to hepatocellular carcinoma (HCC)[4]. Notably, there is an annual incidence of 0.4 cases of HCC per 1000 population-years among patients with NAFLD, making it the third most common cause of HCC in the United States[5]. A diagnosis of NAFLD is associated with not only adverse effects on the liver, but also an increased risk of type 2 diabetes and cardiovascular disease[6,7]. A study suggested that there was a significant increase in mortality associated with liver-specific diseases or cardiovascular diseases in patients with NAFLD compared to controls[8]. For patients who received hepatectomy, hepatic steatosis can increase incidence of postoperative complications and death[9]. The risk of graft failure for patients undergoing liver transplantation increases when hepatic steatosis exceeds 30%[10].

As NAFLD poses substantial risks of HCC, liver-associated complications and other adverse events to patients, it is of great importance to diagnose and quantify hepatic fat content early[4]. NAFLD is likely to be reversible in its early stage even with simple treatments, for example, lifestyle changes[11]. In addition, the main factor contributing to disease progression in patients with NAFLD is liver fibrosis[1, 3]. Abundant liver fat accumulation can trigger and accelerate hepatic fibrosis, thus contributing to disease progression[12,13]. Therefore, in patients with NAFLD, quantitative measurements of liver steatosis could be useful for prognostic assessment and treatment[4]. Although high level of liver fat can lead to fibrosis progression, it is of note that the level of liver fat is not always parallel to the grade of fibrosis. It has been suggested that patients without fibrosis or in the early stages of fibrosis may demonstrate obvious disease progression with high level of liver fat content; however, the fat content decreases when disease progresses to advanced fibrosis or cirrhosis[14-16]. Therefore, when evaluating the value of measuring hepatic steatosis for assessing disease progression and prognosis, the fibrosis status should first be taken into account[17].

When it comes to diagnosing diffuse hepatic disease, liver histopathologic examination is the most precise method. With liver biopsy, quantification of the liver fat level is classified into four grades (grade 0, < 5%; grade 1, 5%-33%; grade 2, 33%-66%; grade 3, > 66%)[18]. Although the use of liver biopsy correctly evaluates liver steatosis, its limitations include its invasiveness, sampling error, which make biopsy impractical for patients who have only simple steatosis[19,20]. Therefore, noninvasive methods to diagnose the presence of steatosis and to monitor changes in hepatic steatosis are needed (Table 1). Conventional gray-scale ultrasound can be applied to diagnose liver steatosis. However, its inability to provide accurate quantification of liver fat has limited its use in the diagnostic pathway of liver steatosis[21]. At present, a number of imaging techniques for the evaluation of hepatic fat content, including MR- and ultrasound-based methods, have been developed. In this review, we summarize the available imaging methods for the quantified measurement of hepatic fat content. In addition, we briefly discuss the clinical performance of these methods.

ULTRASOUND-BASED METHODS TO DIAGNOSE AND QUANTIFY HEPATIC STEATOSIS

Table 2 summarizes published diagnostic utility metrics and optimal cutoff values of quantitative ultrasound methods for quantified measurement of hepatic fat content.

Table 1 Characteristics of imaging techniques for hepatic steatosis evaluation

Techniques	Clinical characteristics	Limitations
CAP	Low cost; High availability; Time-saving	High measurement failure rate
	Allows simultaneous evaluation of steatosis and fibrosis	Measurement without B-mode ultrasound image
	Moderate to high diagnostic accuracy for detecting and grading steatosis	The cutoff value for diagnosing steatosis is poorly standardized
	Moderate to high repeatability and reproducibility	
	Well validated	
ATI, ATT and UGAP	Outperform or have comparable diagnostic accuracy compared with CAP	The measurement may be influenced by liver fibrosis
	High repeatability and reproducibility	Fairly small number of studies
	Strong correlation with liver histology or MRI-PDFF	
	Low measurement failure rate	
	Measured on B-mode ultrasound images	
Att. PLUS	Measurement is obtained at the same time as the sound speed measurement	Fairly small number of studies
	Comparable diagnostic accuracy with CAP	No study comparing this technique with liver histology or MRI-PDFF
TAI and TSI	High diagnostic accuracy for detecting and grading steatosis	Fairly small number of studies
	Strong correlation with MRI-PDFF	
	High repeatability and reproducibility	
BSC	Uses a reference phantom to reduce sources of variability due to ultrasound systems or operators	Fairly small number of studies
	High diagnostic accuracy for detecting and grading steatosis	
	Strong correlation with liver histology or MRI-PDFF	
	High repeatability and reproducibility	
UDFF	Is a combination of both attenuation coefficient and backscatter coefficient	Fairly small number of studies
	UDFF approximates MRI-PDFF	
ASQ and NLV	Moderate to high diagnostic accuracy for detecting and grading steatosis	Weak correlation with liver histology
	Strong correlation with CAP	The correlation with MR-based techniques is controversial
		The influence of fibrosis on measurement is controversial
		Fairly small number of studies
SS	Moderate to high diagnostic accuracy for detecting and grading steatosis	Fairly small number of studies
	Strong correlation with CAP	
MRS and MRI-PDFF	High diagnostic accuracy for detecting and grading steatosis	High cost; low availability
	Considered as the reference standard	Time-consuming

CAP: Controlled attenuation parameter; ATI: Attenuation imaging; ATT: Attenuation measurement function; UGAP: Ultrasound-guided attenuation parameter; Att. PLUS: Attenuation plane-wave ultrasound; TAI: Tissue attenuation imaging; TSI: Tissue scatter distribution imaging; BSC: Backscatter coefficient; UDFF: Ultrasound-derived fat fraction; ASQ: Acoustic structure quantification; NLV: Normalized local variance; SS: Speed of sound; MRS: Magnetic resonance spectroscopy; MRI-PDFF: Magnetic resonance imaging-proton density fat fraction.

Conventional gray scale ultrasound

Due to its low price and availability, gray scale ultrasound is a traditional diagnostic method for diagnosing and monitoring liver steatosis[22]. When using this method, fatty infiltration is indicated by the following signs: Hyperechogenicity of the liver parenchyma, liver-to-kidney comparison, ultrasound beam attenuation, and impaired visualization of the intrahepatic structures[23]. However, it is difficult for operators to grade liver steatosis solely based on the gray scale ultrasound[24]. Degree of liver fat content can be classified into 4 grades (normal, mild, moderate, and severe)[22]. For moderate to severe hepatic steatosis, gray scale ultrasound has a high diagnostic accuracy. A meta-analysis enrolling a total of 2815 patients and using hepatic histopathologic results as the golden standard demonstrated that the overall sensitivity and specificity of gray scale ultrasound to distinguish normal liver and moderate steatosis were 85% and 93%[25]. However, gray scale ultrasound has restricted diagnostic performance for mild steatosis[24]. Another limitation is that gray scale ultrasound is based on qualitative visual features, and the intraobserver and interobserver reproducibility vary with different operators[26,27].

Hepatorenal index

To improve the diagnostic performance of using gray scale ultrasound for the measurement of liver content, hepatorenal index (HRI) was developed[28] (Figure 1). This metric calculates the rate of parenchymal echo of the liver and the renal cortex[28]. Previous studies found that HRI had a significant correlation with histologic steatosis[29-31]. Marshall *et al*[32] reported a sensitivity, confirmed by liver biopsy, of 100% with an HRI cutoff of 1.27 for detecting more than 5% steatosis. Borges *et al*[33] reported for diagnosing fatty liver, the cutoff value of 1.24 revealed 93% sensitivity and specificity, but this study only used healthy volunteers as the control group. Stahlschmidt *et al*[34] suggested in livers with advanced fibrosis, HRI should not be used to measure steatosis because fibrosis replaces fat as NAFLD progresses. Similarly, patients suffering from chronic kidney disease may present increased echo of the renal cortex, which makes the HRI unreliable for grading steatosis[35]. Furthermore, Kjaergaard *et al*[36] found that HRI presented a higher incidence of failure (12%) compared to controlled attenuation parameter (CAP, 2%). In addition, it can be challenging to diagnose mild steatosis by HRI[33].

Quantitative ultrasound techniques

Mechanism of quantitative ultrasound techniques: Conventional gray scale ultrasound and HRI cannot provide quantitative information about liver fat content. Essentially, quantitative methods are used to model the relationship between physical properties of hepatic tissue and the echo signals that are scattered by it. The impedance difference of fat vesicles in hepatocytes causes increased scattering magnitudes and signal attenuation. A frequency-dependent analysis of signal attenuation and backscatter is performed on signals returned by tissue[37].

The quantitative ultrasound techniques used for the measurement of hepatic fat quantification included the spectral-based techniques and the techniques based on envelope statistics. Estimation of either attenuation coefficient (AC) or the backscatter coefficient (BSC) is used for spectral based techniques. The AC measures energy loss as ultrasound wave passes through tissue and the BSC measures the returned ultrasound energy when ultrasound wave strikes the microstructure of tissue. Techniques based on the envelope statistics of the backscattered ultrasound include the acoustic structure quantification (ASQ), normalized local variance (NLV), and estimation of sound speed[38]. Techniques according to envelope statistics are relatively novel. Microstructural characteristics of tissues can be determined by the shape and attributes of backscattered ultrasound[38].

Current commercial techniques and their mechanism of hepatic steatosis quantification are presented in Table 3.

CAP: CAP was the initial available technique for quantified measurement of hepatic fat content. Attenuation of the ultrasound beam is applied to generate the CAP amount[39,40]. Typically, two types of probes, the medium probe and the extra-large probe, can be utilized. The choice of optimal probe is automatically controlled according to skin-to-liver capsule distance (SCD). When the SCD exceeds 2.5 cm, the extra-large probe is more effective than the M probe. The CAP is presented in units of decibels per meter (dB/m)[41].

More than 160 studies have discussed the efficacy of CAP as a metric for quantified measurement of liver fat content, and acceptable accuracy was found. The general diagnostic accuracy evaluated by the area under the receiver operating curve (AUROC) of CAP for detecting presence of steatosis has been displayed to range from 0.64 to 0.97[42-44]. A meta-analysis including 19 studies found that CAP had good diagnostic performance with AUROCs of 0.823 for distinguishing steatosis grade > S0, 0.865 for distinguishing steatosis grade > S1, 0.882 for distinguishing steatosis grade > S2. The corresponding optimal cutoff values for > S0, > S1, > S2 were 248, 268 and 280 dB/m. Moreover, they found that there was a potential link between NAFLD, diabetes mellitus, and body mass index with the CAP value[45]. Although the diagnostic utility of CAP for differentiating patients with and without hepatic steatosis has been fully validated, the optimal cutoff value to determine the presence of steatosis varies significantly between studies[17]. A meta-analysis of 2346 participants with different diffused hepatic diseases demonstrated that CAP cutoffs varied according to the etiology of the hepatic diseases,

Table 2 Summary of studies using ultrasound methods to evaluate hepatic steatosis

Ref.	No.	Method	Reference standard	Grade of steatosis	Optimal cutoff value	AUROC
Bae *et al*[59], 2019	108	ATI	LB	≥ S1	0.64	0.84
				≥ S2	0.70	0.89
				≥ S3	0.75	0.93
Bae *et al*[60], 2022	120	ATI	LB	≥ S1	0.66	0.91
				≥ S2	0.66	0.91
Tada *et al*[62], 2019	148	ATI	LB	≥ S1	0.66	0.85
				≥ S2	0.67	0.91
				≥ S3	0.68	0.91
Tada *et al*[63], 2020	119	ATI	MRI-PDFF	≥ S1	0.63	0.81
				≥ S2	0.73	0.87
				≥ S3	0.75	0.94
Jeon *et al*[61], 2019	87	ATI	MRI-PDFF	≥ S1	0.59	0.76
Ferraioli *et al*[65], 2019	129	ATI	MRI-PDFF	≥ S1	0.63	0.91
				≥ S2	0.72	0.95
Ferraioli *et al*[66], 2021	72	ATI-GEN	MRI-PDFF	≥ S1	0.62	0.92
		ATI-PEN	MRI-PDFF	≥ S1	0.69	0.90
Sugimoto *et al*[67], 2021	111	ATI	LB	≥ S1	0.67	0.88
				≥ S2	0.72	0.86
				≥ S3	0.86	0.79
Hsu *et al*[70], 2021	28	ATI	LB	≥ S1	0.69	0.97
				≥ S2	0.78	0.99
				≥ S3	0.82	0.97
Kwon *et al*[57], 2021	100	ATI	MRI-PDFF	≥ S1	0.62	0.91
				≥ S2	0.72	0.94
Jang *et al*[58], 2022	57	ATI	LB	≥ S1	0.62	0.81
Koizumi *et al*[73], 2019	89	ATT	LB	≥ S1	0.68	0.74
				≥ S2	0.72	0.80
				≥ S3	0.78	0.96
Tamaki *et al*[54], 2018	351	ATT	LB	≥ S1	0.63	0.79
				≥ S2	0.69	0.87
				≥ S3	0.85	0.96
Fujiwara *et al*[75], 2018	163	UGAP	LB	≥ S1	0.53	0.90
				≥ S2	0.60	0.95
				≥ S3	0.65	0.96
Imajo *et al*[76], 2022	1010	UGAP	MRI-PDFF	≥ S1	0.65	0.91
				≥ S2	0.71	0.91
				≥ S3	0.77	0.89
Kuroda *et al*[79], 2021	202	UGAP	LB	≥ S1	0.49	0.89
				≥ S2	0.65	0.91

				≥ S3	0.69	0.92
Tada *et al*[80], 2019	126	UGAP	MRI-PDFF	≥ S1	0.60	0.92
				≥ S2	0.69	0.87
				≥ S3	0.69	0,89
Jeon *et al*[83], 2021	120	TAI	MRI-PDFF	≥ S1	0.88	0.86
		TSI	MRI-PDFF	≥ S1	91.2	0.96
Rónaszéki *et al*[84], 2022	110	TAI	MRI-PDFF	≥ S1	0.59	0.92
		TSI	MRI-PDFF	≥ S1	99.7	0.91
Şendur *et al*[85], 2023	80	TAI	MRI-PDFF	≥ S1	0.75	0.95
				≥ S2	0.86	0.97
				≥ S3	0.96	0.97
		TSI	MRI-PDFF	≥ S1	92.44	0.96
				≥ S2	96.64	0.91
				≥ S3	99.45	0.94
Lin *et al*[91], 2015	204	BSC	MRI-PDFF	≥ S1	0.0038	0.98
Dillman *et al*[94], 2022	56	UDFF	MRI-PDFF	≥ S1	5%	0.90
Labyed *et al*[37], 2020	101	UDFF	LB	≥ S1	8.1%	0.94
				≥ S2	15.9%	0.88
				≥ S3	16.1%	0.83

AUROC: Area under the receiver operating characteristic curve; LB: Liver biopsy; MRI-PDFF: Magnetic resonance imaging-proton density fat fraction; ATI: Attenuation imaging; ATT: Attenuation measurement function; UGAP: Ultrasound-guided attenuation parameter; TAI: Tissue attenuation imaging; TSI: Tissue scatter distribution imaging; BSC: Backscatter coefficient; UDFF: Ultrasound-derived fat fraction.

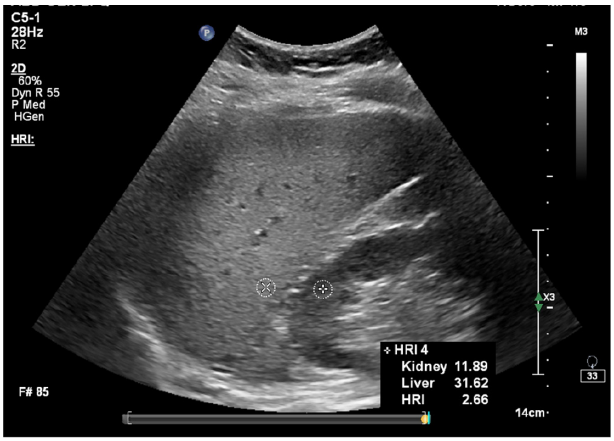

DOI: 10.3748/wjg.v29.i17.2534

Figure 1 Hepatorenal index. In this case, the result was 2.66, indicating severe hepatic steatosis.

including NAFLD, chronic viral hepatitis, alcoholic liver disease[46].

The CAP value demonstrated a moderate to strong correlation with magnetic resonance (MR)-based techniques for liver steatosis quantification[47,48]. However, compared with MR-based methods, the CAP has inferior diagnostic ability in grading liver steatosis. Diagnostic effectiveness of MR spectroscopy (MRS) over CAP for diagnosing S1 was significantly higher (AUROC, 0.77 *vs* 0.99)[49]. Imajo *et al*[50] demonstrated suboptimal diagnostic performance of CAP compared to MRI-proton density fat fraction (MRI-PDFF) in grading liver steatosis.

However, CAP has the limitation of failure rate up to 7.7%. According to previous reports, an association was found between measurement failure and sex, body mass index, and metabolic syndrome[51]. Use of the extra-large probe can reduce the failure rate because it is designed for patients

Table 3 Summary of techniques for liver fat quantification and their mechanisms

Technique	Mechanism for liver fat quantification	Principle of the techniques
CAP	Spectral based technique (AC)	CAP measures the attenuation of or reduction in the amplitude of the ultrasound waves on their way through the liver
ATI	Spectral based technique (AC)	ATI quantifies the degree of the ultrasound beam attenuation. The attenuation of the ultrasound beam is calculated by analyzing echo signals received by the transducer
ATT	Spectral based technique (AC)	Two ultrasonic waves of different frequencies (F0, F1; F0 < F1) are transmitted to the same beamline and the received signal is obtained. ATT estimates the attenuation coefficient it by calculating the slope of the received signal ratio (F0/F1)
UGAP	Spectral based technique (AC)	UGAP compares the measured liver signal and the referential signal (measured on the reference phantom with known attenuation and backscatter coefficients)
Att. PLUS	Spectral based technique (AC)	Att. PLUS measures the decrease in amplitude of ultrasound waves as they propagate throughout the tissue
TAI	Spectral based technique (AC)	TAI is determined based on the attenuation properties of different frequency components in the tissue, and the spectrum of radiofrequency signals provides a downshift of the center frequency according to depth. The TAI parameter indicates the slope of the ultrasound center frequency downshift
BSC	Spectral based technique (BSC)	BSC measures the ultrasound energy returned from the tissue
UDFF	Spectral based technique (BSC)	UDFF is obtained by combining both AC and BSC and the result is presented as the percentage of hepatic steatosis. Reference phantom data is integrated into the ultrasound system and fixed-acquisition region of interest is applied
TSI	Envelope Statistic based technique	The TSI is based on the shape parameter of the Nakagami distribution which reflects the local concentration and arrangement of ultrasound scatterers
ASQ	Envelope Statistic based technique	ASQ measures the FD ratio, which is based on the difference between theoretical and real echo amplitude distributions
NLV	Envelope Statistic based technique	NLV parameter was derived from ASQ, which analyzed ultrasound amplitudes sampled from gray-scale ultrasound images
SS	Envelope Statistic based technique	SS calculates the speed of sound through the liver
SSp.PLUS	Envelope Statistic based technique	SSp.PLUS is a novel technique that allows quantification of the intrahepatic speed of sound which is correlated with the liver fat content

AC: Attenuation coefficient; BSC: Backscatter coefficient; CAP: Controlled attenuation parameter; ATI: Attenuation imaging; ATT: Attenuation measurement function; UGAP: Ultrasound-guided attenuation parameter; Att.PLUS: Attenuation plane-wave ultrasound; TAI: Tissue attenuation imaging; UDFF: Ultrasound-derived fat fraction; TSI: Tissue scatter distribution imaging; ASQ: Acoustic structure quantification; NLV: Normalized local variance; SS: Speed of sound; SSp.PLUS: Sound speed plane-wave ultrasound; FD: Focal disturbance.

with obesity[4].

Quantification of attenuation using ultrasound imaging: Several techniques aiming to evaluate the attenuation coefficient applying ultrasound guidance have been exploited, including attenuation imaging (ATI), attenuation measurement function (ATT), and ultrasound guided attenuation parameter (UGAP). CAP has a disadvantage that it lacks the guidance of gray scale ultrasound images in choosing the area for measurement. In contrast, the ATI, ATT, and UGAP techniques are characterized by evaluating liver steatosis on gray scale ultrasonography images with accurate placement of region of interest[17]. When using these techniques, conventional gray scale ultrasound images can be evaluated simultaneously, and the exact region of interest can be placed to avoid the vessels, bile duct, masses or cysts. Therefore, the technical success rate using these methods is high[52-55]. Another advantage of ATI, ATT, and UGAP is that these techniques have high intraobserver and interobserver agreement. A range of 0.81 to 0.98 is found for the intraobserver agreement of ATI, and a range of 0.79 to 0.92 is found for the interobserver agreement. Although there are few studies investigating the topic, the intraobserver and interobserver agreement of UGAP is reported to be 0.86 and 0.84, respectively. In addition, ATI measurements among different operators demonstrated high agreement (intraclass correlation coefficients: 0.91)[17,44,56].

ATI is a kind of two-dimensional attenuation imaging technique (Figure 2)[57,58]. ATI assesses the attenuation of ultrasound beams in a region of interest using color-coded maps in real time. dB/cm/MHz is the unit of measurement for the attenuation coefficient[35]. In addition, to ensure a high technique success rate, the ATI is equipped with a reliability index (R^2), and an R^2 value ≥ 0.80 is considered a reliable measurement[59-61]. In the reported measurements, the cutoff values ranged from 0.63 to 0.69 dB/cm/MHz for detecting ≥ S1, 0.66-0.72 dB/cm/MHz for detecting ≥ S2, and 0.68-0.86 dB/

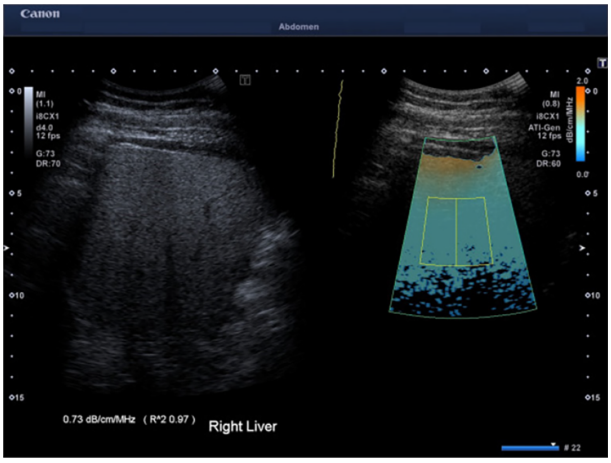

Figure 2 Attenuation imaging technique by Canon with reliability indicator (R^2)[40]. The Gray scale image and the corresponding attenuation imaging image are shown side by side. The attenuation coefficient measurement of the images shown here is 0.73 dB/cm/MHz with an R^2 of 0.97, indicating a valid measurement. Citation: Seneviratne N, Fang C, Sidhu PS. Ultrasound-based hepatic fat quantification: current status and future directions. *Clin Radiol* 2023; 78: 187-200. Copyright© The Author(s) 2023. Published by Elsevier Ltd. The authors have obtained the permission for figure using (Supplementary material).

cm/MHz for detecting = S3. The reported AUROCs were 0.80-0.97 for detecting ≥ S1, 0.86-0.99 for detecting ≥ S2, and 0.79-0.99 for detecting = S3[59-70]. It has been found that ATI measurements have a significant correlation with histological steatosis grade determined by liver biopsy[59,60,67]. Additionally, in case where MRI-PDFF was applied as the gold standard, the ATI demonstrated positive correlation with it (r = 0.70-0.83)[57,65,66]. The ATI also outperformed the CAP in evaluating the grades of hepatic steatosis. A study including 72 consecutive adult patients found that the AUROC for detecting S0 *vs* S1-S3 of CAP was lower than that of ATI (0.85 *vs* 0.92, respectively)[66].

ATT is a technique developed by Fujifilm Health Care company (previously Hitachi Medical Systems, Japan) (Figure 3). In ATT, a beamline is connected to an ultrasonic transmitter with two ultrasonic waves of different frequencies (F0, F1) at once. The received signal is obtained, and attenuation coefficients are determined by the slope of the received signal ratio (F0/F1). The results are presented in units of dB/cm/MHz[54,55,71-73]. A study enrolled 351 patients and biopsy specimens were examined quantitatively for fat content. In terms of fat area, ATT had a significant correlation (r = 0.50, P < 0.001). The cutoff values were 0.62 dB/cm/MHz for S ≥ 1, 0.67 dB/cm/MHz for S ≥ 2 and 0.73 dB/cm/MHz for S ≥ 3 and corresponding AUROCs were 0.79, 0.87 and 0.96[54]. An analysis of 94 patients who received both ATT and CAP examinations when undergoing liver histopathologic examination revealed that ATT exhibited diagnostic accuracy equivalent to that of CAP for grading histological steatosis[73].

With known attenuation and BSC, an ultrasound system uses a phantom method to calculate attenuation coefficients measurement implemented in UGAP (Figure 4). Using this method, the US system's transmitting and receiving beamforming characteristics can be compensated. The result is presented in units of dB/cm/MHz[4,74-76]. Several studies reported good diagnostic efficacy of UGAP for liver fat content quantification applying hepatic histological results as the gold standard, and a positive association was found between UGAP and steatosis percentage (correlation coefficient: 0.78-0.81). The reported AUROCs were 0.89-0.92 for detecting steatosis grade ≥ S1, 0.90–0.95 for detecting steatosis grade ≥ S2, and 0.88-0.96 for detecting steatosis grade = S3[75,77-79]. Several other studies compared UGAP with MR-based methods, and a significant correlation between MR-based methods and attenuation coefficient values by UGAP was found (correlation coefficient: 0.72-0.77)[76,80]. Imajo *et al*[76] conducted a multicentric study with 1010 patients and reported that UGAP had good diagnostic efficacy for making quantified measurement of liver fat content. In their study, the AUROCs were 0.910 for detecting MRI-PDFF ≥ 5.2%, 0.912 for MRI-PDFF ≥ 11.3%, and 0.894 for MRI-PDFF ≥17.1%[76]. Fujiwara *et al*[75] reported that as compared to CAP, UGAP achieved significantly higher AUROCs for identifying ≥ S2 (0.950 *vs* 0.841) and ≥ S3 (0.959 *vs* 0.817). In addition, they also reported 5.2% of CAP patients had measurement failures, while no UGAP patients did. Tada *et al*[81] reported that there was no effect of liver stiffness on UGAP attenuation coefficient values.

Attenuation plane-wave ultrasound: Attenuation Plane-Wave Ultrasound (Att. PLUS) presents information on ultraphonic beam attenuation through a region of interest. The ultrasound beam attenuation is calculated in a region of interest at a constant depth. The attenuation coefficient results are displayed in units of dB/cm/MHz[56]. The Att. PLUS measurement is combined with the sound speed measurement for each acquisition. It is the median of five measurements taken consecutively that determines the final result[35]. Only one published study regarding this method was found. Popa *et al*[82] carried out a study aiming to assess the clinical value of Att. PLUS of noninvasive measurement of fatty liver with the CAP value considered as control. They reported that the cutoff value to detect S2-S3

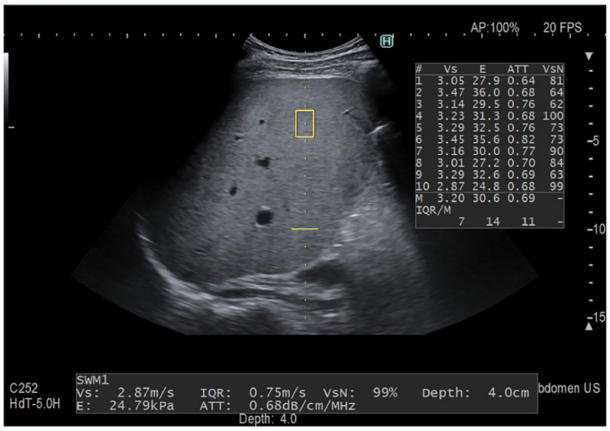

Figure 3 The attenuation measurement function technique was developed by Fujifilm Health Care company[4]. The attenuation coefficient (0.68 dB/cm/MHz) is measured in a fixed area (yellow box) along the same axis as the liver stiffness measurement. Ten acquisitions are performed, and the median value is utilized as the final metric. Citation: Ferraioli G, Berzigotti A, Barr RG, Choi BI, Cui XW, Dong Y, Gilja OH, Lee JY, Lee DH, Moriyasu F, Piscaglia F, Sugimoto K, Wong GL, Wong VW, Dietrich CF. Quantification of Liver Fat Content with Ultrasound: A WFUMB Position Paper. *Ultrasound Med Biol* 2021; 47: 2803-2820. Copyright© The Author(s) 2021. Published by Elsevier Ltd. The authors have obtained the permission for figure using (Supplementary material).

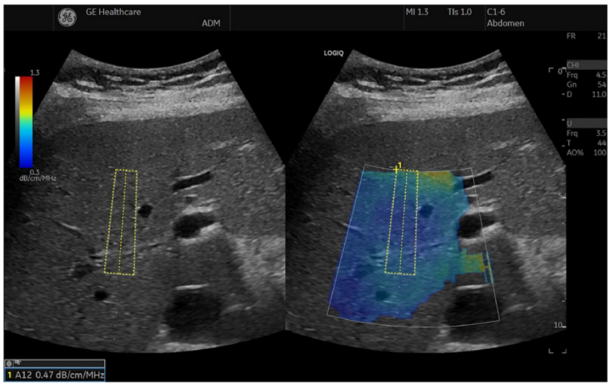

Figure 4 The ultrasound-guided attenuation parameter method implemented in the LOGIQ E9 XDclear 2.0 US scanner[4]. The attenuation coefficient is 0.47 dB/cm/MHz, indicating less than 5% steatosis. Citation: Ferraioli G, Berzigotti A, Barr RG, Choi BI, Cui XW, Dong Y, Gilja OH, Lee JY, Lee DH, Moriyasu F, Piscaglia F, Sugimoto K, Wong GL, Wong VW, Dietrich CF. Quantification of Liver Fat Content with Ultrasound: A WFUMB Position Paper. *Ultrasound Med Biol* 2021; 47: 2803-2820. Copyright© The Author(s) 2021. Published by Elsevier Ltd. The authors have obtained the permission for figure using (Supplementary material).

was 0.5 dB/cm/MHz (sensitivity 53.1%, specificity 82.0%), and the AUROC was 0.72.

Tissue attenuation imaging and tissue scatter distribution imaging: Tissue attenuation imaging (TAI) parameter indicates slope of the ultrasound central frequency downshift along depth, which is able to be utilized to calculate acoustic attenuation. The tissue scatter distribution imaging (TSI) parameter is a measurement of the Nakagami parameters in the region of interest, which reflects the concentration of ultrasound scatterers and their arrangement locally[35,83].

We found three studies comparing TAI and TSI with MRI-PDFF, and these studies revealed that both TAI and TSI revealed correlation with MRI-PDFF[84-86]. Jeon *et al*[86] enrolled 120 patients to assess feasibility of TAI and TSI for hepatic steatosis quantification utilizing MRI-PDFF as the reference. According to MRI-PDFF, the participants were classified into three groups (≤ 5%, 5%-10%, and ≥ 10%). They found that both methods had excellent utility for diagnosing and evaluating the degree of hepatic steatosis. For diagnosing fatty quantification of ≥ 5% and ≥ 10%, the AUROCs of TAI were 0.861 and 0.835, and those of TSI were 0.964 and 0.935, respectively[86]. Rónaszéki *et al*[84] compared TAI with TSI utilizing MRI-PDFF as gold standard enrolling 101 participants and found that TAI provided better diagnostic performance than TSI for diagnosing ≥ 5% MRI-PDFF (AUROC: 0.89 *vs* 0.87) and ≥ 10% (AUROC: 0.93 *vs* 0.86). TAI and TSI revealed good intra- and interobserver agreement. In TAI, the intra- and interobserver ICCs were reported at 0.994 and 0.975, respectively, while in TSI, they were reported at 0.991 and 0.947[87].

Techniques based on ultrasound BSC: Using the BSC, we can determine amount of ultrasound energy reflected by the tissue. Applying computer algorithm and a reference phantom, the BSC can be

estimated with less changeability resulted from ultrasound systems and operators. The right liver lobe was used to obtain gray scale images, and in the same liver region, a continuous series of 10 frames of transducer signals was captured. Then, in the tissue-imitating reference phantom, which mimics the acoustic properties of human hepatic tissue, consecutive frames were noted without changing scanner settings[35,88-90].

The diagnostic accuracy of the BSC has been evaluated by Lin *et al*[91] by analyzing 204 participants. They found that BSC was positively correlated with MRI-PDFF (Spearman's $\rho = 0.80$; $P < 0.0001$). BSC had an AUROC of 0.98 with a cutoff value of 0.00381/cm-steradian for detecting patients with hepatic steatosis. In addition, when using the optimal BSC cutoff value, in the training group, hepatic steatosis was detected with 93% sensitivity and 97% specificity, while in the validation group, it was detected with 87% sensitivity and 91% specificity[91].

Han *et al*[89,90,92,93] published several studies focusing on the use of the BSC. In a study including 102 participants, they revealed moderate correlation of the BSC with MRI-PDFF (Pearson's $r = 0.58$, $P < 0.001$)[93]. In addition, they enrolled 41 participants to study the repeatability and reproducibility of BSC and found that ICC were 0.87-0.95 for BSC acquired without participant repositioning and 0.69-0.82 with participant repositioning, suggesting that BSC measurement is repeatable and reproducible in patients with NAFLD[89].

Ultrasound-derived fat fraction

The ultrasound-derived fat fraction (UDFF) technique is a coalition of attenuation coefficient and BSC, and a percentage of liver fat content is reported as the result. Data from reference phantoms is integrated into the ultrasound system, and a fixed-acquisition region of interest is utilized[4] (Figure 5). Labyed and Milkowski[37] designed the UDFF method and conducted a study including 101 participants. They found that the UDFF was positively correlated with the MRI-PDFF (Pearson's $r = 0.87$). Using the histology results as the gold standard, the AUROCs of UDFF were 0.94 for detecting S ≥ 1, 0.88 for S ≥ 2 and 0.83 for S = 3. When using MRI-PDFF to be the gold standard, AUROCs of UDFF were 0.97 for diagnosing MRI-PDFF higher than 5%, 0.95 for diagnosing MRI-PDFF higher than 10% [37]. Similarly, Dillman *et al*[94] reported that liver fat content quantification applying UDFF showed a significant correlation with MRI-PDFF (Spearman's $\rho = 0.82$; $P < 0.001$).

ASQ: Quantifying the acoustic structure of an environment by comparing theoretical and real echo amplitude distributions is referred to as ASQ. In order to compute the theoretical echo amplitude distribution of the hepatic section imaged, the Rayleigh distribution function, assuming that solely ultrasound beam interference from small scattering objects generates the speckle pattern, is applied. However, actual echo amplitude distribution of the liver parenchyma does not follow the Rayleigh distribution. Because ultrasound beams are scattered by small structures, for example the walls of hepatic vessels, resulting in heterogeneity in echo amplitudes[95,96]. However, when diffuse liver diseases cause changes in parenchymal echotexture, ASQ can provide quantitative information by comparing theoretical echo amplitude distribution to a real distribution[97]. Kuroda *et al*[98] tested the ASQ-derived focal disturbance ratio (FD ratio) with 9 Leptin-deficient mice in comparison with histopathological results and found that the FD ratio had significant negative correlations with the fat droplet area (Spearman $r = -0.72$, $P = 0.0017$) and fat droplet size (Spearman $r = -0.98$, $P = 0.0052$), suggesting that the FD ratio can be used to quantify steatosis grade in an animal model and may be a quantitative metric of hepatic steatosis[98]. Karlas *et al*[95] conducted a cohort study to compare ASQ with MRS, and negative correlation was found between FD ratio and MRS (Spearman $r = -0.43$, $P = 0.004$). Similarly, in a prospective study including 36 patients with suspected fatty liver disease, the FD ratio showed a strong, negative correlation with the MRS in 36 patients[99]. Son *et al*[100] also reported FD ratio is comparable to hepatic fat fraction by MRS to make quantified measurement of liver fat content and diagnose liver fat content more than 10% in donor liver patients. Keller *et al*[96] found significant negative correlation between ASQ and steatosis level obtained by histological examination ($r = -0.55$, $P < 0.0001$). Nevertheless, they found no correlation between histologically determined fibrosis stage and any measurements of ASQ.

NLV: The NLV is derived from ASQ and analyzes ultrasound amplitudes sampled from grayscale ultrasound images[4,101]. Bae *et al*[102] assessed the clinical value of the NLV in the measurement of liver fat content in comparison with MRS in 40 male mice using histopathology as the golden standard and found that the AUROCs for diagnosing mild, moderate, and severe hepatic steatosis were 0.953, 0.896, and 0.735, and the NLV value performed similarly to MRS in detecting mild or moderate hepatic steatosis. The same authors also conducted a study with 194 patients to assess the diagnostic efficacy of the NLV for diagnosing and grading liver fat content using liver histopathology as the reference standard. They demonstrated the NLV had excellent diagnostic efficacy in detecting and grading fatty liver with AUROCs of 0.911 for ≥ steatosis grade 1, 0.974 for ≥ steatosis grade 2, and 0.954 ≥ steatosis grade 3[103].

Speed of sound: A speed of sound (SS) estimation is based on the fact that sound speed varies with fat content in soft tissues, and that the relationship between sound speed and liver fat percentage can be

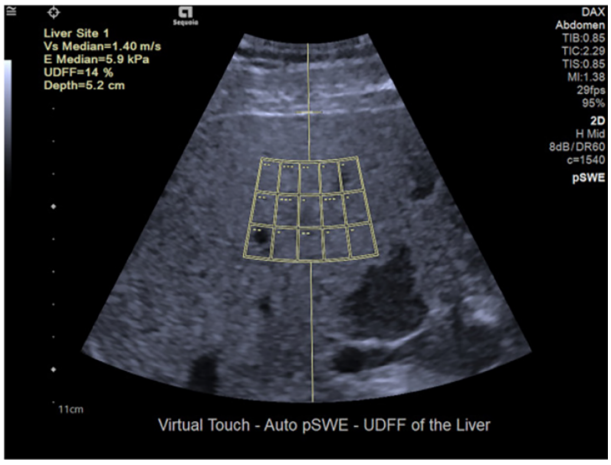

Figure 5 Ultrasound-derived fat fraction method[40]. The ultrasound-derived fat fraction method approximates the magnetic resonance imaging-derived proton density fat fraction and is based on the combination of the attenuation and backscatter coefficient. The method provides both liver stiffness measurement (5.9 kPa in this case) and the percentage of fat accumulation (14% in this case). Citation: Seneviratne N, Fang C, Sidhu PS. Ultrasound-based hepatic fat quantification: current status and future directions. *Clin Radiol* 2023; 78: 187-200. Copyright© The Author(s) 2023. Published by Elsevier Ltd. The authors have obtained the permission for figure using (Supplementary material).

identified[104]. Dioguardi Burgio *et al*[104] carried out a study aiming to explore the value of SS for detecting and quantifying liver steatosis and included 100 patients who underwent both SS and abdominal MR. They found that, in the training cohort, a cut-off value of less than 1.537mm/s led to 87% sensitivity and 95.7% specificity for diagnosing any steatosis with an AUROC of 0.882%. Based on an SS cut-off value of 1.511mm/s, the sensitivity was 100% and specificity was 95.6% for detecting moderate to severe steatosis and the AUROC was 0.989[104].

Sound speed plane-wave ultrasound (SSp.PLUS) is a novel technique for measuring intrahepatic sound speed which is correlated with the liver fat content. The measurement of SSp.PLUS is expressed in m/s[82]. Popa *et al*[82] performed a study with 215 patients to test the value of SSp.PLUS in detecting and grading hepatic fat level applying the CAP value as the gold standard. As a first finding, SSp.PLUS is more closely correlated with CAP values than Att.PLUS: (r = -0.74) *vs* (r = 0.45). Furthermore, the SSp.PLUS cut-off of less than 1516 m/s indicated 98.36% specificity and 58.74% sensitivity for predicting the presence of significant steatosis (S2-S3)[82].

CONCLUSION

Quantification ultrasound techniques can provide objective continuous number associated with liver fat content and past records can be found when patients receiving check-ups to evaluate change of degree of fatty liver, which is useful for follow-up to monitor the impact of any clinical interventions. Besides, as hepatic steatosis may pose adverse effects to prognosis of patients, quantification of liver fat holds clinical significance. For example, substantial hepatic fat accumulation may contribute to rapid disease progression toward NASH or liver fibrosis[105]. Patients with liver resections are more likely to suffer postoperative complications and die due to liver fat accumulation. Compared with patients without steatosis, those with ≤ 30% steatosis have a significantly increased risk of postoperative complications and patients with > 30% steatosis have an increased risk of postoperative death[9,106,107]. It is worth to be mentioned that simple steatosis may lead to poor prognosis. A study carried out in a nationwide Swedish cohort from 1966 to 2017 including 10568 patients found that simple steatosis, non-fibrotic NASH, non-cirrhotic fibrosis, and cirrhosis were associated with significant higher hazard ratio for mortality risk compared with controls. The all-cause mortalities of cohorts with simple steatosis, non-fibrotic NASH, non-cirrhotic fibrosis, and cirrhosis were 2.52% person-years, 3.03% person-years, 3.53% person-years, and 7.05% person-years respectively whereas the mortality of population comparators was 1.69% person-years[108]. Association between imaging quantification method and clinical prognosis is another issue. In patients with chronic hepatitis C, CAP value ≤ 221 dB/m is associated with higher risk of HCC and in patients with NAFLD, CAP value ≤ 265 dB/m is associated with higher risk of HCC[109]. Similarly, in another cross-sectional study including 130 patients (HCC) and 54 patients (chronic hepatitis C), the authors reported that CAP value of chronic hepatitis C group was significantly higher than that of HCC group (259.96 dB/m *vs* 209.57 dB/m, P < 0.001)[110].

While serving as the conventional reference standard, liver histopathologic test has the limitations of invasiveness, sampling error, and high cost. Issues including availability, cost, accuracy and reliability should be taken into consideration when choosing the optimal noninvasive methods. The further

application of noninvasive methods is desirable for detecting and grading hepatic steatosis at the initial diagnosis and monitoring changes in liver fat content during follow-up after receiving clinical therapies.

MRS and MRI-PDFF are reported to be the most accurate imaging modalities for quantified measurement of liver fat content. However, their low accessibility and high cost make it impossible to use MR-based techniques as repeatable methods to monitor the process of liver steatosis. Therefore, ultrasound-based techniques are more desirable with the advantages of portability and cost-effectiveness. CAP is the first method based on attenuation of the ultrasound beam, and its performance has been validated in several studies. However, the limitations of CAP are nonnegligible in that due to its blindness, it has a high rate of measurement failures because it cannot determine the exact location of the region of interest. UGAP, ATT and ATI have been developed to improve this situation, and these metrics can be used to evaluate degree of fatty liver on gray scale ultrasonography in real-time with a correct region of interest. The CAP measurement also showed suboptimal performance in quantifying liver fat content especially in mild steatosis, which limited its use as a golden standard to evaluate the efficacy of novel imaging methods for liver fat content quantification. In addition, techniques derived from other principles, such as ASQ, TSI and UDFF, have been developed. These techniques are reported to have nice clinical efficacy for liver fat quantification. Nevertheless, studies exploring value of such techniques enrolled a small number of participants. Therefore, future studies enrolling more participants are needed to test the utility of such techniques. Besides, imaging-based techniques may have some limitations. For example, CAP, ATI and MRI-PDFF may be unable to differentiate grade 2 with grade 3 liver steatosis.

Several hepatic steatosis quantification tools are launched by commercial platforms. Larger clinical studies are needed to compare the efficacy among different products. For patients with NAFLD, except for steatosis, inflammation and fibrosis are also significant features which are associated with prognosis. The steatosis measurement is able to be obtained together with the stiffness value by some tools. In this way, comprehensive evaluation of patients with NAFLD can be made. Except for elastography tools, ASQ has also been studied to evaluate liver stiffness. Hepatic steatosis measurement and stiffness measurement, in conjunction with other ultrasound methods, are promising tools for patients with diffuse liver disease to supervise curative effect and disease progression. Developing such a multiparametric ultrasound modality will require future studies.

ACKNOWLEDGEMENTS

We thank all medical staff and technicians who agreed to participate in this review.

FOOTNOTES

Author contributions: Lu Q conceived and designed the protocol; Zeng KY performed the literature search; Bao WYG and Wang YH selected the studies and extracted relevant information; Liao M, Yang J and Huang JY prepared the figures and tables; Zeng KY wrote the first version of draft; Lu Q critically revised successive drafts of the paper and approved the final version.

Conflict-of-interest statement: The authors have no financial relationships to disclose.

Country/Territory of origin: China

ORCID number: Ke-Yu Zeng 0000-0002-0836-3186; Wu-Yong-Ga Bao 0000-0001-7693-5804; Yun-Han Wang 0000-0002-5885-1356; Min Liao 0000-0002-0923-9419; Jie Yang 0000-0002-6819-146X; Jia-Yan Huang 0000-0002-1918-2874; Qiang Lu 0000-0002-4057-1997.

S-Editor: Yan JP
L-Editor: A
P-Editor: Zhao S

REFERENCES

1 **Younossi Z**, Anstee QM, Marietti M, Hardy T, Henry L, Eslam M, George J, Bugianesi E. Global burden of NAFLD and NASH: trends, predictions, risk factors and prevention. *Nat Rev Gastroenterol Hepatol* 2018; **15**: 11-20 [PMID: 28930295 DOI: 10.1038/nrgastro.2017.109]

2 **Powell EE**, Wong VW, Rinella M. Non-alcoholic fatty liver disease. *Lancet* 2021; **397**: 2212-2224 [PMID: 33894145 DOI: 10.1016/S0140-6736(20)32511-3]

3 **Chalasani N**, Younossi Z, Lavine JE, Charlton M, Cusi K, Rinella M, Harrison SA, Brunt EM, Sanyal AJ. The diagnosis and management of nonalcoholic fatty liver disease: Practice guidance from the American Association for the Study of Liver Diseases. *Hepatology* 2018; **67**: 328-357 [PMID: 28714183 DOI: 10.1002/hep.29367]

4 **Ferraioli G**, Berzigotti A, Barr RG, Choi BI, Cui XW, Dong Y, Gilja OH, Lee JY, Lee DH, Moriyasu F, Piscaglia F, Sugimoto K, Wong GL, Wong VW, Dietrich CF. Quantification of Liver Fat Content with Ultrasound: A WFUMB Position Paper. *Ultrasound Med Biol* 2021; **47**: 2803-2820 [PMID: 34284932 DOI: 10.1016/j.ultrasmedbio.2021.06.002]

5 **Younossi ZM**, Koenig AB, Abdelatif D, Fazel Y, Henry L, Wymer M. Global epidemiology of nonalcoholic fatty liver disease-Meta-analytic assessment of prevalence, incidence, and outcomes. *Hepatology* 2016; **64**: 73-84 [PMID: 26707365 DOI: 10.1002/hep.28431]

6 **El-Serag HB**, Tran T, Everhart JE. Diabetes increases the risk of chronic liver disease and hepatocellular carcinoma. *Gastroenterology* 2004; **126**: 460-468 [PMID: 14762783 DOI: 10.1053/j.gastro.2003.10.065]

7 **Adams LA**, Lymp JF, St Sauver J, Sanderson SO, Lindor KD, Feldstein A, Angulo P. The natural history of nonalcoholic fatty liver disease: a population-based cohort study. *Gastroenterology* 2005; **129**: 113-121 [PMID: 16012941 DOI: 10.1053/j.gastro.2005.04.014]

8 **Musso G**, Gambino R, Cassader M, Pagano G. Meta-analysis: natural history of non-alcoholic fatty liver disease (NAFLD) and diagnostic accuracy of non-invasive tests for liver disease severity. *Ann Med* 2011; **43**: 617-649 [PMID: 21039302 DOI: 10.3109/07853890.2010.518623]

9 **Leandro G**, Mangia A, Hui J, Fabris P, Rubbia-Brandt L, Colloredo G, Adinolfi LE, Asselah T, Jonsson JR, Smedile A, Terrault N, Pazienza V, Giordani MT, Giostra E, Sonzogni A, Ruggiero G, Marcellin P, Powell EE, George J, Negro F; HCV Meta-Analysis (on) Individual Patients' Data Study Group. Relationship between steatosis, inflammation, and fibrosis in chronic hepatitis C: a meta-analysis of individual patient data. *Gastroenterology* 2006; **130**: 1636-1642 [PMID: 16697727 DOI: 10.1053/j.gastro.2006.03.014]

10 **Linares I**, Hamar M, Selzner N, Selzner M. Steatosis in Liver Transplantation: Current Limitations and Future Strategies. *Transplantation* 2019; **103**: 78-90 [PMID: 30418431 DOI: 10.1097/TP.0000000000002466]

11 **Hossain N**, Kanwar P, Mohanty SR. A Comprehensive Updated Review of Pharmaceutical and Nonpharmaceutical Treatment for NAFLD. *Gastroenterol Res Pract* 2016; **2016**: 7109270 [PMID: 27006654 DOI: 10.1155/2016/7109270]

12 **Ajmera V**, Park CC, Caussy C, Singh S, Hernandez C, Bettencourt R, Hooker J, Sy E, Behling C, Xu R, Middleton MS, Valasek MA, Faulkner C, Rizo E, Richards L, Sirlin CB, Loomba R. Magnetic Resonance Imaging Proton Density Fat Fraction Associates With Progression of Fibrosis in Patients With Nonalcoholic Fatty Liver Disease. *Gastroenterology* 2018; **155**: 307-310.e2 [PMID: 29660324 DOI: 10.1053/j.gastro.2018.04.014]

13 **Stine JG**, Munaganuru N, Barnard A, Wang JL, Kaulback K, Argo CK, Singh S, Fowler KJ, Sirlin CB, Loomba R. Change in MRI-PDFF and Histologic Response in Patients With Nonalcoholic Steatohepatitis: A Systematic Review and Meta-Analysis. *Clin Gastroenterol Hepatol* 2021; **19**: 2274-2283.e5 [PMID: 32882428 DOI: 10.1016/j.cgh.2020.08.061]

14 **Vilar-Gomez E**, Calzadilla-Bertot L, Wai-Sun Wong V, Castellanos M, Aller-de la Fuente R, Metwally M, Eslam M, Gonzalez-Fabian L, Alvarez-Quiñones Sanz M, Conde-Martin AF, De Boer B, McLeod D, Hung Chan AW, Chalasani N, George J, Adams LA, Romero-Gomez M. Fibrosis Severity as a Determinant of Cause-Specific Mortality in Patients With Advanced Nonalcoholic Fatty Liver Disease: A Multi-National Cohort Study. *Gastroenterology* 2018; **155**: 443-457.e17 [PMID: 29733831 DOI: 10.1053/j.gastro.2018.04.034]

15 **Permutt Z**, Le TA, Peterson MR, Seki E, Brenner DA, Sirlin C, Loomba R. Correlation between liver histology and novel magnetic resonance imaging in adult patients with non-alcoholic fatty liver disease - MRI accurately quantifies hepatic steatosis in NAFLD. *Aliment Pharmacol Ther* 2012; **36**: 22-29 [PMID: 22554256 DOI: 10.1111/j.1365-2036.2012.05121.x]

16 **Wildman-Tobriner B**, Middleton MM, Moylan CA, Rossi S, Flores O, Chang ZA, Abdelmalek MF, Sirlin CB, Bashir MR. Association Between Magnetic Resonance Imaging-Proton Density Fat Fraction and Liver Histology Features in Patients With Nonalcoholic Fatty Liver Disease or Nonalcoholic Steatohepatitis. *Gastroenterology* 2018; **155**: 1428-1435.e2 [PMID: 30031769 DOI: 10.1053/j.gastro.2018.07.018]

17 **Tamaki N**, Ajmera V, Loomba R. Non-invasive methods for imaging hepatic steatosis and their clinical importance in NAFLD. *Nat Rev Endocrinol* 2022; **18**: 55-66 [PMID: 34815553 DOI: 10.1038/s41574-021-00584-0]

18 **Kleiner DE**, Brunt EM, Van Natta M, Behling C, Contos MJ, Cummings OW, Ferrell LD, Liu YC, Torbenson MS, Unalp-Arida A, Yeh M, McCullough AJ, Sanyal AJ; Nonalcoholic Steatohepatitis Clinical Research Network. Design and validation of a histological scoring system for nonalcoholic fatty liver disease. *Hepatology* 2005; **41**: 1313-1321 [PMID: 15915461 DOI: 10.1002/hep.20701]

19 **Davison BA**, Harrison SA, Cotter G, Alkhouri N, Sanyal A, Edwards C, Colca JR, Iwashita J, Koch GG, Dittrich HC. Suboptimal reliability of liver biopsy evaluation has implications for randomized clinical trials. *J Hepatol* 2020; **73**: 1322-1332 [PMID: 32610115 DOI: 10.1016/j.jhep.2020.06.025]

20 **Wong VW**, Adams LA, de Lédinghen V, Wong GL, Sookoian S. Noninvasive biomarkers in NAFLD and NASH - current progress and future promise. *Nat Rev Gastroenterol Hepatol* 2018; **15**: 461-478 [PMID: 29844588 DOI: 10.1038/s41575-018-0014-9]

21 **Castera L**, Friedrich-Rust M, Loomba R. Noninvasive Assessment of Liver Disease in Patients With Nonalcoholic Fatty Liver Disease. *Gastroenterology* 2019; **156**: 1264-1281.e4 [PMID: 30660725 DOI: 10.1053/j.gastro.2018.12.036]

22 **Barr RG**. Ultrasound of Diffuse Liver Disease Including Elastography. *Radiol Clin North Am* 2019; **57**: 549-562 [PMID:

30928077 DOI: 10.1016/j.rcl.2019.01.003]
23 **Saadeh S**, Younossi ZM, Remer EM, Gramlich T, Ong JP, Hurley M, Mullen KD, Cooper JN, Sheridan MJ. The utility of radiological imaging in nonalcoholic fatty liver disease. *Gastroenterology* 2002; **123**: 745-750 [PMID: 12198701 DOI: 10.1053/gast.2002.35354]
24 **Dasarathy S**, Dasarathy J, Khiyami A, Joseph R, Lopez R, McCullough AJ. Validity of real time ultrasound in the diagnosis of hepatic steatosis: a prospective study. *J Hepatol* 2009; **51**: 1061-1067 [PMID: 19846234 DOI: 10.1016/j.jhep.2009.09.001]
25 **Hernaez R**, Lazo M, Bonekamp S, Kamel I, Brancati FL, Guallar E, Clark JM. Diagnostic accuracy and reliability of ultrasonography for the detection of fatty liver: a meta-analysis. *Hepatology* 2011; **54**: 1082-1090 [PMID: 21618575 DOI: 10.1002/hep.24452]
26 **Strauss S**, Gavish E, Gottlieb P, Katsnelson L. Interobserver and intraobserver variability in the sonographic assessment of fatty liver. *AJR Am J Roentgenol* 2007; **189**: W320-W323 [PMID: 18029843 DOI: 10.2214/AJR.07.2123]
27 **Cengiz M**, Sentürk S, Cetin B, Bayrak AH, Bilek SU. Sonographic assessment of fatty liver: intraobserver and interobserver variability. *Int J Clin Exp Med* 2014; **7**: 5453-5460 [PMID: 25664055]
28 **Osawa H**, Mori Y. Sonographic diagnosis of fatty liver using a histogram technique that compares liver and renal cortical echo amplitudes. *J Clin Ultrasound* 1996; **24**: 25-29 [PMID: 8655663 DOI: 10.1002/(SICI)1097-0096(199601)24:1<25::AID-JCU4>3.0.CO;2-N]
29 **Mancini M**, Prinster A, Annuzzi G, Liuzzi R, Giacco R, Medagli C, Cremone M, Clemente G, Maurea S, Riccardi G, Rivellese AA, Salvatore M. Sonographic hepatic-renal ratio as indicator of hepatic steatosis: comparison with (1)H magnetic resonance spectroscopy. *Metabolism* 2009; **58**: 1724-1730 [PMID: 19716568 DOI: 10.1016/j.metabol.2009.05.032]
30 **Webb M**, Yeshua H, Zelber-Sagi S, Santo E, Brazowski E, Halpern Z, Oren R. Diagnostic value of a computerized hepatorenal index for sonographic quantification of liver steatosis. *AJR Am J Roentgenol* 2009; **192**: 909-914 [PMID: 19304694 DOI: 10.2214/AJR.07.4016]
31 **Shiralkar K**, Johnson S, Bluth EI, Marshall RH, Dornelles A, Gulotta PM. Improved method for calculating hepatic steatosis using the hepatorenal index. *J Ultrasound Med* 2015; **34**: 1051-1059 [PMID: 26014325 DOI: 10.7863/ultra.34.6.1051]
32 **Marshall RH**, Eissa M, Bluth EI, Gulotta PM, Davis NK. Hepatorenal index as an accurate, simple, and effective tool in screening for steatosis. *AJR Am J Roentgenol* 2012; **199**: 997-1002 [PMID: 23096171 DOI: 10.2214/AJR.11.6677]
33 **Borges VF**, Diniz AL, Cotrim HP, Rocha HL, Andrade NB. Sonographic hepatorenal ratio: a noninvasive method to diagnose nonalcoholic steatosis. *J Clin Ultrasound* 2013; **41**: 18-25 [PMID: 22997020 DOI: 10.1002/jcu.21994]
34 **Stahlschmidt FL**, Tafarel JR, Menini-Stahlschmidt CM, Baena CP. Hepatorenal index for grading liver steatosis with concomitant fibrosis. *PLoS One* 2021; **16**: e0246837 [PMID: 33577616 DOI: 10.1371/journal.pone.0246837]
35 **Bozic D**, Podrug K, Mikolasevic I, Grgurevic I. Ultrasound Methods for the Assessment of Liver Steatosis: A Critical Appraisal. *Diagnostics (Basel)* 2022; **12** [PMID: 36291976 DOI: 10.3390/diagnostics12102287]
36 **Kjaergaard M**, Lindvig KP, Hansen CD, Detlefsen S, Krag A, Thiele M. Hepatorenal Index by B-Mode Ratio Versus Imaging and Fatty Liver Index to Diagnose Steatosis in Alcohol-Related and Nonalcoholic Fatty Liver Disease. *J Ultrasound Med* 2023; **42**: 487-496 [PMID: 35475550 DOI: 10.1002/jum.15991]
37 **Labyed Y**, Milkowski A. Novel Method for Ultrasound-Derived Fat Fraction Using an Integrated Phantom. *J Ultrasound Med* 2020; **39**: 2427-2438 [PMID: 32525261 DOI: 10.1002/jum.15364]
38 **Oelze ML**, Mamou J. Review of Quantitative Ultrasound: Envelope Statistics and Backscatter Coefficient Imaging and Contributions to Diagnostic Ultrasound. *IEEE Trans Ultrason Ferroelectr Freq Control* 2016; **63**: 336-351 [PMID: 26761606 DOI: 10.1109/TUFFC.2015.2513958]
39 **Sasso M**, Beaugrand M, de Ledinghen V, Douvin C, Marcellin P, Poupon R, Sandrin L, Miette V. Controlled attenuation parameter (CAP): a novel VCTE™ guided ultrasonic attenuation measurement for the evaluation of hepatic steatosis: preliminary study and validation in a cohort of patients with chronic liver disease from various causes. *Ultrasound Med Biol* 2010; **36**: 1825-1835 [PMID: 20870345 DOI: 10.1016/j.ultrasmedbio.2010.07.005]
40 **Seneviratne N**, Fang C, Sidhu PS. Ultrasound-based hepatic fat quantification: current status and future directions. *Clin Radiol* 2023; **78**: 187-200 [PMID: 36411088 DOI: 10.1016/j.crad.2022.10.003]
41 **Ferraioli G**, Soares Monteiro LB. Ultrasound-based techniques for the diagnosis of liver steatosis. *World J Gastroenterol* 2019; **25**: 6053-6062 [PMID: 31686762 DOI: 10.3748/wjg.v25.i40.6053]
42 **de Lédinghen V**, Vergniol J, Foucher J, Merrouche W, le Bail B. Non-invasive diagnosis of liver steatosis using controlled attenuation parameter (CAP) and transient elastography. *Liver Int* 2012; **32**: 911-918 [PMID: 22672642 DOI: 10.1111/j.1478-3231.2012.02820.x]
43 **Caussy C**, Brissot J, Singh S, Bassirian S, Hernandez C, Bettencourt R, Rizo E, Richards L, Sirlin CB, Loomba R. Prospective, Same-Day, Direct Comparison of Controlled Attenuation Parameter With the M vs the XL Probe in Patients With Nonalcoholic Fatty Liver Disease, Using Magnetic Resonance Imaging-Proton Density Fat Fraction as the Standard. *Clin Gastroenterol Hepatol* 2020; **18**: 1842-1850.e6 [PMID: 31843596 DOI: 10.1016/j.cgh.2019.11.060]
44 **Park J**, Lee JM, Lee G, Jeon SK, Joo I. Quantitative Evaluation of Hepatic Steatosis Using Advanced Imaging Techniques: Focusing on New Quantitative Ultrasound Techniques. *Korean J Radiol* 2022; **23**: 13-29 [PMID: 34983091 DOI: 10.3348/kjr.2021.0112]
45 **Karlas T**, Petroff D, Sasso M, Fan JG, Mi YQ, de Lédinghen V, Kumar M, Lupsor-Platon M, Han KH, Cardoso AC, Ferraioli G, Chan WK, Wong VW, Myers RP, Chayama K, Friedrich-Rust M, Beaugrand M, Shen F, Hiriart JB, Sarin SK, Badea R, Jung KS, Marcellin P, Filice C, Mahadeva S, Wong GL, Crotty P, Masaki K, Bojunga J, Bedossa P, Keim V, Wiegand J. Individual patient data meta-analysis of controlled attenuation parameter (CAP) technology for assessing steatosis. *J Hepatol* 2017; **66**: 1022-1030 [PMID: 28039099 DOI: 10.1016/j.jhep.2016.12.022]
46 **Petroff D**, Blank V, Newsome PN, Shalimar, Voican CS, Thiele M, de Lédinghen V, Baumeler S, Chan WK, Perlemuter G, Cardoso AC, Aggarwal S, Sasso M, Eddowes PJ, Allison M, Tsochatzis E, Anstee QM, Sheridan D, Cobbold JF, Naveau S, Lupsor-Platon M, Mueller S, Krag A, Irles-Depe M, Semela D, Wong GL, Wong VW, Villela-Nogueira CA,

Garg H, Chazouillères O, Wiegand J, Karlas T. Assessment of hepatic steatosis by controlled attenuation parameter using the M and XL probes: an individual patient data meta-analysis. *Lancet Gastroenterol Hepatol* 2021; **6**: 185-198 [PMID: 33460567 DOI: 10.1016/S2468-1253(20)30357-5]

47 **Caussy C**, Alquiraish MH, Nguyen P, Hernandez C, Cepin S, Fortney LE, Ajmera V, Bettencourt R, Collier S, Hooker J, Sy E, Rizo E, Richards L, Sirlin CB, Loomba R. Optimal threshold of controlled attenuation parameter with MRI-PDFF as the gold standard for the detection of hepatic steatosis. *Hepatology* 2018; **67**: 1348-1359 [PMID: 29108123 DOI: 10.1002/hep.29639]

48 **Shao CX**, Ye J, Dong Z, Li F, Lin Y, Liao B, Feng S, Zhong B. Steatosis grading consistency between controlled attenuation parameter and MRI-PDFF in monitoring metabolic associated fatty liver disease. *Ther Adv Chronic Dis* 2021; **12**: 20406223211033119 [PMID: 34408822 DOI: 10.1177/20406223211033119]

49 **Runge JH**, Smits LP, Verheij J, Depla A, Kuiken SD, Baak BC, Nederveen AJ, Beuers U, Stoker J. MR Spectroscopy-derived Proton Density Fat Fraction Is Superior to Controlled Attenuation Parameter for Detecting and Grading Hepatic Steatosis. *Radiology* 2018; **286**: 547-556 [PMID: 28915103 DOI: 10.1148/radiol.2017162931]

50 **Imajo K**, Kessoku T, Honda Y, Tomeno W, Ogawa Y, Mawatari H, Fujita K, Yoneda M, Taguri M, Hyogo H, Sumida Y, Ono M, Eguchi Y, Inoue T, Yamanaka T, Wada K, Saito S, Nakajima A. Magnetic Resonance Imaging More Accurately Classifies Steatosis and Fibrosis in Patients With Nonalcoholic Fatty Liver Disease Than Transient Elastography. *Gastroenterology* 2016; **150**: 626-637.e7 [PMID: 26677985 DOI: 10.1053/j.gastro.2015.11.048]

51 **de Lédinghen V**, Vergniol J, Capdepont M, Chermak F, Hiriart JB, Cassinotto C, Merrouche W, Foucher J, Brigitte le B. Controlled attenuation parameter (CAP) for the diagnosis of steatosis: a prospective study of 5323 examinations. *J Hepatol* 2014; **60**: 1026-1031 [PMID: 24378529 DOI: 10.1016/j.jhep.2013.12.018]

52 **Yoo J**, Lee JM, Joo I, Lee DH, Yoon JH, Kang HJ, Ahn SJ. Reproducibility of ultrasound attenuation imaging for the noninvasive evaluation of hepatic steatosis. *Ultrasonography* 2020; **39**: 121-129 [PMID: 31693842 DOI: 10.14366/usg.19034]

53 **Yuri M**, Nishimura T, Tada T, Yoshida M, Fujiwara A, Kawata S, Yoshihara K, Yoshioka R, Ota S, Nakano R, Yuri Y, Takashima T, Aizawa N, Ikeda N, Shiomi H, Ide YH, Enomoto H, Yasuhiro F, Yano H, Iijima H. Diagnosis of hepatic steatosis based on ultrasound attenuation imaging is not influenced by liver fibrosis. *Hepatol Res* 2022; **52**: 1009-1019 [PMID: 36018852 DOI: 10.1111/hepr.13831]

54 **Tamaki N**, Koizumi Y, Hirooka M, Yada N, Takada H, Nakashima O, Kudo M, Hiasa Y, Izumi N. Novel quantitative assessment system of liver steatosis using a newly developed attenuation measurement method. *Hepatol Res* 2018; **48**: 821-828 [PMID: 29679473 DOI: 10.1111/hepr.13179]

55 **Tamaki N**, Kurosaki M, Yasui Y, Tsuchiya K, Izumi N. Attenuation coefficient (ATT) measurement for liver fat quantification in chronic liver disease. *J Med Ultrason (2001)* 2021; **48**: 481-487 [PMID: 34165645 DOI: 10.1007/s10396-021-01103-4]

56 **Ferraioli G**, Kumar V, Ozturk A, Nam K, de Korte CL, Barr RG. US Attenuation for Liver Fat Quantification: An AIUM-RSNA QIBA Pulse-Echo Quantitative Ultrasound Initiative. *Radiology* 2022; **302**: 495-506 [PMID: 35076304 DOI: 10.1148/radiol.210736]

57 **Kwon EY**, Kim YR, Kang DM, Yoon KH, Lee YH. Usefulness of US attenuation imaging for the detection and severity grading of hepatic steatosis in routine abdominal ultrasonography. *Clin Imaging* 2021; **76**: 53-59 [PMID: 33549920 DOI: 10.1016/j.clinimag.2021.01.034]

58 **Jang JK**, Kim SY, Yoo IW, Cho YB, Kang HJ, Lee DH. Diagnostic performance of ultrasound attenuation imaging for assessing low-grade hepatic steatosis. *Eur Radiol* 2022; **32**: 2070-2077 [PMID: 34549325 DOI: 10.1007/s00330-021-08269-y]

59 **Bae JS**, Lee DH, Lee JY, Kim H, Yu SJ, Lee JH, Cho EJ, Lee YB, Han JK, Choi BI. Assessment of hepatic steatosis by using attenuation imaging: a quantitative, easy-to-perform ultrasound technique. *Eur Radiol* 2019; **29**: 6499-6507 [PMID: 31175413 DOI: 10.1007/s00330-019-06272-y]

60 **Bae JS**, Lee DH, Suh KS, Kim H, Lee KB, Lee JY, Han JK. Noninvasive assessment of hepatic steatosis using a pathologic reference standard: comparison of CT, MRI, and US-based techniques. *Ultrasonography* 2022; **41**: 344-354 [PMID: 34852424 DOI: 10.14366/usg.21150]

61 **Jeon SK**, Lee JM, Joo I, Yoon JH, Lee DH, Lee JY, Han JK. Prospective Evaluation of Hepatic Steatosis Using Ultrasound Attenuation Imaging in Patients with Chronic Liver Disease with Magnetic Resonance Imaging Proton Density Fat Fraction as the Reference Standard. *Ultrasound Med Biol* 2019; **45**: 1407-1416 [PMID: 30975533 DOI: 10.1016/j.ultrasmedbio.2019.02.008]

62 **Tada T**, Iijima H, Kobayashi N, Yoshida M, Nishimura T, Kumada T, Kondo R, Yano H, Kage M, Nakano C, Aoki T, Aizawa N, Ikeda N, Takashima T, Yuri Y, Ishii N, Hasegawa K, Takata R, Yoh K, Sakai Y, Nishikawa H, Iwata Y, Enomoto H, Hirota S, Fujimoto J, Nishiguchi S. Usefulness of Attenuation Imaging with an Ultrasound Scanner for the Evaluation of Hepatic Steatosis. *Ultrasound Med Biol* 2019; **45**: 2679-2687 [PMID: 31277922 DOI: 10.1016/j.ultrasmedbio.2019.05.033]

63 **Tada T**, Kumada T, Toyoda H, Nakamura S, Shibata Y, Yasuda S, Watanuki Y, Tsujii K, Fukuda N, Fujioka M, Takeshima K, Niwa F, Ogawa S, Hashinokuchi S, Kataoka S, Ichikawa H, Iijima H. Attenuation imaging based on ultrasound technology for assessment of hepatic steatosis: A comparison with magnetic resonance imaging-determined proton density fat fraction. *Hepatol Res* 2020; **50**: 1319-1327 [PMID: 32876367 DOI: 10.1111/hepr.13563]

64 **Jeon SK**, Lee JM, Joo I, Yoon JH. Assessment of the inter-platform reproducibility of ultrasound attenuation examination in nonalcoholic fatty liver disease. *Ultrasonography* 2022; **41**: 355-364 [PMID: 34933319 DOI: 10.14366/usg.21167]

65 **Ferraioli G**, Maiocchi L, Raciti MV, Tinelli C, De Silvestri A, Nichetti M, De Cata P, Rondanelli M, Chiovato L, Calliada F, Filice C. Detection of Liver Steatosis With a Novel Ultrasound-Based Technique: A Pilot Study Using MRI-Derived Proton Density Fat Fraction as the Gold Standard. *Clin Transl Gastroenterol* 2019; **10**: e00081 [PMID: 31609745 DOI: 10.14309/ctg.0000000000000081]

66 **Ferraioli G**, Maiocchi L, Savietto G, Tinelli C, Nichetti M, Rondanelli M, Calliada F, Preda L, Filice C. Performance of the Attenuation Imaging Technology in the Detection of Liver Steatosis. *J Ultrasound Med* 2021; **40**: 1325-1332 [PMID:

32960457 DOI: 10.1002/jum.15512]
67 **Sugimoto K**, Abe M, Oshiro H, Takahashi H, Kakegawa T, Tomita Y, Yoshimasu Y, Takeuchi H, Itoi T. The most appropriate region-of-interest position for attenuation coefficient measurement in the evaluation of liver steatosis. *J Med Ultrason (2001)* 2021; **48**: 615-621 [PMID: 34453648 DOI: 10.1007/s10396-021-01124-z]
68 **Lee DH**. Quantitative assessment of fatty liver using ultrasound attenuation imaging. *J Med Ultrason (2001)* 2021; **48**: 465-470 [PMID: 34453237 DOI: 10.1007/s10396-021-01132-z]
69 **Hsu PK**, Wu LS, Su WW, Su PY, Chen YY, Hsu YC, Yen HH, Wu CL. Comparing the controlled attenuation parameter using FibroScan and attenuation imaging with ultrasound as a novel measurement for liver steatosis. *PLoS One* 2021; **16**: e0254892 [PMID: 34653177 DOI: 10.1371/journal.pone.0254892]
70 **Hsu PK**, Wu LS, Yen HH, Huang HP, Chen YY, Su PY, Su WW. Attenuation Imaging with Ultrasound as a Novel Evaluation Method for Liver Steatosis. *J Clin Med* 2021; **10** [PMID: 33801163 DOI: 10.3390/jcm10050965]
71 **Cerit M**, Şendur HN, Cindil E, Erbaş G, Yalçın MM, Cerit ET, Allahverdiyeva S, Oktar SÖ, Yücel C. Quantification of liver fat content with ultrasonographic attenuation measurement function: Correlation with unenhanced multidimensional computerized tomography. *Clin Imaging* 2020; **65**: 85-93 [PMID: 32387801 DOI: 10.1016/j.clinimag.2020.04.028]
72 **Ferraioli G**, Raimondi A, Maiocchi L, De Silvestri A, Filice C. Quantification of Liver Fat Content with the iATT Algorithm: Correlation with Controlled Attenuation Parameter. *Diagnostics (Basel)* 2022; **12** [PMID: 35892497 DOI: 10.3390/diagnostics12081787]
73 **Koizumi Y**, Hirooka M, Tamaki N, Yada N, Nakashima O, Izumi N, Kudo M, Hiasa Y. New diagnostic technique to evaluate hepatic steatosis using the attenuation coefficient on ultrasound B mode. *PLoS One* 2019; **14**: e0221548 [PMID: 31454369 DOI: 10.1371/journal.pone.0221548]
74 **Bende F**, Sporea I, Şirli R, Bâldea V, Lazăr A, Lupușoru R, Fofiu R, Popescu A. Ultrasound-Guided Attenuation Parameter (UGAP) for the quantification of liver steatosis using the Controlled Attenuation Parameter (CAP) as the reference method. *Med Ultrason* 2021; **23**: 7-14 [PMID: 33220028 DOI: 10.11152/mu-2688]
75 **Fujiwara Y**, Kuroda H, Abe T, Ishida K, Oguri T, Noguchi S, Sugai T, Kamiyama N, Takikawa Y. The B-Mode Image-Guided Ultrasound Attenuation Parameter Accurately Detects Hepatic Steatosis in Chronic Liver Disease. *Ultrasound Med Biol* 2018; **44**: 2223-2232 [PMID: 30077415 DOI: 10.1016/j.ultrasmedbio.2018.06.017]
76 **Imajo K**, Toyoda H, Yasuda S, Suzuki Y, Sugimoto K, Kuroda H, Akita T, Tanaka J, Yasui Y, Tamaki N, Kurosaki M, Izumi N, Nakajima A, Kumada T. Utility of Ultrasound-Guided Attenuation Parameter for Grading Steatosis With Reference to MRI-PDFF in a Large Cohort. *Clin Gastroenterol Hepatol* 2022; **20**: 2533-2541.e7 [PMID: 34768008 DOI: 10.1016/j.cgh.2021.11.003]
77 **Ogino Y**, Wakui N, Nagai H, Igarashi Y. The ultrasound-guided attenuation parameter is useful in quantification of hepatic steatosis in non-alcoholic fatty liver disease. *JGH Open* 2021; **5**: 947-952 [PMID: 34386604 DOI: 10.1002/jgh3.12615]
78 **Kuroda H**, Abe T, Fujiwara Y, Nagasawa T, Takikawa Y. Diagnostic accuracy of ultrasound-guided attenuation parameter as a noninvasive test for steatosis in non-alcoholic fatty liver disease. *J Med Ultrason (2001)* 2021; **48**: 471-480 [PMID: 34415481 DOI: 10.1007/s10396-021-01123-0]
79 **Kuroda H**, Fujiwara Y, Abe T, Nagasawa T, Oguri T, Noguchi S, Kamiyama N, Takikawa Y. Two-dimensional shear wave elastography and ultrasound-guided attenuation parameter for progressive non-alcoholic steatohepatitis. *PLoS One* 2021; **16**: e0249493 [PMID: 33826669 DOI: 10.1371/journal.pone.0249493]
80 **Tada T**, Kumada T, Toyoda H, Kobayashi N, Sone Y, Oguri T, Kamiyama N. Utility of Attenuation Coefficient Measurement Using an Ultrasound-Guided Attenuation Parameter for Evaluation of Hepatic Steatosis: Comparison With MRI-Determined Proton Density Fat Fraction. *AJR Am J Roentgenol* 2019; **212**: 332-341 [PMID: 30476453 DOI: 10.2214/AJR.18.20123]
81 **Tada T**, Kumada T, Toyoda H, Yasuda S, Sone Y, Hashinokuchi S, Ogawa S, Oguri T, Kamiyama N, Chuma M, Akita T, Tanaka J. Liver stiffness does not affect ultrasound-guided attenuation coefficient measurement in the evaluation of hepatic steatosis. *Hepatol Res* 2020; **50**: 190-198 [PMID: 31661724 DOI: 10.1111/hepr.13442]
82 **Popa A**, Bende F, Şirli R, Popescu A, Bâldea V, Lupușoru R, Cotrău R, Fofiu R, Foncea C, Sporea I. Quantification of Liver Fibrosis, Steatosis, and Viscosity Using Multiparametric Ultrasound in Patients with Non-Alcoholic Liver Disease: A "Real-Life" Cohort Study. *Diagnostics (Basel)* 2021; **11** [PMID: 33926073 DOI: 10.3390/diagnostics11050783]
83 **Jeon SK**, Lee JM, Joo I. Clinical Feasibility of Quantitative Ultrasound Imaging for Suspected Hepatic Steatosis: Intra- and Inter-examiner Reliability and Correlation with Controlled Attenuation Parameter. *Ultrasound Med Biol* 2021; **47**: 438-445 [PMID: 33277108 DOI: 10.1016/j.ultrasmedbio.2020.11.009]
84 **Rónaszéki AD**, Budai BK, Csongrády B, Stollmayer R, Hagymási K, Werling K, Fodor T, Folhoffer A, Kalina I, Győri G, Maurovich-Horvat P, Kaposi PN. Tissue attenuation imaging and tissue scatter imaging for quantitative ultrasound evaluation of hepatic steatosis. *Medicine (Baltimore)* 2022; **101**: e29708 [PMID: 35984128 DOI: 10.1097/MD.0000000000029708]
85 **Şendur HN**, Özdemir Kalkan D, Cerit MN, Kalkan G, Şendur AB, Özhan Oktar S. Hepatic Fat Quantification With Novel Ultrasound Based Techniques: A Diagnostic Performance Study Using Magnetic Resonance Imaging Proton Density Fat Fraction as Reference Standard. *Can Assoc Radiol J* 2023; **74**: 362-369 [PMID: 36113064 DOI: 10.1177/08465371221123696]
86 **Jeon SK**, Lee JM, Joo I, Park SJ. Quantitative Ultrasound Radiofrequency Data Analysis for the Assessment of Hepatic Steatosis in Nonalcoholic Fatty Liver Disease Using Magnetic Resonance Imaging Proton Density Fat Fraction as the Reference Standard. *Korean J Radiol* 2021; **22**: 1077-1086 [PMID: 33739636 DOI: 10.3348/kjr.2020.1262]
87 **Şendur HN**, Cerit MN, Ibrahimkhanli N, Şendur AB, Özhan Oktar S. Interobserver Variability in Ultrasound-Based Liver Fat Quantification. *J Ultrasound Med* 2023; **42**: 833-841 [PMID: 35778902 DOI: 10.1002/jum.16048]
88 **Coila A**, Oelze ML. Effects of acoustic nonlinearities on the ultrasonic backscatter coefficient estimation. *J Acoust Soc Am* 2019; **146**: 85 [PMID: 31370607 DOI: 10.1121/1.5115355]
89 **Han A**, Andre MP, Deiranieh L, Housman E, Erdman JW Jr, Loomba R, Sirlin CB, O'Brien WD Jr. Repeatability and Reproducibility of the Ultrasonic Attenuation Coefficient and Backscatter Coefficient Measured in the Right Lobe of the

Liver in Adults With Known or Suspected Nonalcoholic Fatty Liver Disease. *J Ultrasound Med* 2018; **37**: 1913-1927 [PMID: 29359454 DOI: 10.1002/jum.14537]

90 **Han A**, Zhang YN, Boehringer AS, Andre MP, Erdman JW Jr, Loomba R, Sirlin CB, O'Brien WD Jr. Inter-platform reproducibility of ultrasonic attenuation and backscatter coefficients in assessing NAFLD. *Eur Radiol* 2019; **29**: 4699-4708 [PMID: 30783789 DOI: 10.1007/s00330-019-06035-9]

91 **Lin SC**, Heba E, Wolfson T, Ang B, Gamst A, Han A, Erdman JW Jr, O'Brien WD Jr, Andre MP, Sirlin CB, Loomba R. Noninvasive Diagnosis of Nonalcoholic Fatty Liver Disease and Quantification of Liver Fat Using a New Quantitative Ultrasound Technique. *Clin Gastroenterol Hepatol* 2015; **13**: 1337-1345.e6 [PMID: 25478922 DOI: 10.1016/j.cgh.2014.11.027]

92 **Han A**, Labyed Y, Sy EZ, Boehringer AS, Andre MP, Erdman JW Jr, Loomba R, Sirlin CB, O'Brien WD Jr. Inter-sonographer reproducibility of quantitative ultrasound outcomes and shear wave speed measured in the right lobe of the liver in adults with known or suspected non-alcoholic fatty liver disease. *Eur Radiol* 2018; **28**: 4992-5000 [PMID: 29869170 DOI: 10.1007/s00330-018-5541-9]

93 **Han A**, Zhang YN, Boehringer AS, Montes V, Andre MP, Erdman JW Jr, Loomba R, Valasek MA, Sirlin CB, O'Brien WD Jr. Assessment of Hepatic Steatosis in Nonalcoholic Fatty Liver Disease by Using Quantitative US. *Radiology* 2020; **295**: 106-113 [PMID: 32013792 DOI: 10.1148/radiol.2020191152]

94 **Dillman JR**, Thapaliya S, Tkach JA, Trout AT. Quantification of Hepatic Steatosis by Ultrasound: Prospective Comparison With MRI Proton Density Fat Fraction as Reference Standard. *AJR Am J Roentgenol* 2022; **219**: 784-791 [PMID: 35674351 DOI: 10.2214/AJR.22.27878]

95 **Karlas T**, Berger J, Garnov N, Lindner F, Busse H, Linder N, Schaudinn A, Relke B, Chakaroun R, Tröltzsch M, Wiegand J, Keim V. Estimating steatosis and fibrosis: Comparison of acoustic structure quantification with established techniques. *World J Gastroenterol* 2015; **21**: 4894-4902 [PMID: 25945002 DOI: 10.3748/wjg.v21.i16.4894]

96 **Keller J**, Kaltenbach TE, Haenle MM, Oeztuerk S, Graeter T, Mason RA, Seufferlein T, Kratzer W. Comparison of Acoustic Structure Quantification (ASQ), shearwave elastography and histology in patients with diffuse hepatopathies. *BMC Med Imaging* 2015; **15**: 58 [PMID: 26637242 DOI: 10.1186/s12880-015-0100-1]

97 **Lin YH**, Wan YL, Tai DI, Tseng JH, Wang CY, Tsai YW, Lin YR, Chang TY, Tsui PH. Considerations of Ultrasound Scanning Approaches in Non-alcoholic Fatty Liver Disease Assessment through Acoustic Structure Quantification. *Ultrasound Med Biol* 2019; **45**: 1955-1969 [PMID: 31130411 DOI: 10.1016/j.ultrasmedbio.2019.04.018]

98 **Kuroda H**, Kakisaka K, Kamiyama N, Oikawa T, Onodera M, Sawara K, Oikawa K, Endo R, Takikawa Y, Suzuki K. Non-invasive determination of hepatic steatosis by acoustic structure quantification from ultrasound echo amplitude. *World J Gastroenterol* 2012; **18**: 3889-3895 [PMID: 22876042 DOI: 10.3748/wjg.v18.i29.3889]

99 **Lee DH**, Lee JY, Park MS, Han JK. Non-invasive monitoring of hepatic steatosis *via* acoustic structure quantification of ultrasonography with MR spectroscopy as the reference standard. *Ultrasonography* 2020; **39**: 70-78 [PMID: 31639886 DOI: 10.14366/usg.19002]

100 **Son JY**, Lee JY, Yi NJ, Lee KW, Suh KS, Kim KG, Lee JM, Han JK, Choi BI. Hepatic Steatosis: Assessment with Acoustic Structure Quantification of US Imaging. *Radiology* 2016; **278**: 257-264 [PMID: 26121121 DOI: 10.1148/radiol.2015141779]

101 **Zhao Y**, Zhang C, Xu S, Zhang H, Wei S, Huang P, Zhang L, Wong YN, Xu W. Quantitative evaluation of hepatic steatosis using novel ultrasound technology normalized local variance (NLV) and its standard deviation with different ROIs in patients with metabolic-associated fatty liver disease: a pilot study. *Abdom Radiol (NY)* 2022; **47**: 693-703 [PMID: 34958409 DOI: 10.1007/s00261-021-03394-0]

102 **Bae JS**, Lee JY, Lee DH, Kim H, Lee Y, Han JK. Quantitative Evaluation of Hepatic Steatosis Using Normalized Local Variance in a Rat Model: Comparison with Histopathology as the Reference Standard. *Korean J Radiol* 2019; **20**: 1399-1407 [PMID: 31464118 DOI: 10.3348/kjr.2019.0068]

103 **Bae JS**, Lee DH, Lee JY, Kim H, Yu SJ, Lee JH, Cho EJ, Lee YB, Han JK, Choi BI. Quantitative Assessment of Fatty Liver using Ultrasound with Normalized Local Variance Technique. *Ultraschall Med* 2021; **42**: 599-606 [PMID: 32323278 DOI: 10.1055/a-1143-3091]

104 **Dioguardi Burgio M**, Imbault M, Ronot M, Faccinetto A, Van Beers BE, Rautou PE, Castera L, Gennisson JL, Tanter M, Vilgrain V. Ultrasonic Adaptive Sound Speed Estimation for the Diagnosis and Quantification of Hepatic Steatosis: A Pilot Study. *Ultraschall Med* 2019; **40**: 722-733 [PMID: 30396216 DOI: 10.1055/a-0660-9465]

105 **Suliman I**, Abdelgelil N, Kassamali F, Hassanein TI. The Effects of Hepatic Steatosis on the Natural History of HBV Infection. *Clin Liver Dis* 2019; **23**: 433-450 [PMID: 31266618 DOI: 10.1016/j.cld.2019.05.001]

106 **Abdalla EK**, Vauthey JN. Steatosis as a risk factor in liver surgery. *Ann Surg* 2007; **246**: 340-1; author reply 341 [PMID: 17667519 DOI: 10.1097/SLA.0b013e31811ea9d2]

107 **Spitzer AL**, Lao OB, Dick AA, Bakthavatsalam R, Halldorson JB, Yeh MM, Upton MP, Reyes JD, Perkins JD. The biopsied donor liver: incorporating macrosteatosis into high-risk donor assessment. *Liver Transpl* 2010; **16**: 874-884 [PMID: 20583086 DOI: 10.1002/lt.22085]

108 **Simon TG**, Roelstraete B, Khalili H, Hagström H, Ludvigsson JF. Mortality in biopsy-confirmed nonalcoholic fatty liver disease: results from a nationwide cohort. *Gut* 2021; **70**: 1375-1382 [PMID: 33037056 DOI: 10.1136/gutjnl-2020-322786]

109 **Izumi T**, Sho T, Morikawa K, Shigesawa T, Suzuki K, Nakamura A, Ohara M, Kawagishi N, Umemura M, Shimazaki T, Kimura M, Nakai M, Suda G, Natsuizaka M, Ogawa K, Kudo Y, Nishida M, Ono K, Baba M, Furuya K, Sakamoto N. Assessing the risk of hepatocellular carcinoma by combining liver stiffness and the controlled attenuation parameter. *Hepatol Res* 2019; **49**: 1207-1217 [PMID: 31219667 DOI: 10.1111/hepr.13391]

110 **Abdelaziz AO**, Shousha HI, Said EM, Soliman ZA, Shehata AA, Nabil MM, Abdelmaksoud AH, Elbaz TM, Abdelsalam FM. Evaluation of liver steatosis, measured by controlled attenuation parameter, in patients with hepatitis C-induced advanced liver fibrosis and hepatocellular carcinoma. *Eur J Gastroenterol Hepatol* 2018; **30**: 1384-1388 [PMID: 30179227 DOI: 10.1097/MEG.0000000000001196]

World Journal of Gastroenterology

Submit a Manuscript: https://www.f6publishing.com

World J Gastroenterol 2023 May 7; 29(17): 2551-2570

DOI: 10.3748/wjg.v29.i17.2551

ISSN 1007-9327 (print) ISSN 2219-2840 (online)

REVIEW

Alcohol-related hepatitis: A review article

Hunza Chaudhry, Aalam Sohal, Humzah Iqbal, Marina Roytman

Specialty type: Gastroenterology and hepatology

Provenance and peer review: Invited article; Externally peer reviewed.

Peer-review model: Single blind

Peer-review report's scientific quality classification

Grade A (Excellent): 0
Grade B (Very good): 0
Grade C (Good): C, C, C
Grade D (Fair): 0
Grade E (Poor): 0

P-Reviewer: Li M, China; Liu W, China

Received: December 26, 2022
Peer-review started: December 26, 2022
First decision: March 8, 2023
Revised: March 10, 2023
Accepted: April 13, 2023
Article in press: April 13, 2023
Published online: May 7, 2023

Hunza Chaudhry, Humzah Iqbal, Department of Internal Medicine, University of California, San Francisco, Fresno, CA 93701, United States

Aalam Sohal, Department of Hepatology, Liver Institute Northwest, Seattle, WA 98105, United States

Marina Roytman, Department of Gastroenterology and Hepatology, University of California, San Francisco, Fresno, CA 93701, United States

Corresponding author: Hunza Chaudhry, MD, Staff Physician, Department of Internal Medicine, University of California, San Francisco, 155 N. Fresno St, Fresno, CA 93701, United States. hunza.chaudhry@ucsf.edu

Abstract

Alcohol-related hepatitis (ARH) is a unique type of alcohol-associated liver disease characterized by acute liver inflammation caused by significant alcohol use. It ranges in severity from mild to severe and carries significant morbidity and mortality. The refinement of scoring systems has enhanced prognostication and guidance of clinical decision-making in the treatment of this complex disease. Although treatment focuses on supportive care, steroids have shown benefit in select circumstances. There has been a recent interest in this disease process, as coronavirus disease 2019 pandemic led to substantial rise in cases. Although much is known regarding the pathogenesis, prognosis remains grim due to limited treatment options. This article summarizes the epidemiology, genetics, pathogenesis, diagnosis and treatment of ARH.

Key Words: Alcohol; Hepatitis; Epidemiology; Prevalence; Treatment; Clinical trials

Core Tip: The aim of this article is to review alcohol-related hepatitis (ARH). Despite the increased understanding of the pathogenesis of this disease process, treatment options remain limited. Our review article focuses on epidemiology, genetics, pathogenesis, diagnosis and treatment. We also discuss complications of ARH along with their optimal management and ongoing clinical trials. Further research evaluating therapeutic targets for its management are warranted.

Citation: Chaudhry H, Sohal A, Iqbal H, Roytman M. Alcohol-related hepatitis: A review article. *World J Gastroenterol* 2023; 29(17): 2551-2570
URL: https://www.wjgnet.com/1007-9327/full/v29/i17/2551.htm
DOI: https://dx.doi.org/10.3748/wjg.v29.i17.2551

INTRODUCTION

The burden of alcohol-associated liver disease continues to grow with rising cases during and even after the coronavirus disease 2019 (COVID-19) pandemic[1-2]. Some experts believe that the rise in cases during the COVID-19 pandemic will have long lasting effects on society and healthcare. Alcohol is an integral part of American culture and its widespread use cuts across socioeconomic and racial lines. Alcohol-related liver disease (ALD) can range from hepatic steatosis to end-stage liver disease. Alcohol-related hepatitis (ARH), a form of ALD, is an acute inflammatory syndrome of jaundice and liver injury occurring in patients with significant alcohol use. The severity can range from subclinical to acute severe illness, which is associated with high mortality. The recent trends in ARH hospitalizations in the United States suggest its importance in the current realm of clinical practice[1-4].

The prevalence of ARH has been on a rise even prior to COVID-19 pandemic[4]. Studies have shown a 53% increase in ARH from 2019 to 2020 with a 64% increase in the latter phase of the pandemic[2]. Multiple other studies have shown that the societal disruptions associated with the pandemic have further intensified the rise in cases of ARH. ARH can resolve with abstinence and supportive therapy; however, these measures do not guarantee recovery in all patients. Acute-on-chronic liver failure (ACLF) and development of cirrhosis are the most feared complications of ARH and is associated with significant morbidity and mortality. Thus, identifying patients early during the course of the disease is critical.

PREVALENCE

The true prevalence of ARH is difficult to assess as patients can be asymptomatic and remain undiagnosed. A study by Jinjuvadia *et al*[5] evaluating the temporal trends in ARH hospitalizations reported an increase in patients with ARH from 249884 in 2002 to 326403 in 2010. Their study included hospitalizations with a primary and secondary diagnosis of ARH. To estimate true prevalence, Ali *et al* [4] included patients only with a primary diagnosis of ARH and reported an increase in the total hospitalizations from 67070 in 2009 to 125540 in 2019. They also reported an increase in inpatient mortality from 2.48% in 2009 to 3.78% in 2019. The increase in the cases of ARH has been further intensified during the COVID-19 pandemic, especially in younger patients and in women.

ARH is also associated with a significant risk of mortality. Mortality has been estimated to be around 15% at 30 d and 39% at 1 year and has been linked to the severity of the disease[5]. Patients with mild liver injury have a 20% mortality, while patients with severe liver injury have an overall 40% mortality [6]. Mortality in patients with higher Maddrey's discriminant function (MDF) score (> 30), a surrogate marker of severity, is estimated to be between 30%-50%[7-8].

In previous years, there has also been an increase in the healthcare burden of ARH hospitalizations. An increase was noted in the mean inpatient cost for ARH hospitalizations from $31189 in 2009 to $62229 in 2019[4]. A study by Thompson *et al*[9], using commercial insurance claims, examined hospitalized patients between 2006-2013 and reported the average cost per patient is $145000 in their cohort of 15546 patients. They also reported the cost surrounding death of ARH was 200%-300% higher than the average cost surrounding death.

EPIDEMIOLOGY

Alcohol intake: The amount of alcohol consumption that places patients at risk of ARH is largely unknown. The estimates of the amount of alcohol consumed by patients may not be accurate as they are based on interviewing patients and family members[9]. The majority of patients with ARH consume more than 100 g/d of alcohol[10]. American Association for the Study of Liver Disease (AASLD) practice guidelines recommend suspecting ARH in women who consume > 40 g of alcohol and in men who consume > 60 g/d for ≥ 6 mo[11-12]. It is also pertinent to note that not all patients who drink heavily develop ALD. In a study by Friedman *et al*[13], 35% of the patients developed steatohepatitis and ARH, while only 10% of the patient's developed cirrhosis.

The pattern of drinking as well as the type of alcohol consumed also contributes to the risk of developing ARH. Drinking spirits or beer, binge drinking as well as drinking outside of the typical mealtimes has been associated with a higher risk of developing ALD[13-15] (Figure 1).

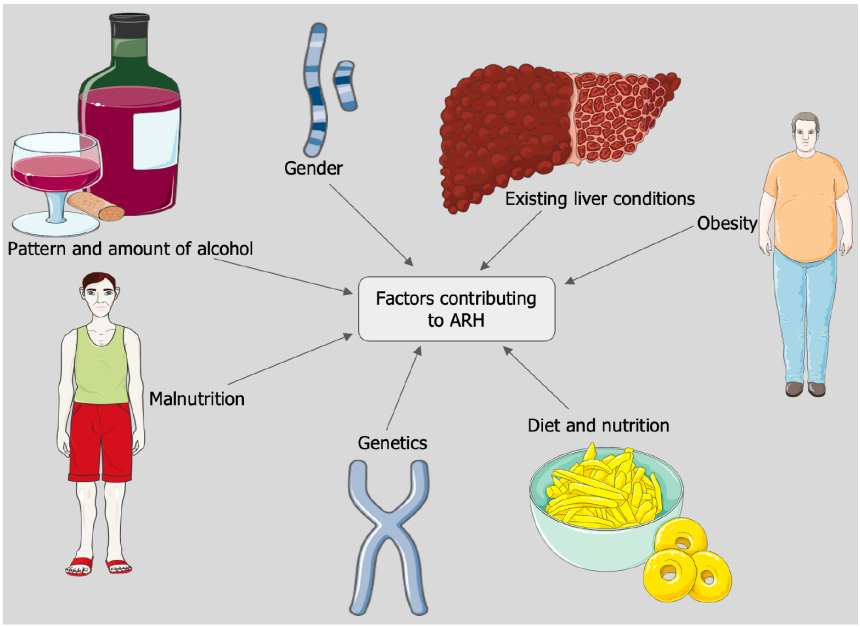

DOI: 10.3748/wjg.v29.i17.2551

Figure 1 Risk factors of alcohol-related hepatitis. ARH: Alcohol-related hepatitis.

Gender: There are significant differences based on gender. Women are at a higher risk of developing ARH at a lower threshold compared to men. This is attributed to differences in the variability of alcohol dehydrogenase activity, sex hormones, body fat distribution and liver volume between the two genders [16-18]. There has been an increase in the cases of ARH in women in recent years. A study conducted between 2009-2019 showed an increase in the proportion of women being admitted with ARH from 29.1% to 34.1%[4].

Malnutrition: Patients who consume alcohol excessively are often malnourished and can suffer from vitamin deficiencies[19]. Mortality has been closely related to the severity of protein-energy malnutrition. Patients with severe malnutrition and ARH have an estimated mortality of 80%[20]. Additionally, depletion of hepatic vitamin A and vitamin E can aggravate liver disease[21]. Zinc deficiency in patients with excessive alcohol can lead to disruption of mucosal permeability which may play a role in the pathogenesis of ARH.

Concurrent liver disease: It is well established that the combination of alcohol misuse and chronic hepatitis C (HCV) increases the incidence of cirrhosis and hepatocellular carcinoma (HCC) and is associated with reduced survival compared to patients with either HCV or alcohol use alone[22]. Consuming upward of 50 g/d of alcohol increases the relative risk of liver disease compared to patients with HCV who do not consume alcohol[23]. Patients with chronic HCV have been noted to have worse outcomes and higher in-hospital mortality when admitted with ARH[24].

While the literature clearly demonstrated worse outcomes in patients with concomitant alcohol misuse and chronic HCV, the data regarding the effect of alcohol use on patients with chronic hepatitis B (HBV) remains understudied. A study by Iida-Ueno *et al*[25] revealed that patients with light to moderate alcohol consumption had a 1.5-fold increase of chronic HBV infection while patients with heavy alcohol consumption had significantly accelerated progression to cirrhosis and HCC with 1.3 to 8.4-fold increased risk. Although the mechanism by which alcohol enhances disease progression is less studied in patients with chronic HBV in comparison to patients with HCV, patients with either chronic HCV and HBV should be counseled to avoid alcohol consumption to minimize chances of liver disease progression.

Obesity, diabetes mellitus and metabolic syndrome-underlying non-alcoholic fatty liver disease, a hepatic manifestation of metabolic syndrome, can be additive to the damage sustained through alcohol misuse and lead to worse outcomes. A study by Siddiqui *et al*[26] reported obesity to be an independent predictor of mortality in ARH.

Seasonality: Studies have shown that there might be a seasonal trend to admissions with alcohol use. We have previously reported that in the United States, ARH was highest in the summer months, as compared to the common opinion that ARH hospitalizations are higher in the winter season[27].

GENETICS

Significant variability has been noted among patients in regard to the susceptibility of developing ARH as well as the severity of symptoms. This variability has prompted several studies exploring a possible genetic basis for individual response to ARH. Studies have found an alteration in the expression of claudins, osteopontin, CD209, selenoprotein, and bile duct proliferation genes in patients with ARH compared to patients with alcoholic steatosis and healthy controls without liver disease[28]. Colmenero *et al*[29] identified several genes that were upregulated in ARH including extracellular matrix proteins, fibrogenesis mediators, inflammatory cytokines, and apoptosis regulators. Cytochrome p450 2E1 and angiotensinogen were found to be downregulated. Additionally, certain genes were found to be correlated with the severity of disease features including tissue inhibitors of metalloproteinases-1 and growth-related oncogene α. Epigenetic studies have also shown that a liver affected by ARH has significant alterations in HNF4α-dependent genes, which play a role in impairing metabolic and synthetic function[30]. A cohort study by Beaudoin *et al*[31] demonstrated an increased risk for developing ARH with a higher total bilirubin in patients with variants in the patatin-like phospholipase domain-containing protein 3 (*PNPLA3*) and the haptoglobin genes as compared to other genetic variants associated with chronic liver disease states[32].

The *PNPLA3* gene in particular has been identified to play a significant role in the pathogenesis of several liver diseases, as it belongs to a group of lipid-metabolizing enzymes. The I148M variant, a single-nucleotide polymorphism of the gene, is associated with an increased risk for developing hepatic steatosis, non-alcoholic steatohepatitis (NASH), ALD, cirrhosis, and HCC[33]. Despite these correlations, the precise function of the *PNPLA3* gene is yet to be fully understood. Palmer *et al*[33] demonstrated that variants in the *PNPLA3* gene in Hispanic-American and African-American patients is significantly associated with the development of hepatic steatosis, and other studies have shown that these groups suffer from higher mortality rates due to ALD. Levy *et al*[34] reported that patients of Hispanic ancestry presented with ALD at a significantly earlier age than patients of Caucasian or African-American background, though the mechanisms remain unclear and may be related to the gene variants described by Palmer *et al*[33] as well as health care disparities. Future studies can help to elucidate the underlying mechanisms of these discrepancies and the potential of gene-targeted therapy in the management of ARH.

PATHOGENESIS

The pathogenesis of ARH involves acute inflammation superimposed on chronic ALD. Initial hepatic injury results from the metabolism of ethanol into acetaldehyde by alcohol dehydrogenase and cytochrome P450 2E1 (CYP2E1). As ethanol builds up as a result of increased consumption, acetaldehyde also accumulates in the liver and begins to exert toxic effects[35]. Acetaldehyde leads to the formation of adducts, in the form of bonds with proteins, lipids, and DNA. This in turn impairs the normal function of the affected proteins and lipids and leads to DNA damage. CYP2E1 further contributes to liver injury by the production of reactive oxygen species which leads to hepatocyte injury [36]. This is thought to occur as a result of lipid peroxidation and interaction with proteins and nucleic acids, leading to hepatocyte necrosis[37] (Figure 2).

The oxidation of ethanol and acetaldehyde leads to an increase in the levels of nicotinamide adenine dinucleotide, which enhances lipogenesis in the liver[38]. Fatty infiltration of the liver is also a result of increased gut permeability due to alcohol ingestion, leading to higher levels of lipopolysaccharides present in the portal circulation[39]. Endotoxin, a lipopolysaccharide present in cell walls of gut microbiota, forms a protein complex and binds to the CD14 receptor on Kupffer cells in the liver[40]. The activation of Kupffer cells leads to the release of tumor necrosis factor-α (TNF-α), a pro-inflammatory cytokine[41]. TNF-α exerts its hepatotoxic effects by causing hepatocyte apoptosis and stimulating the release of other cytokines[42]. Higher levels of TNF-α are correlated with increased severity of ARH, demonstrating the significance of the cytokine in the pathogenesis of ARH[43].

The stimulation of Kupffer cells also lead to an increase in polymorphonuclear leukocyte infiltrate in the liver, as a result of chemotactic factors such as interleukin-8[44]. The multifactorial process of inflammation superimposed on alcohol-induced hepatic damage leads to the impairment of liver function observed as systemic illness and laboratory abnormalities in ARH. A thorough understanding of the pathogenesis of ARH can aid in its treatment, and further studies elucidating the precise mechanisms involved may improve treatment modalities and outcomes.

DIAGNOSIS

Physical Examination

Physical examination can range from benign to profoundly abnormal[45]. Patients may have signs of

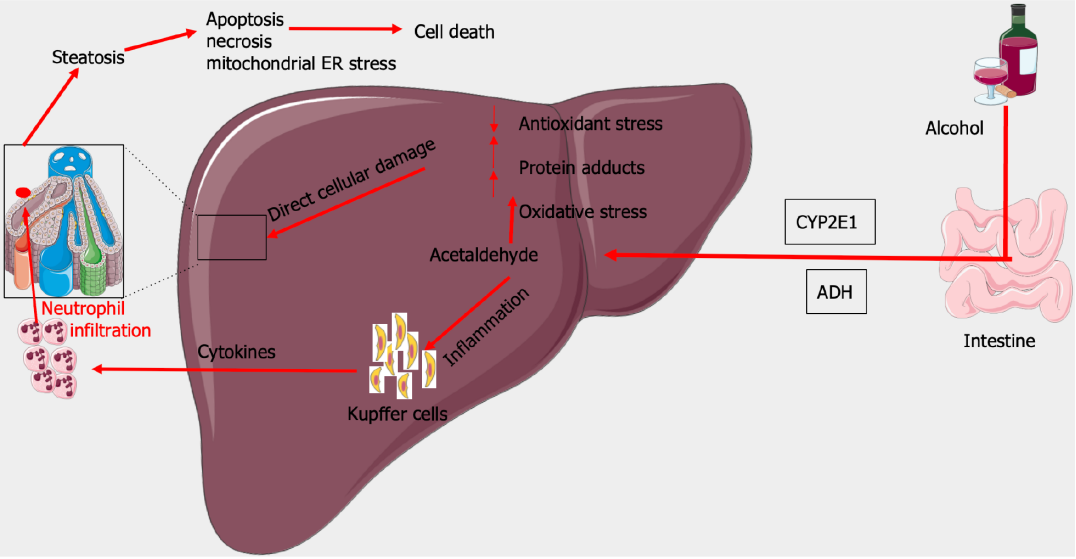

DOI: 10.3748/wjg.v29.i17.2551

Figure 2 Pathogenesis of alcohol-related hepatitis. ADH: Alcohol dehydrogenase.

malnutrition/sarcopenia manifested as temporal or thenar muscle wasting. Jaundice and scleral icterus may be apparent in patients with more severe disease while subtle signs of jaundice can be noted sublingually or in the tympanic membranes in patients with less severe disease. The presence of spider angiomas, gynecomastia in men and caput medusa is uncommon in patients with ARH in the absence of cirrhosis. Right upper quadrant tenderness to palpation along the enlarged hepatic border is common, with the liver edge extending into the pelvis and crossing the midline in severe cases. Some studies have reported a bruit over the liver as a feature of severe ARH in > 50% of patients[46]. Splenomegaly can often be appreciated as well even in the absence of cirrhosis. Fluid wave, shifting dullness and frank abdominal distention signifying large-volume ascites can be seen in severe cases. Lower extremity swelling progressing to anasarca can also be seen in severe cases. Finally, asterixis can be seen in patients with significant hepatic dysfunction.

Laboratory findings

Patients with suspected ARH should undergo a broad laboratory workup including comprehensive metabolic panel, complete blood count, international normalized ratio (INR), and gamma glutamyl transferase (GGT). Serologies for HAV, HBV and HCV should also be obtained to rule out alternative/concomitant infectious causes. Typical laboratory findings in ARH consist of elevated white blood cell count, thrombocytopenia, low sodium, potassium and magnesium. Other findings include total bilirubin > 3 mg/dL, elevated alanine transaminase (ALT) and aspartate transaminase (AST) with levels usually < 400 U/L, AST:ALT ratio > 2, GGT > 100 U/mL, INR > 1.5, and albumin < 3.0 g/L[47]. Other sequelae of chronic alcohol use such as macrocytic anemia can also be seen (Figure 3).

It is pertinent to rule out alternative/concomitant causes of liver disease such as Wilson's disease, autoimmune liver diseases and iron overload syndromes. This is especially important in patients with severe disease who may be considered for liver transplantation, as these diagnoses will have significant implications on patient's ability to qualify for an urgent transplant as well as pre-and post-transplant management. Making these diagnoses can be challenging as patients with ARH may have multiple metabolic derangements. For example, patients with ARH may have decreased ceruloplasmin levels in the setting of hepatic dysfunction leading to suspicion of Wlison's disease. If there is a significant clinical concern for Wilson's disease, patients should undergo a slit lamp examination for Kayser-Fleischer rings as well as a 24-h urine copper collection. Ferritin levels as well as iron saturations in patients with ARH can be markedly elevated in ARH therefore genetic testing for *HFE* gene mutation should be considered[48]. A clinical suspicion of autoimmune liver disease, especially in the setting of elevated autoimmune markers [antinuclear antibody (ANA), anti-smooth muscle antibody (SMA), antimitochondrial antibody, anti-liver kidney microsomal antibody], should prompt consideration of liver biopsy. Alpha-1-antitrypsin levels can be artificially elevated in the setting of acute illness; genetic testing should be considered if clinical suspicion is sufficiently high.

Imaging

Abdominal imaging can be effective in the initial evaluation of suspected ARH however, it cannot serve as the sole basis for the diagnosis. Abdominal ultrasound (US) computed tomography scan and/or magnetic resonance imaging will likely reveal and enlarged liver with smooth contours and decreased

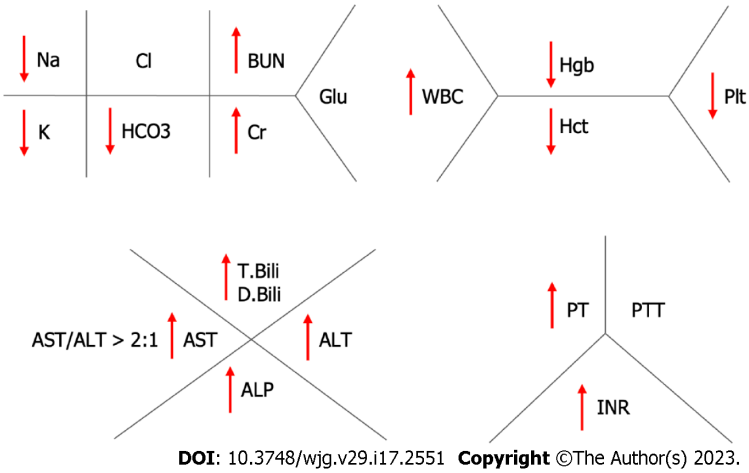

DOI: 10.3748/wjg.v29.i17.2551

Figure 3 Fishnet diagram showing laboratory abnormalities, commonly seen in patients with alcohol-related hepatitis. BUN: Blood urea nitrogen; WBC: White blood cell; Glu: Glucose; Hgb: Hemoglobin; Hct: Hematocrit; Plt: Platelet; T.Bili: Total bilirubin; D.Bili: Direct bilirubin; AST: Aspartate transaminase; ALT: Alanine transaminase; ALP: Alkaline phosphatase; PT: Prothrombin time; PTT: Partial thromboplastin time; INR: International normalized ratio.

attenuation, and in more severe cases, an enlarged spleen, ascites and other sequelae of portal hypertension. The presence of smooth hepatic borders, as opposed to the nodular contour, can help to differentiate ARH from cirrhosis[49] (Figure 4).

BIOPSY

The European Association for the Study of the Liver clinical practice guideline in 2014 stated that the "presence of acute steatohepatitis can be suspected on the clinical and biochemical grounds, but a definitive diagnosis of acute steatohepatitis requires liver biopsy"[50]. AASLD practice guidelines in 2019 recommend performing biopsy for confirmation if there are potential confounding factors such as [11]: (1) Ischemic hepatitis (*e.g.* severe upper GI bleed, cocaine use within 7 d or hypotension); (2) Suspected drug-induced liver disease; (3) Uncertain alcohol use assessment; and (4) Atypical laboratory tests (AST < 50 or > 400 IU/L, AST/ALT < 1.5), ANA > 1:160 or SMA > 1:80. Liver biopsy is controversial, especially in patients with coagulopathy and ascites. Percutaneous biopsy may be performed in most patients, but transjugular biopsy is preferred in patients with severe thrombocytopenia and prolonged INR. Liver biopsy is also recommended in patients suspected of having additional etiology for ACLF.

HISTOLOGY

Histology in patients with ALD can range from steatosis to steatofibrosis[51-52]. Steatofibrosis is defined as steatosis with fibrosis, with or without hepatitis. Histological features include steatosis, hepatocyte ballooning, neutrophil-rich inflammation in the lobular parenchyma, necrosis, apoptosis and Mallory-Denk bodies (MDB)[53]. The predominant mode of hepatocyte injury is *via* ballooning degeneration, followed by lytic necrosis and apoptosis. The hepatocytes become swollen, with clumping of intermediate filaments and loss of cytokeratin 8 and 18[51]. The swelling in hepatocytes can be attributed to severe ATP depletion and an increase in intra-cellular calcium, resulting in loss of plasma membrane volume control, oncotic necrosis and disruption of the intermediate filament network. The majority of changes in ALD are seen in the centrilobular region of hepatic lobe as they contain enzymes such as alcohol dehydrogenase, which are critical in alcohol metabolism[54].

It is pertinent to note there are histological similarities between NASH and ARH[53]. The differentiation is based on clinical information regarding alcohol intake; however some features are seen more commonly in ARH as compared to NASH (Table 1).

Apoptosis can be triggered by oxidative stress. Apoptotic hepatocytes, also known as councilman bodies or acidophil bodies, are visualized as shrunken cells, chromatin condensation and cellular fragmentation[55]. MDB contain eosinophilic material, located primarily in the perinuclear location in the cytoplasm of hepatocytes[56]. They are formed due to the misfolding of aggregated keratin filaments. MDB demonstrate immunoreactivity with antibodies to keratin 8, 18 and p62. Portal inflammation is milder as compared to other etiologies of liver disease. Portal inflammation, when present, is accompanied by ductular reaction and periportal inflammation[57]. Other features of this disease

Table 1 Histological differences between non-alcoholic steatohepatitis and alcohol-related hepatitis

Histological features	NASH	ARH
Canalicular cholestasis	Less common	More common
Mallory denk body	Less common	More common
Ductular reaction	Less common	More common
Fibrosis in portal tract	Less common	More common
Sclerosing hyaline necrosis	Less common	More common
Veno-occlusive lesions	Less common	More common
Severe steatosis	More common	Less common
Glycogenated nuclei	More common	Less common
Lipogranulomas	More common	Less common
Fibrosis	Lattice pattern	Solid pattern

NASH: Non-alcoholic steatohepatitis; ARH: Alcohol-related hepatitis.

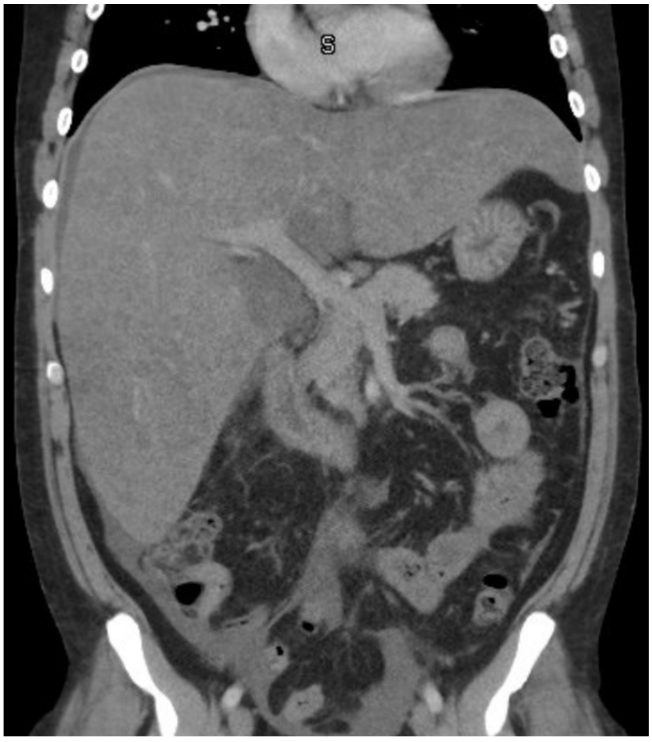

DOI: 10.3748/wjg.v29.i17.2551

Figure 4 Computerized tomography showing enlarged liver with smooth contour.

include glycogenated nuclei, megamitochondria, cholestasis and hemosiderin deposits[58]. Iron deposition can also occur in patients with ALD[59-60]. Based on the index of suspicion, concomitant hereditary hemochromatosis should be ruled out.

As the disease progresses, fibrosis begins in perivenular region (Zone 3) and extends to the perisinusoidal region in patients giving classic "chicken-wire fibrosis". Trichrome stain visualizes the fibrosis. If the injury continues, fibrosis progresses resulting in nodule formation and finally cirrhosis. An orcein stain, can be beneficial in later stages to differentiate broad bands of fibrosis from areas of collapse, which can occur in superimposed ARH[54].

A histological severity score including cytokeratin 8 and 18, has shown good accuracy in predicting 90-d survival[61]. Alcoholic hepatitis histologic score was created using parameters such as degree of fibrosis, degree of neutrophil inflammation, type of bilirubin stasis, and presence of mitochondria[62]. This score has been shown to be predictive of 90-d mortality. Trépo *et al*[63] combined the expression patterns of 123 genes with the model for end-stage liver disease (MELD) score to create gene-signature

plus MELD scoring system. This helped in discriminating patients with poor and good 90-d survival with an area under the curve of 0.86. This score outperformed other models including MELD plus Lille. This is not yet commercially available for use, however, may hold promise for the future.

COMPLICATIONS

Complications of ARH include infection, kidney injury, gastrointestinal bleeding, and acute liver failure amongst others (Figure 5).

Infection

Patients with ascites are at risk for developing spontaneous bacterial peritonitis (SBP), a life-threatening infection of the peritoneal cavity. SBP is almost exclusively seen in patients with ascites and is a result of bacterial translocation of enteric microflora into the ascitic fluid with concurrent failure of liver-related defensive mechanisms due to cirrhosis[64]. Additionally, patients with ARH are often treated with corticosteroids, further suppressing the immune response and increasing the risk of serious infection. Treatment of SBP is usually with a third-generation cephalosporin, such as ceftriaxone, which can also be used prophylactically in patients with decompensated cirrhosis or known patient with cirrhosis who presents with gastrointestinal bleeding.

Despite the well-known association of SBP with ALD, several studies demonstrate that infection due to pneumonia and urinary tract infection (UTI) is more common in severe ARH than SBP[65]. Infection overall is a major cause of mortality in severe ARH, with the majority being bacterial in nature[66-67]. A recent meta-analysis[68] found pneumonia to be the most common infection in severe ARH at 23%, followed by UTI at 10%. In comparison, SBP accounted for only 7% of infections. Patients with acute severe ARH have also been shown to have a greater level of immunosuppression compared to patients with cirrhosis, as they were found to have reduced T-lymphocyte and neutrophil activity[69]. Furthermore, obesity has been associated with increased susceptibility to infection in patients with ARH [70]. A high index of suspicion is needed in monitoring infectious signs and symptoms in patients with ARH as these patients often lack typical signs of infection such as fever or abdominal pain and may present instead with progressive hepatic decompensation. A low threshold for initiation of antibiotic therapy is advised and can be initiated empirically while infectious work-up is in progress.

Acute kidney injury

Acute kidney injury (AKI) is a common complication in hospitalized patients with ARH and can be due to pre-renal, intrinsic renal and post-renal causes. Pre-renal AKI continues to be the most common etiology, while the most feared etiology is hepatorenal syndrome (HRS). These entities can be differentiated *via* volume expansion challenge (25% albumin 1 g/kg for 48 h). Renal US can be used to rule out post-renal causes. Diuretics should be discontinued in patients with AKI.

Another etiology that should be considered in patients with ARH is acute tubular necrosis (ATN) secondary to cholemic nephrosis, or bile salt nephropathy and should be suspected in patients with prolonged severe cholestasis. Hyperbilirubinemia can also lead to formation of tubular casts, which can lead to ATN[71]. Evaluation of fractional excretion of sodium/urea as well as urine microscopy is beneficial to identify the etiology of kidney disease. Workup for AKI in patients with ARH is presented in Figure 6.

The most feared complication, HRS, results from renal artery vasoconstriction secondary to splanchnic vasodilation seen in liver disease[72]. Patients with ARH and other ALD often develop dilation of the splanchnic vasculature in response to increased hepatic resistance, which in turn leads to activation of the renin-angiotensin-aldosterone system, sympathetic nervous system, and arginine vasopressin system. The activation of these vasoconstrictor systems leads to constriction of the renal arteries and subsequent AKI due to decreased renal blood flow often in the setting of decreased cardiac output[73]. The development of AKI in patients with ARH is associated with a significantly higher mortality rate compared to patients without AKI, 65% *vs* 7% ($P < 0.0001$) respectively[74].

Treatment of HRS is complex, with most studies supporting the use of vasoconstrictors in combination with albumin administration. Terlipressin, a vasopressin analogue, has shown promising results in the treatment of HRS as it was found to be superior to both placebo and octreotide[75]. It has recently been approved in the United States by the Food and Drug Administration for the management of HRS. Liver transplantation (LT) is the treatment of choice in patients with HRS as renal dysfunction is potentially reversible with the correction of hepatic failure[76]. Interestingly, obesity has been found to be associated with decreased survival in acute ARH, and this is thought to be due to an increased risk of developing renal failure[77].

Acute on chronic liver failure

Severe ARH can lead to ACLF, a condition that is associated with increased mortality in patients with ARH and is commonly seen during the course of the disease[78]. ACLF manifests as worsening jaundice and coagulopathy and is usually triggered by a precipitating event. Current literature shows that ARH

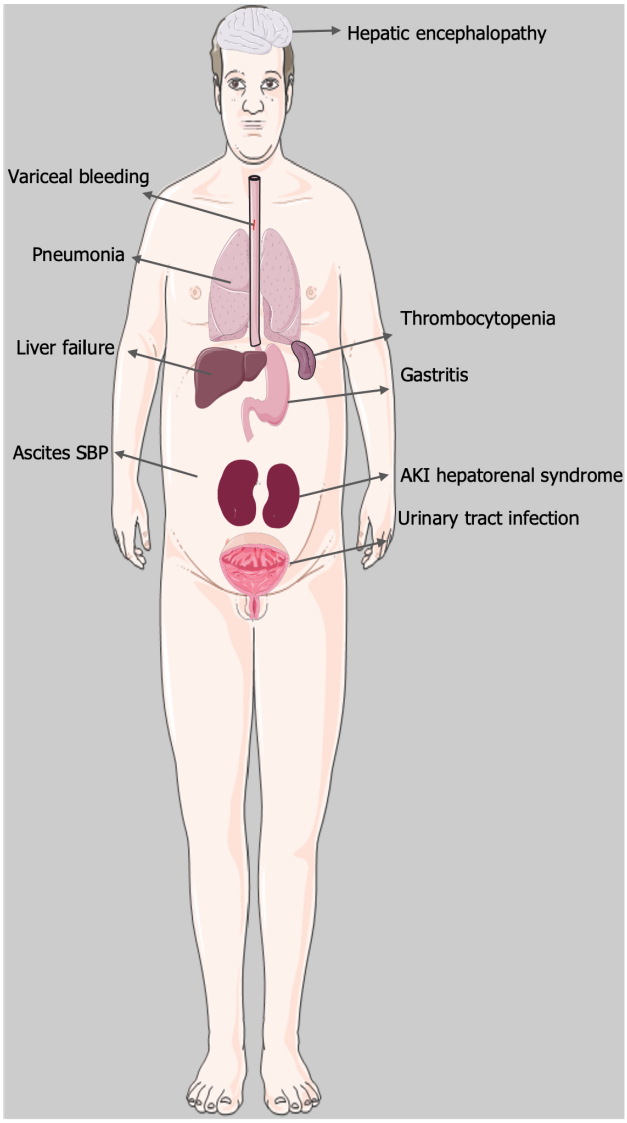

DOI: 10.3748/wjg.v29.i17.2551

Figure 5 Complications and clinical features in patients with alcohol-related hepatitis. SBP: Spontaneous bacterial peritonitis; AKI: Acute kidney injury.

serves as a common precipitating event for the development of ACLF[76]. Studies have demonstrated that 65% of patients with severe ARH had ACLF at the time of diagnosis or within a 6-mo follow-up period[77]. Given the poor prognosis of ACLF, early liver transplantation is becoming more commonplace in the treatment of severe ARH, with recent literature supporting its use with stringent patient selection criteria[79-80].

Portal hypertension and cirrhosis

Many patients with ARH also have portal hypertension or will develop portal hypertension at some point during their disease course potentially leading to variceal hemorrhage. Overall one-month mortality in moderate to severe ARH is 23%, with the most common causes of death being liver failure, gastrointestinal bleeding, and infection[81] The one-month mortality in non-severe ARH is 6%, however the rate increases to 13% after one year[82].

Long-term follow-up in patients with ARH over 4 years revealed the probability of developing cirrhosis to be 10%-20% per year and up to 70% of patients will ultimately develop cirrhosis[83]. In another study, about 40% of the patients were diagnosed with cirrhosis on biopsy, 5 years after the episode of ARH[84]. The probability of developing cirrhosis is associated with continued alcohol use, as Rehm *et al*[85] demonstrated in a meta-analysis that there is a close dose-dependent relationship between ongoing alcohol use and the risk of progression of ALD to liver cirrhosis. Parés *et al*[86] found an 18% risk of progression to cirrhosis in patients who abstained from alcohol after 20 mo compared to 23% in patients with continued alcohol consumption.

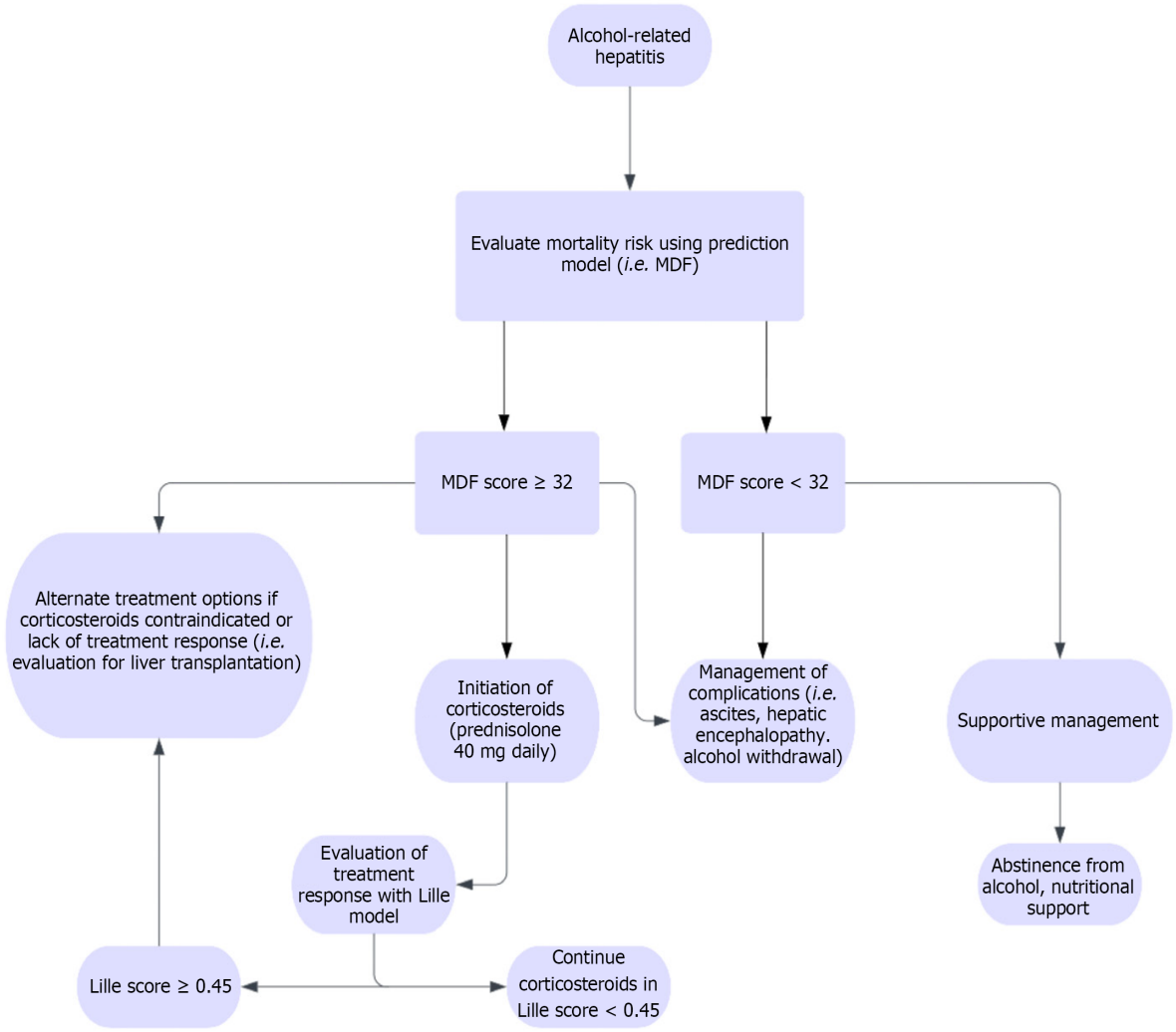

DOI: 10.3748/wjg.v29.i17.2551

Figure 6 Diagnostic workup for acute kidney injury in patients with alcohol-related hepatitis. MDF: Maddrey's discriminant function.

PREDICTION MODELS

MDF is a commonly used prognostic indicator in the management of ARH as it is specific for ARH and has shown to be relatively accurate in predicting short-term outcomes[87]. The MDF score incorporates two of the major indices of liver function, prothrombin time (PT) and total bilirubin with the formula 4.6 × (prolongation of PT in seconds) + bilirubin (μmol/L)/17. MDF score of < 32 signifies mild to moderate ARH with 30-d survival estimated at 80%-100%. MDF score ≥ 32 is considered to be severe ARH with a 30-d survival of only 50%, and these patients warrant corticosteroid administration for treatment of their disease[87] (Table 2).

Lille Model is used to evaluate treatment response to corticosteroids and includes age, initial serum albumin, change in total serum bilirubin at day 7 of treatment, renal insufficiency, and initial MDF score [88]. Patients with a Lille score of < 0.45 had an average 6-mo survival rate of 85%, compared to just 25% in patients who scored ≥ 0.45 after 7 d of treatment (P < 0.0001). The Lille model is primarily used in conjunction with the MDF to guide treatment of ARH. Patients who score ≥ 0.45 after receiving corticosteroid therapy for 7 d are considered for discontinuation of steroids and initiation of alternative treatment modalities, as continuation of steroids is of little benefit in these patients.

MELD was initially created to assess the mortality risk in patients with portal hypertension undergoing transjugular intrahepatic portosystemic shunts procedure however, it has now become a validated tool in assessing patients with a variety of liver pathologies[89]. MELD differs from MDF in that it incorporates serum creatinine and uses INR rather than PT. The formula for MELD is 9.57 × loge (creatinine) + 3.78 × loge (total bilirubin) + 11.2 × loge (INR) + 6.43. In comparison to the MDF, the MELD has been shown to be superior in predicting outcomes of patients with ARH. Several studies have demonstrated this effect, further supporting the use of MELD in patients with ARH[90-94]. Patients with a MELD score ≤ 11 have mild disease associated with a very low mortality rate. Patients who score > 21 are considered to have severe ARH.

Table 2 Prediction models for alcohol-related hepatitis

Score	Variables	Mortality rate
MDF	PT, total bilirubin	50% at 30 d for score ≥ 32
Lille model	Age, albumin, change in total bilirubin, renal insufficiency, MDF score	75% at 6 mo for score ≥ 0.45
Model for end-stage liver disease	Creatinine, total bilirubin, INR	20% at 90 d for score > 21
Glasgow alcoholic hepatitis score	Age, white blood cell count, BUN, total bilirubin, PT	48% at 28 d for score ≥ 9
ABIC score	Age, total bilirubin, creatinine, INR	75% at 90 d for score > 9

PT: Prothrombin time; BUN: Blood urea nitrogen; INR: International normalized ratio; ABIC: Age, serum bilirubin, international normalized ratio, serum creatinine; MDF: Maddrey discriminant function.

Glasgow alcoholic hepatitis score (GAHS) was developed in order to present a model with increased specificity than MDF and a more accurate cutoff score than MELD. The GAHS incorporates many of the same parameters as the MDF and MELD, but differs in its inclusion of the peripheral white blood cell count[95]. The inclusion of an inflammatory component is thought to provide a more accurate predictor of mortality in ARH and has been shown to be superior to MDF in predicting 28-d and 84-d mortality. The cutoff point delineating severe ARH from non-severe is a GAHS score of ≥ 9.

Age, serum bilirubin, INR, serum creatinine (ABIC) score is another scoring system that was developed to predict mortality in patients with ARH[96]. The ABIC score includes liver function as well as kidney function and has a formula of (age × 0.1) + (serum bilirubin × 0.08) + (serum creatinine × 0.3) + (INR × 0.8). This model is validated for predicting 3-mo survival rates in ARH based on stratification of the severity of disease. Patients are classified based on their ABIC score into low (< 6.71), intermediate (6.71-8.99), and high (> 9.0) mortality risk. These classes correspond to a 90-d mortality of 0%, 30%, and 75%, respectively. Despite its efficacy in death risk stratification, the ABIC score does not play a major role in treatment or in determining whether corticosteroid administration is indicated.

TREATMENT

The management of ARH involves reducing hepatic inflammation by targeting pro-inflammatory and immunologic substances acutely and reversing alcohol-induced hepatotoxicity in the long term. The mainstay of treatment in ALD is abstinence from alcohol. A retrospective study by Lackner *et al*[97] demonstrated a 5-year mortality rate of 13% in early ALD and 43% in decompensated ALD. Abstaining from alcohol showed an improvement in survival in patients with both early and decompensated ALD. A meta-analysis by Xie *et al*[98] determined that patients with ALD see an improvement in survival rates after approximately 1.5 years of abstinence. However, studies have also shown that histological improvements in ALD can be observed in patients as soon as 2 wk after discontinuation of alcohol consumption[99].

Many of the traditional pharmacologic agents used to promote abstinence from alcohol such as disulfiram, naltrexone, acamprosate, and topiramate are of limited use in ALD as they may be hepatotoxic and lack data supporting their usage[100]. Baclofen, a selective gamma-aminobutyric acid B receptor agonist, has been studied as a potential agent of choice in patients with ALD as it has minimal hepatic clearance. A recent multi-site randomized control trial[101] of patients with and without ALD demonstrated that low-medium dose baclofen at 30-75 mg daily led to a significant improvement in alcohol abstinence.

Nutritional supplementation is a vital component in the treatment of ALD. Malnutrition is common in patients with ALD, and the severity of malnourishment is correlated with the severity of liver disease [102]. The AASLD recommends a diet of at least 2000 kcal/d with at least 1.5 g protein/kg/d in patients with ALD[103]. These patients suffer from nutritional deficiencies and appropriate nutritional supplementation should be provided as nutritional deficiencies have been shown to be associated with worse outcomes[104].

Treatment of mild to moderate ARH, as defined by an MDF score < 32, consists mainly of supportive care and management of complications such as ascites, hepatic encephalopathy, and acute alcohol withdrawal syndrome[105]. Ascites is managed primarily through sodium restriction and diuresis. Patients with ascites generally have decreased sodium excretion, warranting a daily sodium restriction of 2-4 g/d. AASLD guidelines recommend that for the first episode of ascites, aldosterone antagonists alone can generate an adequate response with few side effects[106]. On the contrary, if the patient has long-standing ascites, anasarca or hepatic hydrothorax, the recommended regimen is a combination of an aldosterone antagonist and loop diuretic.

Hepatic encephalopathy is managed primarily with lactulose and rifaximin in order to promote the excretion of toxic metabolites *via* stool and improve the biodiversity of gut flora. Acute alcohol withdrawal is treated with benzodiazepines such as lorazepam on a scheduled regimen or symptom-triggered dose in accordance with protocols such as the Clinical Institute Withdrawal Assessment. Lorazepam has been shown to be the safest agent in its class in patients with liver disease due to minimal hepatotoxicity and is therefore the drug of choice[107]. Use of long-acting benzodiazepines, such as chlordiazepoxide, should be avoided in patients with significant hepatic dysfunction due to decreased rate of hepatic metabolism and potential for rapid accumulation leading to progressive decline in mental status[108].

The most well-studied treatment modality in severe ARH, classified as an MDF score ≥ 32, is the use of corticosteroids. Its use was validated in the "Steroids or pentoxifylline for alcoholic hepatitis" (STOPAH)[109] trial, which included 1053 subjects with ARH. There was a 28-d mortality benefit in patients treated with prednisolone. On the contrary, no mortality benefit was observed in the prednisolone group after 90 d or 1 year, adding further evidence that the positive effects of steroids in severe ARH are limited to short-term (Figure 7).

A meta-analysis of 5 randomized control trials[110] revealed a significant improvement in 28-d survival among patients with severe ARH treated with corticosteroids (79.97% ± 2.8% *vs* 65.7% ± 3.4%, $P = 0.0005$). A more recent meta-analysis[111] of 11 randomized control trials found similar results in short-term mortality benefit, however also demonstrated that corticosteroid treatment did not decrease mortality rate after 6 mo. The primary mechanism by which corticosteroids exert their effect in severe ARH is by blunting the immune response and inflammation that contributes to mortality[112]. The standard regimen for treatment of severe ARH is administration of prednisolone 40 mg daily[113]. Contraindications to steroid administration include active infection, gastrointestinal bleeding, acute pancreatitis, and renal failure, as steroids can acutely exacerbate these conditions[114].

STOPAH109 trial reported that incidence of serious infections occurred in 13% of patients in the prednisolone group compared to 7% in patients who were not treated with prednisolone ($P = 0.002$). However, a recent meta-analysis[115] found that corticosteroid administration in severe ARH reduced 28-d mortality from liver-related death with no significant change in mortality from bacterial infection or gastrointestinal bleeding. The study also found a higher incidence of fungal infection in steroid-treated patients. Pentoxifylline was previously used in the management of ARH. Its use has been limited based on the results of STOPAH trial, in which use of pentoxifylline was not associated with mortality benefit.

LT has been controversial in the treatment of ARH, as patients with ALD have historically been considered poor candidates for transplantation due to concern for continued alcohol use after transplantation. However, recent trends have shown an opportunity for LT to gain a larger role in the treatment of ARH with strict selection criteria for candidates, as demonstrated in several studies[116]. A prospective trial by Mathurin *et al*[117] showed a significantly improved 6-mo survival rate in patients with severe ARH (MDF > 32, Lillie > 0.45) who received LT compared to controls without LT (77% and 23% respectively, $P < 0.001$). However, selection criteria were remarkably strict, as only patients with no prior episodes of hepatic decompensation, strong family support, complete commitment to abstinence, and consensus among all care providers were accepted for LT, which was less than 2% of all patients admitted with ARH during the study period. A more recent trial by Weeks *et al*[118] demonstrated a 97% 1-year survival rate in patients who received LT for severe ARH, however had an alcohol use relapse rate at 17% due to less strict inclusion requirements (including patients with recent hepatic decompensation). A recent large multi-center retrospective analysis (ACCELERATE-AH)[119] found a 94% 1-year survival rate and 84% 3-year survival rate with a 11% relapse rate. Of note, median MELD score was 39 and median Lille score was 0.82 for patients who received LT.

In summary, LT should be considered for patients with life-threatening ARH who have failed medical therapy and who have a low likelihood of alcohol relapse based on predetermined medical and social criteria. The proportion of candidates meeting these criteria may be relatively low, however stringent patient selection can aid in avoiding improper use of donor organs while dramatically improving survival rates. A study reported that the rates of relapse-free survival and hazardous relapse-free survival did not differ between the patients who received early transplantation compared to those who were transplanted after 6 mo of abstinence[120].

THERAPIES/CLINICAL TRIALS UNDER INVESTIGATION

Multiple therapies are currently under clinical trial for the management of ARH. While the discussion regarding all the therapies under investigation is beyond the scope of this article, information regarding the various mechanisms and clinical trials currently targeting this disease is presented in Table 3 below.

Table 3 Clinical trials under investigation

Drugs	Mechanisms	Clinical trials
Anakinra and Canakinumab	Reduce hepatic inflammation	NCT01809132[121], NCT04072822[122], NCT03775109[123]
N-acetyl cysteine, S-adenosyl methionine (SAM-E)	Reduce oxidative stress	NCT03069300[124], NCT00851981[125], NCT02024295[126]
DUR-928	Epigenetic modulation of lipid homeostasis, inflammation, cell survival, tissue regeneration	NCT03432260[127], NCT03917407[128]
Granulocyte colony stimulating growth factors, interleukin-22 and obeticholic acid	Boosts liver regeneration	NCT02442180[129], NCT03703674[130], NCT04066179[131], NCT02655510[132], NCT01918462[133], NCT02039219[134]
Rifaximin, zinc supplementation, bovine colostrum, probiotics, and fecal microbiota transplant	Targets the gut-liver axis	NCT02116556[135], NCT02485106[136], NCT01968382[137], NCT02473341[138], NCT01922895[139], NCT02335632[140], NCT02458079[141], NCT03091010[142], NCT03827772[143]

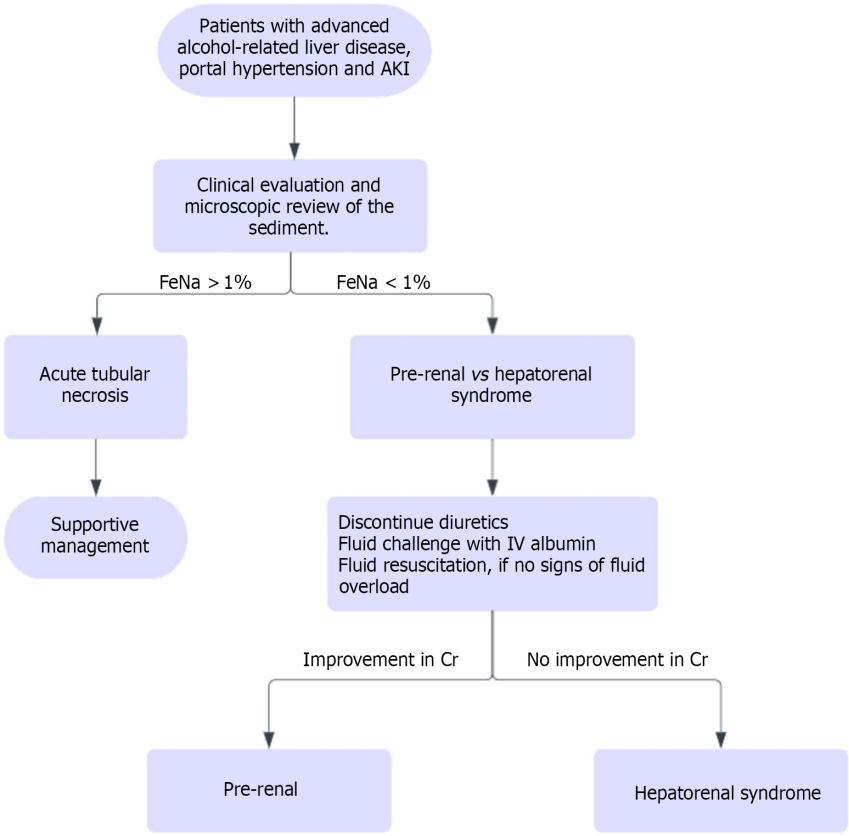

DOI: 10.3748/wjg.v29.i17.2551

Figure 7 Treatment algorithm for alcohol-related hepatitis. AKI: Acute kidney injury.

CONCLUSION

ARH remains a disease process with high morbidity and mortality. Despite research advances in pathogenesis of this disease process, limited progress has been made in management of this condition. Abstinence remains critical in maximizing the chances of hepatic recovery; corticosteroids continue to play a role in select populations. Given the grim prognosis and increasing prevalence of ARH, research efforts are aiming at inhibiting inflammatory cytokine pathways that lead to progressive hepatic damage. In the meantime, many centers around the world are resorting to liver transplantation as salvage therapy. The COVID-19 pandemic exacerbated the pre-existing trend of rising cases of ARH. Urgent societal and government interventions are needed to prevent the ongoing rise in ARH cases in addition to intensifying research efforts in identifying and testing therapeutic targets for this complex disease process.

ACKNOWLEDGEMENTS

We thank Dino Dukovic for his expertise and assistance in writing the manuscript.

FOOTNOTES

Author contributions: Chaudhry H, Sohal A and Iqbal H reviewed the literature, drafted the manuscript, revised it for important intellectual content and were involved in the final approval of the version to be published; Roytman M revised the article for important intellectual content and was involved in the final approval of the version to be published; All authors have read and approved the final manuscript.

Conflict-of-interest statement: All the authors report no relevant conflicts of interest for this article.

Country/Territory of origin: United States

ORCID number: Hunza Chaudhry 0000-0001-7769-0394.

S-Editor: Li L
L-Editor: A
P-Editor: Zhang XD

REFERENCES

1 **Moon AM**, Curtis B, Mandrekar P, Singal AK, Verna EC, Fix OK. Alcohol-Associated Liver Disease Before and After COVID-19-An Overview and Call for Ongoing Investigation. *Hepatol Commun* 2021; **5**: 1616-1621 [PMID: 34510833 DOI: 10.1002/hep4.1747]
2 **Sohal A**, Khalid S, Green V, Hagino J, Chaudhry H, Gulati A, Roytman M. Soaring rates of alcohol-related hepatitis in the latter phase of the COVID-19 pandemic: A new normal? *JGH Open* 2023; **7**: 148-151 [PMID: 36852146 DOI: 10.1002/jgh3.12864]
3 **Gonzalez HC**, Zhou Y, Nimri FM, Rupp LB, Trudeau S, Gordon SC. Alcohol-related hepatitis admissions increased 50% in the first months of the COVID-19 pandemic in the USA. *Liver Int* 2022; **42**: 762-764 [PMID: 35094494 DOI: 10.1111/liv.15172]
4 **Ali H**, Pamarthy R, Bolick NL, Farooq MF. Ten-year trends and prediction model of 30-day inpatient mortality for alcoholic hepatitis in the United States. *Ann Gastroenterol* 2022; **35**: 427-433 [PMID: 35784634 DOI: 10.20524/aog.2022.0718]
5 **Jinjuvadia R**, Liangpunsakul S; Translational Research and Evolving Alcoholic Hepatitis Treatment Consortium. Trends in Alcoholic Hepatitis-related Hospitalizations, Financial Burden, and Mortality in the United States. *J Clin Gastroenterol* 2015; **49**: 506-511 [PMID: 25198164 DOI: 10.1097/MCG.0000000000000161]
6 **Mathurin P**, Duchatelle V, Ramond MJ, Degott C, Bedossa P, Erlinger S, Benhamou JP, Chaput JC, Rueff B, Poynard T. Survival and prognostic factors in patients with severe alcoholic hepatitis treated with prednisolone. *Gastroenterology* 1996; **110**: 1847-1853 [PMID: 8964410 DOI: 10.1053/gast.1996.v110.pm8964410]
7 **Morgan MY**. The prognosis and outcome of alcoholic liver disease. *Alcohol Alcohol Suppl* 1994; **2**: 335-343 [PMID: 8974353]
8 **Shah NJ**, Royer A, John S. Alcoholic Hepatitis. 2023. In: StatPearls [Internet]. Treasure Island (FL): StatPearls Publishing; 2023 [PMID: 29262136]
9 **Thompson JA**, Martinson N, Martinson M. Mortality and costs associated with alcoholic hepatitis: A claims analysis of a commercially insured population. *Alcohol* 2018; **71**: 57-63 [PMID: 30048829 DOI: 10.1016/j.alcohol.2018.02.003]
10 **Midanik L**. The validity of self-reported alcohol consumption and alcohol problems: a literature review. *Br J Addict* 1982; **77**: 357-382 [PMID: 6762224 DOI: 10.1111/j.1360-0443.1982.tb02469.x]
11 **Naveau S**, Giraud V, Borotto E, Aubert A, Capron F, Chaput JC. Excess weight risk factor for alcoholic liver disease. *Hepatology* 1997; **25**: 108-111 [PMID: 8985274 DOI: 10.1002/hep.510250120]
12 **Crabb DW**, Im GY, Szabo G, Mellinger JL, Lucey MR. Diagnosis and Treatment of Alcohol-Associated Liver Diseases: 2019 Practice Guidance From the American Association for the Study of Liver Diseases. *Hepatology* 2020; **71**: 306-333 [PMID: 31314133 DOI: 10.1002/hep.30866]
13 **Friedman SL**, Neuschwander-Tetri BA, Rinella M, Sanyal AJ. Mechanisms of NAFLD development and therapeutic strategies. *Nat Med* 2018; **24**: 908-922 [PMID: 29967350 DOI: 10.1038/s41591-018-0104-9]
14 **Barrio E**, Tomé S, Rodríguez I, Gude F, Sánchez-Leira J, Pérez-Becerra E, González-Quintela A. Liver disease in heavy drinkers with and without alcohol withdrawal syndrome. *Alcohol Clin Exp Res* 2004; **28**: 131-136 [PMID: 14745311 DOI: 10.1097/01.ALC.0000106301.39746.EB]

15 **Wechsler H**, Austin SB. Binge drinking: the five/four measure. *J Stud Alcohol* 1998; **59**: 122-124 [PMID: 9498324 DOI: 10.15288/jsa.1998.59.122]

16 **Mezey E**, Kolman CJ, Diehl AM, Mitchell MC, Herlong HF. Alcohol and dietary intake in the development of chronic pancreatitis and liver disease in alcoholism. *Am J Clin Nutr* 1988; **48**: 148-151 [PMID: 3389321 DOI: 10.1093/ajcn/48.1.148]

17 **Bellentani S**, Saccoccio G, Costa G, Tiribelli C, Manenti F, Sodde M, Saveria Crocè L, Sasso F, Pozzato G, Cristianini G, Brandi G. Drinking habits as cofactors of risk for alcohol induced liver damage. The Dionysos Study Group. *Gut* 1997; **41**: 845-850 [PMID: 9462221 DOI: 10.1136/gut.41.6.845]

18 **Lu XL**, Luo JY, Tao M, Gen Y, Zhao P, Zhao HL, Zhang XD, Dong N. Risk factors for alcoholic liver disease in China. *World J Gastroenterol* 2004; **10**: 2423-2426 [PMID: 15285035 DOI: 10.3748/wjg.v10.i16.2423]

19 **Mendenhall CL**, Moritz TE, Roselle GA, Morgan TR, Nemchausky BA, Tamburro CH, Schiff ER, McClain CJ, Marsano LS, Allen JI. Protein energy malnutrition in severe alcoholic hepatitis: diagnosis and response to treatment. The VA Cooperative Study Group #275. *JPEN J Parenter Enteral Nutr* 1995; **19**: 258-265 [PMID: 8523623 DOI: 10.1177/0148607195019004258]

20 **Mendenhall C**, Roselle GA, Gartside P, Moritz T. Relationship of protein calorie malnutrition to alcoholic liver disease: a reexamination of data from two Veterans Administration Cooperative Studies. *Alcohol Clin Exp Res* 1995; **19**: 635-641 [PMID: 7573786 DOI: 10.1111/j.1530-0277.1995.tb01560.x]

21 **Leevy CM**, Moroianu SA. Nutritional aspects of alcoholic liver disease. *Clin Liver Dis* 2005; **9**: 67-81 [PMID: 15763230 DOI: 10.1016/j.cld.2004.11.003]

22 **Singal AK**, Anand BS. Mechanisms of synergy between alcohol and hepatitis C virus. *J Clin Gastroenterol* 2007; **41**: 761-772 [PMID: 17700425 DOI: 10.1097/MCG.0b013e3180381584]

23 **Poynard T**, Bedossa P, Opolon P. Natural history of liver fibrosis progression in patients with chronic hepatitis C. The OBSVIRC, METAVIR, CLINIVIR, and DOSVIRC groups. *Lancet* 1997; **349**: 825-832 [PMID: 9121257 DOI: 10.1016/S0140-6736(96)07642-8]

24 **Singal AK**, Sagi S, Kuo YF, Weinman S. Impact of hepatitis C virus infection on the course and outcome of patients with acute alcoholic hepatitis. *Eur J Gastroenterol Hepatol* 2011; **23**: 204-209 [PMID: 21258239 DOI: 10.1097/MEG.0b013e328343b085]

25 **Iida-Ueno A**, Enomoto M, Tamori A, Kawada N. Hepatitis B virus infection and alcohol consumption. *World J Gastroenterol* 2017; **23**: 2651-2659 [PMID: 28487602 DOI: 10.3748/wjg.v23.i15.2651]

26 **Siddiqui T**, Trieu J, Bilal M, Mehta D, Gollapudi LA, Nabors C, Wolf DC. Obesity Has Significant Impact on Mortality in Patients With Acute Alcoholic Hepatitis. *Am. J. Gastroenterol***113**: S591-S593 [DOI: 10.14309/00000434-201810001-01037]

27 **Sohal A**, Bains K, Dhaliwal A, Chaudhry H, Sharma R, Singla P, Gupta G, Dukovic D, Sandhu S, Roytman M, Tringali S. Seasonal Variations of Hospital Admissions for Alcohol-Related Hepatitis in the United States. *Gastroenterology Res* 2022; **15**: 75-81 [PMID: 35572478 DOI: 10.14740/gr1506]

28 **Seth D**, Gorrell MD, Cordoba S, McCaughan GW, Haber PS. Intrahepatic gene expression in human alcoholic hepatitis. *J Hepatol* 2006; **45**: 306-320 [PMID: 16797773 DOI: 10.1016/j.jhep.2006.04.013]

29 **Colmenero J**, Bataller R, Sancho-Bru P, Bellot P, Miquel R, Moreno M, Jares P, Bosch J, Arroyo V, Caballería J, Ginès P. Hepatic expression of candidate genes in patients with alcoholic hepatitis: correlation with disease severity. *Gastroenterology* 2007; **132**: 687-697 [PMID: 17258719 DOI: 10.1053/j.gastro.2006.12.036]

30 **Argemi J**, Latasa MU, Atkinson SR, Blokhin IO, Massey V, Gue JP, Cabezas J, Lozano JJ, Van Booven D, Bell A, Cao S, Vernetti LA, Arab JP, Ventura-Cots M, Edmunds LR, Fondevila C, Stärkel P, Dubuquoy L, Louvet A, Odena G, Gomez JL, Aragon T, Altamirano J, Caballeria J, Jurczak MJ, Taylor DL, Berasain C, Wahlestedt C, Monga SP, Morgan MY, Sancho-Bru P, Mathurin P, Furuya S, Lackner C, Rusyn I, Shah VH, Thursz MR, Mann J, Avila MA, Bataller R. Defective HNF4alpha-dependent gene expression as a driver of hepatocellular failure in alcoholic hepatitis. *Nat Commun* 2019; **10**: 3126 [PMID: 31311938 DOI: 10.1038/s41467-019-11004-3]

31 **Beaudoin JJ**, Liang T, Tang Q, Banini BA, Shah VH, Sanyal AJ, Chalasani NP, Gawrieh S. Role of candidate gene variants in modulating the risk and severity of alcoholic hepatitis. *Alcohol Clin Exp Res* 2021; **45**: 709-719 [PMID: 33616244 DOI: 10.1111/acer.14581]

32 **Bruschi FV**, Tardelli M, Claudel T, Trauner M. PNPLA3 expression and its impact on the liver: current perspectives. *Hepat Med* 2017; **9**: 55-66 [PMID: 29158695 DOI: 10.2147/HMER.S125718]

33 **Palmer ND**, Musani SK, Yerges-Armstrong LM, Feitosa MF, Bielak LF, Hernaez R, Kahali B, Carr JJ, Harris TB, Jhun MA, Kardia SL, Langefeld CD, Mosley TH Jr, Norris JM, Smith AV, Taylor HA, Wagenknecht LE, Liu J, Borecki IB, Peyser PA, Speliotes EK. Characterization of European ancestry nonalcoholic fatty liver disease-associated variants in individuals of African and Hispanic descent. *Hepatology* 2013; **58**: 966-975 [PMID: 23564467 DOI: 10.1002/hep.26440]

34 **Levy R**, Catana AM, Durbin-Johnson B, Halsted CH, Medici V. Ethnic differences in presentation and severity of alcoholic liver disease. *Alcohol Clin Exp Res* 2015; **39**: 566-574 [PMID: 25702770 DOI: 10.1111/acer.12660]

35 **Setshedi M**, Wands JR, Monte SM. Acetaldehyde adducts in alcoholic liver disease. *Oxid Med Cell Longev* 2010; **3**: 178-185 [PMID: 20716942 DOI: 10.4161/oxim.3.3.12288]

36 **Lieber CS**. Cytochrome P-4502E1: its physiological and pathological role. *Physiol Rev* 1997; **77**: 517-544 [PMID: 9114822 DOI: 10.1152/physrev.1997.77.2.517]

37 **Gao B**, Bataller R. Alcoholic liver disease: pathogenesis and new therapeutic targets. *Gastroenterology* 2011; **141**: 1572-1585 [PMID: 21920463 DOI: 10.1053/j.gastro.2011.09.002]

38 **Osna NA**, Donohue TM Jr, Kharbanda KK. Alcoholic Liver Disease: Pathogenesis and Current Management. *Alcohol Res* 2017; **38**: 147-161 [PMID: 28988570]

39 **Abenavoli L**, Masarone M, Federico A, Rosato V, Dallio M, Loguercio C, Persico M. Alcoholic Hepatitis: Pathogenesis, Diagnosis and Treatment. *Rev Recent Clin Trials* 2016; **11**: 159-166 [PMID: 27457347 DOI: 10.2174/1574887111666160724183409]

40 **Su GL**, Klein RD, Aminlari A, Zhang HY, Steinstraesser L, Alarcon WH, Remick DG, Wang SC. Kupffer cell activation

by lipopolysaccharide in rats: role for lipopolysaccharide binding protein and toll-like receptor 4. *Hepatology* 2000; **31**: 932-936 [PMID: 10733550 DOI: 10.1053/he.2000.5634]

41 **Morgan TR**, McClain CJ. Pentoxifylline and alcoholic hepatitis. *Gastroenterology* 2000; **119**: 1787-1791 [PMID: 11113103 DOI: 10.1053/gast.2000.20826]

42 **Bradham CA**, Plümpe J, Manns MP, Brenner DA, Trautwein C. Mechanisms of hepatic toxicity. I. TNF-induced liver injury. *Am J Physiol* 1998; **275**: G387-G392 [PMID: 9724248 DOI: 10.1152/ajpgi.1998.275.3.G387]

43 **McClain C**, Hill D, Schmidt J, Diehl AM. Cytokines and alcoholic liver disease. *Semin Liver Dis* 1993; **13**: 170-182 [PMID: 8337603 DOI: 10.1055/s-2007-1007347]

44 **Bird G**. Interleukin-8 in alcoholic liver disease. *Acta Gastroenterol Belg* 1994; **57**: 255-259 [PMID: 7810274]

45 **Dugum M**, Zein N, McCullough A, Hanouneh I. Alcoholic hepatitis: Challenges in diagnosis and management. *Cleve Clin J Med* 2015; **82**: 226-236 [PMID: 25955457 DOI: 10.3949/ccjm.82a.14048]

46 **Hardison JE**. Auscultation of the Liver. In: Clinical Methods: The History, Physical, and Laboratory Examinations. Boston: Butterworths; 1990 [PMID: 21250262]

47 **Keating M**, Lardo O, Hansell M. Alcoholic Hepatitis: Diagnosis and Management. *Am Fam Physician* 2022; **105**: 412-420 [PMID: 35426628]

48 **Atkinson SR**, Hamesch K, Spivak I, Guldiken N, Cabezas J, Argemi J, Theurl I, Zoller H, Cao S, Mathurin P, Shah VH, Trautwein C, Bataller R, Thursz MR, Strnad P. Serum Transferrin Is an Independent Predictor of Mortality in Severe Alcoholic Hepatitis. *Am J Gastroenterol* 2020; **115**: 398-405 [PMID: 31985531 DOI: 10.14309/ajg.0000000000000492]

49 **Grillet F**, Calame P, Cervoni JP, Weil D, Thevenot T, Ronot M, Delabrousse E. Non-invasive diagnosis of severe alcoholic hepatitis: Usefulness of cross-sectional imaging. *Diagn Interv Imaging* 2021; **102**: 247-254 [PMID: 33069642 DOI: 10.1016/j.diii.2020.09.009]

50 **European Association for the Study of the Liver**. EASL Clinical Practice Guidelines: Management of alcohol-related liver disease. *J Hepatol* 2018; **69**: 154-181 [PMID: 29628280 DOI: 10.1016/j.jhep.2018.03.018]

51 **Crawford JM**. Histologic findings in alcoholic liver disease. *Clin Liver Dis* 2012; **16**: 699-716 [PMID: 23101978 DOI: 10.1016/j.cld.2012.08.004]

52 **Lefkowitch JH**. Morphology of alcoholic liver disease. *Clin Liver Dis* 2005; **9**: 37-53 [PMID: 15763228 DOI: 10.1016/j.cld.2004.11.001]

53 **Sakhuja P**. Pathology of alcoholic liver disease, can it be differentiated from nonalcoholic steatohepatitis? *World J Gastroenterol* 2014; **20**: 16474-16479 [PMID: 25469015 DOI: 10.3748/wjg.v20.i44.16474]

54 **Theise ND**. Histopathology of alcoholic liver disease. *Clin Liver Dis (Hoboken)* 2013; **2**: 64-67 [PMID: 30992826 DOI: 10.1002/cld.172]

55 **Feldstein AE**, Gores GJ. Apoptosis in alcoholic and nonalcoholic steatohepatitis. *Front Biosci* 2005; **10**: 3093-3099 [PMID: 15970563 DOI: 10.2741/1765]

56 **Denk H**, Stumptner C, Zatloukal K. Mallory bodies revisited. *J Hepatol* 2000; **32**: 689-702 [PMID: 10782920 DOI: 10.1016/S0168-8278(00)80233-0]

57 **Yeh MM**, Brunt EM. Pathology of nonalcoholic fatty liver disease. *Am J Clin Pathol* 2007; **128**: 837-847 [PMID: 17951208 DOI: 10.1309/RTPM1PY6YGBL2G2R]

58 **Tiniakos DG**. Liver biopsy in alcoholic and non-alcoholic steatohepatitis patients. *Gastroenterol Clin Biol* 2009; **33**: 930-939 [PMID: 19646834 DOI: 10.1016/j.gcb.2009.05.009]

59 **Kowdley KV**. Iron Overload in Patients With Chronic Liver Disease. *Gastroenterol Hepatol (N Y)* 2016; **12**: 695-698 [PMID: 28035198]

60 **Eng SC**, Taylor SL, Reyes V, Raaka S, Berger J, Kowdley KV. Hepatic iron overload in alcoholic end-stage liver disease is associated with iron deposition in other organs in the absence of HFE-1 hemochromatosis. *Liver Int* 2005; **25**: 513-517 [PMID: 15910487 DOI: 10.1111/j.1478-3231.2005.01004.x]

61 **Mookerjee RP**, Lackner C, Stauber R, Stadlbauer V, Deheragoda M, Aigelsreiter A, Jalan R. The role of liver biopsy in the diagnosis and prognosis of patients with acute deterioration of alcoholic cirrhosis. *J Hepatol* 2011; **55**: 1103-1111 [PMID: 21376092 DOI: 10.1016/j.jhep.2011.02.021]

62 **Altamirano J**, Miquel R, Katoonizadeh A, Abraldes JG, Duarte-Rojo A, Louvet A, Augustin S, Mookerjee RP, Michelena J, Smyrk TC, Buob D, Leteurtre E, Rincón D, Ruiz P, García-Pagán JC, Guerrero-Marquez C, Jones PD, Barritt AS 4th, Arroyo V, Bruguera M, Bañares R, Ginès P, Caballería J, Roskams T, Nevens F, Jalan R, Mathurin P, Shah VH, Bataller R. A histologic scoring system for prognosis of patients with alcoholic hepatitis. *Gastroenterology* 2014; **146**: 1231-9.e1 [PMID: 24440674 DOI: 10.1053/j.gastro.2014.01.018]

63 **Trépo E**, Goossens N, Fujiwara N, Song WM, Colaprico A, Marot A, Spahr L, Demetter P, Sempoux C, Im GY, Saldarriaga J, Gustot T, Devière J, Thung SN, Minsart C, Sersté T, Bontempi G, Abdelrahman K, Henrion J, Degré D, Lucidi V, Rubbia-Brandt L, Nair VD, Moreno C, Deltenre P, Hoshida Y, Franchimont D. Combination of Gene Expression Signature and Model for End-Stage Liver Disease Score Predicts Survival of Patients With Severe Alcoholic Hepatitis. *Gastroenterology* 2018; **154**: 965-975 [PMID: 29158192 DOI: 10.1053/j.gastro.2017.10.048]

64 **Koulaouzidis A**, Bhat S, Saeed AA. Spontaneous bacterial peritonitis. *World J Gastroenterol* 2009; **15**: 1042-1049 [PMID: 19266595 DOI: 10.3748/wjg.15.1042]

65 **Karakike E**, Moreno C, Gustot T. Infections in severe alcoholic hepatitis. *Ann Gastroenterol* 2017; **30**: 152-160 [PMID: 28243035 DOI: 10.20524/aog.2016.0101]

66 **Orntoft NW**, Sandahl TD, Jepsen P, Vilstrup H. Short-term and long-term causes of death in patients with alcoholic hepatitis in Denmark. *Clin Gastroenterol Hepatol* 2014; **12**: 1739-44.e1 [PMID: 24780287 DOI: 10.1016/j.cgh.2014.04.020]

67 **Markwick LJ**, Riva A, Ryan JM, Cooksley H, Palma E, Tranah TH, Manakkat Vijay GK, Vergis N, Thursz M, Evans A, Wright G, Tarff S, O'Grady J, Williams R, Shawcross DL, Chokshi S. Blockade of PD1 and TIM3 restores innate and adaptive immunity in patients with acute alcoholic hepatitis. *Gastroenterology* 2015; **148**: 590-602.e10 [PMID: 25479137 DOI: 10.1053/j.gastro.2014.11.041]

68 **Falagas ME**, Kompoti M. Obesity and infection. *Lancet Infect Dis* 2006; **6**: 438-446 [PMID: 16790384 DOI: 10.1016/S1473-3099(06)70523-0]

69 **Leclerc M**, Lanot A, Béchade C, Le Naoures C, Comoz F, Lobbedez T. [Bile salt nephropathy/cholemic nephrosis]. *Nephrol Ther* 2016; **12**: 460-462 [PMID: 27262935 DOI: 10.1016/j.nephro.2016.03.002]

70 **Ginès P**, Solà E, Angeli P, Wong F, Nadim MK, Kamath PS. Hepatorenal syndrome. *Nat Rev Dis Primers* 2018; **4**: 23 [PMID: 30213943 DOI: 10.1038/s41572-018-0022-7]

71 **Francoz C**, Durand F, Kahn JA, Genyk YS, Nadim MK. Hepatorenal Syndrome. *Clin J Am Soc Nephrol* 2019; **14**: 774-781 [PMID: 30996046 DOI: 10.2215/CJN.12451018]

72 **Altamirano J**, Fagundes C, Dominguez M, García E, Michelena J, Cárdenas A, Guevara M, Pereira G, Torres-Vigil K, Arroyo V, Caballería J, Ginès P, Bataller R. Acute kidney injury is an early predictor of mortality for patients with alcoholic hepatitis. *Clin Gastroenterol Hepatol* 2012; **10**: 65-71.e3 [PMID: 21946124 DOI: 10.1016/j.cgh.2011.09.011]

73 **Wang H**, Liu A, Bo W, Feng X, Hu Y. Terlipressin in the treatment of hepatorenal syndrome: A systematic review and meta-analysis. *Medicine (Baltimore)* 2018; **97**: e0431 [PMID: 29668606 DOI: 10.1097/MD.0000000000010431]

74 **Parker R**, Kim SJ, Im GY, Nahas J, Dhesi B, Vergis N, Sinha A, Ghezzi A, Rink MR, McCune A, Aithal GP, Newsome PN, Weston CJ, Holt A, Gao B. Obesity in acute alcoholic hepatitis increases morbidity and mortality. *EBioMedicine* 2019; **45**: 511-518 [PMID: 31278069 DOI: 10.1016/j.ebiom.2019.03.046]

75 **Liang W**, Chikritzhs T, Pascal R, Binns CW. Mortality rate of alcoholic liver disease and risk of hospitalization for alcoholic liver cirrhosis, alcoholic hepatitis and alcoholic liver failure in Australia between 1993 and 2005. *Intern Med J* 2011; **41**: 34-41 [PMID: 20546060 DOI: 10.1111/j.1445-5994.2010.02279.x]

76 **Jalan R**, Gines P, Olson JC, Mookerjee RP, Moreau R, Garcia-Tsao G, Arroyo V, Kamath PS. Acute-on chronic liver failure. *J Hepatol* 2012; **57**: 1336-1348 [PMID: 22750750 DOI: 10.1016/j.jhep.2012.06.026]

77 **Michelena J**, Altamirano J, Abraldes JG, Affò S, Morales-Ibanez O, Sancho-Bru P, Dominguez M, García-Pagán JC, Fernández J, Arroyo V, Ginès P, Louvet A, Mathurin P, Mehal WZ, Caballería J, Bataller R. Systemic inflammatory response and serum lipopolysaccharide levels predict multiple organ failure and death in alcoholic hepatitis. *Hepatology* 2015; **62**: 762-772 [PMID: 25761863 DOI: 10.1002/hep.27779]

78 **Arroyo V**, Moreau R, Jalan R. Acute-on-Chronic Liver Failure. *N Engl J Med* 2020; **382**: 2137-2145 [PMID: 32459924 DOI: 10.1056/NEJMra1914900]

79 **Bodzin AS**, Baker TB. Liver Transplantation Today: Where We Are Now and Where We Are Going. *Liver Transpl* 2018; **24**: 1470-1475 [PMID: 30080954 DOI: 10.1002/lt.25320]

80 **Jadlowiec CC**, Taner T. Liver transplantation: Current status and challenges. *World J Gastroenterol* 2016; **22**: 4438-4445 [PMID: 27182155 DOI: 10.3748/wjg.v22.i18.4438]

81 **Yu CH**, Xu CF, Ye H, Li L, Li YM. Early mortality of alcoholic hepatitis: a review of data from placebo-controlled clinical trials. *World J Gastroenterol* 2010; **16**: 2435-2439 [PMID: 20480532 DOI: 10.3748/wjg.v16.i19.2435]

82 **Bennett K**, Enki DG, Thursz M, Cramp ME, Dhanda AD. Systematic review with meta-analysis: high mortality in patients with non-severe alcoholic hepatitis. *Aliment Pharmacol Ther* 2019; **50**: 249-257 [PMID: 31231848 DOI: 10.1111/apt.15376]

83 **Bird GL**, Williams R. Factors determining cirrhosis in alcoholic liver disease. *Mol Aspects Med* 1988; **10**: 97-105 [PMID: 3067028 DOI: 10.1016/0098-2997(88)90017-9]

84 **Alexander JF**, Lischner MW, Galambos JT. Natural history of alcoholic hepatitis. II. The long-term prognosis. *Am J Gastroenterol* 1971; **56**: 515-525 [PMID: 5134879]

85 **Rehm J**, Taylor B, Mohapatra S, Irving H, Baliunas D, Patra J, Roerecke M. Alcohol as a risk factor for liver cirrhosis: a systematic review and meta-analysis. *Drug Alcohol Rev* 2010; **29**: 437-445 [PMID: 20636661 DOI: 10.1111/j.1465-3362.2009.00153.x]

86 **Parés A**, Caballería J, Bruguera M, Torres M, Rodés J. Histological course of alcoholic hepatitis. Influence of abstinence, sex and extent of hepatic damage. *J Hepatol* 1986; **2**: 33-42 [PMID: 3950362 DOI: 10.1016/S0168-8278(86)80006-X]

87 **Maddrey WC**, Boitnott JK, Bedine MS, Weber FL Jr, Mezey E, White RI Jr. Corticosteroid therapy of alcoholic hepatitis. *Gastroenterology* 1978; **75**: 193-199 [PMID: 352788]

88 **Louvet A**, Naveau S, Abdelnour M, Ramond MJ, Diaz E, Fartoux L, Dharancy S, Texier F, Hollebecque A, Serfaty L, Boleslawski E, Deltenre P, Canva V, Pruvot FR, Mathurin P. The Lille model: a new tool for therapeutic strategy in patients with severe alcoholic hepatitis treated with steroids. *Hepatology* 2007; **45**: 1348-1354 [PMID: 17518367 DOI: 10.1002/hep.21607]

89 **Kamath PS**, Kim WR; Advanced Liver Disease Study Group. The model for end-stage liver disease (MELD). *Hepatology* 2007; **45**: 797-805 [PMID: 17326206 DOI: 10.1002/hep.21563]

90 **Morales-Arráez D**, Ventura-Cots M, Altamirano J, Abraldes JG, Cruz-Lemini M, Thursz MR, Atkinson SR, Sarin SK, Kim W, Chavez-Araujo R, Higuera-de la Tijera MF, Singal AK, Shah VH, Kamath PS, Duarte-Rojo A, Charles EA, Vargas V, Jager M, Rautou PE, Rincon D, Zamarripa F, Restrepo-Gutiérrez JC, Torre A, Lucey MR, Arab JP, Mathurin P, Louvet A, García-Tsao G, González JA, Verna EC, Brown RS Jr, Argemi J, Fernández-Carrillo C, Clemente A, Alvarado-Tapias E, Forrest E, Allison M, Bataller R. The MELD Score Is Superior to the Maddrey Discriminant Function Score to Predict Short-Term Mortality in Alcohol-Associated Hepatitis: A Global Study. *Am J Gastroenterol* 2022; **117**: 301-310 [PMID: 34962498 DOI: 10.14309/ajg.0000000000001596]

91 **Srikureja W**, Kyulo NL, Runyon BA, Hu KQ. MELD score is a better prognostic model than Child-Turcotte-Pugh score or Discriminant Function score in patients with alcoholic hepatitis. *J Hepatol* 2005; **42**: 700-706 [PMID: 15826720 DOI: 10.1016/j.jhep.2004.12.022]

92 **Dunn W**, Jamil LH, Brown LS, Wiesner RH, Kim WR, Menon KV, Malinchoc M, Kamath PS, Shah V. MELD accurately predicts mortality in patients with alcoholic hepatitis. *Hepatology* 2005; **41**: 353-358 [PMID: 15660383 DOI: 10.1002/hep.20503]

93 **Sheth M**, Riggs M, Patel T. Utility of the Mayo End-Stage Liver Disease (MELD) score in assessing prognosis of patients with alcoholic hepatitis. *BMC Gastroenterol* 2002; **2**: 2 [PMID: 11835693 DOI: 10.1186/1471-230X-2-2]

94 **Peng Y**, Qi X, Guo X. Child-Pugh Versus MELD Score for the Assessment of Prognosis in Liver Cirrhosis: A Systematic

Review and Meta-Analysis of Observational Studies. *Medicine (Baltimore)* 2016; **95**: e2877 [PMID: 26937922 DOI: 10.1097/MD.0000000000002877]

95 **Forrest EH**, Evans CD, Stewart S, Phillips M, Oo YH, McAvoy NC, Fisher NC, Singhal S, Brind A, Haydon G, O'Grady J, Day CP, Hayes PC, Murray LS, Morris AJ. Analysis of factors predictive of mortality in alcoholic hepatitis and derivation and validation of the Glasgow alcoholic hepatitis score. *Gut* 2005; **54**: 1174-1179 [PMID: 16009691 DOI: 10.1136/gut.2004.050781]

96 **Dominguez M**, Rincón D, Abraldes JG, Miquel R, Colmenero J, Bellot P, García-Pagán JC, Fernández R, Moreno M, Bañares R, Arroyo V, Caballería J, Ginès P, Bataller R. A new scoring system for prognostic stratification of patients with alcoholic hepatitis. *Am J Gastroenterol* 2008; **103**: 2747-2756 [PMID: 18721242 DOI: 10.1111/j.1572-0241.2008.02104.x]

97 **Lackner C**, Spindelboeck W, Haybaeck J, Douschan P, Rainer F, Terracciano L, Haas J, Berghold A, Bataller R, Stauber RE. Histological parameters and alcohol abstinence determine long-term prognosis in patients with alcoholic liver disease. *J Hepatol* 2017; **66**: 610-618 [PMID: 27894795 DOI: 10.1016/j.jhep.2016.11.011]

98 **Xie YD**, Feng B, Gao Y, Wei L. Effect of abstinence from alcohol on survival of patients with alcoholic cirrhosis: A systematic review and meta-analysis. *Hepatol Res* 2014; **44**: 436-449 [PMID: 23607793 DOI: 10.1111/hepr.12131]

99 **Diehl AM**. Alcoholic liver disease: natural history. *Liver Transpl Surg* 1997; **3**: 206-211 [PMID: 9346741 DOI: 10.1002/Lt.500030303]

100 **Dugum M**, McCullough A. Diagnosis and Management of Alcoholic Liver Disease. *J Clin Transl Hepatol* 2015; **3**: 109-116 [PMID: 26356792 DOI: 10.14218/JCTH.2015.00008]

101 **Morley KC**, Baillie A, Fraser I, Furneaux-Bate A, Dore G, Roberts M, Abdalla A, Phung N, Haber PS. Baclofen in the treatment of alcohol dependence with or without liver disease: multisite, randomised, double-blind, placebo-controlled trial. *Br J Psychiatry* 2018; **212**: 362-369 [PMID: 29716670 DOI: 10.1192/bjp.2018.13]

102 **McClain CJ**, Barve SS, Barve A, Marsano L. Alcoholic liver disease and malnutrition. *Alcohol Clin Exp Res* 2011; **35**: 815-820 [PMID: 21284673 DOI: 10.1111/j.1530-0277.2010.01405.x]

103 **Bertha M**, Choi G, Mellinger J. Diagnosis and Treatment of Alcohol-Associated Liver Disease: A Patient-Friendly Summary of the 2019 AASLD Guidelines. *Clin Liver Dis (Hoboken)* 2021; **17**: 418-423 [PMID: 34386207 DOI: 10.1002/cld.1129]

104 **DiCecco SR**, Francisco-Ziller N. Nutrition in alcoholic liver disease. *Nutr Clin Pract* 2006; **21**: 245-254 [PMID: 16772542 DOI: 10.1177/0115426506021003245]

105 **Mitchell MC**, Friedman LS, McClain CJ. Medical Management of Severe Alcoholic Hepatitis: Expert Review from the Clinical Practice Updates Committee of the AGA Institute. *Clin Gastroenterol Hepatol* 2017; **15**: 5-12 [PMID: 27979049 DOI: 10.1016/j.cgh.2016.08.047]

106 **Biggins SW**, Angeli P, Garcia-Tsao G, Ginès P, Ling SC, Nadim MK, Wong F, Kim WR. Diagnosis, Evaluation, and Management of Ascites, Spontaneous Bacterial Peritonitis and Hepatorenal Syndrome: 2021 Practice Guidance by the American Association for the Study of Liver Diseases. *Hepatology* 2021; **74**: 1014-1048 [PMID: 33942342 DOI: 10.1002/hep.31884]

107 Benzodiazepines. 2017. In: LiverTox: Clinical and Research Information on Drug-Induced Liver Injury [Internet]. Bethesda (MD): National Institute of Diabetes and Digestive and Kidney Diseases; 2012 [PMID: 31643176]

108 **Peppers MP**. Benzodiazepines for alcohol withdrawal in the elderly and in patients with liver disease. *Pharmacotherapy* 1996; **16**: 49-57 [PMID: 8700792]

109 **Thursz MR**, Richardson P, Allison M, Austin A, Bowers M, Day CP, Downs N, Gleeson D, MacGilchrist A, Grant A, Hood S, Masson S, McCune A, Mellor J, O'Grady J, Patch D, Ratcliffe I, Roderick P, Stanton L, Vergis N, Wright M, Ryder S, Forrest EH; STOPAH Trial. Prednisolone or pentoxifylline for alcoholic hepatitis. *N Engl J Med* 2015; **372**: 1619-1628 [PMID: 25901427 DOI: 10.1056/NEJMoa1412278]

110 **Mathurin P**, O'Grady J, Carithers RL, Phillips M, Louvet A, Mendenhall CL, Ramond MJ, Naveau S, Maddrey WC, Morgan TR. Corticosteroids improve short-term survival in patients with severe alcoholic hepatitis: meta-analysis of individual patient data. *Gut* 2011; **60**: 255-260 [PMID: 20940288 DOI: 10.1136/gut.2010.224097]

111 **Louvet A**, Thursz MR, Kim DJ, Labreuche J, Atkinson SR, Sidhu SS, O'Grady JG, Akriviadis E, Sinakos E, Carithers RL Jr, Ramond MJ, Maddrey WC, Morgan TR, Duhamel A, Mathurin P. Corticosteroids Reduce Risk of Death Within 28 Days for Patients With Severe Alcoholic Hepatitis, Compared With Pentoxifylline or Placebo-a Meta-analysis of Individual Data From Controlled Trials. *Gastroenterology* 2018; **155**: 458-468.e8 [PMID: 29738698 DOI: 10.1053/j.gastro.2018.05.011]

112 **Levitsky J**, Mailliard ME. Diagnosis and therapy of alcoholic liver disease. *Semin Liver Dis* 2004; **24**: 233-247 [PMID: 15349802 DOI: 10.1055/s-2004-832937]

113 **Sohail U**, Satapathy SK. Diagnosis and management of alcoholic hepatitis. *Clin Liver Dis* 2012; **16**: 717-736 [PMID: 23101979 DOI: 10.1016/j.cld.2012.08.005]

114 **Sougioultzis S**, Dalakas E, Hayes PC, Plevris JN. Alcoholic hepatitis: from pathogenesis to treatment. *Curr Med Res Opin* 2005; **21**: 1337-1346 [PMID: 16197651 DOI: 10.1185/030079905X56493]

115 **Hmoud BS**, Patel K, Bataller R, Singal AK. Corticosteroids and occurrence of and mortality from infections in severe alcoholic hepatitis: a meta-analysis of randomized trials. *Liver Int* 2016; **36**: 721-728 [PMID: 26279269 DOI: 10.1111/liv.12939]

116 **Im GY**, Cameron AM, Lucey MR. Liver transplantation for alcoholic hepatitis. *J Hepatol* 2019; **70**: 328-334 [PMID: 30658734 DOI: 10.1016/j.jhep.2018.11.007]

117 **Mathurin P**, Moreno C, Samuel D, Dumortier J, Salleron J, Durand F, Castel H, Duhamel A, Pageaux GP, Leroy V, Dharancy S, Louvet A, Boleslawski E, Lucidi V, Gustot T, Francoz C, Letoublon C, Castaing D, Belghiti J, Donckier V, Pruvot FR, Duclos-Vallée JC. Early liver transplantation for severe alcoholic hepatitis. *N Engl J Med* 2011; **365**: 1790-1800 [PMID: 22070476 DOI: 10.1056/NEJMoa1105703]

118 **Weeks SR**, Sun Z, McCaul ME, Zhu H, Anders RA, Philosophe B, Ottmann SE, Garonzik Wang JM, Gurakar AO, Cameron AM. Liver Transplantation for Severe Alcoholic Hepatitis, Updated Lessons from the World's Largest Series. *J*

Am Coll Surg 2018; **226**: 549-557 [PMID: 29409981 DOI: 10.1016/j.jamcollsurg.2017.12.044]

119 **Lee BP**, Mehta N, Platt L, Gurakar A, Rice JP, Lucey MR, Im GY, Therapondos G, Han H, Victor DW, Fix OK, Dinges L, Dronamraju D, Hsu C, Voigt MD, Rinella ME, Maddur H, Eswaran S, Hause J, Foley D, Ghobrial RM, Dodge JL, Li Z, Terrault NA. Outcomes of Early Liver Transplantation for Patients With Severe Alcoholic Hepatitis. *Gastroenterology* 2018; **155**: 422-430.e1 [PMID: 29655837 DOI: 10.1053/j.gastro.2018.04.009]

120 **Herrick-Reynolds KM**, Punchhi G, Greenberg RS, Strauss AT, Boyarsky BJ, Weeks-Groh SR, Krach MR, Anders RA, Gurakar A, Chen PH, Segev DL, King EA, Philosophe B, Ottman SE, Wesson RN, Garonzik-Wang JM, Cameron AM. Evaluation of Early vs Standard Liver Transplant for Alcohol-Associated Liver Disease. *JAMA Surg* 2021; **156**: 1026-1034 [PMID: 34379106 DOI: 10.1001/jamasurg.2021.3748]

121 **Mitchell M**. Efficacy study of anakinra, pentoxifylline, and zinc compared to methylprednisolone in severe acute alcoholic hepatitis. [accessed 2022 Dec 16]. In: ClinicalTrials.gov [Internet]. Bethesda (MD): U.S. National Library of Medicine. Available from: https://clinicaltrials.gov/ct2/show/NCT01809132 ClinicalTrials.gov Identifier: NCT01809132

122 **Gawrieh S**. Trial of Anakinra (Plus Zinc) or Prednisone in Patients With Severe Alcoholic Hepatitis. [accessed 2022 Dec 16]. In: ClinicalTrials.gov [Internet]. Bethesda (MD): U.S. National Library of Medicine. Available from: https://clinicaltrials.gov/ct2/show/NCT04072822 ClinicalTrials.gov Identifier: NCT04072822

123 **Imperial College London**. IL-1 Signal Inhibition in Alcoholic Hepatitis [accessed 2022 Dec 16]. In: ClinicalTrials.gov [Internet]. Bethesda (MD): U.S. National Library of Medicine. Available from: https://clinicaltrials.gov/ct2/show/NCT03775109 ClinicalTrials.gov Identifier: NCT03775109

124 **Imperial College London**. N-ACetylcysteine to Reduce Infection and Mortality for Alcoholic Hepatitis [accessed 2022 Dec 16]. In: ClinicalTrials.gov [Internet]. Bethesda (MD): U.S. National Library of Medicine. Available from: https://clinicaltrials.gov/ct2/show/NCT03069300 ClinicalTrials.gov Identifier: NCT03069300

125 **Mendler MH**. Randomized, Controlled Trial of S-adenosylmethionine in Alcoholic Liver Disease. [accessed 2022 Dec 16]. In: ClinicalTrials.gov [Internet]. Bethesda (MD): U.S. National Library of Medicine. Available from: https://clinicaltrials.gov/ct2/show/NCT00851981 ClinicalTrials.gov Identifier: NCT00851981

126 **Cheng J**. Efficacy and Safety of S-adenosyl-l-methionine in Treatment of Alcoholic Hepatitis With Cholestasis. [accessed 2022 Dec 16]. In: ClinicalTrials.gov [Internet]. Bethesda (MD): U.S. National Library of Medicine. Available from: https://clinicaltrials.gov/ct2/show/NCT02024295 ClinicalTrials.gov Identifier: NCT02024295

127 **Gordon R**. A Research Study to Assess the Safety, Pharmacokinetics and Pharmacodynamics of DUR-928 in Patients With Alcoholic Hepatitis. [accessed 2022 Dec 16]. In: ClinicalTrials.gov [Internet]. Bethesda (MD): U.S. National Library of Medicine. Available from: https://clinicaltrials.gov/ct2/show/NCT03432260 ClinicalTrials.gov Identifier: NCT03432260

128 **McClain CJ**. DUR-928 in Patients With Alcoholic Hepatitis. [accessed 2022 Dec 16]. In: ClinicalTrials.gov [Internet]. Bethesda (MD): U.S. National Library of Medicine. Available from: https://clinicaltrials.gov/ct2/show/NCT03917407 ClinicalTrials.gov Identifier: NCT03917407

129 **Kim DJ**. Efficacy and Safety of G-CSF in Patients With Severe Alcoholic Hepatitis With Null or Partial Response to Steroid. [accessed 2022 Dec 16]. In: ClinicalTrials.gov [Internet]. Bethesda (MD): U.S. National Library of Medicine. Available from: https://clinicaltrials.gov/ct2/show/NCT02442180 ClinicalTrials.gov Identifier: NCT02442180

130 **Singh V**. GCSF in Alcoholic Hepatitis. [accessed 2022 Dec 16]. In: ClinicalTrials.gov [Internet]. Bethesda (MD): U.S. National Library of Medicine. Available from: https://clinicaltrials.gov/ct2/show/NCT03703674 ClinicalTrials.gov Identifier: NCT03703674

131 **Mishra A**. Efficacy of Monotherapy vs Combination Therapy of Corticosteroids With GCSF in Severe Alcoholic Hepatitis Patients. [accessed 2022 Dec 16]. In: ClinicalTrials.gov [Internet]. Bethesda (MD): U.S. National Library of Medicine. Available from: https://clinicaltrials.gov/ct2/show/NCT04066179 ClinicalTrials.gov Identifier: NCT04066179

132 **Shah V**. Use of F-652 in Patients With Alcoholic Hepatitis [accessed 2022 Dec 16]. In: ClinicalTrials.gov [Internet]. Bethesda (MD): U.S. National Library of Medicine. Available from: https://clinicaltrials.gov/ct2/show/NCT02655510 ClinicalTrials.gov Identifier: NCT02655510

133 **Stoy S**. Protective Immune Mechanisms in Alcoholic Hepatitis. [accessed 2022 Dec 16]. In: ClinicalTrials.gov [Internet]. Bethesda (MD): U.S. National Library of Medicine. Available from: https://clinicaltrials.gov/ct2/show/NCT01918462 ClinicalTrials.gov Identifier: NCT01918462

134 **Chalasani N**. Trial of Obeticholic Acid in Patients With Moderately Severe Alcoholic Hepatitis (AH). [accessed 2022 Dec 16]. In: ClinicalTrials.gov [Internet]. Bethesda (MD): U.S. National Library of Medicine. Available from: https://clinicaltrials.gov/ct2/show/NCT02039219 ClinicalTrials.gov Identifier: NCT02039219

135 **Vargas V**. Effects of Rifaximin in Patients With Acute Alcoholic Hepatitis. [accessed 2022 Dec 16]. In: ClinicalTrials.gov [Internet]. Bethesda (MD): U.S. National Library of Medicine. Available from: https://clinicaltrials.gov/ct2/show/NCT02116556 ClinicalTrials.gov Identifier: NCT02116556

136 **Song DS**. Rifaximin Use in Severe Alcoholic Hepatitis. [accessed 2022 Dec 16]. In: ClinicalTrials.gov [Internet]. Bethesda (MD): U.S. National Library of Medicine. Available from: https://clinicaltrials.gov/ct2/show/NCT02485106 ClinicalTrials.gov Identifier: NCT02485106

137 **Sanyal A**. Safety and Efficacy of IMM 124-E for Patients With Severe Alcoholic Hepatitis. [accessed 2022 Dec 16]. In: ClinicalTrials.gov [Internet]. Bethesda (MD): U.S. National Library of Medicine. Available from: https://clinicaltrials.gov/ct2/show/NCT01968382 ClinicalTrials.gov Identifier: NCT01968382

138 **Sidhu S**. Comparison of Bovine Colostrum Versus Placebo in Treatment of Severe Alcoholic Hepatitis: A Randomized Double Blind Controlled Trial. [accessed 2022 Dec 16]. In: ClinicalTrials.gov [Internet]. Bethesda (MD): U.S. National Library of Medicine. Available from: https://clinicaltrials.gov/ct2/show/NCT02473341 ClinicalTrials.gov Identifier: NCT02473341

139 **Mitchell M**. Novel Therapies in Moderately Severe Acute Alcoholic Hepatitis. [accessed 2022 Dec 16]. In: ClinicalTrials.gov [Internet]. Bethesda (MD): U.S. National Library of Medicine. Available from: https://clinicaltrials.gov/ct2/show/NCT01922895 ClinicalTrials.gov Identifier: NCT01922895

140 **Suk KT**. Effect of Probiotics on Gut-Liver Axis of Alcoholic Hepatitis. [accessed 2022 Dec 16]. In: ClinicalTrials.gov [Internet]. Bethesda (MD): U.S. National Library of Medicine. Available from: https://clinicaltrials.gov/ct2/show/NCT02335632 ClinicalTrials.gov Identifier: NCT02335632

141 **Institute of Liver and Biliary Sciences**. Pentoxyphilline Versus Fecal Microbiota Therapy in Severe Alcoholic Hepatitis. [accessed 2022 Dec 16]. In: ClinicalTrials.gov [Internet]. Bethesda (MD): U.S. National Library of Medicine. Available from: https://clinicaltrials.gov/ct2/show/NCT02458079 ClinicalTrials.gov Identifier: NCT02458079

142 **Institute of Liver and Biliary Sciences**. A Comparison of Fecal Microbiota Transplantation and Steroid Therapy in Patients With Severe Alcoholic Hepatitis. [accessed 2022 Dec 16]. In: ClinicalTrials.gov [Internet]. Bethesda (MD): U.S. National Library of Medicine. Available from: https://clinicaltrials.gov/ct2/show/NCT03091010 ClinicalTrials.gov Identifier: NCT03091010

143 **Dhiman RK**. Fecal Microbiota Transplantation in Severe Alcoholic Hepatitis- Assessment of Impact on Prognosis and Short-term Outcome. [accessed 2022 Dec 16]. In: ClinicalTrials.gov [Internet]. India: U.S. National Library of Medicine. Available from: https://clinicaltrials.gov/ct2/show/NCT03827772 ClinicalTrials.gov Identifier: NCT03827772

World Journal of Gastroenterology

Submit a Manuscript: https://www.f6publishing.com

World J Gastroenterol 2023 May 7; 29(17): 2571-2599

DOI: 10.3748/wjg.v29.i17.2571

ISSN 1007-9327 (print) ISSN 2219-2840 (online)

REVIEW

Current and novel approaches in the pharmacological treatment of hepatocellular carcinoma

Fernanda Villarruel-Melquiades, María Eugenia Mendoza-Garrido, Claudia M García-Cuellar, Yesennia Sánchez-Pérez, Julio Isael Pérez-Carreón, Javier Camacho

Specialty type: Gastroenterology and hepatology

Provenance and peer review: Invited article; Externally peer reviewed.

Peer-review model: Single blind

Peer-review report's scientific quality classification

Grade A (Excellent): 0
Grade B (Very good): B, B
Grade C (Good): C
Grade D (Fair): 0
Grade E (Poor): 0

P-Reviewer: Bao YZ, China; Han J, China; Wang C, China

Received: December 27, 2022
Peer-review started: December 27, 2022
First decision: January 11, 2023
Revised: January 19, 2023
Accepted: April 11, 2023
Article in press: April 11, 2023
Published online: May 7, 2023

Fernanda Villarruel-Melquiades, Javier Camacho, Departamento de Farmacología, Centro de Investigación y de Estudios Avanzados del Instituto Politécnico Nacional (CINVESTAV-IPN), Mexico City 07360, Mexico

María Eugenia Mendoza-Garrido, Departamento de Fisiología, Biofísica y Neurociencias, Centro de Investigación y de Estudios Avanzados del Instituto Politécnico Nacional (CINVESTAV-IPN), Mexico City 07360, Mexico

Claudia M García-Cuellar, Yesennia Sánchez-Pérez, Subdirección de Investigación Básica, Instituto Nacional de Cancerología (INCan), Mexico City 14080, Mexico

Julio Isael Pérez-Carreón, Instituto Nacional de Medicina Genómica, Instituto Nacional de Medicina Genómica (INMEGEN), Mexico City 14610, Mexico

Corresponding author: Javier Camacho, BSc, MSc, PhD, Research Scientist, Departamento de Farmacología, Centro de Investigación y de Estudios Avanzados del Instituto Politécnico Nacional (CINVESTAV-IPN), Avenida Instituto Politécnico Nacional 2508, Mexico City 07360, Mexico. fcamacho@cinvestav.mx

Abstract

Hepatocellular carcinoma (HCC) is one of the most lethal malignant tumours worldwide. The mortality-to-incidence ratio is up to 91.6% in many countries, representing the third leading cause of cancer-related deaths. Systemic drugs, including the multikinase inhibitors sorafenib and lenvatinib, are first-line drugs used in HCC treatment. Unfortunately, these therapies are ineffective in most cases due to late diagnosis and the development of tumour resistance. Thus, novel pharmacological alternatives are urgently needed. For instance, immune checkpoint inhibitors have provided new approaches targeting cells of the immune system. Furthermore, monoclonal antibodies against programmed cell death-1 have shown benefits in HCC patients. In addition, drug combinations, including first-line treatment and immunotherapy, as well as drug repurposing, are promising novel therapeutic alternatives. Here, we review the current and novel pharmacological approaches to fight HCC. Preclinical studies, as well as approved and ongoing clinical trials for liver cancer treatment, are discussed. The pharmacological opportunities analysed here should lead to significant improvement in HCC therapy.

Key Words: Liver cancer; Systemic therapy; Immunotherapy; Drug repurposing; Drug combinations; Hepatocellular carcinoma

Core Tip: Hepatocellular carcinoma (HCC) is one of the most lethal malignant tumours worldwide. Unfortunately, most HCC cases are diagnosed at an advanced stage, and "curative" options are not suggested for these patients. The best option is to start with drug therapy, with sorafenib and lenvatinib as the first-choice drugs. However, most patients do not respond to these treatments; therefore, new therapeutic strategies are urgently needed. Here, we review current potential and novel pharmacological approaches, including immunotherapy, drug combination, and drug repositioning, that should help to improve the prognosis of HCC patients.

Citation: Villarruel-Melquiades F, Mendoza-Garrido ME, García-Cuellar CM, Sánchez-Pérez Y, Pérez-Carreón JI, Camacho J. Current and novel approaches in the pharmacological treatment of hepatocellular carcinoma. *World J Gastroenterol* 2023; 29(17): 2571-2599
URL: https://www.wjgnet.com/1007-9327/full/v29/i17/2571.htm
DOI: https://dx.doi.org/10.3748/wjg.v29.i17.2571

INTRODUCTION

Liver cancer ranks seventh in incidence and fourth in mortality worldwide. It is one of the malignancies with the highest mortality-to-incidence ratio, reaching up to 91.6%, according to the World Health Organization[1]. This cancer frequently occurs in association with chronic liver disease and is classified according to the cells of origin of the tumour. Hepatocellular carcinoma (HCC) is the most common, originating in hepatocytes and accounting for 75%-85% of all cases[2].

The main risk factors for developing HCC are chronic liver disease, such as non-alcoholic fatty liver disease and non-alcoholic steatohepatitis, as well as hepatitis B (HBV) and C virus (HCV) infections[3]. In addition, some habits, including excessive alcohol consumption and smoking, are also considered major risk factors for developing HCC[2].

The most appropriate management in clinical practice depends on the stage of the disease. At an early or even intermediate stage, the treatment options currently available are surgical methods (liver resection and transplantation), locoregional therapy (radiofrequency ablation), and transarterial chemoembolization therapy[4]. The 5-year survival rate for patients at these stages is 14%, and only 30% can be subjected to curative treatment. Unfortunately, most diagnoses are made when HCC is at an advanced stage, and treatment options are no longer viable[5,6]; pharmacological therapy is suggested in these cases. Chemotherapy is a potential treatment for these patients, but the main disadvantage is that such agents target both cancer and healthy cells, leading to unwanted events that can even endanger the life of the patient. The use of chemotherapeutic agents in monotherapy is ineffective; therefore, more effective and directed drugs are urgently needed. A new generation of treatments called “targeted therapy” (also known as “systemic therapy”) aims to specifically target some molecular features that provide malignant advantages to cancer cells while having low toxicity to non-cancerous cells[7,8]. Table 1 summarizes the recommended HCC management based on the Barcelona Clinic Liver Cancer strategy (BCLC), the most widely used liver cancer staging system. This system has five stages depending on disease extension, liver function, and performance status (Table 1)[9-11].

Systemic therapy is the standard treatment for advanced-stage disease (BCLC stage C). This type of treatment is classified into first- and second-line therapies, and its use in clinical practice depends on the individual patient characteristics. To date, many potential drug targets for the treatment of HCC have been investigated; the most critical targets are listed below and represented in Figure 1[8].

Growth factors and their receptors include vascular endothelial growth factor (VEGF), fibroblast growth factor (FGF), platelet-derived growth factor (PDGF), epidermal growth factor (EGF), mesenchymal-epithelial transition factor (c-Met), insulin-like growth factor, and transforming growth factor α (TGF-α).

Intracellular signalling pathways include phosphoinositide 3-kinase (PI3K)/Akt/mechanistic target of rapamycin (mTOR), RAS/RAF/MEK/ERK, Janus kinase (JAK)/signal transducer and activator of transcription (STAT), and Wnt/β-catenin and the Hedgehog pathway. There are also cell cycle regulators such as CDKs. Transcription factors include nuclear factor kB (NF-kB), activating protein-1 and cyclic AMP response element binding (CREB).

Table 1 Barcelona Clinic Liver Cancer staging system and treatment strategy

Stage	Very early stage (0)	Early stage (A)	Intermediate stage (B)	Advanced stage (C)	Terminal stage (D)
Characteristics	Single nodule < 2 cm, preserved liver function, ECOG PS 0	Single or 2-3 nodules < 3 cm, preserved liver function, ECOG PS 0	Multinodular, unresectable, preserved liver function, ECOG PS 0	Portal invasion/extrahepatic spread, preserved liver function, ECOG PS 1-2	Not transplantable HCC, end-stage liver function, ECOG PS 3-4
Treatment	Ablation, resection, transplant		Chemoembolization	Systemic therapy	Best supportive care
Survival	> 5 yr		> 2.5 yr	> 2 yr	3 mo

ECOG PS: Eastern Cooperative Oncology Group performance status; HCC: Hepatocellular carcinoma.

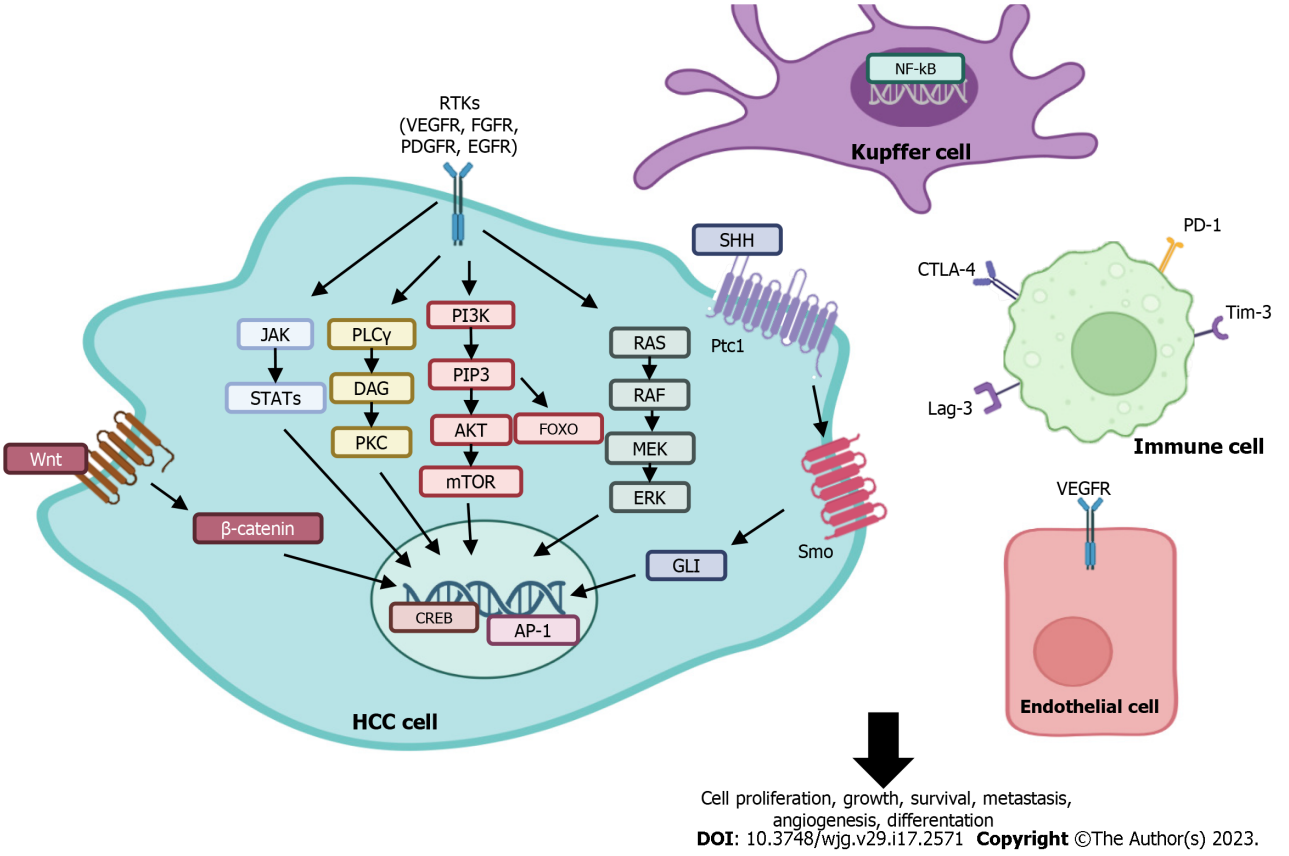

DOI: 10.3748/wjg.v29.i17.2571

Figure 1 Critical signalling pathways involved in hepatocellular carcinoma progression. Systemic therapy primarily targets signalling pathways triggered by tyrosine kinase receptors expressed on tumour cells, which are known to play an essential role in liver carcinogenesis. However, Wnt/B-catenin and Smo (hedgehog pathway) signalling are also important components in liver cancer development. Furthermore, Kupffer cells, immune cells, and endothelial cells are part of the tumour microenvironment, and activation of critical signalling pathways in these cells may also contribute to cancer development. Indeed, the expression of immune checkpoint molecules (cytotoxic T-lymphocyte-associated protein 4, programmed cell death protein 1, Lag-3, Tim-3) on the surface of immune cells play an essential role in the development of hepatocellular carcinoma (discussed in the main text). RTK: Receptor tyrosine kinase; VEGFR: Vascular endothelial growth factor receptor; FGFR: Fibroblast growth factor receptor; PDGFR: Platelet-derived growth factor receptors; EGFR: Endothelial growth factor receptor; JAK: Janus kinase; STAT: Signal transducer and activator of transcription; PLCγ: Phospholipase C-γ; DAG: Diacylglycerol; PKC: Protein kinase C; PI3K: Phosphoinositide 3-kinase; PIP3: phosphatidylinositol 3,4,5-trisphosphate; mTOR: Mechanistic target of rapamycin; FOXO: Forkhead box O; AP-1: Activating protein-1; CREB: Cyclic AMP response element binding; NF-kB: Nuclear factor kB; CTLA-4: Cytotoxic T-lymphocyte-associated protein 4; PD-1: Programmed cell death protein 1.

Next, first- and second-line systemic therapies approved for advanced HCC, as well as those drugs and targets under investigation for treating the disease, are described and discussed in detail and summarized in Table 2.

Table 2 Summary of first and second-line drugs approved for the treatment of advanced hepatocellular carcinoma

Drug	Pharmacological target	Trial (NCT)	Treatment arm	Control arm
First-line				
Systemic therapy				
Sorafenib	VEGF 1-3, PDGF, KIT, FLT3, BRAF, RAF	SHARP (NCT00105443)	Sorafenib (400 mg twice daily)	Placebo
Lenvatinib	VEGFR1-3, FGFR 1-4, PDGR, RET and KIT	REFLECT (NCT01761266)	Lenvatinib (12 mg/day for bodyweight ≥ 60 kg or 8 mg/day for bodyweight < 60 kg)	Sorafenib (400 mg twice-daily in 28-d cycles)
Immunotherapy				
Atezolizumab plus bevacizumab	PD-L1, vEGF	IMbrave150 (NCT03434379)	1200 mg of atezolizumab plus 15 mg per kilogram of body weight of bevacizumab intravenously every 3 wk	Sorafenib (400 mg orally twice daily)
Tremelimumab plus durvalumab	CTLA-4, PD-L1	HIMALAYA (NCT03298451)	STRIDE: Tremelimumab plus durvalumab or durvalumab alone (300 mg, one dose of tremelimumab plus 1500 mg every 4 wk for durvalumab)	Sorafenib (400 mg orally twice daily)
Second-line[1]				
Systemic therapy				
Regorafenib	VEGFR 1-3, PDGFR, FGFR 1-2, RET, RAF	RESORCE (NCT01774344)	Regorafenib (160 mg once daily during weeks 1-3 of each 4-wk cycle)	Placebo
Cabozantinib	VEGFR 1-3, MET and AXL	CELESTIAL (NCT01908426)	Cabozantinib (60 mg once daily)	Placebo
Ramucirumab	VEGFR	REACH-2 (NCT02435433)	Ramucirumab 8 mg/kg intravenous ramucirumab every 2 wk	Placebo
Immunotherapy				
Nivolumab	PD-1	CheckMate-459 (NCT02576509)	Nivolumab (240 mg intravenously every 2 wk)	Sorafenib(400 mg orally twice daily)
Nivolumab plus ipilimumab	PD-1, CTLA-4	CheckMate-040 (NCT01658878)	Nivolumab 1 mg/kg plus ipilimumab 3 mg/kg, administered every 3 wk (4 doses), followed by nivolumab 240 mg every 2 wk (arm A); nivolumab 3 mg/kg plus ipilimumab 1 mg/kg, administered every 3 wk (4 doses), followed by nivolumab 240 mg every 2 wk (arm B); or nivolumab 3 mg/kg every 2 wk plus ipilimumab 1 mg/kg every 6 wk (arm C)	Placebo
Pembrolizumab	PD-1	KEYNOTE-240 (NCT02702401)	Pembrolizumab (200 mg intravenously every 3 wk for at least 35 cycles during approximately 2 yr)	Placebo

[1]Eligible patients who had received previous treatment with sorafenib.

CTLA-4: Cytotoxic T-lymphocyte-associated protein 4; PD-1: Programmed cell death protein 1; VEGFR: Vascular endothelial growth factor receptor; FGFR: Fibroblast growth factor receptor; PDGFR: Platelet-derived growth factor receptors; OS: Overall survival; PFS: Progression-free survival; PD-L1: Programmed death ligand-1.

FIRST-LINE SYSTEMIC THERAPIES

Sorafenib

The need for new and better treatments for patients in advanced stages has led researchers to develop molecules to specifically target components of the carcinogenesis process. Sorafenib was the first oral multikinase inhibitor drug approved by the Food and Drug Administration (FDA) in 2007 to treat advanced HCC. *In vitro* experiments found that this drug inhibited HCC cell line growth and angiogenesis by inhibiting the RAF/MEK/ERK signalling pathway, as well as tyrosine and serine/threonine kinase receptors, including those for VEGF, PDGF, c-KIT, FLT3 and BRAF[12]. This drug is indicated in patients with preserved liver function who are not candidates for surgical or locoregional therapies and those with advanced tumours according to the BCLC classification and the Child-Pugh scale[9].

Sorafenib was the first drug to significantly improve the survival of patients with advanced HCC in the Asia-Pacific region. The median overall survival (OS) was 6.5 mo [95% confidence interval (CI): 5.56-7.56] in patients treated with sorafenib compared to 4.2 mo (3.75-5.46) in patients treated with placebo [13]. Similar results in terms of improved survival were observed in the SHARP clinical trial (ClinicalTrials.gov identifier: NCT00105443), a phase III, double-blind, placebo-controlled study that evaluated the effect of sorafenib on OS and time to symptomatic progression in patients diagnosed with advanced HCC. Here, the median OS was 10.7 mo in the sorafenib group and 7.9 mo in the placebo group. The most frequent adverse events in the sorafenib group were weight loss, diarrhoea, hypophosphataemia, and hand-foot skin reactions. Based on these trials, sorafenib became the first targeted therapy drug to be approved for the treatment of advanced HCC and has been the first-choice drug since its approval. Currently, the treatment of patients with sorafenib until significant radiographic progression and simultaneous treatment with regorafenib (discussed below) are recommended[9]. Unfortunately, only 30% of sorafenib users benefit, and within a short period of time, resistance to sorafenib often develops, rendering further use ineffective[14].

Lenvatinib

Following the approval of sorafenib, research led to the recognition of lenvatinib as another drug targeting important receptors and pathways in HCC. Lenvatinib is an oral receptor tyrosine kinase inhibitor and was approved in 2018 by the FDA as a first-line treatment for unresectable HCC[15]. VEGF receptor (VEGFR), FGF receptor (FGFR), PDGRα, RET, and KIT[16,17] are among its therapeutic targets. In preclinical models, lenvatinib was shown to selectively inhibit the proliferation of human HCC cell lines and *in vivo* tumour growth in xenograft models[18]. The approval of this molecule was based on the REFLECT clinical trial (ClinicalTrials.gov identifier: NCT01761266), a phase III, multicentre, open-label, non-inferiority trial that evaluated the OS of patients diagnosed with advanced HCC treated with lenvatinib *vs* patients treated with sorafenib. Lenvatinib met non-inferiority criteria against sorafenib, as the median survival for lenvatinib was 13.6 mo (95%CI: 12.1-14.9) *vs* 12.3 mo for the sorafenib group [12.3 mo, 10.4-13.9; hazard ratio (HR): 0.92, 95%CI: 0.79-1.06][19]. The most common adverse events in the lenvatinib group in this study were diarrhoea, loss of appetite, and weight loss.

Atezolizumab plus bevacizumab

Atezolizumab is a monoclonal antibody that selectively targets programmed death ligand-1 (PD-L1) to reverse the suppression of T-cell activity[20]. Its activity was assessed through an assay that determined predictive correlates of response to this antibody in cancer patients. According to Herbst *et al*[20], who studied various types of cancer, responses were observed in patients with tumours expressing high levels of PD-L1, mainly when it was expressed on tumour-infiltrating immune cells[20].

Conversely, the monoclonal antibody bevacizumab interferes with angiogenesis and tumour growth by inhibiting VEGF activity[21]. Finn *et al*[22] demonstrated the potential of bevacizumab as a promising anti-VEGF treatment for liver cancer in preclinical trials. They evaluated the effect of this humanized antibody in an orthotopic mouse model of HCC using the Hep3B cell line and found that bevacizumab treatment significantly reduced tumour microvessel density and alpha-fetoprotein (AFP) levels and prolonged time to progression compared to the control group[22].

The combination of atezolizumab and bevacizumab is a therapeutic strategy aiming to simultaneously inhibit PD-L1 (atezolizumab) and VEGF (bevacizumab) signalling in patients with advanced HCC. This combination was evaluated in the Imbrave150 clinical trial (ClinicalTrials.gov identifier: NCT03434379), a global, open-label, phase III study that evaluated the effect of the combination of these two antibodies in patients with unresectable HCC against the effect of sorafenib as a single drug, resulting in improved OS and progression-free survival (PFS) for the combination group [67. 2% (95%CI: 61.3-73.1) and 54.6% for the sorafenib group (95%CI: 45.2-64.0)][23]. A few years later, a longer follow-up of these patients was performed, reporting that the combination maintained the improvement in patients over the effect of sorafenib[24]. Accordingly, atezolizumab plus bevacizumab combination therapy was very recently approved by the FDA (2020) as the initial treatment for advanced HCC, adding a targeted drug combination to the first-line treatment strategies for these patients[25].

Tremelimumab plus durvalumab

In October 2022, the FDA approved the combination of tremelimumab plus durvalumab for treating

patients with unresectable HCC, which could form part of the first-line treatment for this cancer[26].

Tremelimumab is a fully human immunoglobulin G (IgG)2 monoclonal antibody against cytotoxic T-lymphocyte-associated protein 4 (CTLA-4), a receptor that inhibits T-cell activity[27]. Duffy *et al*[28] subjected patients diagnosed with HCC to a study evaluating the efficacy of treatment with tremelimumab plus an ablative procedure performed during week 6 (ClinicalTrials.gov identifier: NCT01853618). The authors observed that such a combination led to the accumulation of intratumoural CD8+ T-cells and suggested it as a potential new treatment for patients with advanced HCC[28]. In contrast, dirvalumab is another human monoclonal antibody that binds to the PD-L1 protein and has been shown to be effective in liver cancer and in small-cell lung cancer, especially when used in combination with another therapeutic agent[29,30].

A phase I/II clinical trial (ClinicalTrials.gov identifier: NCT02519348) evaluated the safety and efficacy of monotherapy and combination treatment of tremelimumab plus durvalumab (300 mg and 1500 mg, respectively) in patients with HCC who had progressed on, were intolerant to, or refused sorafenib. The objective response rates (ORRs) were 24.0% (95%CI: 14.9-35.3) for the combination, 10.6% for durvalumab (5.4-18.1), and 7.2% (2.4-16.1) for tremelimumab, while the median OS was 18.7 (10.8-27.3), 13.6 (8.7-17.6), and 15.1 (11.3-20.5) months, respectively[31]. However, the clinical study that led to the approval of this combination was HIMALAYA (ClinicalTrials.gov identifier: NCT03298451), a phase III and global study with a heterogeneous population representative of HCC patients and no previous systemic treatment, which also evaluated the effect of durvalumab monotherapy and compared it to sorafenib. Here, the median OS was 16.43 mo for the combination (95%CI: 14.16-19.58), 16.56 mo (95%CI: 14.06-19.12) with durvalumab, and 13.77 mo (95%CI: 12.25-16.13) with sorafenib. The combination significantly improved OS over sorafenib, and durvalumab was not inferior to sorafenib in these patients, suggesting that it could be used as a first-line treatment[32].

SECOND-LINE SYSTEMIC THERAPIES AND IMMUNOTHERAPY

Although approximately 30% of patients receiving sorafenib show improvement, resistance to treatment can develop after prolonged use (approximately 6 mo), rendering it ineffective after this period[14]. Therefore, second-line treatments are indicated for patients who either have progressed on previous sorafenib or do not respond to it. Notably, to date, no clinical trials have evaluated second-line therapy after lenvatinib[33].

Regorafenib

Regorafenib is another oral multikinase inhibitor that primarily targets VEGFR, PDGF receptors, FGFR, RET, and RAF and, in preclinical trials, was shown to significantly inhibit liver tumour development [34]. In addition, it activates proteins involved in MAPK signalling, apoptosis, and autophagy[35]. The FDA approved this drug as a second-line treatment for patients who have already been treated with sorafenib. The safety and efficacy of this drug in humans were tested in a multinational, randomized, double-blind, placebo-controlled, phase III clinical trial (RESORCE, ClinicalTrials.gov identifier: NCT01774344), in which the median OS was 10.6 mo (95%CI: 9.1-12.1) for the regorafenib group *vs* 7.8 mo (6.3-8.8) in the placebo group[36]. The most common adverse events reported in this study were hypertension, hand-foot skin reactions, fatigue, and diarrhoea. Thus, because of the survival benefit of regorafenib in HCC patients unresponsive to sorafenib, it was approved by health agencies in several countries, including the United States, Japan, and China.

Cabozantinib

Cabozantinib is a multikinase inhibitor suppressor of tumour growth, metastasis, and angiogenesis that primarily targets VEGFR but also targets MET and AXL, which in addition to being implicated in HCC progression are involved in sorafenib resistance[37]. Initially, this drug showed clinical activity in a phase II study in previously untreated HCC patients and those with progression or no response to sorafenib, resulting in a median OS of 5.5 mo with no significant radiographic responses[38]. However, its approval was based on the results of the CELESTIAL clinical trial (ClinicalTrials.gov identifier: NCT01908426), a randomized, double-blind, phase III trial evaluating cabozantinib *vs* placebo in patients diagnosed with advanced HCC, in which cabozantinib demonstrated significant benefit over placebo in OS and tumour PFS. The median OS was 10.2 mo with cabozantinib and 8.0 mo with placebo (95%CI: 0.63-0.92). The median PFS was 5.2 mo with cabozantinib and 1.9 mo with placebo (95%CI: 0.36-0.52)[39]. In 2019, the FDA approved cabozantinib for treating patients with advanced HCC who were previously treated with sorafenib[40].

Interestingly, this drug is involved in tyrosine kinase inhibition and has also been reported to be an immunomodulator since some of its targets are involved in the immune response. Indeed, in combination with anti-programmed cell death protein 1 (PD-1) therapy, cabozantinib showed a greater antitumour effects than monotherapy or placebo in animal models of HCC. On its own, cabozantinib significantly increased neutrophil infiltration and reduced intratumoural CD8+ PD-1+ T-cell ratios, while the combination further stimulated this effect[41].

Ramucirumab

Ramucirumab is an antiangiogenic anti-VEGFR2 monoclonal antibody[42,43]. The efficacy of this drug was tested in the REACH clinical trial, a randomized, placebo-controlled, double-blind, multicentre, phase III trial (ClinicalTrials.gov identifier: NCT01140347). Here, ramucirumab was tested against placebo in patients diagnosed with advanced HCC who were previously treated with sorafenib and who experienced either progression or intolerance. The median OS for the ramucirumab group was 9.2 mo (95%CI: 8.0-10.6) *vs* 7.6 mo (6.0-9.3) for the placebo group (HR: 0.87; 95%CI: 0.72-1.05; $P = 0.14$). Consistent with these results, second-line treatment with ramucirumab did not significantly improve survival over placebo in patients with advanced HCC[44]. A follow-up trial, REACH-2, was a randomized, double-blind, placebo-controlled, phase III trial comparing ramucirumab *vs* placebo at a 2:1 ratio in the same population, but this time for a preselected population with AFP concentrations ≥ 400 ng/mL. The median OS was 8.5 mo (95%CI: 7.0-10.6) *vs* 7.3 mo (5.4-9.1); HR: 0.71 (95%CI: 0.53-0.95; $P = 0.0199$) and PFS [2.8 mo (2.8-4.1) *vs* 1.6 mo (1.5-2.7); 0.452 (0.33-0.60); $P < 0.0001$] were significantly improved in the ramucirumab group compared with the placebo group. This trial showed improved OS with ramucirumab compared to placebo in patients with HCC and AFP concentrations of at least 400 ng/mL who had previously received sorafenib[45].

Very recently, the clinical relevance of rechallenge treatment with previously administered drugs was evaluated, with five consecutive patients with advanced HCC who received rechallenge treatment with lenvatinib and with failure after treatment with ramucirumab. Here, the radiological findings using the modified Response Evaluation Criteria in Solid Tumours showed stable disease in four patients and a partial response in one. This trial demonstrated that re-exposure to lenvatinib treatment after ramucirumab might be effective for treating advanced HCC[46].

IMMUNOTHERAPY

Unfortunately, cancer cells can develop resistance to systemic therapies. Thus, more and better drug treatments must be devised for these patients. Potential strategies include combination approaches and immunological therapy. In fact, immunotherapy has now been postulated as a possible therapeutic strategy to treat different types of cancer.

Cancer cells can escape the defence mechanisms of immune cells in the tumour microenvironment, thus avoiding detection and elimination by host lymphocytes by downregulating stimulatory immunoreceptors and stimulating inhibitory immunoreceptors. For example, in the case of T cells, tumour cells can modulate stimulatory activity by downregulating MHC-I on the surface. Conversely, inhibitory activity can be modulated by these cells through upregulation of PD-L1 on the surface[47-49]. Such molecules are known as immune checkpoints, which act as modulators of immune responses. These molecules can be used as pharmacological targets to generate various monoclonal antibodies that modulate their activity. Among the most studied immune receptors are PD-1, CTLA-4, LAG3, TIM3, TIGIT, and BTLA[49].

Immunotherapy has been shown to have significant efficacy in the treatment of different types of cancer, including HCC[50], making it an excellent option for patients with cancer progression or for whom systemic therapy with sorafenib was ineffective. Several immune checkpoint inhibitors that primarily target CTLA-4, PD-1, and its ligand PD-L1 have been tested to date. Some ICIs have also been approved by the FDA for the treatment of HCC. PD-L1, also called B7-H1 or CD274, is expressed in many cancer and immune cells and plays an essential role in blocking the "cancer immunity cycle" by binding to PD-1 and B7.1 (CD80), both of which are negative regulators of T-cell activation[51,52].

Antibody-based therapy is the main strategy designed to modulate the tumour immune response, but other cancer immunotherapeutic strategies, such as adoptive cell therapy, chimeric antigen receptor-modified immune cells, engineered cytokines, and therapeutic cancer vaccines, are still under development[53,54].

Nivolumab

Nivolumab is a human IgG4 monoclonal antibody that binds to the PD-1 receptor, inhibiting its interaction with PD-L1 and PD-L2 and restoring T-cell activity[55]. Nivolumab has been shown to be effective in several malignancies, including melanoma, renal Hodgki''s lymphoma, lung cancer, and gastric cancer[56-60].

Nivolumab was evaluated in HCC patients in a study called CheckMate-040 (ClinicalTrials.gov identifier: NCT01658878), a phase I/II, open-label, non-comparative, multicentre trial that included patients with advanced HCC who either had also reported progression after treatment with sorafenib or were sorafenib naive. Patients received intravenous nivolumab 240 mg every 2 wk until unacceptable toxicity or disease progression occurred. In this study, nivolumab showed favourable clinical activity and safety with manageable toxicities, suggesting that it could be suitable for patients with advanced HCC[61].

Subsequently, the activity of nivolumab (240 mg intravenously every 2 wk) was compared to that of sorafenib (400 mg orally twice daily) in a randomized, open-label, phase III trial (CheckMate 459, ClinicalTrials.gov identifier: NCT02576509) until disease progression or unacceptable toxicity. OS was improved from 14.7 mo for sorafenib to 16.4 mo with nivolumab but did not reach statistical significance (P = 0.0752). In addition, there was no significant difference in PFS (3.7 *vs* 3.8 mo). The ORRs for nivolumab and sorafenib were 15% and 7%, respectively. Nivolumab showed relevant clinical activity and a favourable safety profile for patients with advanced HCC. However, nivolumab administered for the first time in these patients was not significantly better than sorafenib in terms of OS[62]. Thus, in September 2017, nivolumab was approved by the FDA as a second-line treatment for patients with advanced HCC. It is worth mentioning that this antibody has only been approved by this institution[63].

Recently, the effect of the combination of nivolumab plus ipilimumab, a fully human IgG1 monoclonal antibody that binds to CTLA-4 on T cells[64], was evaluated. The efficacy of this combination was tested in the CheckMate 040 study (ClinicalTrials.gov identifier: NCT01658878), a multicentre, open-label, multicohort, phase I/II study in which it was shown that the combination of nivolumab plus ipilimumab led to high OS rates and had a manageable safety profile[65]. Based on the results of this trial, in March 2020, the FDA approved the combination of nivolumab plus ipilimumab as a second-line treatment for patients with HCC who had been previously treated with sorafenib[66].

Pembrolizumab

Pembrolizumab is an anti-PD-1 monoclonal antibody that demonstrated clinical efficacy in patients with advanced HCC. This antibody was evaluated in a non-randomized, multicentre, open-label, phase II study in patients with BCLC B-C HCC pre-treated with sorafenib (ClinicalTrials.gov identifier: NCT02702414), and it showed antineoplastic activity with an ORR of 17% and a manageable safety profile[67]. Based on these results, in November 2018, the FDA granted accelerated approval to pembrolizumab for patients with HCC who had been previously treated with sorafenib[68]. A subsequent study was then conducted evaluating pembrolizumab in a randomized, double-blind, phase III study in patients with advanced HCC previously treated with sorafenib (KEYNOTE-240, ClinicalTrials.gov identifier: NCT02702401). Here, the median OS was 13.9 mo (95%CI: 11.6-16.0 mo) for pembrolizumab *vs* 10.6 mo (95%CI: 8.3-13.5 mo) for placebo (HR: 0.781; 95%CI: 0.611-0.998; P = 0.0238). The median PFS for pembrolizumab was 3.0 mo (95%CI: 2.8-4.1 mo) *vs* 2.8 mo (95%CI: 1.6 to 3.0 mo) for placebo[69].

Additionally, the KEYNOTE-394 trial (ClinicalTrials.gov identifier: NCT03062358), a randomized, double-blind, phase III study, evaluated the efficacy of pembrolizumab plus best supportive care *vs* placebo in Asian HCC patients as second-line therapy. Overall, the results were consistent with those seen in previous trials, further supporting the use of pembrolizumab in patients with advanced HCC. Here, the median OS was 14.6 mo (12.6-18.0) for pembrolizumab and 13.0 mo (10.5-15.1) for placebo (95%CI); furthermore, pembrolizumab showed significant improvement of PFS (HR: 0.74, 95%CI: 0.60-0.92, P = 0.0032)[70].

INNOVATIVE STRATEGIES FOR HCC TREATMENT

Drug combination and repurposing

Currently, monotherapies are ineffective in fighting cancer mainly due to the development of resistance of cancer cells to available drugs[71], and preclinical findings may not be replicated in patients. For instance, the monoclonal antibody bortezomib demonstrated promising antineoplastic activity in preclinical assays, but in humans, it did not show notable single-agent activity compared to sorafenib [72]. Thus, more and better treatment options are needed for these patients, and drug combinations are promising options. This strategy consists of simultaneously administering two or more drugs aimed at different cancer-specific drug targets and has shown significant benefits compared to monotherapy[73]. However, combining drugs must become a rational strategy that guarantees significant pharmacological responses, especially for those patients who either did not respond to current therapy or developed resistance.

Several tools have been developed for the identification of potentially useful drug combinations; these tools include dose-response matrices, RNA interference technology, and the wide adaptation of clustered regularly interspaced short palindromic repeats (CRISPR) systems, as well as more novel techniques such as patient-derived xenograft (PDX) models and *ex vivo* primary cell and organoid models[74]. For instance, Lim *et al*[75] used PDXs of HCC, PDX-derived organoids and a hybrid experimental-computational approach–namely, the quadratic phenotypic optimization platform–and found that the combination of the second-generation proteasome inhibitor ixazomib and the CDK inhibitor dinaciclib (Dina), which they tested *in vitro* and *in vivo*, is effective against HCC[75]. Another example of the usefulness of these strategies is CRISPR-Cas9 combinatorial screening, a technique that accelerated the discovery of combination treatment with the approved drug ifenprodil (an NMDA receptor antagonist) and sorafenib as a new therapeutic alternative for advanced HCC[76].

Therefore, implementing the abovementioned strategies should aid the discovery of potentially useful drug combinations. In this manner, medical staff may have different choices and establish a selection order more suitable for each HCC patient in a personalized manner[77,78].

Conversely, it is well known that the discovery of new molecules with pharmacological activity is a process with two main disadvantages: Time and cost. It takes at least 10 years to bring a new drug to the market, and the approximate cost ranges from $314 million to $2.8 billion[79]. Furthermore, in emergency situations such as cancer, the demand for effective treatments is extremely high, and additional strategies are required to obtain novel therapies in an expedited manner. Thanks to advances in pharmacology and genomics, several non-cancer drugs have been shown to have great potential for use in treating multiple cancers. Drug repurposing is a strategy that involves the discovery of already known drugs initially used to treat other diseases but with the potential to treat various malignancies. The main advantage of this approach is that it allows an accelerated and less costly process to identify new cancer treatments since it focuses on the selection of drugs already approved by relevant health institutions[80,81]. Some non-cancer drugs showing antineoplastic activity against HCC and with high repurposing potential are described below and summarized in Table 3.

One of the differences between repositioned drugs and existing drugs approved to treat HCC is that the latter target relatively few signalling pathways; in contrast, repositioned drugs have the enormous advantage of targeting a surprisingly wide variety of signalling pathways involved in liver carcinogenesis (Table 3). For instance, Nair *et al*[82] identified CDC20 as a marker of poor prognosis during the development of early and advanced HCC. Through molecular docking studies, it was determined that labetalol, a beta blocker, binds with high affinity to CDC20[82], suggesting that the effect of labetalol against the development of HCC should be tested. The same research group further investigated this possibility by *in vitro* cytotoxicity studies, in which labetalol significantly inhibited the growth of the HepG2 cell line[83]. Subsequent application of bioinformatics analysis tools to repositioned drugs provides an incredible advantage for the identification of unknown drug targets and signalling pathways potentially involved in liver carcinogenesis.

Antihistamines

Histamine exerts a variety of physiological activities *via* its G protein-coupled receptors, the activation of which has been associated with the progression of different types of cancer[84,85]. It is well known that histamine favours the development of different types of cancer, including liver cancer[86]. Accordingly, overexpression of the histamine H1 receptor (H1HR) is associated with HCC cell proliferation and metastasis by inducing cell cycle progression, lamellipodia production, matrix metalloprotease 2 (MMP2) production and inhibition of apoptosis. Furthermore, suppressing H1HR activity significantly inhibited tumour growth and metastasis in mouse xenograft models[86]. Interestingly, very recently, it was shown that antihistamine consumption is associated with a significant decrease in the developing of liver cancer in patients diagnosed with HBV, HCV or both viruses[87].

Astemizole

Ellegaard *et al*[88] analysed cohort studies and reported that the use of cationic amphiphilic antihistamines, including astemizole (an H1-antihistamine), was associated with a significant reduction in mortality in lung cancer patients[88]. It is worth mentioning that astemizole might affect cancer cell proliferation *via* different molecular mechanisms, including ion channels.

The ether à-go-go-1 (Eag1) potassium channel has been reported to play an important role in the development of several types of cancer, such as liver, cervical, breast, lung and colon cancer[89-93], suggesting that this channel is a potential early biomarker and drug target for these tumours[94]. Eag1 overexpression has been implicated in cell cycle progression and cancer cell proliferation[95], and inhibition of this channel has reduced tumour progression in both *in vitro* and *in vivo* assays in leukaemia and gastric cancer[86-97]. De Guadalupe Chávez-López *et al*[98] found that astemizole inhibited cell proliferation and induced apoptosis in human HCC cell lines[98]. In the same study using an HCC model induced by diethylnitrosamine (DEN) in mice, they found that astemizole inhibited tumour development and decreased Eag1 mRNA and protein levels[98].

Cytochrome P450 2J2 (CYP2J2) is implicated in the development of different types of cancer. In HCC, CYP2J2 is overexpressed, and its activity promotes cell proliferation[99-101]. Interestingly, astemizole and loratadine inhibit CYP2J2 activity[102]. Ellegaard *et al*[88] proposed the possibility that this drug targets this protein, which would partially explain the effect of reduced mortality in lung cancer patients [88].

TRPV2 is a calcium channel expressed in and associated with several types of cancer, including HCC progression. Both mRNA and protein levels of this channel are increased in well-differentiated HCC tumour tissue compared to undifferentiated tissue. There is a strong association between its expression and portal vein invasion. Van den Eynde *et al*[103] reported that TRPV2 is related to endometrial cancer progression and identified astemizole, loratadine, and clemizole as TRPV2 blockers, with loratadine being the most potent antagonist, leading to inhibition of cell proliferation and migration in *in vitro* assays in HEK293 cells[103].

Table 3 Identified drugs and their targets for drug repurposing in hepatocellular carcinoma

Drug	Original therapeutic indication	Molecular targets in HCC	Ref.
Antihistamines	Allergy	H1R-H4R, Eag1, CYP2J2, TRPV2, AP-1, NF-B	[88,91,96,98,102,103,105,109,111,113,115,116]
Raloxifene, bazedoxifene	Breast cancer (raloxifene), osteoporosis	ER-, ER-, GPER, IL-6R, aHR, NF-B, STAT3, PI3K/AKT, MAPK	[135-137,141,142]
Disulfiram	Alcoholism	NF-B, TGF-β, ROS-JNK	[149-151,157]
Clofazimine	Antimycobacterial used to treat leprosy	Wnt/-catenin pathway	[166-178]
Albendazole	Anthelmintic	Tubulin, ERK1/2-HIF-1α-p300/CREB	[175]
Pimozide	Antipsychotic used to manage Tourette's Disorder	STAT3, Wnt/-catenin	[185,188]
Natamycin	Macrolide antifungal	PRDX1	[191]
Metformin	Glycemic control in type 2 diabetes mellitus	PI3K-mTOR pathway, AMPK	[200-202,206,207]
Valproate	Anticonvulsant	HDAC, Notch-1, MAPK pathway, -catenin pathway	[220,221,223]
Atorvastatin	Lower lipid levels and reduce the risk of cardiovascular disease	Mevalonate pathway	[231]
Celebrex	NSAID	COX-2, PNO1	[237,243]
Hydroxychloroquine	Antimalarial	Autophagy inhibition, TLR9 pathway	[247]

NSAID: Non-steroidal anti-inflammatory drug; mTOR: Mechanistic target of rapamycin; HCC: Hepatocellular carcinoma; NF-kB: Nuclear factor kB; AP-1: Activating protein-1; CYP2J2: Cytochrome P450 2J2; ER: Oestrogen receptor; IL-6R: Interleukin-6R; STAT3: Signal transducer and activator of transcription 3; PI3K: Phosphoinositide 3-kinase; TGF-β: Transforming growth factor-β; PRDX1: Peroxiredoxin 1; HDAC: Histone deacetylase; aHR: Adjusted hazard ratio.

Loratadine

Loratadine is a second-generation antihistamine indicated for the treatment of allergic rhinitis and urticaria. It is a selective H1HR receptor antagonist[104]. Fritz *et al*[105,106] evaluated the effect of loratadine through retrospective studies in patients diagnosed with breast cancer and melanoma and found that loratadine use was associated with improved OS[105,106]. In patients diagnosed with lung cancer, a cohort study found that the use of loratadine or its metabolite desloratadine was associated with a significant reduction in mortality; the authors proposed that cancer-related changes in lysosomal membranes could favour the entry of these antihistamines[88,107]. To date, there has been scarce evidence studying the effect of loratadine in HCC. In a thesis from a few years ago, the cytotoxic effect of the combination of loratadine and cisplatin in HCC cell lines was evaluated; loratadine alone had a concentration-dependent cytotoxic effect on liver cancer cell lines, and the combination of loratadine with cisplatin had a synergistic effect[108]. The same thesis showed that loratadine alone and in combination also induced apoptosis and cell cycle arrest in the G2/M phase. Loratadine targets proteins that have been suggested to be involved in the development of HCC. As in the case of astemizole, loratadine might exert antineoplastic effects through H1HR antagonism, lysosomal membrane sensitization, TRPV2 calcium channel blockade and inhibition of CYP2J2 activity[86,88,102,103]. Furthermore, it has been reported that loratadine could exert anti-inflammatory activity by inhibiting the inflammatory response triggered by NF-kB signalling[109], an effect that reduces the levels of proinflammatory components, including interleukin (IL)-6 and tumour necrosis factor (TNF)-α. The effect of loratadine on HCC and its potential mechanisms of action deserve further investigation.

Deptropine

Deptropine is a first-generation H1HR antihistamine indicated to treat asthma[110]. This drug has activity against cancer cells. For example, *in vitro* assays in human liver cancer cells showed that, compared to the activity of other first- and second-generation antihistamines, deptropine was more potent in inhibiting cell proliferation and inducing autophagosome formation by significantly increasing the expression of light chain 3B-II. In mouse xenograft models, deptropine potently inhibited the tumour effect[111].

Cyproheptadine

This antihistamine is a potential anti-HCC agent. Feng *et al*[112] evaluated the activity of cyproheptadine in liver cancer cell viability and found that this drug had a potent inhibitory effect on cell proliferation through cell cycle arrest. Interestingly, a minimal cytotoxic effect was observed in healthy

hepatocytes[112]. Subsequently, a cohort study in Taiwanese patients at different stages of HCC compared patients who received cyproheptadine treatment and those who did not. The adjusted HR (aHR) of all-cause mortality significantly decreased in all stages in the patients who received palliative treatments with cyproheptadine use compared with those who received palliative treatments without cyproheptadine use (all $P < 0.0001$ and aHR = 0.76, 0.80, 0.66, and 0.66 for stages I, II, III, and IV, respectively). The authors suggested that cyproheptadine could improve survival in patients with HCC at any stage[113]. The same research group conducted a case report documenting that a 62-year-old woman with suspected advanced HCC and bone metastases showed disease remission after cyproheptadine monotherapy[114]. A dose of 4 mg of this drug three times daily for 17 mo reduced serum AFP concentrations from 17697.62 ng/mL to 4.3 ng/mL in only 3 mo. A liver biopsy performed two months after starting cyproheptadine treatment showed no malignancy. This outcome was previously observed in another case report in which two patients with HCC and lung metastases were treated with a combination of cyproheptadine plus thalidomide (it should be noted that the cyproheptadine prescription was indicated for skin itching). Computed tomography imaging showed complete remission of HCC in both patients after 6 mo and 6 wk of treatment[115].

A cohort study evaluated the efficacy of the combination of cyproheptadine with sorafenib compared to sorafenib alone in patients with advanced HCC. The median OS was 11 mo in the combination group (95%CI: 6.8-15.1 mo) and 4.8 mo in the sorafenib group (95%CI: 3.1-6.6 mo), while the median PFS time was 7.5 mo (95%CI: 5.1-10.0 mo) in the combination group compared with 1.7 mo (95%CI: 1.4-2.1 mo) in the sorafenib group[116].

Roles of other histamine receptors and antihistamines in HCC

Histamine 2 receptor: Histamine receptor 2 (H2HR) activation has an inhibitory effect on tumour progression in colorectal cancer; gene expression profiling studies in tumour samples from colorectal cancer patients described the elevated expression of this receptor, associated with improved OS outcomes[117]. In human liver cancer cells, H2HR activation leads to the inhibition of IL-6 expression and signalling, arresting cell proliferation[118]. In contrast, there is evidence that H2HR activation in HCC favours the expression of β-catenin and survivin, leading to cell survival[119]. Cimetidine, an H2 antihistamine, decreases intracellular cAMP concentrations, as well as EGF-induced cell proliferation and migration, and it has been suggested as an HCC chemopreventive agent[120]. Additionally, cimetidine treatment was shown to inhibit liver carcinogenesis in rats with DEN-induced HCC[121]. Recently, Crouchet *et al*[122] developed a system in human liver cells that models a clinical prognostic liver signature predicting long-term liver disease progression to HCC, and they identified nizatidine, an H2HR antihistamine, for the treatment of advanced liver disease and prevention of HCC[122].

Histamine 3 receptor: The H3HR receptor has been described to participate in the carcinogenesis of different types of cancer, including colorectal and pancreatic cancer[123,124]. In tumour tissues from HCC patients, H3HR was overexpressed and associated with poor prognosis, and its activation promoted the growth and metastasis of HCC cell lines by inducing lamellipodia formation[125,126]. Zhang *et al*[126] reported that H3HR activation favours HCC progression through an acceleration of the G1-S phase transition, inhibition of apoptosis, and activation of the AMPc/PKA/CREB signalling pathway to downregulate the expression of CDKN1A, a cyclin-dependent kinase inhibitor that has anti-oncogene activity[126]. Thus, the oncogenic role of H3HR might be antagonized as a potential therapy in HCC.

Histamine 4 receptor: Analysis of cancer genomic data from The Cancer Genome Atlas showed that the histamine H4 receptor (H4HR) is slightly but significantly overexpressed in human HCC tumour tissues compared to healthy tissue[84]. Furthermore, patients with increased H4HR protein expression in tumour cells also had increased tumour sizes and more metastasis compared to those with lower receptor expression, suggesting that H4HR levels could be used as a prognostic marker for liver cancer [127]. However, to date, there have been insufficient studies demonstrating the role of H4HR in HCC and its clinical relevance, so it is crucial to investigate its association with this cancer.

ESTROGEN RECEPTOR MODULATORS

According to the Global Cancer Observatory, liver cancer ranks fifth in incidence in men, while in women, it ranks ninth[1]. This fact has attracted the attention of researchers, who have argued that oestrogens explain this difference. Accordingly, oestrogens play a protective role against liver damage and prevent the development of HCC[128-130]. Epidemiological data have indicated that oestrogen deficiency in peri- and postmenopausal women increases the risk of developing liver damage and increases HCC incidence in postmenopausal women; in concordance, oestrogen treatment suppresses this phenomenon[131,132].

Both isoforms of the nuclear oestrogen receptor (ER), ER-α and ER-β, are involved in the development of liver cancer; however, the functions of ER-β have not yet been fully described. Both ER-α and ER-β are expressed in the liver under normal conditions, but their expression is modified during inflammatory

processes. Both are decreased in HCC patients compared to healthy tissue samples[133] and are believed to lose their function during disease progression; indeed, the ER-α isoform might even be considered a predictor of poor prognosis in HCC[128,134]. Conversely, Matsushima *et al*[135] reported that the selective oestrogen receptor modulators (SERMs) raloxifene and bazedoxifene inhibited HCC progression through their specific interaction with ER-β. They proposed that both drugs could activate the ER-β receptor in the liver, which through downstream signal transduction suppresses TGF-induced HCC cell migration *via* inhibition of Akt[135].

Raloxifene is indicated for the treatment of osteoporosis and is used for the treatment and prevention of breast cancer[136]. Raloxifene is a potent inhibitor of the IL-6/GP130 signalling pathway, which is involved in the process of oncogenesis of various cancers, including HCC[137]. This research group observed that raloxifene inhibited cell viability in human liver cancer cell lines. Furthermore, using an *in vivo* model, they also demonstrated that it could inhibit tumour growth.

Because liver cancer frequently develops in the context of chronic inflammatory liver disease, proinflammatory cytokines and immune cells play important roles in carcinogenesis. One of the most relevant cytokines in the development of HCC is IL-6; when overproduced, it has a strong effect on liver carcinogenesis, and its high expression is related to a high rate of metastasis and poor prognosis in HCC [138-140]. Naugler *et al*[141] reported in an animal model that oestrogen administration inhibited IL-6 secretion and significantly reduced DEN-induced injury in males[141]. When IL-6 binds to its receptor, it recruits JAK, leading to activation of STAT3, a transcription factor that favours proliferative processes, angiogenesis, invasion, *etc*[142]. In addition, ER-α could interact directly with NF-kB and inhibit IL-6 secretion, and raloxifene could interact with ER-α and inhibit IL-6 secretion and thus tumour progression[142].

OTHER DRUGS

Disulfiram

Disulfiram is an FDA-approved drug from several years ago and has been extensively used in the treatment of alcoholism[143]. This drug has potential anticancer activity in different types of cancer, including lymphoma[144], breast cancer[145,146], and pancreatic cancer[147]. A phase II, multicentre, randomized, double-blind trial (ClinicalTrials.gov identifier: NCT00312819) evaluated the safety and efficacy of the combination of disulfiram with cisplatin and vinorelbine in patients diagnosed with lung cancer. Interestingly, a significant increase in survival was observed in patients given this combined treatment[148]. Intracellular copper (Cu) levels are significantly elevated in HCC cells and are associated with poor patient prognoses[149,150]. Surprisingly, the increase in Cu concentration might be harnessed for therapeutic use since disulfiram has Cu-dependent anticancer properties. Li *et al*[151] found that disulfiram inhibited the proliferation, migration, and invasion of liver cancer cells; interestingly, Cu enhanced this activity when combined with disulfiram; however, Cu alone did not [151]. In this regard, a phase I clinical trial determined the maximum tolerated dose of Cu administered with disulfiram in patients with liver cancer and found that 250 mg of daily Cu gluconate were well tolerated by these patients[152]. In the same study, temporary disease stabilization was observed in some patients, but there were no objective responses. Disulfiram can penetrate cancer cells and chelate intracellular Cu because Cu levels are elevated in many cancers. This action provides the advantage of specificity for cancer cells compared to healthy cells. Disulfiram might work as a Cu ionophore that induces oxidative stress by promoting reactive oxygen species (ROS) production, resulting in the inhibition of NF-kB[151], a transcription factor involved in the regulation of inflammatory processes and the development of liver injury, as well as HCC progression[153,154]. Blocking NF-kB signalling leads to an increase in ROS-induced toxicity and consequent cell apoptosis[155]. Furthermore, Thiery[156] found that inhibition of NF-kB signalling also resulted in inhibition of liver cancer cell metastasis by reversing the epithelial-to-mesenchymal transition (EMT), an important process in cancer metastasis in which NF-kB and TGF-β are important components[156]. Indeed, in this same study, disulfiram was found to inhibit TGF-kβ signalling. Interestingly, disulfiram plus Cu reversed EMT more effectively than disulfiram alone[151].

Most recently, Zhang *et al*[157] reported that disulfiram plus copper in combination with sorafenib resulted in increased anticancer activity against HCC under *in vitro* and *in vivo* conditions. Moreover, this combination synergistically inhibited the proliferation of human HCC cell lines and significantly increased autophagy and apoptosis compared to sorafenib alone. In addition, in a mouse orthotopic HCC xenograft model, the combination effectively inhibited tumour growth compared to the effect of sorafenib alone[157].

Clofazimine

The canonical Wnt/β-catenin signalling pathway is a crucial component during embryonic development and normal adult homeostasis because it participates in processes such as cell differentiation, polarity, migration, and apoptosis[158]. However, abnormal activation of this pathway (especially of the transcription factor β-catenin) has been linked to cellular malignant transformation

and promotion of carcinogenesis, and it is present in many types of cancer, including HCC[159-161]. Notably, mutations in the *CTNNB1* gene, which codes for β-catenin, are the most frequent mutations during HCC[162,163]. Interestingly, clofazimine, an anti-leprosy agent, could be useful for treating Wnt-dependent cancers. For instance, it has been shown to be effective against triple-negative breast cancer, both *in vitro* and *in vivo*, through inhibition of Wnt/β-catenin signalling[164,165]. Furthermore, Xu *et al* [166] demonstrated that clofazimine could effectively suppress HCC cell growth, inhibiting Wnt/β-catenin canonical signalling[166]. This drug has been evaluated for some years, and the results have suggested that it might work successfully as an antitumour agent. For example, Van Rensburg *et al*[167] found that it inhibited HCC cell line proliferation *in vitro*[167]. In addition, in a phase II clinical trial in patients with unresectable or metastatic liver cancer, 600 mg of this drug were administered daily for two weeks, followed by a dose reduction to 400 mg until progression or death. In this trial, 13 of 30 treated patients had disease stability for up to 20 mo, and the median OS was 13 wk[168]. Furthermore, a phase II clinical trial evaluated the combination of clofazimine plus doxorubicin in patients diagnosed with HCC. Although no patients showed complete or partial response, this combination showed only mild toxic effects, and the authors recommended further studies involving this antileprosy agent[169]. Overall, these trials provided strong evidence to suggest that clofazimine might be useful in treating HCC.

Albendazole

Albendazole is an antiparasitic agent used to treat parenchymal neurocysticercosis and other helminth infections by blocking parasite microtubules, leading to the inhibition of glucose uptake and transport and, ultimately, cell death[170]. Interestingly, this drug has been reported to possess antitumour activity and has been studied in different malignancies, including liver, lung, breast, prostate, and colorectal cancers and melanoma[171-175]. Pourgholami *et al*[176] evaluated the effect of this drug in several liver cancer cell lines and in mouse xenograft models (human SKHEP-1 tumour growth in nude mice), reporting that the drug induced dose-dependent inhibition of [^{3}H] thymidine incorporation in all the cell lines studied and a significant decrease in the number of SKHEP-1 cells significantly inhibiting tumour growth[176].

Pimozide

Pimozide is a dopamine receptor antagonist neuroleptic drug[177] that was approved by the FDA for the treatment of Tourette's syndrome and schizophrenia[178] and it has shown efficacy for the treatment of different types of cancer, such as breast cancer[179,180], prostate cancer[181], brain tumours[182], colorectal cancer[183], and chronic myelogenous leukaemia[184]. In liver cancer, pimozide effectively inhibited cell proliferation of HCC cell lines through disruption of Wnt/β-catenin signalling and reduction of epithelial cell adhesion molecule expression, a marker of both liver stem cells[185] and HCC tumour-initiating cells[186,187]. Furthermore, Chen *et al*[188] found that pimozide was able to inhibit cell proliferation, migration, colony formation, and sphere formation *in vitro* in HCC cell lines and stem-like cells by suppressing STAT3 activity. Additionally, pimozide reduced the tumour burden in a xenograft model in nude mice[188]. Moreover, the same research group found that the antiproliferative effects of pimozide on HCC cell lines were reversible and in line with the involvement of cell quiescence and ROS production. Interestingly, pimozide combined with sorafenib synergistically inhibited HCC cell proliferation *in vitro*[188].

Natamycin

Natamycin is a natural polyene amphoteric macrolide antibiotic with antifungal properties[189]. It has been reported to significantly inhibit the proliferation of prostate cancer cells[190]. Conversely, An *et al* [191] found that natamycin induced apoptosis and inhibited the proliferation of HCC cells by triggering excessive ROS production through the downregulation of peroxiredoxin 1 (PRDX-1). Additionally, they found that the combination of natamycin plus sorafenib exerted a synergistic effect on cell growth suppression compared to the effect of monotherapy[191].

Dysregulation of cellular redox systems is a critical feature of many types of cancer. Increased ROS play a fundamental role in the tumour microenvironment, activating important signalling pathways in carcinogenesis, such as MAPK/ERK, JNK, and PI3K/AKT, and in turn activating NF-kB, MMPs, and VEGF, consequently affecting angiogenesis, metastasis and cell survival in many types of cancer[192-194]. However, at significantly elevated ROS concentrations, cancer cells are able to develop antioxidant defence systems to maintain redox homeostasis and survive[195]. An example of this situation is the participation of the peroxiredoxin family, which consists of peroxidases that break down hydrogen peroxide, protecting the cancer cell from oxidative stress and consequently providing a survival advantage; thus, this family of enzymes are potential targets for tumour growth arrest and cancer therapy[196,197]. It is worth mentioning that the PRDX-1 isoform is the most abundant and positively regulated protein in different types of cancer, and its expression is associated with poor prognosis[198].

Valproic acid

Valproic acid is a drug that possesses anticonvulsant activity and is primarily indicated for the

treatment of epilepsy. However, it is also useful for treating migraine, bipolar disorder, anxiety, and psychiatric disorders[199]. The interest in testing the activity of this drug as an antineoplastic agent came from findings in human neuroblastoma models. This molecule was able to inhibit proliferation and induce differentiation of primitive neuroectodermal tumour cells *in vivo*, providing evidence for using valproic acid as a treatment for neuroblastoma patients[200]. Machado *et al*[201] reported the effect of this drug on human liver cancer cells both *in vitro* and *in vivo*. Valproic acid significantly inhibited cell proliferation in a dose-dependent manner, while in mouse xenograft models, it reduced tumour growth, in addition to negatively regulating Notch-1 mRNA levels[201]. Very recently, Bai *et al*[202] evaluated the effect of valproate in animal models of HCC in rats treated with DEN and found that this drug significantly reduced liver nodules and AFP levels, as well as other important liver enzymes, compared to rats treated with DEN alone. Additionally, valproate reduced inflammatory cytokines, such as TNF-α, IL-6, IL-1β, NF-kB and TGF-β1, in liver tissue[202].

Lee *et al*[203] took advantage of the benefits of combination therapy to evaluate the effects of cytokine-induced killer (CIK) cells with valproic acid. CIK cells are *ex vivo* expanded T lymphocytes expressing natural killer and T-cell markers that are used as adjuvant therapy to reduce HCC recurrence, yet CIK cell monotherapy is insufficient to treat advanced HCC[203-205]. Therefore, this research group determined whether treatment with CIK cells and valproic acid synergized to inhibit tumour growth in mouse models of HCC. After seven days of the combined treatment, there was a synergistic effect on relative tumour volume in the animals since the relative tumour volume in control animals was significantly increased[206].

Additionally, Yu *et al*[207] implemented a therapeutic strategy in HCC cells *in vitro* and *in vivo* that consisted of testing the combined effect of valproic acid with proton and photon irradiation. Histone deacetylase (HDAC) inhibitors, including valproic acid, have shown promising results in the treatment of different cancers[208-210]. However, their use as monotherapy has not been satisfactory, so using them in combination with another therapy is an appealing strategy. HDAC inhibitors can sensitize human cancer cells to ionizing radiation[211], which is a therapeutic strategy for cancer[212]. In a study by Yu *et al*[207], valproic acid prolonged DNA damage and increased proton-induced apoptosis and ROS formation while suppressing the expression of nuclear factor erythroid 2–related factor 2, a transcription factor involved in cellular antioxidant regulation. In tumour xenograft models, valproic acid significantly enhanced tumour growth retardation[207]. In addition, An *et al*[213] reported that valproic acid could induce cellular senescence in HCC cells through its role as an HDAC inhibitor[213].

ONGOING CLINICAL TRIALS USING ONCOLOGY AND NON-ONCOLOGY DRUGS

Table 4 summarizes the ongoing clinical trials for HCC patients. Immunotherapy is currently positioned as the most innovative pharmacological strategy to treat different types of cancer, including liver cancer. In addition, it is interesting to note that most of the ongoing HCC clinical trials are evaluating the effects of combination therapy and that drug repurposing is gaining tremendous interest, as non-oncology molecules are now being tested. Next, the non-oncology drugs used in ongoing clinical trials (Tables 3 and 4) are discussed.

Metformin

This drug is commonly used for the treatment of type 2 diabetes and was approved by the FDA in 1994. Metformin lowers glucose levels and improves insulin sensitivity[214]. Surprisingly, metformin has been shown to have antineoplastic activity in different types of cancer[83,215]. It is one of the most successful non-cancer drugs used in oncology. Several clinical trials are currently investigating the therapeutic potential of this drug in various cancers, including breast, prostate, endometrial, and colorectal cancer[216-219]. In the case of liver cancer, metformin has gained interest as an antineoplastic agent, given the increased risk of developing liver cancer in diabetic patients. Meta-analyses have reported that metformin has a beneficial effect on the incidence and/or survival of patients with liver cancer. For example, Ma *et al*[220] reported the association between metformin use and improved survival in diabetic patients with liver cancer[220]. Afterwards, the same research group reported a meta-analysis of 19 studies in diabetic subjects and suggested that metformin use reduced the proportion of liver cancer by 48% compared to non-users[221]. At the molecular level, metformin reduces insulin levels, activating the PI3K-mTOR signalling pathway and inhibiting cell proliferation in cancers expressing the insulin receptor[222]. Other mechanisms include negative regulation of mTOR *via* AMPK activation[223].

Ongoing clinical trials in HCC patients are evaluating the use of metformin in combination with other molecules, such as vitamin C (ClinicalTrials.gov identifier: NCT04033107), statins (ClinicalTrials.gov identifier: NCT02819869) and Celebrex (ClinicalTrials.gov identifier: NCT03184493).

Statins (atorvastatin)

Statins are agents that decrease the level of low-density lipoprotein cholesterol in the blood. They are specific inhibitors of the mevalonate pathway through inhibition of the conversion of 3-hydroxy-3-

Table 4 Ongoing clinical trials involving monotherapy, drug combination and non-oncology drugs

Study title	NTC number	Study design	Drugs	Status
Monotherapy				
Study of Pembrolizumab (MK-3475) as Monotherapy in Participants With Advanced Hepatocellular Carcinoma (MK-3475-224/KEYNOTE-224)	NCT02702414	Phase II, non-randomized, parallel assignment, open label	Pembrolizumab	Active, not recruiting
An Investigational Immuno-therapy Study of Nivolumab Compared to Sorafenib as a First Treatment in Patients With Advanced Hepatocellular Carcinoma	NCT02576509	Phase III, randomized, parallel assignment, open label	Nivolumab. Sorafenib	Active, not recruiting
Exploratory Study on Combined Conversion Immuno-therapy for Liver Metastasis of MSS Type Initial Unresectable Colorectal Cancer Based on Gene Status	NCT05409417	Phase II, III, single group assignment, open label	Experimental drug	Recruiting
First-in-Human Safety, Tolerability and Antitumour Activity Study of MTL-CEBPA in Patients With Advanced Liver Cancer	NCT02716012	Phase I, non-randomized, parallel assignment, open label	MLT-CEBPA. Sorafenib (200 mg)	Active, not recruiting
Drug combination				
A Phase III, Open-Label, Randomized Study of Atezol-izumab in Combination With Bevacizumab Compared With Sorafenib in Patients With Untreated Locally Advanced or Metastatic Hepatocellular Carcinoma (IMbrave150)	NCT03434379	Phase III, randomized, parallel assignment, open label	Atezolizumab. Bevacizumab. Sorafenib	Active, not recruiting
A Trial of Lenvatinib Plus Pembrolizumab in Participants With Hepatocellular Carcinoma	NCT03006926	Phase I, single group, open label	Lenvatinib. Pembrol-izumab (200 mg)	Active, not recruiting
A Study of Durvalumab or Tremelimumab Monotherapy, or Durvalumab in Combination With Tremelimumab or Bevacizumab in Advanced Hepatocellular Carcinoma	NCT02519348	Phase II, randomized, parallel assignment, open label	Tremelimumab. Durvalumab. Bevacizumab	Active, not recruiting
Pembrolizumab With or Without Elbasvir/Grazoprevir and Ribavirin in Treating Patients With Advanced Refractory Liver Cancer	NCT02940496	Phase II, non-randomized, parallel assignment, open label	Elbasvir/Grazoprevir. Pembrolizumab. Ribavirin	Active, not recruiting
Clinical Recruitment of Patients With First-line Targeted Drug Resistance or Intolerance to Hepatocellular Cancer With PD-1 Inhibitor (Toripalimab, JS001) Detected on the NGS Platform Combined With Anlotinib	NCT05453383	Phase II, single group assignment, open label	Anlotinib. Toripalimab	Recruiting
TACE Combined With Camrelizumab and Apatinib in the Treatment of Advanced Liver Cancer	NCT05550025	Phase II, single group assignment, open label	Camrelizumab. Apatinib	Recruiting
IBR900 Cell Injection Combined With Lenvatinib or Bevacizumab in the Treatment of Advanced Primary Liver Cancer	NCT05411757	Phase I, single group assignment, open label	IBR900. Lenvatinib. Bevacizumab	Not recruiting yet
Trial to Evaluate the Safety of Talimogene Laherparepvec Injected Into Tumors Alone and in Combination With Systemic Pembrolizumab MK-3475-611/Keynote-611	NCT02509507	Phase I, II, non-randomized, sequential assignment, open label	Talimogene. Laherparepvec. Pembrol-izumab	Active, not recruiting
HAIC Sequential TAE Combined With Lenvatinib and Tislelizumab in Unresectable HCC	NCT05532319	Phase II, single group assignment, open label	HAIC sequential TAE. Lenvatinib. Tislelizumab	Not recruiting yet
A Study of E7386 in Combination With Other Anticancer Drug in Participants With Solid Tumor	NCT04008797	Phase I, non-randomized, sequential assignment, open label	E7386. Lenvatinib	Recruiting
An Immuno-therapy Study to Evaluate the Effectiveness, Safety and Tolerability of Nivolumab or Nivolumab in Combination With Other Agents in Patients With Advanced Liver Cancer	NCT01658878	Phase I, II, parallel assignment, open label	Nivolumab. Sorafenib. Ipilimumab. Cabozantinib	Active, not recruiting
A Phase I Clinical Study of Recombinant Humanized Anti-BTLA Monoclonal Antibody (JS004) Injection Combined With Toripalimab Injection in Patients With Advanced Solid Tumors	NCT05427396	Phase I, single group assignment, open label	JS004. Toripalimab	Recruiting
mFOLFOX7 Plus Camrelizumab and Apatinib for Advanced HCC	NCT05412589	Phase II, single group assignment, open label	mFOLFOX7. Camrel-izumab. Apatinib	Recruiting
Trial of PXS-5505 Combined With First Line Atezolizumab Plus Bevacizumab For Treating Patients With Unresectable Hepatocellular Carcinoma	NCT05109052	Phase II, III, single group assignment, open label	PXS-5505. Atezolizumab. Bevacizumab	Not recruiting yet

Combination of Regorafenib and Nivolumab in Unresectable Hepatocellular Carcinoma	NCT04310709	Phase II, single group assignment, open label	Regorafenib. Nivolumab	Recruiting
Phase Ib Trial of Infigratinib In Combination With Atezolizumab And Bevacizumab for The Second-Line Treatment of Advanced Cholangiocarcinoma With FGFR2 Fusion/Amplification	NCT05510427	Phase I, randomized, single group assignment, open label	Infigratinib. Atezolizumab. Bevacizumab	Recruiting
A Study of TAK-500 With or Without Pembrolizumab in Adults With Select Locally Advanced or Metastatic Solid Tumors	NCT05070247	Phase I, non-randomized, parallel assignment, open label	TAK-500. Pembrolizumab	Recruiting
A Study of Nivolumab and Relatlimab in Combination With Bevacizumab in Advanced Liver Cancer	NCT05337137	Phase I, II, randomized, parallel assignment, quadruple (participant care, provider, investigator, outcomes assessor)	Relatlimab. Nivolumab. Bevacizumab	Recruiting
Drug repurposing				
High Dose Vitamin C Combined With Metformin in the Treatment of Malignant Tumors	NCT04033107	Phase II, single group assignment, open label	Vitamin C. Metformin	Recruiting
Statin Combination Therapy in Patients Receiving Sorafenib for Advanced Hepatocellular Carcinoma	NCT03275376	Phase II, randomized, parallel assignment, Quadruple (Participant, Care Provider, Investigator, Outcomes Assessor)	Atorvastatin	Terminated
The Combination Effect of Statin Plus Metformin on Relapse-free	NCT02819869	Phase II, randomized, parallel assignment	Statin. Metfotmin	Terminated
Statin for Preventing Hepatocellular Carcinoma Recurrence After Curative Treatment	NCT03024684	Phase IV, randomized, parallel assignment, triple masking (Participant, Care Provider, Investigator)	Atorvastatin	Recruiting
Meclizine for Hepatocellular Carcinoma	NCT03253289	Phase I, single group assignment, open label	Meclizine	Recruiting
Celebrex and Metformin for Postoperative Hepatocellular Carcinoma	NCT03184493	Phase III, non- randomized, parallel assignment	Celebrex plus metformin	Recruiting
Sorafenib Induced Autophagy Using Hydroxychloroquine in Hepatocellular Cancer	NCT03037437	Phase II, non-randomized, parallel assignment, open label	Sorafenib. Hydroxychloroquine	Recruiting

PD-1: Programmed cell death protein 1; HCC: Hepatocellular carcinoma.

methylglutaryl coenzyme A into mevalonate, which is responsible for cholesterol synthesis[224]. Interestingly, mevalonate signalling is deregulated in several types of cancer and is also involved in the process of tumorigenesis[225,226], making it a potentially useful target for cancer treatment. Preclinical trials have demonstrated that statins can be used as antitumour agents in colorectal cancer[227-229]. It was suggested that statins might reduce the risk of developing HCC[230]. Kim *et al*[231] reported that atorvastatin inhibited the activation of YAP (*via* the mevalonate pathway) and AKT (*via* stabilization of the truncated retinoid X receptor alpha pathway), which are involved in cancer development[231].

Ongoing clinical trials are evaluating the effects of statins in patients with advanced HCC, such as a trial evaluating atorvastatin in patients receiving treatment with sorafenib (ClinicalTrials.gov identifier: NCT03275376) and a clinical trial studying two non-oncology drugs-statins and metformin-either alone or in combination (ClinicalTrials.gov identifier: NCT03024684).

Celebrex

Celebrex (celecoxib) is a cyclooxygenase-2 (COX-2) selective non-steroidal anti-inflammatory drug indicated for the treatment of pain and inflammation caused by osteoarthritis, rheumatoid arthritis, and ankylosing spondylitis[232]. Interestingly, celecoxib anticancer activity is presumed to occur by inhibiting COX-2[233-235] because this cyclooxygenase isoform is frequently expressed in many types of cancer and promotes carcinogenesis and resistance of cancer cells to chemotherapy[236]. Dai *et al*[237] found that celecoxib also targets the RNA-binding protein ""partner of NOB1"" (PNO1) and exerts antitumour activity through the AKT/mTOR pathway[237]. In addition, PNO1 has been reported to participate in the progression of lung, oesophageal, breast, bladder, and colorectal cancer[238-242]. Targeting PNO1 (which is overexpressed in HCC tissues) can inhibit cell apoptosis by promoting autophagy through the ERK/MAPK signalling pathway[243].

A clinical trial is currently ongoing to compare the effect of Celebrex alone, metformin alone, and the combination of both drugs in preventing HCC recurrence after hepatic resection (ClinicalTrials.gov identifier: NCT03184493). In preclinical trials, it was shown that the combination of the two *in vitro* and

in vivo inhibited HCC proliferation more effectively than the effect of each drug alone[244].

Hydroxychloroquine

Hydroxychloroquine is an antimalarial drug that has been evaluated as an antitumour agent in HCC and has even been used for the treatment of other cancers, either alone or in combination with other therapeutic agents[215,245]. This drug targets cancer cells and the tumour microenvironment; among its molecular mechanisms of action, it inhibits autophagosome-lysosome fusion and Toll-like receptor 9 (TLR9) signalling, along with TLR7, which are overexpressed in HCC and are involved in cell proliferation and inhibition of apoptosis[246]. Furthermore, Chen *et al*[247] reported that hydroxychloroquine and miRNA (hsa-miR-30a-5p) target and resensitize sorafenib-resistant HCC cells to sorafenib through impairment of autophagy and DNA damage by oxidative stress *via* the TLR9/SOD1/hsa-miR-30a-5p/Beclin-1 pathway[247]. Since one of the mechanisms of sorafenib resistance is the induction of autophagy, a prospective, phase II clinical trial is currently under way to evaluate the efficacy of sorafenib and hydroxychloroquine treatment in patients with advanced HCC (ClinicalTrials.gov identifier: NCT03037437).

PERSPECTIVES

The high mortality caused by liver cancer remains an important concern in oncology. Therefore, there is an urgent need to implement new therapeutic strategies to provide significant benefits in patients with advanced HCC.

Immunotherapy is a tool that has shown great promise in treating HCC. Nevertheless, it is necessary to continue developing immunotherapy agents, which increase understanding of the role of the immune response in the tumour and take advantage of this process.

In contrast, the use of combination therapy has shown very favourable results compared to the effect of monotherapy, reflected by the diversity of current clinical trials evaluating the impact of the combination of two or more agents in HCC. Drug combinations simultaneously targeting relevant signalling pathways in liver carcinogenesis provide at least four potential advantages: (1) Anticancer synergistic effects; (2) minimization of treatment resistance; (3) reduction of individual drug doses; and (4) the occurrence of minimal adverse events. These advantages should facilitate HCC treatment, making it extremely important to consider possible future drug combinations to achieve greater benefits for HCC patients.

Furthermore, growing evidence has supported that non-cancer drugs possess antineoplastic activity. In emergency situations such as cancer, drug repurposing can be a very useful strategy. Compared to the traditional process of developing new drugs, drug repurposing allows for the rapid and less costly discovery of new treatments, increasing the likelihood of success with the advantage that safety issues in humans have already been described. It is crucial to mention that drug repurposing does not replace the traditional process; both are extremely important. However, repurposing non-oncology drugs is an attractive strategy to obtain more treatment options for advanced HCC.

Simultaneously, implementing non-oncology drug repurposing and proposing combinations of non-oncology drugs with systemic therapy or immunotherapy are very attractive strategies to generate significant benefits in patients with unresectable HCC. In addition, new relevant signalling pathways, critical drug targets, and biomarkers of this cancer might be identified along the way, providing significant advantages for understanding liver carcinogenesis.

CONCLUSION

Currently, approved drug options for treating advanced HCC are limited, and the likelihood of generating resistance is high, making the use of novel pharmacological approaches urgent (Figure 2). Compared to monotherapy, this review demonstrated that combining therapies has resulted in more significant benefits for HCC patients. Furthermore, evidence has been provided indicating that several non-oncology drugs are potentially useful for the treatment of this cancer. In addition, immunotherapy has significant effects in some cases compared to current systemic therapy, making this approach, along with repositioning and combination therapy, promising for the pharmacological treatment of advanced liver cancer.

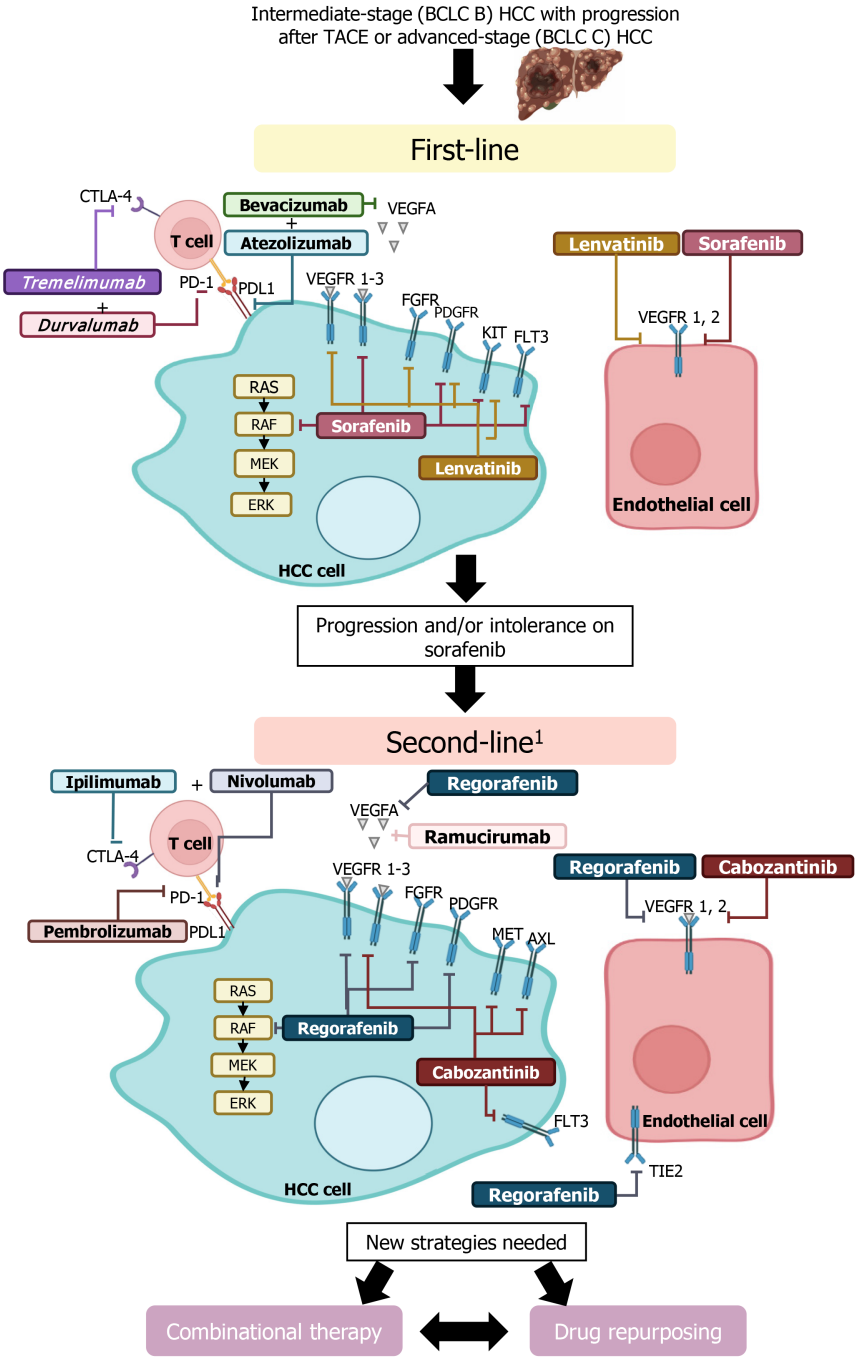

DOI: 10.3748/wjg.v29.i17.2571

Figure 2 Pharmacological strategies for the treatment of advanced hepatocellular carcinoma. When a patient is diagnosed with hepatocellular carcinoma either intermediate (BCLC B) or advanced (BCLC C) stage, surgical and locoregional therapeutic options are no longer indicated. In these cases, the most appropriate treatment option is systemic therapy with first-line treatments with sorafenib and lenvatinib as the initial drugs. However, if the patient develops resistance to sorafenib or disease progression after therapy, treatment with second-line drugs indicated in the schedule is initiated. It is important to note that immunotherapy using monoclonal antibodies is already part of the current and approved drug options. Because current drug treatments are limited and monotherapy is ineffective, the implementation of combination and drug repositioning are two therapeutic strategies to achieve more and better treatments. [1]All agents require prior sorafenib use. BCLC: Barcelona Clinic Liver Cancer; TACE: Transarterial chemoembolization; CTLA-4: Cytotoxic T-lymphocyte-associated protein 4; PD-1: Programmed cell death protein 1; VEGFR: Vascular endothelial growth factor receptor; FGFR: Fibroblast growth factor receptor; PDGFR: Platelet-derived growth factor receptors; HCC: Hepatocellular carcinoma.

FOOTNOTES

Author contributions: Villarruel-Melquiades F and Camacho J wrote the paper and made substantial contributions to conception of the manuscript; Mendoza-Garrido ME, García-Cuellar CM, Sánchez-Pérez Y and Pérez-Carreón JI made critical revisions related to important intellectual content of the manuscript; all authors read and approved the final version of the article to be published.

Supported by CONACyT Fellowship (FV-M), No. 787907.

Conflict-of-interest statement: All the authors report no relevant conflicts of interest for this article.

Country/Territory of origin: Mexico

ORCID number: María Eugenia Mendoza-Garrido 0000-0003-2037-0618; Claudia M García-Cuellar 0000-0001-8080-5797; Yesennia Sánchez-Pérez 0000-0003-0103-9188; Julio Isael Pérez-Carreón 0000-0001-9284-7775; Javier Camacho 0000-0002-8886-086X.

S-Editor: Fan JR
L-Editor: A
P-Editor: Zhao S

REFERENCES

1 **Ferlay J**, Ervik M, Lam F, Colombet M, Mery L, Piñeros M, Znaor A, Soerjomataram I, Bray F (2022). Global Cancer Observatory: Cancer Today. Lyon, France: International Agency for Research on Cancer. [cited 14 October 2022]. Available from: https://gco.iarc.fr/today

2 **Massarweh NN**, El-Serag HB. Epidemiology of Hepatocellular Carcinoma and Intrahepatic Cholangiocarcinoma. *Cancer Control* 2017; **24**: 1073274817729245 [PMID: 28975830 DOI: 10.1177/1073274817729245]

3 **Sung H**, Ferlay J, Siegel RL, Laversanne M, Soerjomataram I, Jemal A, Bray F. Global Cancer Statistics 2020: GLOBOCAN Estimates of Incidence and Mortality Worldwide for 36 Cancers in 185 Countries. *CA Cancer J Clin* 2021; **71**: 209-249 [PMID: 33538338 DOI: 10.3322/caac.21660]

4 **Bruix J**, Han KH, Gores G, Llovet JM, Mazzaferro V. Liver cancer: Approaching a personalized care. *J Hepatol* 2015; **62**: S144-S156 [PMID: 25920083 DOI: 10.1016/j.jhep.2015.02.007]

5 **Khalaf N**, Ying J, Mittal S, Temple S, Kanwal F, Davila J, El-Serag HB. Natural History of Untreated Hepatocellular Carcinoma in a US Cohort and the Role of Cancer Surveillance. *Clin Gastroenterol Hepatol* 2017; **15**: 273-281.e1 [PMID: 27521507 DOI: 10.1016/j.cgh.2016.07.033]

6 **Zhu XD**, Li KS, Sun HC. Adjuvant therapies after curative treatments for hepatocellular carcinoma: Current status and prospects. *Genes Dis* 2020; **7**: 359-369 [PMID: 32884990 DOI: 10.1016/j.gendis.2020.02.002]

7 **Baudino TA**. Targeted Cancer Therapy: The Next Generation of Cancer Treatment. *Curr Drug Discov Technol* 2015; **12**: 3-20 [PMID: 26033233 DOI: 10.2174/1570163812666150602144310]

8 **Chow AK**, Yau SW, Ng L. Novel molecular targets in hepatocellular carcinoma. *World J Clin Oncol* 2020; **11**: 589-605 [PMID: 32879846 DOI: 10.5306/wjco.v11.i8.589]

9 **European Association for the Study of the Liver**. EASL Clinical Practice Guidelines: Management of hepatocellular carcinoma. *J Hepatol* 2018; **69**: 182-236 [PMID: 29628281 DOI: 10.1016/j.jhep.2018.03.019]

10 **Reig M**, Forner A, Rimola J, Ferrer-Fàbrega J, Burrel M, Garcia-Criado Á, Kelley RK, Galle PR, Mazzaferro V, Salem R, Sangro B, Singal AG, Vogel A, Fuster J, Ayuso C, Bruix J. BCLC strategy for prognosis prediction and treatment recommendation: The 2022 update. *J Hepatol* 2022; **76**: 681-693 [PMID: 34801630 DOI: 10.1016/j.jhep.2021.11.018]

11 **Raoul JL**, Sangro B, Forner A, Mazzaferro V, Piscaglia F, Bolondi L, Lencioni R. Evolving strategies for the management of intermediate-stage hepatocellular carcinoma: available evidence and expert opinion on the use of transarterial chemoembolization. *Cancer Treat Rev* 2011; **37**: 212-220 [PMID: 20724077 DOI: 10.1016/j.ctrv.2010.07.006]

12 **Abdelgalil AA**, Alkahtani HM, Al-Jenoobi FI. Sorafenib. *Profiles Drug Subst Excip Relat Methodol* 2019; **44**: 239-266 [PMID: 31029219 DOI: 10.1016/bs.podrm.2018.11.003]

13 **Cheng AL**, Kang YK, Chen Z, Tsao CJ, Qin S, Kim JS, Luo R, Feng J, Ye S, Yang TS, Xu J, Sun Y, Liang H, Liu J, Wang J, Tak WY, Pan H, Burock K, Zou J, Voliotis D, Guan Z. Efficacy and safety of sorafenib in patients in the Asia-Pacific region with advanced hepatocellular carcinoma: a phase III randomised, double-blind, placebo-controlled trial. *Lancet Oncol* 2009; **10**: 25-34 [PMID: 19095497 DOI: 10.1016/S1470-2045(08)70285-7]

14 **Tang W**, Chen Z, Zhang W, Cheng Y, Zhang B, Wu F, Wang Q, Wang S, Rong D, Reiter FP, De Toni EN, Wang X. The mechanisms of sorafenib resistance in hepatocellular carcinoma: theoretical basis and therapeutic aspects. *Signal Transduct Target Ther* 2020; **5**: 87 [PMID: 32532960 DOI: 10.1038/s41392-020-0187-x]

15 **U.S. Food & Drug Administration**. FDA approves lenvatinib for unresectable hepatocellular carcinoma. 2018 Ago 16 [Internet]. [cited 30 October 2022]. Available from: https://www.fda.gov/drugs/resources-information-approved-drugs/fda-approves-lenvatinib-unresectable-hepatocellular-carcinoma

16 **Al-Salama ZT**, Syed YY, Scott LJ. Lenvatinib: A Review in Hepatocellular Carcinoma. *Drugs* 2019; **79**: 665-674 [PMID: 30993651 DOI: 10.1007/s40265-019-01116-x]

17 **Vogel A**, Bathon M, Saborowski A. Advances in systemic therapy for the first-line treatment of unresectable HCC. *Expert Rev Anticancer Ther* 2021; **21**: 621-628 [PMID: 33499684 DOI: 10.1080/14737140.2021.1882855]

18 **Matsuki M**, Hoshi T, Yamamoto Y, Ikemori-Kawada M, Minoshima Y, Funahashi Y, Matsui J. Lenvatinib inhibits angiogenesis and tumor fibroblast growth factor signaling pathways in human hepatocellular carcinoma models. *Cancer*

Med 2018; **7**: 2641-2653 [PMID: 29733511 DOI: 10.1002/cam4.1517]

19 **Kudo M**, Finn RS, Qin S, Han KH, Ikeda K, Piscaglia F, Baron A, Park JW, Han G, Jassem J, Blanc JF, Vogel A, Komov D, Evans TRJ, Lopez C, Dutcus C, Guo M, Saito K, Kraljevic S, Tamai T, Ren M, Cheng AL. Lenvatinib versus sorafenib in first-line treatment of patients with unresectable hepatocellular carcinoma: a randomised phase 3 non-inferiority trial. *Lancet* 2018; **391**: 1163-1173 [PMID: 29433850 DOI: 10.1016/S0140-6736(18)30207-1]

20 **Herbst RS**, Soria JC, Kowanetz M, Fine GD, Hamid O, Gordon MS, Sosman JA, McDermott DF, Powderly JD, Gettinger SN, Kohrt HE, Horn L, Lawrence DP, Rost S, Leabman M, Xiao Y, Mokatrin A, Koeppen H, Hegde PS, Mellman I, Chen DS, Hodi FS. Predictive correlates of response to the anti-PD-L1 antibody MPDL3280A in cancer patients. *Nature* 2014; **515**: 563-567 [PMID: 25428504 DOI: 10.1038/nature14011]

21 **Ferrara N**, Hillan KJ, Novotny W. Bevacizumab (Avastin), a humanized anti-VEGF monoclonal antibody for cancer therapy. *Biochem Biophys Res Commun* 2005; **333**: 328-335 [PMID: 15961063 DOI: 10.1016/j.bbrc.2005.05.132]

22 **Finn RS**, Bentley G, Britten CD, Amado R, Busuttil RW. Targeting vascular endothelial growth factor with the monoclonal antibody bevacizumab inhibits human hepatocellular carcinoma cells growing in an orthotopic mouse model. *Liver Int* 2009; **29**: 284-290 [PMID: 18482274 DOI: 10.1111/j.1478-3231.2008.01762.x]

23 **Finn RS**, Qin S, Ikeda M, Galle PR, Ducreux M, Kim TY, Kudo M, Breder V, Merle P, Kaseb AO, Li D, Verret W, Xu DZ, Hernandez S, Liu J, Huang C, Mulla S, Wang Y, Lim HY, Zhu AX, Cheng AL; Imbrave150 Investigators. Atezolizumab plus Bevacizumab in Unresectable Hepatocellular Carcinoma. *N Engl J Med* 2020; **382**: 1894-1905 [PMID: 32402160 DOI: 10.1056/NEJMoa1915745]

24 **Cheng AL**, Qin S, Ikeda M, Galle PR, Ducreux M, Kim TY, Lim HY, Kudo M, Breder V, Merle P, Kaseb AO, Li D, Verret W, Ma N, Nicholas A, Wang Y, Li L, Zhu AX, Finn RS. Updated efficacy and safety data from Imbrave150: Atezolizumab plus bevacizumab vs. sorafenib for unresectable hepatocellular carcinoma. *J Hepatol* 2022; **76**: 862-873 [PMID: 34902530 DOI: 10.1016/j.jhep.2021.11.030]

25 **U.S. Food & Drug Administration**. FDA approves atezolizumab plus bevacizumab for unresectable hepatocellular carcinoma. 2020 Jun 01 [Internet]. [cited 30 October 2022]. Available from: https://www.fda.gov/drugs/resources-information-approved-drugs/fda-approves-atezolizumab-plus-bevacizumab-unresectable-hepatocellular-carcinoma

26 **U.S. Food & Drug Administration**. FDA approves tremelimumab in combination with durvalumab for unresectable hepatocellular carcinoma. 2022 Oct 10 [Internet]. [cited 30 October 2022]. Available from: https://www.fda.gov/drugs/resources-information-approved-drugs/fda-approves-tremelimumab-combination-durvalumab-unresectable-hepatocellular-carcinoma

27 **Tarhini AA**. Tremelimumab: a review of development to date in solid tumors. *Immunotherapy* 2013; **5**: 215-229 [PMID: 23444951 DOI: 10.2217/imt.13.9]

28 **Duffy AG**, Ulahannan SV, Makorova-Rusher O, Rahma O, Wedemeyer H, Pratt D, Davis JL, Hughes MS, Heller T, ElGindi M, Uppala A, Korangy F, Kleiner DE, Figg WD, Venzon D, Steinberg SM, Venkatesan AM, Krishnasamy V, Abi-Jaoudeh N, Levy E, Wood BJ, Greten TF. Tremelimumab in combination with ablation in patients with advanced hepatocellular carcinoma. *J Hepatol* 2017; **66**: 545-551 [PMID: 27816492 DOI: 10.1016/j.jhep.2016.10.029]

29 **Al-Salama ZT**. Durvalumab: A Review in Extensive-Stage SCLC. *Target Oncol* 2021; **16**: 857-864 [PMID: 34731446 DOI: 10.1007/s11523-021-00843-0]

30 **Antonia SJ**, Villegas A, Daniel D, Vicente D, Murakami S, Hui R, Yokoi T, Chiappori A, Lee KH, de Wit M, Cho BC, Bourhaba M, Quantin X, Tokito T, Mekhail T, Planchard D, Kim YC, Karapetis CS, Hiret S, Ostoros G, Kubota K, Gray JE, Paz-Ares L, de Castro Carpeño J, Wadsworth C, Melillo G, Jiang H, Huang Y, Dennis PA, Özgüroğlu M; PACIFIC Investigators. Durvalumab after Chemoradiotherapy in Stage III Non-Small-Cell Lung Cancer. *N Engl J Med* 2017; **377**: 1919-1929 [PMID: 28885881 DOI: 10.1056/NEJMoa1709937]

31 **Kelley RK**, Sangro B, Harris W, Ikeda M, Okusaka T, Kang YK, Qin S, Tai DW, Lim HY, Yau T, Yong WP, Cheng AL, Gasbarrini A, Damian S, Bruix J, Borad M, Bendell J, Kim TY, Standifer N, He P, Makowsky M, Negro A, Kudo M, Abou-Alfa GK. Safety, Efficacy, and Pharmacodynamics of Tremelimumab Plus Durvalumab for Patients With Unresectable Hepatocellular Carcinoma: Randomized Expansion of a Phase I/II Study. *J Clin Oncol* 2021; **39**: 2991-3001 [PMID: 34292792 DOI: 10.1200/JCO.20.03555]

32 **Abou-Alfa GK**, Lau G, Kudo M, Chan SL, Kelley RK, Furuse J, Sukeepaisarnjaroen W, Kang YK, Van Dao T, De Toni EN, Rimassa L, Breder V, Vasilyev A, Heurgué A, Tam VC, Mody K, Thungappa SC, Ostapenko Y, Yau T, Azevedo S, Varela M, Chrng AL, Qin S, Galle PR, Ali S, Marcovitz M, Makowsky M, He P, Kurland JF, Negro A, Sangro B. Tremelimumab plus Durvalumab in Unresectable Hepatocellular Carcinoma. *NEJM Evidence* 2022; 1 [DOI: 10.1056/EVIDoa2100070]

33 **Frenette C**, Blanc JF, Cheng AL, Finn R, Galle, P, Pfiffer T, Sun HC. The importance of systemic treatment sequencing in improving survival for patients with hepatocellular carcinoma. Bayer. [cited 10 September 2020]. Available from: https://www.bayer.com/sites/default/files/Bayer_HCC_Expert_Statement_1.pdf

34 **Wilhelm SM**, Dumas J, Adnane L, Lynch M, Carter CA, Schütz G, Thierauch KH, Zopf D. Regorafenib (BAY 73-4506): a new oral multikinase inhibitor of angiogenic, stromal and oncogenic receptor tyrosine kinases with potent preclinical antitumor activity. *Int J Cancer* 2011; **129**: 245-255 [PMID: 21170960 DOI: 10.1002/ijc.25864]

35 **Carr BI**, Cavallini A, Lippolis C, D'Alessandro R, Messa C, Refolo MG, Tafaro A. Fluoro-Sorafenib (Regorafenib) effects on hepatoma cells: growth inhibition, quiescence, and recovery. *J Cell Physiol* 2013; **228**: 292-297 [PMID: 22777740 DOI: 10.1002/jcp.24148]

36 **Bruix J**, Qin S, Merle P, Granito A, Huang YH, Bodoky G, Pracht M, Yokosuka O, Rosmorduc O, Breder V, Gerolami R, Masi G, Ross PJ, Song T, Bronowicki JP, Ollivier-Hourmand I, Kudo M, Cheng AL, Llovet JM, Finn RS, LeBerre MA, Baumhauer A, Meinhardt G, Han G; RESORCE Investigators. Regorafenib for patients with hepatocellular carcinoma who progressed on sorafenib treatment (RESORCE): a randomised, double-blind, placebo-controlled, phase 3 trial. *Lancet* 2017; **389**: 56-66 [PMID: 27932229 DOI: 10.1016/S0140-6736(16)32453-9]

37 **Yakes FM**, Chen J, Tan J, Yamaguchi K, Shi Y, Yu P, Qian F, Chu F, Bentzien F, Cancilla B, Orf J, You A, Laird AD, Engst S, Lee L, Lesch J, Chou YC, Joly AH. Cabozantinib (XL184), a novel MET and VEGFR2 inhibitor, simultaneously suppresses metastasis, angiogenesis, and tumor growth. *Mol Cancer Ther* 2011; **10**: 2298-2308 [PMID: 21926191 DOI:

10.1158/1535-7163.MCT-11-0264]
38 **Kelley RK**, Verslype C, Cohn AL, Yang TS, Su WC, Burris H, Braiteh F, Vogelzang N, Spira A, Foster P, Lee Y, Van Cutsem E. Cabozantinib in hepatocellular carcinoma: results of a phase 2 placebo-controlled randomized discontinuation study. *Ann Oncol* 2017; **28**: 528-534 [PMID: 28426123 DOI: 10.1093/annonc/mdw651]
39 **Abou-Alfa GK**, Meyer T, Cheng AL, El-Khoueiry AB, Rimassa L, Ryoo BY, Cicin I, Merle P, Chen Y, Park JW, Blanc JF, Bolondi L, Klümpen HJ, Chan SL, Zagonel V, Pressiani T, Ryu MH, Venook AP, Hessel C, Borgman-Hagey AE, Schwab G, Kelley RK. Cabozantinib in Patients with Advanced and Progressing Hepatocellular Carcinoma. *N Engl J Med* 2018; **379**: 54-63 [PMID: 29972759 DOI: 10.1056/NEJMoa1717002]
40 **U.S. Food & Drug Administration**. FDA approves cabozantinib for hepatocellular carcinoma. 2019 Mar 03 [Internet]. [cited 30 October 2022]. Available from: https://www.fda.gov/drugs/fda-approves-cabozantinib-hepatocellular-carcinoma
41 **Esteban-Fabró R**, Willoughby CE, Piqué-Gili M, Montironi C, Abril-Fornaguera J, Peix J, Torrens L, Mesropian A, Balaseviciute U, Miró-Mur F, Mazzaferro V, Pinyol R, Llovet JM. Cabozantinib Enhances Anti-PD1 Activity and Elicits a Neutrophil-Based Immune Response in Hepatocellular Carcinoma. *Clin Cancer Res* 2022; **28**: 2449-2460 [PMID: 35302601 DOI: 10.1158/1078-0432.CCR-21-2517]
42 **Syed YY**. Ramucirumab: A Review in Hepatocellular Carcinoma. *Drugs* 2020; **80**: 315-322 [PMID: 32034692 DOI: 10.1007/s40265-020-01263-6]
43 **Turkes F**, Chau I. Ramucirumab and its use in the treatment of hepatocellular carcinoma. *Future Oncol* 2019; **15**: 979-988 [PMID: 30644314 DOI: 10.2217/fon-2018-0822]
44 **Zhu AX**, Park JO, Ryoo BY, Yen CJ, Poon R, Pastorelli D, Blanc JF, Chung HC, Baron AD, Pfiffer TE, Okusaka T, Kubackova K, Trojan J, Sastre J, Chau I, Chang SC, Abada PB, Yang L, Schwartz JD, Kudo M; REACH Trial Investigators. Ramucirumab versus placebo as second-line treatment in patients with advanced hepatocellular carcinoma following first-line therapy with sorafenib (REACH): a randomised, double-blind, multicentre, phase 3 trial. *Lancet Oncol* 2015; **16**: 859-870 [PMID: 26095784 DOI: 10.1016/S1470-2045(15)00050-9]
45 **Zhu AX**, Kang YK, Yen CJ, Finn RS, Galle PR, Llovet JM, Assenat E, Brandi G, Pracht M, Lim HY, Rau KM, Motomura K, Ohno I, Merle P, Daniele B, Shin DB, Gerken G, Borg C, Hiriart JB, Okusaka T, Morimoto M, Hsu Y, Abada PB, Kudo M; REACH-2 study investigators. Ramucirumab after sorafenib in patients with advanced hepatocellular carcinoma and increased α-fetoprotein concentrations (REACH-2): a randomised, double-blind, placebo-controlled, phase 3 trial. *Lancet Oncol* 2019; **20**: 282-296 [PMID: 30665869 DOI: 10.1016/S1470-2045(18)30937-9]
46 **Komatsu S**, Yano Y, Kido M, Kuramitsu K, Gon H, Fukushima K, Urade T, So S, Yanagimoto H, Toyama H, Kodama Y, Fukumoto T. Lenvatinib Rechallenge After Ramucirumab Treatment Failure for Hepatocellular Carcinoma. *Anticancer Res* 2021; **41**: 4555-4562 [PMID: 34475083 DOI: 10.21873/anticanres.15268]
47 **Das S**, Johnson DB. Immune-related adverse events and anti-tumor efficacy of immune checkpoint inhibitors. *J Immunother Cancer* 2019; **7**: 306 [PMID: 31730012 DOI: 10.1186/s40425-019-0805-8]
48 **Franzin R**, Netti GS, Spadaccino F, Porta C, Gesualdo L, Stallone G, Castellano G, Ranieri E. The Use of Immune Checkpoint Inhibitors in Oncology and the Occurrence of AKI: Where Do We Stand? *Front Immunol* 2020; **11**: 574271 [PMID: 33162990 DOI: 10.3389/fimmu.2020.574271]
49 **He X**, Xu C. Immune checkpoint signaling and cancer immunotherapy. *Cell Res* 2020; **30**: 660-669 [PMID: 32467592 DOI: 10.1038/s41422-020-0343-4]
50 **Keilson JM**, Knochelmann HM, Paulos CM, Kudchadkar RR, Lowe MC. The evolving landscape of immunotherapy in solid tumors. *J Surg Oncol* 2021; **123**: 798-806 [PMID: 33595890 DOI: 10.1002/jso.26416]
51 **Onuma AE**, Zhang H, Huang H, Williams TM, Noonan A, Tsung A. Immune Checkpoint Inhibitors in Hepatocellular Cancer: Current Understanding on Mechanisms of Resistance and Biomarkers of Response to Treatment. *Gene Expr* 2020; **20**: 53-65 [PMID: 32340652 DOI: 10.3727/105221620X15880179864121]
52 **Xu F**, Jin T, Zhu Y, Dai C. Immune checkpoint therapy in liver cancer. *J Exp Clin Cancer Res* 2018; **37**: 110 [PMID: 29843754 DOI: 10.1186/s13046-018-0777-4]
53 **Lai E**, Astara G, Ziranu P, Pretta A, Migliari M, Dubois M, Donisi C, Mariani S, Liscia N, Impera V, Persano M, Tolu S, Balconi F, Pinna G, Spanu D, Pireddu A, Saba G, Camera S, Musio F, Puzzoni M, Pusceddu V, Madeddu C, Casadei Gardini A, Scartozzi M. Introducing immunotherapy for advanced hepatocellular carcinoma patients: Too early or too fast? *Crit Rev Oncol Hematol* 2021; **157**: 103167 [PMID: 33271389 DOI: 10.1016/j.critrevonc.2020.103167]
54 **Liu Z**, Liu X, Liang J, Liu Y, Hou X, Zhang M, Li Y, Jiang X. Immunotherapy for Hepatocellular Carcinoma: Current Status and Future Prospects. *Front Immunol* 2021; **12**: 765101 [PMID: 34675942 DOI: 10.3389/fimmu.2021.765101]
55 **Finkelmeier F**, Waidmann O, Trojan J. Nivolumab for the treatment of hepatocellular carcinoma. *Expert Rev Anticancer Ther* 2018; **18**: 1169-1175 [PMID: 30304963 DOI: 10.1080/14737140.2018.1535315]
56 **Ansell SM**, Lesokhin AM, Borrello I, Halwani A, Scott EC, Gutierrez M, Schuster SJ, Millenson MM, Cattry D, Freeman GJ, Rodig SJ, Chapuy B, Ligon AH, Zhu L, Grosso JF, Kim SY, Timmerman JM, Shipp MA, Armand P. PD-1 blockade with nivolumab in relapsed or refractory Hodgkin's lymphoma. *N Engl J Med* 2015; **372**: 311-319 [PMID: 25482239 DOI: 10.1056/NEJMoa1411087]
57 **Borghaei H**, Paz-Ares L, Horn L, Spigel DR, Steins M, Ready NE, Chow LQ, Vokes EE, Felip E, Holgado E, Barlesi F, Kohlhäufl M, Arrieta O, Burgio MA, Fayette J, Lena H, Poddubskaya E, Gerber DE, Gettinger SN, Rudin CM, Rizvi N, Crinó L, Blumenschein GR, Antonia SJ, Dorange C, Harbison CT, Finckenstein FG, Brahmer JR. Nivolumab vs Docetaxel in Advanced Nonsquamous Non–Small-Cell Lung Cancer. *N Engl J Med* 2015; **373**: 1627-1639 [PMID: 26412456 DOI: 10.1056/NEJMoa1507643]
58 **Kang YK**, Boku N, Satoh T, Ryu MH, Chao Y, Kato K, Chung HC, Chen JS, Muro K, Kang WK, Yeh KH, Yoshikawa T, Oh SC, Bai LY, Tamura T, Lee KW, Hamamoto Y, Kim JG, Chin K, Oh DY, Minashi K, Cho JY, Tsuda M, Chen LT. Nivolumab in patients with advanced gastric or gastro-oesophageal junction cancer refractory to, or intolerant of, at least two previous chemotherapy regimens (ONO-4538-12, ATTRACTION-2): a randomised, double-blind, placebo-controlled, phase 3 trial. *Lancet* 2017; **390**: 2461-2471 [PMID: 28993052 DOI: 10.1016/S0140-6736(17)31827-5]
59 **Motzer RJ**, Escudier B, McDermott DF, George S, Hammers HJ, Srinivas S, Tykodi SS, Sosman JA, Procopio G, Plimack ER, Castellano D, Choueiri TK, Gurney H, Donskov F, Bono P, Wagstaff J, Gauler TC, Ueda T, Tomita Y,

Schutz FA, Kollmannsberger C, Larkin J, Ravaud A, Simon JS, Xu LA, Waxman IM, Sharma P; CheckMate 025 Investigators. Nivolumab versus Everolimus in Advanced Renal-Cell Carcinoma. *N Engl J Med* 2015; **373**: 1803-1813 [PMID: 26406148 DOI: 10.1056/NEJMoa1510665]

60 **Weber JS**, D'Angelo SP, Minor D, Hodi FS, Gutzmer R, Neyns B, Hoeller C, Khushalani NI, Miller WH Jr, Lao CD, Linette GP, Thomas L, Lorigan P, Grossmann KF, Hassel JC, Maio M, Sznol M, Ascierto PA, Mohr P, Chmielowski B, Bryce A, Svane IM, Grob JJ, Krackhardt AM, Horak C, Lambert A, Yang AS, Larkin J. Nivolumab versus chemotherapy in patients with advanced melanoma who progressed after anti-CTLA-4 treatment (CheckMate 037): a randomised, controlled, open-label, phase 3 trial. *Lancet Oncol* 2015; **16**: 375-384 [PMID: 25795410 DOI: 10.1016/S1470-2045(15)70076-8]

61 **Kudo M**, Matilla A, Santoro A, Melero I, Gracián AC, Acosta-Rivera M, Choo SP, El-Khoueiry AB, Kuromatsu R, El-Rayes B, Numata K, Itoh Y, Di Costanzo F, Crysler O, Reig M, Shen Y, Neely J, Tschaika M, Wisniewski T, Sangro B. CheckMate 040 cohort 5: A phase I/II study of nivolumab in patients with advanced hepatocellular carcinoma and Child-Pugh B cirrhosis. *J Hepatol* 2021; **75**: 600-609 [PMID: 34051329 DOI: 10.1016/j.jhep.2021.04.047]

62 **Yau T**, Park JW, Finn RS, Cheng AL, Mathurin P, Edeline J, Kudo M, Harding JJ, Merle P, Rosmorduc O, Wyrwicz L, Schott E, Choo SP, Kelley RK, Sieghart W, Assenat E, Zaucha R, Furuse J, Abou-Alfa GK, El-Khoueiry AB, Melero I, Begic D, Chen G, Neely J, Wisniewski T, Tschaika M, Sangro B. Nivolumab versus sorafenib in advanced hepatocellular carcinoma (CheckMate 459): a randomised, multicentre, open-label, phase 3 trial. *Lancet Oncol* 2022; **23**: 77-90 [PMID: 34914889 DOI: 10.1016/S1470-2045(21)00604-5]

63 **U.S. Food & Drug Administration**. FDA grants accelerated approval to nivolumab for HCC previously treated with sorafenib. 2017 Sep 25 [Internet]. [cited 30 October 2022]. Available from: https://www.fda.gov/drugs/resources-information-approved-drugs/fda-grants-accelerated-approval-nivolumab-hcc-previously-treated-sorafenib

64 **Tsang J**, Wong JSL, Kwok GGW, Li BCW, Leung R, Chiu J, Cheung TT, Yau T. Nivolumab + Ipilimumab for patients with hepatocellular carcinoma previously treated with Sorafenib. *Expert Rev Gastroenterol Hepatol* 2021; **15**: 589-598 [PMID: 33666530 DOI: 10.1080/17474124.2021.1899808]

65 **Yau T**, Kang YK, Kim TY, El-Khoueiry AB, Santoro A, Sangro B, Melero I, Kudo M, Hou MM, Matilla A, Tovoli F, Knox JJ, Ruth He A, El-Rayes BF, Acosta-Rivera M, Lim HY, Neely J, Shen Y, Wisniewski T, Anderson J, Hsu C. Efficacy and Safety of Nivolumab Plus Ipilimumab in Patients With Advanced Hepatocellular Carcinoma Previously Treated With Sorafenib: The CheckMate 040 Randomized Clinical Trial. *JAMA Oncol* 2020; **6**: e204564 [PMID: 33001135 DOI: 10.1001/jamaoncol.2020.4564]

66 **U.S. Food & Drug Administration**. FDA grants accelerated approval to nivolumab and ipilimumab combination for hepatocellular carcinoma. 2020 Mar 03 [Internet]. [cited 31 October 2022]. Available from: https://www.fda.gov/drugs/resources-information-approved-drugs/fda-grants-accelerated-approval-nivolumab-and-ipilimumab-combination-hepatocellular-carcinoma

67 **Zhu AX**, Finn RS, Edeline J, Cattan S, Ogasawara S, Palmer D, Verslype C, Zagonel V, Fartoux L, Vogel A, Sarker D, Verset G, Chan SL, Knox J, Daniele B, Webber AL, Ebbinghaus SW, Ma J, Siegel AB, Cheng AL, Kudo M; KEYNOTE-224 investigators. Pembrolizumab in patients with advanced hepatocellular carcinoma previously treated with sorafenib (KEYNOTE-224): a non-randomised, open-label phase 2 trial. *Lancet Oncol* 2018; **19**: 940-952 [PMID: 29875066 DOI: 10.1016/S1470-2045(18)30351-6]

68 **U.S. Food & Drug Administration**. FDA grants accelerated approval to pembrolizumab for hepatocellular carcinoma. 2018 Dic 14 [Internet]. [cited 31 October 2022]. Available from: https://www.fda.gov/drugs/fda-grants-accelerated-approval-pembrolizumab-hepatocellular-carcinoma

69 **Finn RS**, Ryoo BY, Merle P, Kudo M, Bouattour M, Lim HY, Breder V, Edeline J, Chao Y, Ogasawara S, Yau T, Garrido M, Chan SL, Knox J, Daniele B, Ebbinghaus SW, Chen E, Siegel AB, Zhu AX, Cheng AL; KEYNOTE-240 investigators. Pembrolizumab As Second-Line Therapy in Patients With Advanced Hepatocellular Carcinoma in KEYNOTE-240: A Randomized, Double-Blind, Phase III Trial. *J Clin Oncol* 2020; **38**: 193-202 [PMID: 31790344 DOI: 10.1200/JCO.19.01307]

70 **Qin S**, Chen Z, Fang W, Ren Z, Xu R, Ryoo BY, Meng Z, Bai Y, Chen X, Liu X, Xiao J, Ho GF, Mao Y, Ye X, Ying J, Li J, Zhong WY, Zhou Y, Siegel AB, Hao C. Pembrolizumab plus best supportive care vs placebo plus best supportive care as second-line therapy in patients in Asia with advanced hepatocellular carcinoma (HCC): Phase 3 KEYNOTE-394 study. *J Clin Oncol* 2022; **40** Suppl 4: 383-383 [DOI: 10.1200/JCO.2022.40.4_suppl.383]

71 **Bayat Mokhtari R**, Homayouni TS, Baluch N, Morgatskaya E, Kumar S, Das B, Yeger H. Combination therapy in combating cancer. *Oncotarget* 2017; **8**: 38022-38043 [PMID: 28410237 DOI: 10.18632/oncotarget.16723]

72 **Kim GP**, Mahoney MR, Szydlo D, Mok TS, Marshke R, Holen K, Picus J, Boyer M, Pitot HC, Rubin J, Philip PA, Nowak A, Wright JJ, Erlichman C. An international, multicenter phase II trial of bortezomib in patients with hepatocellular carcinoma. *Invest New Drugs* 2012; **30**: 387-394 [PMID: 20839030 DOI: 10.1007/s10637-010-9532-1]

73 **He B**, Lu C, Zheng G, He X, Wang M, Chen G, Zhang G, Lu A. Combination therapeutics in complex diseases. *J Cell Mol Med* 2016; **20**: 2231-2240 [PMID: 27605177 DOI: 10.1111/jcmm.12930]

74 **Pemovska T**, Bigenzahn JW, Superti-Furga G. Recent advances in combinatorial drug screening and synergy scoring. *Curr Opin Pharmacol* 2018; **42**: 102-110 [PMID: 30193150 DOI: 10.1016/j.coph.2018.07.008]

75 **Lim JJ**, Hooi L, Dan YY, Bonney GK, Zhou L, Chow PK, Chee CE, Toh TB, Chow EK. Rational drug combination design in patient-derived avatars reveals effective inhibition of hepatocellular carcinoma with proteasome and CDK inhibitors. *J Exp Clin Cancer Res* 2022; **41**: 249 [PMID: 35971164 DOI: 10.1186/s13046-022-02436-9]

76 **Xu F**, Tong M, Tong CSW, Chan BKC, Chu HY, Wong TL, Fong JHC, Cheung MSH, Mak KH, Pardeshi L, Huang Y, Wong KH, Choi GCG, Ma S, Wong ASL. A Combinatorial CRISPR-Cas9 Screen Identifies Ifenprodil as an Adjunct to Sorafenib for Liver Cancer Treatment. *Cancer Res* 2021; **81**: 6219-6232 [PMID: 34666996 DOI: 10.1158/0008-5472.CAN-21-1017]

77 **Canzoneri R**, Lacunza E, Abba MC. Genomics and bioinformatics as pillars of precision medicine in oncology. *Medicina (B Aires)* 2019; **79**: 587-592 [PMID: 31864231]

78 **Suwinski P**, Ong C, Ling MHT, Poh YM, Khan AM, Ong HS. Advancing Personalized Medicine Through the Application

of Whole Exome Sequencing and Big Data Analytics. *Front Genet* 2019; **10**: 49 [PMID: 30809243 DOI: 10.3389/fgene.2019.00049]

79 **Wouters OJ**, McKee M, Luyten J. Estimated Research and Development Investment Needed to Bring a New Medicine to Market, 2009-2018. *JAMA* 2020; **323**: 844-853 [PMID: 32125404 DOI: 10.1001/jama.2020.1166]

80 **Corsello SM**, Nagari RT, Spangler RD, Rossen J, Kocak M, Bryan JG, Humeidi R, Peck D, Wu X, Tang AA, Wang VM, Bender SA, Lemire E, Narayan R, Montgomery P, Ben-David U, Garvie CW, Chen Y, Rees MG, Lyons NJ, McFarland JM, Wong BT, Wang L, Dumont N, O'Hearn PJ, Stefan E, Doench JG, Harrington CN, Greulich H, Meyerson M, Vazquez F, Subramanian A, Roth JA, Bittker JA, Boehm JS, Mader CC, Tsherniak A, Golub TR. Discovering the anti-cancer potential of non-oncology drugs by systematic viability profiling. *Nat Cancer* 2020; **1**: 235-248 [PMID: 32613204 DOI: 10.1038/s43018-019-0018-6]

81 **Shah RR**, Stonier PD. Repurposing old drugs in oncology: Opportunities with clinical and regulatory challenges ahead. *J Clin Pharm Ther* 2019; **44**: 6-22 [PMID: 30218625 DOI: 10.1111/jcpt.12759]

82 **Nair G**, Saraswathy GR, Hema Sree GNS. 48P Target mining and drug repurposing for hepatocellular carcinoma *via* bioinformatic and computational approaches. *Ann Oncol* 2021; **32**: S19 [DOI: 10.1016/j.annonc.2021.01.063]

83 **Nair G**, Hema Sree GNS, Saraswathy GR, Marise VLP, Krishna Murthy TP. Application of comprehensive bioinformatics approaches to reconnoiter crucial genes and pathways underpinning hepatocellular carcinoma: a drug repurposing endeavor. *Med Oncol* 2021; **38**: 145 [PMID: 34687371 DOI: 10.1007/s12032-021-01576-w]

84 **Massari NA**, Nicoud MB, Medina VA. Histamine receptors and cancer pharmacology: an update. *Br J Pharmacol* 2020; **177**: 516-538 [PMID: 30414378 DOI: 10.1111/bph.14535]

85 **Nguyen PL**, Cho J. Pathophysiological Roles of Histamine Receptors in Cancer Progression: Implications and Perspectives as Potential Molecular Targets. *Biomolecules* 2021; **11** [PMID: 34439898 DOI: 10.3390/biom11081232]

86 **Zhao J**, Hou Y, Yin C, Hu J, Gao T, Huang X, Zhang X, Xing J, An J, Wan S, Li J. Upregulation of histamine receptor H1 promotes tumor progression and contributes to poor prognosis in hepatocellular carcinoma. *Oncogene* 2020; **39**: 1724-1738 [PMID: 31740780 DOI: 10.1038/s41388-019-1093-y]

87 **Shen YC**, Hsu HC, Lin TM, Chang YS, Hu LF, Chen LF, Lin SH, Kuo PI, Chen WS, Lin YC, Chen JH, Liang YC, Chang CC. H1-Antihistamines Reduce the Risk of Hepatocellular Carcinoma in Patients With Hepatitis B Virus, Hepatitis C Virus, or Dual Hepatitis B Virus-Hepatitis C Virus Infection. *J Clin Oncol* 2022; **40**: 1206-1219 [PMID: 35044851 DOI: 10.1200/JCO.21.01802]

88 **Ellegaard AM**, Dehlendorff C, Vind AC, Anand A, Cederkvist L, Petersen NHT, Nylandsted J, Stenvang J, Mellemgaard A, Østerlind K, Friis S, Jäättelä M. Repurposing Cationic Amphiphilic Antihistamines for Cancer Treatment. *EbioMedicine* 2016; **9**: 130-139 [PMID: 27333030 DOI: 10.1016/j.ebiom.2016.06.013]

89 **Ortiz CS**, Montante-Montes D, Saqui-Salces M, Hinojosa LM, Gamboa-Dominguez A, Hernández-Gallegos E, Martínez-Benítez B, Del Rosario Solís-Pancoatl M, Garcia-Villa E, Ramírez A, Aguilar-Guadarrama R, Gariglio P, Pardo LA, Stühmer W, Camacho J. Eag1 potassium channels as markers of cervical dysplasia. *Oncol Rep* 2011; **26**: 1377-1383 [PMID: 21887469 DOI: 10.3892/or.2011.1441]

90 **Chen J**, Xuan Z, Song W, Han W, Chen H, Du Y, Xie H, Zhao Y, Zheng S, Song P. EAG1 enhances hepatocellular carcinoma proliferation by modulating SKP2 and metastasis through pseudopod formation. *Oncogene* 2021; **40**: 163-176 [PMID: 33097858 DOI: 10.1038/s41388-020-01522-6]

91 **García-Quiroz J**, Camacho J. Astemizole: an old anti-histamine as a new promising anti-cancer drug. *Anticancer Agents Med Chem* 2011; **11**: 307-314 [PMID: 21443504 DOI: 10.2174/187152011795347513]

92 **Hemmerlein B**, Weseloh RM, Mello de Queiroz F, Knötgen H, Sánchez A, Rubio ME, Martin S, Schliephacke T, Jenke M, Heinz-Joachim-Radzun, Stühmer W, Pardo LA. Overexpression of Eag1 potassium channels in clinical tumours. *Mol Cancer* 2006; **5**: 41 [PMID: 17022810 DOI: 10.1186/1476-4598-5-41]

93 **Toplak Ž**, Hendrickx LA, Abdelaziz R, Shi X, Peigneur S, Tomašič T, Tytgat J, Peterlin-Mašič L, Pardo LA. Overcoming challenges of HERG potassium channel liability through rational design: Eag1 inhibitors for cancer treatment. *Med Res Rev* 2022; **42**: 183-226 [PMID: 33945158 DOI: 10.1002/med.21808]

94 **Rodríguez-Rasgado JA**, Acuña-Macías I, Camacho J. Eag1 channels as potential cancer biomarkers. *Sensors (Basel)* 2012; **12**: 5986-5995 [PMID: 22778627 DOI: 10.3390/s120505986]

95 **Asher V**, Sowter H, Shaw R, Bali A, Khan R. Eag and HERG potassium channels as novel therapeutic targets in cancer. *World J Surg Oncol* 2010; **8**: 113 [PMID: 21190577 DOI: 10.1186/1477-7819-8-113]

96 **Smith GA**, Tsui HW, Newell EW, Jiang X, Zhu XP, Tsui FW, Schlichter LC. Functional up-regulation of HERG K+ channels in neoplastic hematopoietic cells. *J Biol Chem* 2002; **277**: 18528-18534 [PMID: 11893742 DOI: 10.1074/jbc.M200592200]

97 **Shao XD**, Wu KC, Hao ZM, Hong L, Zhang J, Fan DM. The potent inhibitory effects of cisapride, a specific blocker for human ether-a-go-go-related gene (HERG) channel, on gastric cancer cells. *Cancer Biol Ther* 2005; **4**: 295-301 [PMID: 15846098 DOI: 10.4161/cbt.4.3.1500]

98 **de Guadalupe Chávez-López M**, Pérez-Carreón JI, Zuñiga-García V, Díaz-Chávez J, Herrera LA, Caro-Sánchez CH, Acuña-Macías I, Gariglio P, Hernández-Gallegos E, Chiliquinga AJ, Camacho J. Astemizole-based anticancer therapy for hepatocellular carcinoma (HCC), and Eag1 channels as potential early-stage markers of HCC. *Tumour Biol* 2015; **36**: 6149-6158 [PMID: 25783527 DOI: 10.1007/s13277-015-3299-0]

99 **Gui L**, Xu Q, Huang J, Wu G, Tang H, Hui L, Hua P, Zhang L, Zhu Y. CYP2J2 promotes the development of hepatocellular carcinoma by increasing the EETs production to improve HIF-1α stability. *Am J Transl Res* 2020; **12**: 7923-7937 [PMID: 33437370]

100 **Hwang GH**, Park SM, Han HJ, Baek KM, Kim JS, Chang W, Lee HJ, Yun SP, Ryu JM, Lee MY. Role of cytochrome P450 2J2 on cell proliferation and resistance to an anticancer agent in hepatocellular carcinoma HepG2 cells. *Oncol Lett* 2017; **14**: 5484-5490 [PMID: 29098037 DOI: 10.3892/ol.2017.6846]

101 **Jeon YJ**, Kim JS, Hwang GH, Wu Z, Han HJ, Park SH, Chang W, Kim LK, Lee YM, Liu KH, Lee MY. Inhibition of cytochrome P450 2J2 by tanshinone IIA induces apoptotic cell death in hepatocellular carcinoma HepG2 cells. *Eur J Pharmacol* 2015; **764**: 480-488 [PMID: 26209360 DOI: 10.1016/j.ejphar.2015.07.047]

102 **Lee CA**, Jones JP 3rd, Katayama J, Kaspera R, Jiang Y, Freiwald S, Smith E, Walker GS, Totah RA. Identifying a selective substrate and inhibitor pair for the evaluation of CYP2J2 activity. *Drug Metab Dispos* 2012; **40**: 943-951 [PMID: 22328583 DOI: 10.1124/dmd.111.043505]

103 **Van den Eynde C**, Held K, Ciprietti M, De Clercq K, Kerselaers S, Marchand A, Chaltin P, Voets T, Vriens J. Loratadine, an antihistaminic drug, suppresses the proliferation of endometrial stromal cells by inhibition of TRPV2. *Eur J Pharmacol* 2022; **928**: 175086 [PMID: 35714693 DOI: 10.1016/j.ejphar.2022.175086]

104 **Sidhu G**, Akhondi H. Loratadine. In StatPearls. StatPearls Publishing 2022. [cited 31 October 2022]. Available from: http://www.ncbi.nlm.nih.gov/books/NBK542278/

105 **Fritz I**, Wagner P, Broberg P, Einefors R, Olsson H. Desloratadine and loratadine stand out among common H(1)-antihistamines for association with improved breast cancer survival. *Acta Oncol* 2020; **59**: 1103-1109 [PMID: 32459128 DOI: 10.1080/0284186X.2020.1769185]

106 **Fritz I**, Wagner P, Olsson H. Improved survival in several cancers with use of H(1)-antihistamines desloratadine and loratadine. *Transl Oncol* 2021; **14**: 101029 [PMID: 33550204 DOI: 10.1016/j.tranon.2021.101029]

107 **Kallunki T**, Olsen OD, Jäättelä M. Cancer-associated lysosomal changes: friends or foes? *Oncogene* 2013; **32**: 1995-2004 [PMID: 22777359 DOI: 10.1038/onc.2012.292]

108 **Adly N**. Evaluation of cytotoxic potential of loratadine and the combination of loratadine and cisplatin on hepatocellular carcinoma cell lines [American University in Cairo (AUC)] 2018. [cited 31 October 2022]. Available from: https://fount.aucegypt.edu/etds/418

109 **Hunto ST**, Kim HG, Baek KS, Jeong D, Kim E, Kim JH, Cho JY. Loratadine, an antihistamine drug, exhibits anti-inflammatory activity through suppression of the NF-(k)B pathway. *Biochem Pharmacol* 2020; **177**: 113949 [PMID: 32251678 DOI: 10.1016/j.bcp.2020.113949]

110 **de Vries TW**, Tobi H, Schirm E, van den Berg P, Duiverman EJ, de Jong-van den Berg LT. The gap between evidence-based medicine and daily practice in the management of paediatric asthma. A pharmacy-based population study from The Netherlands. *Eur J Clin Pharmacol* 2006; **62**: 51-55 [PMID: 16365748 DOI: 10.1007/s00228-005-0065-z]

111 **Liang YC**, Chang CC, Sheu MT, Lin SY, Chung CC, Teng CT, Suk FM. The Antihistamine Deptropine Induces Hepatoma Cell Death through Blocking Autophagosome-Lysosome Fusion. *Cancers (Basel)* 2020; **12** [PMID: 32570749 DOI: 10.3390/cancers12061610]

112 **Feng YM**, Feng CW, Chen SY, Hsieh HY, Chen YH, Hsu CD. Cyproheptadine, an antihistaminic drug, inhibits proliferation of hepatocellular carcinoma cells by blocking cell cycle progression through the activation of P38 MAP kinase. *BMC Cancer* 2015; **15**: 134 [PMID: 25886177 DOI: 10.1186/s12885-015-1137-9]

113 **Hsieh MC**, Lee WH, Wu AT, Chow JM, Chang CL, Yuan KS, Wu SY. Cyproheptadine use in hepatocellular carcinoma. *Am J Cancer Res* 2017; **7**: 584-602 [PMID: 28401014]

114 **Feng YM**, Chen TH, Berman D, Chou CK, Liao KS, Hsieh MC, Chen CY. Efficacy of Cyproheptadine Monotherapy in Hepatocellular Carcinoma With Bone Metastasis: A Case Report. *Front Oncol* 2021; **11**: 620212 [PMID: 34745929 DOI: 10.3389/fonc.2021.620212]

115 **Feng YM**, Feng CW, Chen SC, Hsu CD. Unexpected remission of hepatocellular carcinoma (HCC) with lung metastasis to the combination therapy of thalidomide and cyproheptadine: report of two cases and a preliminary HCC cell line study. *BMJ Case Rep* 2012; **2012** [PMID: 23076705 DOI: 10.1136/bcr-2012-007180]

116 **Feng YM**, Feng CW, Lu CL, Lee MY, Chen CY, Chen SC. Cyproheptadine significantly improves the overall and progression-free survival of sorafenib-treated advanced HCC patients. *Jpn J Clin Oncol* 2015; **45**: 336-342 [PMID: 25646358 DOI: 10.1093/jjco/hyv007]

117 **Shi Z**, Fultz RS, Engevik MA, Gao C, Hall A, Major A, Mori-Akiyama Y, Versalovic J. Distinct roles of histamine H1- and H2-receptor signaling pathways in inflammation-associated colonic tumorigenesis. *Am J Physiol Gastrointest Liver Physiol* 2019; **316**: G205-G216 [PMID: 30462522 DOI: 10.1152/ajpgi.00212.2018]

118 **Merétey K**, Falus A, Taga T, Kishimoto T. Histamine influences the expression of the interleukin-6 receptor on human lymphoid, monocytoid and hepatoma cell lines. *Agents Actions* 1991; **33**: 189-191 [PMID: 1680274 DOI: 10.1007/BF01993163]

119 **Lampiasi N**, Azzolina A, Montalto G, Cervello M. Histamine and spontaneously released mast cell granules affect the cell growth of human hepatocellular carcinoma cells. *Exp Mol Med* 2007; **39**: 284-294 [PMID: 17603279 DOI: 10.1038/emm.2007.32]

120 **Fujikawa T**, Shiraha H, Nakanishi Y, Takaoka N, Ueda N, Suzuki M, Shiratori Y. Cimetidine inhibits epidermal growth factor-induced cell signaling. *J Gastroenterol Hepatol* 2007; **22**: 436-443 [PMID: 17295779 DOI: 10.1111/j.1440-1746.2006.04541.x]

121 **Furuta K**, Sato S, Miyake T, Okamoto E, Ishine J, Ishihara S, Amano Y, Adachi K, Kinoshita Y. Anti-tumor effects of cimetidine on hepatocellular carcinomas in diethylnitrosamine-treated rats. *Oncol Rep* 2008; **19**: 361-368 [PMID: 18202782]

122 **Crouchet E**, Bandiera S, Fujiwara N, Li S, El Saghire H, Fernández-Vaquero M, Riedl T, Sun X, Hirschfield H, Jühling F, Zhu S, Roehlen N, Ponsolles C, Heydmann L, Saviano A, Qian T, Venkatesh A, Lupberger J, Verrier ER, Sojoodi M, Oudot MA, Duong FHT, Masia R, Wei L, Thumann C, Durand SC, González-Motos V, Heide D, Hetzer J, Nakagawa S, Ono A, Song WM, Higashi T, Sanchez R, Kim RS, Bian CB, Kiani K, Croonenborghs T, Subramanian A, Chung RT, Straub BK, Schuppan D, Ankavay M, Cocquerel L, Schaeffer E, Goossens N, Koh AP, Mahajan M, Nair VD, Gunasekaran G, Schwartz ME, Bardeesy N, Shalek AK, Rozenblatt-Rosen O, Regev A, Felli E, Pessaux P, Tanabe KK, Heikenwälder M, Schuster C, Pochet N, Zeisel MB, Fuchs BC, Hoshida Y, Baumert TF. A human liver cell-based system modeling a clinical prognostic liver signature for therapeutic discovery. *Nat Commun* 2021; **12**: 5525 [PMID: 34535664 DOI: 10.1038/s41467-021-25468-9]

123 **Tanaka T**, Kochi T, Shirakami Y, Mori T, Kurata A, Watanabe N, Moriwaki H, Shimizu M. Cimetidine and Clobenpropit Attenuate Inflammation-Associated Colorectal Carcinogenesis in Male ICR Mice. *Cancers (Basel)* 2016; **8** [PMID: 26907350 DOI: 10.3390/cancers8020025]

124 **Cricco GP**, Mohamad NA, Sambuco LA, Genre F, Croci M, Gutiérrez AS, Medina VA, Bergoc RM, Rivera ES, Martín

GA. Histamine regulates pancreatic carcinoma cell growth through H3 and H4 receptors. *Inflamm Res* 2008; **57** Suppl 1: S23-S24 [PMID: 18345506 DOI: 10.1007/s00011-007-0611-5]

125 **Yu D**, Zhao J, Wang Y, Hu J, Zhao Q, Li J, Zhu J. Upregulated histamine receptor H3 promotes tumor growth and metastasis in hepatocellular carcinoma. *Oncol Rep* 2019; **41**: 3347-3354 [PMID: 31002350 DOI: 10.3892/or.2019.7119]

126 **Zhang C**, Yu Y, Ma L, Fu P. Histamine H3 Receptor Promotes Cell Survival *via* Regulating PKA/CREB/CDKN1A Signal Pathway in Hepatocellular Carcinoma. *Onco Targets Ther* 2020; **13**: 3765-3776 [PMID: 32440145 DOI: 10.2147/OTT.S250655]

127 **Nicoud MB**, Formoso K, Medina VA. Pathophysiological Role of Histamine H4 Receptor in Cancer: Therapeutic Implications. *Front Pharmacol* 2019; **10**: 556 [PMID: 31231212 DOI: 10.3389/fphar.2019.00556]

128 **Shi L**, Feng Y, Lin H, Ma R, Cai X. Role of estrogen in hepatocellular carcinoma: is inflammation the key? *J Transl Med* 2014; **12**: 93 [PMID: 24708807 DOI: 10.1186/1479-5876-12-93]

129 **Villa E**. Role of estrogen in liver cancer. *Womens Health (Lond)* 2008; **4**: 41-50 [PMID: 19072450 DOI: 10.2217/17455057.4.1.41]

130 **Wei Q**, Guo P, Mu K, Zhang Y, Zhao W, Huai W, Qiu Y, Li T, Ma X, Liu Y, Chen X, Han L. Estrogen suppresses hepatocellular carcinoma cells through Erβ-mediated upregulation of the NLRP3 inflammasome. *Lab Invest* 2015; **95**: 804-816 [PMID: 26006022 DOI: 10.1038/labinvest.2015.63]

131 **Brady CW**. Liver disease in menopause. *World J Gastroenterol* 2015; **21**: 7613-7620 [PMID: 26167064 DOI: 10.3748/wjg.v21.i25.7613]

132 **Shimizu I**. Impact of oestrogens on the progression of liver disease. *Liver Int* 2003; **23**: 63-69 [PMID: 12640729 DOI: 10.1034/j.1600-0676.2003.00811.x]

133 **Sukocheva OA**. Estrogen, estrogen receptors, and hepatocellular carcinoma: Are we there yet? *World J Gastroenterol* 2018; **24**: 1-4 [PMID: 29358876 DOI: 10.3748/wjg.v24.i1.1]

134 **Villa E**, Colantoni A, Cammà C, Grottola A, Buttafoco P, Gelmini R, Ferretti I, Manenti F. Estrogen receptor classification for hepatocellular carcinoma: comparison with clinical staging systems. *J Clin Oncol* 2003; **21**: 441-446 [PMID: 12560432 DOI: 10.1200/JCO.2003.11.051]

135 **Matsushima-Nishiwaki R**, Yamada N, Hattori Y, Hosokawa Y, Tachi J, Hori T, Kozawa O. SERMs (selective estrogen receptor modulator), acting as estrogen receptor β agonists in hepatocellular carcinoma cells, inhibit the transforming growth factor-α-induced migration *via* specific inhibition of AKT signaling pathway. *PloS One* 2022; **17**: e0262485 [PMID: 35007301 DOI: 10.1371/journal.pone.0262485]

136 **Pinkerton JV**. Selective Estrogen Receptor Modulators in Gynecology Practice. *Clin Obstet Gynecol* 2021; **64**: 803-812 [PMID: 34310353 DOI: 10.1097/GRF.0000000000000647]

137 **Wang Y**, Ma H, Zhao C, Liu T, Yan D, Jou D, Li H, Zhang C, Lü J, Li C, Lin J, Li S, Lin L. Growth-suppressive activity of raloxifene on liver cancer cells by targeting IL-6/GP130 signaling. *Oncotarget* 2017; **8**: 33683-33693 [PMID: 28430601 DOI: 10.18632/oncotarget.16898]

138 **Hsia CY**, Huo TI, Chiang SY, Lu MF, Sun CL, Wu JC, Lee PC, Chi CW, Lui WY, Lee SD. Evaluation of interleukin-6, interleukin-10 and human hepatocyte growth factor as tumor markers for hepatocellular carcinoma. *Eur J Surg Oncol* 2007; **33**: 208-212 [PMID: 17140760 DOI: 10.1016/j.ejso.2006.10.036]

139 **Nakagawa H**, Maeda S, Yoshida H, Tateishi R, Masuzaki R, Ohki T, Hayakawa Y, Kinoshita H, Yamakado M, Kato N, Shiina S, Omata M. Serum IL-6 levels and the risk for hepatocarcinogenesis in chronic hepatitis C patients: an analysis based on gender differences. *Int J Cancer* 2009; **125**: 2264-2269 [PMID: 19585572 DOI: 10.1002/ijc.24720]

140 **Xu J**, Lin H, Wu G, Zhu M, Li M. IL-6/STAT3 Is a Promising Therapeutic Target for Hepatocellular Carcinoma. *Front Oncol* 2021; **11**: 760971 [PMID: 34976809 DOI: 10.3389/fonc.2021.760971]

141 **Naugler WE**, Sakurai T, Kim S, Maeda S, Kim K, Elsharkawy AM, Karin M. Gender disparity in liver cancer due to sex differences in MyD88-dependent IL-6 production. *Science* 2007; **317**: 121-124 [PMID: 17615358 DOI: 10.1126/science.1140485]

142 **Svinka J**, Mikulits W, Eferl R. STAT3 in hepatocellular carcinoma: new perspectives. *Hepat Oncol* 2014; **1**: 107-120 [PMID: 30190945 DOI: 10.2217/hep.13.7]

143 **Mutschler J**, Grosshans M, Soyka M, Rösner S. Current Findings and Mechanisms of Action of Disulfiram in the Treatment of Alcohol Dependence. *Pharmacopsychiatry* 2016; **49**: 137-141 [PMID: 26987743 DOI: 10.1055/s-0042-103592]

144 **Zha J**, Chen F, Dong H, Shi P, Yao Y, Zhang Y, Li R, Wang S, Li P, Wang W, Xu B. Disulfiram targeting lymphoid malignant cell lines *via* ROS-JNK activation as well as Nrf2 and NF-kB pathway inhibition. *J Transl Med* 2014; **12**: 163 [PMID: 24915933 DOI: 10.1186/1479-5876-12-163]

145 **Liu P**, Kumar IS, Brown S, Kannappan V, Tawari PE, Tang JZ, Jiang W, Armesilla AL, Darling JL, Wang W. Disulfiram targets cancer stem-like cells and reverses resistance and cross-resistance in acquired paclitaxel-resistant triple-negative breast cancer cells. *Br J Cancer* 2013; **109**: 1876-1885 [PMID: 24008666 DOI: 10.1038/bjc.2013.534]

146 **Wang Y**, Li W, Patel SS, Cong J, Zhang N, Sabbatino F, Liu X, Qi Y, Huang P, Lee H, Taghian A, Li JJ, DeLeo AB, Ferrone S, Epperly MW, Ferrone CR, Ly A, Brachtel EF, Wang X. Blocking the formation of radiation-induced breast cancer stem cells. *Oncotarget* 2014; **5**: 3743-3755 [PMID: 25003837 DOI: 10.18632/oncotarget.1992]

147 **Cong J**, Wang Y, Zhang X, Zhang N, Liu L, Soukup K, Michelakos T, Hong T, DeLeo A, Cai L, Sabbatino F, Ferrone S, Lee H, Levina V, Fuchs B, Tanabe K, Lillemoe K, Ferrone C, Wang X. A novel chemoradiation targeting stem and nonstem pancreatic cancer cells by repurposing disulfiram. *Cancer Lett* 2017; **409**: 9-19 [PMID: 28864067 DOI: 10.1016/j.canlet.2017.08.028]

148 **Nechushtan H**, Hamamreh Y, Nidal S, Gotfried M, Baron A, Shalev YI, Nisman B, Peretz T, Peylan-Ramu N. A phase Iib trial assessing the addition of disulfiram to chemotherapy for the treatment of metastatic non-small cell lung cancer. *Oncologist* 2015; **20**: 366-367 [PMID: 25777347 DOI: 10.1634/theoncologist.2014-0424]

149 **Davis CI**, Gu X, Kiefer RM, Ralle M, Gade TP, Brady DC. Altered copper homeostasis underlies sensitivity of hepatocellular carcinoma to copper chelation. *Metallomics* 2020; **12**: 1995-2008 [PMID: 33146201 DOI: 10.1039/d0mt00156b]

150 **Denoyer D**, Masaldan S, La Fontaine S, Cater MA. Targeting copper in cancer therapy: 'Copper That Cancer'. *Metallomics* 2015; **7**: 1459-1476 [PMID: 26313539 DOI: 10.1039/c5mt00149h]

151 **Li Y**, Wang LH, Zhang HT, Wang YT, Liu S, Zhou WL, Yuan XZ, Li TY, Wu CF, Yang JY. Disulfiram combined with copper inhibits metastasis and epithelial-mesenchymal transition in hepatocellular carcinoma through the NF-κB and TGF-β pathways. *J Cell Mol Med* 2018; **22**: 439-451 [PMID: 29148232 DOI: 10.1111/jcmm.13334]

152 **Kelley KC**, Grossman KF, Brittain-Blankenship M, Thorne KM, Akerley WL, Terrazas MC, Kosak KM, Boucher KM, Buys SS, McGregor KA, Werner TL, Agarwal N, Weis JR, Sharma S, Ward JH, Kennedy TP, Sborov DW, Shami PJ. A Phase 1 dose-escalation study of disulfiram and copper gluconate in patients with advanced solid tumors involving the liver using S-glutathionylation as a biomarker. *BMC Cancer* 2021; **21**: 510 [PMID: 33957901 DOI: 10.1186/s12885-021-08242-4]

153 **Czauderna C**, Castven D, Mahn FL, Marquardt JU. Context-Dependent Role of NF-κB Signaling in Primary Liver Cancer-from Tumor Development to Therapeutic Implications. *Cancers (Basel)* 2019; **11** [PMID: 31349670 DOI: 10.3390/cancers11081053]

154 **Luedde T**, Schwabe RF. NF-κB in the liver–linking injury, fibrosis and hepatocellular carcinoma. *Nat Rev Gastroenterol Hepatol* 2011; **8**: 108-118 [PMID: 21293511 DOI: 10.1038/nrgastro.2010.213]

155 **Yip NC**, Fombon IS, Liu P, Brown S, Kannappan V, Armesilla AL, Xu B, Cassidy J, Darling JL, Wang W. Disulfiram modulated ROS-MAPK and NFκB pathways and targeted breast cancer cells with cancer stem cell-like properties. *Br J Cancer* 2011; **104**: 1564-1574 [PMID: 21487404 DOI: 10.1038/bjc.2011.126]

156 **Thiery JP**. Epithelial-mesenchymal transitions in tumour progression. *Nat Rev Cancer* 2002; **2**: 442-454 [PMID: 12189386 DOI: 10.1038/nrc822]

157 **Zhang G**, Wang Y, Fuchs BC, Guo W, Drum DL, Erstad DJ, Shi B, DeLeo AB, Zheng H, Cai L, Zhang L, Tanabe KK, Wang X. Improving the Therapeutic Efficacy of Sorafenib for Hepatocellular Carcinoma by Repurposing Disulfiram. *Front Oncol* 2022; **12**: 913736 [PMID: 35912209 DOI: 10.3389/fonc.2022.913736]

158 **Komiya Y**, Habas R. Wnt signal transduction pathways. *Organogenesis* 2008; **4**: 68-75 [PMID: 19279717 DOI: 10.4161/org.4.2.5851]

159 **Duchartre Y**, Kim YM, Kahn M. The Wnt signaling pathway in cancer. *Crit Rev Oncol Hematol* 2016; **99**: 141-149 [PMID: 26775730 DOI: 10.1016/j.critrevonc.2015.12.005]

160 **Zhan T**, Rindtorff N, Boutros M. Wnt signaling in cancer. *Oncogene* 2017; **36**: 1461-1473 [PMID: 27617575 DOI: 10.1038/onc.2016.304]

161 **Zhang Y**, Wang X. Targeting the Wnt/β-catenin signaling pathway in cancer. *J Hematol Oncol* 2020; **13**: 165 [PMID: 33276800 DOI: 10.1186/s13045-020-00990-3]

162 **Arzumanian VA**, Kiseleva OI, Poverennaya EV. The Curious Case of the HepG2 Cell Line: 40 Years of Expertise. *Int J Mol Sci* 2021; **22** [PMID: 34884942 DOI: 10.3390/ijms222313135]

163 **He S**, Tang S. WNT/β-catenin signaling in the development of liver cancers. *Biomed Pharmacother* 2020; **132**: 110851 [PMID: 33080466 DOI: 10.1016/j.biopha.2020.110851]

164 **Ahmed K**, Koval A, Xu J, Bodmer A, Katanaev VL. Towards the first targeted therapy for triple-negative breast cancer: Repositioning of clofazimine as a chemotherapy-compatible selective Wnt pathway inhibitor. *Cancer Lett* 2019; **449**: 45-55 [PMID: 30771433 DOI: 10.1016/j.canlet.2019.02.018]

165 **Koval AV**, Vlasov P, Shichkova P, Khunderyakova S, Markov Y, Panchenko J, Volodina A, Kondrashov FA, Katanaev VL. Anti-leprosy drug clofazimine inhibits growth of triple-negative breast cancer cells *via* inhibition of canonical Wnt signaling. *Biochem Pharmacol* 2014; **87**: 571-578 [PMID: 24355563 DOI: 10.1016/j.bcp.2013.12.007]

166 **Xu J**, Koval A, Katanaev VL. Beyond TNBC: Repositioning of Clofazimine Against a Broad Range of Wnt-Dependent Cancers. *Front Oncol* 2020; **10**: 602817 [PMID: 33363033 DOI: 10.3389/fonc.2020.602817]

167 **Van Rensburg CE**, Van Staden AM, Anderson R. The riminophenazine agents clofazimine and B669 inhibit the proliferation of cancer cell lines in vitro by phospholipase A2-mediated oxidative and nonoxidative mechanisms. *Cancer Res* 1993; **53**: 318-323 [PMID: 7678073]

168 **Ruff P**, Chasen MR, Long JE, van Rensburg CE. A phase II study of oral clofazimine in unresectable and metastatic hepatocellular carcinoma. *Ann Oncol* 1998; **9**: 217-219 [PMID: 9553669 DOI: 10.1023/a:1008204911774]

169 **Sato B**. Can an autocrine loop explain sex-hormone-dependent tumor growth? *Oncology* 1999; **57** Suppl 2: 3-6 [PMID: 10545797 DOI: 10.1159/000012036]

170 **Venkatesan P**. Albendazole. *J Antimicrob Chemother* 1998; **41**: 145-147 [PMID: 9533454 DOI: 10.1093/jac/41.2.145]

171 **Kim U**, Shin C, Kim CY, Ryu B, Kim J, Bang J, Park JH. Albendazole exerts antiproliferative effects on prostate cancer cells by inducing reactive oxygen species generation. *Oncol Lett* 2021; **21**: 395 [PMID: 33777218 DOI: 10.3892/ol.2021.12656]

172 **Patel K**, Doudican NA, Schiff PB, Orlow SJ. Albendazole sensitizes cancer cells to ionizing radiation. *Radiat Oncol* 2011; **6**: 160 [PMID: 22094106 DOI: 10.1186/1748-717X-6-160]

173 **Petersen JSSM**, Baird SK. Treatment of breast and colon cancer cell lines with anti-helmintic benzimidazoles mebendazole or albendazole results in selective apoptotic cell death. *J Cancer Res Clin Oncol* 2021; **147**: 2945-2953 [PMID: 34148157 DOI: 10.1007/s00432-021-03698-0]

174 **Zhou F**, Du J, Wang J. Albendazole inhibits HIF-1α-dependent glycolysis and VEGF expression in non-small cell lung cancer cells. *Mol Cell Biochem* 2017; **428**: 171-178 [PMID: 28063005 DOI: 10.1007/s11010-016-2927-3]

175 **Zhu L**, Yang Q, Hu R, Li Y, Peng Y, Liu H, Ye M, Zhang B, Zhang P, Liu-Smith F, Li H, Liu J. Novel therapeutic strategy for melanoma based on albendazole and the CDK4/6 inhibitor palbociclib. *Sci Rep* 2022; **12**: 5706 [PMID: 35383224 DOI: 10.1038/s41598-022-09592-0]

176 **Pourgholami MH**, Woon L, Almajd R, Akhter J, Bowery P, Morris DL. In vitro and in vivo suppression of growth of hepatocellular carcinoma cells by albendazole. *Cancer Lett* 2001; **165**: 43-49 [PMID: 11248417 DOI: 10.1016/S0304-3835(01)00382-2]

177 **Smyj R**, Wang XP, Han F. Pimozide. *Profiles Drug Subst Excip Relat Methodol* 2012; **37**: 287-311 [PMID: 22469321 DOI: 10.1016/B978-0-12-397220-0.00007-6]

178 **Egolf A**, Coffey BJ. Current pharmacotherapeutic approaches for the treatment of Tourette syndrome. *Drugs Today (Barc)* 2014; **50**: 159-179 [PMID: 24619591 DOI: 10.1358/dot.2014.50.2.2097801]

179 **Dakir el-H**, Pickard A, Srivastava K, McCrudden CM, Gross SR, Lloyd S, Zhang SD, Margariti A, Morgan R, Rudland PS, El-Tanani M. The anti-psychotic drug pimozide is a novel chemotherapeutic for breast cancer. *Oncotarget* 2018; **9**: 34889-34910 [PMID: 30405882 DOI: 10.18632/oncotarget.26175]

180 **Li J**, Qu P, Zhou XZ, Ji YX, Yuan S, Liu SP, Zhang QG. Pimozide inhibits the growth of breast cancer cells by alleviating the Warburg effect through the P53 signaling pathway. *Biomed Pharmacother* 2022; **150**: 113063 [PMID: 35658233 DOI: 10.1016/j.biopha.2022.113063]

181 **Kim U**, Kim CY, Lee JM, Ryu B, Kim J, Shin C, Park JH. Pimozide Inhibits the Human Prostate Cancer Cells Through the Generation of Reactive Oxygen Species. *Front Pharmacol* 2019; **10**: 1517 [PMID: 32009948 DOI: 10.3389/fphar.2019.01517]

182 **Ranjan A**, Kaushik I, Srivastava SK. Pimozide Suppresses the Growth of Brain Tumors by Targeting STAT3-Mediated Autophagy. *Cells* 2020; **9** [PMID: 32971907 DOI: 10.3390/cells9092141]

183 **Ren Y**, Tao J, Jiang Z, Guo D, Tang J. Pimozide suppresses colorectal cancer *via* inhibition of Wnt/β-catenin signaling pathway. *Life Sci* 2018; **209**: 267-273 [PMID: 30107167 DOI: 10.1016/j.lfs.2018.08.027]

184 **Nelson EA**, Walker SR, Weisberg E, Bar-Natan M, Barrett R, Gashin LB, Terrell S, Klitgaard JL, Santo L, Addorio MR, Ebert BL, Griffin JD, Frank DA. The STAT5 inhibitor pimozide decreases survival of chronic myelogenous leukemia cells resistant to kinase inhibitors. *Blood* 2011; **117**: 3421-3429 [PMID: 21233313 DOI: 10.1182/blood-2009-11-255232]

185 **Fako V**, Yu Z, Henrich CJ, Ransom T, Budhu AS, Wang XW. Inhibition of wnt/β-catenin Signaling in Hepatocellular Carcinoma by an Antipsychotic Drug Pimozide. *Int J Biol Sci* 2016; **12**: 768-775 [PMID: 27313491 DOI: 10.7150/ijbs.14718]

186 **Noh CK**, Wang HJ, Kim CM, Kim J, Yoon SY, Lee GH, Cho HJ, Yang MJ, Kim SS, Hwang JC, Cho SW, Roh J, Kim YB, Kim SJ, Kim BW, Cheong JY. EpCAM as a Predictive Marker of Tumor Recurrence and Survival in Patients Who Underwent Surgical Resection for Hepatocellular Carcinoma. *Anticancer Res* 2018; **38**: 4101-4109 [PMID: 29970536 DOI: 10.21873/anticanres.12700]

187 **Vasanthakumar S**, Sasikala P, Padma M, Balachandar V, Venkatesh B, Ganesan S. EpCAM as a novel therapeutic target for hepatocellular carcinoma. *J Oncol Sci* 2017; **3**: 71-76 [DOI: 10.1016/j.jons.2017.04.002]

188 **Chen JJ**, Zhang LN, Cai N, Zhang Z, Ji K. Antipsychotic agent pimozide promotes reversible proliferative suppression by inducing cellular quiescence in liver cancer. *Oncol Rep* 2019; **42**: 1101-1109 [PMID: 31322218 DOI: 10.3892/or.2019.7229]

189 **National Center for Biotechnology Information (2022)**. PubChem Compound Summary for CID 5284447, Natamycin. [cited 9 November 2022]. Available from: https://pubchem.ncbi.nlm.nih.gov/compound/Natamycin

190 **Vasquez JL**, Lai Y, Annamalai T, Jiang Z, Zhang M, Lei R, Zhang Z, Liu Y, Tse-Dinh YC, Agoulnik IU. Inhibition of base excision repair by natamycin suppresses prostate cancer cell proliferation. *Biochimie* 2020; **168**: 241-250 [PMID: 31756402 DOI: 10.1016/j.biochi.2019.11.008]

191 **An Y**, Jiang J, Zhou L, Shi J, Jin P, Li L, Peng L, He S, Zhang W, Huang C, Zou B, Xie N. Peroxiredoxin 1 is essential for natamycin-triggered apoptosis and protective autophagy in hepatocellular carcinoma. *Cancer Lett* 2021; **521**: 210-223 [PMID: 34428517 DOI: 10.1016/j.canlet.2021.08.023]

192 **Aggarwal V**, Tuli HS, Varol A, Thakral F, Yerer MB, Sak K, Varol M, Jain A, Khan MA, Sethi G. Role of Reactive Oxygen Species in Cancer Progression: Molecular Mechanisms and Recent Advancements. *Biomolecules* 2019; **9** [PMID: 31766246 DOI: 10.3390/biom9110735]

193 **Reczek CR**, Chandel NS. The Two Faces of Reactive Oxygen Species in Cancer. *Annu Rev Cancer Biol* 2017; **1**: 79-98 [DOI: 10.1146/annurev-cancerbio-041916-065808]

194 **Singh R**, Manna PP. Reactive oxygen species in cancer progression and its role in therapeutics. *Explor Med* 2022; 43-57 [DOI: 10.37349/emed.2022.00073]

195 **Harris IS**, DeNicola GM. The Complex Interplay between Antioxidants and ROS in Cancer. *Trends Cell Biol* 2020; **30**: 440-451 [PMID: 32303435 DOI: 10.1016/j.tcb.2020.03.002]

196 **Hampton MB**, Vick KA, Skoko JJ, Neumann CA. Peroxiredoxin Involvement in the Initiation and Progression of Human Cancer. *Antioxid Redox Signal* 2018; **28**: 591-608 [PMID: 29237274 DOI: 10.1089/ars.2017.7422]

197 **Kim Y**, Jang HH. The Role of Peroxiredoxin Family in Cancer Signaling. *J Cancer Prev* 2019; **24**: 65-71 [PMID: 31360686 DOI: 10.15430/JCP.2019.24.2.65]

198 **Sun YL**, Cai JQ, Liu F, Bi XY, Zhou LP, Zhao XH. Aberrant expression of peroxiredoxin 1 and its clinical implications in liver cancer. *World J Gastroenterol* 2015; **21**: 10840-10852 [PMID: 26478675 DOI: 10.3748/wjg.v21.i38.10840]

199 **Ghodke-Puranik Y**, Thorn CF, Lamba JK, Leeder JS, Song W, Birnbaum AK, Altman RB, Klein TE. Valproic acid pathway: pharmacokinetics and pharmacodynamics. *Pharmacogenet Genomics* 2013; **23**: 236-241 [PMID: 23407051 DOI: 10.1097/FPC.0b013e32835ea0b2]

200 **Cinatl J Jr**, Cinatl J, Driever PH, Kotchetkov R, Pouckova P, Kornhuber B, Schwabe D. Sodium valproate inhibits in vivo growth of human neuroblastoma cells. *Anticancer Drugs* 1997; **8**: 958-963 [PMID: 9436639 DOI: 10.1097/00001813-199711000-00007]

201 **Machado MC**, Bellodi-Privato M, Kubrusly MS, Molan NA, Tharcisio T Jr, de Oliveira ER, D'Albuquerque LA. Valproic acid inhibits human hepatocellular cancer cells growth in vitro and in vivo. *J Exp Ther Oncol* 2011; **9**: 85-92 [PMID: 21699015]

202 **Bai X**, Liu L, Wang Y. Valproate Ameliorates Diethylnitrosamine/Phenobarbital- Induced Hepatic Cancer *via* the Role of TNF-α and TGF-β1. *Int J Pharmacol* 2021; **17**: 156-168 [DOI: 10.3923/ijp.2021.156.168]

203 **Lee JH**, Lee JH, Lim YS, Yeon JE, Song TJ, Yu SJ, Gwak GY, Kim KM, Kim YJ, Lee JW, Yoon JH. Adjuvant immunotherapy with autologous cytokine-induced killer cells for hepatocellular carcinoma. *Gastroenterology* 2015; **148**: 1383-91.e6 [PMID: 25747273 DOI: 10.1053/j.gastro.2015.02.055]

204 **Lee JH**, Lee JH, Lim YS, Yeon JE, Song TJ, Yu SJ, Gwak GY, Kim KM, Kim YJ, Lee JW, Yoon JH. Sustained efficacy of adjuvant immunotherapy with cytokine-induced killer cells for hepatocellular carcinoma: an extended 5-year follow-up.

Cancer Immunol Immunother 2019; **68**: 23-32 [PMID: 30232520 DOI: 10.1007/s00262-018-2247-4]

205 **Ma Y**, Xu YC, Tang L, Zhang Z, Wang J, Wang HX. Cytokine-induced killer (CIK) cell therapy for patients with hepatocellular carcinoma: efficacy and safety. *Exp Hematol Oncol* 2012; **1**: 11 [PMID: 23210562 DOI: 10.1186/2162-3619-1-11]

206 **Lee DH**, Nam JY, Chang Y, Cho H, Kang SH, Cho YY, Cho E, Lee JH, Yu SJ, Kim YJ, Yoon JH. Synergistic effect of cytokine-induced killer cell with valproate inhibits growth of hepatocellular carcinoma cell in a mouse model. *Cancer Biol Ther* 2017; **18**: 67-75 [PMID: 28055304 DOI: 10.1080/15384047.2016.1276132]

207 **Yu JI**, Choi C, Shin SW, Son A, Lee GH, Kim SY, Park HC. Valproic Acid Sensitizes Hepatocellular Carcinoma Cells to Proton Therapy by Suppressing NRF2 Activation. *Sci Rep* 2017; **7**: 14986 [PMID: 29118323 DOI: 10.1038/s41598-017-15165-3]

208 **Lane AA**, Chabner BA. Histone Deacetylase Inhibitors in Cancer Therapy. *J Clin Oncol* 2009; **27**: 5459-5468 [PMID: 19826124 DOI: 10.1200/JCO.2009.22.1291]

209 **Li G**, Tian Y, Zhu WG. The Roles of Histone Deacetylases and Their Inhibitors in Cancer Therapy. *Front Cell Dev Biol* 2020; **8**: 576946 [PMID: 33117804 DOI: 10.3389/fcell.2020.576946]

210 **West AC**, Johnstone RW. New and emerging HDAC inhibitors for cancer treatment. *J Clin Invest* 2014; **124**: 30-39 [PMID: 24382387 DOI: 10.1172/JCI69738]

211 **Munshi A**, Tanaka T, Hobbs ML, Tucker SL, Richon VM, Meyn RE. Vorinostat, a histone deacetylase inhibitor, enhances the response of human tumor cells to ionizing radiation through prolongation of gamma-H2AX foci. *Mol Cancer Ther* 2006; **5**: 1967-1974 [PMID: 16928817 DOI: 10.1158/1535-7163.MCT-06-0022]

212 **Chen W**, Chiang CL, Dawson LA. Efficacy and safety of radiotherapy for primary liver cancer. *Chin Clin Oncol* 2021; **10**: 9 [PMID: 32576017 DOI: 10.21037/cco-20-89]

213 **An HM**, Xue YF, Shen YL, Du Q, Hu B. Sodium valproate induces cell senescence in human hepatocarcinoma cells. *Molecules* 2013; **18**: 14935-14947 [PMID: 24304587 DOI: 10.3390/molecules181214935]

214 **Pernicova I**, Korbonits M. Metformin–mode of action and clinical implications for diabetes and cancer. *Nat Rev Endocrinol* 2014; **10**: 143-156 [PMID: 24393785 DOI: 10.1038/nrendo.2013.256]

215 **Zhang Z**, Zhou L, Xie N, Nice EC, Zhang T, Cui Y, Huang C. Overcoming cancer therapeutic bottleneck by drug repurposing. *Signal Transduct Target Ther* 2020; **5**: 113 [PMID: 32616710 DOI: 10.1038/s41392-020-00213-8]

216 **Akce M**, Rupji M, Switchenko JM, Shaib WL, Wu C, Alese OB, Diab M, Lesinski GB, El-Rayes BF. Phase II trial of nivolumab and metformin in patients with treatment refractory microsatellite stable metastatic colorectal cancer. *J Clin Oncol* 2021; **39** Suppl 3: 95 [DOI: 10.1200/JCO.2021.39.3_suppl.95]

217 **Goodwin PJ**, Chen BE, Gelmon KA, Whelan TJ, Ennis M, Lemieux J, Ligibel JA, Hershman DL, Mayer IA, Hobday TJ, Bliss JM, Rastogi P, Rabaglio-Poretti M, Mukherjee SD, Mackey JR, Abramson VG, Oja C, Wesolowski R, Thompson AM, Rea DW, Stos PM, Shepherd LE, Stambolic V, Parulekar WR. Effect of Metformin vs Placebo on Invasive Disease-Free Survival in Patients With Breast Cancer: The MA.32 Randomized Clinical Trial. *JAMA* 2022; **327**: 1963-1973 [PMID: 35608580 DOI: 10.1001/jama.2022.6147]

218 **Soliman PT**, Westin SN, Iglesias DA, Fellman BM, Yuan Y, Zhang Q, Yates MS, Broaddus RR, Slomovitz BM, Lu KH, Coleman RL. Everolimus, Letrozole, and Metformin in Women with Advanced or Recurrent Endometrioid Endometrial Cancer: A Multi-Center, Single Arm, Phase II Study. *Clin Cancer Res* 2020; **26**: 581-587 [PMID: 31628143 DOI: 10.1158/1078-0432.CCR-19-0471]

219 **Wilson BE**, Armstrong AJ, de Bono J, Sternberg CN, Ryan CJ, Scher HI, Smith MR, Rathkopf D, Logothetis CJ, Chi KN, Jones RJ, Saad F, De Porre P, Tran N, Hu P, Gillessen S, Carles J, Fizazi K, Joshua AM. Effects of metformin and statins on outcomes in men with castration-resistant metastatic prostate cancer: Secondary analysis of COU-AA-301 and COU-AA-302. *Eur J Cancer* 2022; **170**: 296-304 [PMID: 35568679 DOI: 10.1016/j.ejca.2022.03.042]

220 **Ma SJ**, Zheng YX, Zhou PC, Xiao YN, Tan HZ. Metformin use improves survival of diabetic liver cancer patients: systematic review and meta-analysis. *Oncotarget* 2016; **7**: 66202-66211 [PMID: 27494848 DOI: 10.18632/oncotarget.11033]

221 **Ma S**, Zheng Y, Xiao Y, Zhou P, Tan H. Meta-analysis of studies using metformin as a reducer for liver cancer risk in diabetic patients. *Medicine (Baltimore)* 2017; **96**: e6888 [PMID: 28489794 DOI: 10.1097/MD.0000000000006888]

222 **Pollak M**. Overcoming Drug Development Bottlenecks With Repurposing: Repurposing biguanides to target energy metabolism for cancer treatment. *Nat Med* 2014; **20**: 591-593 [PMID: 24901568 DOI: 10.1038/nm.3596]

223 **Howell JJ**, Hellberg K, Turner M, Talbott G, Kolar MJ, Ross DS, Hoxhaj G, Saghatelian A, Shaw RJ, Manning BD. Metformin Inhibits Hepatic mTORC1 Signaling *via* Dose-Dependent Mechanisms Involving AMPK and the TSC Complex. *Cell Metab* 2017; **25**: 463-471 [PMID: 28089566 DOI: 10.1016/j.cmet.2016.12.009]

224 **Stancu C**, Sima A. Statins: mechanism of action and effects. *J Cell Mol Med* 2001; **5**: 378-387 [PMID: 12067471 DOI: 10.1111/j.1582-4934.2001.tb00172.x]

225 **Clendening JW**, Pandyra A, Boutros PC, El Ghamrasni S, Khosravi F, Trentin GA, Martirosyan A, Hakem A, Hakem R, Jurisica I, Penn LZ. Dysregulation of the mevalonate pathway promotes transformation. *Proc Natl Acad Sci U S A* 2010; **107**: 15051-15056 [PMID: 20696928 DOI: 10.1073/pnas.0910258107]

226 **Mullen PJ**, Yu R, Longo J, Archer MC, Penn LZ. The interplay between cell signalling and the mevalonate pathway in cancer. *Nat Rev Cancer* 2016; **16**: 718-731 [PMID: 27562463 DOI: 10.1038/nrc.2016.76]

227 **Jiang W**, Hu JW, He XR, Jin WL, He XY. Statins: a repurposed drug to fight cancer. *J Exp Clin Cancer Res* 2021; **40**: 241 [PMID: 34303383 DOI: 10.1186/s13046-021-02041-2]

228 **Kodach LL**, Jacobs RJ, Voorneveld PW, Wildenberg ME, Verspaget HW, van Wezel T, Morreau H, Hommes DW, Peppelenbosch MP, van den Brink GR, Hardwick JC. Statins augment the chemosensitivity of colorectal cancer cells inducing epigenetic reprogramming and reducing colorectal cancer cell 'stemness' *via* the bone morphogenetic protein pathway. *Gut* 2011; **60**: 1544-1553 [PMID: 21551187 DOI: 10.1136/gut.2011.237495]

229 **Longo J**, van Leeuwen JE, Elbaz M, Branchard E, Penn LZ. Statins as Anticancer Agents in the Era of Precision Medicine. *Clin Cancer Res* 2020; **26**: 5791-5800 [PMID: 32887721 DOI: 10.1158/1078-0432.CCR-20-1967]

230 **Mansourian PG**, Yoneda M, Krishna Rao M, Martinez FJ, Thomas E, Schiff ER. Effects of statins on the risk of

hepatocellular carcinoma. *Gastroenterol Hepatol (N Y)* 2014; **10**: 417-426 [PMID: 25904829]

231 **Kim MH**, Kim MY, Salloum S, Qian T, Wong LP, Xu M, Lee Y, Shroff SG, Sadreyev RI, Corey KE, Baumert TF, Hoshida Y, Chung RT. Atorvastatin favorably modulates a clinical hepatocellular carcinoma risk gene signature. *Hepatol Commun* 2022; **6**: 2581-2593 [PMID: 35712812 DOI: 10.1002/hep4.1991]

232 **Krasselt M**, Baerwald C. Celecoxib for the treatment of musculoskeletal arthritis. *Expert Opin Pharmacother* 2019; **20**: 1689-1702 [PMID: 31339385 DOI: 10.1080/14656566.2019.1645123]

233 **Khafaga AF**, Shamma RN, Abdeen A, Barakat AM, Noreldin AE, Elzoghby AO, Sallam MA. Celecoxib repurposing in cancer therapy: molecular mechanisms and nanomedicine-based delivery technologies. *Nanomedicine (Lond)* 2021; **16**: 1691-1712 [PMID: 34264123 DOI: 10.2217/nnm-2021-0086]

234 **Sobolewski C**, Legrand N. Celecoxib Analogues for Cancer Treatment: An Update on OSU-03012 and 2,5-Dimethyl-Celecoxib. *Biomolecules* 2021; **11** [PMID: 34356673 DOI: 10.3390/biom11071049]

235 **Tołoczko-Iwaniuk N**, Dziemiańczyk-Pakieła D, Nowaszewska BK, Celińska-Janowicz K, Miltyk W. Celecoxib in Cancer Therapy and Prevention – Review. *Curr Drug Targets* 2019; **20**: 302-315 [PMID: 30073924 DOI: 10.2174/1389450119666180803121737]

236 **Hashemi Goradel N**, Najafi M, Salehi E, Farhood B, Mortezaee K. Cyclooxygenase-2 in cancer: A review. *J Cell Physiol* 2019; **234**: 5683-5699 [PMID: 30341914 DOI: 10.1002/jcp.27411]

237 **Dai H**, Zhang S, Ma R, Pan L. Celecoxib Inhibits Hepatocellular Carcinoma Cell Growth and Migration by Targeting PNO1. *Med Sci Monit* 2019; **25**: 7351-7360 [PMID: 31568401 DOI: 10.12659/MSM.919218]

238 **Li J**, Liu L, Chen Y, Wu M, Lin X, Shen Z, Cheng Y, Chen X, Weygant N, Wu X, Wei L, Sferra TJ, Han Y, Shen A, Peng J. Ribosome assembly factor PNO1 is associated with progression and promotes tumorigenesis in triplenegative breast cancer. *Oncol Rep* 2022; **47** [PMID: 35445733 DOI: 10.3892/or.2022.8319]

239 **Lin C**, Yuan H, Wang W, Zhu Z, Lu Y, Wang J, Feng F, Wu J. Importance of PNO1 for growth and survival of urinary bladder carcinoma: Role in core-regulatory circuitry. *J Cell Mol Med* 2020; **24**: 1504-1515 [PMID: 31800162 DOI: 10.1111/jcmm.14835]

240 **Liu D**, Lin L, Wang Y, Chen L, He Y, Luo Y, Qi L, Guo Y, Han Z, Li G, Li Q, Liu Z, Chen P, Guo H. PNO1, which is negatively regulated by miR-340-5p, promotes lung adenocarcinoma progression through Notch signaling pathway. *Oncogenesis* 2020; **9**: 58 [PMID: 32483111 DOI: 10.1038/s41389-020-0241-0]

241 **Shen Z**, Chen Y, Li L, Liu L, Peng M, Chen X, Wu X, Sferra TJ, Wu M, Lin X, Cheng Y, Chu J, Shen A, Peng J. Transcription Factor EBF1 Over-Expression Suppresses Tumor Growth in vivo and in vitro *via* Modulation of the PNO1/p53 Pathway in Colorectal Cancer. *Front Oncol* 2020; **10**: 1035 [PMID: 32676457 DOI: 10.3389/fonc.2020.01035]

242 **Wang G**, Li Q, Li C, Duan G, Sang H, Dong H, Yang Y, Ma C, Tao T. Knockdown of PNO1 inhibits esophageal cancer progression. *Oncol Rep* 2021; **45** [PMID: 33864661 DOI: 10.3892/or.2021.8036]

243 **Han Z**, Liu D, Chen L, He Y, Tian X, Qi L, Luo Y, Chen Z, Hu X, Li G, Zhan L, Wang Y, Li Q, Chen P, Liu Z, Guo H. PNO1 regulates autophagy and apoptosis of hepatocellular carcinoma *via* the MAPK signaling pathway. *Cell Death Dis* 2021; **12**: 552 [PMID: 34050137 DOI: 10.1038/s41419-021-03837-y]

244 **Hu JW**, Chen B, Zhang J, Qi YP, Liang JH, Zhong JH, Xiang BD. Novel combination of celecoxib and metformin improves the antitumor effect by inhibiting the growth of Hepatocellular Carcinoma. *J Cancer* 2020; **11**: 6437-6444 [PMID: 33033527 DOI: 10.7150/jca.47532]

245 **Levy JMM**, Towers CG, Thorburn A. Targeting autophagy in cancer. *Nat Rev Cancer* 2017; **17**: 528-542 [PMID: 28751651 DOI: 10.1038/nrc.2017.53]

246 **Mohamed FE**, Al-Jehani RM, Minogue SS, Andreola F, Winstanley A, Olde Damink SW, Habtesion A, Malagó M, Davies N, Luong TV, Dhillon AP, Mookerjee RP, Dhar DK, Jalan R. Effect of toll-like receptor 7 and 9 targeted therapy to prevent the development of hepatocellular carcinoma. *Liver Int* 2015; **35**: 1063-1076 [PMID: 24990399 DOI: 10.1111/liv.12626]

247 **Chen MY**, Yadav VK, Chu YC, Ong JR, Huang TY, Lee KF, Lee KH, Yeh CT, Lee WH. Hydroxychloroquine (HCQ) Modulates Autophagy and Oxidative DNA Damage Stress in Hepatocellular Carcinoma to Overcome Sorafenib Resistance *via* TLR9/SOD1/hsa-miR-30a-5p/Beclin-1 Axis. *Cancers (Basel)* 2021; **13** [PMID: 34203465 DOI: 10.3390/cancers13133227]

World Journal of Gastroenterology

Submit a Manuscript: https://www.f6publishing.com

World J Gastroenterol 2023 May 7; 29(17): 2600-2615

DOI: 10.3748/wjg.v29.i17.2600

ISSN 1007-9327 (print) ISSN 2219-2840 (online)

MINIREVIEWS

Difficult colorectal polypectomy: Technical tips and recent advances

Sukit Pattarajierapan, Hiroyuki Takamaru, Supakij Khomvilai

Specialty type: Gastroenterology and hepatology

Provenance and peer review: Invited article; Externally peer reviewed.

Peer-review model: Single blind

Peer-review report's scientific quality classification

Grade A (Excellent): 0
Grade B (Very good): B, B, B
Grade C (Good): C
Grade D (Fair): D
Grade E (Poor): 0

P-Reviewer: Argyriou K, Greece; Gao SG, China; Ichita C, Japan; Rasa K, Turkey

Received: January 29, 2023
Peer-review started: January 29, 2023
First decision: February 14, 2023
Revised: February 24, 2023
Accepted: April 12, 2023
Article in press: April 12, 2023
Published online: May 7, 2023

Sukit Pattarajierapan, Supakij Khomvilai, Surgical Endoscopy Colorectal Division, Department of Surgery, Faculty of Medicine, Chulalongkorn University, Bangkok 10330, Thailand

Hiroyuki Takamaru, Endoscopy Division, National Cancer Center Hospital, Tokyo 104-0045, Japan

Corresponding author: Sukit Pattarajierapan, MD, Doctor, Surgeon, Surgical Endoscopy Colorectal Division, Department of Surgery, Faculty of Medicine, Chulalongkorn University, 1873 Rama IV Road, Pathumwan, Bangkok 10330, Thailand. sukit.p@chulahospital.org

Abstract

Colonoscopy has been shown to be an effective modality to prevent colorectal cancer (CRC) development. CRC reduction is achieved by detecting and removing adenomas, which are precursors of CRC. Most colorectal polyps are small and do not pose a significant challenge for trained and skilled endoscopists. However, up to 15% of polyps are considered "difficult", potentially causing life-threatening complications. A difficult polyp is defined as any polyp that is challenging for the endoscopist to remove owing to its size, shape, or location. Advanced polypectomy techniques and skills are required to resect difficult colorectal polyps. There were various polypectomy techniques for difficult polyps such as endoscopic mucosal resection (EMR), underwater EMR, Tip-in EMR, endoscopic submucosal dissection (ESD), or endoscopic full-thickness resection. The selection of the appropriate modality depends on the morphology and endoscopic diagnosis. Several technologies have been developed to aid endoscopists in performing safe and effective polypectomies, especially complex procedures such as ESD. These advances include video endoscopy system, equipment assisting in advanced polypectomy, and closure devices/techniques for complication management. Endoscopists should know how to use these devices and their availability in practice to enhance polypectomy performance. This review describes several useful strategies and tips for managing difficult colorectal polyps. We also propose the stepwise approach for difficult colorectal polyps.

Key Words: Adenoma; Colonic polyps; Colonoscopy; Endoscopic mucosal resection; Endoscopic submucosal dissection; Polypectomy

Core Tip: Most colorectal polyps are small and do not pose a significant challenge to resection. However, up to 15% of polyps are considered "difficult" because of their size, shape, or location. Advanced polypectomy techniques and skills are required for the resection of difficult colorectal polyps. Recent advancements in techniques and devices for endoscopic mucosal resection, endoscopic submucosal dissection, and endoscopic full-thickness resection allow curative therapy of these difficult polyps and avoid unnecessary surgery that carries the risk of morbidity and mortality. However, the proper selection of adjunct endoscopic devices/techniques and stepwise training for skill improvement are critical for successful advanced polypectomy.

Citation: Pattarajierapan S, Takamaru H, Khomvilai S. Difficult colorectal polypectomy: Technical tips and recent advances. *World J Gastroenterol* 2023; 29(17): 2600-2615
URL: https://www.wjgnet.com/1007-9327/full/v29/i17/2600.htm
DOI: https://dx.doi.org/10.3748/wjg.v29.i17.2600

INTRODUCTION

In 2020, colorectal cancer (CRC) was the fourth most common malignancy worldwide, with 1.9 million new cases recorded[1]. Colonoscopy has been shown to be an effective modality to prevent CRC development. Previous studies have shown a 60%-90% reduction in CRC incidence after screening colonoscopy[2,3]. CRC reduction is achieved by detecting and removing adenomas, which are precursors of CRC. Most colorectal polyps detected during colonoscopy are small, benign, and easily resected by skilled endoscopists. However, 10%-15% of colorectal polyps are classified as "difficult" colorectal polyps[4,5]. Generally, difficult colorectal polyps are defined as any polyps that are technically challenging for endoscopic resection because of their size (> 20 mm), morphology (pedunculated polyp with a thick stalk, laterally spreading tumor), or location (ileocecal valve, appendiceal orifice, dentate line)[5,6].

Endoscopic resection of difficult polyps is associated with an increased risk of incomplete resection and serious adverse events, including intra-procedural massive bleeding and perforation. Therefore, difficult polypectomy should be performed or supervised by an experienced endoscopist. This review describes helpful strategies and tips for dealing with difficult colorectal polyps.

THE STEPWISE APPROACH FOR DIFFICULT COLORECTAL POLYPS

Lesion assessment

The first step in managing colorectal polyps is lesion assessment. Dye-based chromoendoscopy and image-enhanced endoscopy (IEE) with magnifying observation should be used to distinguish benign lesions, adenomas, and adenocarcinomas. Dye-based chromoendoscopy with indigo carmine and crystal violet enables pit pattern diagnosis based on Kudo's classification[7]. However, IEE techniques such as narrow-band imaging (NBI) and blue laser imaging are more common than chromoendoscopy in clinical practice outside Japan. IEE can diagnose lesions by visualizing surface patterns and microvessels based on the NBI International Colorectal Endoscopic (NICE) and Japan NBI Expert Team (JNET) classification[8,9] (Table 1). The accuracy of discriminating non-neoplastic from neoplastic lesions was 95% for magnifying observation with IEE and 96%-98% for pit pattern observation with chromoendoscopy, while the accuracy for discriminating adenomas from adenocarcinomas was 70%-90% for both IEE and chromoendoscopy[10].

Colorectal cancers with submucosal invasion have a 7%-14% risk of lymph node metastasis[11-14]. For submucosal cancers, it is crucial to differentiate between superficial (< 1000 μm) and deep submucosal invasive (≥ 1000 μm) cancer. Current evidence strongly supports the theory that superficial cancer with submucosal invasion < 1000 μm without lymphovascular invasion, grade 2/3 tumor budding, or poorly differentiated component have no risk of lymph node metastasis[15,16]. A Japanese study suggested that magnifying chromoendoscopy with crystal violet is the best modality for estimating the invasion depth in early colorectal lesions. Matsuda *et al*[17] found that the diagnostic accuracy of the invasive pattern in magnifying chromoendoscopy with crystal violet to differentiate superficial (< 1000 μm) and deep submucosal invasive (≥ 1000 μm) cancers was 98.8%. Patients with submucosal invasive cancer should undergo radical colectomy considering the risk of nodal metastasis, whereas patients with adenoma or cancer with submucosal superficial invasion are candidates for endoscopic resection. It should be noted that experienced examiners performed magnifying chromoendoscopy in this study; therefore, the effectiveness of magnifying chromoendoscopy should be revalidated in general endoscopists. Togashi *et al*[18] reported a minimum experience of observing 200

Table 1 The Japan Narrow-band Imaging Expert Team classification[8]

	Type 1	Type 2A	Type 2B	Type 3
Vessel pattern	Invisible	Regular caliber, regular distribution (meshed/spiral pattern)	Variable caliber, irregular distribution	Loose vessel areas, interruption of thick vessels
Surface pattern	Regular dark or white spots, similar to surrounding normal mucosa	Regular (tubular/branched/papillary)	Irregular or obscure	Amorphous areas
Suspected pathology	Hyperplastic polyp/sessile serrated polyp	Low grade intramucosal neoplasia	High grade intramucosal neoplasia/shallow submucosal invasive cancer	Deep submucosal invasive cancer

lesions with magnifying chromoendoscopy is needed to understand pit pattern diagnosis. Moreover, the limited availability of crystal violet outside Japan makes this approach difficult to apply in clinical practice.

Identification of the causes of difficult polypectomy

Table 2 shows the causes of difficult polypectomy. The difficulty might arise from the size, location, morphology, or other specific conditions. Possible solutions for each complex polyp character or situation are described in the following subsections.

The Size, Morphology, Site, Access (SMSA) classification system has been proposed by Gupta *et al*[19] for stratifying lesion complexity (Table 3). This stratifies polyps into 4 levels of difficulty, with level 1 being the easiest to resect by all endoscopists and level 4 being very difficult to resect. Longcroft-Wheaton *et al*[20] validated the SMSA system in a prospective study of 220 lesions ≥ 20 mm in diameter. They found that lesions with SMSA level 4 had higher complication rates (8.6% *vs* 0%, $P = 0.007$) and lower complete resection rates (87.5% *vs* 97.5%, $P = 0.009$) than the lesions with SMSA level 2 and 3. European Society of Gastrointestinal Endoscopy guideline for colorectal polypectomy and endoscopic mucosal resection (EMR) recommends using the SMSA system to assess large and complex polyps. If the lesions have SMSA level 4, they should be resected by experts at a high-volume tertiary care center [21].

Basic techniques of colorectal polypectomy

Endoscopists should have the appropriate basic skills to conduct a colorectal polypectomy. First, looping on the colonoscope should be unwound by shortening before performing polypectomy; otherwise, colonoscope manipulation would be paradoxical and troublesome. Second, endoscopists should position the polyp at 5-6 o'clock on the monitor because the instrument exits the colonoscope channel at 5 o'clock (Figure 1A). Finally, the base of the polyp, particularly that of a pedunculated polyp, should lie opposite to gravity. Polyp stretching by gravity improves the visualization of the polyp base, and this maneuver prevents blood pooling at the resected site (Figure 1B and C).

Selection of therapeutic modality for large colorectal polyps

The selection of the appropriate modality from various polypectomy techniques depends on the morphology and endoscopic diagnosis. Large pedunculated polyps are mainly resected by polypectomy with a prophylactic strategy against bleeding. The selection of a therapeutic modality for large non-pedunculated polyps, mostly laterally spreading tumors (LSTs), is highly debated. LST is defined as a lesion ≥ 10 mm in diameter, extending laterally with a low vertical axis[22]. The comparison between EMR and endoscopic submucosal dissection (ESD) is an important issue for large LSTs. ESD has higher *en bloc* resection and lower recurrence rates than EMR because the snare EMR method tends to result in piecemeal resection for large lesions[23,24]. Moreover, ESD allows accurate histopathologic diagnosis regarding the depth of invasion without segmentation of the carcinomatous part, which compromises the pathological diagnosis[25]. Nevertheless, colorectal ESD is one of the most challenging endoscopic procedures with high complications. The learning curve of colorectal ESD is steep, with approximately 80 procedures required to gain proficiency in large polyp resection[26]. Recently, Tip-in EMR was proposed as a promising modified EMR technique for the resection of large nonpedunculated polyps [27,28]. After the submucosal injection, the snare tip with a cut current was used to make a spot-shaped mucosal incision at the proximal side of the tumor. The small incision helps fix the snare tip in the submucosal layer during the snare placement; therefore, endoscopists could place the snare flexibly and repeatedly in the appropriate position. Takada *et al*[29] compared Tip-in EMR with ESD for the resection of 20- to 30-mm nonpedunculated polyp using propensity score matching. They found that Tip-in EMR had a lower *en bloc* resection (85% *vs* 99%, $P < 0.001$) and R0 resection rates (63% *vs* 91%, $P < 0.001$) than ESD; however, Tip-in had a shorter procedural time (8 min *vs* 60 min, $P < 0.001$) and comparable local recurrence rate (2% *vs* 0%, $P = 0.386$). They concluded that Tip-in EMR could be a feasible alternative to ESD for 20- to 30-mm nonpedunculated polyps.

Table 2 Characteristics of the difficult colorectal polyps

Size	> 20 mm
Location	Near or involving the appendiceal orifice
	Ileocecal valve
	Anorectal junction
	Behind the fold
	Angulated segment
Morphology	Pedunculated polyp with thick stalk and large head
	Laterally spreading tumor
	Submucosal fibrosis or positive non-lifting sign
Special situation	Recurrent lesion
	Strong colonic peristalsis

Table 3 Size/Morphology/Site/Access scoring system[19]

Parameter	Range	Score
Size	< 1 cm	1
	1.0-1.9 cm	3
	2.0-2.9 cm	5
	3.0-3.9 cm	7
	> 4 cm	9
Morphology	Pedunculated	1
	Sessile	2
	Flat	3
Site	Left	1
	Right	2
Access	Easy	1
	Difficult	3

Size/Morphology/Site/Access (SMSA) level 1: 4-5 points, level 2: 6-8 points, level 3: 9-12 points, level 4: > 12 points.

LST is classified as granular type (LST-G), which has a nodular surface, or non-granular type (LST-NG), which has a smooth surface. These two types have different patterns of submucosal invasion. In a large retrospective cohort study by Yamada *et al*[30], 19% of the LST-G cases had submucosal invasion; the invasion site was the large nodule in 56%, the depression area in 28%, and multifocal in 16%. LST-NG showed 39% submucosal invasion, and the invasion site was 10% at submucosal mass-like elevation, 45% at depression, or 45% multifocal. Because of the substantial risk of multifocal submucosal invasion, ESD is warranted for LST-NG, and *en bloc* resection is required for large LST-G nodules. Table 4 shows the indications for colorectal ESD suggested by the 2020 Japan Gastroenterological Endoscopy Society (JGES) guidelines for colorectal ESD and EMR[10].

APPROACHES TO DIFFICULT POLYPECTOMY IN SPECIFIC SITUATIONS

Pedunculated polyp with thick stalk and large head

The risk of bleeding after polypectomy of large pedunculated polyps with thick stalk increases due to the possibility of large blood vessels in the stalk. A prospective study found that pedunculated polyps with stalk diameter > 5 mm and polyp size > 17 mm are risk factors for post-polypectomy bleeding[31]. Therefore, prophylactic strategies against bleeding should be implemented prior to polypectomy.

Table 4 Indications for colorectal endoscopic submucosal dissection[10]

	Lesions requiring *en bloc* resection
1	Lesions which *en bloc* resection with EMR is difficult
	LST-NG, particularly LST-NG with pseudo-depressed type
	Lesions with V_I-type pit pattern
	Carcinoma with shallow T1 invasion
	Large depressed-type tumor
	Large protruded-type lesions suspected to be carcinoma
2	Mucosal tumors with submucosal fibrosis
3	Sporadic tumors in conditions of chronic inflammation such as ulcerative colitis
4	Local residual or recurrent early carcinomas after endoscopic resection

EMR: Endoscopic mucosal resection; LST-NG: Laterally spreading tumor non-granular type.

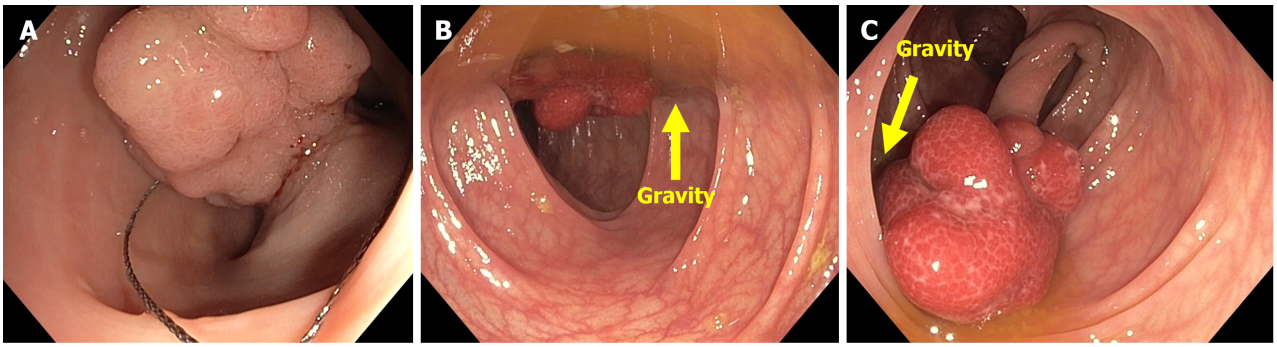

DOI: 10.3748/wjg.v29.i17.2600

Figure 1 Basic maneuvers of polypectomy. A: Positioning the polyp at 5-6 o'clock on the monitor before polypectomy; B: The polyp's base lying on gravity, this leads to poor visualization of the resection area; therefore, the patient's position should be altered; C: The polyp's base lying opposite to gravity after changing the patient's position. This position change allows polyp stretching and avoids blood pooling on the resected site.

A randomized controlled trial (RCT) by Dobrowolski *et al*[32] found that colorectal polyps ≥ 1 cm that underwent prophylactic adrenaline injection at the stalk before polypectomy had a lower immediate bleeding rate than conventional polypectomy (2% *vs* 16%, $P < 0.05$). In contrast, another RCT by Lee *et al*[33] revealed no statistical difference in immediate and delayed post-polypectomy bleeding rates between the prophylactic adrenaline injection and control groups.

A detachable snare (endoloop) was developed by Hachisu to prevent post-polypectomy bleeding from large pedunculated polyps[34]. A nylon-thread loop is tightened around the polyp stalk to ensure hemostasis before polypectomy (Figure 2). Three RCTs confirmed that a detachable snare effectively prevents post-polypectomy bleeding in large colorectal polyps[35-37]. However, endoloop placement might not be possible for all polyps, especially those with a large head or a short stalk. A previous study reported an 8.3% failure rate in endoloop placement[37]. Although the largest available endoloop has an opening diameter of 30 mm, it is floppy and challenging to place at the stalk of large polyps. Moreover, the polyp stalk will be shortened after endoloop tightening; therefore, endoloop-assisted polypectomy might not be suitable for polyps with short stalks due to the possibility of incomplete resection. A case series reported successful ESD for large pedunculated polyps with failed endoloop placement using a scissor-type knife[38], which allows precise dissection with targeted hemostasis. With a scissor-type knife, the tissue and vessels could be grasped between two blades and pre-coagulated before cutting (Figure 3). In addition, a case report described successful ESD with a scissor-type knife for a large pedunculated polyp with a short, thick stalk[39].

Prophylactic clip application at the thick stalk before polypectomy may prevent post-polypectomy bleeding (Figure 4). Soh *et al*[40] conducted an RCT of 137 pedunculated polyps ≥ 1 cm in 116 patients and found that prophylactic clip application before polypectomy significantly decreased immediate bleeding compared with conventional polypectomy [odds ratio (OR): 0.22; 95% confidence interval (95%CI): 0.08-0.57]. The delayed bleeding rate did not differ between the two groups. However, this technique is difficult to apply to polyps with a short thick stalk due to the risk of incomplete resection, and endoscopists should be aware of transmural burns from electrical current conducted by the

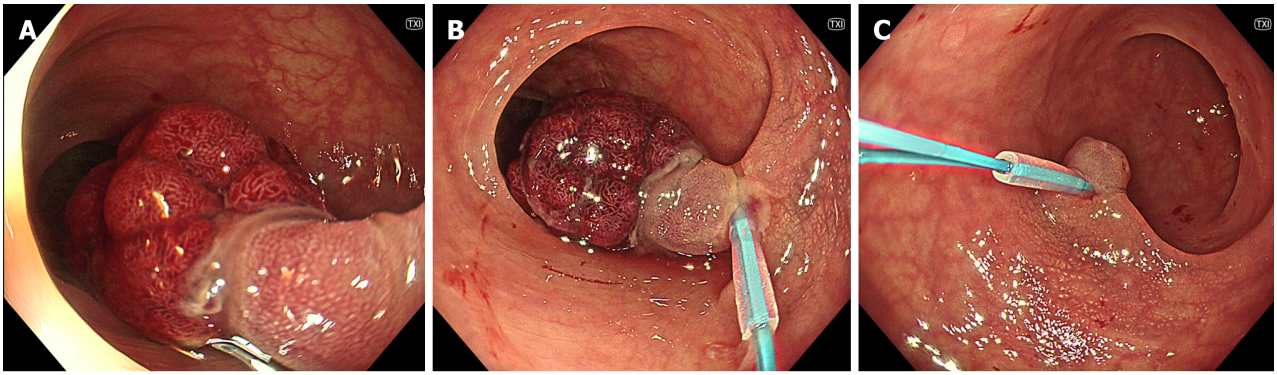

DOI: 10.3748/wjg.v29.i17.2600

Figure 2 Endoloop-assisted polypectomy. A: A pedunculated polyp with a thick stalk; B: Endoloop tightening around the stalk before snaring, the polyp's color turned deep purple due to the ischemia; C: No bleeding evidence after the resection.

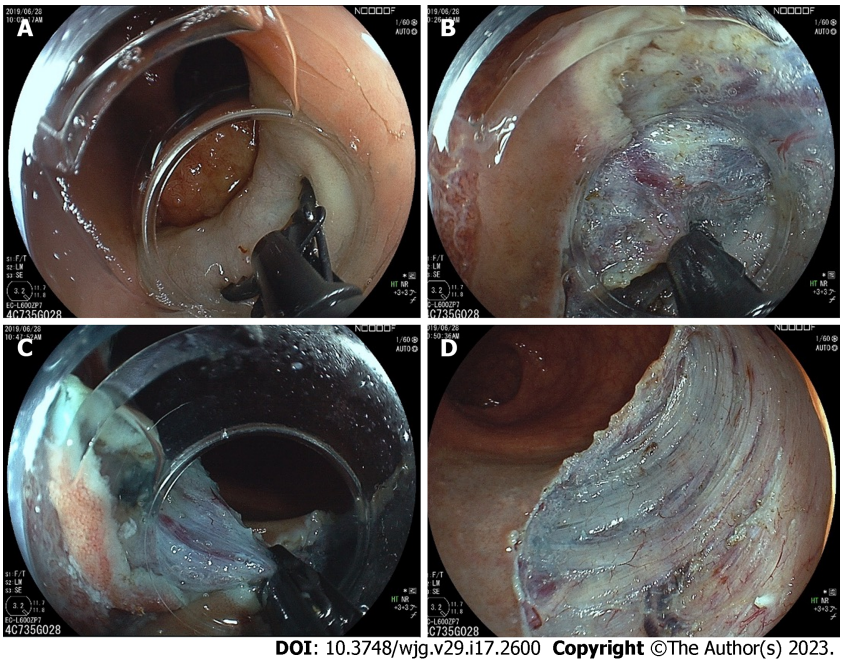

DOI: 10.3748/wjg.v29.i17.2600

Figure 3 Endoscopic submucosal dissection with a scissor-type knife for a large subpedunculated polyp. A: After submucosal injection, a scissor-type knife could be used to perform mucosal incision; B: The tissue and vessels could be grasped between two blades and precoagulated before cutting; C: Final cut of the procedure; D: Mucosal defect after completed endoscopic submucosal dissection.

endoscopic clip.

A meta-analysis of 15 RCTs involving 3,462 patients found that both prophylactic adrenaline injection and mechanical therapy reduced the risk of early post-polypectomy bleeding [injection therapy, risk ratio (RR): 0.32; 95%CI: 0.11-0.67; mechanical therapy: RR: 0.13; 95%CI: 0.03-0.37], although no prophylactic therapy decreased the risk of delayed bleeding[41]. In conclusion, prophylactic therapy, including adrenaline injection, detachable snare, or clipping, should be performed before the resection of a pedunculated polyp with a thick stalk or large head. However, detachable snare placement or prophylactic clipping may not be possible for polyps with a short, thick stalk, which may be suitably resected using ESD.

Polyps involving the appendiceal orifice

Endoscopic resection of polyps involving the appendiceal orifice is technically challenging because of the poor-lifting nature of submucosal fibrosis, thin cecal wall, and inability to access the lesion extending deep into the appendiceal orifice. Traditionally, these polyps have been managed surgically. However, recent advances have allowed endoscopists to perform a safe endoscopic resection for these polyps.

A Japanese retrospective study revealed the safety and effectiveness of ESD for the treatment of polyps involving the appendiceal orifice. For a total of 76 lesions, the authors reported a 95.0% *en bloc*

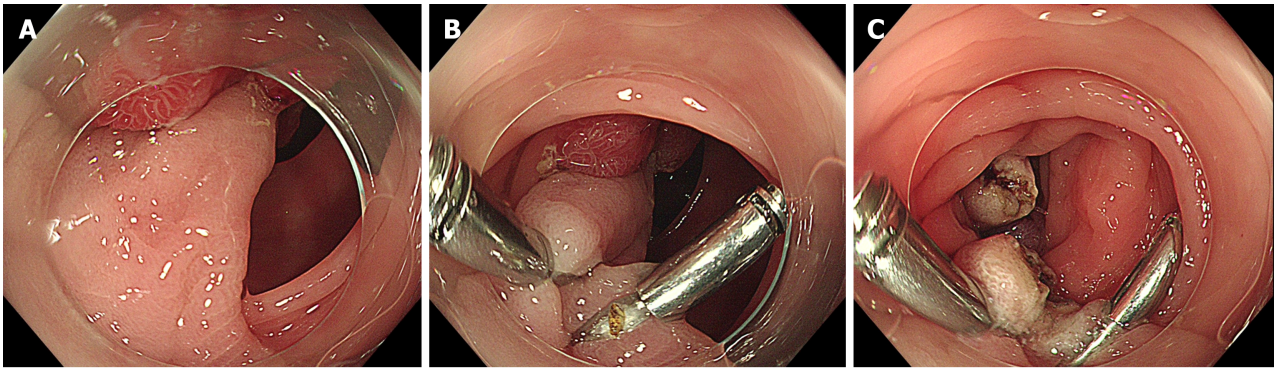

DOI: 10.3748/wjg.v29.i17.2600

Figure 4 Prophylactic clip application at the stalk before polypectomy. A: A pedunculated polyp with a thick stalk and large head. There were failed attempts placing the endoloop due to the large polyp head; B: Clip application before snaring; C: No bleeding evidence after the resection.

resection rate, 1.3% perforation, and 2.6% post-ESD appendicitis rate. However, they excluded patients with lesions deeply involving the orifice and without a history of appendectomy. The authors emphasized that ESD should be performed by experienced and skilled endoscopists in this situation[42].

Binmoeller *et al*[43] suggested the usefulness of underwater endoscopic mucosal resection (UEMR) without submucosal injection for polyps involving the appendiceal orifice. With a water-filled lumen, the floating effect facilitated snare capture (Figure 5). They reported an 89% success ratio for UEMR in 27 polyps involving the appendiceal orifice (rim, 5 patients; extending deep inside, 22 patients). There was no perforation or post-resection appendicitis; however, 7% of the patients had post-polypectomy syndrome. During surveillance, 10% of the patients had residual adenomas that could be treated endoscopically.

Endoscopic full-thickness resection (EFTR) has recently been employed for difficult polyps and is another suitable modality for polyps involving the appendiceal orifice. In a multicenter retrospective study, Schmidbaur *et al*[44] found that EFTR achieved R0 resection in 64% of 50 lesions involving the appendiceal orifice. However, 14% of patients developed acute appendicitis, and 42% of those with appendicitis required appendectomy. Similarly, a multicenter retrospective study by Ichkhanian *et al*[45], including 66 appendiceal orifice lesions (61% polyps extending deep into the appendiceal lumen) with a mean size of 14.5 mm, found that EFTR achieved an 89% technical success ratio and 93% R0 resection of the neoplastic lesions. Post-resection appendicitis occurred in 17% of patients without a prior history of appendectomy, and 60% (six patients) required appendectomy. Even with the promising outcomes of EFTR, the authors of both studies emphasized that patients must be counseled about the risk of post-resection appendicitis.

In summary, ESD is a viable option for polyps involving the rim of the appendiceal orifice for experienced endoscopists. However, ESD may not be feasible for lesions with a deep extension into the appendiceal orifice. UEMR is also a decent modality that is less technically demanding and has a high success rate. For lesions with deep extension into the appendiceal orifice, EFTR is the suitable option due to the high R0 resection rate. However, patients must be counseled regarding the risk of post-resection appendicitis.

Polyps on the ileocecal valve

Polyps on the ileocecal valve are technically challenging for endoscopic resection because the valve shape and orifice make it difficult to approach the lesions. Moreover, lesions may extend from the valve orifice to the terminal ileum. Therefore, resection is extremely difficult and associated with a high risk of recurrence[46]. A large retrospective study revealed a high complete resection rate (76.3%) of piecemeal EMR for polyps on the ileocecal valve, and the rate increased to 93.0% in the most recent eight years. Delayed bleeding and perforation occurred in 3.3% and 0% of the patients, and residual polyps were found in 16.5% and 18.6% during the first and second surveillance, respectively. They suggested four EMR keys for polyps on the ileocecal valve: (1) Use of a high-definition colonoscope; (2) use of a cap on the distal end of the scope; (3) inclusion of a dye in the injection fluid; and (4) initiating injection at the margin of the polyp with the valve orifice[47].

ESD for polyps on the ileocecal valve may be necessary for lesions suspected to be early carcinomas. However, ESD in this area is technically challenging because of the valve anatomy and composition. The ileocecal valve has abundant submucosal fatty tissue; consequently, the colonoscope lens often becomes cloudy during dissection. Yoshizaki *et al*[48] found no difference in the *en bloc* resection and perforation rates between ESD of lesions involving the ileocecal valve and lesions that did not involve it. Lesions involving the ileocecal valve were reported to have a 97% *en bloc* resection rate without perforation. The authors highlighted the critical steps for successful ESD. The mucosal incision should be started on the ileal side of the tumor to prevent the tumor from prolapsing into the terminal ileum.

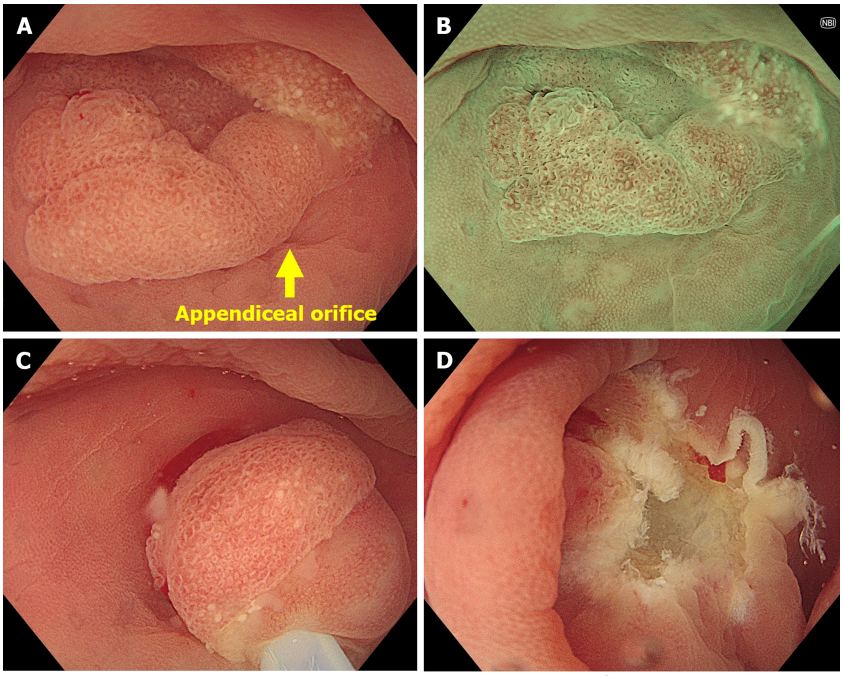

DOI: 10.3748/wjg.v29.i17.2600

Figure 5 Underwater endoscopic mucosal resection for a polyp involving appendiceal orifice. A: Endoscopic image showing a 15-mm sessile polyp involving the appendiceal orifice; B: Magnifying narrow-band image showing a type 1 polyp of the Japan Narrow-band Imaging Expert Team classification with open pit pattern. The most likely diagnosis was sessile serrated lesion; C: Underwater snaring without submucosal injection; D: Mucosal defect after completed underwater endoscopic mucosal resection.

For areas with abundant submucosal fatty tissue, the electrical setting should be changed from the forced coagulation mode to the endocut or swift coagulation mode to enhance tissue cutting. Recently, Tanaka *et al*[49] conducted a study to evaluate the outcomes of ESD for polyps of the ileocecal valve with extension into the terminal ileum. They found that ESD of lesions with or without extension into the terminal ileum showed no difference in the *en bloc* resection rate (95% *vs* 94%, $P = 0.79$), R0 resection rate (90% *vs* 89%, $P = 0.89$), postoperative bleeding (5% *vs* 3%, $P = 0.79$), intraoperative perforation (0% *vs* 4%, $P = 0.34$), or delayed perforation (0% *vs* 0%, respectively). Therefore, ESD for polyps involving the ileocecal valve with extension into the terminal ileum is safe and effective in expert hands.

Polyps at the anorectal junction

Polyps close to the dentate line can be challenging to resect because of the risk of bleeding from the hemorrhoids. Polypectomy in this area is painful due to the sensory nerves in the squamous epithelium below the dentate line. Moreover, the anatomy of the anal sphincter makes it difficult to maintain good visualization[50]. For polyps at the anorectal junction that are indicated for ESD, Imai *et al*[51] proposed the following strategies: (1) Using a cap on the distal end of the scope to maintain good visualization in the narrow space of the anal canal; (2) addition of 1% lidocaine to the submucosal injection solution to prevent pain; (3) employing a horizontal approach with an endoscopic knife to minimize thermal damage to the muscular layer; and (4) performing preventive hemostasis when thick hemorrhoidal vessels are observed. With these strategies, they reported an *en bloc* resection rate of 95.6% and an R0 resection rate of 53.3%. The low R0 resection rate was due to burning artifacts on the anal side of the specimens. They reported a 4.4% perforation and a 2.2% postoperative bleeding rate. Tamaru *et al*[52] investigated the outcomes of ESD for polyps at the anorectal junction in patients with and without hemorrhoids. They found no differences in *en bloc* resection (93% *vs* 95%) or postoperative bleeding (16% *vs* 11%) rates between patients with and without hemorrhoids. Therefore, ESD is safe and effective for patients with lesions near the anorectal junction and hemorrhoids. Similarly, several studies have shown the safety and effectiveness of ESD for polyps at the anorectal junction[53-55]. In conclusion, ESD for polyps at the anorectal junction is safe even in the presence of hemorrhoids, and special strategies to prevent bleeding and pain should be implemented (Figure 6).

Locally recurrent colorectal polyps

Locally recurrent polyps mostly result from incomplete resections. A systematic review and meta-analysis found that local recurrence after EMR of non-pedunculated polyps occurred in 3% of *en bloc* resections and 20% of piecemeal resections, and 90% of recurrences were detected within 6 mo after EMR[56]. Locally recurrent polyps without risk factors for lymph node metastasis and positive vertical margins can be resected endoscopically[57]. However, endoscopic resection of locally recurrent polyps

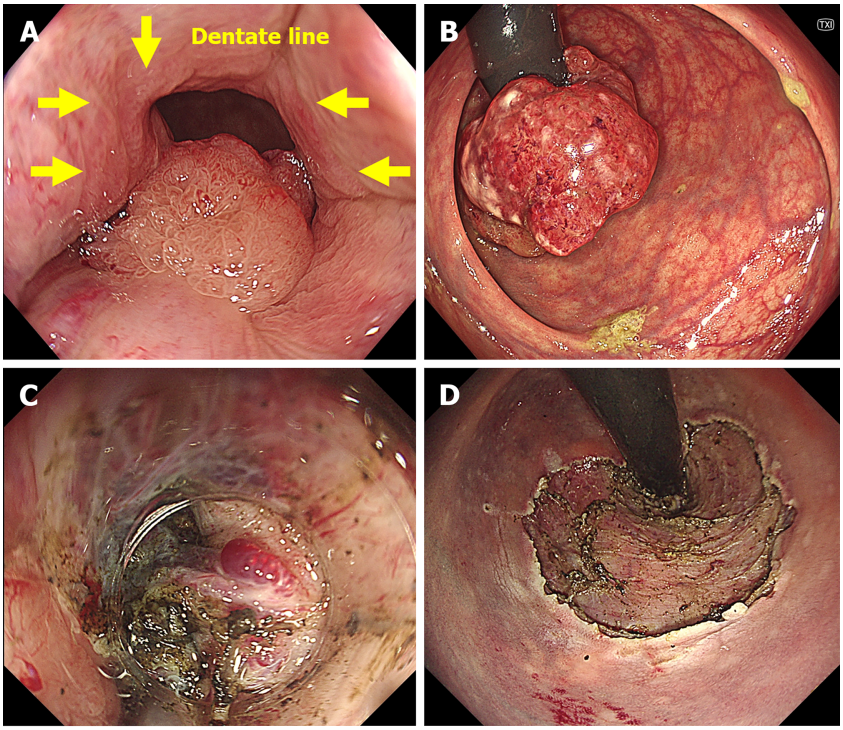

DOI: 10.3748/wjg.v29.i17.2600

Figure 6 Endoscopic submucosal dissection for a polyp involving the anorectal junction. A: Endoscopic image showing a 6-cm laterally spreading tumor involving the dentate line; B: Retroflexed view of the same polyp; C: Hemorrhoidal plexus at the anus makes the endoscopic submucosal dissection (ESD) challenging with the bleeding risk; D: Mucosal defect after completed ESD.

is extraordinarily challenging because it is associated with poor lifting with submucosal injection from submucosal fibrosis[58].

The 2020 JGES guidelines for colorectal ESD and EMR suggest that local recurrence of early carcinoma after endoscopic resection is an indication of ESD[10]. A Japanese retrospective study revealed that ESD had a higher *en bloc* resection rate than EMR for locally recurrent lesions (56% *vs* 39%, respectively), although the lesions in the ESD group were significantly larger than those in the EMR group (mean size; 25.3 mm *vs* 7.8 mm, $P = 0.001$)[59]. Perforations were not observed in the ESD group. However, this study was conducted at a single center with expertise in ESD. ESD for locally recurrent lesions is technically demanding and requires high operator skills. It is noted that the *en bloc* resection rate of locally recurrent polyps was much lower than their previous report of colorectal ESD (168/200 patients, 84%)[60]. Ide *et al*[61] conducted a retrospective study comparing ESD with the pocket-creation method using a traction device and conventional ESD for locally recurrent lesions. They found that ESD using the pocket-creation method with a traction device had higher *en bloc* resection and R0 resection rates than conventional ESD (100% *vs* 78%, $P = 0.008$, and 97% *vs* 66%, $P=0.001$, respectively). Therefore, the combination of the pocket creation method and traction device is a promising strategy for the resection of locally recurrent polyps.

UEMR without submucosal injection has been reported as a promising technique for the salvage treatment of recurrent adenomas. Fibrosis prevents elevation of the recurrent lesion after submucosal injection, while the surrounding normal mucosa still elevates around the non-lifting lesion after the injection. This makes snare capture difficult. The floating effect after UEMR facilitates snare capture with minimal risk of perforation because the colonic muscularis propria remains circular with a water-filling lumen. Kim *et al*[62] conducted a retrospective, cross-sectional study involving patients with recurrent adenomas after piecemeal resection of colorectal LSTs. They found that the *en bloc* resection and complete resection rates were higher in the UEMR group than in the EMR group (47.2% *vs* 15.9%, $P = 0.002$, and 88.9% *vs* 31.8%, $P < 0.001$, respectively). The recurrence rate on surveillance colonoscopy was lower in the UEMR group than in the EMR group (10.0% *vs* 39.4%, $P = 0.020$). In this study, UEMR was an independent predictor of *en bloc* resection and complete removal.

In summary, ESD and UEMR are the appropriate modalities for treating locally recurrent colorectal polyps. Previous studies have shown a higher *en bloc* resection rate with ESD than with UEMR and ESD using the pocket-creation method and a traction device is a promising strategy for locally recurrent polyps. However, ESD for locally recurrent lesions is only suitable for centers with high ESD expertise because it is technically difficult, even with advances in ESD devices and techniques. In extremely difficult cases, endoscopists may consider surgery if the anticipated risk of complications is too high.

Polypectomy in patients with strong colonic peristalsis

Strong colonic spasm is a common obstacle during colorectal polypectomy, limiting visualization and scope manipulation. In this situation, endoscopists generally use antispasmodic drugs. Hyoscine butylbromide is the most common antispasmodic agent in practice, and the recommended dose is 20 mg *via* intravenous injection. Hyoscine butylbromide exerts an antimuscarinic anticholinergic effect that reduces the smooth muscle tone at multiple sites in the gastrointestinal tract. Contraindications of hyoscine butylbromide include cardiovascular disease, glaucoma, myasthenia gravis, and hypersensitivity to the drug[63]. In patients with these contraindications, other antispasmodic agents, including glucagon or peppermint oil, should be administered. The dose of glucagon is 1 mg *via* intravenous injection, which is contraindicated in patients with pheochromocytoma[64]. Peppermint oil was administered *via* intraluminal application of 20 mL of 1.6% L-menthol solution without contraindications[65]. Topical lidocaine, a local anesthetic, also functions as an antispasmodic agent by blocking the Na^+ channels. It was administered *via* the intraluminal application of 30 mL of 2% lidocaine hydrochloride. An RCT found no difference in the inhibitory duration between topical lidocaine and peppermint oil; however, topical lidocaine significantly decreased rebound spasm[66].

In specific situations with intense colonic spasms, even with the administration of antispasmodic drugs, UEMR may be a decent modality. Another advantage of the water-filled lumen in UEMR is the stabilized visualization of the lumen. Pattarajierapan *et al*[67] reported successful UEMR for rectal adenoma in the non-distensible rectum due to severe fecal incontinence and intense colonic peristalsis. Therefore, UEMR may be a suitable option for patients with intense colonic spasms who have failed medication.

RECENT ADVANCES IN POLYPECTOMY DEVICES AND TECHNIQUES

Several technologies have been developed to aid endoscopists in performing safe and effective polypectomies, especially complex procedures such as ESD. These advances include video endoscopy system, equipment assisting in advanced polypectomy, and closure devices/techniques for complication management. Endoscopists should know how to use these devices and their availability in practice to enhance polypectomy performance, particularly in challenging cases.

Video endoscopy system

Red dichromatic imaging (RDI) was recently installed in the latest Olympus endoscopy system EVIS X1. RDI utilizes two long-wavelength lights (600 nm and 630 nm), which improve the visibility of thick blood vessels in deep tissues[68,69]. Therefore, easier identification of bleeding sources during polypectomy is expected in the RDI mode (Figure 7). Fujimoto *et al*[69] conducted an RCT comparing hemostatic procedures using RDI and white-light imaging (WLI). Although they found that RDI did not shorten the hemostatic time, it significantly reduced psychological stress compared to WLI. They concluded that it is safe and reasonable to use the RDI during hemostatic procedures to reduce the psychological stress experienced by endoscopists.

Equipment assisting advanced polypectomy

Although ESD has been widely accepted as a standard procedure for colorectal polyps that require *en bloc* resection, a limited number of endoscopists outside East Asia are competent owing to the difficulty of the method[70]. Colorectal ESD is more technically demanding than gastric or esophageal ESD because of its thin colonic wall and narrow colonic lumen, as well as peristalsis and respiratory movement. In addition to good training with experienced endoscopists, the recent development of traction devices and techniques may facilitate the procedure. The lack of traction during dissection contributes to the technical difficulty of ESD; therefore, various traction devices and techniques have been proposed (Figure 8). These devices include the clip-line method[71], S-O clip[72], double clips and rubber band traction[73], and traction wire[74]. To date, there have been no head-to-head comparisons of these traction devices, and the traction method has been selected based on tumor location and preference[75]. The clip-line method is helpful for rectal lesions but may not be feasible for colon lesions. For colonic ESD, endoscopists can use an S-O clip, double clips and rubber band traction, or traction wire. Without traction devices, ESD using the pocket creation method is a special technique that maintains a stable scope position inside the pocket while sustaining good traction[76,77]. This technique starts with an initial small mucosal incision, the creation of a submucosal pocket under most of the tumor, and then the completion of opening the pocket in a step-by-step manner.

Closure devices and techniques for complication management

Perforation is the most feared complication of polypectomy. With advances in closure devices, most perforations after polypectomy can be closed endoscopically, thereby eliminating the need for surgery, which is associated with morbidity and mortality[78]. Endoscopic closure devices can be classified into through-the-scope clips (TTSC), over-the-scope clips (OTSC), and suturing devices. Useful modified

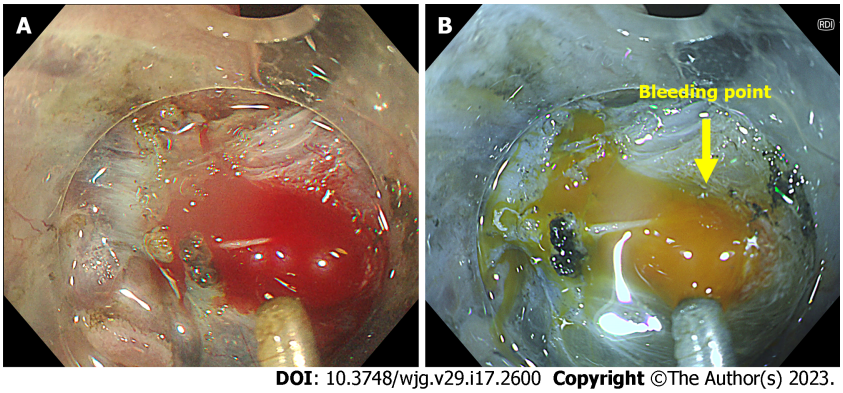

DOI: 10.3748/wjg.v29.i17.2600

Figure 7 Bleeding during endoscopic submucosal dissection. A: Endoscopic image in white light imaging showing the bleeding from the large vessels of the polyp; B: Identification of bleeding sources during polypectomy is easier in the Red Dichromatic Imaging (RDI) mode. RDI mode also reduces the endoscopists' psychological stress by turning the blood color yellow.

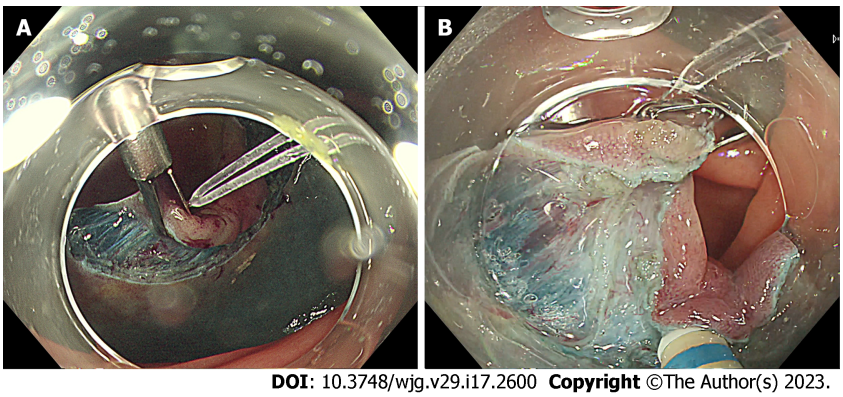

DOI: 10.3748/wjg.v29.i17.2600

Figure 8 Traction device during endoscopic submucosal dissection. A: Rubber band traction clip facilitating endoscopic submucosal dissection of a laterally spreading tumor with submucosal fibrosis; B: Traction force from the device helping during the submucosal dissection.

techniques in TTSC include the hold-and-drag closure technique using reopenable clips[78], mucosal incision method[79], endoloop-assisted clip closure[80], over-the-line clip method[80], and dual-action clip closure[81]. To date, no RCT has compared these closure techniques after colorectal polypectomy. Modified techniques in TTSC help close defects larger than the width of the clips. Therefore, endoscopists should learn these modified techniques, which are feasible for their centers because they may occasionally be necessary.

The OTSC system is a super-elastic nitinol clip that must be mounted at the end of an endoscope before deployment. This results in full-thickness closure of the teeth arranged in a bear-trap shape[78]. The reported successful closure rate for iatrogenic colon perforation for OTSC is 89%-100%[82-85]. However, the limitations of OTSC include lower success rates in the right colon compared with the left side and limited availability.

Endoscopic suturing is a promising method for defect closure with a 100% success rate in a report of 16 patients[86]. The endoscopic suturing device consists of a curved needle placed on the endoscope tip, a catheter-based suture anchor, and an operating handle attached to the neck of the instrument channel of the endoscope[87]. Limitations to the suturing device include the requirement of a double-channel endoscope and special training in endoscopic suturing to become competent in this technique. In addition, endoscopic suturing devices are expensive and limited in availability.

CONCLUSION

Recent advancements in EMR, ESD, and EFTR techniques and devices allow curative therapy of difficult colorectal polyps and prevent unnecessary surgery that carries the risk of morbidity and mortality. Moreover, these advancements also help endoscopists cope with feared complications, such as massive intra-procedural bleeding and perforation. However, proper selection of adjunct endoscopic devices/techniques according to polyp characteristics and step-by-step training for skill improvement are critical for successful advanced polypectomies. Based on current evidence, we summarize the stepwise

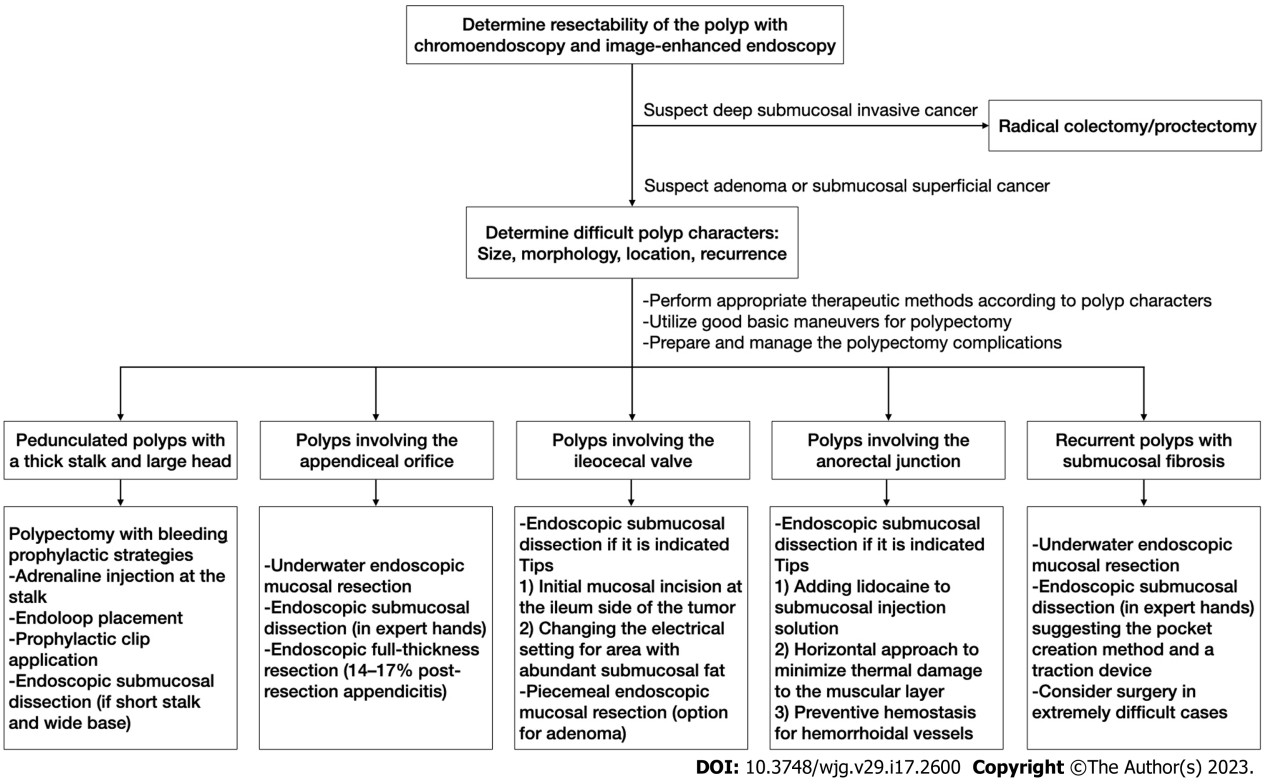

DOI: 10.3748/wjg.v29.i17.2600

Figure 9 Stepwise approach for difficult colorectal polyps.

approach (Figure 9) that might help endoscopists make better decisions for the treatment of difficult colorectal polyps.

FOOTNOTES

Author contributions: Pattarajierapan S wrote the article; Takamaru H and Khomvilai S made substantial contributions to the content, offered critical revisions, and approved the final version of the article.

Conflict-of-interest statement: The authors have no conflicts of interest or financial ties to disclose.

Country/Territory of origin: Thailand

ORCID number: Sukit Pattarajierapan 0000-0003-1042-8476; Hiroyuki Takamaru 0000-0002-7019-6331; Supakij Khomvilai 0000-0002-9703-9627.

Corresponding Author's Membership in Professional Societies: American Society for Gastrointestinal Endoscopy, No. 162994.

S-Editor: Chen YL
L-Editor: A
P-Editor: Cai YX

REFERENCES

1 **Sung H**, Ferlay J, Siegel RL, Laversanne M, Soerjomataram I, Jemal A, Bray F. Global Cancer Statistics 2020: GLOBOCAN Estimates of Incidence and Mortality Worldwide for 36 Cancers in 185 Countries. *CA Cancer J Clin* 2021; **71**: 209-249 [PMID: 33538338 DOI: 10.3322/caac.21660]

2 **Winawer SJ**, Zauber AG, Ho MN, O'Brien MJ, Gottlieb LS, Sternberg SS, Waye JD, Schapiro M, Bond JH, Panish JF. Prevention of colorectal cancer by colonoscopic polypectomy. The National Polyp Study Workgroup. *N Engl J Med* 1993; **329**: 1977-1981 [PMID: 8247072 DOI: 10.1056/NEJM199312303292701]

3 **Baxter NN**, Warren JL, Barrett MJ, Stukel TA, Doria-Rose VP. Association between colonoscopy and colorectal cancer mortality in a US cohort according to site of cancer and colonoscopist specialty. *J Clin Oncol* 2012; **30**: 2664-2669 [PMID: 22689809 DOI: 10.1200/JCO.2011.40.4772]

4 **Gallegos-Orozco JF**, Gurudu SR. Complex colon polypectomy. *Gastroenterol Hepatol (N Y)* 2010; **6**: 375-382 [PMID: 20733940]

5 **Ngamruengphong S**, Pohl H, Haito-Chavez Y, Khashab MA. Update on Difficult Polypectomy Techniques. *Curr Gastroenterol Rep* 2016; **18**: 3 [PMID: 26714965 DOI: 10.1007/s11894-015-0476-7]

6 **Mann R**, Gajendran M, Umapathy C, Perisetti A, Goyal H, Saligram S, Echavarria J. Endoscopic Management of Complex Colorectal Polyps: Current Insights and Future Trends. *Front Med (Lausanne)* 2021; **8**: 728704 [PMID: 35127735 DOI: 10.3389/fmed.2021.728704]

7 **Kudo S**, Tamura S, Nakajima T, Yamano H, Kusaka H, Watanabe H. Diagnosis of colorectal tumorous lesions by magnifying endoscopy. *Gastrointest Endosc* 1996; **44**: 8-14 [PMID: 8836710 DOI: 10.1016/s0016-5107(96)70222-5]

8 **Sano Y**, Tanaka S, Kudo SE, Saito S, Matsuda T, Wada Y, Fujii T, Ikematsu H, Uraoka T, Kobayashi N, Nakamura H, Hotta K, Horimatsu T, Sakamoto N, Fu KI, Tsuruta O, Kawano H, Kashida H, Takeuchi Y, Machida H, Kusaka T, Yoshida N, Hirata I, Terai T, Yamano HO, Kaneko K, Nakajima T, Sakamoto T, Yamaguchi Y, Tamai N, Nakano N, Hayashi N, Oka S, Iwatate M, Ishikawa H, Murakami Y, Yoshida S, Saito Y. Narrow-band imaging (NBI) magnifying endoscopic classification of colorectal tumors proposed by the Japan NBI Expert Team. *Dig Endosc* 2016; **28**: 526-533 [PMID: 26927367 DOI: 10.1111/den.12644]

9 **Hayashi N**, Tanaka S, Hewett DG, Kaltenbach TR, Sano Y, Ponchon T, Saunders BP, Rex DK, Soetikno RM. Endoscopic prediction of deep submucosal invasive carcinoma: validation of the narrow-band imaging international colorectal endoscopic (NICE) classification. *Gastrointest Endosc* 2013; **78**: 625-632 [PMID: 23910062 DOI: 10.1016/j.gie.2013.04.185]

10 **Tanaka S**, Kashida H, Saito Y, Yahagi N, Yamano H, Saito S, Hisabe T, Yao T, Watanabe M, Yoshida M, Saitoh Y, Tsuruta O, Sugihara KI, Igarashi M, Toyonaga T, Ajioka Y, Kusunoki M, Koike K, Fujimoto K, Tajiri H. Japan Gastroenterological Endoscopy Society guidelines for colorectal endoscopic submucosal dissection/endoscopic mucosal resection. *Dig Endosc* 2020; **32**: 219-239 [PMID: 31566804 DOI: 10.1111/den.13545]

11 **Tateishi Y**, Nakanishi Y, Taniguchi H, Shimoda T, Umemura S. Pathological prognostic factors predicting lymph node metastasis in submucosal invasive (T1) colorectal carcinoma. *Mod Pathol* 2010; **23**: 1068-1072 [PMID: 20473277 DOI: 10.1038/modpathol.2010.88]

12 **Yamaoka Y**, Shiomi A, Kagawa H, Hino H, Manabe S, Chen K, Nanishi K, Notsu A. Lymph node metastasis in T1 colorectal cancer with the only high-risk histology of submucosal invasion depth ≥ 1000 μm. *Int J Colorectal Dis* 2022; **37**: 2387-2395 [PMID: 36283994 DOI: 10.1007/s00384-022-04269-6]

13 **Suh JH**, Han KS, Kim BC, Hong CW, Sohn DK, Chang HJ, Kim MJ, Park SC, Park JW, Choi HS, Oh JH. Predictors for lymph node metastasis in T1 colorectal cancer. *Endoscopy* 2012; **44**: 590-595 [PMID: 22638780 DOI: 10.1055/s-0031-1291665]

14 **Kikuchi R**, Takano M, Takagi K, Fujimoto N, Nozaki R, Fujiyoshi T, Uchida Y. Management of early invasive colorectal cancer. Risk of recurrence and clinical guidelines. *Dis Colon Rectum* 1995; **38**: 1286-1295 [PMID: 7497841 DOI: 10.1007/BF02049154]

15 **Kitajima K**, Fujimori T, Fujii S, Takeda J, Ohkura Y, Kawamata H, Kumamoto T, Ishiguro S, Kato Y, Shimoda T, Iwashita A, Ajioka Y, Watanabe H, Watanabe T, Muto T, Nagasako K. Correlations between lymph node metastasis and depth of submucosal invasion in submucosal invasive colorectal carcinoma: a Japanese collaborative study. *J Gastroenterol* 2004; **39**: 534-543 [PMID: 15235870 DOI: 10.1007/s00535-004-1339-4]

16 **Nakadoi K**, Tanaka S, Kanao H, Terasaki M, Takata S, Oka S, Yoshida S, Arihiro K, Chayama K. Management of T1 colorectal carcinoma with special reference to criteria for curative endoscopic resection. *J Gastroenterol Hepatol* 2012; **27**: 1057-1062 [PMID: 22142484 DOI: 10.1111/j.1440-1746.2011.07041.x]

17 **Matsuda T**, Fujii T, Saito Y, Nakajima T, Uraoka T, Kobayashi N, Ikehara H, Ikematsu H, Fu KI, Emura F, Ono A, Sano Y, Shimoda T, Fujimori T. Efficacy of the invasive/non-invasive pattern by magnifying chromoendoscopy to estimate the depth of invasion of early colorectal neoplasms. *Am J Gastroenterol* 2008; **103**: 2700-2706 [PMID: 18853968 DOI: 10.1111/j.1572-0241.2008.02190.x]

18 **Togashi K**, Konishi F, Ishizuka T, Sato T, Senba S, Kanazawa K. Efficacy of magnifying endoscopy in the differential diagnosis of neoplastic and non-neoplastic polyps of the large bowel. *Dis Colon Rectum* 1999; **42**: 1602-1608 [PMID: 10613481 DOI: 10.1007/BF02236215]

19 **Gupta S**, Miskovic D, Bhandari P, Dolwani S, McKaig B, Pullan R, Rembacken B, Riley S, Rutter MD, Suzuki N, Tsiamoulos Z, Valori R, Vance ME, Faiz OD, Saunders BP, Thomas-Gibson S. A novel method for determining the difficulty of colonoscopic polypectomy. *Frontline Gastroenterol* 2013; **4**: 244-248 [PMID: 28839733 DOI: 10.1136/flgastro-2013-100331]

20 **Longcroft-Wheaton G**, Duku M, Mead R, Basford P, Bhandari P. Risk stratification system for evaluation of complex polyps can predict outcomes of endoscopic mucosal resection. *Dis Colon Rectum* 2013; **56**: 960-966 [PMID: 23838864 DOI: 10.1097/DCR.0b013e31829193e0]

21 **Ferlitsch M**, Moss A, Hassan C, Bhandari P, Dumonceau JM, Paspatis G, Jover R, Langner C, Bronzwaer M, Nalankilli K, Fockens P, Hazzan R, Gralnek IM, Gschwantler M, Waldmann E, Jeschek P, Penz D, Heresbach D, Moons L, Lemmers A, Paraskeva K, Pohl J, Ponchon T, Regula J, Repici A, Rutter MD, Burgess NG, Bourke MJ. Colorectal polypectomy and endoscopic mucosal resection (EMR): European Society of Gastrointestinal Endoscopy (ESGE) Clinical Guideline. *Endoscopy* 2017; **49**: 270-297 [PMID: 28212588 DOI: 10.1055/s-0043-102569]

22 **Kudo Se**, Lambert R, Allen JI, Fujii H, Fujii T, Kashida H, Matsuda T, Mori M, Saito H, Shimoda T, Tanaka S, Watanabe H, Sung JJ, Feld AD, Inadomi JM, O'Brien MJ, Lieberman DA, Ransohoff DF, Soetikno RM, Triadafilopoulos G, Zauber

A, Teixeira CR, Rey JF, Jaramillo E, Rubio CA, Van Gossum A, Jung M, Vieth M, Jass JR, Hurlstone PD. Nonpolypoid neoplastic lesions of the colorectal mucosa. *Gastrointest Endosc* 2008; **68**: S3-47 [PMID: 18805238 DOI: 10.1016/j.gie.2008.07.052]

23 **Hotta K**, Fujii T, Saito Y, Matsuda T. Local recurrence after endoscopic resection of colorectal tumors. *Int J Colorectal Dis* 2009; **24**: 225-230 [PMID: 18972121 DOI: 10.1007/s00384-008-0596-8]

24 **Oka S**, Tanaka S, Saito Y, Iishi H, Kudo SE, Ikematsu H, Igarashi M, Saitoh Y, Inoue Y, Kobayashi K, Hisabe T, Tsuruta O, Sano Y, Yamano H, Shimizu S, Yahagi N, Watanabe T, Nakamura H, Fujii T, Ishikawa H, Sugihara K; Colorectal Endoscopic Resection Standardization Implementation Working Group of the Japanese Society for Cancer of the Colon and Rectum, Tokyo, Japan. Local recurrence after endoscopic resection for large colorectal neoplasia: a multicenter prospective study in Japan. *Am J Gastroenterol* 2015; **110**: 697-707 [PMID: 25848926 DOI: 10.1038/ajg.2015.96]

25 **Tanaka S**, Saitoh Y, Matsuda T, Igarashi M, Matsumoto T, Iwao Y, Suzuki Y, Nozaki R, Sugai T, Oka S, Itabashi M, Sugihara KI, Tsuruta O, Hirata I, Nishida H, Miwa H, Enomoto N, Shimosegawa T, Koike K. Evidence-based clinical practice guidelines for management of colorectal polyps. *J Gastroenterol* 2021; **56**: 323-335 [PMID: 33710392 DOI: 10.1007/s00535-021-01776-1]

26 **Hotta K**, Oyama T, Shinohara T, Miyata Y, Takahashi A, Kitamura Y, Tomori A. Learning curve for endoscopic submucosal dissection of large colorectal tumors. *Dig Endosc* 2010; **22**: 302-306 [PMID: 21175483 DOI: 10.1111/j.1443-1661.2010.01005.x]

27 **Chien H**, Imai K, Hotta K, Ito S, Yamaguchi Y, Kawata N, Tanaka M, Takizawa K, Kakushima N, Matsubayashi H, Ono H. Tip-in EMR for R0 resection for a large flat colonic tumor. *Gastrointest Endosc* 2016; **84**: 743 [PMID: 27207826 DOI: 10.1016/j.gie.2016.05.017]

28 **Sato Y**, Ozawa SI, Yasuda H, Kato M, Kiyokawa H, Yamashita M, Matsuo Y, Yamamoto H, Itoh F. Tip-in endoscopic mucosal resection for large colorectal sessile polyps. *Surg Endosc* 2021; **35**: 1820-1826 [PMID: 32356110 DOI: 10.1007/s00464-020-07581-w]

29 **Takada K**, Hotta K, Imai K, Ito S, Kishida Y, Minamide T, Yamamoto Y, Yabuuchi Y, Yoshida M, Maeda Y, Kawata N, Takizawa K, Ishiwatari H, Matsubayashi H, Kawabata T, Ono H. Tip-in EMR as an alternative to endoscopic submucosal dissection for 20- to 30-mm nonpedunculated colorectal neoplasms. *Gastrointest Endosc* 2022; **96**: 849-856.e3 [PMID: 35798055 DOI: 10.1016/j.gie.2022.06.030]

30 **Yamada M**, Saito Y, Sakamoto T, Nakajima T, Kushima R, Parra-Blanco A, Matsuda T. Endoscopic predictors of deep submucosal invasion in colorectal laterally spreading tumors. *Endoscopy* 2016; **48**: 456-464 [PMID: 26919264 DOI: 10.1055/s-0042-100453]

31 **Dobrowolski S**, Dobosz M, Babicki A, Głowacki J, Nałecz A. Blood supply of colorectal polyps correlates with risk of bleeding after colonoscopic polypectomy. *Gastrointest Endosc* 2006; **63**: 1004-1009 [PMID: 16733117 DOI: 10.1016/j.gie.2005.11.063]

32 **Dobrowolski S**, Dobosz M, Babicki A, Dymecki D, Hać S. Prophylactic submucosal saline-adrenaline injection in colonoscopic polypectomy: prospective randomized study. *Surg Endosc* 2004; **18**: 990-993 [PMID: 15108107 DOI: 10.1007/s00464-003-9214-6]

33 **Lee SH**, Chung IK, Kim SJ, Kim JO, Ko BM, Kim WH, Kim HS, Park DI, Kim HJ, Byeon JS, Yang SK, Jang BI, Jung SA, Jeen YT, Choi JH, Choi H, Han DS, Song JS. Comparison of postpolypectomy bleeding between epinephrine and saline submucosal injection for large colon polyps by conventional polypectomy: a prospective randomized, multicenter study. *World J Gastroenterol* 2007; **13**: 2973-2977 [PMID: 17589949 DOI: 10.3748/wjg.v13.i21.2973]

34 **Hachisu T**. A new detachable snare for hemostasis in the removal of large polyps or other elevated lesions. *Surg Endosc* 1991; **5**: 70-74 [PMID: 1948617 DOI: 10.1007/BF00316840]

35 **Di Giorgio P**, De Luca L, Calcagno G, Rivellini G, Mandato M, De Luca B. Detachable snare *vs* epinephrine injection in the prevention of postpolypectomy bleeding: a randomized and controlled study. *Endoscopy* 2004; **36**: 860-863 [PMID: 15452780 DOI: 10.1055/s-2004-825801]

36 **Kouklakis G**, Mpoumponaris A, Gatopoulou A, Efraimidou E, Manolas K, Lirantzopoulos N. Endoscopic resection of large pedunculated colonic polyps and risk of postpolypectomy bleeding with adrenaline injection *vs* endoloop and hemoclip: a prospective, randomized study. *Surg Endosc* 2009; **23**: 2732-2737 [PMID: 19430833 DOI: 10.1007/s00464-009-0478-3]

37 **Paspatis GA**, Paraskeva K, Theodoropoulou A, Mathou N, Vardas E, Oustamanolakis P, Chlouverakis G, Karagiannis I. A prospective, randomized comparison of adrenaline injection in combination with detachable snare *vs* adrenaline injection alone in the prevention of postpolypectomy bleeding in large colonic polyps. *Am J Gastroenterol* 2006; **101**: 2805; quiz 2913 [PMID: 17026560 DOI: 10.1111/j.1572-0241.2006.00855.x]

38 **Jawaid S**, Draganov PV, Yang D. Endoscopic resection of large pedunculated colon polyps using only a scissor-type knife: a case series. *VideoGIE* 2020; **5**: 264-266 [PMID: 32529165 DOI: 10.1016/j.vgie.2020.02.016]

39 **Yamamoto S**, Shafazand M. Endoscopic submucosal dissection with scissor-type knife for pedunculated polyp with short and thick stalk. *VideoGIE* 2018; **3**: 189-190 [PMID: 30128383 DOI: 10.1016/j.vgie.2018.04.001]

40 **Soh JS**, Seo M, Kim KJ. Prophylactic clip application for large pedunculated polyps before snare polypectomy may decrease immediate postpolypectomy bleeding. *BMC Gastroenterol* 2020; **20**: 68 [PMID: 32164613 DOI: 10.1186/s12876-020-01210-5]

41 **Park CH**, Jung YS, Nam E, Eun CS, Park DI, Han DS. Comparison of Efficacy of Prophylactic Endoscopic Therapies for Postpolypectomy Bleeding in the Colorectum: A Systematic Review and Network Meta-Analysis. *Am J Gastroenterol* 2016; **111**: 1230-1243 [PMID: 27402502 DOI: 10.1038/ajg.2016.287]

42 **Jacob H**, Toyonaga T, Ohara Y, Tsubouchi E, Takihara H, Baba S, Yoshizaki T, Kawara F, Tanaka S, Ishida T, Hoshi N, Morita Y, Umegaki E, Azuma T. Endoscopic submucosal dissection of cecal lesions in proximity to the appendiceal orifice. *Endoscopy* 2016; **48**: 829-836 [PMID: 27467815 DOI: 10.1055/s-0042-110396]

43 **Binmoeller KF**, Hamerski CM, Shah JN, Bhat YM, Kane SD. Underwater EMR of adenomas of the appendiceal orifice (with video). *Gastrointest Endosc* 2016; **83**: 638-642 [PMID: 26375437 DOI: 10.1016/j.gie.2015.08.079]

44 **Schmidbaur S**, Wannhoff A, Walter B, Meier B, Schäfer C, Meining A, Caca K. Risk of appendicitis after endoscopic

full-thickness resection of lesions involving the appendiceal orifice: a retrospective analysis. *Endoscopy* 2021; **53**: 424-428 [PMID: 32894866 DOI: 10.1055/a-1227-4555]

45 **Ichkhanian Y**, Barawi M, Seoud T, Thakkar S, Kothari TH, Halabi ME, Ullah A, Edris W, Aepli P, Kowalski T, Shinn B, Shariaha RZ, Mahadev S, Mosko JD, Andrisani G, Di Matteo FM, Albrecht H, Giap AQ, Tang SJ, Naga YM, van Geenen E, Friedland S, Tharian B, Irani S, Ross AS, Jamil LH, Lew D, Nett AS, Farha J, Runge TM, Jovani M, Khashab MA. Endoscopic full-thickness resection of polyps involving the appendiceal orifice: a multicenter international experience. *Endoscopy* 2022; **54**: 16-24 [PMID: 33395714 DOI: 10.1055/a-1345-0044]

46 **Nanda KS**, Tutticci N, Burgess NG, Sonson R, Williams SJ, Bourke MJ. Endoscopic mucosal resection of laterally spreading lesions involving the ileocecal valve: technique, risk factors for failure, and outcomes. *Endoscopy* 2015; **47**: 710-718 [PMID: 25763831 DOI: 10.1055/s-0034-1391732]

47 **Ponugoti PL**, Broadley HM, Garcia J, Rex DK. Endoscopic management of large ileocecal valve lesions over an 18-year interval. *Endosc Int Open* 2019; **7**: E1646-E1651 [PMID: 31788547 DOI: 10.1055/a-0990-9035]

48 **Yoshizaki T**, Toyonaga T, Tanaka S, Ohara Y, Kawara F, Baba S, Tsubouchi E, Takihara H, Watanabe D, Ishida T, Hoshi N, Morita Y, Umegaki E, Azuma T. Feasibility and safety of endoscopic submucosal dissection for lesions involving the ileocecal valve. *Endoscopy* 2016; **48**: 639-645 [PMID: 26990510 DOI: 10.1055/s-0042-102783]

49 **Tanaka H**, Oka S, Kunihiro M, Nagata S, Kitamura S, Kuwai T, Hiraga Y, Furudoi A, Tanaka S. Endoscopic submucosal dissection for tumors involving the ileocecal valve with extension into the terminal ileum: a multicenter study from the Hiroshima GI Endoscopy Research Group. *Surg Endosc* 2023; **37**: 958-966 [PMID: 36070146 DOI: 10.1007/s00464-022-09542-x]

50 **Nakadoi K**, Tanaka S, Hayashi N, Ozawa S, Terasaki M, Takata S, Kanao H, Oka S, Chayama K. Clinical outcomes of endoscopic submucosal dissection for rectal tumor close to the dentate line. *Gastrointest Endosc* 2012; **76**: 444-450 [PMID: 22817799 DOI: 10.1016/j.gie.2012.04.004]

51 **Imai K**, Hotta K, Yamaguchi Y, Shinohara T, Ooka S, Shinoki K, Kakushima N, Tanaka M, Takizawa K, Matsubayashi H, Oishi T, Ono H. Safety and efficacy of endoscopic submucosal dissection of rectal tumors extending to the dentate line. *Endoscopy* 2015; **47**: 529-532 [PMID: 25502418 DOI: 10.1055/s-0034-1391078]

52 **Tamaru Y**, Oka S, Tanaka S, Hiraga Y, Kunihiro M, Nagata S, Furudoi A, Ninomiya Y, Asayama N, Shigita K, Nishiyama S, Hayashi N, Chayama K. Endoscopic submucosal dissection for anorectal tumor with hemorrhoids close to the dentate line: a multicenter study of Hiroshima GI Endoscopy Study Group. *Surg Endosc* 2016; **30**: 4425-4431 [PMID: 26895899 DOI: 10.1007/s00464-016-4761-9]

53 **Tanaka S**, Toyonaga T, Morita Y, Hoshi N, Ishida T, Ohara Y, Yoshizaki T, Kawara F, Umegaki E, Azuma T. Feasibility and safety of endoscopic submucosal dissection for lower rectal tumors with hemorrhoids. *World J Gastroenterol* 2016; **22**: 6268-6275 [PMID: 27468216 DOI: 10.3748/wjg.v22.i27.6268]

54 **Matsumoto S**, Mashima H. The efficacy of endoscopic submucosal dissection for colorectal tumors extending to the dentate line. *Int J Colorectal Dis* 2017; **32**: 831-837 [PMID: 28188417 DOI: 10.1007/s00384-017-2775-y]

55 **Probst A**, Ebigbo A, Märkl B, Ting S, Schaller T, Anthuber M, Fleischmann C, Messmann H. Endoscopic submucosal dissection for rectal neoplasia extending to the dentate line: European experience. *Endosc Int Open* 2018; **6**: E1355-E1362 [PMID: 30410957 DOI: 10.1055/a-0749-8735]

56 **Belderbos TD**, Leenders M, Moons LM, Siersema PD. Local recurrence after endoscopic mucosal resection of nonpedunculated colorectal lesions: systematic review and meta-analysis. *Endoscopy* 2014; **46**: 388-402 [PMID: 24671869 DOI: 10.1055/s-0034-1364970]

57 **Shichijo S**, Takeuchi Y, Uedo N, Ishihara R. Management of local recurrence after endoscopic resection of neoplastic colonic polyps. *World J Gastrointest Endosc* 2018; **10**: 378-382 [PMID: 30631401 DOI: 10.4253/wjge.v10.i12.378]

58 **Sato K**, Ito S, Kitagawa T, Kato M, Tominaga K, Suzuki T, Maetani I. Factors affecting the technical difficulty and clinical outcome of endoscopic submucosal dissection for colorectal tumors. *Surg Endosc* 2014; **28**: 2959-2965 [PMID: 24853849 DOI: 10.1007/s00464-014-3558-y]

59 **Sakamoto T**, Saito Y, Matsuda T, Fukunaga S, Nakajima T, Fujii T. Treatment strategy for recurrent or residual colorectal tumors after endoscopic resection. *Surg Endosc* 2011; **25**: 255-260 [PMID: 20559661 DOI: 10.1007/s00464-010-1169-9]

60 **Saito Y**, Uraoka T, Matsuda T, Emura F, Ikehara H, Mashimo Y, Kikuchi T, Fu KI, Sano Y, Saito D. Endoscopic treatment of large superficial colorectal tumors: a case series of 200 endoscopic submucosal dissections (with video). *Gastrointest Endosc* 2007; **66**: 966-973 [PMID: 17524403 DOI: 10.1016/j.gie.2007.02.053]

61 **Ide D**, Ohya TR, Ishioka M, Enomoto Y, Nakao E, Mitsuyoshi Y, Tokura J, Suzuki K, Yakabi S, Yasue C, Chino A, Igarashi M, Nakashima A, Saruta M, Saito S, Fujisaki J. Efficacy of the pocket-creation method with a traction device in endoscopic submucosal dissection for residual or recurrent colorectal lesions. *Clin Endosc* 2022; **55**: 655-664 [PMID: 35636748 DOI: 10.5946/ce.2022.009]

62 **Kim HG**, Thosani N, Banerjee S, Chen A, Friedland S. Underwater endoscopic mucosal resection for recurrences after previous piecemeal resection of colorectal polyps (with video). *Gastrointest Endosc* 2014; **80**: 1094-1102 [PMID: 25012560 DOI: 10.1016/j.gie.2014.05.318]

63 **Sanagapalli S**, Agnihotri K, Leong R, Corte CJ. Antispasmodic drugs in colonoscopy: a review of their pharmacology, safety and efficacy in improving polyp detection and related outcomes. *Therap Adv Gastroenterol* 2017; **10**: 101-113 [PMID: 28286563 DOI: 10.1177/1756283X16670076]

64 **Hosseinnezhad A**, Black RM, Aeddula NR, Adhikari D, Trivedi N. Glucagon-induced pheochromocytoma crisis. *Endocr Pract* 2011; **17**: e51-e54 [PMID: 21324811 DOI: 10.4158/EP10388.CR]

65 **Inoue K**, Dohi O, Gen Y, Jo M, Mazaki T, Tokita K, Yoshida N, Okayama T, Kamada K, Katada K, Uchiyama K, Ishikawa T, Handa O, Takagi T, Konishi H, Wakabayashi N, Yagi N, Naito Y, Itoh Y. L-menthol improves adenoma detection rate during colonoscopy: a randomized trial. *Endoscopy* 2014; **46**: 196-202 [PMID: 24573731 DOI: 10.1055/s-0034-1365035]

66 **Nemoto D**, Utano K, Isohata N, Endo S, Kumamoto K, Koshimizu TA, Lefor A, Togashi K. Topical lidocaine inhibits spasm during colonoscopy: a double-blind, randomized controlled trial (with video). *Endosc Int Open* 2017; **5**: E402-E407 [PMID: 28573171 DOI: 10.1055/s-0043-105489]

67 **Pattarajierapan S**, Khomvilai S. Underwater endoscopic mucosal resection of a rectal adenoma in the nondistensible rectum from severe fecal incontinence. *VideoGIE* 2021; **6**: 275-276 [PMID: 34141972 DOI: 10.1016/j.vgie.2021.02.014]

68 **Uraoka T**, Igarashi M. Development and clinical usefulness of a unique red dichromatic imaging technology in gastrointestinal endoscopy: A narrative review. *Therap Adv Gastroenterol* 2022; **15**: 17562848221118302 [PMID: 36082177 DOI: 10.1177/17562848221118302]

69 **Fujimoto A**, Saito Y, Abe S, Hoteya S, Nomura K, Yasuda H, Matsuo Y, Uraoka T, Kuribayashi S, Tsuji Y, Ohki D, Maehata T, Kato M, Yahagi N. Clinical usefulness of red dichromatic imaging in hemostatic treatment during endoscopic submucosal dissection: First report from a multicenter, open-label, randomized controlled trial. *Dig Endosc* 2022; **34**: 379-390 [PMID: 34775648 DOI: 10.1111/den.14191]

70 **Ma MX**, Bourke MJ. Endoscopic submucosal dissection in the West: Current status and future directions. *Dig Endosc* 2018; **30**: 310-320 [PMID: 28884493 DOI: 10.1111/den.12960]

71 **Yamasaki Y**, Takeuchi Y, Uedo N, Kanesaka T, Kato M, Hamada K, Tonai Y, Matsuura N, Akasaka T, Hanaoka N, Higashino K, Ishihara R, Okada H, Iishi H. Efficacy of traction-assisted colorectal endoscopic submucosal dissection using a clip-and-thread technique: A prospective randomized study. *Dig Endosc* 2018; **30**: 467-476 [PMID: 29424030 DOI: 10.1111/den.13036]

72 **Sakamoto N**, Osada T, Shibuya T, Beppu K, Matsumoto K, Shimada Y, Konno A, Kurosawa A, Nagahara A, Ohkusa T, Ogihara T, Watanabe S. The facilitation of a new traction device (S-O clip) assisting endoscopic submucosal dissection for superficial colorectal neoplasms. *Endoscopy* 2008; **40** Suppl 2: E94-E95 [PMID: 19085712 DOI: 10.1055/s-2007-995603]

73 **Oung B**, Rivory J, Chabrun E, Legros R, Faller J, Léger-Nguyen F, Rostain F, Ber CE, Hervieu V, Saurin JC, Ponchon T, Jacques J, Pioche M. ESD with double clips and rubber band traction of neoplastic lesions developed in the appendiceal orifice is effective and safe. *Endosc Int Open* 2020; **8**: E388-E395 [PMID: 32118111 DOI: 10.1055/a-1072-4830]

74 **Bhatt A**, Hwang JH, Sharma NR, Waxman I. Traction wire endoscopic submucosal dissection: tips and techniques from 4 institutions. *VideoGIE* 2022; **7**: 21-22 [PMID: 35059534 DOI: 10.1016/j.vgie.2021.08.011]

75 **Abe S**, Wu SYS, Ego M, Takamaru H, Sekiguchi M, Yamada M, Nonaka S, Sakamoto T, Suzuki H, Yoshinaga S, Matsuda T, Oda I, Saito Y. Efficacy of Current Traction Techniques for Endoscopic Submucosal Dissection. *Gut Liver* 2020; **14**: 673-684 [PMID: 31887810 DOI: 10.5009/gnl19266]

76 **Hayashi Y**, Sunada K, Takahashi H, Shinhata H, Lefor AT, Tanaka A, Yamamoto H. Pocket-creation method of endoscopic submucosal dissection to achieve en bloc resection of giant colorectal subpedunculated neoplastic lesions. *Endoscopy* 2014; **46** Suppl 1 UCTN: E421-E422 [PMID: 25314173 DOI: 10.1055/s-0034-1377438]

77 **Hayashi Y**, Miura Y, Yamamoto H. Pocket-creation method for the safe, reliable, and efficient endoscopic submucosal dissection of colorectal lateral spreading tumors. *Dig Endosc* 2015; **27**: 534-535 [PMID: 25708068 DOI: 10.1111/den.12465]

78 **Raju GS**. Closure of Defects and Management of Complications. *Gastrointest Endosc Clin N Am* 2019; **29**: 705-719 [PMID: 31445692 DOI: 10.1016/j.giec.2019.06.005]

79 **Otake Y**, Saito Y, Sakamoto T, Aoki T, Nakajima T, Toyoshima N, Matsuda T, Ono H. New closure technique for large mucosal defects after endoscopic submucosal dissection of colorectal tumors (with video). *Gastrointest Endosc* 2012; **75**: 663-667 [PMID: 22341112 DOI: 10.1016/j.gie.2011.10.037]

80 **Nomura T**, Sugimoto S, Temma T, Oyamada J, Ito K, Kamei A. Suturing techniques with endoscopic clips and special devices after endoscopic resection. *Dig Endosc* 2023; **35**: 287-301 [PMID: 35997063 DOI: 10.1111/den.14427]

81 **Wei MT**, Friedland S. Use of a novel dual-action clip for closure of complex endoscopic resection defects. *VideoGIE* 2022; **7**: 389-391 [PMID: 36407049 DOI: 10.1016/j.vgie.2022.08.005]

82 **Verlaan T**, Voermans RP, van Berge Henegouwen MI, Bemelman WA, Fockens P. Endoscopic closure of acute perforations of the GI tract: a systematic review of the literature. *Gastrointest Endosc* 2015; **82**: 618-28.e5 [PMID: 26005015 DOI: 10.1016/j.gie.2015.03.1977]

83 **Voermans RP**, Le Moine O, von Renteln D, Ponchon T, Giovannini M, Bruno M, Weusten B, Seewald S, Costamagna G, Deprez P, Fockens P; CLIPPER Study Group. Efficacy of endoscopic closure of acute perforations of the gastrointestinal tract. *Clin Gastroenterol Hepatol* 2012; **10**: 603-608 [PMID: 22361277 DOI: 10.1016/j.cgh.2012.02.005]

84 **Gubler C**, Bauerfeind P. Endoscopic closure of iatrogenic gastrointestinal tract perforations with the over-the-scope clip. *Digestion* 2012; **85**: 302-307 [PMID: 22614286 DOI: 10.1159/000336509]

85 **Kirschniak A**, Subotova N, Zieker D, Königsrainer A, Kratt T. The Over-The-Scope Clip (OTSC) for the treatment of gastrointestinal bleeding, perforations, and fistulas. *Surg Endosc* 2011; **25**: 2901-2905 [PMID: 21424197 DOI: 10.1007/s00464-011-1640-2]

86 **Kantsevoy SV**, Bitner M, Hajiyeva G, Mirovski PM, Cox ME, Swope T, Alexander K, Meenaghan N, Fitzpatrick JL, Gushchin V. Endoscopic management of colonic perforations: clips *versus* suturing closure (with videos). *Gastrointest Endosc* 2016; **84**: 487-493 [PMID: 26364965 DOI: 10.1016/j.gie.2015.08.074]

87 **Staudenmann D**, Choi KKH, Kaffes AJ, Saxena P. Current endoscopic closure techniques for the management of gastrointestinal perforations. *Ther Adv Gastrointest Endosc* 2022; **15**: 26317745221076705 [PMID: 35252863 DOI: 10.1177/26317745221076705]

World Journal of Gastroenterology

Submit a Manuscript: https://www.f6publishing.com

World J Gastroenterol 2023 May 7; 29(17): 2616-2627

DOI: 10.3748/wjg.v29.i17.2616

ISSN 1007-9327 (print) ISSN 2219-2840 (online)

ORIGINAL ARTICLE

Basic Study

Cryptotanshinone induces apoptosis of activated hepatic stellate cells *via* modulating endoplasmic reticulum stress

Xiao-Xue Hou, Yu-Wen Li, Jia-Li Song, Wen Zhang, Rui Liu, Hui Yuan, Tian-Tong Feng, Zheng-Yi Jiang, Wen-Ting Li, Chuan-Long Zhu

Specialty type: Gastroenterology and hepatology

Provenance and peer review: Unsolicited article; Externally peer reviewed.

Peer-review model: Single blind

Peer-review report's scientific quality classification

Grade A (Excellent): 0
Grade B (Very good): 0
Grade C (Good): C, C, C, C
Grade D (Fair): 0
Grade E (Poor): 0

P-Reviewer: Maslennikov R, Russia; Perazzo JC, Argentina

Received: November 4, 2022
Peer-review started: November 4, 2022
First decision: February 18, 2023
Revised: February 28, 2023
Accepted: April 10, 2023
Article in press: April 10, 2023
Published online: May 7, 2023

Xiao-Xue Hou, Jia-Li Song, Wen Zhang, Hui Yuan, Tian-Tong Feng, Zheng-Yi Jiang, Chuan-Long Zhu, Department of Infectious Disease, The First Affiliated Hospital of Nanjing Medical University, Nanjing 210009, Jiangsu Province, China

Yu-Wen Li, Department of Pediatrics, The First Affiliated Hospital of Nanjing Medical University, Nanjing 210009, Jiangsu Province, China

Rui Liu, Wen-Ting Li, Department of Infectious and Tropical Diseases, The Second Affiliated Hospital of Hainan Medical University, Haikou 570000, Hainan Province, China

Corresponding author: Chuan-Long Zhu, Founder, Professor, Department of Infectious Disease, The First Affiliated Hospital of Nanjing Medical University, No. 300 Guangzhou Road, Nanjing 210009, Jiangsu Province, China. zhuchuanlong@jsph.org.cn

Abstract

BACKGROUND

Cryptotanshinone (CPT) has wide biological functions, including anti-oxidative, antifibrosis, and anti-inflammatory properties. However, the effect of CPT on hepatic fibrosis is unknown.

AIM

To investigate the effects of CPT treatment on hepatic fibrosis and its underlying mechanism of action.

METHODS

Hepatic stellate cells (HSCs) and normal hepatocytes were treated with different concentrations of CPT and salubrinal. The CCK-8 assay was used to determine cell viability. Flow cytometry was used to measure apoptosis and cell cycle arrest. Reverse transcription polymerase chain reaction (RT-PCR) and Western blot analyses were used to measure mRNA levels and protein expression of endoplasmic reticulum stress (ERS) signaling pathway related molecules, respectively. Carbon tetrachloride (CCL_4) was used to induce *in vivo* hepatic fibrosis in mice. Mice were treated with CPT and salubrinal, and blood and liver samples were collected for histopathological examination.

RESULTS

We found that CPT treatment significantly reduced fibrogenesis by modulating

the synthesis and degradation of the extracellular matrix *in vitro*. CPT inhibited cell proliferation and induced cell cycle arrest at the G2/M phase in cultured HSCs. Furthermore, we found that CPT promoted apoptosis of activated HSCs by upregulating expression of ERS markers (CHOP and GRP78) and activating ERS pathway molecules (PERK, IRE1α, and ATF4), which were inhibited by salubrinal. Inhibition of ERS by salubrinal partially eliminated the therapeutic effect of CPT in our CCL_4-induced hepatic fibrosis mouse model.

CONCLUSION
CPT can promote apoptosis of HSCs and alleviate hepatic fibrosis through modulating the ERS pathway, which represents a promising strategy for treating hepatic fibrosis.

Key Words: Hepatic fibrosis; Endoplasmic reticulum stress; Cryptotanshinone; Hepatic stellate cells; Apoptosis

Core Tip: Hepatic fibrosis is a necessary stage of liver cirrhosis, and there is currently no effective treatment. Cryptotanshinone (CPT), one of the extracts of Chinese herbal medicine Radix Salviae Miltiorrhizae, has a good anti-fibrosis effect. Through this study, we found that CPT can treat hepatic fibrosis by activating endoplasmic reticulum stress and leading to apoptosis of hepatic stellate cells, which provides a new method for the treatment of hepatic fibrosis.

Citation: Hou XX, Li YW, Song JL, Zhang W, Liu R, Yuan H, Feng TT, Jiang ZY, Li WT, Zhu CL. Cryptotanshinone induces apoptosis of activated hepatic stellate cells *via* modulating endoplasmic reticulum stress. *World J Gastroenterol* 2023; 29(17): 2616-2627
URL: https://www.wjgnet.com/1007-9327/full/v29/i17/2616.htm
DOI: https://dx.doi.org/10.3748/wjg.v29.i17.2616

INTRODUCTION

Hepatic fibrosis is a reversible liver injury that occurs in response to viruses, drugs, inflammation, fat deposition, and other causes. The underlying pathological mechanism of hepatic fibrosis involves the deposition of extracellular matrix (ECM), which leads to the replacement of functional liver parenchyma by scar tissue, proliferation and activation of hepatic stellate cells (HSCs), and increased production of collagen and unfolded proteins[1-3]. The endoplasmic reticulum (ER) is an important organelle in eukaryotic cells that is involved in a variety of biological processes, including protein synthesis, processing, modification, folding, and transport, lipid and carbohydrate metabolism, and Ca^{2+} maintenance, among others[4-6]. In some cases, when the physiological function of the ER is disturbed, ER stress (ERS) will be activated to promote cell survival. However, persistent ERS can lead to apoptosis [7,8], which can either promote the occurrence and development of hepatic fibrosis or lead to the activation of HSCs, which can reverse the transformation of hepatic fibrosis[2,9-11].

Cryptotanshinone (CPT) is a diterpene quinone compound that is isolated from Salvia miltiorrhiza. CPT has been shown to have anti-oxidant, anti-inflammatory, and antibacterial properties[12]. Studies have also reported that CPT antifibrotic effects on cardiac and renal tissues[13-15]. These findings suggest that CPT plays a protective role in fibrotic disease. Therefore, we hypothesized that CPT might also protect against hepatic fibrosis. In this study, we treated LX2 cells with different concentrations of CPT and found that cell viability decreased and apoptosis increased in a dose-dependent manner. We also found that expression of proteins related to ERS increased, and inhibiting ERS decreased the apoptosis rate. Based on our findings, we speculate that CPT promotes apoptosis of HSCs through modulating the ERS pathway.

MATERIALS AND METHODS

Reagents and antibodies

CPT (purity ≥ 98% purity by HPLC, Cat No. HY-N0174), were purchased from Med Chem Express LLC (Shanghai, China) (Figure 1A). Primary antibodies for α-SMA, Collagen I, eIF2α, p-eIF2α, p-PERK, PERK, IRE1-α, BAX, BCL2, CHOP, and GRP78/BIP and all secondary antibodies were purchased from Proteintech (China). ATF4, and XBP1 were purchased from Sigma (United States). The primers used in

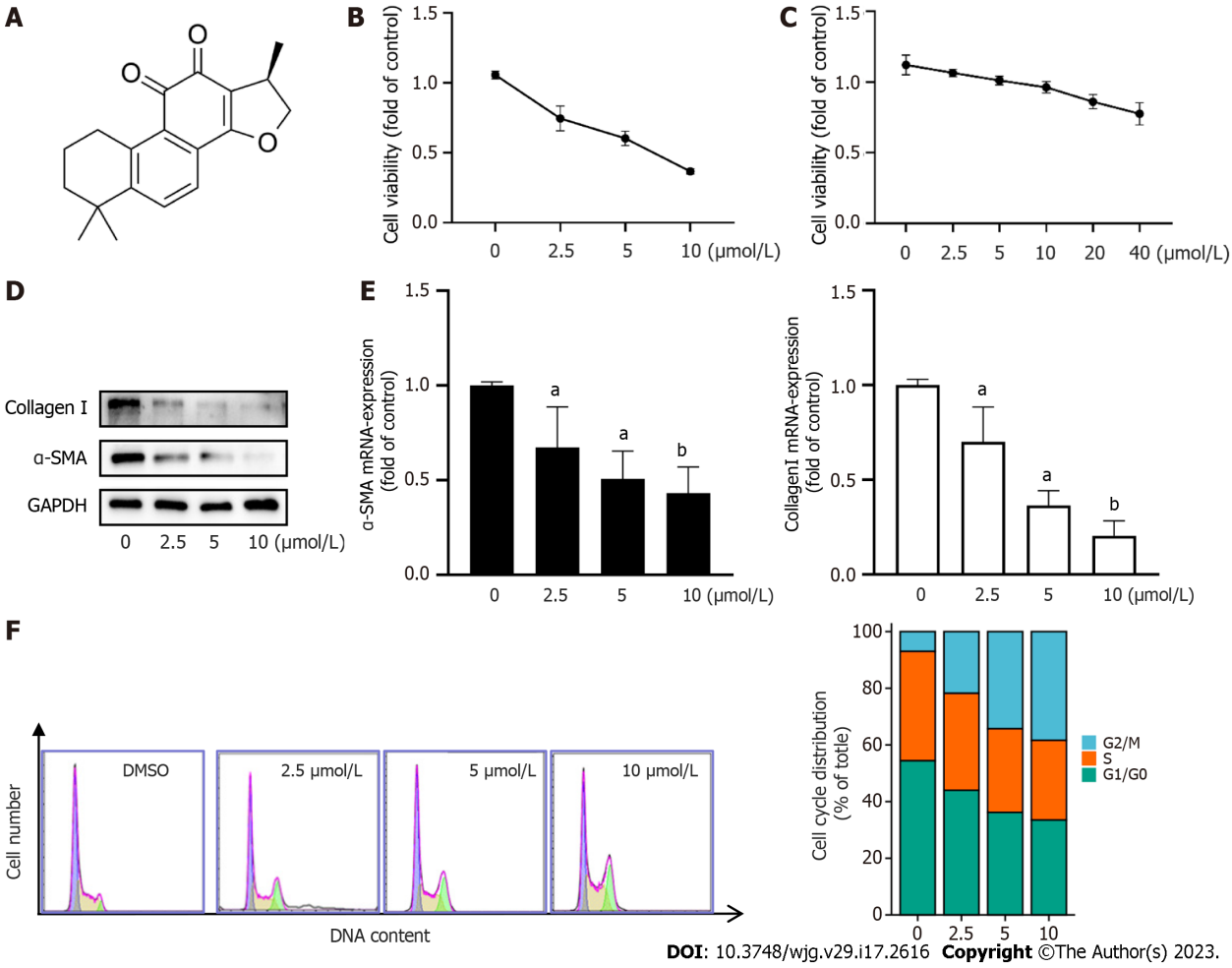

DOI: 10.3748/wjg.v29.i17.2616

Figure 1 Cryptotanshinone reduces collagen deposition and induces cell cycle arrest at the G2/M checkpoint. A: Chemical structure of cryptotanshinone; B: CCK8 assay for LX2 cell viability; C: CCK8 assay for cell viability of LO2; D: Protein levels of collagen I and α-SMA were determined using Western blot analysis; E: mRNA levels of α-SMA and collagen I were determined using reverse transcription polymerase chain reaction (RT-PCR); F: The percentage of cell cycle distribution was determined using flow cytometry. Data are presented as mean ± SD. $^{a}P < 0.05$, $^{b}P < 0.01$ versus control.

quantitative reverse transcription polymerase chain reaction (qRT-PCR) were purchased from Qingke Co. Ltd. (China) (Table 1).

Animals and experimental procedures

All experiments were approved by institutional and local committees. All mice were provided humane care according to the National Institutes of Health (NIH, United States) guidelines[16]. Male C57BL/6 mice (20-25 g) were randomly divided into five groups (n = 8 per group). Group 1 (vehicle control) did not receive carbon tetrachloride (CCL_4) or CPT treatment. Group 2 (model group) received CCL_4. Group 3 received intraperitoneal injections of salubrinal (1 mg/kg). Group 4 received CCL_4 followed by intraperitoneal injections of CPT (40 mg/kg). Group 5 received simultaneous intraperitoneal injections of salubrinal and CPT. Groups 2, 3, 4, and 5 were administered CCL_4 twice a week for 8 wk to induce hepatic fibrosis. Groups 3, 4, and 5 were intraperitoneally injected with CPT or salubrinal every day from 5 wk to 8 wk. CPT and salubrinal were dissolved in physiological saline. After 8 wk of treatment, blood samples and livers were collected. Livers were fixed in 4% buffered paraformaldehyde for histological (hematoxylin and eosin) and Western blot analyses.

Cell culture

The HSC LX2 cell line was donated by Professor Wenting Li. Cells were cultured in high-sugar DMEM medium with 10% fetal bovine serum (FBS) in an incubator at 37 °C[17].

qRT-PCR analysis

RNA was extracted from the LX2 cells using an RNA extraction kit (Biyuntian, China) according to the kit's instructions. The Stepone system was used for qRT-PCR, and the experiment was repeated three times to calculate the mRNA levels of the target genes.

Table 1 Primer sequences

Primer	Sequence
GAPDH-F (human)	AAATCCCATCACCATCTTCCAG
GAPDH-R (human)	AGGGGCCATCCACAGTCTTCT
Bax-F (human)	TGAGCAGATCATGAAGACAGGG
Bax-R (human)	TGAGACACTCGCTCAGCTTC
BCL2-F (human)	TCACTTGTGGCCCAGATAGG
BCL2-R (human)	GATAACGGAGGCTGGGATGC
GRP78-F (human)	CATCACGCCGTCCTATGTCG
GRP78-R (human)	CGTCAAAGACCGTGTTCTCG
CHOP-F (human)	ACCTGAAAGCAGATGTGCT
CHOP-R (human)	GTCCTCATACCAGGCTTCC
α-SMA-F (human)	AAAAGACAGCTACGTGGGTGA
α-SMA-R (human)	GCCATGTTCTATCGGGTACTTC
Col1a1-F (human)	GAGCCAAGACGAAGACATC
Col1a1-R (human)	CAGATCACGTCATCGCACAAC
GAPDH-F (mouse)	TGTCGTGGAGTCTACTGGTG
GAPDH-R (mouse)	ACACCCATCACAAACATGG
α-SMA-F (mouse)	TGACGCTGAAGTATCCGATAGA
α-SMA-R (mouse)	CGAAGCTCGTTATAGAAAGAGTGG
Col1a1-F (mouse)	GATCCTGCCGATGTCGCTAT
Col1a1-R (mouse)	TGTAGGCTAGCTGTTCTTGCA

Western blot analysis

RIPA buffer containing protease and phosphatase inhibitors was used to lyse cells and tissues on ice. Proteins were electrophoresed and transferred to PVDF membranes (Millipore, United States), which were blocked with 5% bovine serum albumin for 2 h. Subsequently, the membranes were incubated with primary antibodies at 4 °C overnight, followed by incubation with second antibodies at room temperature for 2 h. Finally, the PVDF membranes were washed using 1% TBST and detected by the Bio-Rad ChemiDoc Touch Imaging System.

Enzyme-linked immunosorbent assay

Serum levels of interleukin (IL)-6 and IL-10 were determined using enzyme-linked immunosorbent assay (ELISA) kits (LinkTech Biotechnology, China) according to the manufacturer's instructions. The absorbance was observed at 450 nm using a full-wavelength microplate reader.

Transmission electron microscopy

LX2 cells were treated with CPT for 24 h, gently scraped with a cell scraper, washed with PBS three times, precipitated, centrifuged, and fixed overnight with an electron microscopy fixative. The fixed cells were imaged using a transmission electron microscope (Tokyo, Japan).

Biochemical analysis

Serum levels of aspartate aminotransferase (AST) and alanine aminotransferase (ALT) were measured using a liver function analysis kit (Nanjing Chengjian Institute of Bioengineering, China) according to the kit's instructions. The absorbance was measured using an enzyme-labeled instrument.

Cell proliferation assay

The Cell Counting Kit 8 (CCK-8) kit (Biyuntian, China) was used to assay cell proliferation. LX2 cells were inoculated into a 96-well plate at 3000 cells per well and cultured overnight at 37 °C. After 24 h cells were treated with CPT at different concentrations, and 10 μL of the CCK-8 solution was added to each well. The cells were cultured at 37 °C for 2 h. The absorbance of each well was measured at 450 nm using a microplate reader.

TUNEL staining

LX2 cells were inoculated into a 24-well plate. After the cells attached, DMSO, CPT, or salubrinal was added for 24 h. A TUNEL staining kit (Biyuntian, China) was used to detect apoptotic cells according to the kit's instructions. Cell apoptosis was observed with a fluorescent microscope (Nikon).

Flow cytometry analysis of cell cycle and apoptosis

LX2 cells were inoculated into a 6-well plate at a density of 2×10^4 cells/well. On the following day, the cells were treated with CPT at different concentrations for 24 h. Cell cycle was measured using a cell cycle kit (KeyGen Biotech). Cell apoptosis was determined using Annexin V and propidium iodide double staining with fluorescein isothiocyanate. The percentage of apoptotic cells was determined using flow cytometry (FACS Calibur)[17].

Statistical analysis

Experimental data were graphed using Prism 9.0 and statistically analyzed using SPSS26.0. Statistical significance of differences was determined using one-way analysis of variance with the post-hoc Dunnett's test. A P value of <0.05 was considered statistically significant.

RESULTS

CPT inhibits the proliferation of LX2 cells

Hepatic fibrosis is characterized by progressive and excess accumulation of ECM, leading to disruption of normal liver structure and function. HSC activation is a key cellular event in the pathogenesis of hepatic fibrosis[18,19]. In this study, we sought to determine the effects of CPT on hepatic fibrosis. To do so we first investigated the effect of CPT on cell viability. We treated LX2 cells with varying concentrations of CPT (0, 2.5, 5, 10, and 20 μmol/L) for 24 h and assessed cell proliferation using the CCK-8 assay. The results showed that CPT significantly reduced cell viability in a dose-dependent manner (Figure 1B). We also observed that CPT inhibited the vitality of normal hepatocytes (L02) at 40 μm (Figure 1C), which was far in excess of the concentration that affected HSC viability. To further observe the inhibitory effect of CPT on activated LX2 cells *in vitro*, we examined ECM accumulation under different concentrations of CPT. We found that CPT reduced ECM deposition (Figure 1D and E). To further investigate the inhibitory effect of CPT on cell growth, we measured cell cycle distribution using flow cytometry. Cell cycle analysis showed that the number of cells in the G2/M phase significantly increased while those in the G1 phase significantly decreased with higher concentrations of CPT (Figure 1F). Collectively, these findings suggest that CPT can induce HSC growth.

CPT stimulates apoptosis of activated HSCs

Apoptosis of activated HSCs has been shown to reduce the degree of hepatic fibrosis[2,3]. We assessed HSC apoptosis using TUNEL staining and found that CPT induced activated HSC apoptosis in a dose-dependent manner (Figure 2A). We next explored the pathway underlying CPT-induced HSC apoptosis. We observed that CPT dose-dependently reduced Bcl-2/Bax expression in HSCs (Figure 2B and C). We quantitatively evaluated the apoptotic rate using flow cytometry, which demonstrated that CPT dose-dependently increased the apoptotic rate in activated HSCs (Figure 2D). These data indicate that CPT activates HSC apoptosis.

CPT activates the ERS pathway

ERS is a signaling response pathway intended to protect against cell death. However, if the stress response is very strong or prolonged, it can cause cellular damage[20]. We investigated the underlying mechanism of CPT-induced HSC apoptosis by detecting ERS-related mediators. We found that CPT significantly upregulated the mRNA levels and protein expression of GFR78 and CHOP in LX2 cells, resepectively (Figure 3A and B). Subsequently, we examined the expression of GFR78 and CHOP in L02 cells and found that their expression was not significantly altered (Figure 3C and D). These results suggest that CPT promotes ERS in activated HSCs without triggering ERS in normal liver cells. Western blot analysis revealed that CPT significantly upregulated protein expression of ERS regulatory molecules (Figure 3E and F). We also observed the expansion and swelling of the ER lumen in CPT-treated HSCs using electron microscopy. More specifically, we observed a disappearance of the normal sheet-like folded structure and the formation of numerous vacuoles within the ER (Figure 3G).

CPT-induced apoptosis of HSCs requires ERS activation

Salubrinal, an inhibitor of ERS, can protect HSCs from ERS-induced apoptosis[20]. Based on the above experimental results, we next investigated if activation of ERS by CPT leads to apoptosis of LX2 cells. To test this hypothesis, we treated LX2 cells with both CPT and salubrinal and found that CPT did not significantly upregulate the mRNA and Western blot levels of GFR78 and CHOP (Figure 4A and B). We also measured the expression of ECM components at the mRNA and protein levels. Interestingly, The

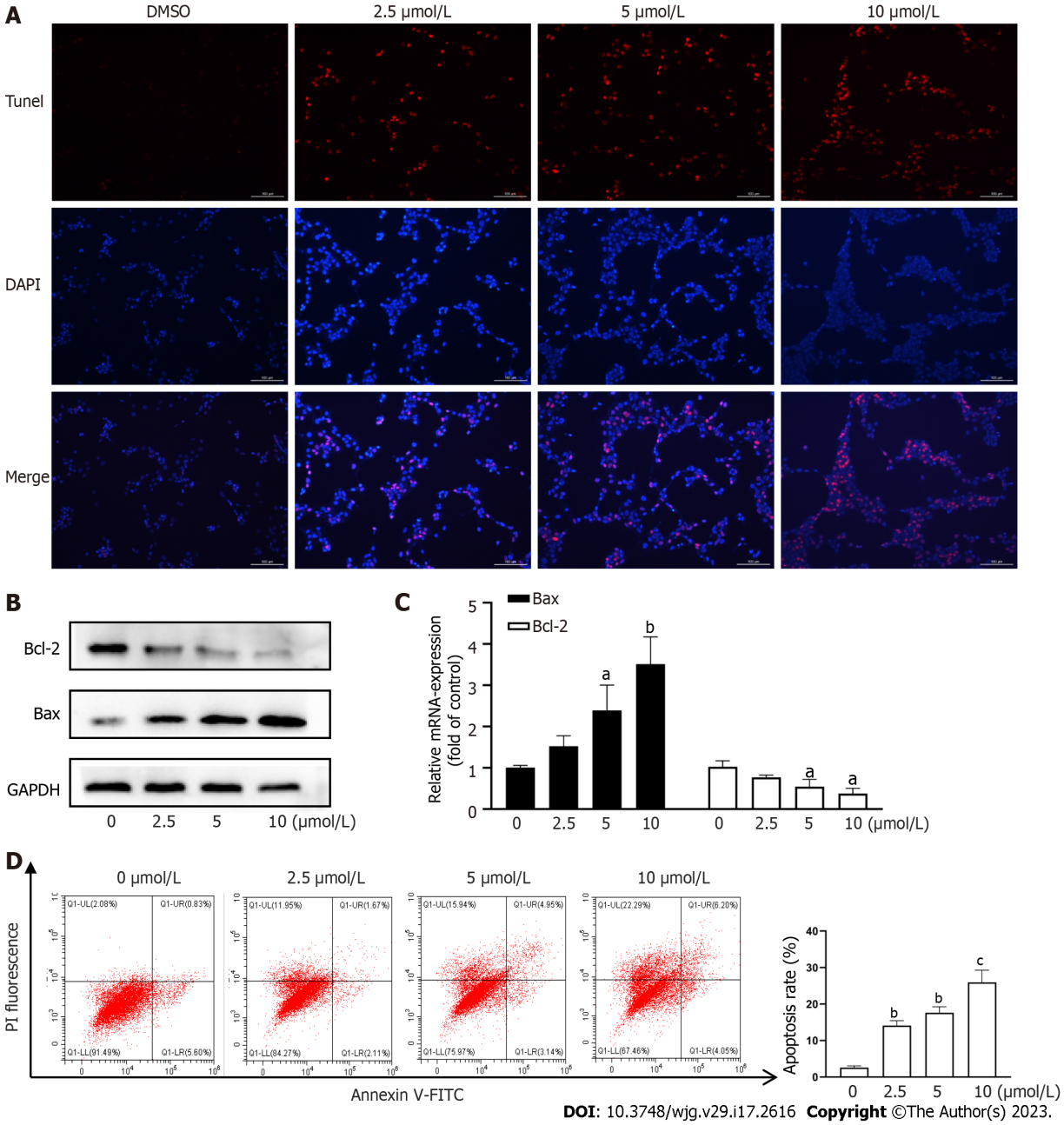

DOI: 10.3748/wjg.v29.i17.2616

Figure 2 Cryptotanshinone induces apoptosis of activated hepatic stellate cells. A: TUNEL staining to assess LX2 apoptosis. Red fluorescence indicates apoptotic cells. Scale baes: 100μm; B: Western blot analysis of Bcl-2 and Bax protein expression in LX2 cells; C: Reverse transcription polymerase chain reaction analysis of Bcl-2 and Bax mRNA levels in LX2 cells; D: Flow cytometric analysis of LX2 cell apoptosis using fluorescein isothiocyanate-labeled Annexin-V/propidium iodide staining. Cells located in the right two quadrants of each figure were considered apoptotic cells. $^{a}P < 0.05$, $^{b}P < 0.01$, $^{c}P < 0.001$ versus control.

decrease of ECM accumulation following CPT treatment was prevented by salubrinal (Figure 4C and D). These results suggest that CPT can activate ERS, leading to apoptosis of LX2 cells, which may be a mechanism to promote HSC clearance. We found that the apoptotic effect of CPT on activated LX2 cells could be reversed by salubrinal (Figure 4E-H). Taken together, these findings suggest that CPT can induce apoptosis of HSCs through modulating ERS, which may be a mechanism for promoting HSCs clearance.

CPT protects mice from CCL_4-induced hepatic fibrosis

CCl_4-induced hepatic fibrosis is a well-established model to investigate hepatic fibrosis *in vivo*. We used this model to confirm the protective effect of CPT in mice(Figure 5A). To this end, we measured protein expression of major markers of hepatic fibrosis including α-SMA and collagen I. CPT effectively diminished expression of these proteins in the CCL_4-induced model of hepatic fibrosis (Figure 5B). In addition, we analyzed biochemical markers of liver injury after 8 wk of CCL_4 treatment. Levels of AST and ALT increased in the model group but were reduced in the CPT groups (Figure 5C and D). During chronic liver disease, hepatic fibrogenesis is commonly accompanied by inflammation. As demonstrated

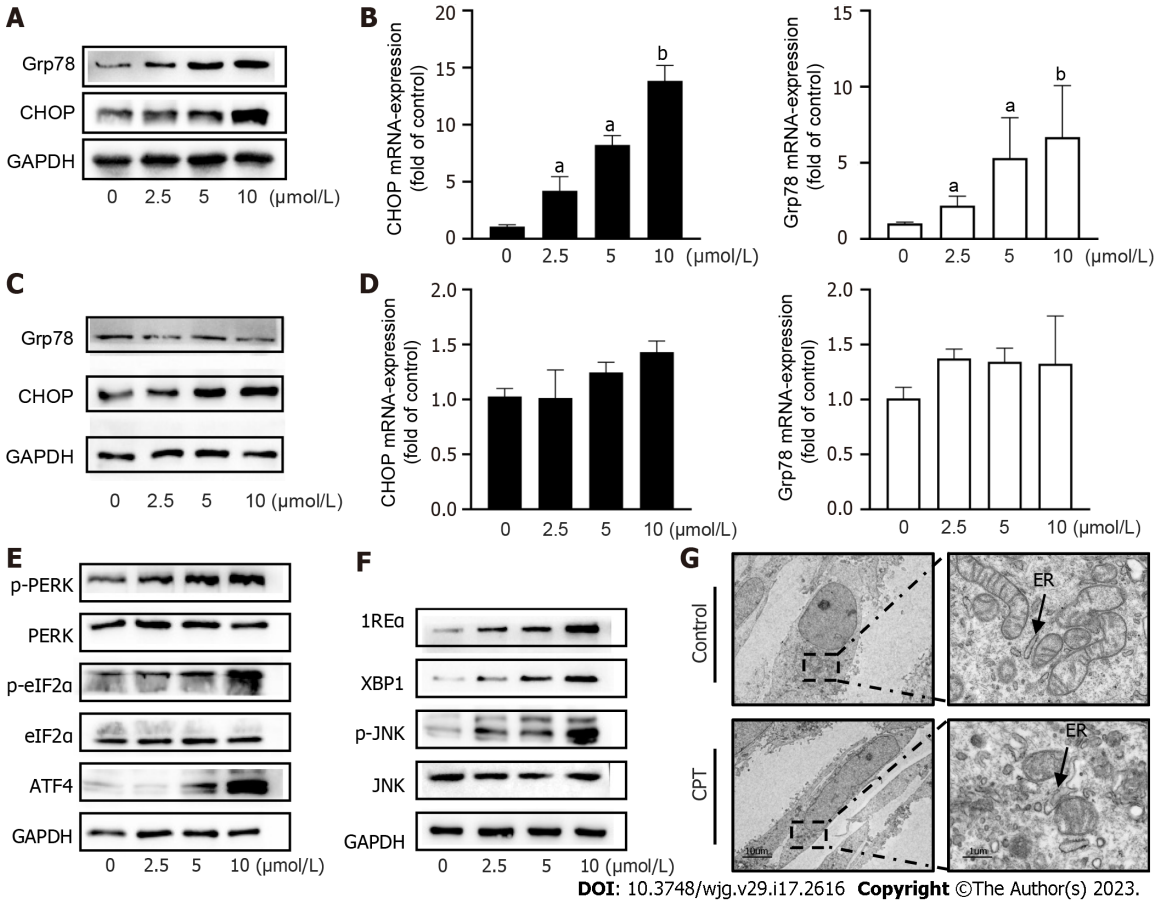

Figure 3 Cryptotanshinone activates the endoplasmic reticulum stress pathway in activated LX2 cells. A: Western blot analysis of endoplasmic reticulum stress (ERS)-related protein expression in LX2 cells; B: Reverse transcription polymerase chain reaction (RT-PCR) analysis of Grp78 and CHOP mRNA levels in LX2 cells; C: Western blot analysis of ERS-related protein expression in LO2 cells; D: RT-PCR analysis of Grp78 and CHOP mRNA levels in LO2 cells; E and F: Western blot analyses of ATF4, PERK, and IRE1 signaling pathways in hepatic stellate cells; G: Transmission electron microscopy showing that CPT caused ER swelling and destruction of the mitochondrial membrane integrity. Data are presented as mean ± SD. $^{a}P < 0.05$, $^{b}P < 0.01$ versus control. ER: Endoplasmic reticulum.

by ELISA, CPT decreased serum levels of IL-6 and IL-10 (Figure 5E and F). Furthermore, the inhibitory effect of CPT on the secretion of pro-inflammatory cytokines was diminished by salubrinal. Thus, we propose that CPT protects against CCL_4-induced liver injury by suppressing inflammation. Next, we analyzed the pathological changes in the liver tissue after CPT treatment. Histological staining showed that treatment with CPT significantly improved morphological changes in liver tissue (Figure 5G). As fibrogenesis is accompanied by accumulation of collagen, liver tissue sections were stained with Masson's reagent and Sirius red to detect collagen deposition. The results showed that collagen was markedly deposited in the CCL_4-injured livers but reduced in the livers of mice in the CPT-treated groups, which was further suppressed by salubrinal (Figure 5G). Taken together, these data provide *in vivo* evidence that activation of ERS signaling can result in reduced collagen accumulation and attenuation of fibrotic damage in a hepatic fibrosis mouse model.

DISCUSSION

Due to their diverse sources and high safety profiles, there has recently been a widespread increase in the use of natural bioactive components from plants for the prevention and treatment of diseases. Salvia miltiorrhiza is a traditional Chinese medicine that has been used to treat many diseases. CPT is one of the main tanshinones extracted from Salvia miltiorrhiza Bunge and is considered an important compound with various pharmacological properties. Specifically, recent studies have shown that CPT has antifibrotic properties in the heart, lung, and kidney[14,15]. However, the relationship between CPT and hepatic fibrosis remains unclear.

Hepatic fibrosis involves inflammatory responses caused by various acute and chronic liver injuries. If left untreated, hepatic fibrosis can progress to liver cirrhosis or even liver cancer. The production of ECM by activated HSCs plays an important role in hepatic fibrosis and cirrhosis[21]. Hepatic fibrosis might be prevented or even reversed by inducing apoptosis of activated HSCs. In this study, we

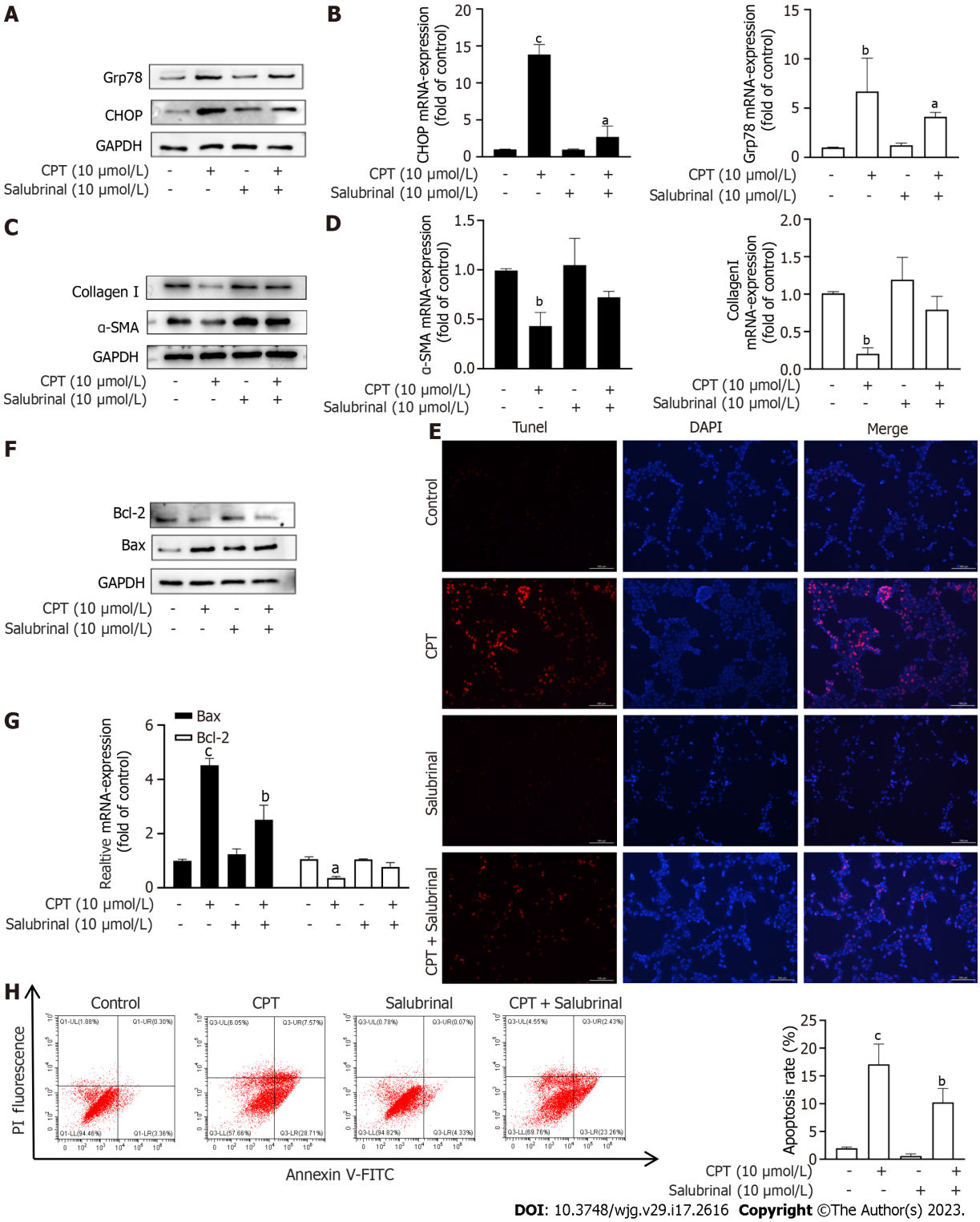

DOI: 10.3748/wjg.v29.i17.2616

Figure 4 The endoplasmic reticulum stress signaling pathway leads to LX2 cell apoptosis and reduces collagen deposition induced by cryptotanshinone. A: Protein expression of Grp78 and CHOP was determined using Western blot analysis; B: mRNA levels of Grp78 and CHOP were determined using reverse transcription polymerase chain reaction (RT-PCR); C: Protein expression of collagen type I and α-SMA was determined using Western blot analysis; D: mRNA levels of α-SMA and collagen I were determined using RT-PCR; E: TUNEL staining was used to assess LX2 cell apoptosis. Red fluorescence indicates apoptotic cells. Scale bars: 100 μm; F: Protein expression of Bax and Bcl2 was determined using Western blot analysis; G: mRNA levels of Bax and Bcl2 were determined using RT-PCR; H: Flow cytometry data are presented as mean ± SD. $^{a}P < 0.05$, $^{b}P < 0.01$, $^{c}P < 0.001$ versus control. CPT: Cryptotanshinone; FITC: Fluorescein isothiocyanate.

established that CPT induces apoptosis through ERS in activated HSCs, which may offer a new strategy for the treatment of hepatic fibrosis. We discovered that CPT decreased both mRNA levels and protein expression of α-SMA and type I collagen in activated HSCs, which resulted in reduced ECM deposition. Furthermore, flow cytometry revealed that CPT dose-dependently induced apoptosis of activated LX2

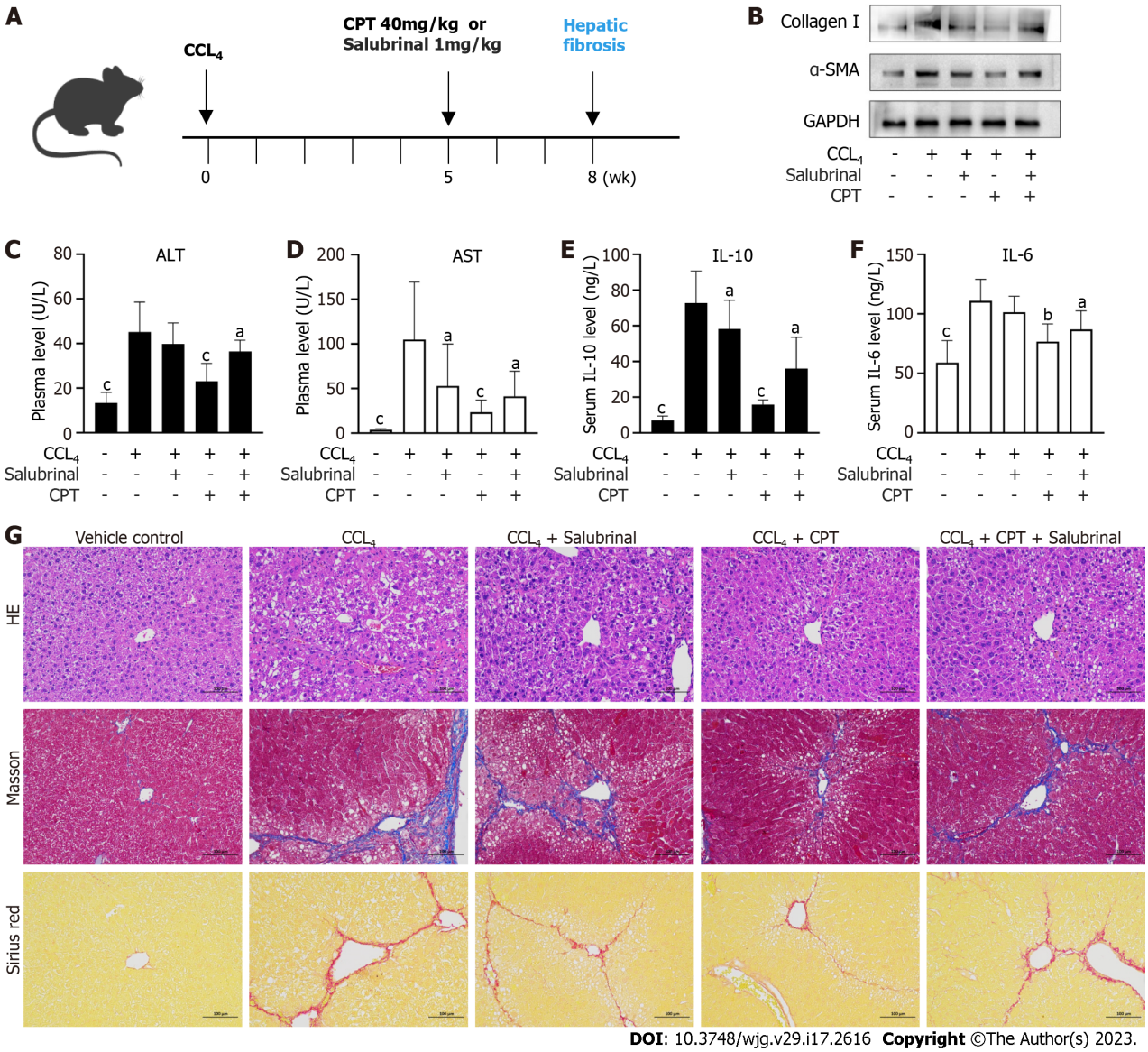

DOI: 10.3748/wjg.v29.i17.2616

Figure 5 Cryptotanshinone protects the liver against carbon tetrachloride-induced injury and inflammation. Cryptotanshinone (CPT) alleviates hepatic fibrotic injury in mice. Mice were injected with carbon tetrachloride (CCL_4) for 8 wk to induce liver fibrosis. During weeks 5 through 8, mice in the treatment groups were given CPT (40 mg/kg) or salubrinal (1 mg/kg). A: CPT treatment protocol in the CCL_4-induced hepatic fibrosis mouse model; B: Western blot analysis of α-SMA and collagen I in the liver tissue; C: Determination of serum alanine aminotransferase levels; D: Determination of serum aspartate aminotransferase levels; E: Enzyme-linked immunosorbent assay (ELISA) measurement of IL-6 levels in the serum; F: ELISA measurement of IL-10 levels in the serum; G: Liver sections were stained with hematoxylin and eosin, Masson reagents, and Sirius red. Scale baes: 100 μm. $^aP < 0.05$, $^bP < 0.01$, $^cP < 0.001$ compared with the CCL_4 group. CPT: Cryptotanshinone; CCL_4: Carbon tetrachloride.

cells. Bax is considered an apoptotic factor, while Bcl2 is an anti-apoptotic molecule that inhibits the release of cytochrome C from the mitochondria and inhibits HSC apoptosis[22]. We found that CPT upregulated the expression of the pro-apoptotic protein Bax and downregulated the expression of the anti-apoptotic protein Bcl2 in activated HSCs, increased the Bax/Bcl ratio, and promoted HSC apoptosis. Interestingly, the pro-apoptotic effect of CPT was more specific for activated HSCs than for normal hepatocytes, which did not undergo apoptosis. This finding is important because it indicates that CPT does not affect normal liver cell activity. Thus, we found that CPT is an effective drug that can induce apoptosis of activated HSCs but have no effect on normal hepatocytes during the treatment of hepatic fibrosis.

Our results demonstrated that CPT upregulated expression of ER-resident chaperone proteins, such as CHOP and GRP78, which are significant markers of ERS[23,24]. In addition, the PERK, IRE1, and ATF6 signaling pathways were activated, all of which can phosphorylate the downstream molecules eIF2α, ATF4, and JNK, modulating the ERS response[25,26]. We also observed ultrastructure changes using electron microscopy. The results showed that the ER cavity of the HSCs was swollen, and the integrity of the mitochondrial membrane was damaged after CPT treatment. The ER and mitochondria are important organelles that cooperate to complete a variety of biological functions through their

interactions with various proteins. In the early stage of ERS, GRP78 is translocated to the mitochondria, and the subsequent damage to the integrity of the mitochondrial membrane becomes an early feature of apoptosis[27,28]. Our results indicate that CPT could promote ERS in HSCs to promote apoptosis. Salubrinal is an ERS inhibitor that selectively induces eIF2α phosphorylation and inhibits its dephosphorylation, ultimately protecting cells from ERS-induced apoptosis[29]. To better understand if CPT-induced HSC apoptosis is regulated by activating the ERS pathway, we incubated HSCs with salubrinal to protect cells from ERS-induced apoptosis. In activated HSCs, salubrinal effectively attenuated CPT-induced apoptosis, reducing secretion of apoptotic proteins. Therefore, these results confirm that targeting ERS can trigger HSCs apoptosis.

To further verify the therapeutic effect of CPT on hepatic fibrosis, we conducted *in vivo* experiments using a CCL_4-induced mouse model of hepatic fibrosis. We found that intraperitoneal injection of CPT reversed the development of hepatic fibrosis in mice, and the therapeutic effect of CPT was reduced after by salubrinal. Interestingly, CCL_4 also induces experimental hepatocarcinoma, which shares common features with hepatic fibrosis, such as increased expression of matricellular proteins (SPARC, BM-40, and osteonectin)[30-32]. However, whether or not CPT also has a significant effect on the treatment of liver cancer requires further investigation.

CONCLUSION

In summary, we found that CPT limited HSC activation through an ERS-dependent pathway *in vivo* and *in vitro*, suggesting that CPT should be further investigated as a prospective therapeutic agent for hepatic fibrosis.

ARTICLE HIGHLIGHTS

Research background

Cryptotanshinone (CPT) has been accepted to be an anti-inflammatory molecule.

Research motivation

Hepatic stellate cell (HSC) activation plays an indispensable role in hepatic fibrosis. Inducing apoptosis of activated HSCs can attenuate or reverse fibrogenesis.

Research objectives

This study investigated the effects of CPT treatment on hepatic fibrosis and its underlying mechanism of action.

Research methods

In vitro, we used reverse transcription polymerase chain reaction, Western blot, TUNEL staining and flow cytometry, which demonstrated that CPT can induce HSC apoptosis through the ERS pathway. *In vivo*, we used liver function kit, enzyme-linked immunosorbent assay, pathological section staining a few columns of technical means to prove that CPT has a certain therapeutic effect on hepatic fibrosis.

Research results

In vitro, CPT was considered to activate HSC apoptosis by promoting endoplasmic reticulum stress (ERS) detrimental response to a certain extent. Main molecules came down to the unfolded protein response signaling pathway. *In vivo*, We found CPT protected the Carbon tetrachloride (CCL_4)-induced hepatic fibrosis. Furthermore, CPT inhibited the levels of the downstream inflammatory cytokines, which were triggered by CCL_4-induced hepatic fibrosis.

Research conclusions

CPT can promote apoptosis of HSCs and alleviate hepatic fibrosis through modulating the ERS pathway, which represents a promising strategy for treating hepatic fibrosis.

Research perspectives

Hepatic fibrosis, cirrhosis and liver cancer are typical "trilogy of liver diseases", which seriously endanger human health. Hepatic fibrosis is reversible in the early stage, but it is difficult to reverse in the late stage of liver cirrhosis. Early treatment is therefore essential. CPT is a diterpene quinone compound that is isolated from Salvia miltiorrhiza. CPT has been shown to have anti-oxidant. In this study, we found that CPT could induce apoptosis of activated HSCs and had good prospects for the treatment of hepatic fibrosis.

FOOTNOTES

Author contributions: Zhu CL and Hou XX designed the research; Hou XX, Li YW and Song JL performed the research; Li WT analyzed data and wrote the article; Zhang W and Feng TT checked the statistical calculations; Yuan H, Liu R and Jiang ZY commented on and revised the paper; all authors have read and approved the final paper.

Supported by Science and Technology Plan of Hainan Province (Clinical Research Center), No. LCYX202103 and No. LCYX202204; Hainan Province Science and Technology Special Fund, No. ZDYF2022SHFZ067; and Hainan Province Clinical Medical Center.

Institutional animal care and use committee statement: All procedures involving animals were reviewed and approved by the Institutional Animal Care and Use Committee of The First Affiliated Hospital of Nanjing Medical University (IACUC protocol number: IACUC-2209028).

Conflict-of-interest statement: All the authors report no relevant conflicts of interest for this article.

Data sharing statement: All data generated or analyzed supporting conclusions are included in the current manuscript.

ARRIVE guidelines statement: The authors have read the ARRIVE Guidelines, and the manuscript was prepared and revised according to the ARRIVE Guidelines.

Country/Territory of origin: China

ORCID number: Chuan-Long Zhu 0000-0001-6557-1654.

S-Editor: Gao CC
L-Editor: A
P-Editor: Zhao S

REFERENCES

1 **Gan C**, Cai Q, Tang C, Gao J. Inflammasomes and Pyroptosis of Liver Cells in Liver Fibrosis. *Front Immunol* 2022; **13**: 896473 [PMID: 35707547 DOI: 10.3389/fimmu.2022.896473]
2 **Tsuchida T**. [Mechanisms of hepatic stellate cell activation as a therapeutic target for the treatment of non-alcoholic steatohepatitis]. *Nihon Yakurigaku Zasshi* 2019; **154**: 203-209 [PMID: 31597900 DOI: 10.1254/fpj.154.203]
3 **Yang F**, Li H, Li Y, Hao Y, Wang C, Jia P, Chen X, Ma S, Xiao Z. Crosstalk between hepatic stellate cells and surrounding cells in hepatic fibrosis. *Int Immunopharmacol* 2021; **99**: 108051 [PMID: 34426110 DOI: 10.1016/j.intimp.2021.108051]
4 **Duwaerts CC**, Maiers JL. ER Disposal Pathways in Chronic Liver Disease: Protective, Pathogenic, and Potential Therapeutic Targets. *Front Mol Biosci* 2021; **8**: 804097 [PMID: 35174209 DOI: 10.3389/fmolb.2021.804097]
5 **Maiers JL**, Malhi H. Endoplasmic Reticulum Stress in Metabolic Liver Diseases and Hepatic Fibrosis. *Semin Liver Dis* 2019; **39**: 235-248 [PMID: 30912096 DOI: 10.1055/s-0039-1681032]
6 **Bravo R**, Parra V, Gatica D, Rodriguez AE, Torrealba N, Paredes F, Wang ZV, Zorzano A, Hill JA, Jaimovich E, Quest AF, Lavandero S. Endoplasmic reticulum and the unfolded protein response: dynamics and metabolic integration. *Int Rev Cell Mol Biol* 2013; **301**: 215-290 [PMID: 23317820 DOI: 10.1016/B978-0-12-407704-1.00005-1]
7 **Iurlaro R**, Muñoz-Pinedo C. Cell death induced by endoplasmic reticulum stress. *FEBS J* 2016; **283**: 2640-2652 [PMID: 26587781 DOI: 10.1111/febs.13598]
8 **Demirtas L**, Guclu A, Erdur FM, Akbas EM, Ozcicek A, Onk D, Turkmen K. Apoptosis, autophagy & endoplasmic reticulum stress in diabetes mellitus. *Indian J Med Res* 2016; **144**: 515-524 [PMID: 28256459 DOI: 10.4103/0971-5916.200887]
9 **Zhang CY**, Yuan WG, He P, Lei JH, Wang CX. Liver fibrosis and hepatic stellate cells: Etiology, pathological hallmarks and therapeutic targets. *World J Gastroenterol* 2016; **22**: 10512-10522 [PMID: 28082803 DOI: 10.3748/wjg.v22.i48.10512]
10 **Koo JH**, Lee HJ, Kim W, Kim SG. Endoplasmic Reticulum Stress in Hepatic Stellate Cells Promotes Liver Fibrosis *via* PERK-Mediated Degradation of HNRNPA1 and Up-regulation of SMAD2. *Gastroenterology* 2016; **150**: 181-193.e8 [PMID: 26435271 DOI: 10.1053/j.gastro.2015.09.039]
11 **Borkham-Kamphorst E**, Steffen BT, Van de Leur E, Haas U, Tihaa L, Friedman SL, Weiskirchen R. CCN1/CYR61 overexpression in hepatic stellate cells induces ER stress-related apoptosis. *Cell Signal* 2016; **28**: 34-42 [PMID: 26515130 DOI: 10.1016/j.cellsig.2015.10.013]

12 **Li H**, Gao C, Liu C, Liu L, Zhuang J, Yang J, Zhou C, Feng F, Sun C, Wu J. A review of the biological activity and pharmacology of cryptotanshinone, an important active constituent in Danshen. *Biomed Pharmacother* 2021; **137**: 111332 [PMID: 33548911 DOI: 10.1016/j.biopha.2021.111332]

13 **Wang X**, Wan W, Lu J, Zhang Y, Quan G, Pan X, Wu Z, Liu P. Inhalable cryptotanshinone spray-dried swellable microparticles for pulmonary fibrosis therapy by regulating TGF-β1/Smad3, STAT3 and SIRT3 pathways. *Eur J Pharm Biopharm* 2022; **172**: 177-192 [PMID: 35202797 DOI: 10.1016/j.ejpb.2022.02.012]

14 **Wang W**, Zhou PH, Hu W, Xu CG, Zhou XJ, Liang CZ, Zhang J. Cryptotanshinone hinders renal fibrosis and epithelial transdifferentiation in obstructive nephropathy by inhibiting TGF-β1/Smad3/integrin β1 signal. *Oncotarget* 2018; **9**: 26625-26637 [PMID: 29928474 DOI: 10.18632/oncotarget.23803]

15 **Lo SH**, Hsu CT, Niu HS, Niu CS, Cheng JT, Chen ZC. Cryptotanshinone Inhibits STAT3 Signaling to Alleviate Cardiac Fibrosis in Type 1-like Diabetic Rats. *Phytother Res* 2017; **31**: 638-646 [PMID: 28176375 DOI: 10.1002/ptr.5777]

16 **Xu W**, Lu C, Zhang F, Shao J, Yao S, Zheng S. Dihydroartemisinin counteracts fibrotic portal hypertension *via* farnesoid X receptor-dependent inhibition of hepatic stellate cell contraction. *FEBS J* 2017; **284**: 114-133 [PMID: 27896916 DOI: 10.1111/febs.13956]

17 **Bian M**, Chen X, Zhang C, Jin H, Wang F, Shao J, Chen A, Zhang F, Zheng S. Magnesium isoglycyrrhizinate promotes the activated hepatic stellate cells apoptosis *via* endoplasmic reticulum stress and ameliorates fibrogenesis *in vitro* and in vivo. *Biofactors* 2017; **43**: 836-846 [PMID: 29048780 DOI: 10.1002/biof.1390]

18 **Garbuzenko DV**. Pathophysiological mechanisms of hepatic stellate cells activation in liver fibrosis. *World J Clin Cases* 2022; **10**: 3662-3676 [PMID: 35647163 DOI: 10.12998/wjcc.v10.i12.3662]

19 **Kisseleva T**, Brenner DA. Hepatic stellate cells and the reversal of fibrosis. *J Gastroenterol Hepatol* 2006; **21** Suppl 3: S84-S87 [PMID: 16958681 DOI: 10.1111/j.1440-1746.2006.04584.x]

20 **Li X**, Wang Y, Wang H, Huang C, Huang Y, Li J. Endoplasmic reticulum stress is the crossroads of autophagy, inflammation, and apoptosis signaling pathways and participates in liver fibrosis. *Inflamm Res* 2015; **64**: 1-7 [PMID: 25286903 DOI: 10.1007/s00011-014-0772-y]

21 **Li X**, Sun S, Appathurai S, Sundaram A, Plumb R, Mariappan M. A Molecular Mechanism for Turning Off IRE1α Signaling during Endoplasmic Reticulum Stress. *Cell Rep* 2020; **33**: 108563 [PMID: 33378667 DOI: 10.1016/j.celrep.2020.108563]

22 **Wolf P**, Schoeniger A, Edlich F. Pro-apoptotic complexes of BAX and BAK on the outer mitochondrial membrane. *Biochim Biophys Acta Mol Cell Res* 2022; **1869**: 119317 [PMID: 35752202 DOI: 10.1016/j.bbamcr.2022.119317]

23 **Bian M**, He J, Jin H, Lian N, Shao J, Guo Q, Wang S, Zhang F, Zheng S. Oroxylin A induces apoptosis of activated hepatic stellate cells through endoplasmic reticulum stress. *Apoptosis* 2019; **24**: 905-920 [PMID: 31538267 DOI: 10.1007/s10495-019-01568-2]

24 **Dubois V**, Gheeraert C, Vankrunkelsven W, Dubois-Chevalier J, Dehondt H, Bobowski-Gerard M, Vinod M, Zummo FP, Güiza F, Ploton M, Dorchies E, Pineau L, Boulinguiez A, Vallez E, Woitrain E, Baugé E, Lalloyer F, Duhem C, Rabhi N, van Kesteren RE, Chiang CM, Lancel S, Duez H, Annicotte JS, Paumelle R, Vanhorebeek I, Van den Berghe G, Staels B, Lefebvre P, Eeckhoute J. Endoplasmic reticulum stress actively suppresses hepatic molecular identity in damaged liver. *Mol Syst Biol* 2020; **16**: e9156 [PMID: 32407006 DOI: 10.15252/msb.20199156]

25 **Mori K**. Evolutionary Aspects of the Unfolded Protein Response. *Cold Spring Harb Perspect Biol* 2022; **14** [PMID: 35940910 DOI: 10.1101/cshperspect.a041262]

26 **Kishino A**, Hayashi K, Maeda M, Jike T, Hidai C, Nomura Y, Oshima T. Caspase-8 Regulates Endoplasmic Reticulum Stress-Induced Necroptosis Independent of the Apoptosis Pathway in Auditory Cells. *Int J Mol Sci* 2019; **20** [PMID: 31771290 DOI: 10.3390/ijms20235896]

27 **Liu Y**, Pan X, Li S, Yu Y, Chen J, Yin J, Li G. Endoplasmic reticulum stress restrains hepatocyte growth factor expression in hepatic stellate cells and rat acute liver failure model. *Chem Biol Interact* 2017; **277**: 43-54 [PMID: 28844859 DOI: 10.1016/j.cbi.2017.08.015]

28 **Senft D**, Ronai ZA. UPR, autophagy, and mitochondria crosstalk underlies the ER stress response. *Trends Biochem Sci* 2015; **40**: 141-148 [PMID: 25656104 DOI: 10.1016/j.tibs.2015.01.002]

29 **Lan B**, He Y, Sun H, Zheng X, Gao Y, Li N. The roles of mitochondria-associated membranes in mitochondrial quality control under endoplasmic reticulum stress. *Life Sci* 2019; **231**: 116587 [PMID: 31220526 DOI: 10.1016/j.lfs.2019.116587]

30 **Dhar D**, Baglieri J, Kisseleva T, Brenner DA. Mechanisms of liver fibrosis and its role in liver cancer. *Exp Biol Med (Maywood)* 2020; **245**: 96-108 [PMID: 31924111 DOI: 10.1177/1535370219898141]

31 **Zadorozhnii PV**, Pokotylo IO, Kiselev VV, Okhtina OV, Kharchenko AV. Molecular docking studies of salubrinal and its analogs as inhibitors of the GADD34:PP1 enzyme. *ADMET DMPK* 2019; **7**: 140-150 [PMID: 35350543 DOI: 10.5599/admet.632]

32 **Madden E**, Logue SE, Healy SJ, Manie S, Samali A. The role of the unfolded protein response in cancer progression: From oncogenesis to chemoresistance. *Biol Cell* 2019; **111**: 1-17 [PMID: 30302777 DOI: 10.1111/boc.201800050]

World Journal of Gastroenterology

Submit a Manuscript: https://www.f6publishing.com

World J Gastroenterol 2023 May 7; 29(17): 2628-2641

DOI: 10.3748/wjg.v29.i17.2628

ISSN 1007-9327 (print) ISSN 2219-2840 (online)

ORIGINAL ARTICLE

Basic Study

Lafoensia pacari alleviates intestinal damage by modulating cyclooxygenase-2: *In silico* and *in vivo* evaluation in a colitis model

Gabrielle Caroline Peiter, Thayene Kamyli Moesch Queiroz, Edson Luiz Michalkiewicz Jr, Raphael Henrique Chappuis, Jennefer Sousa Luz, Luiz Henrique Casagrande Piovezani, Cleison Ferreira Silva, Matheus Nozomi Tsutumi, Augusto Fernandes Chaves, Rafael Messias Luiz, Cinthia Façanha Wendel, Ana Carla Zarpelon-Schutz, Kádima Nayara Teixeira

Specialty type: Immunology

Provenance and peer review: Invited article; Externally peer reviewed.

Peer-review model: Single blind

Peer-review report's scientific quality classification

Grade A (Excellent): 0
Grade B (Very good): B
Grade C (Good): C, C
Grade D (Fair): D
Grade E (Poor): 0

P-Reviewer: Howarth GS, Australia; Petrovic S, Serbia; Wang WJ, China; Yao SK, China

Received: November 19, 2022
Peer-review started: November 19, 2022
First decision: February 1, 2023
Revised: March 12, 2023
Accepted: April 10, 2023
Article in press: April 10, 2023
Published online: May 7, 2023

Gabrielle Caroline Peiter, Kádima Nayara Teixeira, Programa Multicêntrico de Pós-graduação em Biquímica e Biologia Molecular - Setor Palotina, Universidade Federal do Paraná, Palotina 85.950-000, Paraná, Brazil

Thayene Kamyli Moesch Queiroz, Ana Carla Zarpelon-Schutz, Programa de Pós-graduação em Biotecnologia - Setor Palotina, Universidade Federal do Paraná, Palotina 85.950-000, Paraná, Brazil

Edson Luiz Michalkiewicz Jr, Raphael Henrique Chappuis, Jennefer Sousa Luz, Luiz Henrique Casagrande Piovezani, Cleison Ferreira Silva, Matheus Nozomi Tsutumi, Augusto Fernandes Chaves, Rafael Messias Luiz, Cinthia Façanha Wendel, Ana Carla Zarpelon-Schutz, Kádima Nayara Teixeira, Campus Toledo, Universidade Federal do Paraná, Toledo 85.919-899, Paraná, Brazil

Corresponding author: Kádima Nayara Teixeira, PhD, Professor, Campus Toledo, Universidade Federal do Paraná, Max Planck 3796, Toledo 85.919-899, Paraná, Brazil.
kadimateixeira@ufpr.br

Abstract

BACKGROUND

Inflammatory bowel diseases (IBD) are a worldwide health problem and mainly affect young people, consequently affecting the workforce. Available treatments are often associated with side effects, and new therapeutic options are needed. For centuries, plants have represented important substrates in the field of drug development. *Lafoensia pacari* (*L. pacari*) is a plant whose pharmaceutical potential has been described, and may have biological activity relevant to the treatment of IBD symptoms.

AIM

To investigate the activity of keto-alcoholic extracts of *L. pacari* with respect to ameliorating the inflammatory and nociceptive symptoms of acute experimental colitis in mice.

METHODS

Keto-alcoholic extracts of *L. pacari* leaves and bark were administered to male and

female Swiss mice weighing 25 g to 30 g (n = 8 male mice and n = 8 female mice). The effect of these extracts was observed in an acetic acid-induced acute experimental model of colitis with regard to antinociception/analgesia and inflammatory tissue damage. Recorded macroscopic indices included the Wallace score and the colon weight obtained using a precision scale. Mechanical hyperalgesia was determined using an electronic analgesimeter. Behavior related to overt pain was determined by quantifying the number of writhing instances within 20 min of administration of acetic acid. Molecular docking was performed using human and murine cyclooxygenase-2 (COX-2) with 3 flavonoids (ellagic acid, kaempferol, and quercetin) on the AutoDock Vina software. Analysis of variance followed by Tukey's posttest was used with $P < 0.05$ indicating significance.

RESULTS

In this murine model of colitis, administration of extracts from *L. pacari* ameliorated acetic acid-induced writhing and colitis-associated inflammatory pain. These improvements may be attributable to the reduction in edema, inflammation (*e.g.*, ulcers, hyperemia, and bowel wall damage), and the intensity of abdominal hyperalgesia. The keto-alcoholic extracts of *L. pacari* leaves and bark administered at a dose of either 100 mg/kg or 300 mg/kg significantly reduced the number of writhing events when compared to the negative control ($P < 0.05$). Additionally, extracts of *L. pacari* bark also performed better than Dipyrone. Leaf extracts administered at 10 mg/kg, 30 mg/kg, and 100 mg/kg and bark extracts administered at 30 mg/kg significantly reduced or prevented the development of edema in the colon of treated mice, while mesalazine did not. Moreover, using molecular docking, we observed that the flavonoids present in *L. pacari* extracts bind to COX-2, an event not unique to ellagic acid.

CONCLUSION

The results of this study demonstrate a potential novel application of *L. pacari* extracts for the reduction of inflammation and promotion of antinociception/analgesia as demonstrated by our findings in a murine model of colitis. These findings were also corroborated by *in silico* analyses, and suggest that *L. pacari* extracts may be a promising therapeutic agent in the treatment of IBD.

Key Words: Antinociceptive activity; Anti-inflammatory activity; Cyclooxygenase-2; Flavonoids; Inflammatory bowel disease; *Lafoensia pacari*

Core Tip: Keto-alcoholic extracts derived from the leaves and bark of *Lafoensia pacari* (*L. pacari*) demonstrate significant analgesic/antinociceptive activity in a murine acetic acid-induced pain model of colitis. These results can likely be extrapolated to humans, as the identities and structures of mouse and human cyclooxygenase-2 (COX-2) are similar. Furthermore, mouse and human COX-2 interacted in a similar fashion with *L. pacari* extract flavonoids when tested *in silico*. Extracts from both the leaves and bark of *L. pacari* were found to improve inflammation and pain symptoms in mice with acetic acid-induced acute colitis.

Citation: Peiter GC, Moesch Queiroz TK, Michalkiewicz Jr EL, Chappuis RH, Luz JS, Casagrande Piovezani LH, Ferreira Silva C, Nozomi Tsutumi M, Fernandes Chaves A, Luiz RM, Façanha Wendel C, Zarpelon-Schutz AC, Teixeira KN. *Lafoensia pacari* alleviates intestinal damage by modulating cyclooxygenase-2: *In silico* and *in vivo* evaluation in a colitis model. *World J Gastroenterol* 2023; 29(17): 2628-2641

URL: https://www.wjgnet.com/1007-9327/full/v29/i17/2628.htm

DOI: https://dx.doi.org/10.3748/wjg.v29.i17.2628

INTRODUCTION

Inflammatory bowel diseases (IBD) represent a wide spectrum of pathologies that manifest with chronic inflammation of the digestive tract and in many cases may not have a defined etiology[1]. The major diseases under the umbrella of IBD are Crohn's disease and ulcerative colitis, which are both characterized by the presence of an inappropriate immune response against gastrointestinal microbiota and other antigens in the digestive tract lumen[2]. Individual genetic susceptibility and other external factors are also important in the pathogenesis of IBD[3].

IBD occurs worldwide and represents a serious health problem, as it affects young people, frequently relapses, and can often be clinically severe. As such, IBD commonly negatively impacts patient quality of life[4,5].

Conventional pharmacological treatment for IBD is associated with many adverse effects[6] and is often associated with long-term resistance[7]. These phenomena are observed with aminosalicylates, corticosteroids, immunosuppressants, immunomodulators, and antibiotics, all of which are commonly used for induction of remission and are also used for disease maintenance as these drugs reduce inflammatory lesions[8]. Therefore, the search for new drugs to treat IBD is critical. Research on medicinal plants could lead to the discovery of bioactives with anti-inflammatory properties that are capable of curbing the symptoms of IBD with the benefit of avoiding adverse reactions associated with current drugs. *Lafoensia pacari* (*L. pacari*) (Lythraceae), a tree from the Brazilian Cerrado popularly known as dedaleiro, mangava-brava, or pacari, is a fever reducer and promoter of healing according to folk knowledge, and is a candidate for an alternative IBD treatment. Pharmacological trials using extracts derived from the leaves and bark of this plant have demonstrated its antifungal, antimicrobial, and anti-free radical properties. *L. pacari* has also been used in the treatment of gastric ulcers and inflammation [9].

Preclinical models of intestinal inflammation are important tools in the study of bioactives, and can assist in the identification of compounds with therapeutic potential, including drugs used in the treatment of IBD such as mesalazine and sulfasalazine[10].

The most common IBD symptom is abdominal pain, and is even reported in individuals in remission. Yet, IBD-associated abdominal pain is undertreated and there is a scarcity of research on this common issue[11]. Therefore, a drug with antinociceptive (reducing pain *via* modulation of nociceptive pathways [12]) and anti-inflammatory activities would be ideal for IBD therapy.

In view of the colloquial sense of the effects of *L. pacari*, it is possible that its components may be able to help improve the symptomatology of IBD through its antinociceptive and anti-inflammatory actions. Here, we tested this hypothesis using an *in vivo* preclinical mouse model and *in silico* analysis of molecular docking to elucidate the bioactive potential of keto-alcoholic extracts of *L. pacari* leaves and bark.

MATERIALS AND METHODS

Keto-alcoholic extracts of L. pacari

Leaves and bark of *L. pacari* were collected in the cerrado of Presidente Olegário, Minas Gerais, Brazil (coordinates 18°24'56" S; 46°25'17" W) in November 2021. The samples were analyzed by a biologist from the Centro Universitário de Patos de Minas (Minas Gerais, Brazil). The material was processed according to a previously published protocol[13] with some modifications. Leaves and bark of *L. pacari* were sanitized, disinfected, washed, dried at 40 ºC for 72 h, and finally ground.

The keto-alcoholic extracts were prepared according to another previously published protocol[14] with modifications. The ground material was mixed in a 1:1 acetone/methanol solution in a 1:10 plant/solution ratio, sonicated (5 cycles of 5 min on/5 min off), incubated at room temperature for 24 h, filtered, and evaporated. The entire extraction process was carried out in the dark. For the *in vivo* experiments, the extracts were solubilized in dimethyl sulfoxide (DMSO) 2% (v/v) in saline [NaCl 0.9% (w/v)].

Determination of total flavonoid content

Keto-alcoholic extracts were submitted for total flavonoid content determination by spectrophotometry using a methanol solution of $AlCl_3$ 5% (w/v). Quercetin was used as the standard with results expressed as quercetin equivalents[15].

Experimental animals

This study was approved by the Ethics Committee for Animal Use of the Setor de Ciências Biológicas at the Universidade Federal do Paraná, Paraná, Brazil (CEUA no. R.O. 07/2022). Male and female Swiss mice weighing 25 g to 30 g were used in the experiments. The animals were kept in the animal house of the Universidade Federal do Paraná - Toledo Campus in polypropylene boxes (41 cm × 33 cm × 16 cm) with pine shavings. Animals had access to rodent food and chlorinated drinking water *ad libitum* and were kept at a controlled temperature (22 ºC ± 2.0 ºC), in a 12 h light/dark cycle.

Writhing test

Female Swiss mice weighing 25 g to 30 g were used (n = 8 per group). The induction of nociceptive response was achieved by intraperitoneal administration of acetic acid [0.8% (v/v)] in saline (10 mL/kg). The noxious stimulus was given 30 min after administration *via* gavage of keto-alcoholic extracts of *L. pacari* leaves and bark (10 mg/kg, 30 mg/kg, 100 mg/kg, or 300 mg/kg), saline (negative control), dipyrone monohydrate 100 mg/kg (positive control), DMSO 2% (v/v), or ellagic acid (a flavonoid found in *L. pacari)* in DMSO 2% (v/v) in saline (1.6 mg/kg)[16]. The mice were individually housed in

glass cylinders and writhing and paw extension events were recorded over a span of 20 min. The intensity of the contortional response was expressed by the cumulative number of contortions over this 20 min period[17,18].

Induction of experimental acute colitis

The following experiment lasted for 14 h. After 24 h of solid fasting, male Swiss mice weighing 25 g to 30 g (*n* = 8 per group) were anesthetized with isoflurane (1.5% in 100% oxygen). At hour 0 and hour 6, the mice were pretreated with keto-alcoholic extracts of *L. pacari* leaves and bark (10 mg/kg, 30 mg/kg, 100 mg/kg, or 300 mg/kg), mesalazine 200 mg/kg (positive control), or saline (negative control). Mice in which colitis was not induced were used as controls. At hour 9, saline enema was performed on all animals. At hour 10, induction of experimental acute colitis was achieved with 7.5% (v/v) acetic acid administered rectally.

The intracolonic injection was performed with a polyethylene cannula measuring 3 cm in length[19]. At hour 12, treatment was administered using the same protocol as for pretreatment. At hour 13, the animals were subjected to mechanical hyperstimulation (Von Frey nociception test). At hour 14, the animals were euthanized by overdose of isoflurane followed by cervical dislocation.

The distal colon of each animal was collected and washed with saline to remove fecal debris. Macroscopic evaluation of each specimen was performed and the severity of lesions was rated using a numerical score (from 0 to 6)[20]. The presence of edema was also evaluated[19,21] by weighing a 2 cm colonic segment using a precision digital scale.

Von Frey test

Visceral mechanical hyperalgesia was assessed using the electronic Von Frey test[22]. Mice were allocated to a box in a temperature-controlled room for at least 45 min prior to testing. Withdrawal reflexes were elicited with a portable force transducer (Digital Algesimeter EFF 310; Insight Ltda, São Paulo, Brazil) fitted to a 0.7 mm^2 polypropylene tip. This apparatus was applied to the lower abdomen up to the mid-abdomen of each animal. After tip removal, the pressure intensity was automatically recorded (recording values from the average of 3 measurements).

Statistical analysis

The means of the values obtained for each group in each experiment were calculated and analyzed using Prism 9.0.1 software. One-way analysis of variance was used to compare groups according to treatment dose followed by Tukey's test. Significance was set at $P < 0.05$.

Bioinformatic analysis by molecular docking

In order to better understand the results of the *in vivo* antinociceptive testing, an *in silico* molecular docking technique was used to evaluate the activity of flavonoids present in *L. pacari*[23] with respect to murine cyclooxygenase-2 (COX-2). The same simulations were performed with human COX-2 for extrapolation of the murine data. Primary sequences of both murine and human COX-2 were analyzed by global alignment using ClustalX 2.1 software[24] for obtaining identity data.

The structure files of the flavonoids (ligands) were obtained from the ZINC database (zinc.docking.org). The 2-dimensional ".sdf" files were converted into 3-dimensional ".pdb" files using the ViewerLite 5.0 software (Accelrys Inc., San Diego, CA, United States). The 3-dimensional structure of murine COX-2 (receptor) was obtained from the Protein Data Bank (PDB) (rcsb.org).

Molecular docking was performed using flexible ligandrigid receptor methodology[25]. For the execution of molecular docking, the AutoDock Tools 4[26] and AutoDock Vina v.1.2.0[27] programs were used. Preparation of molecules was performed, which included the detection of torsion points and calculation of the torsion angles of the ligands, besides the delimitation of the region where the docking was performed (Grid box).

RESULTS

Total flavonoids from L. pacari leaves and bark

The determination of total flavonoid content indicated 97.38 ± 0.0091 (97.38%) and 47.95 ± 0.0035 (47.95%) quercetin/g dry mass equivalents in *L. pacari* leaves or bark, respectively (*i.e.* 97.38 g and 47.95 mg of total flavonoids/g dry mass of leaves or bark, respectively).

Antinociceptive activity of keto-alcoholic extract of L. pacari leaves and bark

The writhing test revealed that DMSO 2% (v/v) did not influence the number of painful contortions when compared to the acetic acid noxious stimulus. A statistically significant decrease in the number of writhing events was observed in mice treated with dipyrone when compared to negative controls (Figure 1).

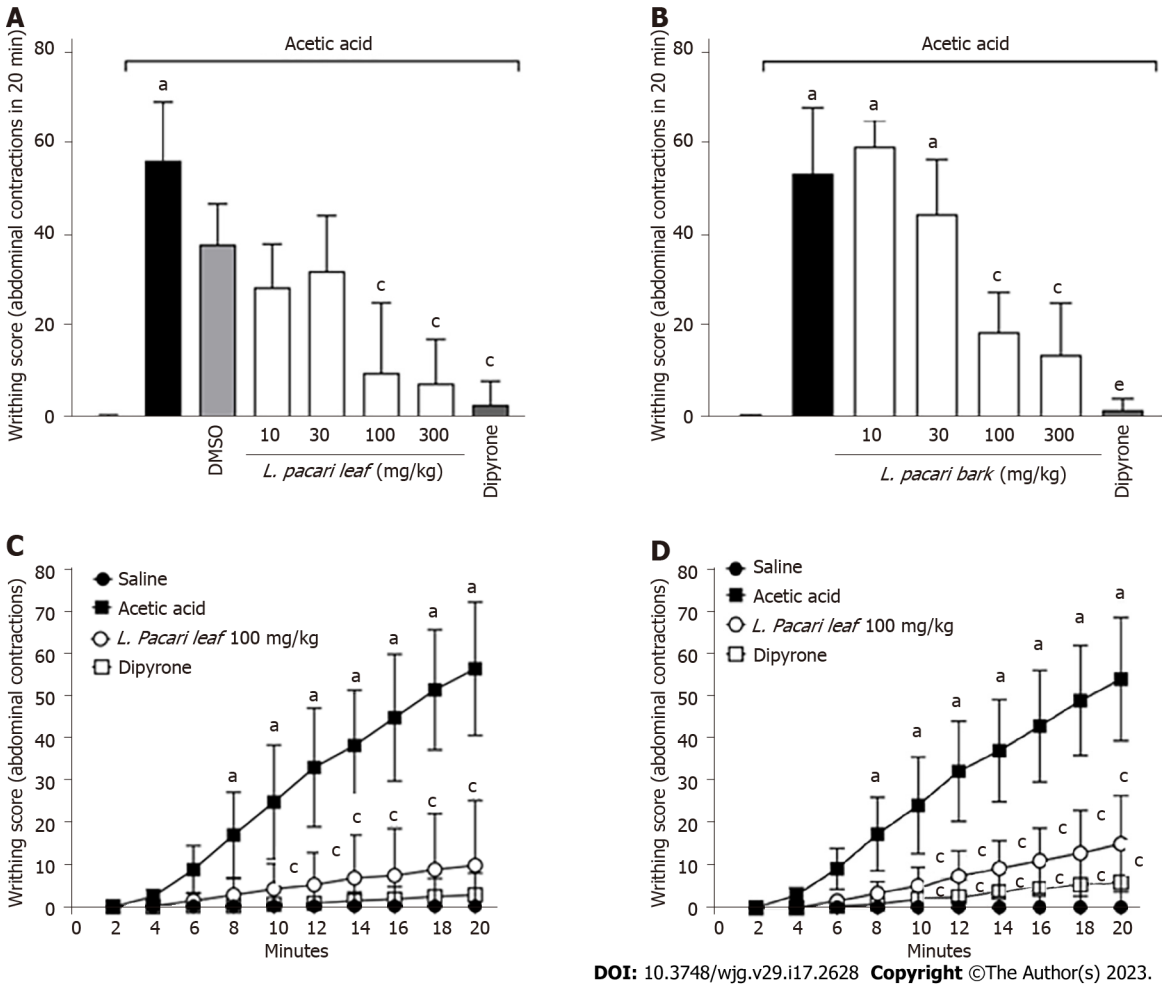

DOI: 10.3748/wjg.v29.i17.2628

Figure 1 Antinociceptive activity of keto-alcoholic extracts of *Lafoensia pacari*. A: Keto-alcoholic extracts of leaves; B: Keto-alcoholic extracts of bark; C: Time-dependent action of the keto-alcoholic extract of *Lafoensia pacari* (*L. pacari*) leaves at 100 mg/kg; D: Time-dependent action of the keto-alcoholic extract of *L. pacari* bark at 100 mg/kg. Results presented ± representative error of 8 animals per group. $^{a}P < 0.05$ *vs* saline group; $^{c}P < 0.05$ *vs* DMSO 2% (v/v), acetic acid; $^{e}P < 0.05$ *vs* all groups except the saline group. One-way analysis of variance followed by Tukey's *t*-test. Error bar: Standard error of the mean; *L. pacari*: *Lafoensia pacari*.

With respect to the keto-alcoholic extracts of *L. pacari* leaves, doses of 100 mg/kg and 300 mg/kg reduced the number of acetic acid-induced writhing events significantly as compared to negative controls, but positive controls (dipyrone-treated; Figure 1A). The keto-alcoholic extracts of *L. pacari* bark at 100 mg/kg and 300 mg/kg significantly reduced the number of acetic-acid induced writhing events as compared to negative controls and also when compared to dipyrone (Figure 1B).

No statistically significant difference was observed between the antinociceptive potential of the low and high *L. pacari* leaves or bark extract doses (100 mg/kg and 300 mg/kg, respectively). The lower dose (100 mg/kg) was found to act in a time-dependent manner, exhibiting effects 10 min after administration (Figure 1C and D). Ellagic acid alone, administered at 1.6 mg/kg, did not significantly reduce the number of contortions (Figure 2).

Activity of keto-alcoholic extracts of L. pacari leaves and bark in acute colitis

Colitis-induced edema was observed and quantified by weighing the removed colonic segment. Colon segment weight of colitis mice was higher than that of healthy mice with no colitis induction. Keto-alcoholic extracts of *L. pacari* leaves administered at doses of 10 mg/kg, 30 mg/kg, and 100 mg/kg significantly reduced or prevented the development of colonic edema in treated mice (Figure 3A); similar results were observed in mice treated with the keto-alcoholic extracts of *L. pacari* bark administered at 30 mg/kg (Figure 3B), as evidenced by the weight of colonic segments of these animals being similar to that of healthy mice. Treatment with mesalazine did not improve edema.

Numerical lesional severity scores as assigned by gross assessment of colonic segments ranged from 0 to 2 (0 = no lesion; 1 = hyperemia without ulceration; 2 = ulceration without intestinal wall hypertrophy). No control mice were found to have lesions (score 0), and untreated mice with induced colitis demonstrated scores of 1 or 2 (Figure 4). Gross assessment of colonic segments of mice treated with keto-alcoholic extracts of *L. pacari* bark at 30 mg/kg, 100 mg/kg, and 300 mg/kg had fewer lesions

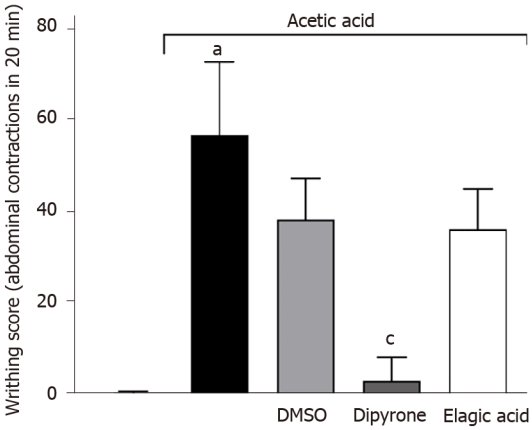

DOI: 10.3748/wjg.v29.i17.2628

Figure 2 Writhing score for ellagic acid. Results presented ± representative error of 8 animals per group. [a]*P* < 0.05 *vs* saline group, [c]*P* < 0.05 *vs* ellagic acid, DMSO 2% (v/v), acetic acid. One-way analysis of variance followed by Tukey's *t*-test. Error bar: Standard error of the mean.

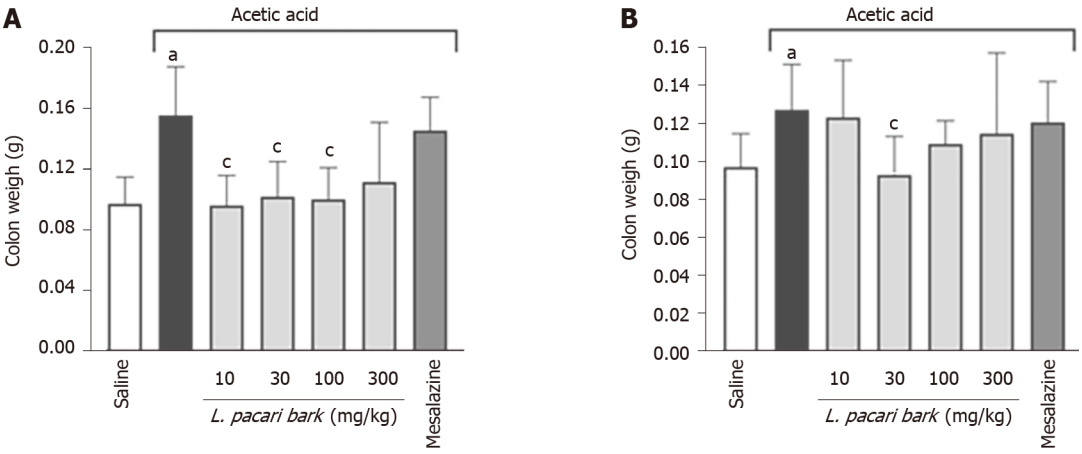

DOI: 10.3748/wjg.v29.i17.2628

Figure 3 Anti-inflammatory activity of the keto-alcoholic extract of *Lafoensia pacari* on colonic edema. A: Keto-alcoholic extract of *Lafoensia pacari* (*L. pacari*) leaves; B: Keto-alcoholic extract of *L. pacari* bark. Results presented ± representative error of 8 animals per group. [a]*P* < 0.05 *vs* saline group; [c]*P* < 0.05 *vs* acetic acid and mesalazine. One-way analysis of variance followed by Tukey's *t*-test. Error bar: Standard error of the mean; *L. pacari*: *Lafoensia pacari*.

than untreated mice (Figure 4B); similar results were observed in mice treated with keto-alcoholic extracts of *L. pacari* leaves at 10 mg/kg (scores = 0 or 1; Figure 4A). In general, the keto-alcoholic extracts of *L. pacari* showed anti-inflammatory activity in the colon of animals with acute colitis. Mice treated with mesalazine showed intestinal lesions with scores of 1 or 2, suggesting poorer performance of this drug when compared to keto-alcoholic extracts of *L. pacari* leaves or bark.

Activity of keto-alcoholic extracts of L. pacari leaves and bark in hyperalgesia

Results of the Von Frey test were expressed as the difference between the intensity required to elicit a positive response before and after the induction of acute colitis by acetic acid. Mice treated with the keto-alcoholic extract of *L. pacari* leaves at 30 mg/kg, 100 mg/kg, or 300 mg/kg or mesalazine showed greater analgesic effect when compared to untreated mice. The keto-alcoholic extract of the leaves administered at 100 mg/kg or 300 mg/kg performed better than the extract administered at 30 mg/kg or mesalazine (Figure 5A).

With respect to the keto-alcoholic extract of *L. pacari* bark, mice treated with 100 mg/kg or 300 mg/kg or mesalazine required a higher intensity of stimulus to elicit a positive response when compared to negative controls. No significant difference was observed among these 3 treatments, although both 100 mg/kg and 300 mg/kg doses of the extract trended toward higher analgesic activity when compared to mesalazine (Figure 5B).

In silico analysis

The 3-dimensional structures of murine COX-2 (PDB: 3LN0) and human COX-2 (PDB: 5 LKQ) were selected from PDB; these were originally complexed to compound 5c-S and meclofenamic acid,

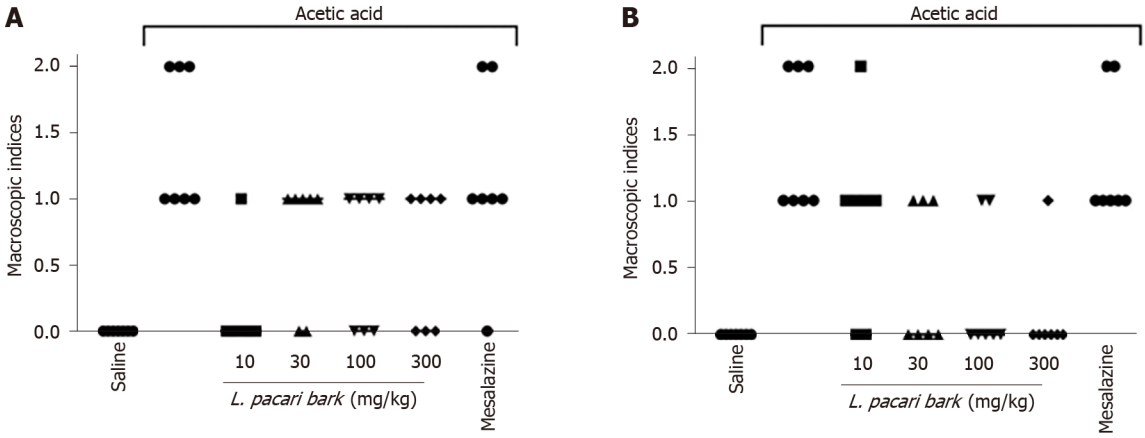

DOI: 10.3748/wjg.v29.i17.2628

Figure 4 Macroscopic indices of colonic segments from mice with induced colitis post-treatment. Scores: 0 = no lesion; 1 = hyperemia without ulceration; 2 = ulceration without hypertrophy of the intestinal wall, according to Wallace *et al*[20]. Error bar: Standard error of the mean; *L. pacari*: *Lafoensia pacari*.

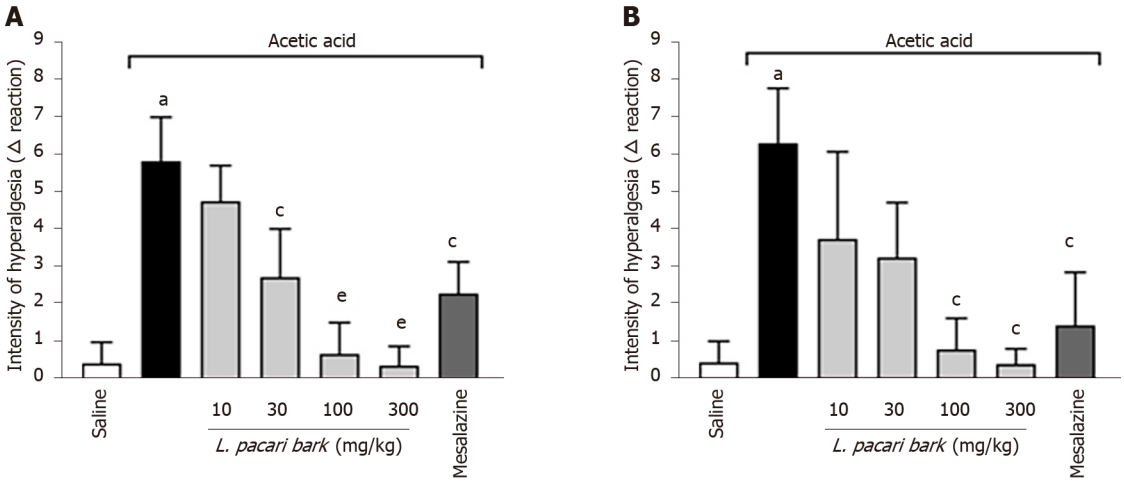

DOI: 10.3748/wjg.v29.i17.2628

Figure 5 Antinociceptive activity of the keto-alcoholic extract of *Lafoensia pacari* in the acute colitis model. A: Keto-alcoholic extract of *Lafoensia pacari* (*L. pacari*) leaves; B: Keto-alcoholic extract of *L. pacari* bark. Results presented ± representative error of 8 animals per group. $^{a}P < 0.05$ *vs* saline group; $^{c}P < 0.05$ *vs* acetic acid; $^{e}P < 0.05$ *vs* mesalazine. One-way analysis of variance followed by Tukey's *t*-test. Error bar: Standard error of the mean; *L. pacari*: *Lafoensia pacari*.

respectively. These compounds were removed for analysis in this study. Human and murine COX-2 are homologous and have similar structures. The number of total residues in the primary sequence of both is 604, and the number of residues resolved by X-ray diffraction of human COX-2 and murine COX-2 is 551 and 587, respectively. After global alignment analysis, it was observed that these enzymes have 86.6% primary sequence identity.

Molecular docking simulations with COX-2 were performed with 3 flavonoids: ellagic acid (ZINC000003872446), kaempferol (ZINC000003869768) and quercetin (ZINC000003869685). It was observed that all flavonoids bind to chain A, the catalytic monomer of COX-2, with significant affinity (Table 1) and possibly, under physiological conditions, the interaction is stable and negatively affects enzyme activity.

Ellagic acid was bound to 2 amino acid residues of murine COX-2 (3 bonds; 2.0-2.8 Å) and to 4 residues of human COX-2 (5 bonds; 2.1-3.3 Å; Figure 6A and B). Kaempferol bound to 3 residues of murine COX-2 (3 bonds; 2.5-4.3 Å) and 2 residues of human COX-2 (3 bonds; 3.1-5.0 Å; Figure 6C and D), and quercetin bound to 6 residues of murine COX-2 (8 bonds; 2.3-4.3 Å) and 4 residues of human COX-2 (4 bonds; 2.0-3.3 Å; Figure 6E and F). None of the flavonoids were bound to the prosthetic group (heme group) of COX-2. The values of the affinity energies are similar to each other, the most significant interactions were between ellagic acid and murine COX-2 and between quercetin and human COX-2.

Table 1 Energy of affinity of cyclooxygenase-2/flavonoid complexes

Flavonoid	Energy of affinity in kcal/mol	
	Human COX-2	Murine COX-2
Ellagic acid	-9.7	-9.9
Kaempferol	-9.9	-8.8
Quercetin	-10.1	-9.5

COX-2: Cyclooxygenase-2.

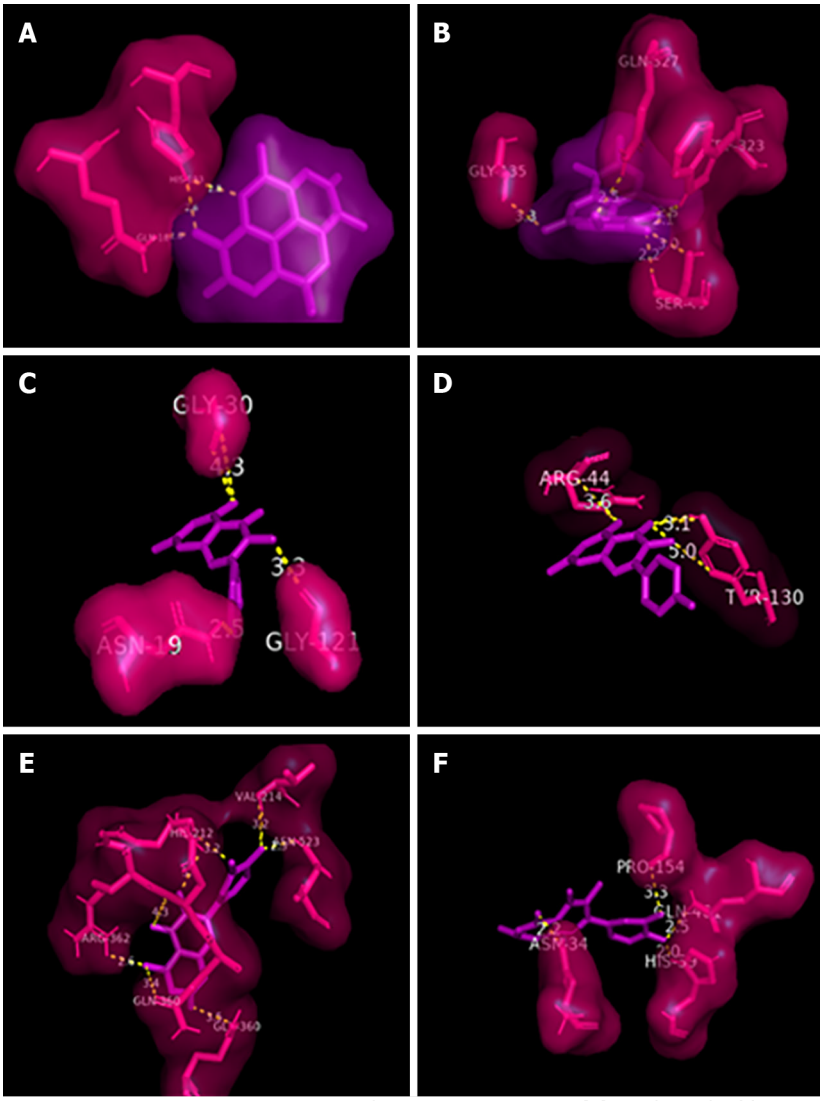

DOI: 10.3748/wjg.v29.i17.2628

Figure 6 Complexes formed by cyclooxygenase-2 and flavonoids from *Lafoensia pacari*. A, C and E: Murine cyclooxygenase-2 (COX-2) bound to ellagic acid, kaempferol, and quercetin, respectively; B, D and F: Human COX-2 bound to ellagic acid, kaempferol, and quercetin, respectively. Lilac: Flavonoid; Pink: Amino acid residues; The dashed lines represent chemical interactions. The name of the amino acid is represented by the three-letter code followed by their number in the primary sequence. The numbers next to the dashed lines are the bond lengths in Angstrom.

DISCUSSION

Using extraction in acetone/methanol solution, 97.38 ± 0.0091 mg total flavonoids/g dry mass of the leaves and 47.95 ± 0.0035 mg total flavonoids/g dry mass of the bark of *L. pacari* were obtained; in crude hydroalcoholic and methanolic extracts of leaves, 15.7 ± 0.02 and 14.4 ± 0.04 equivalents of quercetin were obtained, respectively[28]. In another study[29] 13.61% ± 0.72 equivalents of quercetin was obtained from an aqueous extraction of the bark of *L. pacari*. Comparatively, the keto-alcoholic

extraction was more efficient in obtaining total flavonoids from both leaves and bark of *L. pacari*.

The antinociceptive effect of the keto-alcoholic extracts of *L. pacari* leaves and bark was demonstrated by the writhing test, an assay of nociception using injection of a noxious agent[30]. When tissues and cells are exposed to a noxious stimulus, chemical mediators are released, which in turn stimulate C-type nerve fibers causing local pain. Acetic acid has properties that can cause pain, in addition to stimulating the release of cytokines (IL-1β, TNF- and IL-8) by macrophages and basophils present in the abdominal cavity[31]. The writhing test is considered a model for studying visceral pain[32]; keto-alcoholic extracts of *L. pacari* leaves and bark decreased the number of writhing events in this test, suggesting the efficacy of these extracts in treating this type of pain.

The extracts of *L. pacari* leaves and bark administered at 100 mg/kg and 300 mg/kg, reduced the number of painful contortions in the murine colitis model; however, there was no significant difference between these dosages in terms of analgesic effect. However, the extract administered at 300 mg/kg (the highest concentration used in this study) did not exert such a potent antinociceptive effect when compared to the positive control group (dipyrone-treated).

The aqueous extract of *L. pacari* bark administered at 0.5 g/kg and 1.0 g/kg had previously shown an antinociceptive effect in the writhing test[33]. In a study using the ethanolic extract of *L. pacari* leaves administered at 1.0 g/kg, the extract reduced the number of writhing events, especially when it was administered subcutaneously; however, this dose caused toxicity and death in treated animals[31]. Therefore, although the dose of 300 mg/kg is still below the accepted toxic value[31], in order to avoid undesirable adverse effects, the 100 mg/kg dose of keto-alcoholic *L. pacari* extract may be more appropriate.

The choice of oral administration of the extracts was based on the better viability and ease of administration considering future drug development from the plant's bioactive compounds. As we observed analgesic activity when extracts were administered orally, it seems that this route of administration is sufficient for absorption of the active compound at a therapeutic level.

In comparison, one study evaluated the analgesic and anti-inflammatory activity of total flavonoids from the leaves of *Juniperus sabina*, a plant commonly known as sabina native to Europe and Asia. This study indicated significant dose-dependent analgesic activity in the acetic acid-induced writhing test, with the highest dose (500 mg total flavonoids/kg animal mass) showing the greatest inhibition of writhing (22.02%)[34]. In the present study, the most effective inhibitory dose was 100 mg/kg of dry mass of *L. pacari* leaves and bark, which is equivalent to 9.738 mg/kg and 4.795 mg/kg total flavonoids, respectively.

Other studies have investigated the ethanolic extract of white willow as an anti-inflammatory and antinociceptive, with results similar to ours in which the plant extract was effective in an animal model, but the positive control treatment was more effective, even at lower concentrations[35]. Another study aimed to elucidate the effects of an ethanolic extract of *L. pacari* on acute peritonitis in mice[9], and demonstrated significant anti-inflammatory activity of this extract. This finding may be akin to the antinociceptive effect of the keto-alcoholic *L. pacari* extracts demonstrated in the present study.

Although this study does not present the rate of inhibition of writhing, the difference in concentration of total flavonoids used per body mass in each study suggests that flavonoids from *L. pacari* are more effective, as analgesia was observed at lower doses. One possible explanation for this observation may be the types of flavonoids present in each plant species analyzed, and those of *L. pacari* may act more synergistically to produce an analgesic effect.

Fractionation of the *L. pacari* bark extract leads to the isolation of ellagic acid as the main flavonoid compound, suggesting that this compound is responsible for the anti-inflammatory and anti-edema activity of the extract observed in mouse models of asthma. Ellagic acid was also identified in *L. pacari* leaves by high performance liquid chromatography[31]. Recently, evidence regarding the efficacy of ellagic acid in the treatment of acute visceral pain has been growing; its analgesic effects are attributed to the inhibition of COX, which synthesizes prostaglandins at sites of peripheral cell damage[36].

Ellagic acid is reported to have several benefits, such as anti-inflammatory, anticancer, and hepatoprotective actions, and is also a promising agent for the treatment of chronic diseases such as ulcerative colitis, Crohn's disease, Alzheimer's disease, and diabetes[37]. However, according to the results obtained in this study, ellagic acid was not the only phenolic compound present in the extract of the *L. pacari* that may be responsible for the observed analgesic effect. In a statistical comparison, its effect resembles that of the 30 mg/kg dosage of leaf extract in the twitch test. The relatively low efficiency of ellagic acid compared to other doses of extract indicates that this flavonoid likely acts synergistically with other compounds present in the plant to confer a more robust analgesic pharmacological effect.

Regarding acute experimental colitis, the keto-alcoholic extracts of *L. pacari* leaves administered at 10 mg/kg, 30 mg/kg, or 100 mg/kg significantly reduced or prevented the development of colonic in treated mice. The same was observed in mice treated with the keto-alcoholic extract of *L. pacari* bark administered at 30 mg/kg as evidenced by similar colonic segment weights between treated and health mice.

Gross evaluation of colonic segments of mice revealed lower lesional severity scores in mice receiving keto-alcoholic extracts of *L. pacari* leaves and bark, with further reduction in the groups that received a higher dose. The mice that received mesalazine had similar lesional severity scores compared to the saline-treated group; this may be due to the fact that mesalazine typically used in the treatment of

chronic inflammatory bowel disease[38,39], and we used an acute colitis model.

The macroscopic findings suggest that the keto-alcoholic extracts of *L. pacari* leaves and bark have an anti-inflammatory effect on the mucosa of the gastrointestinal tract and reduce tissue destruction in this model of acute colitis. In agreement with these findings, one study showed that a methanolic extract of the bark of *L. pacari* had a potent gastroprotective effect against ethanol-, indomethacin-, and stress-induced ulcers[40].

Another study showed that an ethanolic extract of *L. pacari* possesses healing properties when applied to skin wounds, accelerating healing when compared to controls. This is attributed to the inhibition of the proliferation and inflammation phases of the healing process, corroborating the findings in our acute colitis induction experiments, which showed reduced colonic tissue damage in mice treated with *L. pacari* extracts. These data suggest a negative modulation of tissue inflammatory processes[23].

The anti-inflammatory effects of extracts derived from *L. pacari* leaves have also been demonstrated in a murine model of asthma. One study showed a significant reduction in lung inflammation and tissue damage in animals that received the extract as evidenced by gross tissue damage score analysis[41]. These data corroborate the results of the present study, which also demonstrated the anti-inflammatory effects of keto-alcoholic extracts of *L. pacari* leaves and bark in reducing macroscopic damage to colonic tissue.

Both the Von Frey monofilament and the electronic Von Frey tests are used as quantitative sensory assays to explore mechanical hyperalgesia[42]. In this study, pain stimuli were administered to mice using the electronic Von Frey test, and the keto-alcoholic extracts of *L. pacari* leaves administered at 30 mg/kg, 100 mg/kg, or 300 mg/kg or mezalazine showed greater analgesic effect when compared to untreated mice. Among the treatments, the keto-alcoholic extract administered at 100 mg/kg or 300 mg/kg performed better than the extract at 30 mg/kg or mesalazine.

Regarding the keto-alcoholic extract of *L. pacari* bark, mice treated with the doses 100 mg/kg or 300 mg/kg or mesalazine required a higher intensity stimulus to induce a positive response when compared to the negative controls. No significant difference was observed among these 3 treatments, although the keto-alcoholic extract at 100 mg/kg or 300 mg/kg had greater analgesic effect as compared to mesalazine. It is important to emphasize that, since this is a study based on a model of acute colitis, the findings regarding mesalazine are consistent with what is expected, since this drug has a better effect with long-term use[43]. The Von Frey test was one of the first evoked stimulus tests to be developed and continues to be widely used today[44]. This test is an excellent tool for evaluating hyperalgesia, visceral pain, and inflammation[45].

Molecular docking is an important method to complement and help better understand results obtained by *in vivo* testing. In humans, despite being structurally a homodimer, COX-2 functions as a conformational heterodimer, with 1 monomer being catalytic and the other allosteric[46]. In our experiments, the catalytic monomer, composed of the A chain, was the interaction target of ellagic acid, kaempferol, and quercetin in both human and murine COX-2.

We observed that the evaluated flavonoids bind to COX-2, but also that the interactions are strong. Binding affinity is measured by the affinity energy, which when lower than -6.0 kcal/mol indicates interaction in a biological environment[47]. Although the values are expressive, they are all within a narrow range (-8.8 1 kcal/mol to 10.1 kcal/mol). Our data suggest that COX-2 inhibition after interaction with any of the flavonoids tested should not trigger events other than the expected inhibition of prostaglandin production and consequent decrease in pain sensation.

Our findings also demonstrate that ellagic acid is not the only compound of interest with respect to analgesia found in the keto-alcoholic extracts of *L. pacari* leaves and bark. The affinity energy evaluated by molecular docking represents the strength of interaction between 2 or more interacting molecules. The strength of interaction is favorable when it is negative, and the receptor/ligand interaction is greater when the energy is lower.

Corroborating our study, another demonstrated that quercetin is also effective in inhibiting hyperalgesia[48]. This flavonoid showed an analgesic effect in animal models of inflammatory pain, inhibiting hyperalgesia induced by mechanical or thermal stimuli, and reduced the pain behaviors of studied animals. In addition, it also inhibited the development of inflammation-related edema, cytokine production, myeloperoxidase activity, and cell migration[49].

Nonsteroidal anti-inflammatory agents (NSAIDs) are part of a heterogeneous group of compounds from different chemical classes, and have 3 main actions: Anti-inflammation, analgesia, and fever reduction. NSAIDs are the most commonly used therapeutic agents[50]. Although they are effective, their long-term use is limited in most patients, as they are associated with adverse gastrointestinal effects such as abdominal pain, ulcers, bleeding, and even gastric or duodenal perforation. These effects have been attributed to the low specificity of these compounds for COX-2[51]. Acetylsalicylic acid (ASA) promotes the irreversible inhibition of human COX activity by covalent binding to a serine residue within the active site.

In COX-1, ASA acetylates serine 530, preventing the binding of arachidonic acid to the enzyme's active site, thus suppressing the production of prostaglandins. In COX-2, ASA acetylates serine 516, blocking the activity of this isoform[50,51]. In our study, *in silico* analysis showed that these amino acid residues, which are key to the action of some analgesics, showed no direct interaction with the evaluated flavonoids, demonstrating that in this model there are other residues involved in COX-2

inhibition.

CONCLUSION

We demonstrated the anti-inflammatory effects of keto-alcoholic extracts of *L. pacari* leaves and bark in a murine acetic acid-induced colitis model. Both extracts inhibited colitis-induced tissue damage as assessed using the Wallace score and the development of colonic edema; this effect seems to be COX-2-dependent. The flavonoid content of *L. pacari* extracts has been used to treat many diseases, and shows anti-inflammatory, analgesic, and antioxidant properties. However, the effects of this plant on symptoms related to colitis have not been described. Using molecular docking, we showed a strong interaction between ellagic acid, kaempferol or quercetin with both human and murine COX-2; however, the inflammatory and antinociceptive effects of *L. pacari* are not solely attributable to ellagic acid. Taken together, these results suggest the potential of oral *L. pacari* extract administration in the treatment of inflammatory diseases such as colitis.

ARTICLE HIGHLIGHTS

Research background

Therapeutic activities of *Lafoensia pacari* (*L. pacari*) have been reported in folk medicine, and this plant has been used as an antifungal, an anti-ulcer, an antibacterial, an anti-inflammatory, a fever reducer, in the treatment of pneumonia, and in the treatment of stomach pain. Despite the common use of this plant, the mechanisms by which it achieves medicinal effects have not been elucidated.

Research motivation

L. pacari is a tree found in Brazil thought to have beneficial pharmacological properties, with its main bioactive compounds belonging to the flavonoid class. One of the most studied flavonoids found in this plant is ellagic acid, which has been reported to have anti-inflammatory activity. However, *L. pacari* contains numerous flavonoids, and these compounds may also have similar activity to or act synergistically with ellagic acid.

Research objectives

We aimed to evaluate the activity of keto-alcoholic extracts of *L. pacari* leaves and bark, which contain a significant amount of flavonoids, with respect to the improvement of symptoms related to inflammatory bowel diseases (*e.g.*, inflammation of the intestinal mucosa, edema, and abdominal pain).

Research methods

The methodology used in this study was based on protocols already well established in the scientific literature, and, when necessary, some modifications were made. All experiments were performed with a number of mice that allowed for statistical analysis of the data and were performed in duplicate or triplicate depending on statistical requirements.

Research results

Our results corroborated those described by other studies with respect to the beneficial effects of *L. pacari* extracts; however, to our knowledge, we are the first to evaluate the therapeutic potential of these extracts in a murine model of acute colitis. Antinociception/analgesia in this murine model were observed with respect to treatment with extracts derived from *L. pacari* leaves and bark.

Research conclusions

Our findings suggest that keto-alcoholic extracts of *L. pacari* leaves and bark are beneficial for the reduction of symptoms related to inflammatory bowel disease. These effects are attributed to the decrease or inhibition of inflammation in the intestinal mucosa. Regarding pain, bioinformatics techniques indicated that ellagic acid alone is not responsible for these effects, since other flavonoids interact and inhibit with significant affinity cyclooxygenase-2, an enzyme that produces pain mediators.

Research perspectives

This study is part of a larger research project; follow-up experiments are planned using a rat model of chronic colitis, other antinociception tests. Future experiments will also investigate the histology of intestinal segments after induction and treatment of chronic colitis with *L. pacari* extracts.

FOOTNOTES

Author contributions: Peiter GC, Moesch Queiroz TK, Michalkiewicz Jr EL, Chappuis RH, Luz JS, Casagrande Piovezani LH, Ferreira Silva C, Nozomi Tsutumi M, Fernandes Chaves A, Luiz RM and Façanha Wendel C performed the experiments; Zarpelon-Schutz AC, Peiter GC and Teixeira KN analyzed the results and wrote the manuscript; Zarpelon-Schutz AC and Teixeira KN interpreted the data, performed the critical analysis of the results, corrected the manuscript and coordinated the study; All authors approved the final version of the manuscript.

Institutional review board statement: The Institutional Review Board declares knowledge about the study.

Institutional animal care and use committee statement: The Institutional Animal Care and Use Committee declares knowledge and approval about the study.

Conflict-of-interest statement: All the authors report no relevant conflicts of interest for this article.

Data sharing statement: The authors declare that all data are public and can be shared upon reasonable request.

ARRIVE guidelines statement: The authors have read the ARRIVE guidelines, and the manuscript was prepared and revised according to the ARRIVE guidelines.

Country/Territory of origin: Brazil

ORCID number: Gabrielle Caroline Peiter 0000-0001-7965-4434; Thayene Kamyli Moesch Queiroz 0000-0002-2120-4833; Edson Luiz Michalkiewicz Jr 0000-0003-3986-9144; Raphael Henrique Chappuis 0000-0002-1332-4974; Jennefer Sousa Luz 0000-0002-5625-0098; Luiz Henrique Casagrande Piovezani 0000-0003-3526-3292; Cleison Ferreira Silva 0000-0002-2666-3385; Matheus Nozomi Tsutumi 0000-0003-3652-6170; Augusto Fernandes Chaves 0000-0002-1454-0804; Rafael Messias Luiz 0000-0002-5107-7281; Cinthia Façanha Wendel 0000-0003-2183-9748; Ana Carla Zarpelon Schutz 0000-0002-8320-3633; Kádima Nayara Teixeira 0000-0002-2928-9181.

S-Editor: Gong ZM
L-Editor: Filipodia
P-Editor: Yu HG

REFERENCES

1 **Sairenji T**, Collins KL, Evans DV. An Update on Inflammatory Bowel Disease. *Prim Care* 2017; **44**: 673-692 [PMID: 29132528 DOI: 10.1016/j.pop.2017.07.010]
2 **Baumgart DC**, Sandborn WJ. Inflammatory bowel disease: clinical aspects and established and evolving therapies. *Lancet* 2007; **369**: 1641-1657 [PMID: 17499606 DOI: 10.1016/S0140-6736(07)60751-X]
3 **Podolsky DK**. Inflammatory bowel disease. *N Engl J Med* 2002; **347**: 417-429 [PMID: 12167685 DOI: 10.1056/NEJMra020831]
4 **Fakhoury M**, Negrulj R, Mooranian A, Al-Salami H. Inflammatory bowel disease: clinical aspects and treatments. *J Inflamm Res* 2014; **7**: 113-120 [PMID: 25075198 DOI: 10.2147/JIR.S65979]
5 **Figueroa C C**, Quera P R, Valenzuela E J, Jensen B C. [Inflammatory bowel disease: experience of two Chilean centers]. *Rev Med Chil* 2005; **133**: 1295-1304 [PMID: 16446852 DOI: 10.4067/S0034-98872005001100004]
6 **Carter MJ**, Lobo AJ, Travis SP; IBD Section, British Society of Gastroenterology. Guidelines for the management of inflammatory bowel disease in adults. *Gut* 2004; **53** Suppl 5: V1-16 [PMID: 15306569 DOI: 10.1136/gut.2004.043372]
7 **Cai Z**, Wang S, Li J. Treatment of Inflammatory Bowel Disease: A Comprehensive Review. *Front Med (Lausanne)* 2021; **8**: 765474 [PMID: 34988090 DOI: 10.3389/fmed.2021.765474]
8 **Stenson WF**, Korzenik J. Inflammatory bowel disease. In: Yamada T, Alpers DH, Laine L, editors. Yamada's textbook of gastroenterology. 4th ed. Philadelphia: Lippincott Williams & Wilkins Publishers, 2003: 1699–759.
9 **Albuquerque DA**, Juliani JM, Santos JA, Hosida PY, Borges S, Borralho CT. Effect of Lafoensia pacari ethanolic extract on acute peritonitis in mice. In: Program and Proceedings of the 3rd SBPC Special Meeting Coastal Ecosystems - From Knowledge to Management; Santa Catarina, Brazil, 1996: 214
10 **Melo NM da C**, Almeida MVS, Campos DM de O, Oliveira CBS de, Oliveira JIN. Animal models for inducing inflammatory bowel diseases: integrative review. *Revista Ciências em Saúde* 2021; **11**: 80-87 [DOI: 10.21876/rcshci.v11i1.1056]
11 **Norton C**, Czuber-Dochan W, Artom M, Sweeney L, Hart A. Systematic review: interventions for abdominal pain management in inflammatory bowel disease. *Aliment Pharmacol Ther* 2017; **46**: 115-125 [PMID: 28470846 DOI: 10.1111/apt.14108]
12 **Basbaum CB**, Mann JK, Chow AW, Finkbeiner WE. Monoclonal antibodies as probes for unique antigens in secretory

cells of mixed exocrine organs. *Proc Natl Acad Sci U S A* 1984; **81**: 4419-4423 [PMID: 6205396 DOI: 10.1073/pnas.81.14.4419]

13 **Albuquerque ER**, Gossler SC, Piovezan M, Conto LC. Extraction and determination of flavonoids, condensed and total tannins from pine nut bark (Araucaria angustifolia). Educational material. Instituto Federal de Santa Catarina/Brazil. 2017. Available at: http://docente.ifsc.edu.br/michael.nunes/MaterialDidatico/Analises%20Quimicas/TCC%20II/TCC%202017%201/Eduarda%20e%20Sheili.pdf

14 **Oliveira MA**. Extraction of polyphenols from cocoa seed (Theobroma cacao). M.Sc. Thesis, Universidade Federal de Santa Catarina/Brazil. 2005. Available at: https://www.yumpu.com/pt/document/read/10594294/extracao-de-polifenois-da-semente-de-cacau

15 **Dutra RP**, Nogueira AMC, Marques RRO, Costa MCP, Ribeiro MNS. Avaliação farmacognóstica de geoprópolis de *Melipona fasciculata* Smith (tiúba) em municípios da Baixada maranhense, Brasil. *Rev Bras Farmacogn* 2008; **18**: 557-562 [DOI: 10.1590/S0102-695X2008000400010]

16 **Rogerio AP**, Fontanari C, Melo MC, Ambrosio SR, de Souza GE, Pereira PS, França SC, da Costa FB, Albuquerque DA, Faccioli LH. Anti-inflammatory, analgesic and anti-oedematous effects of *Lafoensia pacari* extract and ellagic acid. *J Pharm Pharmacol* 2006; **58**: 1265-1273 [PMID: 16945186 DOI: 10.1211/jpp.58.9.0014]

17 **Valério DA**, Cunha TM, Arakawa NS, Lemos HP, Da Costa FB, Parada CA, Ferreira SH, Cunha FQ, Verri WA Jr. Anti-inflammatory and analgesic effects of the sesquiterpene lactone budlein A in mice: inhibition of cytokine production-dependent mechanism. *Eur J Pharmacol* 2007; **562**: 155-163 [PMID: 17320857 DOI: 10.1016/j.ejphar.2007.01.029]

18 **Verri WA Jr**, Cunha TM, Magro DA, Domingues AC, Vieira SM, Souza GR, Liew FY, Ferreira SH, Cunha FQ. Role of IL-18 in overt pain-like behaviour in mice. *Eur J Pharmacol* 2008; **588**: 207-212 [PMID: 18511039 DOI: 10.1016/j.ejphar.2008.04.010]

19 **Guazelli CF**, Fattori V, Colombo BB, Georgetti SR, Vicentini FT, Casagrande R, Baracat MM, Verri WA Jr. Quercetin-loaded microcapsules ameliorate experimental colitis in mice by anti-inflammatory and antioxidant mechanisms. *J Nat Prod* 2013; **76**: 200-208 [PMID: 23347547 DOI: 10.1021/np300670w]

20 **Wallace JL**, MacNaughton WK, Morris GP, Beck PL. Inhibition of leukotriene synthesis markedly accelerates healing in a rat model of inflammatory bowel disease. *Gastroenterology* 1989; **96**: 29-36 [PMID: 2535830 DOI: 10.1016/0016-5085(89)90760-9]

21 **Colombo BB**. A vimpocetina reduz a colite induzida por ácido acético em camundongos. Universidade Estadual de Londrina, 2017

22 **Cunha TM**, Verri WA Jr, Vivancos GG, Moreira IF, Reis S, Parada CA, Cunha FQ, Ferreira SH. An electronic pressure-meter nociception paw test for mice. *Braz J Med Biol Res* 2004; **37**: 401-407 [PMID: 15060710 DOI: 10.1590/s0100-879x2004000300018]

23 **Pereira LOM**, Vilegas W, Tangerina MMP, Arunachalam K, Balogun SO, Orlandi-Mattos PE, Colodel EM, Martins DTO. *Lafoensia pacari* A. St.-Hil.: Wound healing activity and mechanism of action of standardized hydroethanolic leaves extract. *J Ethnopharmacol* 2018; **219**: 337-350 [PMID: 29501673 DOI: 10.1016/j.jep.2018.02.038]

24 **Thompson JD**, Gibson TJ, Plewniak F, Jeanmougin F, Higgins DG. The CLUSTAL_X windows interface: flexible strategies for multiple sequence alignment aided by quality analysis tools. *Nucleic Acids Res* 1997; **25**: 4876-4882 [PMID: 9396791 DOI: 10.1093/nar/25.24.4876]

25 **Lengauer T**, Rarey M. Computational methods for biomolecular docking. *Curr Opin Struct Biol* 1996; **6**: 402-406 [PMID: 8804827 DOI: 10.1016/s0959-440x(96)80061-3]

26 **Morris GM**, Huey R, Lindstrom W, Sanner MF, Belew RK, Goodsell DS, Olson AJ. AutoDock4 and AutoDockTools4: Automated docking with selective receptor flexibility. *J Comput Chem* 2009; **30**: 2785-2791 [PMID: 19399780 DOI: 10.1002/jcc.21256]

27 **Eberhardt J**, Santos-Martins D, Tillack AF, Forli S. AutoDock Vina 1.2.0: New Docking Methods, Expanded Force Field, and Python Bindings. *J Chem Inf Model* 2021; **61**: 3891-3898 [PMID: 34278794 DOI: 10.1021/acs.jcim.1c00203]

28 **Burque RK**, Francesconi LP, Victorino AT, Mascarenhas MA, Ceresér KM. Determination of phenolic and evaluation of antioxidant activity of *Lafoensia pacari* (Lythraceae). *Revista Eletrônica de Farmácia* 2015; **12**: 1-10 [DOI: 10.5216/ref.v12i1.24645]

29 **Cunha GA**, Bailão EFLC, Borges LL, Almeida LM. Evaluation of the antioxidant potential of Lafoensia pacari. In: Annals of the 5th Congress of Teaching, Research and Extension of the Universidade Estadual de Goiás: Science for reducing inequalities; 2018 Oct 17-19; Goiás, Brazil

30 **Collier HO**, Dinneen LC, Johnson CA, Schneider C. The abdominal constriction response and its suppression by analgesic drugs in the mouse. *Br J Pharmacol Chemother* 1968; **32**: 295-310 [PMID: 4230818 DOI: 10.1111/j.1476-5381.1968.tb00973.x]

31 **Guimarães HA**, Nascimento MVM, Tavares A, Galdino PM, De Paula JR, Costa EA. Effects of ethanolic extract of *Lafoensia pacari* A. St.-Hil., Lythraceae (pacari), in pain and inflammation model. *Brazilian J Pharm* 2010; **20**: 328-333 [DOI: 10.1590/S0102-695X2010000300007]

32 **Silva ABL**, Dias KS, Marques MS, Menezes IAC, Santos TC, Mello ICM, Lisboa ACCD, Cavalcanti SCH, Marçal RM, Antoniolli AR. Evaluation of the analgesic effect and acute toxicity of the aqueous extract of *Hyptis fruticosa* (Salmz. Ex Benth.). *Brazilian J Pharm* 2006; **16**: 475-479 [DOI: 10.1016/j.fct.2019.110940]

33 **de Matos LG**, Santos L da R, Ferreira RN, Pontes IS, de Paula JR, Costa EA. Anti-Inflammatory, Antinociceptive, and Sedating Effects of *Lafoensia pacari*. *Aqueous Extract. Pharm Biol* 2008; **46**: 341-346 [DOI: 10.1080/13880200801887799]

34 **Zhao J**, Maitituersun A, Li C, Li Q, Xu F, Liu T. Evaluation on Analgesic and Anti-Inflammatory Activities of Total Flavonoids from *Juniperus sabina*. *Evid Based Complement Alternat Med* 2018; **2018**: 7965306 [PMID: 30069226 DOI: 10.1155/2018/7965306]

35 **Shara M**, Stohs SJ. Efficacy and Safety of White Willow Bark (Salix alba) Extracts. *Phytother Res* 2015; **29**: 1112-1116 [PMID: 25997859 DOI: 10.1002/ptr.5377]

36 **Naghizadeh B**, Mansouri MT, Ghorbanzadeh B. Ellagic acid enhances the antinociceptive action of carbamazepine in the

acetic acid writhing test with mice. *Pharm Biol* 2016; **54**: 157-161 [PMID: 25898222 DOI: 10.3109/13880209.2015.1025288]

37 **Derosa G**, Maffioli P, Sahebkar A. Ellagic Acid and Its Role in Chronic Diseases. *Adv Exp Med Biol* 2016; **928**: 473-479 [PMID: 27671829 DOI: 10.1007/978-3-319-41334-1_20]

38 **Ministry of Health of Brazil**. Department of Health Care: Clinical protocol and therapeutic guidelines for the treatment of Crohn's disease. In: Diário Oficial da União. Portaria 858/02, 2002; 214: 77-82

39 **Ministry of Health of Brazil**. Department of Health Care: Clinical protocol and therapeutic guidelines for the treatment of ulcerative colitis. In: Diário Oficial da União. Portaria 861/02, 2002; 214: 87-98

40 **Tamashiro Filho P**, Sikiru Olaitan B, Tavares de Almeida DA, Lima JC, Marson-Ascêncio PG, Donizeti Ascêncio S, Rios-Santos F, Martins DT. Evaluation of antiulcer activity and mechanism of action of methanol stem bark extract of *Lafoensia pacari* A. St.-Hil. (Lytraceae) in experimental animals. *J Ethnopharmacol* 2012; **144**: 497-505 [PMID: 23069941 DOI: 10.1016/j.jep.2012.09.019]

41 **Rogerio AP**, Fontanari C, Borducchi E, Keller AC, Russo M, Soares EG, Albuquerque DA, Faccioli LH. Anti-inflammatory effects of *Lafoensia pacari* and ellagic acid in a murine model of asthma. *Eur J Pharmacol* 2008; **580**: 262-270 [PMID: 18021768 DOI: 10.1016/j.ejphar.2007.10.034]

42 **Tena B**, Escobar B, Arguis MJ, Cantero C, Rios J, Gomar C. Reproducibility of Electronic Von Frey and Von Frey monofilaments testing. *Clin J Pain* 2012; **28**: 318-323 [PMID: 22001670 DOI: 10.1097/AJP.0b013e31822f0092]

43 **Sandborn WJ**, Hanauer SB. Systematic review: the pharmacokinetic profiles of oral mesalazine formulations and mesalazine pro-drugs used in the management of ulcerative colitis. *Aliment Pharmacol Ther* 2003; **17**: 29-42 [PMID: 12492730 DOI: 10.1046/j.1365-2036.2003.01408.x]

44 **Deuis JR**, Dvorakova LS, Vetter I. Methods Used to Evaluate Pain Behaviors in Rodents. *Front Mol Neurosci* 2017; **10**: 284 [PMID: 28932184 DOI: 10.3389/fnmol.2017.00284]

45 **Laird JMA**, Martinez-Caro L, Garcia-Nicas E, Cervero F. A new model of visceral pain and referred hyperalgesia in the mouse. *Pain* 2001; **92**: 335-342 [PMID: 11376906 DOI: 10.1016/S0304-3959(01)00275-5]

46 **Dong L**, Vecchio AJ, Sharma NP, Jurban BJ, Malkowski MG, Smith WL. Human cyclooxygenase-2 is a sequence homodimer that functions as a conformational heterodimer. *J Biol Chem* 2011; **286**: 19035-19046 [PMID: 21467029 DOI: 10.1074/jbc.M111.231969]

47 **Pantsar T**, Poso A. Binding Affinity *via* Docking: Fact and Fiction. *Molecules* 2018; **23** [PMID: 30061498 DOI: 10.3390/molecules23081899]

48 **Lin CF**, Leu YL, Al-Suwayeh SA, Ku MC, Hwang TL, Fang JY. Anti-inflammatory activity and percutaneous absorption of quercetin and its polymethoxylated compound and glycosides: the relationships to chemical structures. *Eur J Pharm Sci* 2012; **47**: 857-864 [PMID: 22609526 DOI: 10.1016/j.ejps.2012.04.024]

49 **Souto FO**, Zarpelon AC, Staurengo-Ferrari L, Fattori V, Casagrande R, Fonseca MJ, Cunha TM, Ferreira SH, Cunha FQ, Verri WA Jr. Quercetin reduces neutrophil recruitment induced by CXCL8, LTB4, and fMLP: inhibition of actin polymerization. *J Nat Prod* 2011; **74**: 113-118 [PMID: 21275387 DOI: 10.1021/np1003017]

50 **Malta DJN**. Síntese, elucidação estrutural e atividade biológica de novos derivados imidazolidinônicos. M.Sc. Thesis, Universidade Federal de Pernambuco, 2005. Available at: https://repositorio.ufpe.br/handle/123456789/40873

51 **Carvalho WA**, Carvalho RD, Rios-Santos F. [Specific cyclooxygenase-2 inhibitor analgesics: therapeutic advances.]. *Rev Bras Anestesiol* 2004; **54**: 448-464 [PMID: 19471752 DOI: 10.1590/s0034-70942004000300017]

World Journal of Gastroenterology

Submit a Manuscript: https://www.f6publishing.com

World J Gastroenterol 2023 May 7; 29(17): 2642-2656

DOI: 10.3748/wjg.v29.i17.2642

ISSN 1007-9327 (print) ISSN 2219-2840 (online)

ORIGINAL ARTICLE

Basic Study

Establishment and characterization of a new human ampullary carcinoma cell line, DPC-X1

Hao Xu, Chang-Peng Chai, Xin Miao, Huan Tang, Jin-Jing Hu, Hui Zhang, Wen-Ce Zhou

Specialty type: Gastroenterology and hepatology

Provenance and peer review: Unsolicited article; Externally peer reviewed.

Peer-review model: Single blind

Peer-review report's scientific quality classification

Grade A (Excellent): 0
Grade B (Very good): B, B
Grade C (Good): 0
Grade D (Fair): 0
Grade E (Poor): 0

P-Reviewer: Kode JA, India; Lai SW, Taiwan

Received: December 26, 2022
Peer-review started: December 26, 2022
First decision: February 8, 2023
Revised: February 17, 2023
Accepted: April 13, 2023
Article in press: April 13, 2023
Published online: May 7, 2023

Hao Xu, Chang-Peng Chai, Jin-Jing Hu, The Forth Department of General Surgery, The First Hospital of Lanzhou University, Lanzhou 730000, Gansu Province, China

Xin Miao, State Key Laboratory of Veterinary Etiological Biology, Key Laboratory of Animal Virology of the Ministry of Agriculture, Lanzhou Veterinary Research Institute, Chinese Academy of Agricultural Sciences, Lanzhou 730000, Gansu Province, China

Huan Tang, Wen-Ce Zhou, The Second Clinical Medical College, Lanzhou University, Lanzhou 730000, Gansu Province, China

Hui Zhang, Wen-Ce Zhou, Department of General Surgery, The Second Hospital of Lanzhou University, Lanzhou 730000, Gansu Province, China

Corresponding author: Hao Xu, Doctor, MD, Associate Chief Physician, Surgeon, The Forth Department of General Surgery, The First Hospital of Lanzhou University, No. 1 Donggang West Road, Lanzhou 730000, Gansu Province, China. amoyxu@126.com

Abstract

BACKGROUND

An in-depth study of the pathogenesis and biological characteristics of ampullary carcinoma is necessary to identify appropriate treatment strategies. To date, only eight ampullary cancer cell lines have been reported, and a mixed-type ampullary carcinoma cell line has not yet been reported.

AIM

To establish a stable mixed-type ampullary carcinoma cell line originating from Chinese.

METHODS

Fresh ampullary cancer tissue samples were used for primary culture and subculture. The cell line was evaluated by cell proliferation assays, clonal formation assays, karyotype analysis, short tandem repeat (STR) analysis and transmission electron microscopy. Drug resistances against oxaliplatin, paclitaxel, gemcitabine and 5-FU were evaluated by cell counting kit-8 assay. Subcutaneous injection 1 × 10^6 cells to three BALB/c nude mice for xenograft studies. The hematoxylin-eosin staining was used to detect the pathological status of the cell line. The expression of biomarkers cytokeratin 7 (CK7), cytokeratin 20 (CK20), cytokeratin low molecular weight (CKL), Ki67 and carcinoembryonic antigen

(CEA) were determined by immunocytochemistry assay.

RESULTS

DPC-X1 was continuously cultivated for over a year and stably passaged for more than 80 generations; its population doubling time was 48 h. STR analysis demonstrated that the characteristics of DPC-X1 were highly consistent with those of the patient's primary tumor. Furthermore, karyotype analysis revealed its abnormal sub-tetraploid karyotype. DPC-X1 could efficiently form organoids in suspension culture. Under the transmission electron microscope, microvilli and pseudopods were observed on the cell surface, and desmosomes were visible between the cells. DPC-X1 cells inoculated into BALB/C nude mice quickly formed transplanted tumors, with a tumor formation rate of 100%. Their pathological characteristics were similar to those of the primary tumor. Moreover, DPC-X1 was sensitive to oxaliplatin and paclitaxel and resistant to gemcitabine and 5-FU. Immunohistochemistry showed that the DPC-X1 cells were strongly positive for CK7, CK20, and CKL; the Ki67 was 50%, and CEA was focally expressed.

CONCLUSION

Here, we have constructed a mixed-type ampullary carcinoma cell line that can be used as an effective model for studying the pathogenesis of ampullary carcinoma and drug development.

Key Words: Ampullary carcinoma; Cell line; Xenograft; Drug resistance

Core Tip: A new ampullary carcinoma cell line has been established, making up for the shortage of Chinese ampullary carcinoma cell lines. And this is the the first study to report a mixed-type ampullary carcinoma cell line. The cell line inoculated into BALB/c nude mice can quickly form xenograft tumors. It is an excellent model for studying the mechanisms of invasion, metastasis and other mechanisms of ampullary carcinoma. The cell line is sensitive to oxaliplatin and paclitaxel but is naturally resistant to gemcitabine and fluorouracil, which can be used for drug resistance mechanism research and new drug development.

Citation: Xu H, Chai CP, Miao X, Tang H, Hu JJ, Zhang H, Zhou WC. Establishment and characterization of a new human ampullary carcinoma cell line, DPC-X1. *World J Gastroenterol* 2023; 29(17): 2642-2656
URL: https://www.wjgnet.com/1007-9327/full/v29/i17/2642.htm
DOI: https://dx.doi.org/10.3748/wjg.v29.i17.2642

INTRODUCTION

Ampullary carcinoma is a relatively rare tumor, accounting for 0.2% of gastrointestinal cancers but 20% of all periampullary cancers[1,2]. Recently, the incidence rate of ampullary cancer has gradually increased[3,4]. Ampullary carcinoma can occur at any age; however, it is more common between 60 and 65 years of age, and the sex ratio is approximately 3:2[1,2]. As biliary obstruction symptoms appear early, the surgical resection rate of ampullary carcinoma is higher than that of other periampullary malignant tumors, and approximately 50% of patients are eligible for surgery on diagnosis[1,5,6]. Its operation amount is over one-third of the total operation amount of pancreatoduodenectomy. The prognosis is good, and the 5-year survival rate exceeds 52.8%[7]. Despite a high potential curative resection rate, most patients with ampullary cancer eventually succumb to tumor recurrence[8,9].

In 1994, Kimura *et al*[10] first classified ampullary carcinoma into intestinal and pancreaticobiliary types according to their histological characteristics. The prevalence of the pancreaticobiliary type was 72%, which is much higher than that of the intestinal type[10]. In 2010, according to the morphological and immunohistochemical characteristics, WHO revised the pathological diagnosis criteria of ampullary carcinoma into three different histopathological subtypes: Intestinal-, pancreaticobiliary-, and mixed-type ampullary carcinoma[11,12].

To date, only eight ampullary cancer cell lines have been included in the official databases of ATCC, JCRB, RIKEN, and DSMZ. One is American, one is Italian, two are Korean, and four are Japanese (three of them are from different lesions of the same patient)[13-17] (Table 1). Among them, SNU-869 is an intestinal-type cell line, whereas the remaining are pancreaticobiliary-type cell lines[18]. No mixed-type ampullary carcinoma cell line has yet been reported.

Table 1 Energy of affinity of cyclooxygenase-2/flavonoid complexes

Cell line	Age (years)	Gender	Source of culture	Race	Differentiation	Primary culture	Ref.
MDAAmp-7	40	Male	Abdominal metastases	American	Well differentiated	1989	[13]
RCB1169/TGBC18TKB	79	Female	Primary tumor	Japanese	-	1995	[14]
RCB1280/TGBC50TKB	52	Male	Liver metastasis	Japanese	Poorly differentiatedadenosquamous carcinoma	1996	[15]
RCB1280/TGBC51TKB	525	Male	Ascites	Japanese	Poorly differentiatedadenosquamous carcinoma	1996	[15]
RCB1280/TGBC52TKB	52	Male	Lymph node	Japanese	Poorly differentiatedadenosquamous carcinoma	1996	[15]
SNU478	-	-	-	Korean	Poorly differentiated with signet ring cell	-	[16]
SNU869	-	-	-	Korean	Well differentiated	-	[16]
AVC1	71	Female	Primary tumor	Italian	Moderately differentiated	1997	[17]

No randomized clinical trial for adjuvant chemotherapy of ampullary carcinoma currently exists, and the data based on which doctors choose treatment methods are limited. Presently, adjuvant therapy for ampullary carcinoma is being tailored according to the histological subtypes. Pancreatic biliary ampullary carcinoma is typically treated similarly to pancreatic adenocarcinoma or biliary tract carcinoma. In contrast, patients with intestinal ampulla receive the usual protocol for colorectal cancer. Based on these premises, the optimal treatment plan for ampullary carcinoma in adjuvant therapy and chemotherapy for advanced patients remains to be determined[19,20].

Based on the aforementioned factors, establishing an ampullary carcinoma cell line, conducting in-depth research on the pathogenesis and biological characteristics of ampullary carcinoma, and then investigating therapeutic targets to formulate effective treatment strategies for patients with ampullary carcinoma are currently required.

In this study, we establish a stable mixed-type ampullary carcinoma cell line named DPC-X1 from the tumor tissue of a patient with ampullary carcinoma. Our study findings underscore the effectiveness of DPC-X1 as an experimental model that can be used to explore the molecular mechanism of ampullary carcinoma and develop therapeutic schemes for disease control.

MATERIALS AND METHODS

Tissue source

The tissue samples were collected from a patient with ampullary cancer who was admitted to the First Hospital of Lanzhou University on November 17, 2021, for pancreatoduodenectomy. The patient was a 60-year-old man who presented with jaundice, had a long history of smoking and drinking, and had no history of carrying hepatitis B or C. His carbohydrate antigen 199 levels exceeded 1000 U/mL (reference range: 0–35 U/mL; Figure 1A), and preoperative magnetic resonance imaging + magnetic resonance cholangiopancreatography indicated ampullary carcinoma (Figure 1B and C). The new organisms growing around the ampulla were grayish-white and were taken from the primary focus for primary culture and subculture (Figure 1D and E).

This study was approved by the Medical Ethics Committee of the First Hospital of Lanzhou University (LDYYLL-2022-487), and signed informed consent was obtained from the patient.

Drugs

Gemcitabine was obtained from Jiangsu Haosen Pharmaceutical Group Co., Ltd., oxaliplatin from Jiangsu Hengrui Pharmaceutical Co., Ltd., 5-FU from Tianjin Jinyao Pharmaceutical Co., Ltd., and paclitaxel from Jiangsu Aosaikang Pharmaceutical Co., Ltd.

Nude mice

In this study, experiments were conducted on 4–6-week-old BALB/c nude female mice, weighing 16–20 g. They were obtained from Changzhou Kavens Experimental Animal Co., Ltd. and raised in the SPF laboratory of the Animal Experiment Center of Lanzhou University. The animal protocol was designed to minimize pain or discomfort to the animals. The animals were acclimatized to laboratory conditions (23 °C, 12 h/12 h light/dark, 50% humidity, ad libitum access to food and water) for 2 wk prior to experimentation. All animals were euthanized by barbiturate overdose (intravenous injection, 150 mg/

A

Cell line	Patient age/ethnicity	Gender	Current status (days)	Histopathology/differentiation	Tumor size (cm)	Prior therapy	Culture date	Serum		
								AFP IU/mL (0-5.8)	CEA ng/mL (0-5.2)	CA199 U/mL (0-35)
DPC-X1	60/Asian	Male	D (370)	Moderately-poorly	2×1	None	2021-11-17	1.4	4.5	> 1000

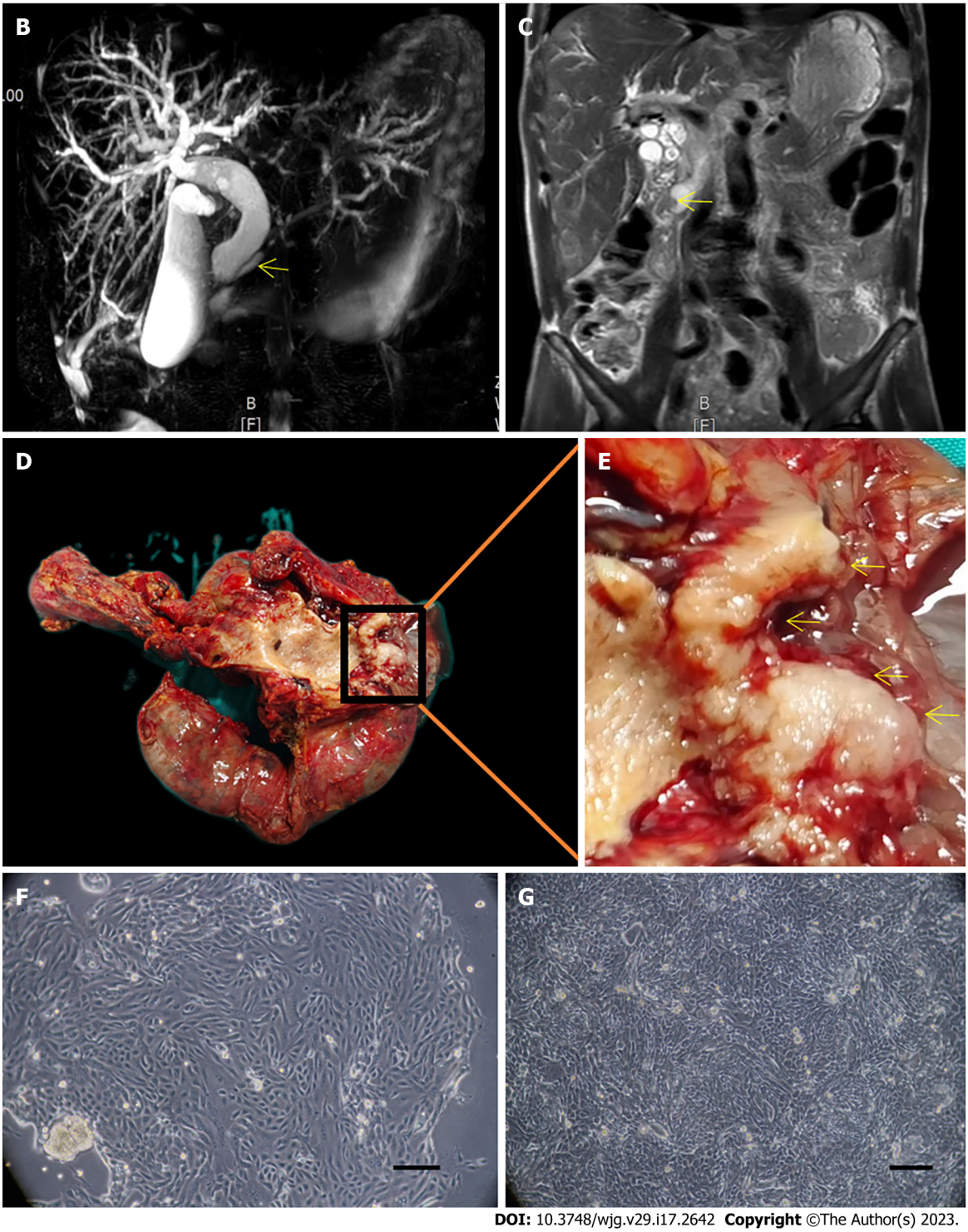

DOI: 10.3748/wjg.v29.i17.2642

Figure 1 Clinical data and cell morphology. A: Clinical data of the patient; B: Magnetic resonance cholangiopancreatography shows the expansion of intrahepatic and extrahepatic bile ducts, gallbladder enlargement, and pancreatic duct expansion (arrow); C: In the coronal view of magnetic resonance imaging, soft tissue shadow (arrow) can be seen in the ampulla, and the upper bile duct is dilated; D: General view of the surgical specimen; E: The enlarged appearance of the ampulla tumor shows the gray-white tumor growing around the ampulla (arrow); F: DPC-X1 primary cell morphology; multinucleated cells and megakaryocytes can be seen; G: DPC-X1 cell morphology of the 80th generation. Scale bars: 100 μm. D: Death; AFP: alpha-fetoprotein; CEA: Carcinoembryonic antigen; CA199:

Carbohydrate antigen 199.

kg pentobarbital sodium) for tissue collection.

All animal experiments were reviewed and approved by the Medical Animal Experiment Ethics Committee of the First Hospital of Lanzhou University (LDYYLL-2022-487). The methods followed in this study were similar or identical to those employed in previous studies[21-23].

Establishment of the cell line

The tumor tissue samples were immersed in sterile phosphate buffered saline (PBS) (Gibco) 3–5 times and sectioned into small pieces. The small woven pieces were mixed with type II collagenase (Gibco) and neutral protease (Invitrogen) and digested in a shaking table at 37 ℃. On digestion of half the tissue block, the supernatant was absorbed, filtered with a 100 mesh filter screen, and centrifuged at 300 × *g* for 3 min. Thereafter, the supernatant was discarded; the sample was resuspended in PBS and centrifugated at 300 × *g* for 3 min. The precipitate was added to a complete medium [RPMI-1640 + 10% fetal bovine serum (FBS) + 1% penicillin–streptomycin, Biological industries (BI)] and uniformly inoculated on a six-well plate (NEST). The medium was refreshed after 48 h. The mixed fibroblasts in the primary culture were removed using differential digestion with 0.25% trypsin. When the cells reached 70% confluency, they were digested and passed on. The cell growth was regularly observed under a light microscope. From the fifth generation, the cells were subcultured in a ratio of 1:2 and frozen with Serum-free rapid cell cryopreservation solution (Mei5 Biotechnology Co., Ltd.).

Cell growth curve

The cell density of DPC-X1 cells in the logarithmic growth phase (P20) was adjusted to 1×10^4/mL after trypsin digestion. After mixing, 0.1 mL of sample was inoculated in each hole in a 96-hole plate cell counting kit-8 (CCK-8) reagent (Dojindo) was added at the same time for 4 consecutive days after inoculation and allowed to react for 2 h. The UV absorbance value at 450 nm wavelength was measured with a microplate reader. The cell doubling time was calculated using the following formula: Td = t × Lg2/Lg (N1/N0). The cell growth curve was plotted with time as the horizontal axis and absorbance value as the vertical axis.

Analysis of short tandem repeats

DPC-X1 cells in the logarithmic growth stage (P10) were collected after trypsin digestion. Together with the primary tumor tissue, they were sent to Suzhou Jianda Biotechnology Company for short tandem repeat (STR) analysis to determine the correlation between the cells and primary tumor tissue.

Karyotype analysis

DPC-X1 cells in the logarithmic growth phase (P40) were treated with 0.25 μg/mL colchicine for 6 h overnight at 37 ℃. The metaphase cells were collected and fixed with methanol glacial acetic acid (3:1). After trypsin digestion, the specimens were stained using Giemsa dye and observed under a microscope. The mitotic phase cells with good dispersion and moderate staining were selected for karyotype analysis.

Organoid culture

DPC-X1 cells in the logarithmic growth phase (P35) were digested, centrifuged, washed twice with PBS, resuspended in a complete culture medium (RPMI-1640 + 10% FBS + 1% penicillin–streptomycin, BI), and inoculated on an ultra-low adsorption cell culture plate (Corning). A thousand cells were added to each well, and 2 mL of culture medium was added for 14 d. The state and number of organ-like cultures were observed under a light microscope.

Transmission electron microscopy

DPC-X1 cells in the logarithmic growth phase (P45) were digested, centrifuged, fixed with an electron microscope fixative, and stored and transported at 4 ℃. Embedding, ultrathin sectioning, and dyeing were performed at Wuhan Servicebio Co., Ltd. Finally, the images were observed under the transmission electron microscope.

Drug sensitivity test

The logarithmically grown DPC-X1 cells (P50) were digested using trypsin to prepare a single-cell suspension. We inoculated 10000 cells/100 μL per well into 96-well plates, and 6 wells in each group were repeated. After the cells adhered to the wall, different concentrations of anti-tumor drugs were added. After 72 h of drug action, 100% X containing 10% (v/v) CCK-8 μL serum-free medium was used to replace the complete medium. The optical density value was measured after 2 h at 450 nm.

Xenograft tumor in nude mice

The cell density of cells in the logarithmic growth phase (P45) was adjusted to 1 × 10^7/mL after trypsin digestion. Thereafter, three BALB/c nude mice each were inoculated with 0.1 mL of this sample. We observed and recorded the tumor growth of the nude mice every alternate day. The mice carrying the tumor were killed after four weeks, and the tumor tissue was excised and fixed with 10% formalin. The surgery was performed under sodium pentobarbital anesthesia, and all efforts were made to minimize suffering. Thereafter, routine histopathological and immunohistochemical examinations were performed.

Immunohistochemical staining

Cells of the 40th generation were digested and inoculated onto sterile slides. After 48 h, the slides were washed with PBS, fixed with 4% paraformaldehyde for 15 min, dried, and treated with 0.5% Triton X-100 for 20 min.

The paraffin sections of primary tumors, transplanted tumors, and organ-like tissues were prepared and incubated at 60 ℃ overnight. The dewaxing, gradient alcohol hydration, and antigen repair processes were completed using Dako's Autostainer Link 48 instrument. Subsequently, 3% hydrogen peroxide solution was incubated at 37 ℃ for 15 min to block the activity of peroxidase; 100 μL of normal goat serum was dripped and then kept sealed at 37 ℃ for 15 min. The first antibody was incubated at 37 ℃ for 1 h with Fuzhou Maxin ready-to-use antibodies [cytokeratin 7 (CK7), cytokeratin 20 (CK20), cytokeratin low molecular weight (CKL), Ki67, and carcinoembryonic antigen (CEA)]. The DAB dye kit (Dako) was used for color development, followed by rinsing with running water for 5 min. Dehydration and xylene transparency were carried out after hematoxylin counterstaining, and the samples were observed under the microscope after neutral resin sealing.

Statistical analyses

All statistical analyses were performed using the SPSS 22.0 software. The data are presented as mean ± SD. Student's *t*-tests and ANOVA were used for group comparisons. Statistical significance was set at $P < 0.05$.

RESULTS

Establishment of the DPC-X1 cell line

Through primary culture and subculture of primary tumor tissue of ampullary carcinoma, an ampullary carcinoma cell line, named DPC-X1, was successfully established. Using light microscopy, we found that DPC-X1 cells adhered to the wall and grew like typical epithelial cells. The cells were mainly short spindle-shaped, with large nuclei and visible nucleoli. The polykaryocytes and megakaryocytes were visible. Loss of contact inhibition between cells likely led to accumulation growth as the cells were closely adherent and grew in clumps and sheets (Figure 1F and Video). The cell morphology and growth mode remained unaltered even though it passed to the 80th generation (Figure 1G).

Cell growth curve

DPC-X1 cells proliferated vigorously and grew stably in RPMI-1640 medium with 10% FBS. Through the CCK-8 method, the doubling time of the DPC-X1 cell population was found to be 48 h using the CCK-8 method. The cell growth curve was plotted using culture time as the abscissa and absorbance values as the ordinate (Figure 2A).

Analysis of STRs

The DNA typing results demonstrated that the two submitted samples were from the same individual with a likelihood ratio = 4.1867 × 10^{20} (Figure 2B and Supplementary material). The results indicate that DPC-X1 is a new human ampullary carcinoma cell line with the same origin as that of the primary tumor tissue and is not contaminated by the existing cell line.

Karyotype analysis

Karyotype analysis showed that DPC-X1 cells were mainly sub-tetraploid, with large differences in chromosome number and morphology. The representative karyotype was 80, XX del (2) (q32) del (5) (p12) del (6) (q24) inv (9) del (10) p (13) del (17) p (12) (Figure 2C).

Organoid culture

After inoculating the DPC-X1 cells on the ultra-low attachment culture plate, the cells were observed to proliferate well and gradually form spherical or cystic organs (Figure 2D). With time, the number of organoid organs gradually increased and appeared spore-like or branch-like (Figure 2E).

A

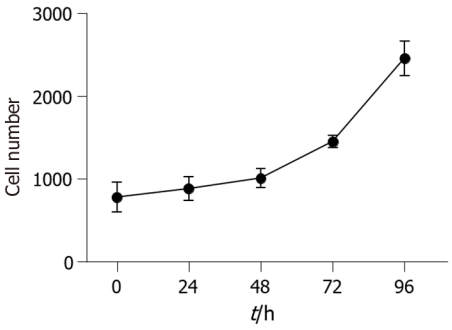

B

Loci	DPC-X1		DPC-X1-tissue		Matching probability
Amelogenin	X	Y	X	Y	/
D3S1358	15		15		0.1225
D13S317	9	10	9	10	0.0338
D7S820	11	12	11	12	0.1538
D16S539	10	13	10	12	-
Penta E	15	16	15	16	0.0109
TPOX	8		8		0.2862
TH01	9		9	9.3	-
D2S1338	18	19	18	19	0.0512
CSF1PO	10		10		0.0420
Penta D	9	10	9	10	0.0744
D19S433	13	15	13	15	0.0244
vWA	16	18	16	18	0.0486
D21S11	29		29		0.0576
D18S51	15		13	15	-
D6S1043	11	19	11	19	0.0330
D8S1179	8	17	8	17	0.0008
D5S818	10	12	10	12	0.0897
D12S391	19	22	19	22	0.0466
FGA	22	25	23	25	-
					4.1867×10^{20}

C

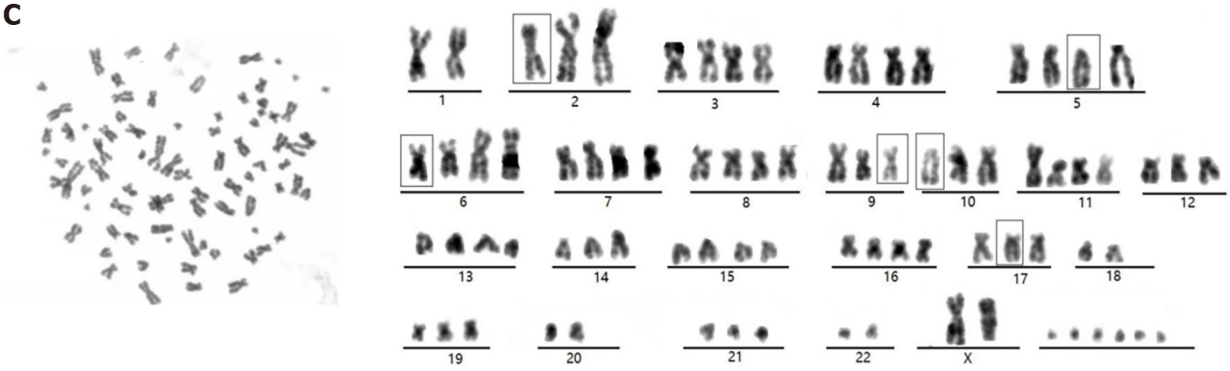

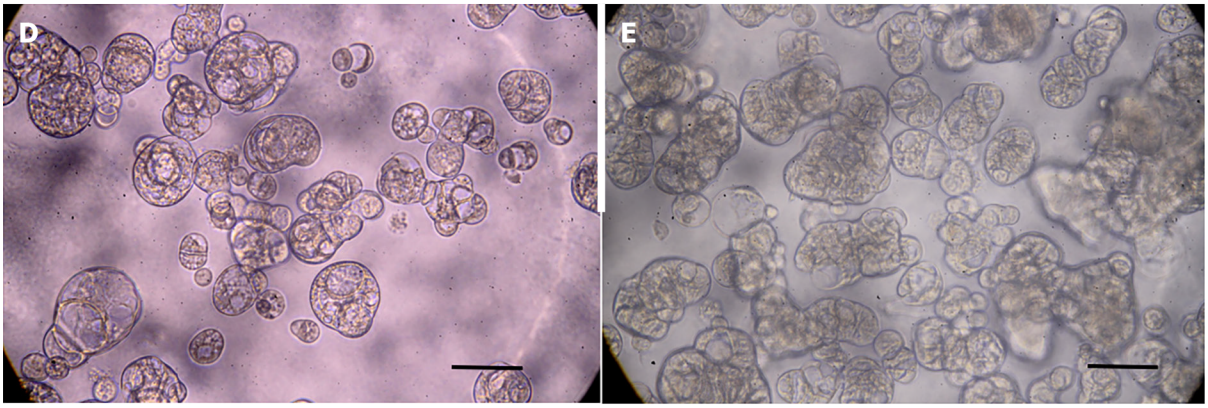

DOI: 10.3748/wjg.v29.i17.2642 **Copyright** ©The Author(s) 2023.

Figure 2 DPC-X1 population doubling time, short tandem repeat detection, karyotype analysis and Organoid culture. A: DPC-X1 growth curve; cell doubling time is 48 h; B: The likelihood ratio between the short tandem repeat results of DPC-X1 and the primary tumor tissue is 4.1867 × 1020. The cells are not contaminated by other cell lines; C: Karyotype analysis shows that DPC-X1 cells are mainly sub-tetraploid, with large differences in chromosome number and morphology. The representative karyotype is 80, XX del (2) (q32) del (5) (p12) del (6) (q24) inv (9) del (10) p (13) del (17) p (12); D: Morphology of DPC-X1organoids after one week. The organoids are spherical or cystic in shape; E: Morphology of DPC-X1 organoids after two weeks. The organoids are spore-like or branch-like in shape. Scale bars: 100 μm.

Transmission electron microscopy

Under the transmission electron microscope, the DPC-X1 nucleus appeared large and deformed, and its number was increased. The nucleolus was clustered in the nuclear membrane, and the cytoplasm was less. Microvilli and pseudopodia were visible on the cell surface (Figure 3A). The endoplasmic reticulum and ribosome were abundantly present in the cells (Figure 3B). Furthermore, the Golgi apparatus was developed, and the mitochondria differed in size and shape (Figure 3C). The desmosome structure was observed between the cells (Figure 3D).

Drug sensitivity test

The chemotherapy drugs gemcitabine and paclitaxel are commonly used for biliary and pancreatic tumors, whereas 5-FU and oxaliplatin are commonly used for gastrointestinal tumors. Our drug

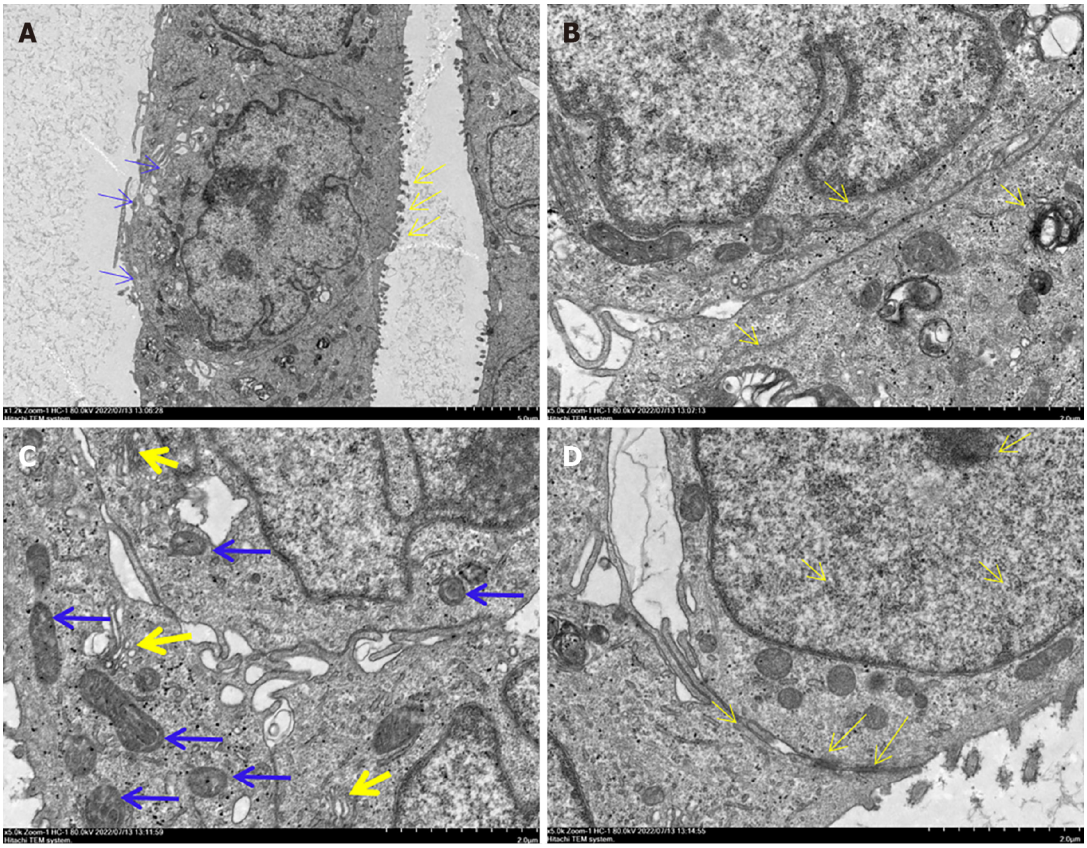

DOI: 10.3748/wjg.v29.i17.2642

Figure 3 Ultrastructure of DPC-X1 under a transmission electron microscope. A: DPC-X1 has a large and deformed nucleus; it is increased in number. The nucleolus is clustered in the nuclear membrane. There are fewer cytoplasm. Microvilli (yellow arrow) and pseudopodia (blue arrow) were visible on the cell surface; B: DPC-X1 cells are rich in the endoplasmic reticulum (yellow arrow) and ribosome; C: DPC-X1 cells have well-developed Golgi apparatus (yellow arrow), and the size and shape of the mitochondria are different (blue arrow); D: DPC-X1 desmosome structure can be seen between the cells (arrow).

sensitivity test revealed that DPC-X1 was sensitive to oxaliplatin [half maximal inhibitory concentration (IC50) = 13.26 μmol/L; Figure 4A] and paclitaxel (IC50 = 0.014 μmol/L; Figure 4B) and resistant to fluorouracil (IC50 = 144.9 μmol/L; Figure 4C) and gemcitabine (IC50 > 600 μmol/L; Figure 4D).

Xenograft tumor formation experiment

To verify the ability of DPC-X1 to form xenograft tumors *in vivo*, 1 × 10^6 DPC-X1 cells were inoculated subcutaneously in three BALB/c nude mice. The results showed that DPC-X1 was able to rapidly form xenograft tumors under the skin of nude mice, and the tumor formation rate was 100% (Figure 5A). The xenograft tumor grew rapidly and showed invasive growth. New blood vessels were visible on the surface of the xenograft tumor (Figure 5B). At four weeks, the diameter of the tumor body exceeded 1 cm (Figure 5C). No metastatic lesions were found in the liver and lungs of the dissected mice (Figure 5D). Tumor growth curve and mouse weight curve are shown in the figure (Figure 5E and F).

Hematoxylin and eosin and immunohistochemical staining

Hematoxylin-eosin staining showed that DPC-X1 cells were of different shapes, primarily short fusiform, with enlarged nuclei, apparent nucleoli, and less cytoplasm. The polykaryocytes and megakaryocytes were visible, exhibiting typical malignant tumor characteristics (Figure 6A).

The DPC-X1 organoids were observed to form irregular gland-like structures; the cells were closely connected, with a gland cavity-like structure inside. The cells in the organoid organs were highly heterotypic and varied in size (Figure 6B), which is highly similar to the histomorphology of the primary tumor tissue.

The xenograft tumor formed an irregular gland-like structure, and its histological morphology was similar to that of the primary tumor. The nucleus of the tumor was large and hyperchromatic, and the megakaryocytes were visible. The mitotic images depicted the vigorous proliferation of the DPC-X1 cells (Figure 6C); this observation is consistent with the characteristics of malignant tumors.

The postoperative pathological diagnosis of the patient's primary tumor showed moderately to poorly differentiated, and the tumor cells were arranged in irregular glandular tubes, strips, and nests (Figure 6D).

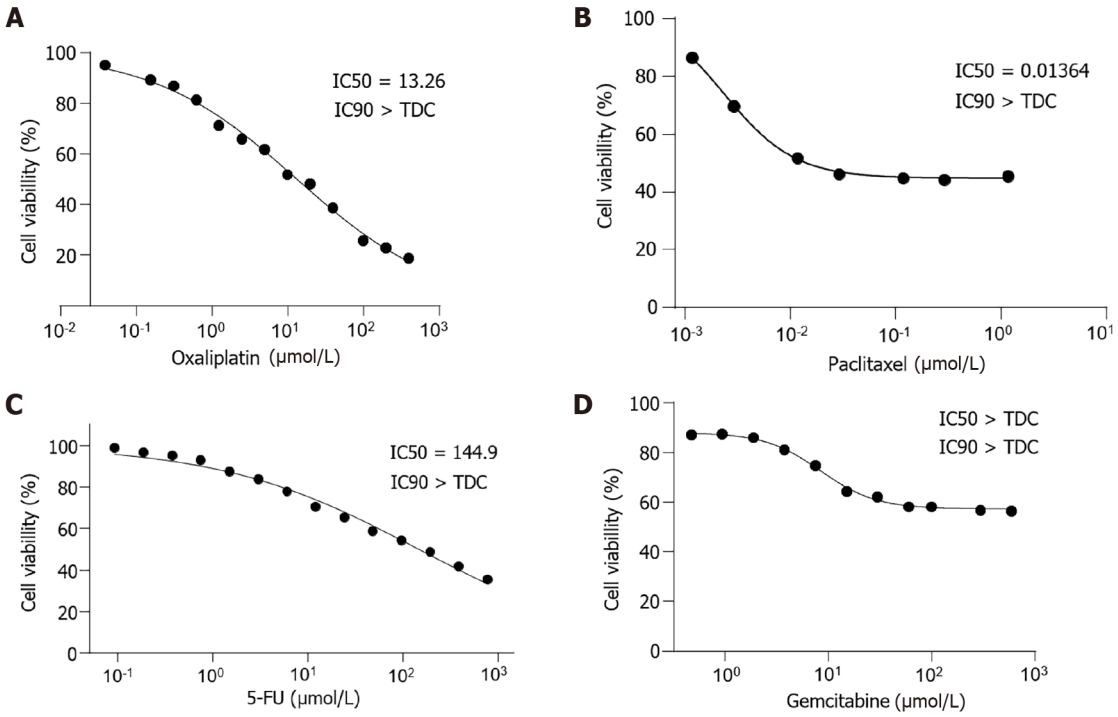

DOI: 10.3748/wjg.v29.i17.2642

Figure 4 Drug sensitivity test. A: DPC-X1 is sensitive to oxaliplatin; IC50 = 13.26 μmol/L; B: DPC-X1 is sensitive to paclitaxel; IC50 = 0.014 μmol/L; C: DPC-X1 is resistant to fluorouracil; IC50 = 144.9 μmol/L; D: DPC-X1 is resistant to gemcitabine; IC50 > 600 μmol/L. IC50: Half maximal inhibitory concentration; TDC: Test drug concentrations.

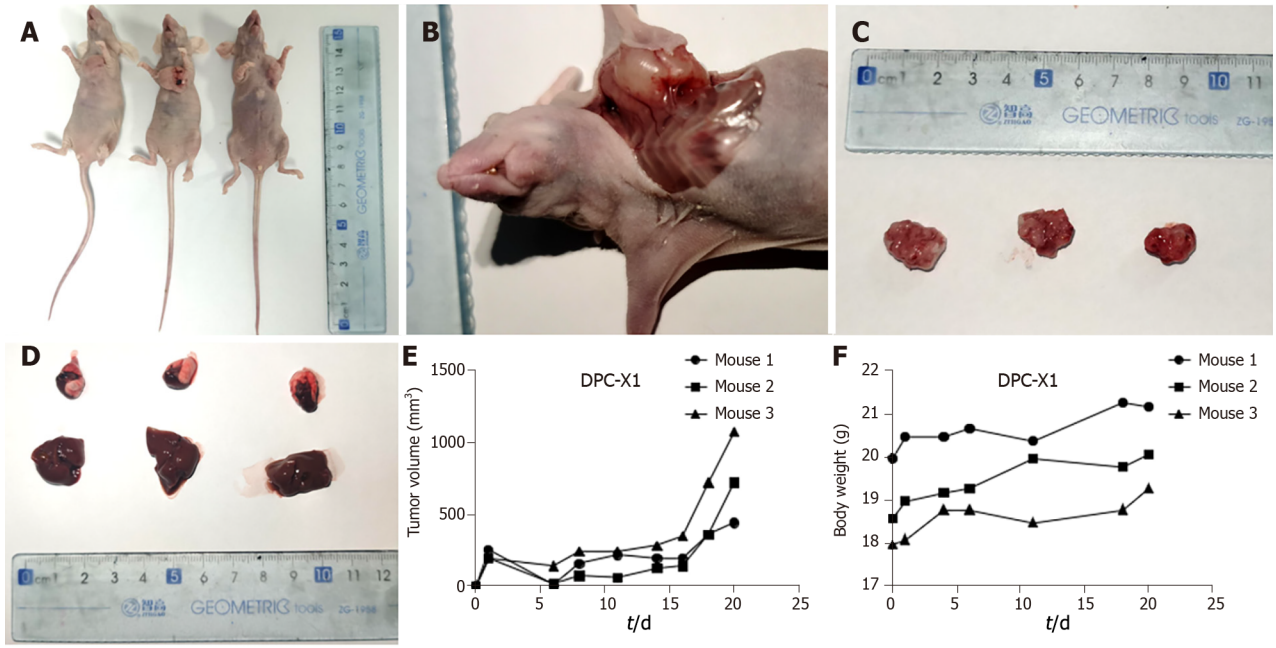

DOI: 10.3748/wjg.v29.i17.2642

Figure 5 Xenograft tumor formation experiment. A: In four weeks, DPC-X1 quickly formed xenograft tumors under the skin of BALB/c nude mice. The tumor formation rate is 100%; B: Anatomically, the xenograft tumor and muscle tissue of the mouse shows invasive growth, and new blood vessels can be seen on the surface of the tumor; C: General view of the xenograft tumor; D: No metastatic lesions were found in the lungs and liver of BALB/c nude mice within four weeks; E: Growth curve of DPC-X1 transplanted tumor; F: Body weight curve of BALB/c nude mice.

Immunohistochemical examination of DPC-X1 cells, organoids, xenograft tumor, and primary tumor showed that CK7 (Figure 6E–H), CK20 (Figure 6I–L), and CKL (Figure 6M–P) were strongly expressed among the four groups, indicating that they had the same origin. Moreover, DPC-X1 cells were found to exhibit both intestinal and pancreaticobiliary characteristics; thus, they were a mixed ampullary carcinoma cell line. Ki67 (Figure 6Q–T) was highly expressed, consistent with the rapid proliferation of

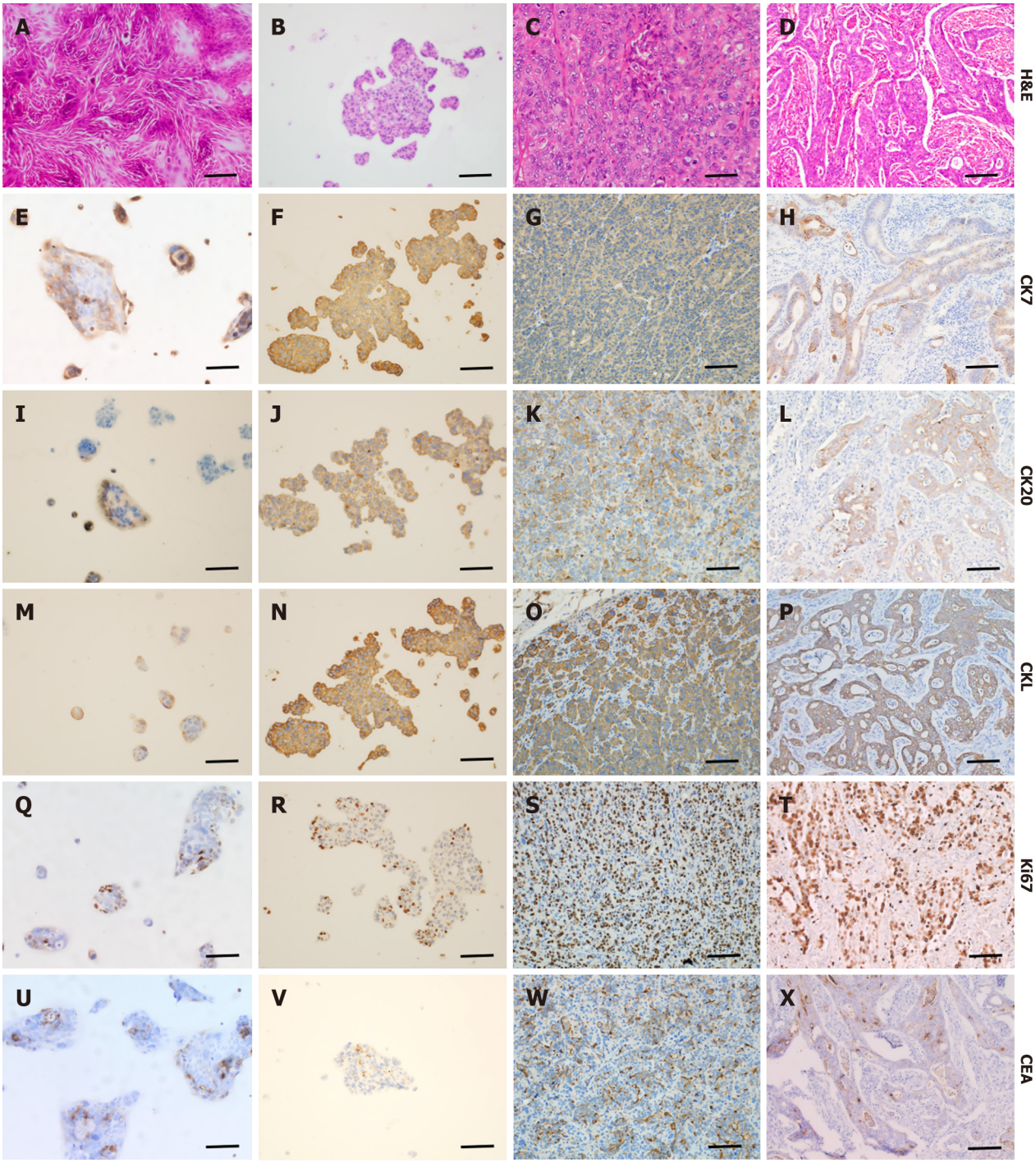

DOI: 10.3748/wjg.v29.i17.2642

Figure 6 Hematoxylin and eosin and immunohistochemical staining of DPC-X1 cells, organoid, xenograft tumor, and primary tumor. A-D: Hematoxylin and eosin staining of DPC-X1 cells, organoids, xenograft tumor, and primary tumor; E-H: Strong cytokeratin (CK)7 positive staining of DPC-X1 cells, organoids, xenograft tumor, and primary tumor; I-L: Strong CK20 positive staining of DPC-X1 cells, organoids, xenograft tumor, and primary tumor; M-P: Strong cytokeratin low molecular weight positive staining of DPC-X1 cells, organoids, xenograft tumor, and primary tumor; Q-T: Ki67 staining of DPC-X1 cells, organoids, xenograft tumor, and primary tumor; U-X: Carcinoembryonic antigen focal staining of DPC-X1 cells, organoids, xenograft tumor, and primary tumor. Scale bars: 100 μm. H&E: Hematoxylin and eosin; CK7: Cytokeratin 7; CK20: Cytokeratin 20; CKL: Cytokeratin low molecular weight; CEA: Carcinoembryonic antigen.

the tumor, and CEA (Figure 6U–X) showed focal expression. These observations are consistent with the characteristics of malignant tumors.

DISCUSSION

In recent years, with development in endoscopy, imaging equipment, and technological progress, an increasing number of ampullary cancer cases have been diagnosed[24-26]. Owing to the lack of cell lines and related research models of ampullary carcinoma, research on the pathogenesis and biological characteristics of ampullary carcinoma remains limited.

In this study, we successfully established a novel ampullary carcinoma cell line named DPC-X1 from the primary tumor tissue of patients with ampullary carcinoma through primary culture and subculture. This cell line was continuously cultured for more than a year and stably passaged for over 80 generations. DPC-X1 cells adhered to the wall and grew like typical epithelial cells. The cells were chiefly short spindle-shaped, with large nuclei and visible nucleoli, and multinucleated cells and megakaryocytes were visible. The cells were closely adherent and grew in clumps and sheets. The characteristics of DPC-X1 were highly consistent with those of the patient's primary tumor, and it was not contaminated by other cell lines and microorganisms. DPC-X1 could efficiently form organoids in suspension culture. The Ki67 of DPC-X1 was 50%, indicating that DPC-X1 has a vigorous proliferation, which is consistent with its population doubling time of 48 h.

CK7 is typically used as a tumor marker of biliary and pancreatic origin, whereas CK20 and villin are used as tumor markers of gastrointestinal origin[18,20,24,27,28]. In this study, DPC-X1 immunohistochemistry showed that CK7, CK20, and CKL were strongly positive, indicating that DPC-X1 was a mixed ampullary carcinoma cell line. To the best of our knowledge, this is the first study to report a mixed-type ampullary carcinoma cell line. Thus, DPC-X1 may provide a useful model for studying mixed-type ampullary carcinoma.

Chromosome instability and chromosomal aneuploidy are common in human cancers and are important characteristics of tumor cells[29-32]. Aneuploid karyotype of tumor cells is closely related to poor prognosis of patients[33,34]. Triploid karyotype may be related to endogenous drug resistance of tumors, whereas tetraploidy of tumors is associated with acquired drug resistance[35]. Spontaneous chromosomal missegregation events in aneuploid cells promote chromosomal instability, thereby increasing the risk of tumor recurrence[36]. Karyotype analysis showed that DPC-X1 cells had a subtetraploid abnormal karyotype, and the representative karyotype was 80, XX del (2) (q32) del (5) (p12) del (6) (q24) inv (9) del (10) p (13) del (17) p (12). The results of drug sensitivity showed that DPC-X1 was sensitive to oxaliplatin and paclitaxel but was naturally resistant to gemcitabine and fluorouracil. The patient underwent four cycles of chemotherapy with the XELOX regimen and two cycles with the AG regimen after surgery; however, he succumbed to tumor recurrence one year after surgery. Our results are highly consistent with that of earlier studies.

Desmosomes are intercellular junction complexes that anchor the intermediate filaments of adjacent cells and provide them with strong cell adhesion; thus, they are essential in maintaining the organizational structure and structural integrity[37]. Much evidence has substantiated the importance of desmosomes and their components in cancer. Desmosome expression is downregulated in poorly differentiated head and neck transitional and squamous cell carcinoma. In these tissues, desmosomes may have the function of inhibiting invasion and metastasis. In colon cancer, no downregulation has been found[38,39]. The change in desmosome component expression may promote tumor progression by altering the intracellular signal transduction pathway or leading to reduced cell adhesion. The loss of desmosome function is a prerequisite for epithelial-mesenchymal transformation, which is related to the transformation of early tumors to invasive cancer[40-44]. When DPC-X1 cells were subcultured, most of them grew in clumps and sheets, and digesting them into single cells in conventional digestion time was difficult, indicating the strong adhesion between the cells. The presence of intercellular desmosomes under transmission electron microscopy provides some ultrastructural evidence for the aforementioned phenomenon. DPC-X1 cells can be used to further study the relationship between tumors and desmosomes.

Animal models are an intermediate step between cell experiments and human clinical trials. They are a powerful tool for studying canceration and tumor progression and for testing the efficacy and toxicity of therapeutic compounds[45]. Suitable animal models not only help to explore the mechanism of ampullary carcinoma occurrence and development but also provide a good platform for exploring new strategies for early clinical diagnosis and precise treatment[46]. DPC-X1 cells inoculated into BALB/C nude mice could quickly form transplanted tumors, with a tumor formation rate of 100%, and the histology of the xenografts resembled that of the original tumor.

CONCLUSION

In summary, we report a novel human mixed-type ampullary carcinoma cell line DPC-X1 developed from a Chinese patient's tumor. This cell line provides a new experimental model for studying the biological and molecular mechanisms of ampullary carcinoma and developing new therapeutic drugs.

ARTICLE HIGHLIGHTS

Research background

To date, only eight ampullary cancer cell lines have been reported, and a mixed-type ampullary carcinoma cell line has not yet been reported.

Research motivation

There is no ampullary cancer cell line of Chinese origin, and there is no report of mixed ampullary cancer cell line.

Research objectives

To establish a stable mixed-type ampullary carcinoma cell line originating from Chinese.

Research methods

Establish cell lines through primary culture and subculture, and identify their biological characteristics.

Research results

In this study, we successfully established and characterized of a mixed-type ampullary carcinoma cell line, DPC-X1, from the primary tumor of a patient with ampullary carcinoma.

Research conclusions

DPC-X1 can be used as an effective model for studying the pathogenesis of ampullary carcinoma and drug development.

Research perspectives

The establishment of ampullary carcinoma cell lines provides suitable experimental models for further study of ampullary carcinoma.

FOOTNOTES

Author contributions: Xu H designed and coordinated the study; Xu H, Chai CP, Miao X and Tang H performed the experiments, acquired and analyzed data; Xu H, Hu JJ and Zhang H interpreted the data; Xu H, Chai CP and Zhou WC wrote the manuscript; All authors have read and approve the final manuscript.

Supported by National Natural Science Foundation of China, No. 82260555; Gansu Provincial Science and Technology Plan, No. 1606RJZA139, No. 21JR11RA096, No. 21JR1RA099, and No. 21JR1RA113; Gansu Health Industry Project, No. GSWSKY2020-21; Traditional Chinese Medicine Scientific Research Project of Gansu Province, No. GZKP-2020-28; Talent Innovation and Entrepreneurship Project of Lanzhou, No. 2020-RC-46; Intra-Hospital Fund of the First Hospital of Lanzhou University, No. ldyyyn2019-97.

Institutional review board statement: The study was conducted according to the guidelines of the Declaration of Helsinki, and approved by the Ethics Committee of the First Hospital of Lanzhou University, No. LDYYLL-2022-487.

Institutional animal care and use committee statement: The animal study was conducted according to the guidelines of the Declaration of Helsinki, and approved by the Ethics Committee of the First Hospital of Lanzhou University, No. LDYYLL-2022-487.

Informed consent statement: All study participants or their legal guardian provided informed written consent about personal and medical data collection prior to study enrolment.

Conflict-of-interest statement: All the authors report no relevant conflicts of interest for this article.

Data sharing statement: The datasets used and/or analysed during the current study are available from the corresponding author upon reasonable request.

ARRIVE guidelines statement: The authors have read the ARRIVE guidelines, and the manuscript was prepared and revised according to the ARRIVE guidelines.

Country/Territory of origin: China

ORCID number: Hao Xu 0000-0001-6459-1063; Chang-Peng Chai 0000-0001-9577-7354; Wen-Ce Zhou 0000-0002-0529-7777.

S-Editor: Fan JR
L-Editor: A
P-Editor: Yu HG

REFERENCES

1 **Ahn DH**, Bekaii-Saab T. Ampullary cancer: an overview. *Am Soc Clin Oncol Educ Book* 2014; 112-115 [PMID: 24857067 DOI: 10.14694/EdBook_AM.2014.34.112]
2 **Zheng-Pywell R**, Reddy S. Ampullary Cancer. *Surg Clin North Am* 2019; **99**: 357-367 [PMID: 30846039 DOI: 10.1016/j.suc.2018.12.001]
3 **Saha SK**, Zhu AX, Fuchs CS, Brooks GA. Forty-Year Trends in Cholangiocarcinoma Incidence in the U.S.: Intrahepatic Disease on the Rise. *Oncologist* 2016; **21**: 594-599 [PMID: 27000463 DOI: 10.1634/theoncologist.2015-0446]
4 **Fischer HP**, Zhou H. Pathogenesis of carcinoma of the papilla of Vater. *J Hepatobiliary Pancreat Surg* 2004; **11**: 301-309 [PMID: 15549428 DOI: 10.1007/s00534-004-0898-3]
5 **de Castro SM**, van Heek NT, Kuhlmann KF, Busch OR, Offerhaus GJ, van Gulik TM, Obertop H, Gouma DJ. Surgical management of neoplasms of the ampulla of Vater: local resection or pancreatoduodenectomy and prognostic factors for survival. *Surgery* 2004; **136**: 994-1002 [PMID: 15523392 DOI: 10.1016/j.surg.2004.03.010]
6 **Yeh CC**, Jeng YM, Ho CM, Hu RH, Chang HP, Tien YW. Survival after pancreaticoduodenectomy for ampullary cancer is not affected by age. *World J Surg* 2010; **34**: 2945-2952 [PMID: 20714897 DOI: 10.1007/s00268-010-0759-y]
7 **Miyakawa S**, Ishihara S, Horiguchi A, Takada T, Miyazaki M, Nagakawa T. Biliary tract cancer treatment: 5,584 results from the Biliary Tract Cancer Statistics Registry from 1998 to 2004 in Japan. *J Hepatobiliary Pancreat Surg* 2009; **16**: 1-7 [PMID: 19110652 DOI: 10.1007/s00534-008-0015-0]
8 **O'Connell JB**, Maggard MA, Manunga J Jr, Tomlinson JS, Reber HA, Ko CY, Hines OJ. Survival after resection of ampullary carcinoma: a national population-based study. *Ann Surg Oncol* 2008; **15**: 1820-1827 [PMID: 18369675 DOI: 10.1245/s10434-008-9886-1]
9 **Partelli S**, Crippa S, Capelli P, Neri A, Bassi C, Zamboni G, Barugola G, Falconi M. Adequacy of lymph node retrieval for ampullary cancer and its association with improved staging and survival. *World J Surg* 2013; **37**: 1397-1404 [PMID: 23546531 DOI: 10.1007/s00268-013-1995-8]
10 **Kimura W**, Futakawa N, Yamagata S, Wada Y, Kuroda A, Muto T, Esaki Y. Different clinicopathologic findings in two histologic types of carcinoma of papilla of Vater. *Jpn J Cancer Res* 1994; **85**: 161-166 [PMID: 7511574 DOI: 10.1111/j.1349-7006.1994.tb02077.x]
11 **Bosman FT**, Carnerio F, Hruban RH, Theise ND. WHO classifcation of tumors of the digestive system. 4th ed. Lyon: IARC, 2010
12 **Sobin LH**, Gospodarowicz MK, Ch W. International Union Against Cancer (UICC). TNM classifcation of malignant tumours, 7th edn. Chichester: Wiley-Blackwell, 2010
13 **Frazier ML**, Brown N, Pathak S, Mackay B, Cleary K, Olive M, Byrd DR, Evans DB, Levin B. Human cell line from an adenocarcinoma of the ampulla of Vater. *In Vitro Cell Dev Biol* 1992; **28A**: 149-153 [PMID: 1582987 DOI: 10.1007/BF02631083]
14 **Liu SQ**, Liu LS, Ohno T. Growth stimulation of tumor-specific cytotoxic T lymphocytes on concanavalin a-immobilized carrier beads. *Cytotechnology* 1998; **26**: 13-21 [PMID: 22359002 DOI: 10.1023/A:1007924430570]
15 **Ghosh M**, Koike N, Tsunoda S, Hirano T, Kaul S, Kashiwagi H, Kawamoto T, Ohkohchi N, Saijo K, Ohno T, Miwa M, Todoroki T. Characterization and genetic analysis in the newly established human bile duct cancer cell lines. *Int J Oncol* 2005; **26**: 449-456 [PMID: 15645130]
16 **Ku JL**, Yoon KA, Kim IJ, Kim WH, Jang JY, Suh KS, Kim SW, Park YH, Hwang JH, Yoon YB, Park JG. Establishment and characterisation of six human biliary tract cancer cell lines. *Br J Cancer* 2002; **87**: 187-193 [PMID: 12107841 DOI: 10.1038/sj.bjc.6600440]
17 **Sorio C**, Moore PS, Ennas MG, Tecchio C, Bonora A, Sartoris S, Balzarini P, Grigolato P, Scarpa A. A novel cell line and xenograft model of ampulla of Vater adenocarcinoma. *Virchows Arch* 2004; **444**: 269-277 [PMID: 14677066 DOI: 10.1007/s00428-003-0936-6]
18 **Lai ZW**, Bolm L, Fuellgraf H, Biniossek ML, Makowiec F, Hopt UT, Werner M, Keck T, Bausch D, Sorio C, Scarpa A, Schilling O, Bronsert P, Wellner UF. Characterization of various cell lines from different ampullary cancer subtypes and cancer associated fibroblast-mediated responses. *BMC Cancer* 2016; **16**: 195 [PMID: 26951071 DOI: 10.1186/s12885-016-2193-5]
19 **Ecker BL**, Vollmer CM Jr, Behrman SW, Allegrini V, Aversa J, Ball CG, Barrows CE, Berger AC, Cagigas MN, Christein JD, Dixon E, Fisher WE, Freedman-Weiss M, Guzman-Pruneda F, Hollis RH, House MG, Kent TS, Kowalsky SJ, Malleo G, Salem RR, Salvia R, Schmidt CR, Seykora TF, Zheng R, Zureikat AH, Dickson PV. Role of Adjuvant Multimodality Therapy After Curative-Intent Resection of Ampullary Carcinoma. *JAMA Surg* 2019; **154**: 706-714 [PMID: 31141112 DOI: 10.1001/jamasurg.2019.1170]
20 **Rizzo A**, Dadduzio V, Lombardi L, Ricci AD, Gadaleta-Caldarola G. Ampullary Carcinoma: An Overview of a Rare Entity and Discussion of Current and Future Therapeutic Challenges. *Curr Oncol* 2021; **28**: 3393-3402 [PMID: 34590592 DOI: 10.3390/curroncol28050293]

21 **Xu H**, Miao X, Chai C, Tang H, Hu J, Zhao Z, Luo W, Zhu K, Zhou W. Establishment and characterization of a new Chinese hepatocellular carcinoma cell line, Hep-X1. *Hum Cell* 2023; **36**: 434-445 [PMID: 36152230 DOI: 10.1007/s13577-022-00797-z]

22 **Peng J**, Xu H, Cai J. Establishment and characterization of a new gastric cancer cell line, XGC-1. *Cancer Cell Int* 2020; **20**: 437 [PMID: 32943986 DOI: 10.1186/s12935-020-01536-w]

23 **Xu H**, Peng JG, Zhuang YF, Chen JJ, Luo QC, Huang WF, Lin CD, Cai JC. Establishment and characterization of an expanding-type gastric cancer cell line by Ming's classification. *Oncol Rep* 2016; **36**: 3030-3036 [PMID: 27633271 DOI: 10.3892/or.2016.5090]

24 **Okano K**, Oshima M, Suto H, Ando Y, Asano E, Kamada H, Kobara H, Masaki T, Suzuki Y. Ampullary carcinoma of the duodenum: current clinical issues and genomic overview. *Surg Today* 2022; **52**: 189-197 [PMID: 33797636 DOI: 10.1007/s00595-021-02270-0]

25 **Albores-Saavedra J**, Schwartz AM, Batich K, Henson DE. Cancers of the ampulla of vater: demographics, morphology, and survival based on 5,625 cases from the SEER program. *J Surg Oncol* 2009; **100**: 598-605 [PMID: 19697352 DOI: 10.1002/jso.21374]

26 **Talamini MA**, Moesinger RC, Pitt HA, Sohn TA, Hruban RH, Lillemoe KD, Yeo CJ, Cameron JL. Adenocarcinoma of the ampulla of Vater. A 28-year experience. *Ann Surg* 1997; **225**: 590-9; discussion 599 [PMID: 9193186 DOI: 10.1097/00000658-199705000-00015]

27 **Perysinakis I**, Minaidou E, Leontara V, Mantas D, Sotiropoulos GC, Tsipras H, Zografos GN, Margaris I, Kouraklis G. Differential Expression of β-Catenin, EGFR, CK7, CK20, MUC1, MUC2, and CDX2 in Intestinal and Pancreatobiliary-Type Ampullary Carcinomas. *Int J Surg Pathol* 2017; **25**: 31-40 [PMID: 27543509 DOI: 10.1177/1066896916664987]

28 **Luchini C**, Veronese N, Nottegar A, Riva G, Pilati C, Mafficini A, Stubbs B, Simbolo M, Mombello A, Corbo V, Cheng L, Yachida S, Wood LD, Lawlor RT, Salvia R, Scarpa A. Perineural Invasion is a Strong Prognostic Moderator in Ampulla of Vater Carcinoma: A Meta-analysis. *Pancreas* 2019; **48**: 70-76 [PMID: 30451797 DOI: 10.1097/MPA.0000000000001194]

29 **Beroukhim R**, Mermel CH, Porter D, Wei G, Raychaudhuri S, Donovan J, Barretina J, Boehm JS, Dobson J, Urashima M, Mc Henry KT, Pinchback RM, Ligon AH, Cho YJ, Haery L, Greulich H, Reich M, Winckler W, Lawrence MS, Weir BA, Tanaka KE, Chiang DY, Bass AJ, Loo A, Hoffman C, Prensner J, Liefeld T, Gao Q, Yecies D, Signoretti S, Maher E, Kaye FJ, Sasaki H, Tepper JE, Fletcher JA, Tabernero J, Baselga J, Tsao MS, Demichelis F, Rubin MA, Janne PA, Daly MJ, Nucera C, Levine RL, Ebert BL, Gabriel S, Rustgi AK, Antonescu CR, Ladanyi M, Letai A, Garraway LA, Loda M, Beer DG, True LD, Okamoto A, Pomeroy SL, Singer S, Golub TR, Lander ES, Getz G, Sellers WR, Meyerson M. The landscape of somatic copy-number alteration across human cancers. *Nature* 2010; **463**: 899-905 [PMID: 20164920 DOI: 10.1038/nature08822]

30 **Gemble S**, Wardenaar R, Keuper K, Srivastava N, Nano M, Macé AS, Tijhuis AE, Bernhard SV, Spierings DCJ, Simon A, Goundiam O, Hochegger H, Piel M, Foijer F, Storchová Z, Basto R. Genetic instability from a single S phase after whole-genome duplication. *Nature* 2022; **604**: 146-151 [PMID: 35355016 DOI: 10.1038/s41586-022-04578-4]

31 **López S**, Lim EL, Horswell S, Haase K, Huebner A, Dietzen M, Mourikis TP, Watkins TBK, Rowan A, Dewhurst SM, Birkbak NJ, Wilson GA, Van Loo P, Jamal-Hanjani M; TRACERx Consortium, Swanton C, McGranahan N. Interplay between whole-genome doubling and the accumulation of deleterious alterations in cancer evolution. *Nat Genet* 2020; **52**: 283-293 [PMID: 32139907 DOI: 10.1038/s41588-020-0584-7]

32 **Bielski CM**, Zehir A, Penson AV, Donoghue MTA, Chatila W, Armenia J, Chang MT, Schram AM, Jonsson P, Bandlamudi C, Razavi P, Iyer G, Robson ME, Stadler ZK, Schultz N, Baselga J, Solit DB, Hyman DM, Berger MF, Taylor BS. Genome doubling shapes the evolution and prognosis of advanced cancers. *Nat Genet* 2018; **50**: 1189-1195 [PMID: 30013179 DOI: 10.1038/s41588-018-0165-1]

33 **Chen Y**, Yang Z, Wang Y, Wang J, Wang C. Karyotyping of circulating tumor cells for predicting chemotherapeutic sensitivity and efficacy in patients with esophageal cancer. *BMC Cancer* 2019; **19**: 651 [PMID: 31269908 DOI: 10.1186/s12885-019-5850-7]

34 **Wang Y**, Liu Y, Zhang L, Tong L, Gao Y, Hu F, Lin PP, Li B, Zhang T. Vimentin expression in circulating tumor cells (CTCs) associated with liver metastases predicts poor progression-free survival in patients with advanced lung cancer. *J Cancer Res Clin Oncol* 2019; **145**: 2911-2920 [PMID: 31646374 DOI: 10.1007/s00432-019-03040-9]

35 **Huang M**, Ma Y, Lv C, Li S, Lu F, Zhang S, Wang DD, Lin PP, Yang Y. Aneuploid Circulating Tumor Cells as a Predictor of Response to Neoadjuvant Chemotherapy in Non-Small Cell Lung Cancer. *Int J Gen Med* 2021; **14**: 6609-6620 [PMID: 34703281 DOI: 10.2147/IJGM.S330361]

36 **Lee AJ**, Endesfelder D, Rowan AJ, Walther A, Birkbak NJ, Futreal PA, Downward J, Szallasi Z, Tomlinson IP, Howell M, Kschischo M, Swanton C. Chromosomal instability confers intrinsic multidrug resistance. *Cancer Res* 2011; **71**: 1858-1870 [PMID: 21363922 DOI: 10.1158/0008-5472.CAN-10-3604]

37 **Brown L**, Wan H. Desmoglein 3: a help or a hindrance in cancer progression? *Cancers (Basel)* 2015; **7**: 266-286 [PMID: 25629808 DOI: 10.3390/cancers7010266]

38 **Garrod DR**. Desmosomes and cancer. *Cancer Surv* 1995; **24**: 97-111 [PMID: 7553665]

39 **Okegawa T**, Li Y, Pong RC, Hsieh JT. Cell adhesion proteins as tumor suppressors. *J Urol* 2002; **167**: 1836-1843 [PMID: 11912444]

40 **Chidgey M**, Dawson C. Desmosomes: a role in cancer? *Br J Cancer* 2007; **96**: 1783-1787 [PMID: 17519903 DOI: 10.1038/sj.bjc.6603808]

41 **Dusek RL**, Attardi LD. Desmosomes: new perpetrators in tumour suppression. *Nat Rev Cancer* 2011; **11**: 317-323 [PMID: 21508970 DOI: 10.1038/nrc3051]

42 **Moh MC**, Shen S. The roles of cell adhesion molecules in tumor suppression and cell migration: a new paradox. *Cell Adh Migr* 2009; **3**: 334-336 [PMID: 19949308 DOI: 10.4161/cam.3.4.9246]

43 **Lamouille S**, Xu J, Derynck R. Molecular mechanisms of epithelial-mesenchymal transition. *Nat Rev Mol Cell Biol* 2014; **15**: 178-196 [PMID: 24556840 DOI: 10.1038/nrm3758]

44 **Davies M**, Robinson M, Smith E, Huntley S, Prime S, Paterson I. Induction of an epithelial to mesenchymal transition in

human immortal and malignant keratinocytes by TGF-beta1 involves MAPK, Smad and AP-1 signalling pathways. *J Cell Biochem* 2005; **95**: 918-931 [PMID: 15861394 DOI: 10.1002/jcb.20458]

45 **Massa A**, Varamo C, Vita F, Tavolari S, Peraldo-Neia C, Brandi G, Rizzo A, Cavalloni G, Aglietta M. Evolution of the Experimental Models of Cholangiocarcinoma. *Cancers (Basel)* 2020; **12** [PMID: 32824407 DOI: 10.3390/cancers12082308]

46 **Li M**, Zhou X, Wang W, Ji B, Shao Y, Du Q, Yao J, Yang Y. Selecting an Appropriate Experimental Animal Model for Cholangiocarcinoma Research. *J Clin Transl Hepatol* 2022; **10**: 700-710 [PMID: 36062286 DOI: 10.14218/JCTH.2021.00374]

World Journal of Gastroenterology

Submit a Manuscript: https://www.f6publishing.com

World J Gastroenterol 2023 May 7; 29(17): 2657-2665

DOI: 10.3748/wjg.v29.i17.2657

ISSN 1007-9327 (print) ISSN 2219-2840 (online)

ORIGINAL ARTICLE

Retrospective Study

Mucosal patterns change after *Helicobacter pylori* eradication: Evaluation using blue laser imaging in patients with atrophic gastritis

Yoshiyuki Nishikawa, Yoshio Ikeda, Hidehiro Murakami, Shin-Ichiro Hori, Megumi Yoshimatsu, Naoki Nishikawa

Specialty type: Gastroenterology and hepatology

Provenance and peer review: Unsolicited article; Externally peer reviewed.

Peer-review model: Single blind

Peer-review report's scientific quality classification

Grade A (Excellent): 0
Grade B (Very good): 0
Grade C (Good): C, C
Grade D (Fair): D
Grade E (Poor): 0

P-Reviewer: Kotelevets SM, Russia; Senchukova M, Russia

Received: February 8, 2023
Peer-review started: February 8, 2023
First decision: February 16, 2023
Revised: March 3, 2023
Accepted: April 7, 2023
Article in press: April 7, 2023
Published online: May 7, 2023

Yoshiyuki Nishikawa, Department of Gastroenterology, Nishikawa Gastrointestinal Clinic, Matsuyama 790-0878, Ehime, Japan

Yoshio Ikeda, Endoscopy Center, Ehime University Hospital, Toon 791-0295, Ehime, Japan

Hidehiro Murakami, Department of Internal Medicine, Saiseikai Matsuyama Hospital, Matsuyama 791-8026, Ehime, Japan

Shin-Ichiro Hori, Department of Gastroenterology, Himeji Red Cross Hospital, Himeji 670-8540, Hyogo, Japan

Megumi Yoshimatsu, Department of Gastroenterology, National Hospital Organization Shikoku Cancer Center, Matsuyama 791-0280, Ehime, Japan

Naoki Nishikawa, Department of Gastroenterology, Matsuyama Shimin Hospital, Matsuyama 790-0067, Ehime, Japan

Corresponding author: Yoshiyuki Nishikawa, MD, PhD, Director, Department of Gastroenterology, Nishikawa Gastrointestinal Clinic, 2-72 Katsuyama-cho, Matsuyama 790-0878, Ehime, Japan. yonishik@ehime.med.or.jp

Abstract

BACKGROUND

Mucosal patterns (MPs) observed on blue laser imaging in patients with atrophic gastritis can be classified as spotty, cracked, and mottled. Furthermore, we hypothesized that the spotty pattern may change to the cracked pattern after *Helicobacter pylori* (*H. pylori*) eradication.

AIM

To further substantiate and comprehensively investigate MP changes after *H. pylori* eradication in a larger number of patients.

METHODS

We included 768 patients who were diagnosed with atrophic gastritis with evaluable MP using upper gastrointestinal endoscopy at the Nishikawa Gas-

trointestinal Clinic, Japan. Among them, 325 patients were *H. pylori*-positive, and of them, 101 patients who underwent upper gastrointestinal endoscopy before and after *H. pylori* eradication were evaluated for post-eradication MP changes. The patients' MPs were interpreted by three experienced endoscopists who were blinded to their clinical features.

RESULTS

Among 76 patients with the spotty pattern before or after *H. pylori* eradication, the pattern disappeared or decreased in 67 patients [88.2%, 95% confidence interval (CI): 79.0%-93.6%), appeared or increased in 8 patients (10.5%, 95%CI: 5.4%-19.4%), and showed no change in 1 patient (1.3%, 95%CI: 0.2%-7.1%). In 90 patients with the cracked pattern before or after *H. pylori* eradication, the pattern disappeared or decreased in 7 patients (7.8%, 95%CI: 3.8%-15.2%), appeared or increased in 79 patients (87.8%, 95%CI: 79.4%-93.0%), and showed no change in 4 patients (4.4%, 95%CI: 1.7%-10.9%). In 70 patients with the mottled pattern before or after *H. pylori* eradication, the pattern disappeared or decreased in 28 patients (40.0%, 95%CI: 29.3%-51.7%), appeared or increased in 35 patients (50.0%, 95%CI: 38.6%-61.4%), and showed no change in 7 patients (10.0%, 95%CI: 4.9%-19.2%).

CONCLUSION

After *H. pylori* eradication, MPs changed from spotty to cracked in most patients, which may help endoscopists easily and precisely evaluate *H. pylori*-related gastritis status.

Key Words: Atrophic gastritis; *Helicobacter pylori*; Gastrointestinal endoscopy; Image enhancement; Classification

Core Tip: We investigated whether the mucosal patterns on blue laser imaging may change from spotty to cracked after *Helicobacter pylori* (*H. pylori*) eradication. The spotty pattern disappeared or decreased in 88.2% of patients, while the cracked pattern appeared or increased in 87.8% of patients. These suggest that the spotty pattern observed in *H. pylori*-positive patients is likely to disappear after eradication and may be replaced by the cracked pattern. These observations may help endoscopists easily and precisely evaluate *H. pylori*-related gastritis status.

Citation: Nishikawa Y, Ikeda Y, Murakami H, Hori SI, Yoshimatsu M, Nishikawa N. Mucosal patterns change after *Helicobacter pylori* eradication: Evaluation using blue laser imaging in patients with atrophic gastritis. *World J Gastroenterol* 2023; 29(17): 2657-2665
URL: https://www.wjgnet.com/1007-9327/full/v29/i17/2657.htm
DOI: https://dx.doi.org/10.3748/wjg.v29.i17.2657

INTRODUCTION

Helicobacter pylori (*H. pylori*) infection and related atrophic gastritis is closely associated with the development of gastric cancer[1]. Therefore, it is critical to observe the gastric mucosa to precisely judge the infection status as "current," "previous," or "none." Recently, various types of image-enhanced endoscopy have been used to ensure the accurate evaluation of *H. pylori* infection[2-6].

In our previous study[7], we classified mucosal patterns (MPs) into three types (spotty, cracked, and mottled) using blue laser imaging (BLI)[8,9] in patients with *H. pylori*-related gastritis. We found that the spotty pattern indicated the possibility of *H. pylori* infection, the cracked pattern indicated a post-inflammatory change after *H. pylori* eradication, and the mottled pattern indicated an intestinal metaplasia resulting from the progression of *H. pylori*-related gastritis. Thus, we hypothesized that the spotty pattern would disappear or decrease and the cracked pattern would newly appear or increase after *H. pylori* eradication.

To further explore these changes, we quantitatively analyzed the changes to determine whether each pattern would increase, decrease, or remain unchanged. Since little is known concerning the pattern changes after *H. pylori* eradication, clarification of these changes may help endoscopists diagnose the existing pattern as being pre- or post-eradication and understand the MP changes more precisely. Thus, this study aimed to clarify the significance and diagnostic viability of each MP using BLI.

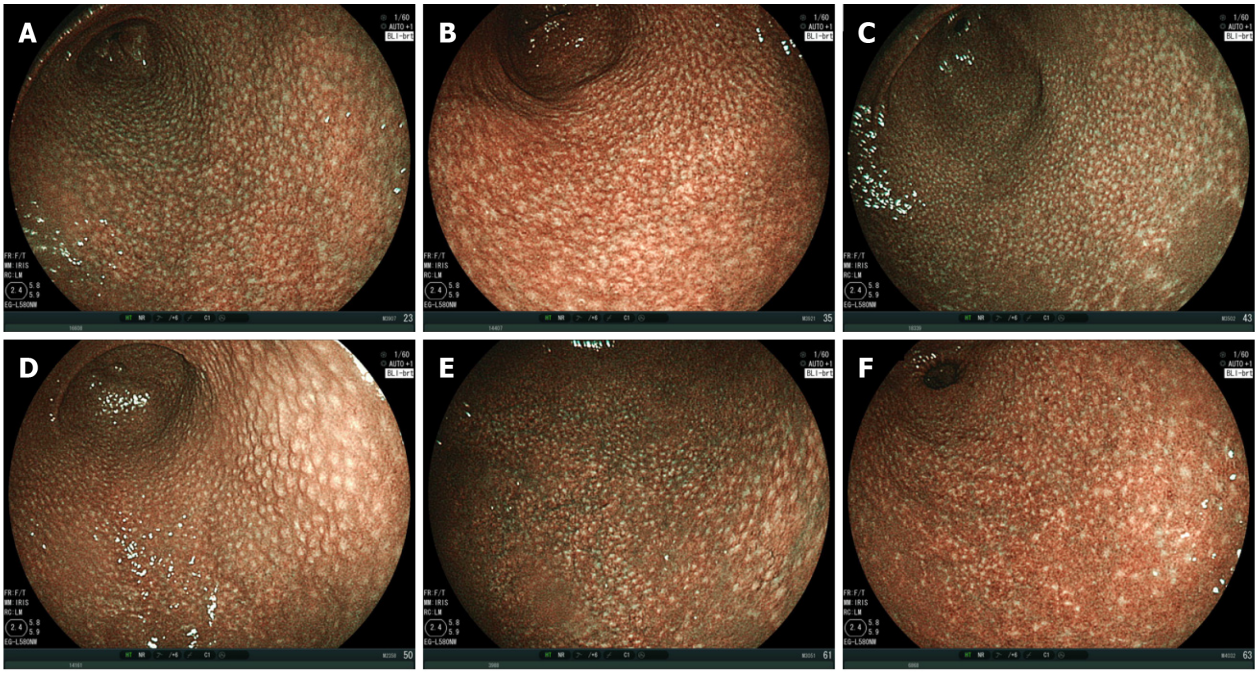

DOI: 10.3748/wjg.v29.i17.2657

Figure 1 Spotty pattern. Representative images of the spotty pattern shown as white spots of 1-2 mm in diameter in the gastric antrum of 6 patients infected with *Helicobacter pylori* (*H. pylori*) observed using blue laser imaging-bright mode. A: 45-year-old female, *H. pylori*-positive; B: 51-year-old female, *H. pylori*-positive; C: 27-year-old female, *H. pylori*-positive; D: 59-year-old female, *H. pylori*-positive, nodular gastritis; E: 49-year-old male, *H. pylori*-positive; F: 66-year-old female, *H. pylori*-positive.

MATERIALS AND METHODS

Patients and methods

A total of 2242 patients underwent upper gastrointestinal (GI) endoscopy at the Nishikawa Gastrointestinal Clinic, Ehime, Japan from April 1, 2015 to March 31, 2017. Of these, 768 patients were endoscopically diagnosed with atrophic gastritis. The presence or absence of *H. pylori* infection was confirmed. Among them, 325 patients were *H. pylori*-positive, and of them, 101 patients who underwent *H. pylori* eradication and subsequent endoscopy were examined for MP changes.

An EG-L580NW nasal upper GI endoscope (FUJIFILM Medical Co. Ltd., Tokyo, Japan) was used orally or nasally. The BLI bright mode was used to evaluate MPs in the intermediate or distant views.

This study was approved by the Ethics Committee of Ehime University Hospital (No: 1605010; August 22, 2016). Prior to receiving an endoscopic examination, all patients agreed that the data obtained in this study might be published in academic papers.

Classification of MPs

The MPs were classified into three types: The spotty pattern, which consists of 1-2 mm diameter spots (Figure 1); the cracked pattern, which consists of net-like cracks (Figure 2); and the mottled pattern, which has a mottled appearance (Figure 3)[7].

Evaluation of the MP changes after H. pylori eradication

The MP patterns were evaluated as follows: (1) Three expert GI endoscopists, with at least 25 years of experience, evaluated the mucosal changes after *H. pylori* eradication; (2) They were blinded to the patients' endoscopic data, including the patterns obtained before and/or after *H. pylori* eradication; (3) They compared two randomly listed endoscopic image groups and evaluated which image group was dominant, less dominant, equal, or absent for the spotty, cracked, and mottled patterns; (4) When two or all endoscopists agreed on a particular pattern, that pattern was adopted for analysis. When they had conflicting pattern determinations, the final determination was reached through a joint discussion; and (5) *H. pylori* infection was diagnosed using the anti-*H. pylori* IgG antibody serology tests[10,11], urea breath tests[12-15], and biopsies.

Statistical analysis

Student's *t*-test was used for the analysis of age, and the χ^2 test was used for the analyses of other variables. Statistical significance was set at $P < 0.05$. A 95% confidence interval (CI) was calculated to determine the uncertainty of the sample estimates. All statistical analyses were performed using

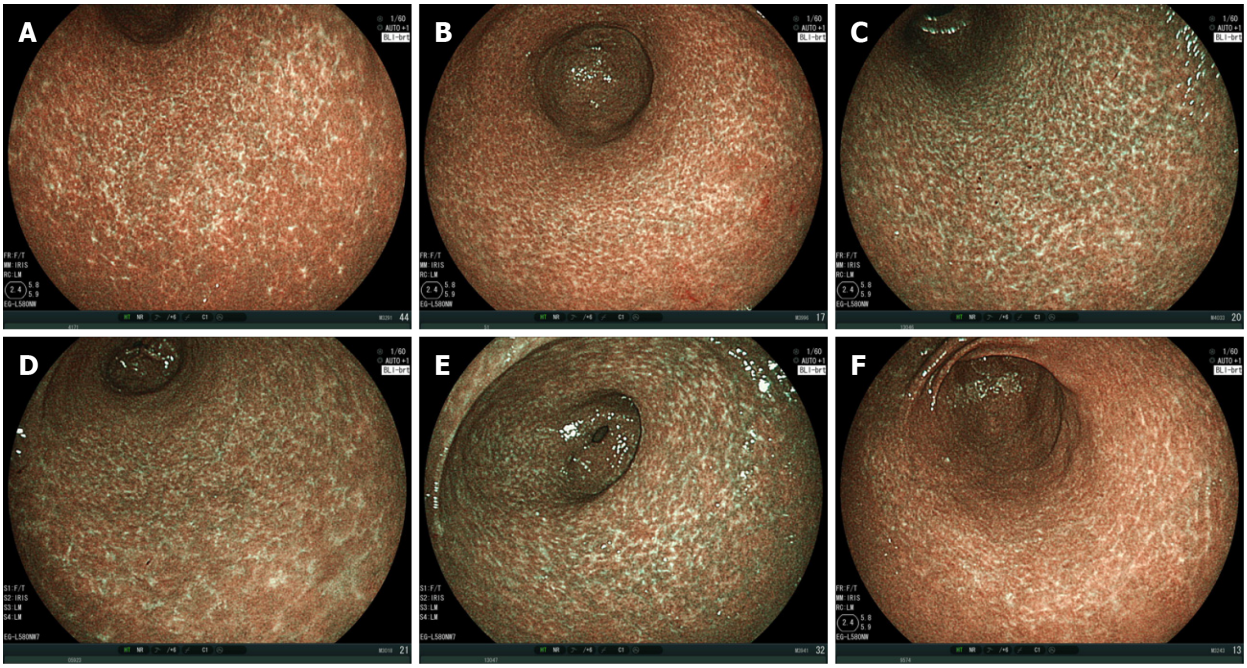

DOI: 10.3748/wjg.v29.i17.2657

Figure 2 Cracked pattern. Representative images of the cracked pattern as white net-like cracks consisting of lines in the gastric antrum of 6 patients after *Helicobacter pylori* (*H. pylori*) eradication observed using blue laser imaging-bright mode. A: 69-year-old female, *H. pylori*-negative, 2 years, 11 mo after eradication; B: 75-year-old female, *H. pylori*-negative, 6 years, 0 mo after eradication; C: 63-year-old female, *H. pylori*-negative, 1 year, 2 mo after eradication; D: 72-year-old female, *H. pylori*-negative, 1 year, 0 mo after eradication; E: 63-year-old female, *H. pylori*-negative, 1 year, 2 mo after eradication; F: 52-year-old male, *H. pylori*-negative, 2 years, 1 mo after eradication.

Microsoft Excel 2016, version 1907, Build 11901.20176 (Microsoft Corporation, Redmond, WA, United States), and the statistical methods of this study were reviewed by Dr. Natsumi Yamashita from Clinical Research Center, National Hospital Organization Shikoku Cancer Center.

RESULTS

Patient characteristics

The number of patients evaluated was 768 (480 females and 288 males) with a mean age of 65.8 ± 12.9 (standard deviation) years. The numbers of patients with and without *H. pylori* infection were 325 (204 females and 121 males) and 443 (276 females and 167 males), respectively.

The mean ages of patients with and without *H. pylori* infection were 61.6 ± 14.3 years and 68.9 ± 10.7 years, respectively, with significant differences among them ($P < 0.001$). No significant difference was observed between the proportions of female and male patients with and without *H. pylori* infection ($P = 0.895$; Table 1).

Changes in MPs after H. pylori eradication

Upper GI endoscopy was performed for 101 patients (females: 75; males: 26; mean age: 57.5 ± 14.1 years) who successfully underwent *H. pylori* eradication, and the endoscopic mucosal changes were evaluated. Patients in whom evaluation was difficult because there were no comparable images of the specific parts were excluded from the analysis. The mean interval between *H. pylori* eradication and post-eradication endoscopy was 27.1 ± 13.1 mo.

In our study, multiple patterns commonly coexisted in many patients, with some patients having all three patterns. Of the 101 patients, 38 patients showed all three patterns (spotty, cracked, and mottled), 59 had two patterns (spotty and cracked, 28; spotty and mottled, 7; and cracked and mottled, 24), and 4 patients presented with only one pattern (spotty, 3; cracked, 0; and mottled, 1) either before or after eradication.

In 76 patients with a spotty pattern before or after *H. pylori* eradication, the pattern disappeared or decreased in 67 patients (88.2%, 95%CI: 79.0%-93.6%) and appeared or increased in 8 patients (10.5%, 95%CI: 5.4%-19.4%). In 1 patient (1.3%, 95%CI: 0.2%-7.1%), no change was observed after *H. pylori* eradication.

In 90 patients with a cracked pattern before or after *H. pylori* eradication, the pattern disappeared or decreased in 7 patients (7.8%, 95%CI: 3.8%-15.2%) and appeared or increased in 79 patients (87.8%,

Table 1 Patient characteristics

Item	Patients with atrophic gastritis	Patients with *H. pylori* infection	Patients underwent both *H. pylori* eradication and follow up endoscopy
No. of patients	768	325	101
Age, mean ± SD	65.8 ± 12.9	61.6 ± 14.3	57.5 ± 14.1
Female	480	204	75
Male	288	121	26

SD: Standard deviation; *H. pylori: Helicobacter pylori*.

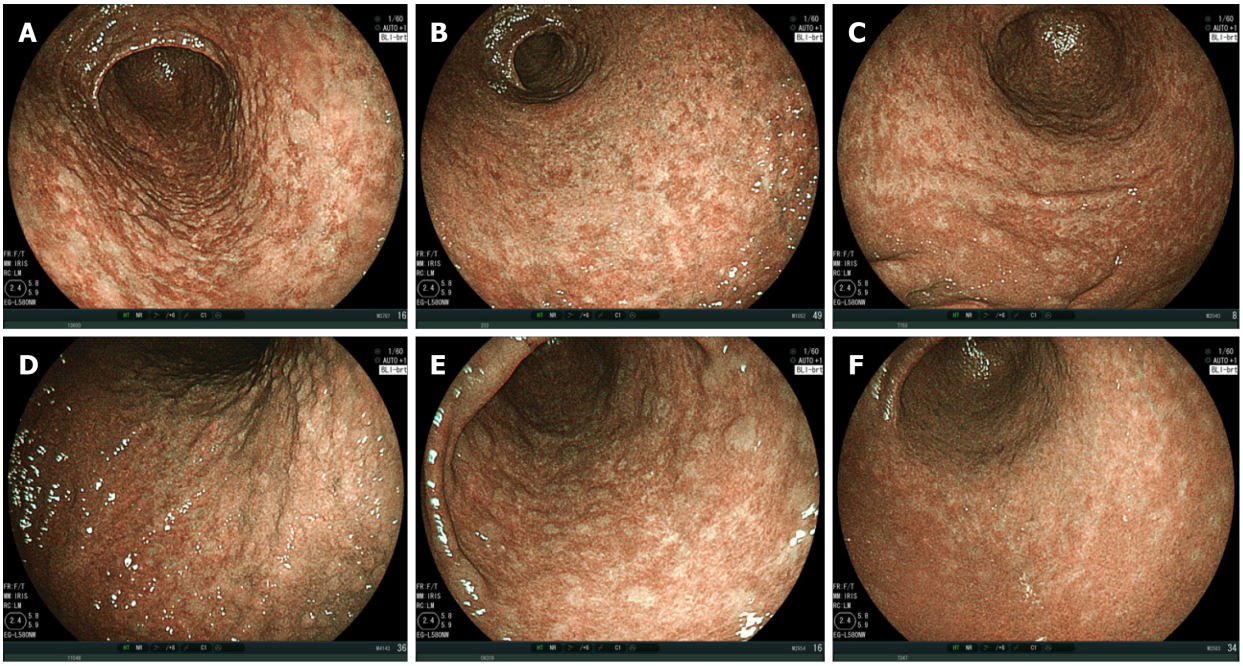

DOI: 10.3748/wjg.v29.i17.2657

Figure 3 Mottled pattern. Representative images of the mottled pattern observed using blue laser imaging-bright mode in the gastric antrum of 6 patients. The whitish-colored mottled areas varied from small to large. Only panel A shows the pattern of a patient infected with *Helicobacter pylori* (*H. pylori*). A: 67-year-old male, *H. pylori*-positive, before eradication; B: 74-year-old male, *H. pylori*-negative, no eradication; C: 73-year-old female, *H. pylori*-negative, 2 years, 11 mo after eradication; D: 87-year-old male, *H. pylori*-negative, no eradication; E: 83-year-old male, *H. pylori*-negative, 5 years, 2 mo after eradication; F: 60-year-old female, *H. pylori*-negative, 2 years, 2 mo after eradication.

95%CI: 79.4%-93.0%). In 4 patients (4.4%, 95%CI: 1.7%-10.9%), no change was observed after *H. pylori* eradication.

In 70 patients with a mottled pattern before or after *H. pylori* eradication, the pattern disappeared or decreased in 28 patients (40.0%, 95%CI: 29.3%-51.7%) and appeared or increased in 35 patients (50.0%, 95%CI: 38.6%-61.4%). In 7 patients (10.0%, 95%CI: 4.9%-19.2%), no change was observed after *H. pylori* eradication (Figure 4).

We investigated the relationship between the spotty and cracked patterns before and after eradication. The spotty pattern disappeared or decreased in 67 out of the 76 patients who had a spotty pattern before or after eradication. Of the 67 patients, the cracked pattern appeared or increased in 55 patients. Among the 8 patients with spotty patterns that appeared or increased after eradication, the cracked pattern appeared or increased in 5 patients. The cracked pattern appeared or increased in most of the 25 patients who did not have a spotty pattern before or after eradication (Figure 5).

We further investigated the difference in MP changes due to *H. pylori* eradication between the short-term (8-24 mo) and long-term (25-60 mo) observation groups. The spotty pattern disappeared or decreased in 88.6% and 87.8% (short-term *vs* long-term) of the patients. The cracked pattern newly appeared or increased in 88.9% and 86.7% (short-term *vs* long-term) of the patients. No significant differences were observed between the patients under short-term and long-term observations.

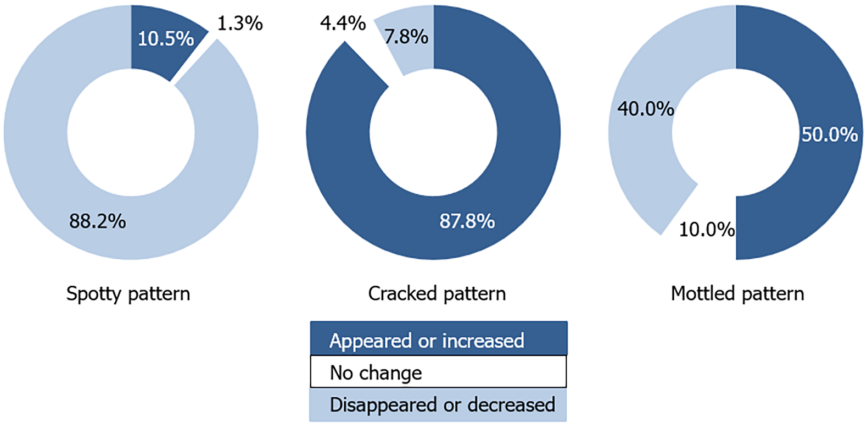

DOI: 10.3748/wjg.v29.i17.2657

Figure 4 Change in mucosal pattern after *Helicobacter pylori* eradication. The spotty pattern tended to disappear or decrease, the cracked pattern appeared or increased, and the mottled pattern exhibited no specific tendency.

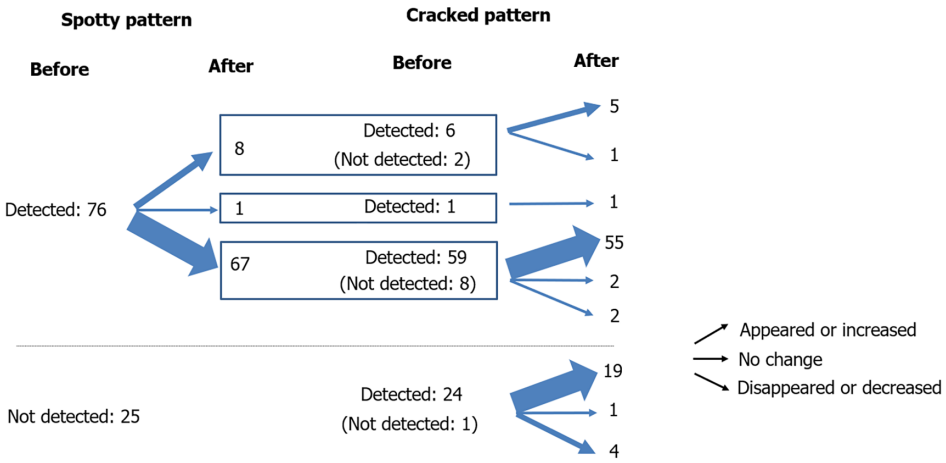

DOI: 10.3748/wjg.v29.i17.2657

Figure 5 Relationship between the spotty and cracked patterns before and after *Helicobacter pylori* eradication.

DISCUSSION

We investigated the use of BLI, an image-enhanced endoscopy, for the diagnosis of *H. pylori*-related gastritis, with a focus on the MP changes after *H. pylori* eradication. The Kyoto Classification of Gastritis was established in 2014 for the endoscopic diagnosis of *H. pylori*-related gastritis[16,17]. The classification of MPs observed on BLI in this study is simpler and easier to use in endoscopic assessment than the Kyoto classification and thus has the potential to become a new standard method with the addition of new diagnostic information to the Kyoto classification. We previously reported the efficacy of MPs on BLI in an intermediate-to-distant view evaluation of *H. pylori* infection and had the benefits of easy detection of atrophic gastritis and easy diagnosis of infection status (current, previous, or no infection) [7].

The results obtained in the current study indicate that the disappearance of the spotty pattern is evidence of *H. pylori* clearance, while newly-appearing cracked pattern is evidence of post-gastritis healing. The mottled pattern may reflect "intestinal metaplasia," as identified in our previous study using biopsies.

Knowledge of the endoscopic changes after *H. pylori* eradication is helpful in clarifying the meaning of each MP. The spotty pattern disappeared or decreased in 88.2% of patients, whereas the cracked pattern appeared or increased in 87.8% of patients after *H. pylori* eradication. The mottled pattern exhibited no specific tendency. As indicated in Figure 5, the spotty pattern observed in *H. pylori*-positive patients before eradication may disappear and may be replaced by the cracked pattern. Based on these observations, we can diagnose the *H. pylori* infection status as current, previous, or no infection. No difference was detected between the short-term and long-term observations of MP changes after *H. pylori* eradication, suggesting that the changes in MP would occur relatively quickly after eradication. The primary tendency of MP changes after *H. pylori* eradication have been clarified in this study. Irregular pattern changes (those other than spotty to cracked pattern) were observed after eradication in

a limited number of patients. Further verification is necessary.

CONCLUSION

In conclusion, the spotty pattern may indicate *H. pylori* infection, the cracked pattern may indicate post-inflammatory changes after *H. pylori* eradication, and the mottled pattern may indicate intestinal metaplasia resulting from the progression of *H. pylori*-related gastritis. We verified that MPs on BLI may change from a spotty to a cracked pattern after *H. pylori* eradication. These observations may help endoscopists easily and precisely evaluate the status of *H. pylori*-related gastritis. We hope that MP changes on BLI will be routinely used to confirm the diagnosis of *H. pylori*-related gastritis in the future.

ARTICLE HIGHLIGHTS

Research background

Determination of the presence or absence of *Helicobacter pylori* (*H. pylori*) infection is important in the diagnosis of atrophic gastritis. Various studies have been conducted to distinguish these two conditions.

Research motivation

In our previous study, we reported that *H. pylori* eradication may lead to the disappearance of the spotty pattern and the appearance of the cracked pattern.

Research objectives

To further substantiate and comprehensively investigate mucosal pattern changes after *H. pylori* eradication in a larger number of patients.

Research methods

Among the patients with atrophic gastritis in whom *H. pylori* positivity was confirmed, we investigated 101 patients who underwent both *H. pylori* eradication and follow-up endoscopy and evaluated the change of patterns before and after eradication.

Research results

The spotty pattern tended to disappear or decrease, and the cracked pattern tended to appear or increase after *H. pylori* eradication, while the mottled pattern exhibited no specific tendency.

Research conclusions

The spotty pattern likely changes to the cracked pattern after *H. pylori* eradication.

Research perspectives

In future studies, it will be necessary to examine the morphological and histological changes of each mucosal pattern, compare these pattern changes with the Kyoto classification, examine the relationship with other classifications of atrophic gastritis, and clarify the meaning of the mucosal pattern changes.

FOOTNOTES

Author contributions: Nishikawa Y conceived and designed the study; Nishikawa Y, Ikeda Y, Murakami H, Hori S, and Yoshimatsu M analyzed and interpreted the data; Nishikawa Y and Nishikawa N drafted the manuscript; Nishikawa Y, Ikeda Y, Murakami H, Hori S, Yoshimatsu M, and Nishikawa N critically revised the manuscript for important intellectual content; Nishikawa Y gave final approval of the manuscript; all authors approved the final version of the article to be published.

Institutional review board statement: This study was approved by the Ethics Committee of Ehime University Hospital (No. 1605010; August 22, 2016).

Informed consent statement: This study was conducted retrospectively from data obtained for clinical purposes. The study was approved by the institutional review board at the Ethics Committee of Ehime University Hospital. Prior to receiving an endoscopic examination, all patients agreed that the data obtained in this study might be published in academic papers.

Conflict-of-interest statement: None of the authors have any financial relationships to disclose with relevance to this article.

Data sharing statement: Data presented in this study is available on request from the corresponding author.

Country/Territory of origin: Japan

ORCID number: Yoshiyuki Nishikawa 0000-0001-8162-9369; Yoshio Ikeda 0009-0009-8832-7852; Hidehiro Murakami 0000-0002-6261-2964; Shin-Ichiro Hori 0000-0002-9393-4413; Megumi Yoshimatsu 0009-0005-8227-0905; Naoki Nishikawa 0009-0003-7489-9071.

S-Editor: Yan JP
L-Editor: A
P-Editor: Chen YX

REFERENCES

1 **Uemura N**, Okamoto S, Yamamoto S, Matsumura N, Yamaguchi S, Yamakido M, Taniyama K, Sasaki N, Schlemper RJ. Helicobacter pylori infection and the development of gastric cancer. *N Engl J Med* 2001; **345**: 784-789 [PMID: 11556297 DOI: 10.1056/NEJMoa001999]

2 **Dohi O**, Majima A, Naito Y, Yoshida T, Ishida T, Azuma Y, Kitae H, Matsumura S, Mizuno N, Yoshida N, Kamada K, Itoh Y. Can image-enhanced endoscopy improve the diagnosis of Kyoto classification of gastritis in the clinical setting? *Dig Endosc* 2020; **32**: 191-203 [PMID: 31550395 DOI: 10.1111/den.13540]

3 **Glover B**, Teare J, Patel N. A systematic review of the role of non-magnified endoscopy for the assessment of H. pylori infection. *Endosc Int Open* 2020; **8**: E105-E114 [PMID: 32010741 DOI: 10.1055/a-0999-5252]

4 **Alaboudy AA**, Elbahrawy A, Matsumoto S, Yoshizawa A. Conventional narrow-band imaging has good correlation with histopathological severity of Helicobacter pylori gastritis. *Dig Dis Sci* 2011; **56**: 1127-1130 [PMID: 20857197 DOI: 10.1007/s10620-010-1414-z]

5 **Tongtawee T**, Kaewpitoon S, Kaewpitoon N, Dechsukhum C, Loyd RA, Matrakool L. Correlation between Gastric Mucosal Morphologic Patterns and Histopathological Severity of Helicobacter pylori Associated Gastritis Using Conventional Narrow Band Imaging Gastroscopy. *Biomed Res Int* 2015; **2015**: 808505 [PMID: 26120585 DOI: 10.1155/2015/808505]

6 **Takeda T**, Asaoka D, Nojiri S, Nishiyama M, Ikeda A, Yatagai N, Ishizuka K, Hiromoto T, Okubo S, Suzuki M, Nakajima A, Nakatsu Y, Komori H, Akazawa Y, Nakagawa Y, Izumi K, Matsumoto K, Ueyama H, Sasaki H, Shimada Y, Osada T, Hojo M, Kato M, Nagahara A. Linked Color Imaging and the Kyoto Classification of Gastritis: Evaluation of Visibility and Inter-Rater Reliability. *Digestion* 2020; **101**: 598-607 [PMID: 31302654 DOI: 10.1159/000501534]

7 **Nishikawa Y**, Ikeda Y, Murakami H, Hori SI, Hino K, Sasaki C, Nishikawa M. Classification of atrophic mucosal patterns on Blue LASER Imaging for endoscopic diagnosis of Helicobacter pylori-related gastritis: A retrospective, observational study. *PLoS One* 2018; **13**: e0193197 [PMID: 29596454 DOI: 10.1371/journal.pone.0193197]

8 **Yoshida N**, Yagi N, Inada Y, Kugai M, Okayama T, Kamada K, Katada K, Uchiyama K, Ishikawa T, Handa O, Takagi T, Konishi H, Kokura S, Yanagisawa A, Naito Y. Ability of a novel blue laser imaging system for the diagnosis of colorectal polyps. *Dig Endosc* 2014; **26**: 250-258 [PMID: 23731034 DOI: 10.1111/den.12127]

9 **Osawa H**, Yamamoto H. Present and future status of flexible spectral imaging color enhancement and blue laser imaging technology. *Dig Endosc* 2014; **26** Suppl 1: 105-115 [PMID: 24373002 DOI: 10.1111/den.12205]

10 **Feldman RA**, Deeks JJ, Evans SJ. Multi-laboratory comparison of eight commercially available Helicobacter pylori serology kits. Helicobacter pylori Serology Study Group. *Eur J Clin Microbiol Infect Dis* 1995; **14**: 428-433 [PMID: 7556232 DOI: 10.1007/BF02114899]

11 **Loy CT**, Irwig LM, Katelaris PH, Talley NJ. Do commercial serological kits for Helicobacter pylori infection differ in accuracy? *Am J Gastroenterol* 1996; **91**: 1138-1144 [PMID: 8651160]

12 **Graham DY**, Klein PD, Evans DJ Jr, Evans DG, Alpert LC, Opekun AR, Boutton TW. Campylobacter pylori detected noninvasively by the 13C-urea breath test. *Lancet* 1987; **1**: 1174-1177 [PMID: 2883491 DOI: 10.1016/s0140-6736(87)92145-3]

13 **Logan RP**, Polson RJ, Misiewicz JJ, Rao G, Karim NQ, Newell D, Johnson P, Wadsworth J, Walker MM, Baron JH. Simplified single sample 13Carbon urea breath test for Helicobacter pylori: comparison with histology, culture, and ELISA serology. *Gut* 1991; **32**: 1461-1464 [PMID: 1773948 DOI: 10.1136/gut.32.12.1461]

14 **Ohara S**, Kato M, Asaka M, Toyota T. Studies of 13C-urea breath test for diagnosis of Helicobacter pylori infection in Japan. *J Gastroenterol* 1998; **33**: 6-13 [PMID: 9497214 DOI: 10.1007/pl00009968]

15 **Gisbert JP**, Pajares JM. Review article: 13C-urea breath test in the diagnosis of Helicobacter pylori infection -- a critical review. *Aliment Pharmacol Ther* 2004; **20**: 1001-1017 [PMID: 15569102 DOI: 10.1111/j.1365-2036.2004.02203.x]

16 **Haruma K**, Kato M, Inoue K, Murakami K, Kamada T. Kyoto Classification of Gastritis. Tokyo: Nihon Medical Center, Ltd., 2014

17 **Toyoshima O**, Nishizawa T, Koike K. Endoscopic Kyoto classification of Helicobacter pylori infection and gastric cancer

risk diagnosis. *World J Gastroenterol* 2020; **26**: 466-477 [PMID: 32089624 DOI: 10.3748/wjg.v26.i5.466]

World Journal of Gastroenterology

Submit a Manuscript: https://www.f6publishing.com

World J Gastroenterol 2023 May 7; 29(17): 2666-2678

DOI: 10.3748/wjg.v29.i17.2666

ISSN 1007-9327 (print) ISSN 2219-2840 (online)

ORIGINAL ARTICLE

Randomized Controlled Trial

Fecal microbiota transplantation for the maintenance of remission in patients with ulcerative colitis: A randomized controlled trial

Perttu Lahtinen, Jonna Jalanka, Eero Mattila, Jyrki Tillonen, Paula Bergman, Reetta Satokari, Perttu Arkkila

Specialty type: Gastroenterology and hepatology

Provenance and peer review: Unsolicited article; Externally peer reviewed.

Peer-review model: Single blind

Peer-review report's scientific quality classification

Grade A (Excellent): 0
Grade B (Very good): 0
Grade C (Good): C, C, C, C
Grade D (Fair): D
Grade E (Poor): 0

P-Reviewer: Triantafillidis J, Greece; Wang LH, China; Zhang Z, China; Zhang F, China

Received: December 27, 2022
Peer-review started: December 27, 2022
First decision: January 22, 2023
Revised: February 6, 2023
Accepted: April 11, 2023
Article in press: April 11, 2023
Published online: May 7, 2023

Perttu Lahtinen, Jyrki Tillonen, Department of Gastroenterology, Päijät-Häme Central Hospital, Lahti 15610, Finland

Perttu Lahtinen, Department of Medicine, University of Helsinki, Helsinki 00014, Finland

Jonna Jalanka, Reetta Satokari, Human Microbiome Research Program, Faculty of Medicine, University of Helsinki, Helsinki 00014, Finland

Eero Mattila, Department of Infectious Diseases, Helsinki University Hospital, Helsinki 00029, Uusimaa, Finland

Paula Bergman, Department of Bioinformatics, Helsinki University Hospital, Helsinki 00014, Finland

Perttu Arkkila, Department of Gastroenterology, University Helsinki, Center Hospital, Helsinki 00029, Uusimaa, Finland

Corresponding author: Perttu Lahtinen, MD, Chief Doctor, Department of Gastroenterology, Päijät-Häme Central Hospital, Keskussairaalankatu 7, Lahti 15610, Finland.
perttu.lahtinen@phhyky.fi

Abstract

BACKGROUND

Fecal microbial transplantation (FMT) is a promising new method for treating active ulcerative colitis (UC), but knowledge regarding FMT for quiescent UC is scarce.

AIM

To investigate FMT for the maintenance of remission in UC patients.

METHODS

Forty-eight UC patients were randomized to receive a single-dose FMT or autologous transplant *via* colonoscopy. The primary endpoint was set to the maintenance of remission, a fecal calprotectin level below 200 μg/g, and a clinical Mayo score below three throughout the 12-mo follow-up. As secondary end-points, we recorded the patient's quality of life, fecal calprotectin, blood chemistry, and endoscopic findings at 12 mo.

RESULTS

The main endpoint was achieved by 13 out of 24 (54%) patients in the FMT group and by 10 out of 24 (41%) patients in the placebo group (log-rank test, P = 0.660). Four months after FMT, the quality-of-life scores decreased in the FMT group compared to the placebo group (P = 0.017). In addition, the disease-specific quality of life measure was higher in the placebo group than in the FMT group at the same time point (P = 0.003). There were no differences in blood chemistry, fecal calprotectin, or endoscopic findings among the study groups at 12 mo. The adverse events were infrequent, mild, and distributed equally between the groups.

CONCLUSION

There were no differences in the number of relapses between the study groups at the 12-mo follow-up. Thus, our results do not support the use of a single-dose FMT for the maintenance of remission in UC.

Key Words: Fecal microbial transplantation; Ulcerative colitis; Quality of life; Maintenance of remission; Inflammatory bowel disease; Fecal calprotectin

Core Tip: This randomized controlled trial compared the efficacy of fecal microbial transplantation *via* colonoscopy and autologous placebo containing patients' own feces for the maintenance of remission in 48 patients with ulcerative colitis. The colitis activity was measured with the clinical Mayo score and fecal calprotectin. There was no significant difference in relapses between the groups at the 12-mo follow-up. Remission remained in 54% of the patients in the fecal microbial transplantation group compared to 41% in the placebo group. There was no difference in the adverse events between the groups.

Citation: Lahtinen P, Jalanka J, Mattila E, Tillonen J, Bergman P, Satokari R, Arkkila P. Fecal microbiota transplantation for the maintenance of remission in patients with ulcerative colitis: A randomized controlled trial. *World J Gastroenterol* 2023; 29(17): 2666-2678
URL: https://www.wjgnet.com/1007-9327/full/v29/i17/2666.htm
DOI: https://dx.doi.org/10.3748/wjg.v29.i17.2666

INTRODUCTION

Ulcerative colitis (UC) is a chronic inflammatory disease with an uncertain etiology. The symptoms of UC include bloody diarrhea and abdominal cramps. The pathophysiology is thought to involve an altered and exaggerated inflammatory response to commensal bacteria in genetically predisposed individuals[1]. An increasing proportion of the population is affected by UC, and the prevalence is highest in North America and Northern Europe. For example, in Finland, the yearly incidence is over 25/100000 and is growing[2]. The lifelong risk of colectomy remains elevated despite new immune response-targeting treatment options[3]. Patients with UC show a reduced quality of life compared to the general population even if the disease is quiescent[4].

UC is associated with decreased gut microbial diversity and stability as well as altered microbiota composition and function[5]. In conditions such as *Clostridioides difficile* infection (CDI) and irritable bowel syndrome (IBS), fecal microbial transplantation (FMT) has been shown to alter the patients' gut microbiota in the long term to resemble that of healthy donors[6-8]. During the last decade, FMT has become a recommended treatment option for recurrent *Clostridioides difficile* infection (rCDI)[9]. The efficacy of FMT for rCDI exceeds 90% using an optimal protocol[10,11]. On this basis, it is worthwhile to investigate FMT in UC patients.

FMT has shown promising efficacy for active UC in placebo-controlled trials, although the methodology has varied between studies[12-15]. Repetitious FMTs have been the most frequently applied approach among these studies, while the applied treatment protocols have been otherwise diverse. Some studies have applied a multidonor approach and prepared each transplant from the feces of multiple donors[14,15]. Anaerobic conditions for manufacturing the fecal transplant have been investigated and shown to yield good results[15], as has the administration of a transplant to each patient as many as 40 times[14]. One study showed a clear difference in efficacy between donors, as transplants from one donor were more effective than transplants from the other five donors[13].

A recent randomized placebo-controlled trial from India investigated the efficacy of FMT in the maintenance of UC remission[16]. In this study, FMT prevented relapses through the administration of transplants during bimonthly colonoscopies, making the implementation of the applied protocol very

laborious in clinical practice. Additionally, the study population consisted of primary responders to FMT treatment; thus, the patients in the trial were a highly selective group.

Given that a single FMT alters the gut microbiota for the long term in rCDI[6] as well as in IBS[8] patients, we aimed to investigate the efficacy of a single FMT *via* colonoscopy to maintain remission in UC patients. Additionally, we aimed to investigate the potential differences in quality of life, fecal calprotectin, blood chemistry [blood count, liver enzymes, creatinine, and C-reactive protein (CRP)], and endoscopic findings during the 12-mo follow-up period.

MATERIALS AND METHODS

Study design

We randomized patients with UC in remission into two groups in a 1:1 ratio to receive either FMT from a healthy donor ("FMT group") or an autologous transplant made from the patient's own feces ("placebo group"). To ensure blinding, all participants donated their stool for the preparation of the placebo transplant, and the FMT group samples were discarded. Bowel lavage was performed using a macrogol solution prior to colonoscopy. The transplant was administered into the cecum of the patient during colonoscopy at baseline.

After the baseline intervention, the patients were followed until a colonoscopy 12 mo later. During the follow-up period, the participants were contacted at 2 mo, 4 mo, and 8 mo after the intervention, at which times the clinical Mayo score[17] was recorded and blood samples were obtained. The quality of life was assessed at baseline as well as at 4 mo and 12 mo[4]. Fecal calprotectin samples were obtained at seven timepoints (baseline and at 2 mo, 4 mo, 6 mo, 8 mo, 10 mo, and 12 mo).

The primary endpoint was sustained remission through the 12-mo follow-up time. Remission was defined as a clinical Mayo score below three and a fecal calprotectin level below 200 μg/g. Additionally, an overt relapse between the measurement points leading to a course of steroids or escalation of maintenance therapy was considered a failure.

This randomized placebo-controlled study was conducted in Finland in the Gastroenterology Departments of Helsinki University Hospital, Helsinki and Päijät-Häme Central Hospital, Lahti. The ethical review board of Helsinki University Hospital approved the study (29/13/03/01/2014). The principles of the Declaration of Helsinki were followed. The trial was registered at ClinicalTrials.gov (NCT03561532).

Participants

Forty-eight patients (21-70-years-old) diagnosed with UC were recruited for the study. The inclusion criteria stated that the patients had to be in remission, and the eligibility criteria included fecal calprotectin levels below 100 μg/g and a clinical Mayo score < 3 at the time of screening. The exclusion criteria included the use of antibiotics within 3 mo prior to study entry, a history of tumor necrosis factor-α blockers or other biologics, the use of a high dose of corticosteroids (prednisolone ≥ 20 mg/d), and pregnancy. The patients were recruited from primary and secondary health care centers of the Helsinki and Lahti regions. At baseline, the majority of the patients were on mesalazine.

After the screening visit and before the start of the trial, some patients experienced minor activation of the disease; 8 patients, 4 in each group, had a clinical Mayo score ≥ 3, and 10 patients, 3 in the FMT group and 7 in the placebo group, had fecal calprotectin levels ≥ 200 μg/g. At baseline, none of these patients experienced significant symptoms, and they did not require escalation of medication. Participants with fecal calprotectin ≥ 200 μg/g or a clinical Mayo score ≥ 3 were analyzed separately as "subgroup B" (n = 15), and the participants without these signs of disease activity at baseline were included in "subgroup A" (n = 33). Among all the recruited patients, 16 patients had minor endoscopic colitis activity with an endoscopic Mayo score of 1 at baseline, while the rest of the patients had an endoscopic Mayo score of 0 at baseline.

Participant recruitment started in October 2014. At the beginning of the study, the inclusion criteria required a diagnosis of UC within 6 mo. However, due to very slowly proceeding recruitment, an amendment to the study protocol was made and approved by the ethical board in October 2016 (HUS/1652/2016). Thereafter, patients with any disease duration were eligible. Recruitment remained slow even after the amendment. The study proceeded using fewer than the desired 80 participants due to time constraints. The follow-up of the last included patient was completed in May 2020 (CONSORT flow diagram in Supplementary Figure 1).

Donors

Transplants from three healthy donors were used in this study. The donors had normal body weights and were healthy without any diagnosed long-term illnesses or medications. All donors had a healthy lifestyle and a diet that included animal products but was rich in vegetables. They were screened according to the best practice at the time[10]; however, the donor screening guidelines have evolved since the start of the trial[9]. The laboratory tests for donor screening are collectively presented in Supplementary Table 1. We applied transplants from a female in her forties ("Donor 1") and a young

adult male ("Donor 2"), both of whom had previously served as donors in our studies[6,8] and in routine clinical practice of FMT to treat rCDI. A male in his fifties ("Donor 3") was a new donor recruited for this study.

Intervention

Half of the participants, 24 out of 48, received FMT *via* colonoscopy into the cecum as described previously[10]. The fecal transplants were produced from 30 g of feces from a healthy donor. We used three universal donors, and the fecal suspensions were prepared as previously described and stored at -80 °C[10].

Briefly, feces were suspended in sterile saline and mixed with glycerol (final concentration of 10%) in a 250 mL screw cap container by using a spatula. The suspension was frozen at -80 °C immediately after preparation and within 2 h of defecation to minimize the time of exposure to oxygen. For FMT application, the suspension was thawed at 37 °C or room temperature, mixed briefly and loaded into syringes to avoid clogging by unsuspended particles. If necessary, the suspension was passed through a presterilized, stainless steel tea strainer to remove particles before loading the syringes. The remaining 24 participants in the placebo group were treated in an otherwise similar manner, but the fecal suspension was made using the participants' own freshly donated stool. Autologous placebo was prepared from fresh feces for practical reasons to prevent an extra visit and minimize inconvenience to the patients.

Power calculation and estimated sample size

The relapse rates during the 12-mo follow-up period were estimated to be 50% in the placebo group and 15% in the FMT group. Previous studies of FMT for maintenance of remission of UC were not published at the time of study design. Due to the lack of available studies, the estimation of outcomes was based on knowledge concerning the maintenance of remission using mesalazine[18] and extrapolating from FMT studies for rCDI[11], in which over 90% efficacy had been achieved.

The calculated sample size using the z-test (95% confidence interval, $\alpha = 0.05$ and $\beta = 0.1$, 90% power) to find a significant treatment effect was 33 patients in each group, and to cover possible dropouts, we aimed for a sample size of 40 participants per group, 80 participants in total[19].

Randomization and blinding

The participants were randomized 1:1 to receive FMT or placebo. The randomization was executed in blocks of 6 patients by a study nurse not involved in the treatment of the patients. The participants and the treating personnel were blinded to the type of feces transplanted. The randomization was decoded only after all the patients had completed the 12-mo follow-up.

Outcomes

The primary outcome was the maintenance of remission through the 12-mo follow-up period. A relapse of colitis was considered a failure to achieve the primary outcome. The patients were followed until the time of the recorded relapse, after which they were dropped from the follow-up. The patients who remained in remission were followed until the study endpoint of 12 mo after baseline.

The secondary endpoints were quality of life, endoscopic and histologic findings at 12 mo, fecal calprotectin, and blood chemistry. General quality of life was assessed with the 15 dimensions (15D) questionnaire, and disease-specific quality of life was assessed with the Inflammatory Bowel Disease Quality of Life Questionnaire (IBDQ) (McMaster University, Hamilton, Canada, license No. IBDQ22-081)[4]. The histologic activity was graded in four categories: histological remission; mild activity (lamina propria or intraepithelial neutrophils); moderate activity (presence of crypt abscess); and strong activity (presence of erosion or ulcer)[20].

The participants donated stool samples every 2nd mo (months 0, 2, 4, 6, 8, 10, and 12) for the detection of fecal calprotectin. Blood samples were obtained at baseline as well as at months 4, 8, and 12. The blood tests included complete blood counts, liver enzymes, creatinine, and CRP. Fecal calprotectin values below 50 μg/g and CRP values below ten were not reported by the laboratory and were coded as null accordingly.

Statistical methods

Descriptive statistics are presented as the means with standard deviations (SDs) for continuous variables and as frequencies and percentages for qualitative variables. Differences between the study groups in the maintenance of remission during the follow-up were assessed using the Kaplan-Meier method. Associations of baseline characteristics with the maintenance of remission were analyzed with univariate Cox regression models. In addition, 15D scores were presented using profile plots, and differences between groups were assessed by *t* tests. Differences in endoscopic and histological colitis activity between the study groups were analyzed with the χ^2 test. *P* values < 0.05 were considered statistically significant for all analyses. SPSS version 27 (IBM Corp. Released 2020. IBM SPSS Statistics for Windows, Version 27.0. Armonk, NY, United States) was used for the statistical analysis.

RESULTS

Baseline characteristics

Forty-nine patients were recruited for this study. After the screening visit and before randomization, 1 patient had overt activation of colitis and was excluded. This left 48 patients to be randomized, with 24 in each group. The patient flow of the study is presented in Supplementary Figure 1, and the baseline characteristics of the patients are presented in Table 1. The placebo group had a longer duration of disease than the FMT group (114 mo *vs* 39 mo, $P = 0.006$). At baseline, the mean fecal calprotectin level was 115.8 (SD: 184.7) in the placebo group and 66.4 (SD: 108.6) in the FMT group ($P = 0.261$). The majority of the patients were on mesalazine: 21 out of 24 patients in the FMT group and 22 out of 24 in the placebo group. Four patients in the placebo group were on thiopurine, but none were in the FMT group. At the study baseline, 2 patients in both groups were still on lower doses of tapering corticosteroid therapy. There were no statistically significant differences between the randomization groups within subgroups A and B, in which the patients had fecal calprotectin < 200 μg/g and a clinical Mayo score < 3 or fecal calprotectin ≥ 200 μg/g and a clinical Mayo score ≥ 3 at baseline, respectively (Table 1).

The primary endpoint-maintenance of remission

The primary endpoint of the study was the maintenance of remission through the 12-mo follow-up, which was achieved by 13 out of 24 (54%) patients in the FMT group and by 10 out of 24 (41%) patients in the placebo group. The difference between the groups was not statistically significant (log-rank test $P = 0.660$). A Kaplan-Meier survival curve of relapses in the FMT and placebo groups is presented in Figure 1A.

A similar result was obtained when the patients were divided into subgroups according to the clinical Mayo score and fecal calprotectin level at baseline. In subgroup A, 6 out of 16 patients relapsed in the placebo group, and 7 out of 17 patients relapsed in the FMT group ($P = 0.703$, Figure 1B). Similarly, subgroup B showed no difference between the placebo and FMT groups ($P = 0.556$) in the number of relapses; all 8 patients in the placebo group and 5 out of 7 patients in the FMT group relapsed (Figure 1C).

To study the possible effect of a specific donor on the patient's outcome, we divided the patients into three groups according to the donor and compared these to the placebo. There were no statistically significant differences in the number of relapses between the different donors (log-rank, $P = 0.517$). At the 12-mo follow-up, 41.7% (10/24) of the patients in the placebo group remained in remission compared to 33.3% (2/6) from Donor 1, 50.0% (5/10) from Donor 2, and 62.5% (5/8) from Donor 3.

We also analyzed the effect of essential baseline characteristics on the maintenance of remission between these donor groups, which included the duration of disease status, fecal calprotectin, clinical Mayo score, total 15D score, and total IBDQ score (Supplementary Table 2). The mean duration of disease was 114 mo in the placebo group, 5 mo in the Donor 1 group, 52 mo in the Donor 2 group, and 49 mo in the Donor 3 group. The disease duration did not have a statistically significant effect on the maintenance of remission in any of the donor groups. There were some statistically significant relationships between baseline characteristics and maintenance of remission. In the placebo group, lower maintenance of remission time was associated with higher baseline fecal calprotectin [Cox regression, hazard ratio (HR): 1.003; 95% confidence interval (CI): 1.001-1.005; $P = 0.010$) and a higher baseline clinical Mayo score (Cox regression, HR: 1.498; 95%CI: 1.067-2.102; $P = 0.020$). In the Donor 2 group, a lower mean 15D total score at baseline was associated with lower maintenance of remission (Cox regression, HR: 0.000; CI: 0.000-0.374; $P = 0.033$). All other analyzed associations were statistically insignificant (Supplementary Table 2).

Secondary endpoint–changes in patient quality of life

We investigated the impact of FMT on patient quality of life as measured with the 15D questionnaire and disease-specific quality of life as measured with the IBDQ questionnaire.

The 15D total score was similar between the placebo and FMT groups at baseline (*t* test, $P = 0.335$) (Figure 2A) and at the 12-mo follow-up after FMT treatment ($P = 0.905$) (Figure 2B). However, there was a significant difference in the 15D total score between the FMT and placebo groups ($P = 0.017$) 4 mo after treatment (Figure 2C). The mean change in the 15D total score from baseline to 4 mo was -0.032 (slightly worse) in the FMT group and -0.009 (no change) in the placebo group. The estimation of the importance of change was performed as presented previously[21]. The mean change in the 15D total score from baseline to 12 mo was -0.008 (no change) in the FMT group and -0.015 (slightly worse) in the placebo group. Additionally, of the 15D, there were statistically significant differences in breathing ($P = 0.049$), usual activities ($P = 0.042$), and vitality ($P = 0.006$), all favoring the placebo group.

The disease-specific quality of life as measured with the IBDQ[22] was also similar between the placebo and FMT groups at baseline ($P = 0.519$) and at 12 mo ($P = 0.868$), but at 4 mo, there was a difference in the IBDQ total score favoring the placebo group ($P = 0.003$). Of the four IBDQ subcategories, there were statistically significant differences in the emotions ($P = 0.008$) and systemic ($P = 0.010$) subcategories.

Table 1 The baseline demographics of patients included in the analysis

Baseline variable	All patients (*n* = 48)		*P* value	Subgroup A (*n* = 33)		*P* value	Subgroup B (*n* = 15)		*P* value
	FMT	Placebo		FMT	Placebo		FMT	Placebo	
Sex as M/F	14/10	12/12	0.562	8/9	8/8	0.866	4/4	5/2	0.608
Age	43.0 (12.9)	43.1 (12.1)	0.982	43.6 (13.0)	44.8 (12.0)	0.781	41.7 (13.6)	39.8 (12.5)	0.775
Disease duration in mo	39.2 (51.0)	114.0 (117.6)	0.006	41.0 (56.2)	125.4 (121.7)	0.015	34.9 (38.7)	91.3 (113.2)	0.233
Fecal calprotectin	66.0 (108.6)	115.8 (184.7)	0.261	34.7 (46.3)	18.9 (44.9)	0.330	142.3 (172.9)	309.6 (208.3)	0.117
15D	0.903 (0.095)	0.928 (0.072)	0.335	0.899 (0.106)	0.939 (0.070)	0.221	0.915 (0.070)	0.907 (0.078)	0.830
IBDQ	169.4 (28.8)	162.7 (39.8)	0.519	166.9 (28.6)	171.4 (32.0)	0.688	175.0 (30.5)	147.4 (49.3)	0.223

Subgroup A included patients with fecal calprotectin < 200 μg/g and a clinical Mayo score < 3 at baseline, and subgroup B included patients with fecal calprotectin ≥ 200 ug/g or a clinical Mayo score ≥ 3 at baseline. Standard deviations are shown in brackets. M: Male; F: Female; 15D: The total score of the 15 dimensions quality of life questionnaire; IBDQ: The total score of the inflammatory bowel disease quality of life questionnaire; FMT: Fecal microbiota transplantation.

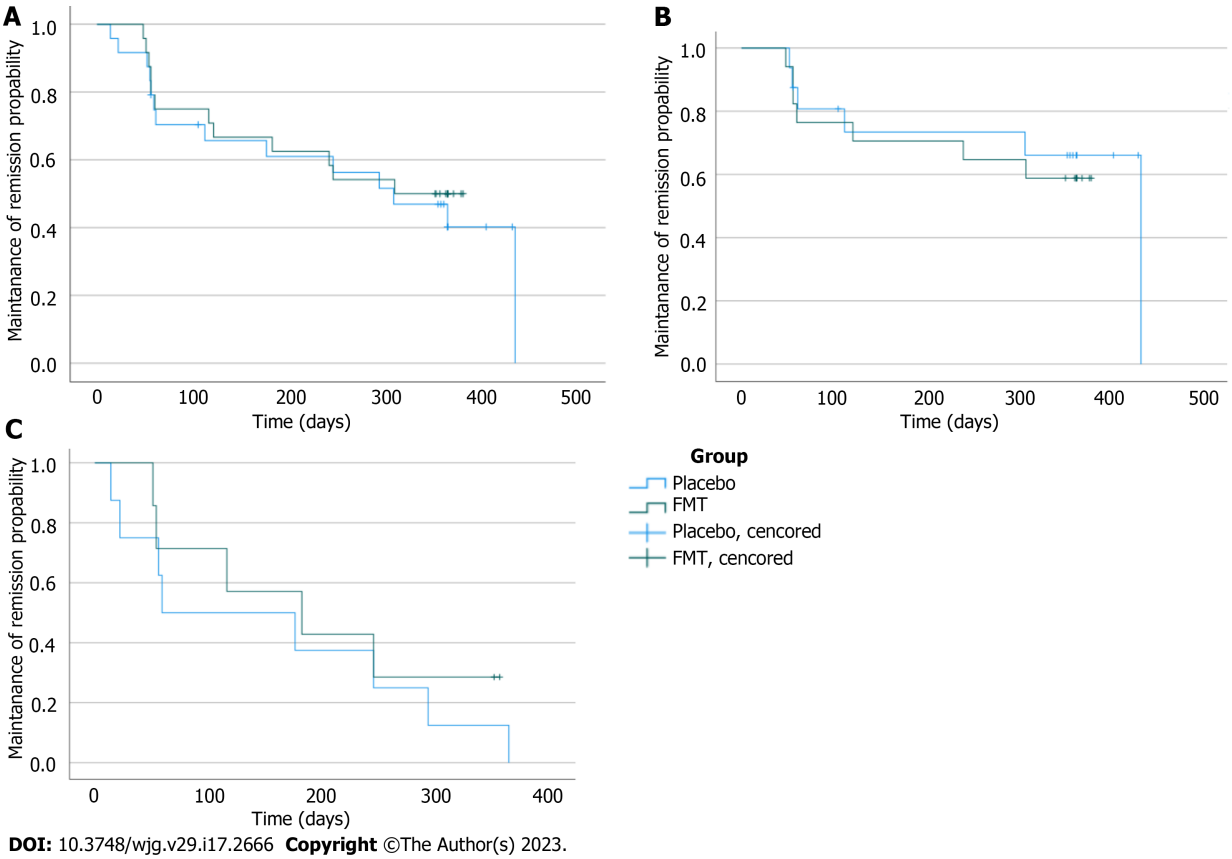

DOI: 10.3748/wjg.v29.i17.2666

Figure 1 Kaplan-Meier survival curve demonstrating the maintenance of remission defined as fecal calprotectin < 200 μg/g and the clinical Mayo score < 3 or an overt relapse in between the measurement points. A: All patients included in analysis (log rank test *P* = 0.660); B: Subgroup A, *i.e.* the patients with fecal calprotectin < 200 μg/g and clinical Mayo score < 3 at the baseline (*P* = 0.703); C: Subgroup B, *i.e.* the patients with fecal calprotectin ≥ 200 μg/g or the clinical Mayo score ≥ 3 at the baseline (*P* = 0.556). Censored means the end of follow-up without a relapse. FMT: Fecal microbiota transplantation.

Secondary endpoint-blood chemistry and fecal calprotectin

The blood chemistry, complete blood count, liver enzymes, and creatinine and CRP levels were analyzed at four different timepoints. Fecal calprotectin was measured every 2nd mo at six different timepoints. There were no clinically significant changes in any of the blood tests compared to the baseline. All laboratory tests at each timepoint showed no statistically significant differences between the FMT and placebo groups ($P > 0.05$). The blood chemistry and fecal calprotectin values are collectively presented in Supplementary Table 3.

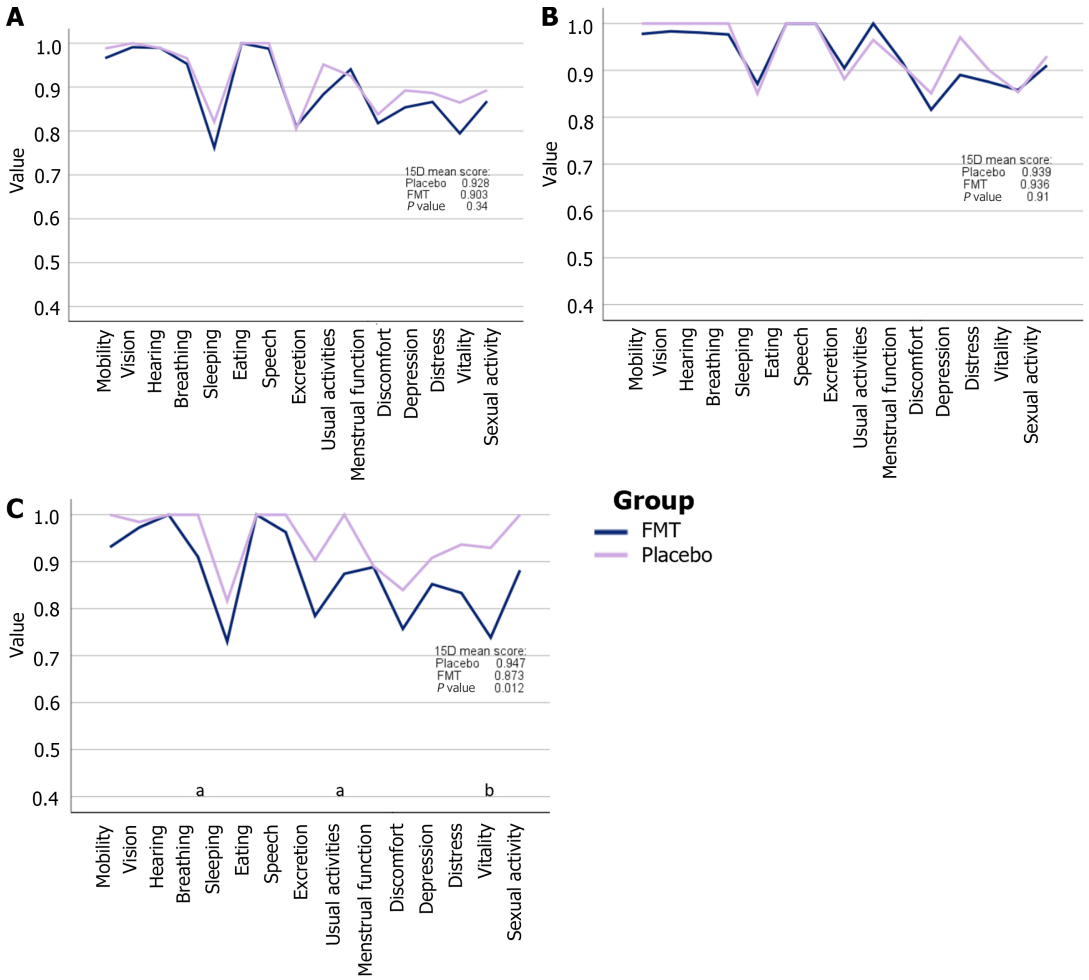

DOI: 10.3748/wjg.v29.i17.2666

Figure 2 The general quality of life of the complete study group shown according to the 15 dimensions and the mean total score and *P* value as expressed numerically within the picture. A: The total score of the 15 dimensions quality of life questionnaire (15D) profiles at the baseline (n = 48); B: 15D profiles at 12 mo (n = 21); C: 15D profiles at 4 mo (n = 30). [a]$P \leq 0.05$ and [b]$P \leq 0.01$. FMT: Fecal microbiota transplantation; 15D: The total score of the 15 dimensions quality of life questionnaire.

Endoscopic and histologic colitis activity at 12 mo

A colonoscopy was performed at the end of the trial, and pinch biopsies were obtained from all 23 patients who reached the primary endpoint and remained in clinical remission throughout the follow-up period. Endoscopic colitis activity was detected in 2 out of 13 patients in the FMT group and in 2 out of 10 patients in the placebo group. Likewise, mild histological colitis activity was detected in the colon pinch biopsies in 2 out of 13 patients in the FMT group and 2 out of 10 patients in the placebo group, indicating chronic inflammation. Thus, the number of patients who were in endoscopic and histologic remission in the follow-up colonoscopy was 11 out of 13 in the FMT group and 8 out of 10 in the placebo group (χ^2, $P = 0.772$).

Adverse events

A similar number of patients experienced UC activation in the FMT and placebo groups (Figure 1). In addition to colitis activation, other adverse events were recorded in 4 patients in the FMT group and 6 patients in the placebo group.

In the FMT group, the adverse events included fatigue through the follow-up period, gastroenteritis at 8 mo after FMT, constipation at 3 wk after FMT and a diagnosis of primary sclerosing cholangitis. In addition, 1 patient reported fatigue and episodes of atrial fibrillation at the 4-mo timepoint, for which he underwent ablation treatment. This patient subsequently developed pneumonia.

In the placebo group, 1 patient with fibromyalgia reported back pain and colitis symptoms simultaneously. Another patient visited the emergency room 6 mo after the procedure and was diagnosed with mitral valve insufficiency. One patient with spondylarthritis experienced arthralgia during the follow-up. One patient experienced an escalation of bloating after the procedure, and 2 patients experienced a prolonged mild respiratory infection. Possible hospitalizations were monitored in all the participants for 12 mo, but none were attributable to FMT.

DISCUSSION

In this placebo-controlled trial, we examined the effect of a single FMT *via* colonoscopy on the maintenance of remission in UC patients. The primary endpoint was sustained remission over a 12-mo follow-up period. A relapse of UC was regarded as a failure to achieve the primary endpoint. We set the cutoff values to differentiate between remission and relapse to a clinically significant level; thus, a clinical Mayo score above three and fecal calprotectin levels above 200 μg/g were considered to indicate colitis activation. There was no statistically significant difference in the number of patients with a relapse of UC during the follow-up period in the FMT and placebo groups. According to the results, a single FMT *via* colonoscopy was ineffective for maintaining UC in remission.

Previously, the impact of the donor on the outcome of FMT was demonstrated in patients with active UC[13]. Including more than one donor in FMT trials enables comparison between the donors. In this trial, we used three donors. Sustainable remission through the follow-up was achieved by 33.3% of the patients who received FMT from Donor 1, whereas the same was achieved by 62.5% of the patients treated with FMT from Donor 3. However, the number of patients in each group was small, and the differences did not reach statistical significance. Furthermore, the Donor 1 treatment was applied at the beginning of the trial when the inclusion criteria were different, requiring new-onset disease, and consequently the baseline activity markers, fecal calprotectin and clinical Mayo score were higher in the patients of Donor 1 than in the patients of Donor 3. For these reasons, the existence or magnitude of the donor effect could not be proven or disproven.

Studies evaluating FMT for active as well as quiescent UC have been encouraging[13,16], but the present data are not sufficient to justify treating UC patients with FMT in clinical practice. Our goal was to investigate whether manipulation of the gut microbiota with FMT early after UC diagnosis would help in the maintenance of remission and the effect on the course of the disease. When planning this study, we aimed to recruit patients whose UC was diagnosed within 6 mo prior to the study baseline. However, due to slow recruitment, we made a change in the study protocol and started including patients with any duration of the disease. Additionally, another center, Päijät-Häme Central Hospital, joined the study in addition to Helsinki University Hospital. Nevertheless, the recruitment remained slow, and we were only able to recruit 48 of the originally planned 80 patients within a reasonable time.

As a result of the change in the protocol, 31% of the patients fulfilled the initial inclusion criteria and had been diagnosed within the previous 6 mo, of whom 6 patients were in the FMT group and 9 patients were in the placebo group. Coincidentally, the patients with the longest duration of the disease were also randomized into the placebo group, resulting in a statistically significant difference in the duration of disease status between the randomization groups. The groups were similar to each other in all other parameters (Table 1). Patients with biologics were not included in the trial; thus, the participants did not have a history of severe and difficult-to-treat disease.

Previously published randomized, placebo-controlled FMT trials investigating patients with UC have included patients with active colitis or patients who have reached clinical remission after several FMT sessions[15,16,23]. The patients in our study had UC in clinical remission but had not previously received FMT therapy. Between the recruitment and the study baseline, a portion of the patients had elevated calprotectin and clinical Mayo score values without overt colitis symptoms and were included in a subgroup analysis (Table 1). Overall, the population of our study represented UC patients in real-world clinical practice.

As a secondary endpoint, we aimed to investigate the effect of FMT on patient quality of life. We evaluated this outcome with the disease-specific IBDQ questionnaire and with the 15D questionnaire, which measures general health-related quality of life. Both questionnaires measure the quality of life in IBD patients with equal reliability[4]. Interestingly, the placebo group presented higher quality-of-life scores 4 mo after the treatment. This may refer to the extraintestinal influence of the gut microbiota, although the difference between the groups may partly be explained by the longer duration of disease in the placebo group and consequently better adaptation to the fluctuating symptoms of the disease. Indeed, the statistically significant differences concerned vitality, usual activities, and breathing in the 15D questionnaire, while intestinal symptoms did not differ between the groups. Additionally, in the IBDQ questionnaire, the subcategories of emotions and systemic symptoms were statistically significantly better in the placebo group at the 4-mo timepoint. We found disease duration and adaptation to be the most plausible explanation for the observed differences since the subscores of the FMT group increased and the differences between treatment groups disappeared at 12 mo. However, changes in microbiota composition and activity extrapolating to extraintestinal effects should also be addressed in future investigations. Previously, we observed a possible link between microbiota, general mental health, and depression in our FMT studies on IBS and rCDI[8,24].

In line with our previous placebo-controlled FMT trial[8], the reported adverse events in this trial were evenly distributed between groups. There were no severe adverse events attributable to FMT, replicating previous reports stating that FMT was safe when performed with high standards[25]. Even as FMT appears safe in randomized controlled trials[8,13,15] and evidence of long-term safety appears encouraging[24], we find it highly important to continue gathering safety data on FMT from randomized trials as well as collecting registry data from clinical practice. The interindividual variability of donors is high concerning microbiota profiles as well as other characteristics, and therefore the

scientific community and clinicians performing FMT for CDI need to stay alert for infectious complications and for possible rare short-term and long-term adverse effects of FMT[26].

Our study had some limitations. First, the number of studied patients remained rather low, with only 48 patients in total due to slow recruitment. Second, after patients experienced a relapse of UC, further data were not recorded. This decreased the amount of obtained data and complicated the comparison of secondary endpoints between the groups, as there were fewer cases left for the analysis with each successive time point. However, after a relapse, some of the patients were given corticosteroids or the medication was changed, which would have misrepresented the true effects of FMT or placebo. Another drawback was that the patients in the placebo group had UC for a longer duration than those in the FMT group and were likely in a more stable phase of the disease. This may have impacted the results of the primary endpoint as well as secondary endpoints; however, there were no statistically significant correlations between the duration of disease and the time to relapse or quality of life in either study group.

Our study also had clear advantages. Its blinded placebo-controlled design is a definite strength. We applied an autologous placebo, which assures very reliable blinding, and the same method has yielded valid results in FMT trials for rCDI[27] and in other conditions such as IBS[8] and Crohn's disease[28]. However, it must be noted that the composition of the fecal microbiota may change when it is exposed to oxygen, and in the case of patient samples, the duration of oxygen exposure could not be carefully controlled, unlike for the donor samples, which were prepared and frozen within 2 h of defecation. The advantage of applying an autologous placebo is that it assures very reliable blinding. Other forms of placebo may be more easily detected by the patient or treating personnel. Another advantage of our study is the sufficiently long follow-up time, which enabled the treatment effect durability to be monitored.

Unlike in rCDI, clinical efficacy may not be achieved in UC by just a single FMT, possibly due to difficulties in modulating the microbiota in the longer term by only one FMT dose. Repeated FMT treatments could possibly enhance efficacy, as shown by Sood *et al*[16] where repeated FMT treatments were associated with maintenance of remission. In that trial, the study population was selected from responders to FMT given for induction of remission, and bimonthly colonoscopic FMTs for 1 year maintained UC in remission better than placebo. Thus, the positive effects of FMT may be maintained by repeated treatments. Repeated FMT treatments have also shown promising results in the induction of remission of active UC[13-15]. Engraftment of the transplanted microbes may be more difficult in an active colitis environment than in a state of remission. From this perspective, repeated FMT can be more justified in active disease.

Moreover, FMT may also exert its efficacy *via* host-derived biomolecules that exert immunoregulatory action or induce transcriptional changes in the affected intestinal epithelium. Action by nonpersisting biomolecules could also explain why multiple FMTs are needed for the induction of remission. On the other hand, if microbiota modulation is considered critical, a single FMT by colonoscopy with our protocol (applying 30 g of donor feces) can induce prolonged microbial engraftment in rCDI patients as well as in IBS patients[6,8].

To our knowledge, our trial is the first controlled trial to investigate a single FMT for the maintenance of remission in UC patients. In future FMT studies on the maintenance of UC remission, repeated treatments seem reasonable. However, other methods to enhance and prolong the effects should also be considered. For example, combining a dietary intervention may improve results and prolong remission [29]. In one recent trial, a dietary intervention resulted in a superior effect on the induction of remission in UC patients compared to FMT[30].

The optimization of donor selection could possibly improve outcomes even with a single FMT given in remission. Additionally, conditions for the engraftment and functioning of beneficial microbiota may be important, particularly when FMT is given to patients in remission. Diet has a great impact on gut microbiota and is likely an important factor affecting the survival and function of transplanted microbes [31]. We suggest prompt documenting of the diet in future FMT studies. Additionally, the combination of FMT with dietary modulation should be addressed in future studies[29,30].

There are many open questions to be answered before we can determine whether FMT may be applied for the maintenance of remission in UC. More research is needed to define the optimal donor characteristics, patient population, and timing for FMT. Additionally, the best route of FMT administration remains undefined. While the colonoscopic route has shown promise[16], FMT with capsules may be considered when high numbers of patients need to be treated[23]. Finally, we do not yet know which stool components are responsible for the positive effects of FMT, and there is much room for future innovative research.

CONCLUSION

In conclusion, there were no statistically significant differences in the number of UC relapses after a single FMT or placebo treatment; therefore, the main outcome of our study was negative. Our results do not support applying a single FMT for the maintenance of UC remission. However, these results must

be interpreted with caution due to the small sample size, and larger studies are warranted.

ARTICLE HIGHLIGHTS

Research background

Ulcerative colitis (UC) is associated with altered gut microbiota. The pathophysiology of UC is thought to involve an altered and exaggerated inflammatory response to commensal bacteria. Fecal microbiota transplantation has yielded good results in the induction of UC remission.

Research motivation

Despite the development in medications for UC, some patients do not respond sufficiently to current treatment options and new treatment modalities are needed. Modulation of gut microbiota *via* fecal microbial transplantation (FMT) is a potential new treatment option for UC patients.

Research objectives

The goal of this trial was to gather information of the role of gut microbiota in maintenance of remission in UC patients, and the aim was to investigate FMT for the maintenance of UC remission.

Research methods

Forty-eight patients with quiescent UC were randomized 1:1 to receive a single FMT *via* colonoscopy or a placebo made from the patient's own stool. The patients were followed for 12 mo, and colitis symptoms were measured as well as fecal calprotectin. As secondary endpoints, quality of life, blood chemistry, and endoscopic findings at 12 mo were measured.

Research results

UC remission was maintained by 13 out of 24 (54%) patients in the FMT group and by 10 out of 24 (41%) patients in the placebo group (log-rank test, $P = 0.660$). The quality of life was lower in the FMT group at 4 mo after FMT as compared to the placebo group ($P = 0.017$). There were no differences in blood chemistry, fecal calprotectin, or endoscopic findings at 12 mo between the groups.

Research conclusions

There were no significant differences in the maintenance of remission between the groups during the 12-mo follow-up. Thus, our results do not support the use of a single-dose FMT for the maintenance of remission in UC patients.

Research perspectives

Many open questions need to be answered before we can determine whether FMT may be applied for the maintenance of remission in UC. We do not yet know which stool components distribute the positive effects of FMT. More research is needed to define the optimal donor characteristics, patient population, and the optimal number and timing of FMT treatments.

ACKNOWLEDGEMENTS

Study nurses Pirkko Tuukkala (Helsinki University Hospital) and Virve Liukkonen (Päijät-Häme Central Hospital) are acknowledged for their contribution to the study with a high level of expertise and commitment.

FOOTNOTES

Author contributions: Lahtinen P wrote the paper; Lahtinen P and Bergman P analyzed the data and designed the figures; Arkkila P, Satokari R, and Mattila E planned the study; Arkkila P, Satokari R, Lahtinen P, and Tillonen J executed the study and collected most of the data; Arkkila P, Lahtinen P, and Tillonen J assessed the colonoscopies; Satokari R administered fecal banking and FMT treatments; Jalanka J, Mattila E, and Tillonen J provided expertise in the study design and components of the article; All authors contributed to drafting the article and revised the manuscript for important intellectual content; All authors had access to the study data and reviewed and approved the final manuscript.

Supported by Academy of Finland (Reetta Satokari), No. 323156; Sigrid Juselius Foundation and University of Helsinki (A Three-year Grant); The Competitive State Research Financing (Perttu Lahtinen), No. 200230042; The Ella and Georg Ehrnrooth Foundation (Perttu Arkkila).

Institutional review board statement: The study was reviewed and approved by the Helsinki University Hospital Institutional Review Board, No. 29/13/03/01/2014.

Clinical trial registration statement: This study is registered at ClinicalTrials.gov. The registration identification number is NCT03561532.

Informed consent statement: All study participants or their legal guardian provided informed written consent about personal and medical data collection prior to study enrolment.

Conflict-of-interest statement: Dr. Lahtinen reports grants from The Competetive State Research Financing, grants from Academy of Finland, grants from Sigrid Juselius Foundation, grants from University of Helsinki, grants from Ella and Georg Ehrnrooth Foundation, during the conduct of the study.

Data sharing statement: The datasets generated and analyzed during the current study are not publicly available because individual privacy could be compromised. However, they are available from the corresponding author on reasonable request.

CONSORT 2010 statement: The authors have read the CONSORT 2010 statement, and the manuscript was prepared and revised according to the CONSORT 2010 statement.

Country/Territory of origin: Finland

ORCID number: Perttu Lahtinen 0000-0001-6430-4642; Jonna Jalanka 0000-0002-3847-8136; Eero Mattila 0000-0001-9787-7674; Jyrki Tillonen 0000-0002-5661-9385; Paula Bergman 0000-0003-4672-2554; Reetta Satokari 0000-0002-4258-3414; Perttu Arkkila 0000-0003-2194-0424.

S-Editor: Fan JR
L-Editor: Filipodia
P-Editor: Cai YX

REFERENCES

1 **Ungaro R**, Mehandru S, Allen PB, Peyrin-Biroulet L, Colombel JF. Ulcerative colitis. *Lancet* 2017; **389**: 1756-1770 [PMID: 27914657 DOI: 10.1016/S0140-6736(16)32126-2]
2 **Jussila A**, Virta LJ, Kautiainen H, Rekiaro M, Nieminen U, Färkkilä MA. Increasing incidence of inflammatory bowel diseases between 2000 and 2007: a nationwide register study in Finland. *Inflamm Bowel Dis* 2012; **18**: 555-561 [PMID: 21425214 DOI: 10.1002/ibd.21695]
3 **Lamb CA**, Kennedy NA, Raine T, Hendy PA, Smith PJ, Limdi JK, Hayee B, Lomer MCE, Parkes GC, Selinger C, Barrett KJ, Davies RJ, Bennett C, Gittens S, Dunlop MG, Faiz O, Fraser A, Garrick V, Johnston PD, Parkes M, Sanderson J, Terry H; IBD guidelines eDelphi consensus group, Gaya DR, Iqbal TH, Taylor SA, Smith M, Brookes M, Hansen R, Hawthorne AB. British Society of Gastroenterology consensus guidelines on the management of inflammatory bowel disease in adults. *Gut* 2019; **68**: s1-s106 [PMID: 31562236 DOI: 10.1136/gutjnl-2019-318484]
4 **Haapamäki J**, Roine RP, Sintonen H, Turunen U, Färkkilä MA, Arkkila PE. Health-related quality of life in inflammatory bowel disease measured with the generic 15D instrument. *Qual Life Res* 2010; **19**: 919-928 [PMID: 20361263 DOI: 10.1007/s11136-010-9650-4]
5 **Manichanh C**, Borruel N, Casellas F, Guarner F. The gut microbiota in IBD. *Nat Rev Gastroenterol Hepatol* 2012; **9**: 599-608 [PMID: 22907164 DOI: 10.1038/nrgastro.2012.152]
6 **Jalanka J**, Mattila E, Jouhten H, Hartman J, de Vos WM, Arkkila P, Satokari R. Long-term effects on luminal and mucosal microbiota and commonly acquired taxa in faecal microbiota transplantation for recurrent Clostridium difficile infection. *BMC Med* 2016; **14**: 155 [PMID: 27724956 DOI: 10.1186/s12916-016-0698-z]
7 **Fuentes S**, van Nood E, Tims S, Heikamp-de Jong I, ter Braak CJ, Keller JJ, Zoetendal EG, de Vos WM. Reset of a critically disturbed microbial ecosystem: faecal transplant in recurrent Clostridium difficile infection. *ISME J* 2014; **8**: 1621-1633 [PMID: 24577353 DOI: 10.1038/ismej.2014.13]
8 **Lahtinen P**, Jalanka J, Hartikainen A, Mattila E, Hillilä M, Punkkinen J, Koskenpato J, Anttila VJ, Tillonen J, Satokari R, Arkkila P. Randomised clinical trial: faecal microbiota transplantation versus autologous placebo administered *via* colonoscopy in irritable bowel syndrome. *Aliment Pharmacol Ther* 2020; **51**: 1321-1331 [PMID: 32343000 DOI: 10.1111/apt.15740]
9 **Cammarota G**, Ianiro G, Tilg H, Rajilić-Stojanović M, Kump P, Satokari R, Sokol H, Arkkila P, Pintus C, Hart A, Segal J, Aloi M, Masucci L, Molinaro A, Scaldaferri F, Gasbarrini G, Lopez-Sanroman A, Link A, de Groot P, de Vos WM,

Högenauer C, Malfertheiner P, Mattila E, Milosavljević T, Nieuwdorp M, Sanguinetti M, Simren M, Gasbarrini A; European FMT Working Group. European consensus conference on faecal microbiota transplantation in clinical practice. *Gut* 2017; **66**: 569-580 [PMID: 28087657 DOI: 10.1136/gutjnl-2016-313017]

10 **Satokari R**, Mattila E, Kainulainen V, Arkkila PE. Simple faecal preparation and efficacy of frozen inoculum in faecal microbiota transplantation for recurrent Clostridium difficile infection--an observational cohort study. *Aliment Pharmacol Ther* 2015; **41**: 46-53 [PMID: 25355279 DOI: 10.1111/apt.13009]

11 **van Nood E**, Vrieze A, Nieuwdorp M, Fuentes S, Zoetendal EG, de Vos WM, Visser CE, Kuijper EJ, Bartelsman JF, Tijssen JG, Speelman P, Dijkgraaf MG, Keller JJ. Duodenal infusion of donor feces for recurrent Clostridium difficile. *N Engl J Med* 2013; **368**: 407-415 [PMID: 23323867 DOI: 10.1056/NEJMoa1205037]

12 **Rossen NG**, Fuentes S, van der Spek MJ, Tijssen JG, Hartman JH, Duflou A, Löwenberg M, van den Brink GR, Mathus-Vliegen EM, de Vos WM, Zoetendal EG, D'Haens GR, Ponsioen CY. Findings From a Randomized Controlled Trial of Fecal Transplantation for Patients With Ulcerative Colitis. *Gastroenterology* 2015; **149**: 110-118.e4 [PMID: 25836986 DOI: 10.1053/j.gastro.2015.03.045]

13 **Moayyedi P**, Surette MG, Kim PT, Libertucci J, Wolfe M, Onischi C, Armstrong D, Marshall JK, Kassam Z, Reinisch W, Lee CH. Fecal Microbiota Transplantation Induces Remission in Patients With Active Ulcerative Colitis in a Randomized Controlled Trial. *Gastroenterology* 2015; **149**: 102-109.e6 [PMID: 25857665 DOI: 10.1053/j.gastro.2015.04.001]

14 **Paramsothy S**, Kamm MA, Kaakoush NO, Walsh AJ, van den Bogaerde J, Samuel D, Leong RWL, Connor S, Ng W, Paramsothy R, Xuan W, Lin E, Mitchell HM, Borody TJ. Multidonor intensive faecal microbiota transplantation for active ulcerative colitis: a randomised placebo-controlled trial. *Lancet* 2017; **389**: 1218-1228 [PMID: 28214091 DOI: 10.1016/S0140-6736(17)30182-4]

15 **Costello SP**, Hughes PA, Waters O, Bryant RV, Vincent AD, Blatchford P, Katsikeros R, Makanyanga J, Campaniello MA, Mavrangelos C, Rosewarne CP, Bickley C, Peters C, Schoeman MN, Conlon MA, Roberts-Thomson IC, Andrews JM. Effect of Fecal Microbiota Transplantation on 8-Week Remission in Patients With Ulcerative Colitis: A Randomized Clinical Trial. *JAMA* 2019; **321**: 156-164 [PMID: 30644982 DOI: 10.1001/jama.2018.20046]

16 **Sood A**, Mahajan R, Singh A, Midha V, Mehta V, Narang V, Singh T, Singh Pannu A. Role of Faecal Microbiota Transplantation for Maintenance of Remission in Patients With Ulcerative Colitis: A Pilot Study. *J Crohns Colitis* 2019; **13**: 1311-1317 [PMID: 30873549 DOI: 10.1093/ecco-jcc/jjz060]

17 **Lewis JD**, Chuai S, Nessel L, Lichtenstein GR, Aberra FN, Ellenberg JH. Use of the noninvasive components of the Mayo score to assess clinical response in ulcerative colitis. *Inflamm Bowel Dis* 2008; **14**: 1660-1666 [PMID: 18623174 DOI: 10.1002/ibd.20520]

18 **Feagan BG**, Macdonald JK. Oral 5-aminosalicylic acid for maintenance of remission in ulcerative colitis. *Cochrane Database Syst Rev* 2012; **10**: CD000544 [PMID: 23076890 DOI: 10.1002/14651858.CD000544.pub3]

19 **Chow SC**. Sample Size Calculations in Clinical Research. 2nd Ed: Chapman & Hall/CRC Biostatistics Series, 2008: 52

20 **D'Haens G**, Sandborn WJ, Feagan BG, Geboes K, Hanauer SB, Irvine EJ, Lémann M, Marteau P, Rutgeerts P, Schölmerich J, Sutherland LR. A review of activity indices and efficacy end points for clinical trials of medical therapy in adults with ulcerative colitis. *Gastroenterology* 2007; **132**: 763-786 [PMID: 17258735 DOI: 10.1053/j.gastro.2006.12.038]

21 **Alanne S**, Roine RP, Räsänen P, Vainiola T, Sintonen H. Estimating the minimum important change in the 15D scores. *Qual Life Res* 2015; **24**: 599-606 [PMID: 25145637 DOI: 10.1007/s11136-014-0787-4]

22 **Guyatt G**, Mitchell A, Irvine EJ, Singer J, Williams N, Goodacre R, Tompkins C. A new measure of health status for clinical trials in inflammatory bowel disease. *Gastroenterology* 1989; **96**: 804-810 [PMID: 2644154]

23 **Haifer C**, Paramsothy S, Kaakoush NO, Saikal A, Ghaly S, Yang T, Luu LDW, Borody TJ, Leong RW. Lyophilised oral faecal microbiota transplantation for ulcerative colitis (LOTUS): a randomised, double-blind, placebo-controlled trial. *Lancet Gastroenterol Hepatol* 2022; **7**: 141-151 [PMID: 34863330 DOI: 10.1016/S2468-1253(21)00400-3]

24 **Jalanka J**, Hillamaa A, Satokari R, Mattila E, Anttila VJ, Arkkila P. The long-term effects of faecal microbiota transplantation for gastrointestinal symptoms and general health in patients with recurrent Clostridium difficile infection. *Aliment Pharmacol Ther* 2018; **47**: 371-379 [PMID: 29226561 DOI: 10.1111/apt.14443]

25 **Baxter M**, Colville A. Adverse events in faecal microbiota transplant: a review of the literature. *J Hosp Infect* 2016; **92**: 117-127 [PMID: 26803556 DOI: 10.1016/j.jhin.2015.10.024]

26 **Osman M**, Budree S, Kelly CR, Panchal P, Allegretti JR, Kassam Z; OpenBiome Collaborators. Effectiveness and Safety of Fecal Microbiota Transplantation for Clostridioides Difficile Infection: Results From a 5344-Patient Cohort Study. *Gastroenterology* 2022; **163**: 319-322 [PMID: 35398345 DOI: 10.1053/j.gastro.2022.03.051]

27 **Kelly CR**, Khoruts A, Staley C, Sadowsky MJ, Abd M, Alani M, Bakow B, Curran P, McKenney J, Tisch A, Reinert SE, Machan JT, Brandt LJ. Effect of Fecal Microbiota Transplantation on Recurrence in Multiply Recurrent Clostridium difficile Infection: A Randomized Trial. *Ann Intern Med* 2016; **165**: 609-616 [PMID: 27547925 DOI: 10.7326/M16-0271]

28 **Sokol H**, Landman C, Seksik P, Berard L, Montil M, Nion-Larmurier I, Bourrier A, Le Gall G, Lalande V, De Rougemont A, Kirchgesner J, Daguenel A, Cachanado M, Rousseau A, Drouet É, Rosenzwajg M, Hagege H, Dray X, Klatzman D, Marteau P; Saint-Antoine IBD Network, Beaugerie L, Simon T. Fecal microbiota transplantation to maintain remission in Crohn's disease: a pilot randomized controlled study. *Microbiome* 2020; **8**: 12 [PMID: 32014035 DOI: 10.1186/s40168-020-0792-5]

29 **Kedia S**, Virmani S, K Vuyyuru S, Kumar P, Kante B, Sahu P, Kaushal K, Farooqui M, Singh M, Verma M, Bajaj A, Markandey M, Sachdeva K, Das P, Makharia GK, Ahuja V. Faecal microbiota transplantation with anti-inflammatory diet (FMT-AID) followed by anti-inflammatory diet alone is effective in inducing and maintaining remission over 1 year in mild to moderate ulcerative colitis: a randomised controlled trial. *Gut* 2022; **71**: 2401-2413 [PMID: 35973787 DOI: 10.1136/gutjnl-2022-327811]

30 **Sarbagili Shabat C**, Scaldaferri F, Zittan E, Hirsch A, Mentella MC, Musca T, Cohen NA, Ron Y, Fliss Isakov N, Pfeffer J, Yaakov M, Fanali C, Turchini L, Masucci L, Quaranta G, Kolonimos N, Godneva A, Weinberger A, Kopylov U, Levine A, Maharshak N. Use of Faecal Transplantation with a Novel Diet for Mild to Moderate Active Ulcerative Colitis: The CRAFT UC Randomised Controlled Trial. *J Crohns Colitis* 2022; **16**: 369-378 [PMID: 34514495 DOI: 10.1093/ecco-jcc/jjab165]

31 **Zmora N**, Suez J, Elinav E. You are what you eat: diet, health and the gut microbiota. *Nat Rev Gastroenterol Hepatol* 2019; **16**: 35-56 [PMID: 30262901 DOI: 10.1038/s41575-018-0061-2]

World Journal of Gastroenterology

Submit a Manuscript: https://www.f6publishing.com

World J Gastroenterol 2023 May 7; 29(17): 2679-2700

DOI: 10.3748/wjg.v29.i17.2679

ISSN 1007-9327 (print) ISSN 2219-2840 (online)

SYSTEMATIC REVIEWS

Different types of fruit intake and colorectal cancer risk: A meta-analysis of observational studies

Zhen-Ying Wu, Jia-Li Chen, Han Li, Ke Su, Yun-Wei Han

Specialty type: Oncology

Provenance and peer review: Unsolicited article; Externally peer reviewed.

Peer-review model: Single blind

Peer-review report's scientific quality classification

Grade A (Excellent): 0
Grade B (Very good): B
Grade C (Good): C, C, C
Grade D (Fair): D
Grade E (Poor): 0

P-Reviewer: Chang YC, Taiwan; Mohamed SY, Egypt; Parthasarathy K, India; Rather AA, India

Received: December 19, 2022
Peer-review started: December 19, 2022
First decision: February 8, 2023
Revised: February 24, 2023
Accepted: March 20, 2023
Article in press: March 20, 2023
Published online: May 7, 2023

Zhen-Ying Wu, Jia-Li Chen, Han Li, Ke Su, Yun-Wei Han, Department of Oncology, The Affiliated Hospital of Southwest Medical University, Luzhou 646099, Sichuan Province, China

Corresponding author: Yun-Wei Han, MD, PhD, Professor, Researcher, Department of Oncology, The Affiliated Hospital of Southwest Medical University, No. 25 Taiping Street, Jiangyang District, Luzhou 646099, Sichuan Province, China. lanpaoxiansheng@126.com

Abstract

BACKGROUND

Multiple studies investigating the relationship between intake of different types of fruit and colorectal cancer (CRC) risk have yielded inconsistent results.

AIM

To perform a meta-analysis of existing studies to assess the association between the intake of different kinds of fruit and the incidence of CRC.

METHODS

We searched online literature databases including PubMed, Embase, WOS, and Cochrane Library for relevant articles available up to August 2022. With data extracted from observational studies, odds ratios (ORs) with 95% confidence intervals (CIs) were assessed using random-effects models. A funnel plot and Egger's test were used to determine publication bias. Furthermore, subgroup analysis and dose-response analysis were performed. All analyses were conducted using R (version 4.1.3).

RESULTS

Twenty-four eligible studies involving 1068158 participants were included in this review. The meta-analysis showed that compared to a low intake, a higher intake of citrus, apples, watermelon, and kiwi reduced the risk of CRC by 9% [OR (95%CI) = 0.91 (0.85-0.97)], 25% [OR (95%CI) = 0.75 (0.66-0.85)], 26% [OR (95%CI) = 0.74 (0.58-0.94)], 13% [OR (95%CI) = 0.87 (0.78-0.96)], respectively. No significant association was observed between the intake of other types of fruit and the risk of CRC. In the dose-response analysis, a nonlinear association was found [R (95%CI) = -0.0031 (-0.0047 to -0.0014)] between citrus intake and CRC risk (P < 0.001), with the risk minimized around 120 g/d (OR = 0.85), while no significant dose-response correlation was observed after continued increase in intake.

CONCLUSION

We found that a higher intake of citrus, apples, watermelon, and kiwi was

negatively associated with the risk of CRC, while the intake of other types of fruits were not significantly associated with CRC. Citrus intake showed a non-linear dose-response relationship with the risk of CRC. This meta-analysis provides further evidence that a higher intake of specific types of fruit is effective in preventing the occurrence of CRC.

Key Words: Colorectal cancer; Fruit; Dose; Systematic review; Meta-analysis

Core Tip: In this study, we summarized and analyzed existing studies on the association between the intake of different types of fruit and the risk of colorectal cancer (CRC). Some specific types of fruit, such as citrus and apples, were found to reduce the incidence of CRC. We also found a nonlinear association between citrus intake and CRC risk in the dose-response analysis. Finally, this study proposed that people should change their diets to lower the risk of CRC, thereby easing the heavy economic burden of cancer worldwide.

Citation: Wu ZY, Chen JL, Li H, Su K, Han YW. Different types of fruit intake and colorectal cancer risk: A meta-analysis of observational studies. *World J Gastroenterol* 2023; 29(17): 2679-2700
URL: https://www.wjgnet.com/1007-9327/full/v29/i17/2679.htm
DOI: https://dx.doi.org/10.3748/wjg.v29.i17.2679

INTRODUCTION

As the third most common cancer, colorectal cancer (CRC) is the third leading cause of cancer death in both men and women, as well as the second leading cause of cancer death in the United States. when men and women are added together[1]. From 2000-2002 to 2014-2016, the incidence of CRC increased by nearly 15% among adults aged 40 to 49 years[2]. The prognosis of CRC varies which mainly depends on the cancer stage, with a 5-year survival rate of about 90% for stage I patients and only 0%-10% for stage IV patients, making the prevention of cancer of great potential and value.

Important risk factors for early-onset CRC include hyperlipidemia, obesity, alcohol consumption and a history of CRC in first-degree relatives[3], of which dietary habits are modifiable. Up to now, various phytochemicals with the potential to prevent cancer have been found in fruits, such as polysaccharides (modified apple polysaccharides, MAP), resveratrol, and flavonoids[4]. MAP inhibits the binding of galectin-3 to its ligand, which is considered to be the promoter of the inflammatory response[5-7], and this may be part of the mechanism by which MAP promotes apoptosis and prevents tumorigenesis[8]. As suggested by Liu *et al*[9], resveratrol regulates PTEN/PI3K/Akt and Wnt/β-catenin signaling pathways, respectively, and thus exhibits growth inhibitory effects in human colon cancer cells. Anticancer properties of flavonoids include modification or inactivation of enzymes that activate or detoxify carcinogens, free radical scavenging, inhibition of transcription factor induction (*e.g.*, activator protein-1 activity), and induction of apoptosis[10]. Epidemiological studies have also highlighted the protective effect of chemicals present in plants and fruits on the risk of CRC[11-14]. For example, data from Jordan and Italy have shown that high intake of flavonoids can reduce CRC risk. Moreover, a considerable number of studies have demonstrated the association between higher intake of fruits and vegetables and lower mortality[15]. However, results from prospective cohorts began to show nonexistent or weak associations[16,17], and a pooled analysis of 14 studies[18] also showed a weak association. Wang *et al*[19] concluded that mortality was not further reduced in those who consumed five servings of fruits and vegetables daily. A meta-analysis showed that increased intake of vegetables, but not fruits, reduced the risk of liver cancer[20]. This finding was also questioned by a large prospective study[21]. Certain types of fruit may be more strongly associated with cancer risk compared with others due to their particular chemical composition and underlying molecular mechanisms, which may be hidden in epidemiological studies. Here, we systematically reviewed the existing evidence and explored potential sources of heterogeneity between study results and whether study results differ by gender, region, and tumor location in order to elucidate the association between intake of different types of fruits and CRC risk.

MATERIALS AND METHODS

The effect of different types of fruit intake on the risk of CRC was reported in this study according to the

Preferred Reporting Items for Systematic Reviews and meta-analyses (PRISMA) statement[22], and it was previously registered with Prospero (study number: CRD42022354620).

Search strategy

Two researchers (Zhen-Ying Wu and Jia-Li Chen) independently conducted a computerized literature search of PubMed, Cochrane, EMBASE, and Web of Science databases until August 2022 for literature on the association of different types of fruit consumption with CRC risk. Studies were identified with the following medical subject heading (MeSH) terms or keywords: (1) Fruit, berry, and plant; (2) cancer, neoplasm, colorectal tumor, CRC, and colorectal neoplasm; and (3) case-control, cohort, and prospective. Titles, abstracts and citations were exported to Endnote 20. The database search strategy is presented in Supplementary Table 1.

Study selection

Two authors (Zhen-Ying Wu and Jia-Li Chen) independently evaluated the titles and abstracts of potentially eligible studies based on the following inclusion criteria: (1) Original articles; (2) human participants; (3) case-control or cohort design; and (4) studies examining the association between intake of different types of fruit and CRC risk. All full-text articles meeting the inclusion criteria were collected. The following exclusion criteria were applied: (1) Articles with confounding of fruits or other food sources; (2) no specific indication of fruit type; (3) no corresponding 95% confidence interval (95%CI) for the relative risk (RR), odds ratio (OR), or hazard ratio (HR) for estimating the highest to lowest levels of fruit consumption; and (4) systematic reviews, meta-analyses, and reviews. Differences between reviewers were resolved through discussion.

Data extraction

For each included potential study, selection evaluation, data extraction and quality assessment were performed independently by two researchers. We extracted the following data from the included studies: The surname of the first author, study area and design, year of publication, sample size (number of cases and controls; cohort size and incident cases), age, follow-up time of the cohort studies, dietary assessment methods, comparison of exposure levels, OR/RR/HR estimates corresponding to fruit intake, and 95%CIs for the highest and lowest fruit intake. We extracted the estimation models that adjusted the most for confounding factors when multiple estimates were reported in the article. If there were independent risk estimates for men and women in a study, or risk estimates for cancers at different sites such as the colon and rectum, we treated them as separate studies.

The number of cases and person-years or non-cases for each category of data are required to calculate the slope of the dose-response curve[23]. With citrus intake in each study divided into at least three groups, we took the mean or median consumption under each category and assigned it to the corresponding RR. The midpoint of the upper and lower boundaries was used as the dose for the corresponding category if the study only reported interval ranges for citrus consumption[24]. When the range of intake was unlimited, we assumed the same level as the adjacent category[25]. For instance, the median for the lowest group was 0, while the median for the highest group was 1.5 times the lower limit for that group. For most studies in the meta-analysis, we used 80 g/serving to calculate intake if the study reported intake in servings[26]. Discrepancies between researchers on included studies were resolved through discussion or consultation with the third author.

Assessment of study quality

We assessed the quality of included studies and their potential risk of bias using the Risk of Bias In Non-randomized Studies of Interventions (ROBINS-I) tool[27]. This assessment tool contains seven domains covering pre-intervention (Bias due to confounding, Bias due to selection of participants), at intervention (Bias in classification of interventions) and post-intervention (Bias due to deviations from intended interventions, Bias due to missing data, Bias in measurement of outcomes and Bias in selection of the reported result). The categories for risk of bias judgements are "low risk", "moderate risk", "serious risk", "critical risk", and "no information". The risk of bias was determined independently by two reviewers, and their disagreements were resolved by mutual consensus.

Statistical methods

The meta-analysis was conducted by comparing the risk of CRC reported in the highest and lowest fruit intake groups. Considering a risk of less than 10% for CRC and a small OR, the RR/HR we calculated was approximately equal to the OR[28]. For the overall estimation, the meta-analysis was performed according to the case where all types of rates were OR. The heterogeneity of the results across studies was evaluated with the I^2 test. Since observational study results are inevitably affected by various sources of heterogeneity such as statistical heterogeneity and conceptual heterogeneity in the real world, we followed the Cochrane Handbook for Systematic Reviews of Interventions and used combined results from random-effects models. The effect of individual studies on risk estimates was investigated through sensitivity analyses by omitting each study in turn. We also conducted sensitivity analyses based on quality assessment to improve the reliability of the results. When an outcome indicator was

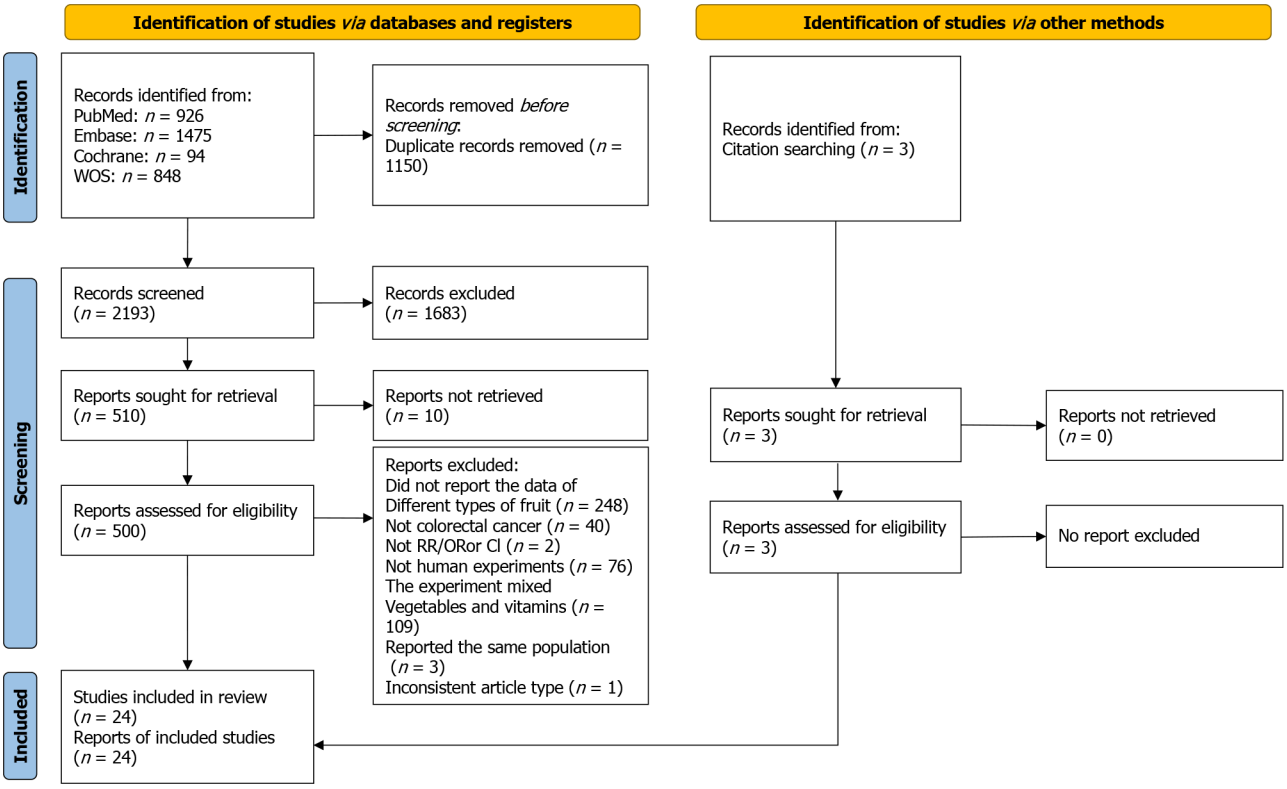

DOI: 10.3748/wjg.v29.i17.2679

Figure 1 PRISMA flow chart of literature search and selection. RR: Relative risk; OR: Odds ratio; CI: Confidence intervals.

reported in more than 10 included studies, publication bias analysis was conducted using Egger's linear regression test and funnel plots. Significant publication bias was considered to exist if the intercept of the Egger's regression line deviated from zero and the *P* value < 0.05. In the present study, we performed pre-specified subgroup analyses based on study design type, location of CRC occurrence, geographic region, and gender. To check for possible non-linear relationships, we also carried out pre-specified dose-response analyses by calculating restrictive three-times sample bars for each study for three or more exposure categories[25]. All analyses were performed by R (version 4.1.3), with two-tailed *P* < 0.05 considered statistically significant.

RESULTS

Included studies

A total of 3343 articles were obtained by the initial literature screening, and after removing 1150 duplicate articles, we identified 2193 articles that were potentially eligible for review. Then 1683 irrelevant entries were eliminated by screening titles and abstracts. Of the remaining 510 articles, 486 were eliminated according to the exclusion criteria. In particular, three studies[29-31] were all from the same study, so only the one with the most complete data was included[29]. Another two studies[32,33] were also from the same study, and similarly the one with the most complete data was included[32]. The results of Tuyns *et al*[34] and Tajima *et al*[35] were removed due to lack of OR and corresponding 95%CI for citrus intake and CRC risk. Three additional[36-38] studies that met the inclusion criteria were identified by manually searching the reference list. The 24 articles were ultimately included in the current meta-analysis[29,32,36-57]. The flow chart for study selection is presented in Figure 1.

Characteristics of the studies

Detailed characteristics of the studies investigating the intake of different types of fruit and CRC risk are shown in Table 1. The final analysis included 16 case-control studies[29,32,37-39,41-49,56,57] and 8 cohort studies[36,40,50-55]. The articles were published between 1996 and 2017, with a total of 1068158 participants aged under 80 years. One study involved only men[50] and one study involved only women[55]. Seven articles distinguished between tumor locations such as rectum and colon (even into proximal and distal colon cancer)[29,38,39,44,50,53,54]. Five articles conducted the research with the classification of gender[36,38,39,52,56]. As for the regional distribution of the study population, nine studies were conducted in Europe[29,32,37,40,43,45,47,49,53], two studies in South America[38,57],

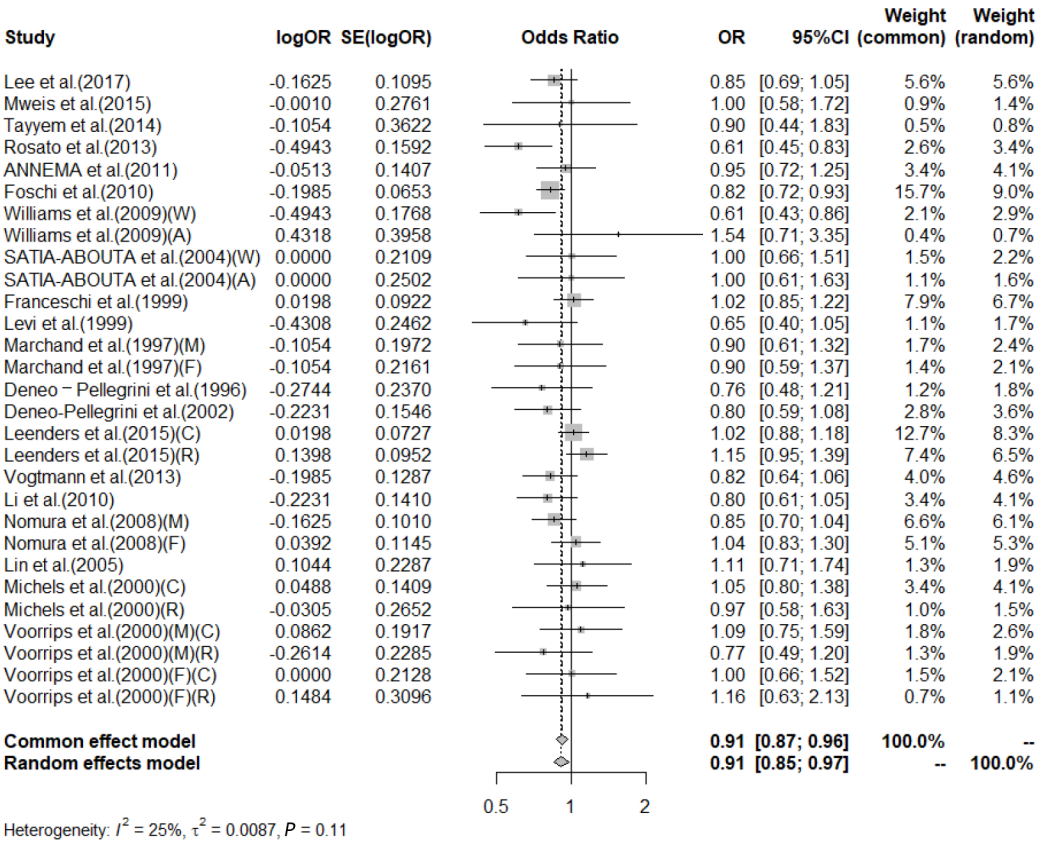

DOI: 10.3748/wjg.v29.i17.2679

Figure 2 Meta-analysis of the risk of colorectal cancer in the highest *vs* lowest category of Citrus intake. F: Female, M: Male; W: Whites, A: African-Americans; C: Colon cancer, R: Rectal cancer. OR: Odds ratio; CI: Confidence intervals.

seven studies in North America[36,46,48,52,54-56], five studies in Asia[39,41,42,50,51], and one study in Australia[44]. Most studies matched or adjusted for age and energy intake; several studies adjusted for BMI (body mass index), smoking status, alcohol use, history of disease associated with CRC, and physical activity; other adjusting factors included gender, education level, and red meat intake (Table 2). Based on the ROBINS-I tool, we identified all studies as having moderate risk of bias. Most of the problems found were regarding confounding and missing data. There was a moderate bias in the classification of interventions in five studies and a moderate bias in the selection of participants in five studies. Among all observational studies, Bias due to deviations from intended interventions, outcomes measurement bias and selection of reported results were considered low. Risk of bias assessment results are summarized in Table 3.

Heterogeneity and pooled results

High *vs* low analysis: Citrus: For 20 included articles[29,38-46,48-57], the overall outcome analysis found that higher citrus intake was related to a lower risk of CRC [I^2 = 25%, P = 0.11, REM; OR (95%CI) = 0.91 (0.85-0.97), P < 0.01] (Figure 2). Further subgroup analysis based on study design showed that citrus intake may reduce the risk of CRC by 15% in case-control studies [I^2 = 17%, P = 0.26, REM; OR (95%CI) = 0.85 (0.78-0.93)], whereas a similar association was not found in cohort studies [I^2 = 0%, P = 0.48, REM; OR (95%CI) = 0.98 (0.90-1.06)] (Figure 3). We also performed a subgroup analysis of 7 included articles based on the specific location of tumorigenesis, which were divided into a total of four locations, namely distal colon, proximal colon, colon, and rectum, but the results suggested no significant association between citrus intake and proximal colon [I^2 = 0%, P = 0.64, REM; OR (95%CI) = 0.93 (0.65-1.32)], distal colon [I^2 = 0%, P = 0.89, REM; OR (95%CI) = 0.80 (0.57-1.12)], colon [I^2 = 0%, P = 0.60, REM; OR (95%CI) = 0.97 (0.91-1.05)], and rectum [I^2 = 55%, P = 0.03, REM; OR (95%CI) = 0.90 (0.78-1.05)] (Figure 4). In the analysis stratified by region, an association between citrus consumption and lower CRC risk was demonstrated only in studies conducted in Asia [I^2 = 0%, P = 0.96, REM; OR (95%CI) = 0.84 (0.73-0.96)], whereas no association was found in studies conducted in North/South America [I^2 = 1%, P = 0.43, REM; OR (95%CI) = 0.91 (0.83-1.01)] and Europe [I^2 = 60%, P < 0.01, REM; OR (95%CI) = 0.92 (0.81-1.05)] (Figure 5). Finally, our stratified analysis of gender in 6 included articles found the protective effect of citrus was only present in men [I^2 = 30%, P = 0.22, REM; OR (95%CI) = 0.84 (0.75-0.96)] but not in women [I^2 = 47%, P = 0.11, REM; OR (95%CI) = 0.98 (0.78-1.25)] (Figure 6).

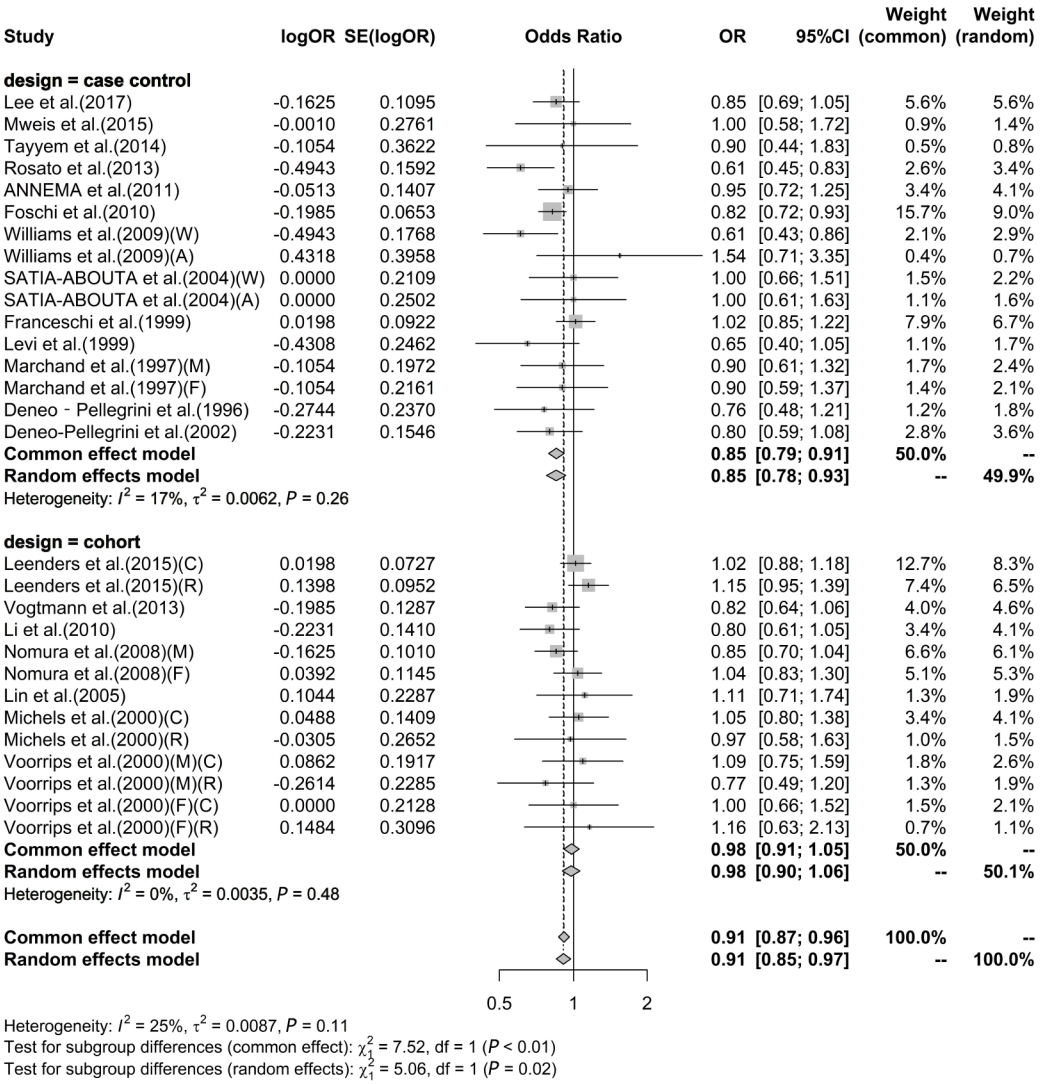

DOI: 10.3748/wjg.v29.i17.2679

Figure 3 Subgroup analysis of the risk of colorectal cancer in the highest *vs* lowest category of Citrus intake by study type. F: Female; M: Male; W: Whites; A: African-Americans; C: Colon cancer; R: Rectal cancer; OR: Odds ratio; CI: Confidence intervals.

Apple: The analysis of the results in 9 included articles[29,32,36,37,41,42,44,47,57] showed that greater intake of apples led to a significant 25% reduction in CRC risk [I^2 = 49%, P = 0.04, REM; OR (95%CI) = 0.75 (0.66-0.85), P < 0.01] (Figure 7). When studies were stratified by region, a significant association was found between apple intake and reduced risk of CRC in the European population [I^2 = 62%, P = 0.03, REM; OR (95%CI) = 0.77 (0.67-0.90)], while no association was observed in the Asian population [I^2 = 0%, P = 0.69, REM; OR (95%CI) = 0.87 (0.55-1.38)] and the North/South American population [I^2 = 76%, P = 0.04, REM; OR (95%CI) = 0.56 (0.30-1.03)] (Supplementary Figure 1).

Banana: The analysis results of six included articles[29,38,41,42,56,57] demonstrated that consuming more bananas did not contribute to reduced risk of CRC [I^2 = 79%, P < 0.01, REM; OR (95%CI) = 0.74 (0.55-1.00), P = 0.05] (Supplementary Figure 2). When stratified by region, banana intake was found to be related to a lower risk of CRC in North/South American populations [I^2 = 58%, P = 0.07, REM; OR (95%CI) = 0.54 (0.39-0.76)], whereas no association was revealed in European populations [I^2 = 0%, P = 1.00, REM; OR (95%CI) = 1.00 (0.92-1.09)] and Asian populations [I^2 = 0%, P = 0.95, REM; OR (95%CI) = 1.16 (0.70-1.92)] (Supplementary Figure 3). When stratified by gender, we found a protective effect of Bananas for both men [I^2 = 0%, P = 0.59, REM; OR (95%CI) = 0.65 (0.49-0.86)] and women [I^2 = 0%, P = 1.00, REM; OR (95%CI) = 0.60 (0.43-0.83)] (Supplementary Figure 4). In a stratified analysis of tumor sites, high banana intake did not show the association with the risk of malignancy in either the colon [I^2 = 86%, P < 0.01, REM; OR (95%CI) = 0.90 (0.72-1.12)] or the rectum [I^2 = 0%, P = 0.36, REM; OR (95%CI) = 0.95 (0.85-1.06)] (Supplementary Figure 5).

Peach: For the four included articles[29,40,42,57], the total analysis results showed that consuming more peaches did not reduce the risk of CRC [I^2 = 62%, P = 0.02, REM; OR (95%CI) = 0.95 (0.83-1.09), P = 0.50]

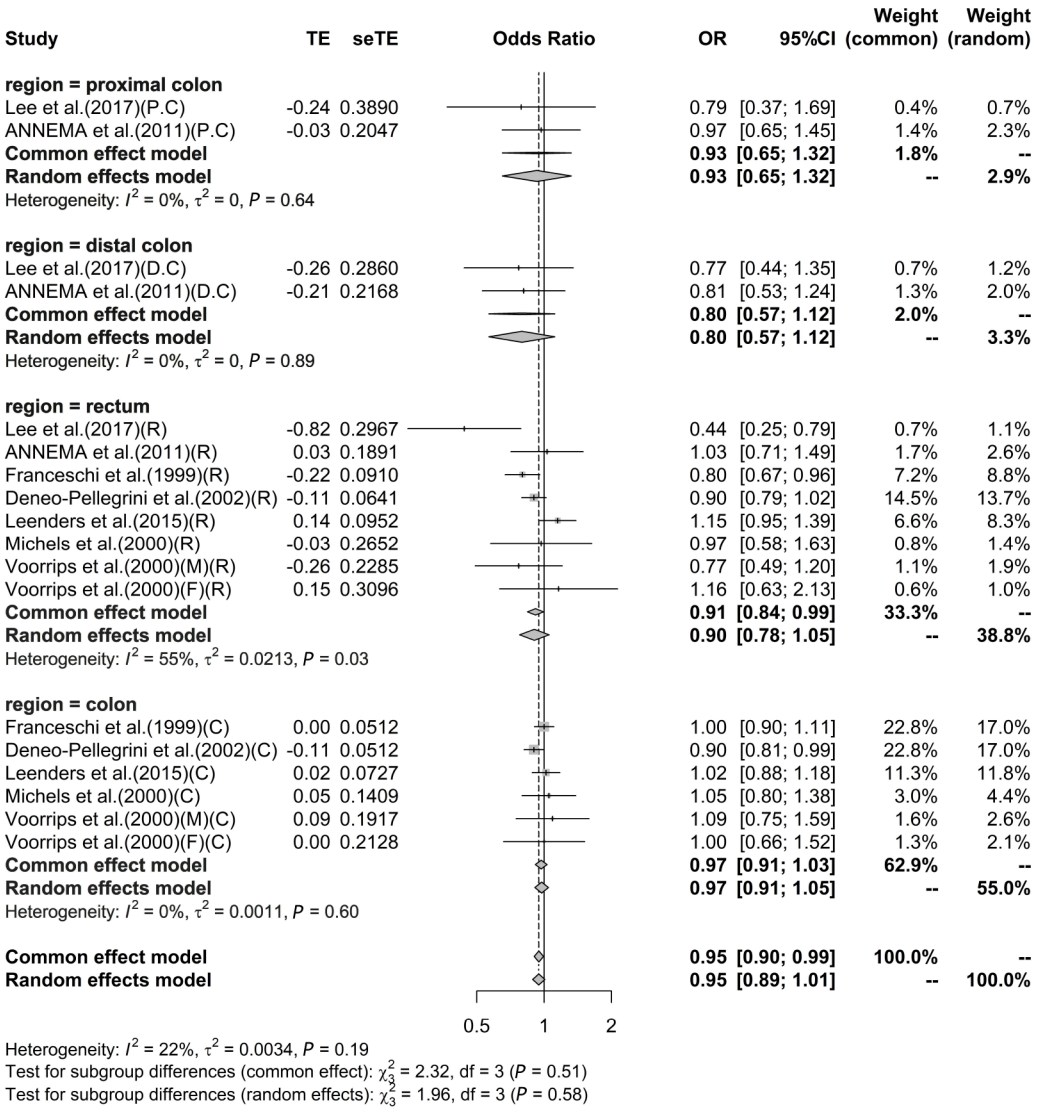

DOI: 10.3748/wjg.v29.i17.2679

Figure 4 Subgroup analysis of the risk of colorectal cancer in the highest *vs* lowest category of Citrus intake by region of cancer. PC: Proximal colon cancer; DC: Distal colon cancer; C: Colon cancer; R: Rectal cancer; F: Female; M: Male; OR: Odds ratio; CI: Confidence intervals.

(Supplementary Figure 6). When stratified by study type, both case-control studies [I^2 = 86%, P = 0.03, REM; OR (95%CI) = 0.90 (0.75-1.07)] and cohort studies [I^2 = 47%, P = 0.17, REM; OR (95%CI) = 1.06 (0.87-1.29)] indicated that peach intake was not related to CRC risk (Supplementary Figure 7). The subgroup analysis based on tumor sites revealed that greater peach intake was not associated with the risk of malignancy in the colon [I^2 = 0%, P = 0.77, REM; OR (95%CI) = 0.99 (0.91-1.08)] and rectum [I^2 = 88%, P < 0.01, REM; OR (95%CI) = 0.96 (0.65-1.42)] (Supplementary Figure 8).

Strawberry: With three articles included in the analysis[29,40,42], overall results demonstrated no reduction in CRC risk even with higher intake of strawberries [I^2 = 58%, P = 0.05, REM; OR (95%CI) = 0.97 (0.90-1.05)], P = 0.42] (Supplementary Figure 9). In the stratified analysis of tumor sites, strawberry intake was not related to cancer risk in either the rectum [I^2 = 34%, P = 0.22, REM; OR (95%CI) = 0.93 (0.83-1.04)] or colon [I^2 = 0%, P = 0.67, REM; OR (95%CI) = 1.00 (0.95-1.06)] (Supplementary Figure 10). In the stratified analysis by study type, case-control studies [I^2 = 75%, P = 0.02, REM; OR (95%CI) = 0.95 (0.86-1.05)] and cohort studies [I^2 = 0%, P = 1.00, REM; OR (95%CI) = 1.04 (0.91-1.19)] showed that strawberry consumption was not associated with CRC risk (Supplementary Figure 11).

Grape: With four articles included[29,40,42,57], overall analysis results indicated that the intake of large amounts of grapes was not related to a reduced risk of CRC [I^2 = 51%, P = 0.07, REM; OR (95%CI) = 1.00 (0.91-1.10), P = 0.97] (Supplementary Figure 12). Subgroup analysis by tumor site showed that grape intake was not significantly associated with malignancy in both the rectum [I^2 = 0%, P = 0.52, REM; OR (95%CI) = 0.91 (0.83-1.01)] and colon [I^2 = 57%, P = 0.13, REM; OR (95%CI) = 1.05 (0.92-1.19)] (Supplementary Figure 13). Stratified by study type, case-control studies [I^2 = 59%, P = 0.06, REM; OR

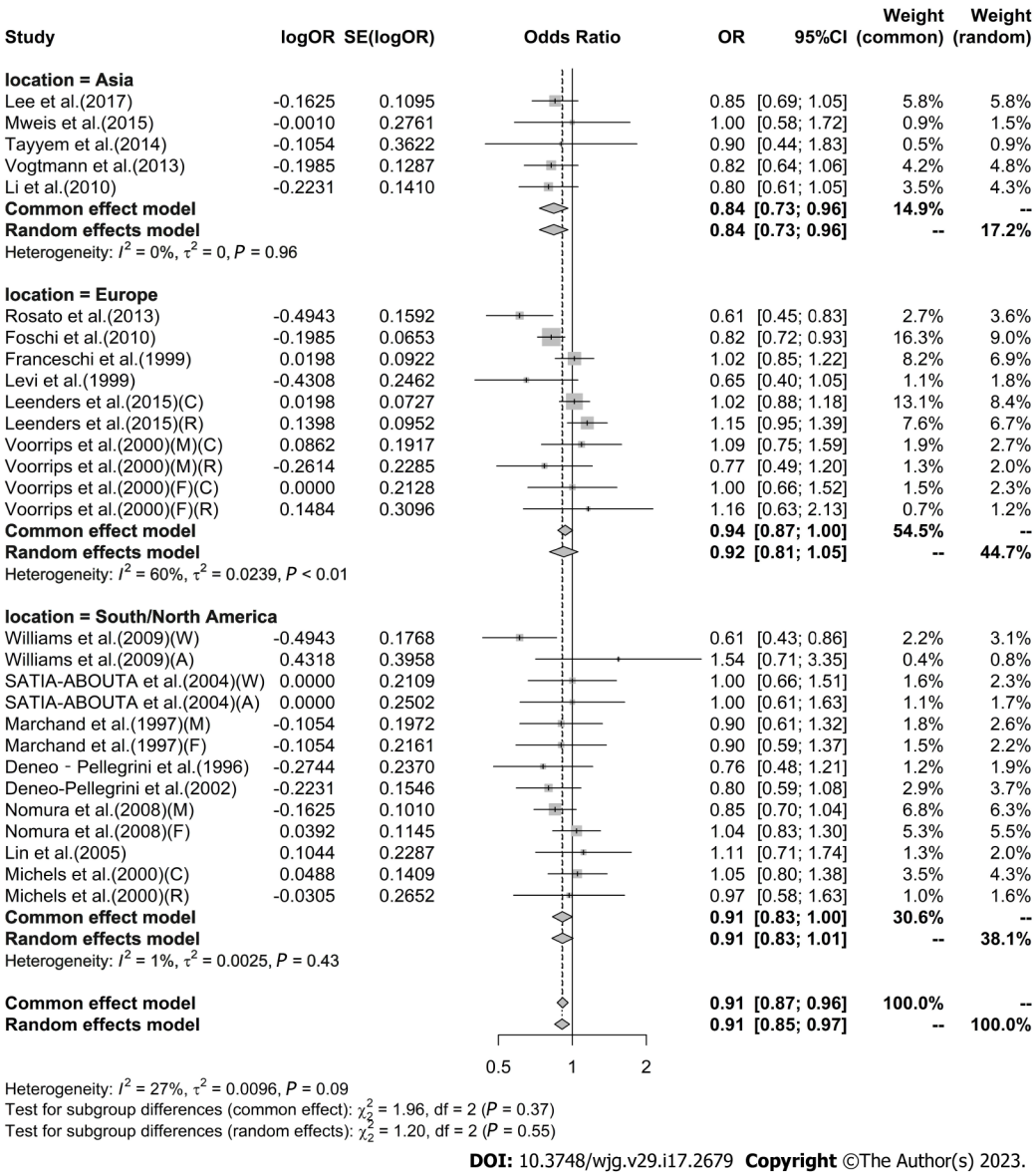

DOI: 10.3748/wjg.v29.i17.2679

Figure 5 Subgroup analysis of the risk of colorectal cancer in the highest *vs* lowest category of Citrus intake by location. F: Female; M: Male; W: Whites; A: African-Americans; C: Colon cancer; R: Rectal cancer; OR: Odds ratio; CI: Confidence intervals.

(95%CI) = 0.97 (0.87-1.08)] and cohort studies [I^2 = 13%, P = 0.28, REM; OR (95%CI) = 1.08 (0.93-1.26)] revealed no reduction in the risk of CRC with grape consumption (Supplementary Figure 14).

Other fresh Fruits: Watermelon[42,50] [I^2 = 0%, P = 0.37, REM; OR (95%CI) = 0.74 (0.58-0.94), P = 0.02] (Supplementary Figure 15) and kiwi[29,42] [I^2 = 0%, P = 0.51, REM; OR (95%CI) = 0.87 (0.78-0.96), P < 0.01] (Supplementary Figure 16) were related to a reduced risk of CRC. Pears[42,57] [I^2 = 0%, P = 0.88, REM; OR (95%CI) = 1.08 (0.72-1.62), P = 0.70] (Supplementary Figure 17), melons[29,42] [I^2 = 34%, P = 0.22, REM; OR (95%CI) = 0.96 (0.87-1.06), P = 0.39] (Supplementary Figure 18), and figs[42,57] [I^2 = 80%, P = 0.03, REM; OR (95%CI) = 0.83 (0.32-2.17), P = 0.70] (Supplementary Figure 19) were not associated with a reduced risk of CRC.

Dose-response meta-analysis

The dose-response analysis of citrus intake included seven articles[39,42,44-46,51,54] (Figure 8). A nonlinear relationship was observed between citrus intake and CRC risk [R (95%CI) = -0.0031 (-0.0047 to -0.0014), P < 0.001]. Based on the above meta-analyses results, a citrus intake of (0 g/d) was used as a reference group and the risk was minimized around 120 g/d (OR = 0.85), whereas no significant dose-response correlation was observed after continuing to increase intake, with correlations only assessed in the range of 0-248 g/d. Dose-response relationships between intake and CRC risk could not be calculated for other types of fruits due to the paucity of available data.

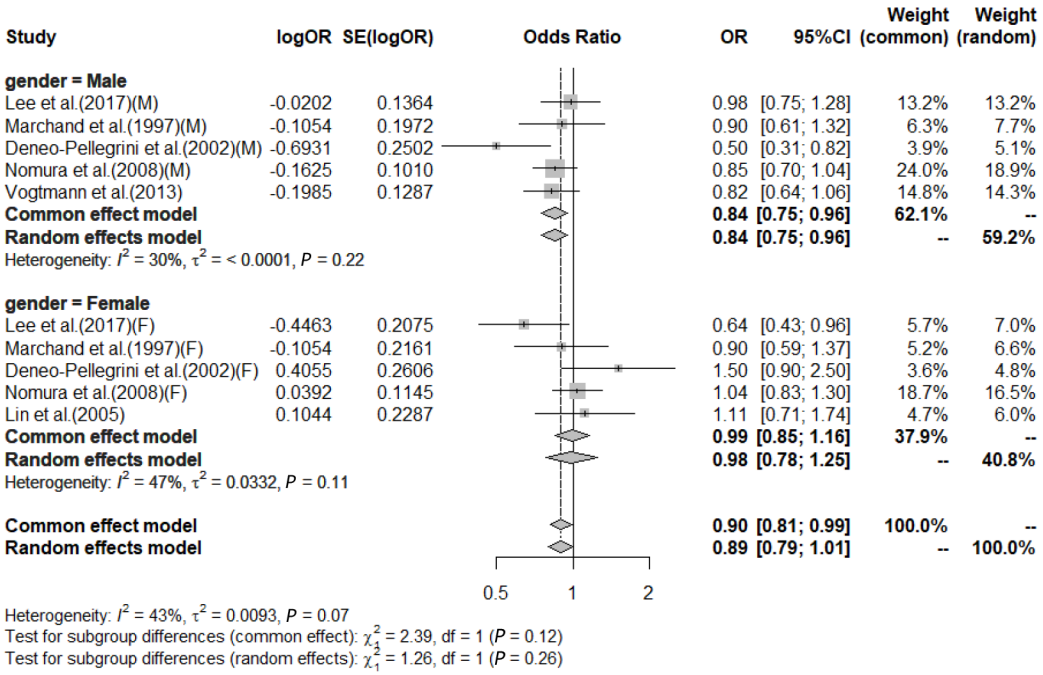

DOI: 10.3748/wjg.v29.i17.2679

Figure 6 Subgroup analysis of the risk of colorectal cancer in the highest *vs* lowest category of Citrus intake by gender. F: Female; M: Male; OR: Odds ratio; CI: Confidence intervals.

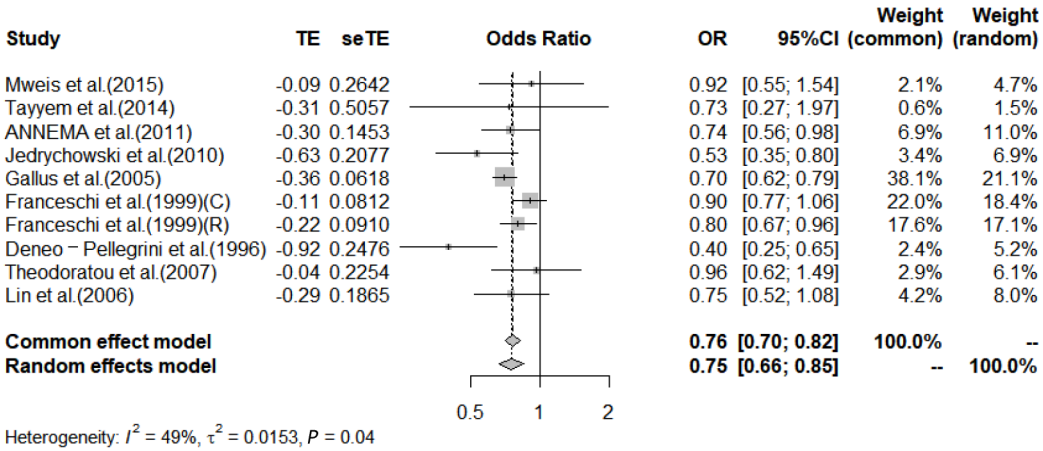

DOI: 10.3748/wjg.v29.i17.2679

Figure 7 Meta-analysis of the risk of colorectal cancer in the highest *vs* lowest category of Apple intake. C: Colon cancer; R: Rectal cancer; OR: Odds ratio; CI: Confidence intervals.

Sensitivity analysis and publication bias

A sensitivity analysis was conducted for all outcome indicators with more than 50% heterogeneity and P < 0.05, and the results showed that the combined results were stable for heterogeneity. A sensitivity analysis based on quality assessment was also conducted. After articles with relatively low quality of evidence (three domains were graded as moderate risk) were excluded, the remaining data were pooled and analyzed again, and the outcome showed that our combined results were robust (Supplementary Figures 20 and 21). No potential publication bias was found. For the analysis of high and low fruit intake, the P value of the citrus Egger's test was 0.8467 (Figure 9A), and the P value for the apple Egger's test was 0.6068 (Figure 9B). Other types of fruits were not tested for publication bias as the number of articles was less than 10.

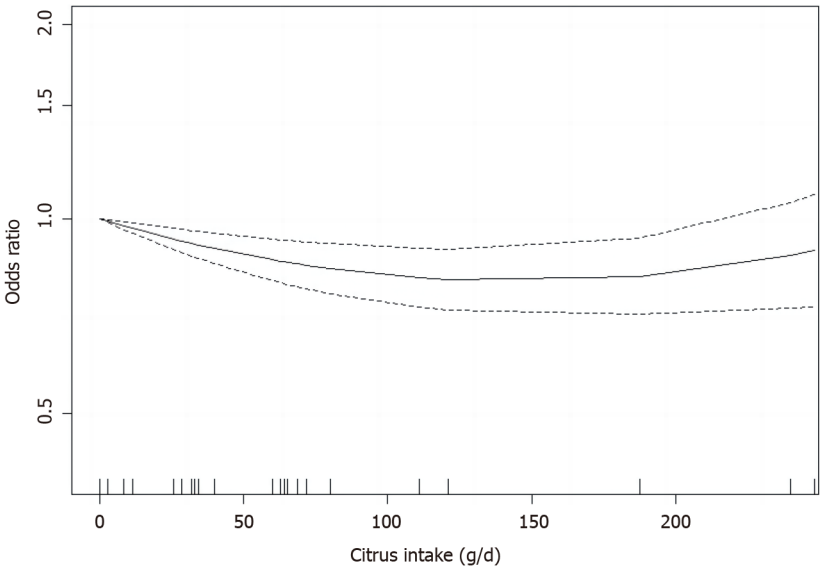

DOI: 10.3748/wjg.v29.i17.2679

Figure 8 Nonlinear relation between Citrus fruit intake and the risk of colorectal cancer.

DISCUSSION

The main findings of this meta-analysis demonstrated that compared to low intakes, higher intakes of citrus, apples, watermelon, and kiwi reduced the risk of CRC by 9%, 25%, 26%, and 13%, respectively, while bananas, grapes, strawberries, peaches, pears, figs, and other melons did not exhibit an association with CRC risk. A nonlinear dose-response relationship was observed between citrus and CRC risk in the present study. To our knowledge, this study is the first meta-analysis to investigate the association between different fruit intake and CRC risk, and the first to perform a dose-response analysis between citrus intake and CRC risk.

The results of this meta-analysis are supported by relevant biological theories. Citrus has many chemopreventive effects on CRC[58]. Nobiletin, a compound extracted from citrus, blocks the cell cycle, inhibits cell proliferation, induces apoptosis, prevents tumor formation, reduces inflammatory effects and limits angiogenesis[59]. Naringenin, which is rich in citrus, inhibits the proliferation of HT-29 colon cancer cells[60] and also reduces the severity of colorectal adenomas and colitis by inhibiting pro-inflammatory mediators GM-CSF/M-CSF, bone marrow-derived suppressor cells, IL-6 and TNF-α, and NF-κB/IL-6/STAT3 cascade in colorectal tissues[61]. Neohesperidin, derived from citrus fruits, has also been confirmed to prevent colorectal tumors by altering the intestinal microbiota[62]. Moreover, APs contained in apples have been verified to prevent AOM/dss-induced colitis-associated CRC (CACC) in ICR mice. APs modulate intestinal flora composition, reduce infiltration of neutrophils, macrophages and T cells in the colon, and more importantly, inhibit the entry of β-catenin into the nucleus, which in turn retards the Wnt/β-catenin pathway[63]. APs also induce apoptosis in colon cancer cells through microactivating the NF-κB pathway, and inhibit CRC cell migration and invasiveness by targeting the LPS/TLR4/NF-κB pathway[64,65]. It has also been shown that apple polyphenols and apple anthocyanin Cy3Gal inhibit and reduce the appearance of precancerous markers of CRC[66] as well as tumor lesions in AOM-induced CRC mice[67]. In addition, apple polyphenols affect the initiation of apoptosis in human colon cancer cells and the activity of protein kinase C[68]. That other fruits did not show protective effects may be owing to the small number of original studies, resulting in large heterogeneity and wide confidence intervals, which masked their anticancer effects. It could also be possible that the intake was too small to show a protective effect, and more research is needed for verification.

There are many reasons contributing to inconsistent results in several subgroup analyses. In citrus, case-control studies tended to show protective factors, while cohort studies did not. In other types of fruits, no correlation was seen in the subgroup analysis of the study type. Generally speaking, case-control studies have several weaknesses, such as a control group that may not be representative of the general population or more problems with reverse causality and recall bias. On the other side, dietary assessment questionnaires used in a prospective study setting may not be as accurate as those used in a retrospective case-control setting. Meanwhile, it is difficult for individuals to accurately report their fruit intake, and this low correlation has been confirmed in some studies (Spearman's correlation coefficient of 0.6 for fruit consumption[69,70]), which may have weakened the estimates of the associated risk. Thus, the true association may be stronger than what we observed, reinforcing the conclusion of protective effect. In another subgroup analysis of studies' geographic location, a negative association between citrus intake and CRC risk was observed in Asia but not in North/South America or Europe,

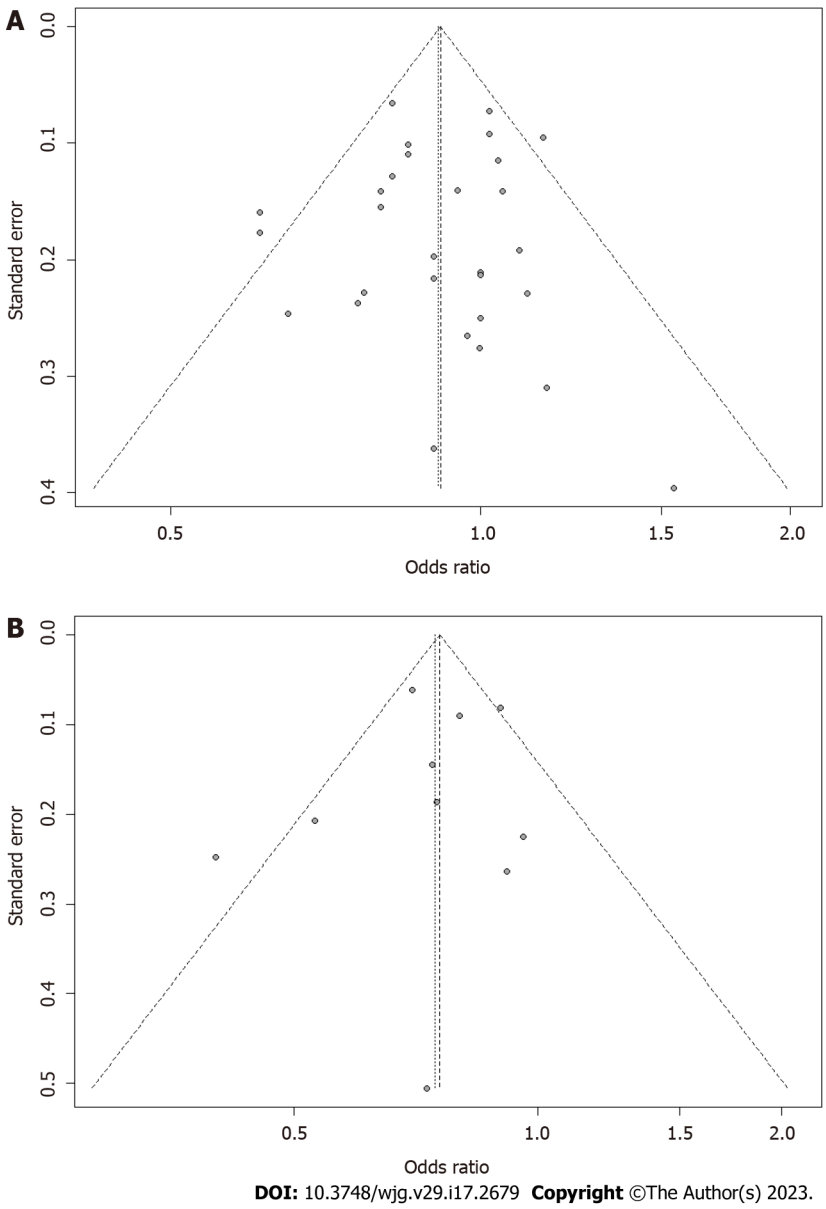

DOI: 10.3748/wjg.v29.i17.2679

Figure 9 Funnel plot. A: Funnel plot of studies evaluating for the association between Citrus fruit intake and risk of colorectal cancer. Dotted lines on both sides indicate 95% pseudo-confidence intervals; B: Funnel plot of studies evaluating for the association between Apple intake and risk of colorectal cancer. OR: Odds ratio; CI: Confidence intervals.

and a negative association for bananas only in North/South America and apples in Europe. These results may be attributed to the varied consumption patterns of fruits and vegetables among countries, leading to errors in the measurement of dietary intake[71]. According to our pooled results, the specific sites of tumor occurrence, such as the distal colon, proximal colon, and rectum, were not significantly associated with the risk and benefit of fruit intake, indicating that fruits improve the function of the entire intestine or regulate the microbial flora of the entire digestive tract, but do not target specific sites, so there is no correlation with the specific location of tumors. No significant risk benefit was seen for men or women in the gender-based subgroup analysis either, possibly due to an insufficient number of included original studies or dietary measurement errors. From the dose-response analysis, the risk of CRC was found to be minimized at a citrus intake of 120 g/d, while the risk of CRC did not decrease further after continuing to increase intake. The underlying mechanism may be related to the availability and digestibility of nutrients from citrus fruits[72,73]. However, further studies are needed to validate our results.

Surgery, chemoradiotherapy and targeted drugs currently used to treat CRC are not only expensive but also highly toxic. Through this Meta-analysis, we can prioritize fruits with proven protective effects to prevent CRC. If cancer prevention can be achieved by changing dietary habits such as fruit supplementation, it will certainly reduce the huge economic burden and mortality of cancer in the world. As for future research directions, we hope to find the key components of anti-cancer through research and make element-specific nutritional preparations to help people better prevent cancer. More prospective

Table 1 Characteristic of eligible studies included in the meta-analysis assessing the relationship between different types of fruit intake and the risk of colorectal cancers

Ref.	Country	No. of cases/controls (age)	Dietary assessment	Comparison of exposure level	Category, OR/RR (95%CI)	Confounding factors
Lee *et al*[39], 2017	-	923 (625 males, 298 females)/1846 (1250 males, 596 females)	SQFFQ, 106 food items	Orange/yellow fruits (g/d); males: T3 (≥ 47.9) *vs* T1 (< 15.9); females: T3 (≥ 90.6) *vs* T1 (< 32.5); proximal colon/distal colon/rectum: T3 (≥ 90.6) *vs* T1 (< 32.5)	Males: 0.98 (0.75-1.28); females: 0.64 (0.43-0.97); total: 0.85 (0.69-1.06); proximal colon: 0.79 (0.37-1.70); distal colon: 0.77 (0.44-1.35); rectum: 0.44 (0.25-0.80)	Age, education, alcohol consumption, BMI, regular exercise, red meat, processed meat, total EI
Leenders *et al* [40], 2015	Ten European countries (Denmark, France, Germany, Greece, Italy, The Netherlands, Norway, Spain, Sweden, and United Kingdom	442961 cohort; 3082 incident cases (2128 colon cancer (954 proximal, 965 distal), 1242 rectal cancer cases); 51.2 (38.3-63.0) years; follow-up 8 years	Center-specific dietary questionnaire	Medians of consumption per quartiles; berries: 21 g/d *vs* 1 g/d; citrus fruits: 110 g/d *vs* 7 g/d; grapes: 32 g/d *vs* 1 g/d; hard fruits: 153 g/d *vs* 10 g/d; stone fruits: 83 g/d *vs* 2 g/d	Colon cancer; berries: 1.04 (0.88-1.24); citrus fruits: 1.02 (0.88-1.17); grapes: 1.15 (0.97-1.37); stone fruits: 0.97 (0.81-1.15); rectal cancer: Berries: 1.04 (0.83-1.30); citrus fruits: 1.15 (0.95-1.38); grapes: 0.98 (0.78-1.25); stone fruits: 1.19 (0.94-1.50)	All other fruit and vegetable consumption, height, weight, dietary calcium consumption, dietary alcohol consumption, dietary cereal fiber consumption, smoking status, time since stopped smoking, duration of smoking, number of cigarettes smoked per day and PA
Abu Mweis *et al*[41], 2015	Jordan	167/240, NA	FFQ, 109 food items	≥ 3 times/wk (high) *vs* ≥ 2 times/wk (low)	Apples: 0.915 (0.545-1.535); bananas: 1.167 (0.670-2.033); oranges: 0.999 (0.581-1.715)	Age, sex, total EI, metabolic equivalent, smoking, education level, marital status, work, income, and family history of CRC
Tayyem *et al* [42], 2014	Jordan	220/281 (248 males, 253 females); males: mean age 55.27 years; females: mean age 48.67 years	NA; 42 food items	Daily (high) *vs* ≤ rarely (low)	Apple: 0.73 (0.27-1.96); banana: 1.12 (0.34-3.67); orange: 0.90 (0.44-1.82); pear: 1.13 (0.56-2.29); peach: 0.64 (0.32-1.25); grape: 0.62 (0.27-1.40); melon: 0.82 (0.38-1.78); watermelon: 0.54 (0.26-1.11); strawberry: 0.75 (0.26-2.13); fig: 0.51 (0.28-0.92); kiwi: 1.14 (0.25-5.06); dried Fruit: 1.42 (0.55-3.67)	Age, sex, total EI, MET minutes/week, tobacco use, education level, marital status, work, income, PA, marital status, family history of CRC
Rosato *et al* [43], 2013	Italia and Swiss	329/1361, median age 40 yr	FFQ; 78 food items	High *vs* Low	Citrus fruit: 0.61 (0.45-0.84)	Age, sex, center, study, year of interview, education, family history, alcohol consumption, EI
Vogtmann *et al*[50], 2013	China	61274 male's cohort (40-74 years); 398 incident cases (236 colon, 162 rectal); follow-up 2002-2006 to 2010	Validated FFQ; 46 food items	Citrus fruit intake g/day: ≥ 12.61 (high) *vs* < 2.70 (low); watermelon intake g/day: ≥ 93.33 (high) *vs* < 33.33 (low)	Citrus fruit: Colorectal cancer: 0.82 (0.64-1.06); colon cancer: 0.86 (0.62-1.19); rectal cancer: 0.76 (0.51-1.14); watermelon: Colorectal cancer: 0.77 (0.59-0.99); colon cancer: 0.76 (0.55-1.06); rectal cancer 0.77 (0.51-1.15)	Age, total EI, red meat intake, total meat intake, education, income, occupation, smoking status, alcohol consumption, BMI, MET hours of exercise participation, history of diabetes mellitus, family history of CRC
Annema *et al* [44], 2011	Western Australia	834 (64.9 yr ± 8.9 yr)/939 (64.6 yr ± 9.4 yr)	FFQ; 74 food items	Servings/d) ≥ 0.50 (high) *vs* < 0.07 (low)	Total: Citrus fruit: 0.95 (0.72-1.25); apples: 0.74 (0.56-0.99); fruit juice: 1.38 (1.08-1.75); citrus fruit: Proximal Colon: 0.97 (0.65-1.45); distal Colon: 0.81 (0.53-1.24); rectum: 1.03 (0.71-1.49); apples: Proximal Colon: 1.13 (0.72-1.77); distal colon: 0.51 (0.34-0.77); rectum: 0.73 (0.49-1.08); fruit	Sex, age, BMI at age 20 yr, EI, multiv-itamin use, alcohol consumption, PA, smoking, diabetes, socioeconomic status

					juice: Proximal Colon: 1.06 (0.74-1.49); distal colon: 1.41 (0.99-2.01); rectum: 1.74 (1.24-2.45)	
Foschi *et al* [45], 2010	Italy and Switzerland	3634 (median age 62 yr)/6804 (median age 57 yr)	Validated FFQ; 78 food items	Citrus fruit or citrus fruit juice intake: ≥ 4 portions/wk *vs* < 1 portion/wk	Citrus: 0.82 (0.72-0.93)	Age, sex, study center, tobacco smoking, alcohol, education, BMI, PA, EI
Li *et al*[51], 2010	Japan	42470 cohort (40-79 yr) (20222 males, 22248 females); 665 incident cases; follow-up 9 years	FFQ; 40 food items	Citrus consumption daily *vs* ≤ 2 times/wk	Citrus: 0.80 (0.61-1.06)	Age, sex, job status, years of education, BMI, time engaging in sports or exercise, time spent walking, cigarette smoking, alcohol drinking, history of hypertension, diabetes mellitus and gastric ulcer, family history of cancer, daily total EI, consumption of rice/miso soup/soybean products/total meat/total fish/dairy products/other fruits/total vegetables/oolong tea/black tea/coffee /green tea
Jedrychowski *et al*[32], 2010	Poland	592/765; NA	EPIC-FFQ148 food items	Apples, servings/d: > 1.50 (Q5; high) *vs* < 0.18 (Q1; low)	Apples: 0.53 (0.35-0.79)	Age, gender, place of residency, marital status, tobacco smoking, total EI, intake of vegetables, fruits excluding apples
Williams *et al* [46], 2009	North Carolina	945/959; 40-79 yr; whites (n = 1520); African-Americans (n = 384)	Diet history questionnaire; 124 food items	Citrus fruit (servings/wk): White: 16.4 Q4 (high) *vs* 1.89 Q1 (low); African-Americans: 21.7 Q4 (high) *vs* 2.3 Q1 (low)	Whites: 0.61 (0.43-0.86); African-Americans: 1.54 (0.71-3.35)	Age, sex, education, income, BMI 1 yr ago, PA, family history, nonsteroidal anti-inflammatory drug use, total EI
Nomura *et al* [52], 2008	Hawaii and Los Angeles	191011 cohort (85903 males, 105108 females); 2110 incident cases (1138 males, 972 females) (1571 of the colon, 515 of the rectum, 24 cases both sites) (45-75 yr); follow-up 7.3 years	Self-administered quantitative FFQ (QFFQ); 180 food items	Citrus fruit were quantified as g × 1000 kcal-1 × d-1; Q5 (high) *vs* Q1 (low)	Citrus fruit: Male: 0.85 (0.70-1.04); female: 1.04 (0.83-1.30)	Ethnicity, age, family history of CRC, history of colorectal polyp, pack-years of cigarette smoking, BMI, hours of vigorous activity, aspirin use, multivitamin use, replacement hormone use (women), log EI, alcohol, red meat, folate, vitamin D, calcium
Gallus *et al* [47], 2005	Italy	1953 (1225 of the colon, 728 of the rectum)/4154	Validated FFQ 78 food items	Average consumption of apples per day ≥ 1 (high) *vs* < 1 (low)	Apples: 0.70 (0.62-0.79)	Age, sex, study center, education, BMI, tobacco smoking, alcohol drinking, total EI, vegetable consumption, PA, other fruit
Lin *et al*[55], 2005	United States	39876 female cohort (mean age 45 years); 240 incident cases; follow-up 10 years	FFQ; 131 food items	Citrus fruit (serving/day) Median intake; 1.6 (Q5) high *vs* 0.1 (Q1) low	Citrus fruit: 1.11 (0.71-1.74)	Age, randomized treatment assignment, BMI, family history of CRC in a first-degree relative, history of

						colon polyps, PA, smoking status, baseline aspirin use, red meat intake, alcohol consumption, total EI, menopausal status and baseline post-menopausal HT use, folate intake, multivitamin use
Satia-Abouta *et al*[48], 2004	United States	613 (337 Caucasians, 276 African-Americans)/996(596 Caucasians, 400 African-Americans) (40-80 years)	Validated FFQ; 100 food items	Citrus fruits and juices: Median g/d: Caucasians: 4th quartile (high) 168 g *vs* 1st quartile 0 g (low); African-Americans: 4th quartile (high) 173 g *vs* 1st quartile 0 g (low)	Caucasians: 1.0 (0.7-1.6); African-Americans: 1.0 (0.6-1.6)	Age, gender, total EI, education, BMI, smoking history, PA, family history of colon cancer, NSAID use, fat, carbohydrates, dietary fiber, vitamin C, vitamin E, beta-carotene, calcium, folate, fruits, vegetables
Voorrips *et al* [53], 2000	Netherlands	4087 cohort; 620 colon cancer cases (332 males, 288 females), 344 rectal cancer cases (217 males, 127 females); follow-up 6.3 years	Validated FFQ; 150 food items	Citrus fruit Median intake (g/d); male: Q5 (167 g/dk) (high) *vs* Q1 (0g/dk) (low); female: Q5 (187 g/dk) (high) *vs* Q1 (8 g/dk) (low)	Male: Colon cancer: 1.09 (0.75-1.59) Rectal cancer: 0.77 (0.49-1.20); female: Colon cancer: 1.00 (0.66-1.52); rectal cancer: 1.16 (0.63-2.12)	Age, family history of CRC, category of alcohol intake
Michels *et al* [54], 2000	United States	136089 cohort (88764 females (30-55 years), 47325 males (40-75years); 1181 incident cases (937 colon cancer, 244 rectal cancer); follow-up 16 years	Validated FFQs; 61 food items	Citrus fruit: Frequencies of intake ≥ 2 servings/d *vs* 1 serving/wk or fewer	Colon cancer: 1.05 (0.80-1.39); rectal cancer: 0.97 (0.58-1.64)	Age, family history of CRC, sigmoidoscopy, height, BMI, pack-years of smoking, alcohol intake, PA, menopausal status, postmenopausal hormone use, aspirin use, vitamin supplement intake, total caloric intake, red meat consumption
Franceschi *et al*[29], 1998	Italy	1953 (1225 colon cancer, 728 rectal cancer)/4154 (2073 males, 2081 females)	Validated FFQ; 78 food items	Mean weekly servings: Citrus fruit Q5 7.5 (high)/Q1 1.0 (low); apples/pears: Q5 15.0 (high)/Q1 3.0 (low); bananas: Q5 3.0 (high)/Q1 0.5 (low); kiwi: Q5 4.0 (high)/Q1 0.5 (low); peaches/apricots/prunes: Q5 5.0 (high)/Q1 0.8 (low); melon: Q5 0.5 (high)/Q1 0.1 (low); grapes: Q5 1.0 (high)/Q1 0.2 (low); Strawberries/cherries: Q5 0.4 (high)/Q1 0.1 (low)	Citrus: Total: 1.02 (0.85-1.22), colon: 1.0 (0.9-1.1), rectal: 0.8 (0.7-1.0); apples/pears: Colon: 0.9 (0.8-1.1) rectal: 0.8 (0.7-1.0); bananas: Colon 1.0 (0.9-1.1), rectal 1.0 (0.8-1.1); kiwi: colon 0.9 (0.8-1.0) rectal 0.8 (0.7-1.0); peaches/apricots/prunes: Colon 1.0 (0.9-1.1) rectal 0.8 (0.7-0.9); melon: Colon 1.0 (0.9-1.0) rectal 0.9 (0.8-1.0); grapes: colon 1.0 (0.9-1.0) rectal 0.9 (0.8-1.0); strawberries/cherries: Colon 1.0 (0.9-1.0) rectal 0.9 (0.9-1.0)	Age, sex, centre, education, PA, total EI
Levi *et al*[49], 1999	Swiss	223 (males 142, females 81) (119 colon cancer, 104 rectal cancer, median age 63 yr)/491 (211 males, 280 females, median age 58 yr)	FFQ; 79 food items	Citrus fruits (Servings per week): Q3 (> 3.5/wk) *vs* Q1 (1.5/wk)	Citrus fruits: 0.65 (0.40-1.05)	Age, sex, education, smoking, alcohol, BMI, PA, meat and vegetable consumption, total EI
Le Marchand *et al*[56], 1997	Hawaii	1192 (698 males, 494 females) (mean age 66 yr)/1192 (698 males, 494 females) (mean age 66 yr)	Validated FFQ; 282 food items	Bananas: Male ≥ 55 g/d (Q4 high) *vs* ≤ 9 g/d (Q1 low), female: ≥ 54 g/d (Q4 high) *vs* ≤ 11 g/d (Q1 low); citrus fruits: Male ≥ 52 g/d (Q4 high) *vs* ≤ 4 g/d (Q1 low), female: ≥ 58 g/d (Q4 high) *vs* ≤ 8 g/d (Q1 low)	Bananas: Male: 0.7 (0.5-1.1), female: 0.6 (0.4-0.9); citrus fruits: Male: 0.9 (0.6-1.3), female: 0.9 (0.6-1.4)	Age, family history of CRC, alcoholic drinks per week, pack-years of cigarette smoking, lifetime recreational activity, Quetelet index 5 years earlier, total calories, egg,

						and calcium
Deneo-Pellegrini *et al*[57], 1996	Uruguay	160 (71 rectal cancer, 89 colon cancer)/221	FFQ; 61 food items	(T3; high) *vs* (T1; low)	Orange: 0.76 (0.47-1.19); apple: 0.40 (0.25-0.66); peach: 1.05 (0.65-1.69); pear: 1.06 (0.65-1.74); grape: 1.61 (0.94-2.74); fig: 1.36 (0.73-2.54); banana: 0.28 (0.16-0.50)	Age, sex, residence, education, BMI, total EI, alcohol intake
Lin *et al*[36], 2006	United States (NHS and HPFS)	71976 female cohort; 498 incident cases (30-55 yr); 35425 male cohort; 380 incident cases (40-75 yr); follow-up 10 yr	Validated FFQ; 131 food items	Apple: ≥ 2 servings/d (Q5; high) *vs* 0-2 servings/wk (Q1; low)	Total: 0.75 (0.52-1.08); NHS females: 0.64 (0.35-1.17); HPFS males: 0.82 (0.51-1.30)	Age, BMI, PA, history of CRC, previous colorectal polyps, prior screening sigmoidoscopy or colonoscopy, smoking, multiv-itamin use, current aspirin use, alcohol, EI, red meat, total Ca, total folate, total fibre
Theodoratou *et al*[37], 2007	United Kingdom	1456 (mean 63.9 yr ± 9.6 yr) yr)/1456 (64.7 yr ± 9.5 yr)	Validated FFQ; 150 food items	Apples: Q4 (high) *vs* Q1 (low)	Apples: 0.96 (0.62-1.50)	Age, sex, residence area, family history of CRC, total EI, fibre, alcohol, NSAID, smoking, BMI, PA
Deneo-Pellegrini *et al*[38], 2002	Uruguay	484 (260 colon cancer, 224 rectal cancer)/1452	FFQ; 64 food items	Citrus fruits estimate: Q4 (high) *vs* Q1 (low); banana estimate: Q4 (high) *vs* Q1 (low)	Total: Citrus fruits: 0.8 (0.6-1.1), banana: 0.6 (0.4-0.8); citrus fruits: Male: 0.5 (0.3-0.8), female: 1.5 (0.9-2.5); colon: 0.9 (0.9-1.1); rectum: 0.9 (0.7-0.9); banana: male: 0.6 (0.4-0.9), female: 0.6 (0.3-0.9); colon: 0.8 (0.7-0.9); rectum: 0.9 (0.8-1.1)	Age, residence, urban/rural status, education, family history of colon cancer for first-degree relatives, BMI, total EI and red meat intakes

NA: Not available; EI: Energy intake; PA: Physical activity; CRC: Colorectal cancer; BMI: Body mass index; MET: Metabolic equivalentr; NSAID: Non-steroidal anti-inflammatory drugs; NHS: Nurses' Health Study; HPFS: Health professionals follow-up study.

studies are also expected to verify the anti-cancer effects of other kinds of fruits.

We observed low heterogeneity between studies. Despite moderate heterogeneity in the studies on bananas and peaches, further sensitivity analysis indicated robust primary outcome and the heterogeneity was acceptable. The funnel plots and Egger's test we adopted produced consistent results, suggesting no publication bias. Moreover, the meta-analysis involved more than 1.06 million subjects, which makes it possible to explore associations between different subgroups, such as gender, geographic location and tumor location. Besides, a significant dose-response relationship was observed between citrus intake and CRC risk, further strengthening the association.

Nevertheless, there are some limitations of our study. First, synthetic results are limited due to the lack of research data on many types of fruits (*e.g.*, grapes, pears, and figs, *etc.*). This is coupled with the fact that dietary assessments of the frequency/amount of fruit intake varies so much that the protective effect against cancer cannot be truly captured. Additional potential bias may exist due to the diversity of designs and inconsistency of adjustment factors in the studies we analyzed. Although we extracted data with the most comprehensive adjustment for confounders, a subset of studies still did not adjust for potential dietary confounding variables (*e.g.*, meat, fiber, income status, and occupation). The limited range of citrus intake in the dose-response meta-analysis may have led to incomplete results. And limited available data for other fruits and the small number of original studies and made it impossible to investigate dose-response relationships between their intake and cancer risk.

CONCLUSION

Taken together, our results support the hypothesis that citrus, apple, watermelon and kiwi intake may contribute to a reduced risk of CRC. A nonlinear dose-response relationship was also observed between citrus intake and CRC risk within a certain range. However, the relationship between other types of fruit intake and CRC risk may be obscured by the various limitations mentioned above. Therefore, future prospective studies are required to further explore the effects of measurement error and control for important confounders, and thus reveal the true relationship between fruit and CRC.

Table 2 The main adjusted factors of studies included in the meta-analysis

Ref.	Adjusted confounders									
	Age	Sex	Energy intake	BMI	Family history of CRC	Alcohol use	Smoking status	Physical activity	Education level	Red meat
Lee *et al*[39], 2017	√		√	√		√		√	√	√
Leenders *et al*[40], 2015				√		√	√	√		
Abu Mweis *et al*[41], 2015	√	√	√		√		√		√	
Tayyem *et al*[42], 2014	√	√	√		√		√	√	√	
Rosato *et al*[43], 2013	√	√	√		√	√			√	
Vogtmann *et al*[50], 2013	√		√	√	√	√	√	√	√	√
Annema *et al*[44], 2011	√	√	√	√		√	√	√		
Foschi *et al*[45], 2010	√	√	√	√		√	√	√	√	
Li *et al*[51], 2010	√	√	√	√	√	√	√	√	√	
Jedrychowski *et al*[32], 2010	√	√	√				√			
Williams *et al*[46], 2009	√	√	√	√	√			√	√	
Nomura *et al*[52], 2008	√		√	√	√	√	√	√		√
Gallus *et al*[47], 2005	√	√	√	√		√	√	√	√	
Lin *et al*[55], 2005	√		√	√	√	√	√	√		√
Satia-Abouta *et al*[48], 2004	√	√	√	√	√		√	√	√	
Voorrips *et al*[53], 2000	√				√	√				
Michels *et al*[54], 2000	√		√	√	√	√	√	√		√
Franceschi *et al*[29], 1998	√	√	√					√	√	
Levi *et al*[49], 1999	√	√	√	√		√	√	√	√	
Le Marchand *et al*[56], 1997	√		√		√	√	√			
Deneo-Pellegrini *et al*[57], 1996	√	√	√	√		√			√	
Lin *et al*[55], 2005	√		√	√	√	√	√	√		√
Theodoratou *et al*[37], 2007	√	√	√	√	√	√	√	√		
Deneo-Pellegrini *et al*[38], 2002	√		√	√	√				√	√

BMI: Body mass index; CRC: Colorectal cancer.

Table 3 Risk of bias of 24 included studies, based on the Risk of Bias In Non-randomized Studies of Interventions-I tool

Ref.	Confounding	Selection of participants	Classification of interventions	Deviations from intended interventions	Bias due to missing data	Measurement of outcomes	Selection of reported result	Overall rating
Lee *et al*[39], 2017	Moderate	Low	Low	Low	Moderate	Low	Low	Moderate
Abu Mweis *et al*[41], 2015	Moderate	Low	Moderate	Low	Moderate	Low	Low	Moderate
Leenders *et al*[40], 2015	Moderate	Moderate	Low	Low	Moderate	Low	Low	Moderate
Tayyem *et al*[42], 2014	Moderate	Low	Low	Low	Low	Low	Low	Moderate
Rosato *et al*[43], 2013	Moderate	Low	Low	Low	Moderate	Low	Low	Moderate
Vogtmann *et al*[50], 2013	Low	Low	Low	Low	Moderate	Low	Low	Moderate
Annema *et al*[44], 2011	Moderate	Low	Low	Low	Moderate	Low	Low	Moderate
Foschi *et al*[45], 2010	Moderate	Moderate	Low	Low	Moderate	Low	Low	Moderate
Jedrychowski *et al*[32], 2010	Moderate	Low	Moderate	Low	Moderate	Low	Low	Moderate
Williams *et al*[46], 2009	Moderate	Low	Low	Low	Moderate	Low	Low	Moderate
Li *et al*[51], 2010	Moderate	Low	Low	Low	Moderate	Low	Low	Moderate
Gallus *et al*[47], 2005	Moderate	Low	Moderate	Low	Moderate	Low	Low	Moderate
Lin *et al*[36], 2006	Low	Moderate	Low	Low	Moderate	Low	Low	Moderate
Satia-Abouta *et al*[48], 2004	Moderate	Low	Low	Low	Moderate	Low	Low	Moderate
Voorrips *et al*[53], 2000	Moderate	Moderate	Low	Low	Moderate	Low	Low	Moderate
Franceschi *et al*[29], 1998	Moderate	Low	Moderate	Low	Moderate	Low	Low	Moderate
Levi *et al*[49], 1999	Moderate	Low	Low	Low	Moderate	Low	Low	Moderate
Le Marchand *et al*[56], 1997	Moderate	Low	Moderate	Low	Moderate	Low	Low	Moderate
Deneo-Pellegrini *et al*[57], 1996	Moderate	Low	Low	Low	Moderate	Low	Low	Moderate
Theodoratou *et al*[37], 2007	Moderate	Low	Low	Low	Moderate	Low	Low	Moderate
Deneo-Pellegrini *et al*[38], 2002	Moderate	Low	Low	Low	Moderate	Low	Low	Moderate
Nomura *et al*[52], 2008	Moderate	Low	Low	Low	Moderate	Low	Low	Moderate
Lin *et al*[55], 2005	Moderate	Low	Low	Low	Moderate	Low	Low	Moderate
Michels *et al*[54], 2000	Moderate	Moderate	Low	Low	Moderate	Low	Low	Moderate

ARTICLE HIGHLIGHTS

Research background

Colorectal cancer (CRC) is the third most prevalent cancer, and the prevalence of CRC in adults aged 40-49 has increased by approximately 15% between 2000-2002 and 2014-2016. However, inconsistent findings have been reported in different studies on the association between the intake of different types of fruits and CRC. Given their different chemical compositions and underlying molecular mechanisms, some types of fruits may have a closer correlation with CRC risk than others. This meta-analysis provides more reliable evidence that a higher intake of certain fruits is more effective in CRC prevention.

Research motivation

The main topic of this study is exploring the association between intake of different types of fruits and CRC risk. The key problem to be solved is to compare the CRC risk in the highest and lowest intake groups and conduct a meta-analysis. The significance of this study is that we have found that certain types of fruits can effectively reduce CRC risk.

Research objectives

To help people improve their lifestyles and dietary habits to live a healthy life. The most important goal is to ease the CRC-related social and economic burden worldwide. In terms of goal realized, through this meta-analysis, we have found that eating more citrus, apple, watermelon and kiwi fruit can effectively reduce CRC risk. Implications of achieving the goals: Further analysis of specific types of fruit is needed to explore key anti-cancer components.

Research methods

This meta-analysis was conducted by comparing the reported CRC risk between the highest and lowest fruit intake groups. Considering that CRC is rare, the risk is less than 10%, and the OR is small, the RR/HR we have calculated is approximately equal to the OR. Heterogeneity of results across studies was assessed by the I^2 test. Publication bias was determined using funnel plots and Egger's linear regression test. A dose-response analysis of citrus fruits was also conducted to examine a possible nonlinear relationship. All analyses were performed using R (version 4.1.3). Characteristics and novelty of the research method: No research has used this method to explore this topic before. This research direction is very suitable for this research method.

Research results

Findings: High intakes of citrus, apple, watermelon, and kiwi reduced CRC risk by 9%, 25%, 26%, and 13%, respectively, compared with low intakes. However, other types of fruit did not show an association with CRC risk. A non-linear dose-response relationship was found between citrus and CRC risk. Contribution to the field: This study performed a meta-analysis of previous data in a scientific context and identified the fruit types most effective in reducing CRC risk. Unresolved issues: More prospective studies are needed in the future to further elucidate the association between fruit and CRC.

Research conclusions

The results of this study underpin the hypothesis that certain types of fruit are effective in preventing CRC. This meta-analysis is based on the reported CRC risk of the highest and lowest fruit intake groups. It convincingly demonstrates the real association between fruit and CRC.

Research perspectives

In future research, we hope to find out the key anti-cancer components of specific types of fruits, so as to help people prevent cancer more effectively.

ACKNOWLEDGEMENTS

We would like to thank the researchers and study participants for their contributions.

FOOTNOTES

Author contributions: Wu ZY and Han YW contributed to conceptualization; Wu ZY contributed to methodology; Chen JL contributed to software; Wu ZY, Chen JL, and Li H contributed to validation; Wu ZY contributed to formal analysis; Su K contributed to investigation; Su K contributed to resources; Li H contributed to data curation; Wu ZY, Chen JL, and Han YW contributed to writing-original draft preparation; all authors contributed to writing-review

and editing; Chen JL contributed to visualization; Han YW contributed to supervision; Han YW contributed to project administration; all authors have read and agreed to the published version of the manuscript.

Conflict-of-interest statement: The authors declare that they have no conflict of interest.

PRISMA 2009 Checklist statement: The authors have read the PRISMA 2009 Checklist, and the manuscript was prepared and revised according to the PRISMA 2009 Checklist.

Country/Territory of origin: China

ORCID number: Zhen-Ying Wu 0000-0002-2269-8804; Jia-Li Chen 0000-0002-2692-8179; Han Li 0000-0003-0846-3846; Ke Su 0000-0002-7948-6335; Yun-Wei Han 0000-0002-0942-9095.

S-Editor: Chen YL
L-Editor: A
P-Editor: Yuan YY

REFERENCES

1 **El-Shami K**, Oeffinger KC, Erb NL, Willis A, Bretsch JK, Pratt-Chapman ML, Cannady RS, Wong SL, Rose J, Barbour AL, Stein KD, Sharpe KB, Brooks DD, Cowens-Alvarado RL. American Cancer Society Colorectal Cancer Survivorship Care Guidelines. *CA Cancer J Clin* 2015; **65**: 428-455 [PMID: 26348643 DOI: 10.3322/caac.21286]

2 **Haghighat S**, Sussman DA, Deshpande A. US Preventive Services Task Force Recommendation Statement on Screening for Colorectal Cancer. *JAMA* 2021; **326**: 1328 [PMID: 34609459 DOI: 10.1001/jama.2021.13466]

3 **O'Sullivan DE**, Sutherland RL, Town S, Chow K, Fan J, Forbes N, Heitman SJ, Hilsden RJ, Brenner DR. Risk Factors for Early-Onset Colorectal Cancer: A Systematic Review and Meta-analysis. *Clin Gastroenterol Hepatol* 2022; **20**: 1229-1240.e5 [PMID: 33524598 DOI: 10.1016/j.cgh.2021.01.037]

4 **Li YH**, Niu YB, Sun Y, Zhang F, Liu CX, Fan L, Mei QB. Role of phytochemicals in colorectal cancer prevention. *World J Gastroenterol* 2015; **21**: 9262-9272 [PMID: 26309353 DOI: 10.3748/wjg.v21.i31.9262]

5 **François C**, van Velthoven R, De Lathouwer O, Moreno C, Peltier A, Kaltner H, Salmon I, Gabius HJ, Danguy A, Decaestecker C, Kiss R. Galectin-1 and galectin-3 binding pattern expression in renal cell carcinomas. *Am J Clin Pathol* 1999; **112**: 194-203 [PMID: 10439799 DOI: 10.1093/ajcp/112.2.194]

6 **Piantelli M**, Iacobelli S, Almadori G, Iezzi M, Tinari N, Natoli C, Cadoni G, Lauriola L, Ranelletti FO. Lack of expression of galectin-3 is associated with a poor outcome in node-negative patients with laryngeal squamous-cell carcinoma. *J Clin Oncol* 2002; **20**: 3850-3856 [PMID: 12228204 DOI: 10.1200/jco.2002.01.078]

7 **Nakahara S**, Oka N, Raz A. On the role of galectin-3 in cancer apoptosis. *Apoptosis* 2005; **10**: 267-275 [PMID: 15843888 DOI: 10.1007/s10495-005-0801-y]

8 **Li Y**, Liu L, Niu Y, Feng J, Sun Y, Kong X, Chen Y, Chen X, Gan H, Cao S, Mei Q. Modified apple polysaccharide prevents against tumorigenesis in a mouse model of colitis-associated colon cancer: role of galectin-3 and apoptosis in cancer prevention. *Eur J Nutr* 2012; **51**: 107-117 [PMID: 21516492 DOI: 10.1007/s00394-011-0194-3]

9 **Liu YZ**, Wu K, Huang J, Liu Y, Wang X, Meng ZJ, Yuan SX, Wang DX, Luo JY, Zuo GW, Yin LJ, Chen L, Deng ZL, Yang JQ, Sun WJ, He BC. The PTEN/PI3K/Akt and Wnt/β-catenin signaling pathways are involved in the inhibitory effect of resveratrol on human colon cancer cell proliferation. *Int J Oncol* 2014; **45**: 104-112 [PMID: 24756222 DOI: 10.3892/ijo.2014.2392]

10 **Moon YJ**, Wang X, Morris ME. Dietary flavonoids: effects on xenobiotic and carcinogen metabolism. *Toxicol In Vitro* 2006; **20**: 187-210 [PMID: 16289744 DOI: 10.1016/j.tiv.2005.06.048]

11 **Arafa MA**, Waly MI, Jriesat S, Al Khafajei A, Sallam S. Dietary and lifestyle characteristics of colorectal cancer in Jordan: a case-control study. *Asian Pac J Cancer Prev* 2011; **12**: 1931-1936 [PMID: 22292627]

12 **van Duijnhoven FJ**, Bueno-De-Mesquita HB, Ferrari P, Jenab M, Boshuizen HC, Ros MM, Casagrande C, Tjønneland A, Olsen A, Overvad K, Thorlacius-Ussing O, Clavel-Chapelon F, Boutron-Ruault MC, Morois S, Kaaks R, Linseisen J, Boeing H, Nöthlings U, Trichopoulou A, Trichopoulos D, Misirli G, Palli D, Sieri S, Panico S, Tumino R, Vineis P, Peeters PH, van Gils CH, Ocké MC, Lund E, Engeset D, Skeie G, Suárez LR, González CA, Sánchez MJ, Dorronsoro M, Navarro C, Barricarte A, Berglund G, Manjer J, Hallmans G, Palmqvist R, Bingham SA, Khaw KT, Key TJ, Allen NE, Boffetta P, Slimani N, Rinaldi S, Gallo V, Norat T, Riboli E. Fruit, vegetables, and colorectal cancer risk: the European Prospective Investigation into Cancer and Nutrition. *Am J Clin Nutr* 2009; **89**: 1441-1452 [PMID: 19339391 DOI: 10.3945/ajcn.2008.27120]

13 **Dahm CC**, Keogh RH, Spencer EA, Greenwood DC, Key TJ, Fentiman IS, Shipley MJ, Brunner EJ, Cade JE, Burley VJ, Mishra G, Stephen AM, Kuh D, White IR, Luben R, Lentjes MA, Khaw KT, Rodwell Bingham SA. Dietary fiber and colorectal cancer risk: a nested case-control study using food diaries. *J Natl Cancer Inst* 2010; **102**: 614-626 [PMID: 20407088 DOI: 10.1093/jnci/djq092]

14 **Fung TT**, Hu FB, Wu K, Chiuve SE, Fuchs CS, Giovannucci E. The Mediterranean and Dietary Approaches to Stop

Hypertension (DASH) diets and colorectal cancer. *Am J Clin Nutr* 2010; **92**: 1429-1435 [PMID: 21097651 DOI: 10.3945/ajcn.2010.29242]

15 **Wang DD**, Li Y, Bhupathiraju SN, Rosner BA, Sun Q, Giovannucci EL, Rimm EB, Manson JE, Willett WC, Stampfer MJ, Hu FB. Fruit and Vegetable Intake and Mortality: Results From 2 Prospective Cohort Studies of US Men and Women and a Meta-Analysis of 26 Cohort Studies. *Circulation* 2021; **143**: 1642-1654 [PMID: 33641343 DOI: 10.1161/CIRCULATIONAHA.120.048996]

16 **Fuchs CS**, Giovannucci EL, Colditz GA, Hunter DJ, Stampfer MJ, Rosner B, Speizer FE, Willett WC. Dietary fiber and the risk of colorectal cancer and adenoma in women. *N Engl J Med* 1999; **340**: 169-176 [PMID: 9895396 DOI: 10.1056/nejm199901213400301]

17 **Flood A**, Velie EM, Chaterjee N, Subar AF, Thompson FE, Lacey JV Jr, Schairer C, Troisi R, Schatzkin A. Fruit and vegetable intakes and the risk of colorectal cancer in the Breast Cancer Detection Demonstration Project follow-up cohort. *Am J Clin Nutr* 2002; **75**: 936-943 [PMID: 11976170 DOI: 10.1093/ajcn/75.5.936]

18 **Koushik A**, Hunter DJ, Spiegelman D, Beeson WL, van den Brandt PA, Buring JE, Calle EE, Cho E, Fraser GE, Freudenheim JL, Fuchs CS, Giovannucci EL, Goldbohm RA, Harnack L, Jacobs DR Jr, Kato I, Krogh V, Larsson SC, Leitzmann MF, Marshall JR, McCullough ML, Miller AB, Pietinen P, Rohan TE, Schatzkin A, Sieri S, Virtanen MJ, Wolk A, Zeleniuch-Jacquotte A, Zhang SM, Smith-Warner SA. Fruits, vegetables, and colon cancer risk in a pooled analysis of 14 cohort studies. *J Natl Cancer Inst* 2007; **99**: 1471-1483 [PMID: 17895473 DOI: 10.1093/jnci/djm155]

19 **Wang X**, Ouyang Y, Liu J, Zhu M, Zhao G, Bao W, Hu FB. Fruit and vegetable consumption and mortality from all causes, cardiovascular disease, and cancer: systematic review and dose-response meta-analysis of prospective cohort studies. *BMJ* 2014; **349**: g4490 [PMID: 25073782 DOI: 10.1136/bmj.g4490]

20 **Yang Y**, Zhang D, Feng N, Chen G, Liu J, Zhu Y. Increased intake of vegetables, but not fruit, reduces risk for hepatocellular carcinoma: a meta-analysis. *Gastroenterology* 2014; **147**: 1031-1042 [PMID: 25127680 DOI: 10.1053/j.gastro.2014.08.005]

21 **Norat T**, Aune D, Chan D, Romaguera D. Fruits and vegetables: updating the epidemiologic evidence for the WCRF/AICR lifestyle recommendations for cancer prevention. *Cancer Treat Res* 2014; **159**: 35-50 [PMID: 24114473 DOI: 10.1007/978-3-642-38007-5_3]

22 **Liberati A**, Altman DG, Tetzlaff J, Mulrow C, Gøtzsche PC, Ioannidis JP, Clarke M, Devereaux PJ, Kleijnen J, Moher D. The PRISMA statement for reporting systematic reviews and meta-analyses of studies that evaluate health care interventions: explanation and elaboration. *PLoS Med* 2009; **6**: e1000100 [PMID: 19621070 DOI: 10.1371/journal.pmed.1000100]

23 **Aune D**, Chan DS, Lau R, Vieira R, Greenwood DC, Kampman E, Norat T. Dietary fibre, whole grains, and risk of colorectal cancer: systematic review and dose-response meta-analysis of prospective studies. *BMJ* 2011; **343**: d6617 [PMID: 22074852 DOI: 10.1136/bmj.d6617]

24 **Rong Y**, Chen L, Zhu T, Song Y, Yu M, Shan Z, Sands A, Hu FB, Liu L. Egg consumption and risk of coronary heart disease and stroke: dose-response meta-analysis of prospective cohort studies. *BMJ* 2013; **346**: e8539 [PMID: 23295181 DOI: 10.1136/bmj.e8539]

25 **Vieira AR**, Abar L, Vingeliene S, Chan DS, Aune D, Navarro-Rosenblatt D, Stevens C, Greenwood D, Norat T. Fruits, vegetables and lung cancer risk: a systematic review and meta-analysis. *Ann Oncol* 2016; **27**: 81-96 [PMID: 26371287 DOI: 10.1093/annonc/mdv381]

26 **Riboli E**, Norat T. Epidemiologic evidence of the protective effect of fruit and vegetables on cancer risk. *Am J Clin Nutr* 2003; **78**: 559S-569S [PMID: 12936950 DOI: 10.1093/ajcn/78.3.559S]

27 **Sterne JA**, Hernán MA, Reeves BC, Savović J, Berkman ND, Viswanathan M, Henry D, Altman DG, Ansari MT, Boutron I, Carpenter JR, Chan AW, Churchill R, Deeks JJ, Hróbjartsson A, Kirkham J, Jüni P, Loke YK, Pigott TD, Ramsay CR, Regidor D, Rothstein HR, Sandhu L, Santaguida PL, Schünemann HJ, Shea B, Shrier I, Tugwell P, Turner L, Valentine JC, Waddington H, Waters E, Wells GA, Whiting PF, Higgins JP. ROBINS-I: a tool for assessing risk of bias in non-randomised studies of interventions. *BMJ* 2016; **355**: i4919 [PMID: 27733354 DOI: 10.1136/bmj.i4919]

28 **Localio AR**, Margolis DJ, Berlin JA. Relative risks and confidence intervals were easily computed indirectly from multivariable logistic regression. *J Clin Epidemiol* 2007; **60**: 874-882 [PMID: 17689803 DOI: 10.1016/j.jclinepi.2006.12.001]

29 **Franceschi S**, Parpinel M, La Vecchia C, Favero A, Talamini R, Negri E. Role of different types of vegetables and fruit in the prevention of cancer of the colon, rectum, and breast. *Epidemiology* 1998; **9**: 338-341 [PMID: 9583427]

30 **Franceschi S**, Favero A. The role of energy and fat in cancers of the breast and colon-rectum in a southern European population. *Ann Oncol* 1999; **10** Suppl 6: 61-63 [PMID: 10676554]

31 **Franceschi S**, Favero A, Parpinel M, Giacosa A, La Vecchia C. Italian study on colorectal cancer with emphasis on influence of cereals. *Eur J Cancer Prev* 1998; **7** Suppl 2: S19-S23 [PMID: 9696938 DOI: 10.1097/00008469-199805000-00004]

32 **Jedrychowski W**, Maugeri U, Popiela T, Kulig J, Sochacka-Tatara E, Pac A, Sowa A, Musial A. Case-control study on beneficial effect of regular consumption of apples on colorectal cancer risk in a population with relatively low intake of fruits and vegetables. *Eur J Cancer Prev* 2010; **19**: 42-47 [PMID: 19926998 DOI: 10.1097/CEJ.0b013e328333d0cc]

33 **Jedrychowski W**, Maugeri U, Pac A, Sochacka-Tatara E, Galas A. Reduced risk of colorectal cancer and regular consumption of apples: Hospital based case-control study in Poland. *CEJ Med* 2009; **4**: 320-326 [DOI: 10.2478/s11536-009-0033-6]

34 **Tuyns AJ**, Kaaks R, Haelterman M. Colorectal cancer and the consumption of foods: a case-control study in Belgium. *Nutr Cancer* 1988; **11**: 189-204 [PMID: 3405870 DOI: 10.1080/01635588809513986]

35 **Tajima K**, Tominaga S. Dietary habits and gastro-intestinal cancers: a comparative case-control study of stomach and large intestinal cancers in Nagoya, Japan. *Jpn J Cancer Res* 1985; **76**: 705-716 [PMID: 3930448]

36 **Lin J**, Zhang SM, Wu K, Willett WC, Fuchs CS, Giovannucci E. Flavonoid intake and colorectal cancer risk in men and women. *Am J Epidemiol* 2006; **164**: 644-651 [PMID: 16923774 DOI: 10.1093/aje/kwj296]

37 **Theodoratou E**, Kyle J, Cetnarskyj R, Farrington SM, Tenesa A, Barnetson R, Porteous M, Dunlop M, Campbell H.

Dietary flavonoids and the risk of colorectal cancer. *Cancer Epidemiol Biomarkers Prev* 2007; **16**: 684-693 [PMID: 17416758 DOI: 10.1158/1055-9965.Epi-06-0785]

38 **Deneo-Pellegrini H**, Boffetta P, De Stefani E, Ronco A, Brennan P, Mendilaharsu M. Plant foods and differences between colon and rectal cancers. *Eur J Cancer Prev* 2002; **11**: 369-375 [PMID: 12195164 DOI: 10.1097/00008469-200208000-00009]

39 **Lee J**, Shin A, Oh JH, Kim J. Colors of vegetables and fruits and the risks of colorectal cancer. *World J Gastroenterol* 2017; **23**: 2527-2538 [PMID: 28465637 DOI: 10.3748/wjg.v23.i14.2527]

40 **Leenders M**, Siersema PD, Overvad K, Tjønneland A, Olsen A, Boutron-Ruault MC, Bastide N, Fagherazzi G, Katzke V, Kühn T, Boeing H, Aleksandrova K, Trichopoulou A, Lagiou P, Klinaki E, Masala G, Grioni S, Santucci De Magistris M, Tumino R, Ricceri F, Peeters PH, Lund E, Skeie G, Weiderpass E, Quirós JR, Agudo A, Sánchez MJ, Dorronsoro M, Navarro C, Ardanaz E, Ohlsson B, Jirström K, Van Guelpen B, Wennberg M, Khaw KT, Wareham N, Key TJ, Romieu I, Huybrechts I, Cross AJ, Murphy N, Riboli E, Bueno-de-Mesquita HB. Subtypes of fruit and vegetables, variety in consumption and risk of colon and rectal cancer in the European Prospective Investigation into Cancer and Nutrition. *Int J Cancer* 2015; **137**: 2705-2714 [PMID: 26077137 DOI: 10.1002/ijc.29640]

41 **Abu Mweis SS**, Tayyem RF, Shehadah I, Bawadi HA, Agraib LM, Bani-Hani KE, Al-Jaberi T, Al-Nusairr M. Food groups and the risk of colorectal cancer: results from a Jordanian case-control study. *Eur J Cancer Prev* 2015; **24**: 313-320 [PMID: 25415835 DOI: 10.1097/CEJ.0000000000000089]

42 **Tayyem RF**, Shehadah I, Abu-Mweis SS, Bawadi HA, Bani-Hani KE, Al-Jaberi T, Al-Nusairr M, Heath DD. Fruit and vegetable intake among Jordanians: results from a case-control study of colorectal cancer. *Cancer Control* 2014; **21**: 350-360 [PMID: 25310217 DOI: 10.1177/107327481402100412]

43 **Rosato V**, Bosetti C, Levi F, Polesel J, Zucchetto A, Negri E, La Vecchia C. Risk factors for young-onset colorectal cancer. *Cancer Causes Control* 2013; **24**: 335-341 [PMID: 23224326 DOI: 10.1007/s10552-012-0119-3]

44 **Annema N**, Heyworth JS, McNaughton SA, Iacopetta B, Fritschi L. Fruit and vegetable consumption and the risk of proximal colon, distal colon, and rectal cancers in a case-control study in Western Australia. *J Am Diet Assoc* 2011; **111**: 1479-1490 [PMID: 21963014 DOI: 10.1016/j.jada.2011.07.008]

45 **Foschi R**, Pelucchi C, Dal Maso L, Rossi M, Levi F, Talamini R, Bosetti C, Negri E, Serraino D, Giacosa A, Franceschi S, La Vecchia C. Citrus fruit and cancer risk in a network of case-control studies. *Cancer Causes Control* 2010; **21**: 237-242 [PMID: 19856118 DOI: 10.1007/s10552-009-9454-4]

46 **Williams CD**, Satia JA, Adair LS, Stevens J, Galanko J, Keku TO, Sandler RS. Dietary patterns, food groups, and rectal cancer risk in Whites and African-Americans. *Cancer Epidemiol Biomarkers Prev* 2009; **18**: 1552-1561 [PMID: 19423533 DOI: 10.1158/1055-9965.EPI-08-1146]

47 **Gallus S**, Talamini R, Giacosa A, Montella M, Ramazzotti V, Franceschi S, Negri E, La Vecchia C. Does an apple a day keep the oncologist away? *Ann Oncol* 2005; **16**: 1841-1844 [PMID: 16091428 DOI: 10.1093/annonc/mdi361]

48 **Satia-Abouta J**, Galanko JA, Martin CF, Ammerman A, Sandler RS. Food groups and colon cancer risk in African-Americans and Caucasians. *Int J Cancer* 2004; **109**: 728-736 [PMID: 14999782 DOI: 10.1002/ijc.20044]

49 **Levi F**, Pasche C, La Vecchia C, Lucchini F, Franceschi S. Food groups and colorectal cancer risk. *Br J Cancer* 1999; **79**: 1283-1287 [PMID: 10098773 DOI: 10.1038/sj.bjc.6690206]

50 **Vogtmann E**, Xiang YB, Li HL, Levitan EB, Yang G, Waterbor JW, Gao J, Cai H, Xie L, Wu QJ, Zhang B, Gao YT, Zheng W, Shu XO. Fruit and vegetable intake and the risk of colorectal cancer: results from the Shanghai Men's Health Study. *Cancer Causes Control* 2013; **24**: 1935-1945 [PMID: 23913012 DOI: 10.1007/s10552-013-0268-z]

51 **Li WQ**, Kuriyama S, Li Q, Nagai M, Hozawa A, Nishino Y, Tsuji I. Citrus consumption and cancer incidence: the Ohsaki cohort study. *Int J Cancer* 2010; **127**: 1913-1922 [PMID: 20104526 DOI: 10.1002/ijc.25203]

52 **Nomura AM**, Wilkens LR, Murphy SP, Hankin JH, Henderson BE, Pike MC, Kolonel LN. Association of vegetable, fruit, and grain intakes with colorectal cancer: the Multiethnic Cohort Study. *Am J Clin Nutr* 2008; **88**: 730-737 [PMID: 18779290 DOI: 10.1093/ajcn/88.3.730]

53 **Voorrips LE**, Goldbohm RA, van Poppel G, Sturmans F, Hermus RJ, van den Brandt PA. Vegetable and fruit consumption and risks of colon and rectal cancer in a prospective cohort study: The Netherlands Cohort Study on Diet and Cancer. *Am J Epidemiol* 2000; **152**: 1081-1092 [PMID: 11117618 DOI: 10.1093/aje/152.11.1081]

54 **Michels KB**, Edward Giovannucci, Joshipura KJ, Rosner BA, Stampfer MJ, Fuchs CS, Colditz GA, Speizer FE, Willett WC. Prospective study of fruit and vegetable consumption and incidence of colon and rectal cancers. *J Natl Cancer Inst* 2000; **92**: 1740-1752 [PMID: 11058617 DOI: 10.1093/jnci/92.21.1740]

55 **Lin J**, Zhang SM, Cook NR, Rexrode KM, Liu S, Manson JE, Lee IM, Buring JE. Dietary intakes of fruit, vegetables, and fiber, and risk of colorectal cancer in a prospective cohort of women (United States). *Cancer Causes Control* 2005; **16**: 225-233 [PMID: 15947874 DOI: 10.1007/s10552-004-4025-1]

56 **Le Marchand L**, Hankin JH, Wilkens LR, Kolonel LN, Englyst HN, Lyu LC. Dietary fiber and colorectal cancer risk. *Epidemiology* 1997; **8**: 658-665 [PMID: 9345666 DOI: 10.1097/00001648-199710000-00008]

57 **Deneo-Pellegrini H**, De Stefani E, Ronco A. Vegetables, fruits, and risk of colorectal cancer: a case-control study from Uruguay. *Nutr Cancer* 1996; **25**: 297-304 [PMID: 8771572 DOI: 10.1080/01635589609514453]

58 **Jaganathan SK**, Vellayappan MV, Narasimhan G, Supriyanto E. Role of pomegranate and citrus fruit juices in colon cancer prevention. *World J Gastroenterol* 2014; **20**: 4618-4625 [PMID: 24782614 DOI: 10.3748/wjg.v20.i16.4618]

59 **Goh JXH**, Tan LT, Goh JK, Chan KG, Pusparajah P, Lee LH, Goh BH. Nobiletin and Derivatives: Functional Compounds from Citrus Fruit Peel for Colon Cancer Chemoprevention. *Cancers (Basel)* 2019; **11** [PMID: 31234411 DOI: 10.3390/cancers11060867]

60 **Frydoonfar HR**, McGrath DR, Spigelman AD. The variable effect on proliferation of a colon cancer cell line by the citrus fruit flavonoid Naringenin. *Colorectal Dis* 2003; **5**: 149-152 [PMID: 12780904 DOI: 10.1046/j.1463-1318.2003.00444.x]

61 **Zhang YS**, Wang F, Cui SX, Qu XJ. Natural dietary compound naringin prevents azoxymethane/dextran sodium sulfate-induced chronic colorectal inflammation and carcinogenesis in mice. *Cancer Biol Ther* 2018; **19**: 735-744 [PMID: 29580144 DOI: 10.1080/15384047.2018.1453971]

62 **Gong Y**, Dong R, Gao X, Li J, Jiang L, Zheng J, Cui S, Ying M, Yang B, Cao J, He Q. Neohesperidin prevents colorectal tumorigenesis by altering the gut microbiota. *Pharmacol Res* 2019; **148**: 104460 [PMID: 31560944 DOI: 10.1016/j.phrs.2019.104460]

63 **Li Y**, Wang S, Sun Y, Xu W, Zheng H, Wang Y, Tang Y, Gao X, Song C, Long Y, Liu J, Liu L, Mei Q. Apple polysaccharide protects ICR mice against colitis associated colorectal cancer through the regulation of microbial dysbiosis. *Carbohydr Polym* 2020; **230**: 115726 [PMID: 31887919 DOI: 10.1016/j.carbpol.2019.115726]

64 **Zhang D**, Sun Y, Yue Z, Li Q, Meng J, Liu J, Hekong X, Jiang F, Mi M, Liu L, Mei Q. Apple polysaccharides induce apoptosis in colorectal cancer cells. *Int J Mol Med* 2012; **30**: 100-106 [PMID: 22470124 DOI: 10.3892/ijmm.2012.953]

65 **Zhang D**, Li YH, Mi M, Jiang FL, Yue ZG, Sun Y, Fan L, Meng J, Zhang X, Liu L, Mei QB. Modified apple polysaccharides suppress the migration and invasion of colorectal cancer cells induced by lipopolysaccharide. *Nutr Res* 2013; **33**: 839-848 [PMID: 24074742 DOI: 10.1016/j.nutres.2013.06.004]

66 **Bars-Cortina D**, Martínez-Bardají A, Macià A, Motilva MJ, Piñol-Felis C. Consumption evaluation of one apple flesh a day in the initial phases prior to adenoma/adenocarcinoma in an azoxymethane rat colon carcinogenesis model. *J Nutr Biochem* 2020; **83**: 108418 [PMID: 32592950 DOI: 10.1016/j.jnutbio.2020.108418]

67 **Marzo F**, Milagro FI, Barrenetxe J, Díaz MT, Martínez JA. Azoxymethane-Induced Colorectal Cancer Mice Treated with a Polyphenol-Rich Apple Extract Show Less Neoplastic Lesions and Signs of Cachexia. *Foods* 2021; **10** [PMID: 33921048 DOI: 10.3390/foods10040863]

68 **Kern M**, Pahlke G, Balavenkatraman KK, Böhmer FD, Marko D. Apple polyphenols affect protein kinase C activity and the onset of apoptosis in human colon carcinoma cells. *J Agric Food Chem* 2007; **55**: 4999-5006 [PMID: 17542601 DOI: 10.1021/jf063158x]

69 **Steevens J**, Schouten LJ, Goldbohm RA, van den Brandt PA. Vegetables and fruits consumption and risk of esophageal and gastric cancer subtypes in the Netherlands Cohort Study. *Int J Cancer* 2011; **129**: 2681-2693 [PMID: 21960262 DOI: 10.1002/ijc.25928]

70 **Yamaji T**, Inoue M, Sasazuki S, Iwasaki M, Kurahashi N, Shimazu T, Tsugane S; Japan Public Health Center-based Prospective Study Group. Fruit and vegetable consumption and squamous cell carcinoma of the esophagus in Japan: the JPHC study. *Int J Cancer* 2008; **123**: 1935-1940 [PMID: 18688852 DOI: 10.1002/ijc.23744]

71 **Bae JM**, Lee EJ, Guyatt G. Citrus fruit intake and stomach cancer risk: a quantitative systematic review. *Gastric Cancer* 2008; **11**: 23-32 [PMID: 18373174 DOI: 10.1007/s10120-007-0447-2]

72 **Holst B**, Williamson G. Nutrients and phytochemicals: from bioavailability to bioefficacy beyond antioxidants. *Curr Opin Biotechnol* 2008; **19**: 73-82 [PMID: 18406129 DOI: 10.1016/j.copbio.2008.03.003]

73 **Oh H**, Kim H, Lee DH, Lee A, Giovannucci EL, Kang SS, Keum N. Different dietary fibre sources and risks of colorectal cancer and adenoma: a dose-response meta-analysis of prospective studies. *Br J Nutr* 2019; **122**: 605-615 [PMID: 31495339 DOI: 10.1017/S0007114519001454]

World Journal of Gastroenterology

Submit a Manuscript: https://www.f6publishing.com

World J Gastroenterol 2023 May 7; 29(17): 2701-2703

DOI: 10.3748/wjg.v29.i17.2701

ISSN 1007-9327 (print) ISSN 2219-2840 (online)

LETTER TO THE EDITOR

T cells in pancreatic cancer stroma: Tryptophan metabolism plays an important role in immunoregulation

Ting Yang, Qiao-Qi Li, Yong-Mei Liu, Biao Yang

Specialty type: Gastroenterology and hepatology

Provenance and peer review: Unsolicited article; Externally peer reviewed.

Peer-review model: Single blind

Peer-review report's scientific quality classification

Grade A (Excellent): A
Grade B (Very good): B
Grade C (Good): 0
Grade D (Fair): 0
Grade E (Poor): 0

P-Reviewer: Liu X, China; Zeng C, United States

Received: December 7, 2022
Peer-review started: December 7, 2022
First decision: January 22, 2023
Revised: February 10, 2023
Accepted: April 4, 2023
Article in press: April 4, 2023
Published online: May 7, 2023

Ting Yang, Qiao-Qi Li, Biao Yang, Department of Abdominal Oncology, Division of Medical Oncology, Cancer Center, West China Hospital, Sichuan University, Chengdu 610041, Sichuan Province, China

Yong-Mei Liu, Division of Radiation Oncology, Cancer Center, West China Hospital, Sichuan University, Chengdu 610041, Sichuan Province, China

Corresponding author: Biao Yang, MD, PhD, Professor, Surgeon, Teacher, Department of Abdominal Oncology, Division of Medical Oncology, Cancer Center, West China Hospital, Sichuan University, No. 37 Guoxue Alley, Chengdu 610041, Sichuan Province, China.
landayb@163.com

Abstract

Several studies have shown that the immune system is highly regulated by tryptophan metabolism, which serves as an immunomodulatory factor. The indoleamine 2,3-dioxygenase 1 (IDO1), as an intracellular enzyme that participates in metabolism of the essential amino acid tryptophan in the kynurenine pathway, is an independent prognostic marker for pancreatic cancer (PC). First, overexpression of IDO1 inhibits the maturation of dendritic cells and T-cell proliferation in the liver and spleen. Second, the high expression of kynurenine induces and activates the aryl hydrocarbon receptor, resulting in upregulated programmed cell death protein 1 expression. Third, the induction of IDO1 can lead to loss of the T helper 17 cell/regulatory T cell balance, mediated by the proximal tryptophan catabolite from IDO metabolism. In our study, we found that overexpression of IDO1 upregulated CD8+ T cells and reduced natural killer T cells in pancreatic carcinoma in mice. Hence, it may be essential to pay more attention to tryptophan metabolism in patients, especially those who are tolerant to immunotherapy for PC.

Key Words: Immunosuppression; Pancreatic cancer stroma; T cell; Tryptophan metabolism; Xxx

Core Tip: There are numerous lines for evidence for tryptophan metabolism, which serves as an immunomodulatory factor. Indoleamine2,3-dioxygenase1 (IDO1) overexpression inhibits the maturation of dendritic cells and T-cell proliferation in the spleen. The high expression of kynurenine induces and activates the aryl hydrocarbon receptor, resulting in upregulated programmed cell death protein 1 expression. The induction of IDO1 can lead to loss of T helper 17 cell/regulatory T cell balance. We also found that overexpression of IDO1 upregulated CD8+ T cells and reduced natural killer T cells in PC in mice.

Citation: Yang T, Li QQ, Liu YM, Yang B. T cells in pancreatic cancer stroma: Tryptophan metabolism plays an important role in immunoregulation. *World J Gastroenterol* 2023; 29(17): 2701-2703
URL: https://www.wjgnet.com/1007-9327/full/v29/i17/2701.htm
DOI: https://dx.doi.org/10.3748/wjg.v29.i17.2701

TO THE EDITOR

We have an interest in the recently published article by Goulart *et al*[1],which summarized the pancreatic cancer (PC) immune landscape, T-cell interactions and immune dysfunction, T-cell phenotype and functions, T-cell exhaustion, and immunotherapy in PC. In this review, Goulart *et al* stated that immune cells including CD8+ T, natural killer (NK) cells, T helper 17 cells (Th17), and regulatory T cells (Tregs) are regulated by different cytokine factors. However, several studies have shown that the immune system is highly regulated by tryptophan metabolism. Indoleamine 2,3-dioxygenase 1 (IDO1), as an intracellular enzyme that participates in the metabolism of the essential amino acid tryptophan in the kynurenine (Kyn) pathway, is an independent prognostic marker for PC. There are numerous lines of evidence for tryptophan metabolism, which serves as an immunomodulatory factor. First, IDO1 overexpression inhibits the maturation of CD11c and dendritic cells, and T-cell proliferation in the liver and spleen[2]. Second, the high expression of Kyn induces and activates the aryl hydrocarbon receptor (AhR), resulting in upregulated programmed cell death protein 1 expression. Inhibition of the Kyn-AhR pathway can enhance the efficacy of antitumor adoptive T-cell therapy and reduce the rate of migration and invasion in both tumor-bearing mice and patients with cancer[3]. In *in vivo* experiments, inactivation of the Kyn-AhR pathway showed amelioration of IDO1-mediated immunosuppression[4]. In a clinical study, high expression of the AhR transcript was correlated with reduced CD8 T-cell infiltration and worse outcomes in patients with PC[5]. Third, the induction of IDO1 can lead to loss of the Th17/Treg balance *in vivo*. Similarly, loss of the Th17/Treg balance is mediated by the proximal tryptophan catabolite from IDO metabolism[6]. In our study, we found that overexpression of IDO1 upregulated CD8+ T cells and reduced NK T cells in both hepatic cancer and PC in mice. Hence, it may be essential to pay more attention to tryptophan metabolism in patients with PC, especially those who are tolerant to immunotherapy.

FOOTNOTES

Author contributions: Yang T, Li QQ, Liu YM, and Yang B designed the research study; Yang T and Li QQ performed the research; Yang T, Li QQ, and Yang B analyzed the data and wrote the manuscript; All authors read and approved the final manuscript.

Supported by National Natural Science Foundation of China, No. 82200695.

Conflict-of-interest statement: The authors have no conflicts of interest to declare.

Country/Territory of origin: China

ORCID number: Yong-Mei Liu 0000-0002-0346-1158; Biao Yang 0000-0003-2150-8690.

S-Editor: Liu GL
L-Editor: Filipodia

P-Editor: Liu GL

REFERENCES

1 **Goulart MR**, Stasinos K, Fincham REA, Delvecchio FR, Kocher HM. T cells in pancreatic cancer stroma. *World J Gastroenterol* 2021; **27**: 7956-7968 [PMID: 35046623 DOI: 10.3748/wjg.v27.i46.7956]

2 **Mo C**, Xie S, Liu B, Zhong W, Zeng T, Huang S, Lai Y, Deng G, Zhou C, Yan W, Chen Y, Gao L, Lv Z. Indoleamine 2,3-dioxygenase 1 limits hepatic inflammatory cells recruitment and promotes bile duct ligation-induced liver fibrosis. *Cell Death Dis* 2021; **12**: 16 [PMID: 33414436 DOI: 10.1038/s41419-020-03277-0]

3 **Liu Y**, Liang X, Dong W, Fang Y, Lv J, Zhang T, Fiskesund R, Xie J, Liu J, Yin X, Jin X, Chen D, Tang K, Ma J, Zhang H, Yu J, Yan J, Liang H, Mo S, Cheng F, Zhou Y, Wang J, Li J, Chen Y, Cui B, Hu ZW, Cao X, Xiao-Feng Qin F, Huang B. Tumor-Repopulating Cells Induce PD-1 Expression in CD8(+) T Cells by Transferring Kynurenine and AhR Activation. *Cancer Cell* 2018; **33**: 480-494.e7 [PMID: 29533786 DOI: 10.1016/j.ccell.2018.02.005]

4 **Liang H**, Li T, Fang X, Xing Z, Zhang S, Shi L, Li W, Guo L, Kuang C, Liu H, Yang Q. IDO1/TDO dual inhibitor RY103 targets Kyn-AhR pathway and exhibits preclinical efficacy on pancreatic cancer. *Cancer Lett* 2021; **522**: 32-43 [PMID: 34520819 DOI: 10.1016/j.canlet.2021.09.012]

5 **Newman AC**, Falcone M, Huerta Uribe A, Zhang T, Athineos D, Pietzke M, Vazquez A, Blyth K, Maddocks ODK. Immune-regulated IDO1-dependent tryptophan metabolism is source of one-carbon units for pancreatic cancer and stellate cells. *Mol Cell* 2021; **81**: 2290-2302.e7 [PMID: 33831358 DOI: 10.1016/j.molcel.2021.03.019]

6 **Favre D**, Mold J, Hunt PW, Kanwar B, Loke P, Seu L, Barbour JD, Lowe MM, Jayawardene A, Aweeka F, Huang Y, Douek DC, Brenchley JM, Martin JN, Hecht FM, Deeks SG, McCune JM. Tryptophan catabolism by indoleamine 2,3-dioxygenase 1 alters the balance of TH17 to regulatory T cells in HIV disease. *Sci Transl Med* 2010; **2**: 32ra36 [PMID: 20484731 DOI: 10.1126/scitranslmed.3000632]

Published by **Baishideng Publishing Group Inc**
7041 Koll Center Parkway, Suite 160, Pleasanton, CA 94566, USA
Telephone: +1-925-3991568
E-mail: bpgoffice@wjgnet.com
Help Desk: https://www.f6publishing.com/helpdesk
https://www.wjgnet.com